Structural diversity of Cu(I), Ag(I) and Cu(II) coordination polymers with the ligand ethanediyl bis(isonicotinate)

Inauguraldissertation

Zur
Erlangung der Würde eines Doktors der Philosophie
vorgelegt der
Philosophisch-Naturwissenschaftlichen Fakultät
der Universität Basel

Von

Adeline ROBIN

Aus Romilly-sur-Seine, Frankreich

BASEL, 2005

Genehmigt von der Philosophisch-Naturwissenschaftlichen Fakultät

Auf Antrag von

Prof. Dr. Katharina FROMM
Prof. Dr. Edwin CONSTABLE

Basel, den 26. Juli 2005

Prof. Dr. Hans-Jakob Wirz

Pour Yveline et Gisèle

Acknowledgements

The presented works have been performed in the laboratories of the “Département de Chimie Minérale, Analytique et Appliquée - CHIAM -“ at the University of Genève and in the “Anorganische Chemie Institut” at the University of Basel under the supervision of Prof. Dr. Katharina Fromm. I would like to thank her for allowing me to join her group and for her confidence towards my thesis project. I am glad I had the opportunity to present my work at the four edges of the world (Germany, Italy, Switzerland, Mexico) and to be entrust with the management of the diffractometer. It was a pleasure to belong to this young but dynamic group and to participate to its expansion.

I thank also Prof. Dr. Edwin Constable for judging this thesis work and Prof. Dr. Markus Meuwly for accepting to be foreman of my Ph.D. examining board and for his help in DFT calculations.

I thank also people with whom I could not carry this work to a successful conclusion: Dr. Gérald Bernardinelli, University of Genève, Dr. Helmut Goesmann, University of Karlsruhe, the crystallographers who measured some of the crystals for the determination of the structures by single crystal X-ray diffraction; Dr. Markus Neuburger, University of Basel, for his help towards the Stoe diffractometer; Dr. Antonia Neels, University of Fribourg, for the resolution of one structure from powder X-ray diffraction; Dr. Hansjörg Eder, University of Genève, Werner Kirsch, University of Basel for the elementary analysis; people of the “Laboratoire de Spectrométrie de Masse”, University of Genève, Dr.phil. Sigmund Gunzenhauser for the mass spectroscopy.

I sincerely thank the persons who help me for the technical and administrative problems: Beatrice Erismann and Odile Hirth, Serge Rodak and Dr. Bernhard Jung, François Bujard and Franz Stehlin, Markus Hauri.

I spend a very good time during the last four years with the members of the “CHIAM” in Genève and of the “Anorganische Chemie group” in Basel. I can’t obviously mentioned every people, but I want to thank those who become my friends: Estelle and Gilles, my first Ph.D colleagues for their support and for the “raclette-discussion” parties; Martine, for her friendship gained in the course of some mountain paths; Pascal for completing the Geneva’s band; Remi, for our surrealistic conversations; Lolo, for his contribution to this work, the two wonderful copper structures and of course for his friendship and the DJ role in the lab; Val C, for the singing “Uni-Parties” and Tünde, for her “female” support even if we had unfortunately not enough time to know each other.

I want finally to thank my family, especially my parents, my brother and Emeline and my friends who didn’t forget me in spite of the distance: Valérie, François, Laurent and Françoise, Cyril, Thibault, Cyril, Nancia, Kathrin.

And the most important for the end: I thank Jérôme, for his support at the end of my thesis and much more….

I thank also the Fond national Suisse and the Departement de l’Instruction Publique (DIP) of the Canton de Genève for the financial support, as well as the fonds Frédéric Firmenich et Philippe Chuit, the Fond Marc Birkigt and the Reisefonds der Universität Basel for allowing me to participate to international conferences.

Some of these results have been reported in these publications [1-3]:

- Structural relationship of two coordination polymers of Cu(I) with the ligand ethanediyl bis(isonicotinate), *CrystEngComm*, **2003**, *5*, 405.

- How many structures are there for {[AgL](NO_3)(H_2O)$_n$}? Water-content dependent variations in the structure of {[AgL](NO_3)(H_2O_n)}, n = 0, 1, 2; L = ethanediyl bis(isonicotinate), *CrystEngComm*, **2004**, *6*, 336.

- Recent advances in the chemistry of clusters and coordination polymers of alkali, alkaline earth metal and group 11 compounds, *Z.Anorg. Allg. Chem*, **2005**, *631*, 1725-1740.

Contents

A - Introduction

The expression „Coordination Polymer“ was first used by J.C. Bailar in 1967, when he compared organic polymers with inorganic compounds which can be considered as polymeric species. In comparison he established rules for the building and the required properties of new species involving metal ions and organic ligands. [4] During the last fifteen years the number of publications concerning coordination polymers has dramatically increased from 100 articles per year to 1000 in 2004. What really are coordination polymers? Why do these huge developments happen?

I - About coordination polymers?

Polymers are defined as high molecular weight molecules formed by the repetition of monomeric units linked with covalent bonds. In comparison, coordination polymers are infinite systems build up with metal ions and organic ligands as main elementary units linked via coordination bonds and other weak chemical bonds. These compounds are also named metal-organic coordination networks or metal-organic frameworks (MOF). [5]

Polymeric coordination networks syntheses could be considered as “construction games”: the final architecture depends on the building modules (organic ligands, metal centres, their counter ions, solvent molecules) and their compatibilities. Analyses of the final geometries, of the diverse interactions and optimization of the growth processes are described as crystal engineering. In appropriate circumstances, crystals can be considered as the sum of a series of reproducible molecular recognition events. This means that control of the overall arrangement of the modules can be conceivable with prediction of topology and dimensionality, but not of the exact crystal structure (cell parameters). This approach could be compared to the supramolecular chemistry and self-assembly feature, if crystals are regarded as single chemical entities [6]. Self assembly is based on complementary and explicit interactions between the building blocks in order to generate the final product. [7]

The arrangement of the components in coordination polymers mostly only exist in the solid state [5]: the building blocks interact through coordination interactions and weaker forces such as hydrogen bonds, π-π stacking or Van der Waals interactions in solution giving some small molecular units, and then, thanks to self-assembly processes coordination polymers grow based on the same interactions. (Figure A-1) [8] We can speak of reversible arrangements due to non covalent bonds. Metal ions are generally called nodes whereas the ligands are the linkers.

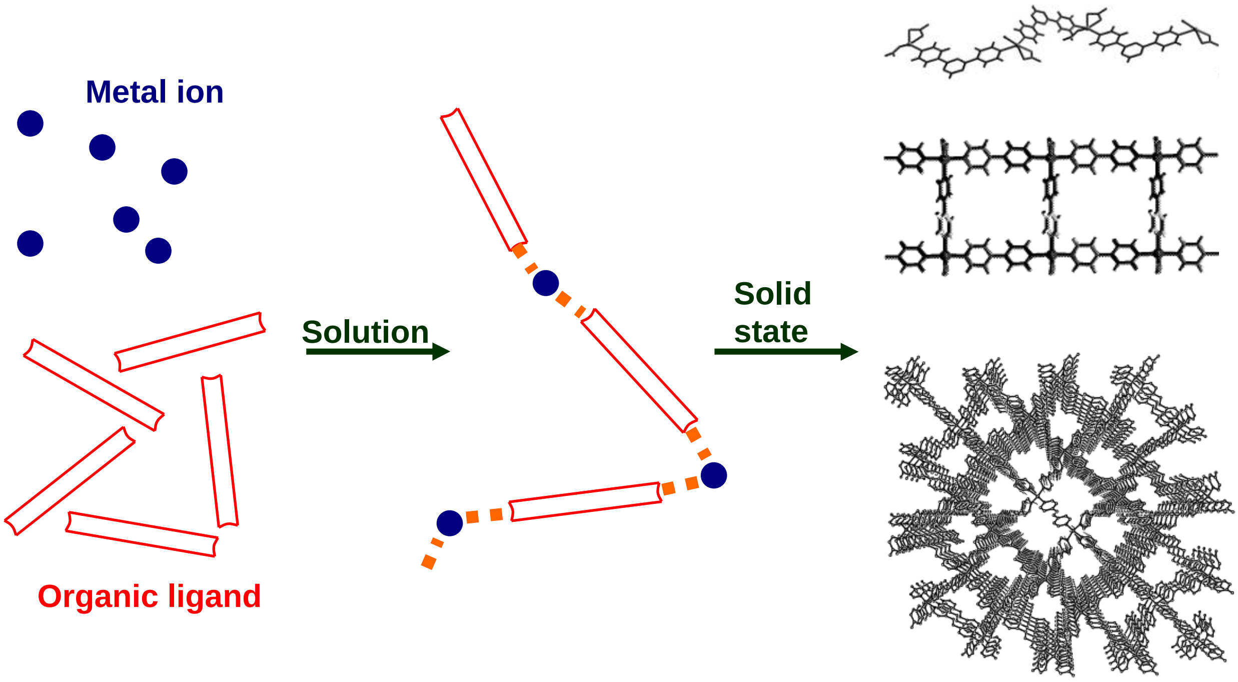

Figure A-1: Formation of coordination polymers [9, 10]

The solid products are generally insoluble or degrade upon dissolution. Structures of coordination polymers can only be determined by X-ray crystallographic methods and characterizations in solution only prove the existence of oligomeric fragments.

I.1 - Interests

The numerous literature contributions in the field of coordination polymers are due to several points:

- Incorporating metal ions in supramolecular networks permits the control of the metal atoms position in the materials, giving them some desired properties. Types of metal centres and distances between them can be chosen so that stable functional solid materials can be tuned.
- The variety of “nodes and linkers” offers to the chemists infinite possibilities for building new species with intriguing architectures and topologies. Moreover, the studies of crystals become much easier thanks to the technologic improvements in the field of X-ray measurements and computational resolution techniques.

I.2 - Interactions

The coordination polymer building is principally directed by the coordination bonding. Coordination bonds are the donation of a lone electron pair of the ligand (Lewis base) to the metal cation (Lewis acid). The energy of such interactions is usually evaluated around 50 kJ.mol^{-1} [11]. Weaker interactions also strongly influence the formation of coordination polymers.

Hydrogen bonds are defined by Steiner [12] as follows: *An D-H···A interaction is called a "hydrogen bond", if 1. it constitutes a local bond, and 2. D-H acts as proton donor to A.* For hydrogen bonds of weak to intermediate strengths, hydrogen bonds may be described with an "electrostatic plus Van der Waals" model. For the strongest types of hydrogen bonds (rarely found in coordination polymers), their quasi-covalent nature has to be fully considered. Some systematic studies have been performed, with the use of structural database (especially the Cambridge Structural Database), in order to understanding the strength and the directional preferences of hydrogen bonds [12-15]. The H···A distance, should be, for instance, in the range 1.5-2.2 Å for strong O-H···O/N hydrogen bonds (with D-H···A angle in the range 140-180°) and 2.0-3.0 Å for weak C-H···O/N contacts (with D-H···A angle in the range 120-180°). The energy of such interactions varies from 15 to 40 kJ.mol^{-1} for moderate hydrogen bonds.

π-π interactions can be of predominant importance during the coordination polymer formation. Janiack reviews this kind of interactions in metal complexes with aromatic nitrogen-containing ligands [16]. Aromatic-aromatic interactions involve face-to-face alignment (with or without offset) and edge-to-face orientations (C-H···π interactions). These interactions are the sum of a lot of contributions (electrostatic, Van der Waals interactions, repulsion, charge transfer), and the aromatic rings stack in an optimal way to minimize all the interaction components. In Figure A-2 and Figure A-3, the geometrical parameters of aromatic-aromatic stacking are defined.

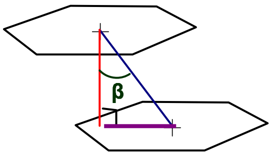

distance geometrical center-geometrical center of the two ring: $\mathbf{d_{H-R}}$

perpendicular distance of a center ring on the other ring: $\mathbf{pd_{H-R}}$

"shift angle": **β**

inclination angle between the two ring planes: α

offset

Figure A-2: schematic representation of aromatic-aromatic interactions (face-to-face) (the designation of distances and angles will be used during this work)

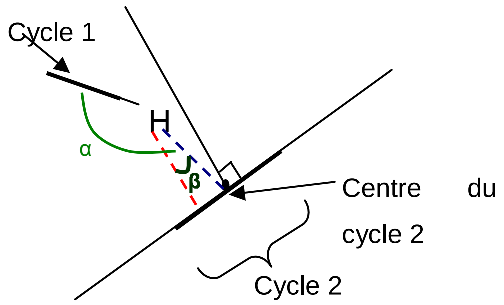

distance H-geometrical center of the second ring: $\mathbf{d_{H-R}}$

perpendicular distance of H on the ring: $\mathbf{pd_{H-R}}$

"shift angle": **β**

inclination angle between the two rings: α

Figure A-3: schematic representation of aromatic-aromatic interactions (edge-to-face) (the designation of distances and angles will be used during this work)

The investigation of the Cambridge Structural Database allows to determine the main parameters for π-π stacking in metal complexes with aromatic nitrogen-containing ligands [16]. For face-to-face interactions, the centroid-centroid distance is found between 3.4 and 3.8 Å (with an inclination angle between the two ring planes as short as possible) and an offset angle ranged between 16 and 40°. Their energy is estimated at 5-10 kJ.mol^{-1}.

Metal-metal interactions can be discussed in some coordination polymers based on d^{10} metal cations (see chapter IV.3 -). The energy of these bonds was roughly estimated at *ca.* 5 kJ.mol^{-1} for a silver-silver interaction [17].

Metal-aromatic interactions can be formed when metal cations accept π-electrons from unsaturated organic molecules. The geometrical parameters of this interaction are given in Figure A-4. For Ag^{I}, the main distances Ag-ring are ranged from 2.8 to 3.3 Å [11]. The energy of metal-aromatic interactions is not well-known, but evaluated around 5-10 kJ.mol^{-1}.

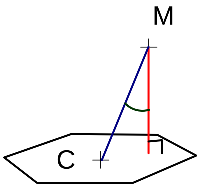

distance Metal-geometrical center of the ring: $\mathbf{d_{M-R}}$

perpendicular distance of M on the ring: $\mathbf{pd_{M-R}}$

"shift angle": **β**

Figure A-4: schematic representation of aromatic-metal interactions (the designation of distances and angles will be used during this work)

I.3 - Synthetic methods

Four main synthetic methods of coordination polymers are known from the literature. [8, 18] Improvement of the synthesis is essential in order to get good quality single crystals suitable for X-ray measurement. It's important to remind that several processes can be investigated for the same starting materials, leading sometimes to different products: isomeric or polymorphic species will be discussed later.

Self-assembly occurs, as written before, when the reagents are mixed together. Molecular recognition permits the construction of products following pre-determined rules. This technique needs convenient conditions:

- Crystals grow in saturated solutions. Good concentration can be achieved by *slow evaporation* of the mother liquor.
- Solubility increases with temperature and crystals could appear during the *cooling* step, which has to be well controlled: speed of cooling, final temperature.

Diffusion methods are preferential methods to get single crystals suitable for X-ray diffraction analysis instead of non- or poly-crystalline products, especially if products are poorly soluble. The principle of this method is to slowly bring into contact the different species:

- One approach can be the *solvent liquid diffusion*: layers are formed; one contains the product in an adequate solvent, another is the precipitant solvent and both are separated with a solvent layer. The precipitant solvent slowly moves into the separate layer and crystal growth occurs at the interface.
- The other approach always concerning diffusion of compounds in solution is the *slow diffusion of reactants*. This technique is similar to the one before, the only difference is that the reactants are dissolved each in one of the two solutions; the separation between both solutions can be a solution layer and/or physical barriers.

Hydro(solvo)thermal methods are originally used for the synthesis of zeolithes, but have been adopted for the formation of coordination polymers. They exploit the self-assembly of products from soluble precursors. The running temperature range is usually 120-260°C inside a closed space (autoclave) under autogenous pressure. Under these conditions the reduced viscosity of water enhances the diffusion process and thus extraction of solids and crystal growth from solution are favoured. As the difference of solubility between organic and inorganic components in the same solvent is often a barrier in the formation of single crystals, hydrothermal experiments can be a good alternative. This crystallization technique way is a non-equilibrium synthesis and may lead to metastable products.

Microwave and Ultrasonic methods are less used methods for the coordination polymer formation. These methods are also based on the improvement of solubilities in order to better react or crystallize the involved species and products.

II - Overview of the diversity of coordination polymers

II.1 - Building blocks

There are four different kinds of building bricks used for the formation of infinite metal-organic frameworks:

Organic ligands act as bridging organic groups between the metal ions. Typical organic ligand molecules are shown on Figure A-5. For possible infinite expansion, ligand molecules have to be multidentate with at least two donor atoms, mostly N-donors, O-donors, S-donors or cyano donors. Ligand molecules may differ from each other in their charges: most used ligands are neutral and anionic. Another determining point is the "body" of the organic ligands: their shapes (rigid or not); their lengths (distance between the coordination functions will be important); their functionalities (further presence of heteroatoms, aromatic rings, alkyl chains…). And finally the ligand molecules can be symmetric, chiral or not, *i.e.* with different donor functions on the same molecule.

Metal ions will be involved in the structure depending on their size, hardness/softness, ligand-field stabilization energy and coordination geometries (linear, trigonal-planar, T-shaped, tetrahedral, square-planar, square-pyramidal, octahedral, trigonal-prismatic, pentagonal-bipyramidal or trigonal-bipyramidal). Different kind of metal atoms have been studied: transition metal ions, lanthanide ions.

Transition metal ions are mostly used: choosing one or another metal element means choosing the coordination geometry *i.e.* the node shape, as well as choosing the potentially required properties of the future materials. Ag^I and Cu^I ions have a d^{10} electronic configuration and thus are more "flexible": their coordination sphere can change depending on the synthesis conditions. Thus Ag^I is found in a wide range of coordination environments: linear, trigonal, tetrahedral, square-planar, square pyramidal and octahedral; for Cu^I, it is usually tetrahedral or trigonal. The transition metals with other electronic configurations have defined coordination environments, for instance, Ni^{II} is tetrahedrally coordinated, Cu^{II} has octahedral coordination geometry (and eventually square planar or square pyramidal), Co^{II} an octahedral geometry , Pt^{II} an square planar geometry, so that a large number of combinations are possible.

Lanthanide ions are less used because of the too important flexibility of their coordination environments. Their coordination numbers can vary from 7 to 10. But with these connectors some original topology can be formed and particular applications become conceivable.

Counter ions are present in the structure when neutral ligands are used. They can influence the metal ion environment (more or less coordinating counter ions) but also the overall structure, being involved in weak interactions or acting as guest molecules in void spaces in the solid state.

Solvent molecules may co-crystallize, increasing the number of possible weak interactions in the final packing, and can also act as guest molecules in the vacant space between the polymer construct.

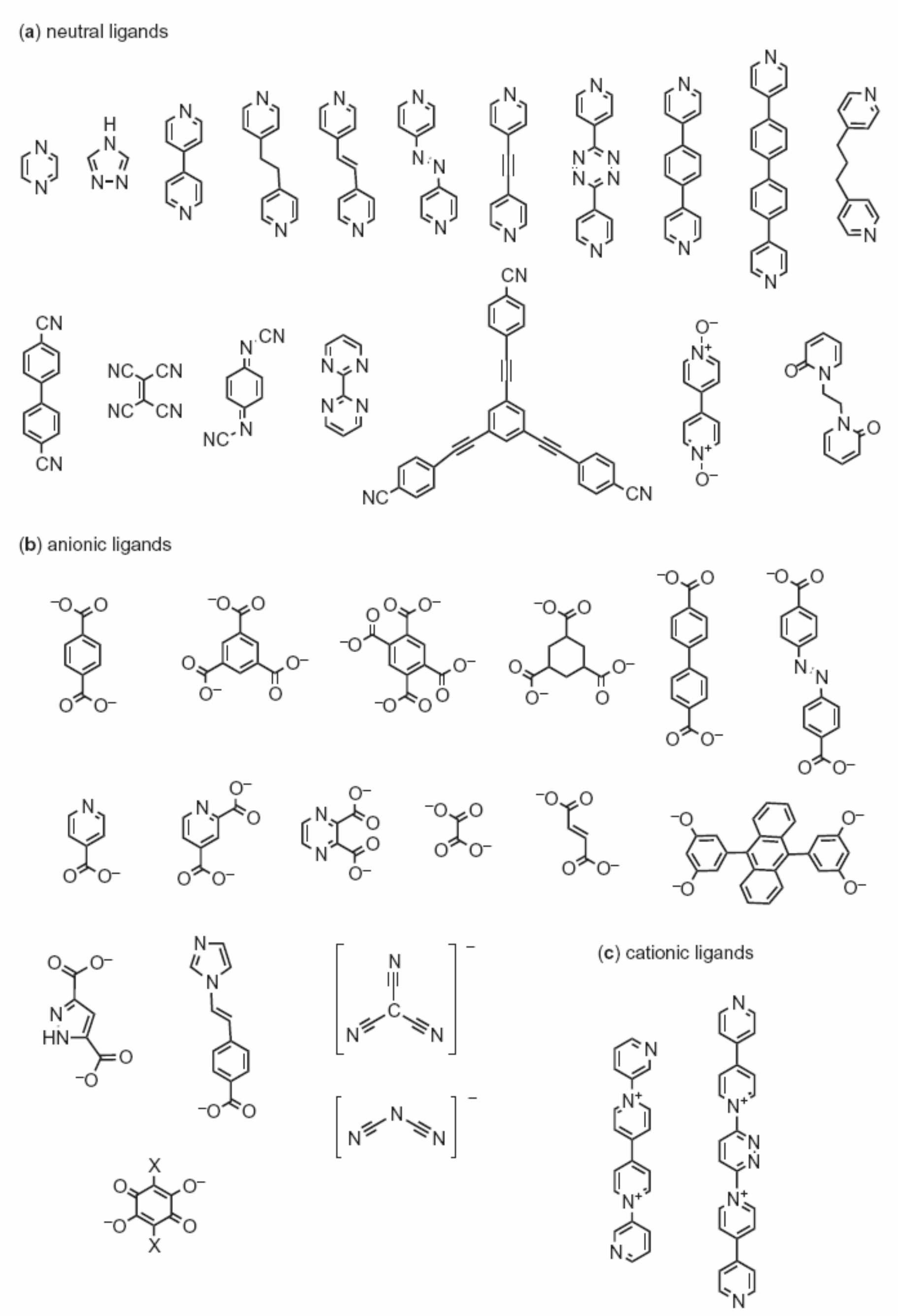

Figure A-5: Typical used organic molecules as organic linkers in coordination polymers [8]

II.2 - Dimensionality and motifs

The organisation of the building blocks together can lead to metal-organic frameworks of different dimensionality: one-, two-, or three-dimensional architectures. The Figure A-6 represents the simplest ways of organisation in order to construct these three architecture types. Linear organic ligands with two donors systems (D) and the spacer (S) are here schematized in red, metal ions are shown in blue, and only the coordination interactions are considered. Dimensionality is often determined by the nodes (metal centres): in one-dimensional motifs the metal ion is coordinated with two ligand molecules, metal ions and organic ligands alternate “infinitely”, leading to a chain; two-dimensional compounds are obtained with three or four ligand molecules coordinating around the metal ion and the elementary motif expands now in two directions; with metal ions of higher coordination number (tetrahedral or octahedral nodes), three-dimensional structures can be built.

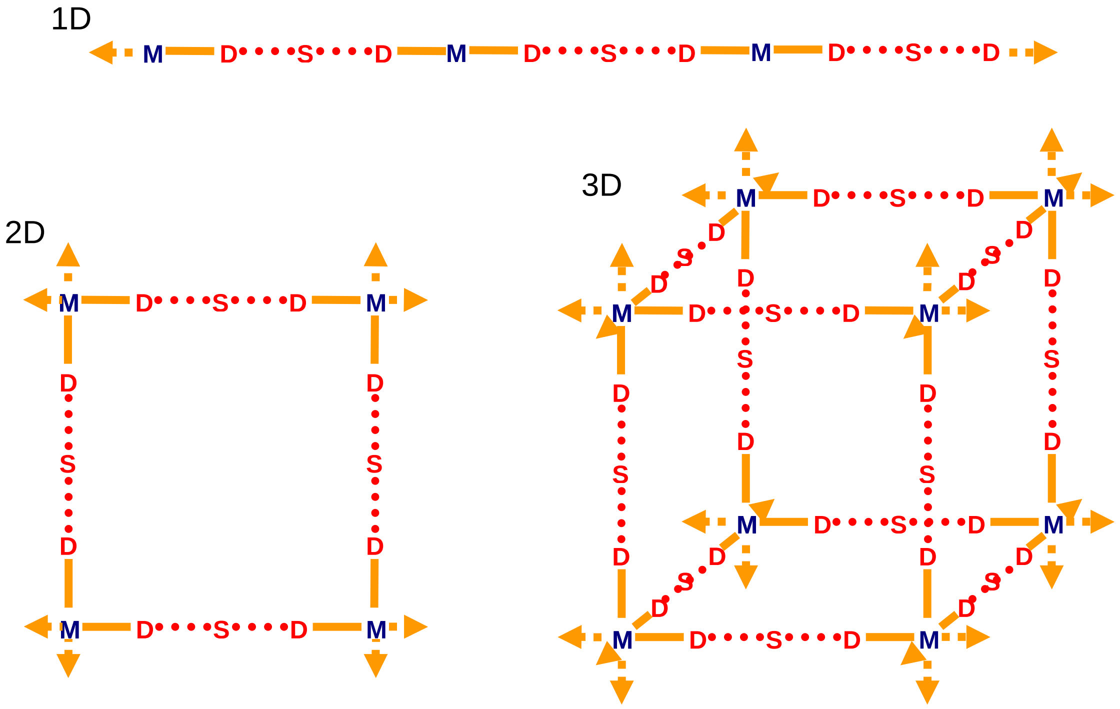

Figure A-6: Dimensionality of the metal-organic frameworks (M: metal ions, D: donor groups of the ligand, S: spacer inside the ligand) [5]

Obviously the elementary units are not always so simple and there are a lot of one-, two-, or three-dimensional architectural types depending on the building blocks and the experimental conditions. These architectures can be schematized only using nodes and links: Figure A-7, Figure A-8 and Figure A-9 [8] represent respectively some of the most important known motifs. Along this thesis, we will often discuss and refer to these network motifs.

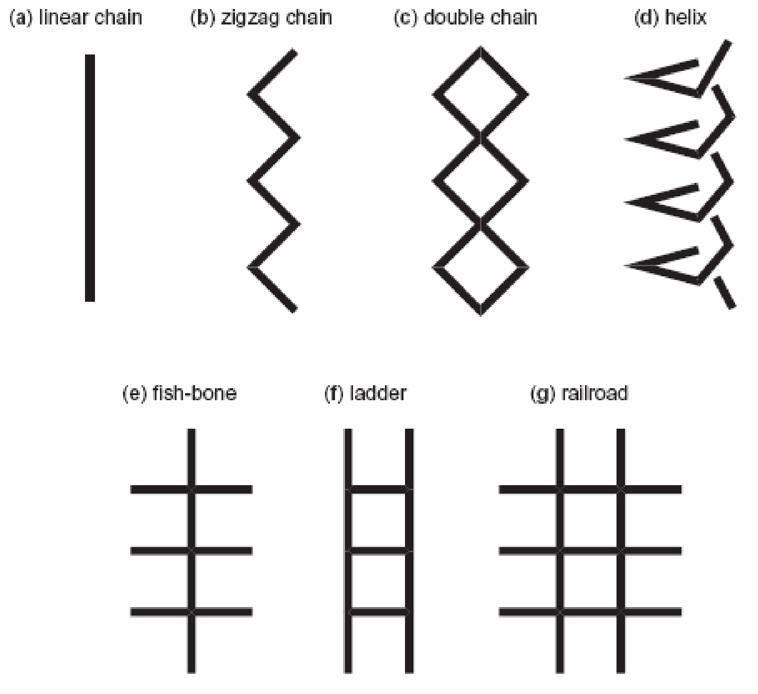

Figure A-7: 1D coordination polymer motifs

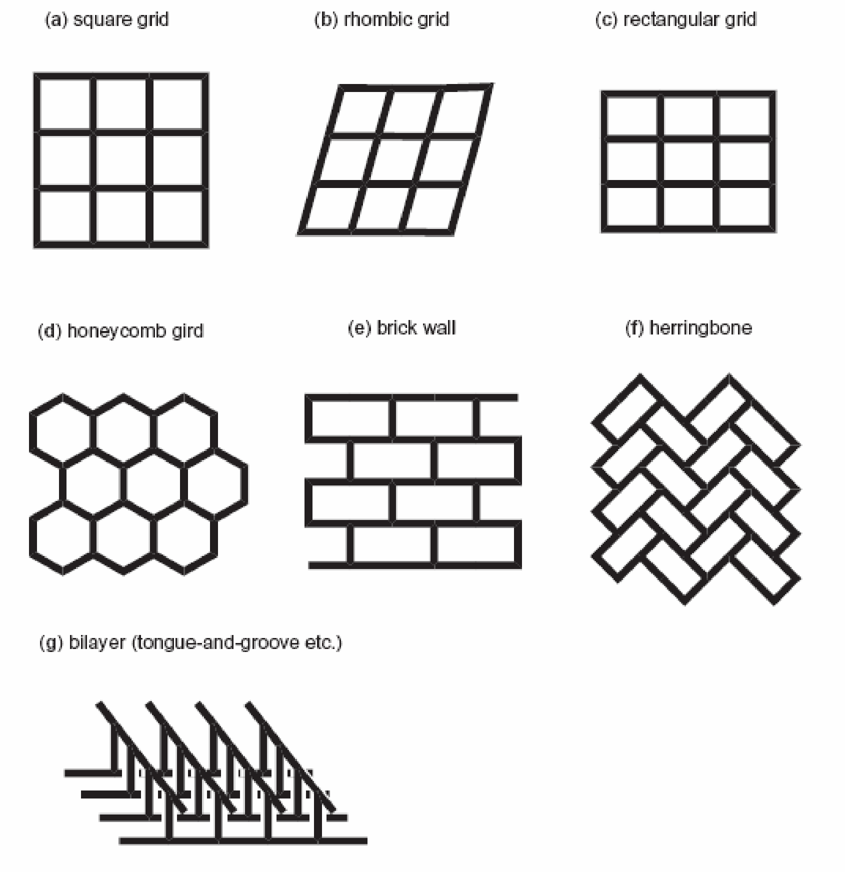

Figure A-8: 2D coordination polymer motifs

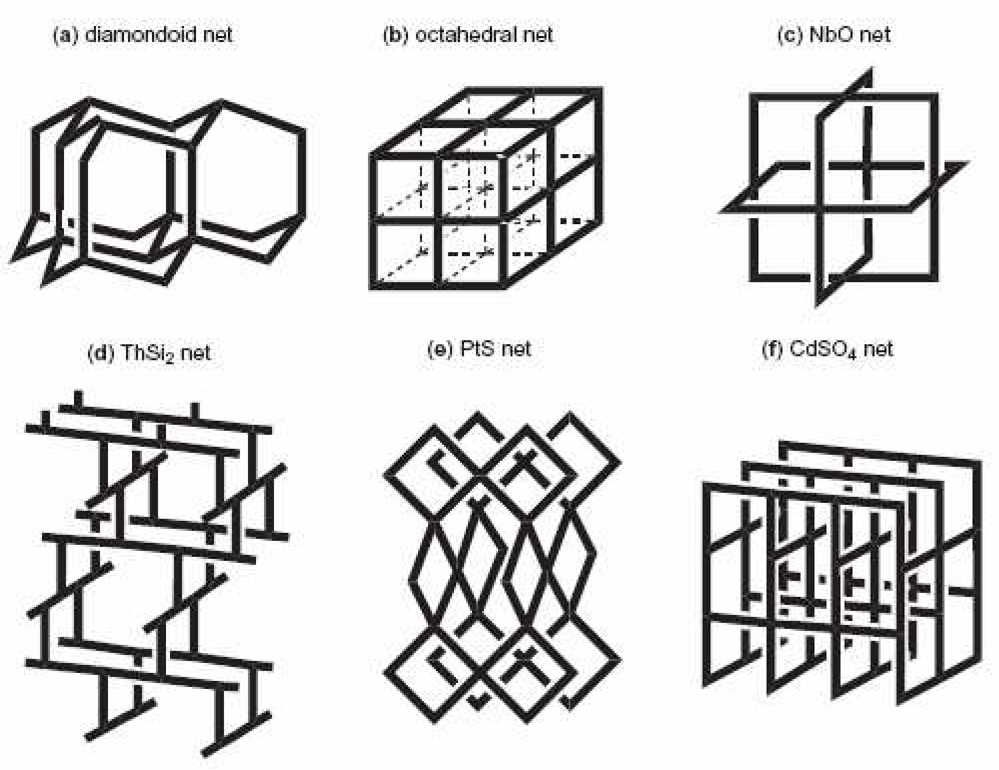

Figure A-9: 3D coordination polymer motifs

One other important feature concerning the analyses of coordination polymers architectures is the interpenetration, in which two- or three-dimensional motifs are interweaving. [19] Some examples are shown on the Figure A-10.

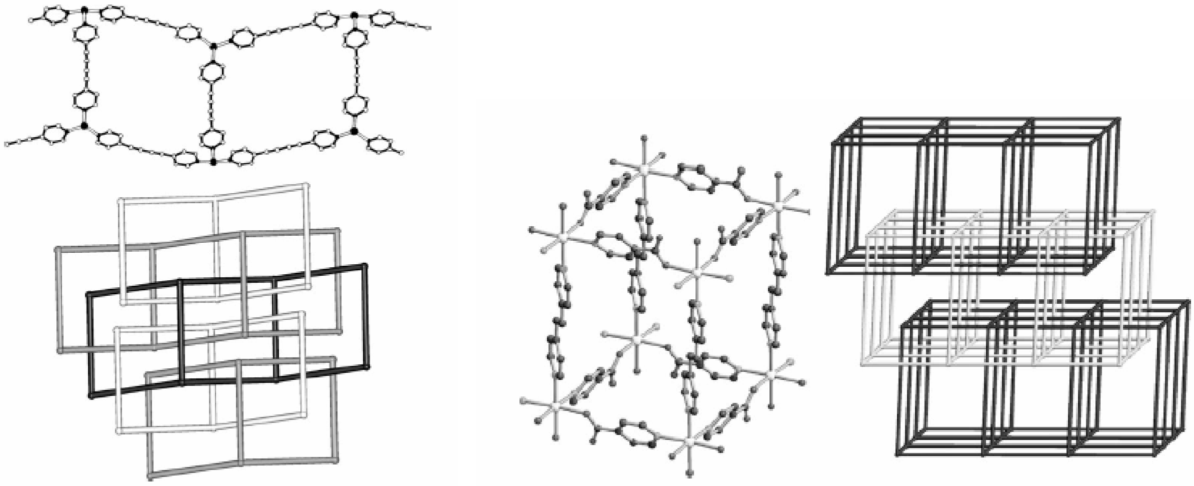

Figure A-10: Two examples of interpenetrated systems

Considering the huge choice of possible building units, we can easily imagine the diversity of new synthesizable materials. In order to illustrate the wild diversity of related coordination polymers, some examples of metal-organic frameworks will be presented; the aim of the following paragraphs is not to make an exhaustive list but only to present an overview of the coordination polymer features. They are classified along their dimensionalities. The shown motifs are the most typical ones and are based on coordination interactions between ligand molecules and metal ions. It is clear that other interactions play also an important role during the formation of the crystals, but the definition of the final compounds dimensionality is based on the metal complexation. Due to the abundance of metal-organic known systems, we will only report the systems containing one type of ligand and one type of metal ions.

II.3 - One-dimensional motifs

Mind will implicitly associate one-dimensional motifs with **linear chains**, like a regular bicolour necklace. This simplest one-dimensional motif exists obviously.

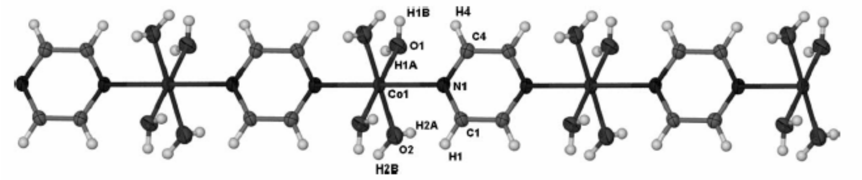

Figure A-11: One-dimensional polymer chain of $\{[Co(H_2O)_4(pyrazine)](NO_3)_2{\cdot}2H_2O\}_n$

For instance crystals of $\{[Co(H_2O)_4(pyrazine)](NO_3)_2{\cdot}2H_2O\}_n$ appear from a heated mixture of pyrazine in acetonitrile and $Co(NO_3)_2{\cdot}6H_2O$ in ethanol [20]. They show a one-dimensional linear chain structure alternating pyrazine molecules and $Co(H_2O)_4$ units. (Figure A-11) Cobalt atoms are hexa-coordinated, the oxygen atoms of the four coordinated water molecules occupying the equatorial positions and the nitrogen atoms of two different ligand molecules the axial positions.

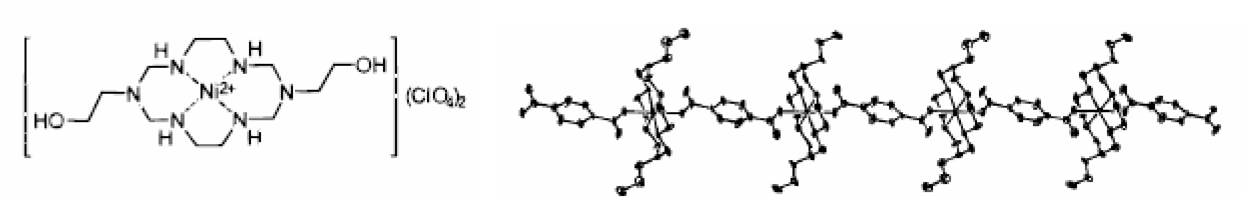

Figure A-12: one-dimensional polymer $\{[Ni(C_{12}H_{30}N_6O_2)(C_8H_4O_4)]{\cdot}4H_2O\}_n$

This arrangement is due to the coordination site occupation of the hexa-coordinating metal ions (*trans*-arrangement of two different ligand molecules in axial positions, and the equatorial positions occupied with counter anions, solvents molecules or other co-crystallizing molecules) and to the fact that the ligand is linear and symmetric. We can observe analogous arrangements in $\{[Ni(C_{12}H_{30}N_6O_2)(C_8H_4O_4)]{\cdot}4H_2O\}_n$ [21] where the ligand molecule is the terephthalate dianion and the equatorial positions are occupied by a macrocycle (Figure A-12) or in $\{[Mn(C_{12}N_2H_{10})(NCS)_2(CH_3OH)_2]\}_n$ [22] in which Mn^{II} is coordinated by two *trans*-1,2-bis(4-pyridyl)ethane, two isothiocyanate ions and two methanol molecules (Figure A-13).

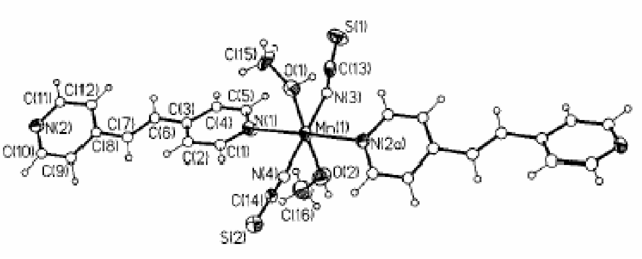

Figure A-13: Coordination mode of Mn^{II} in $\{[Mn(C_{12}N_2H_{10})(NCS)_2(CH_3OH)_2]\}_n$

Some other linear chain motifs can be achieved by a more original organisation of the ligand molecules with the metal ions. The compound $\{[Cu_3(cpida)_2(H_2O)_4]\cdot 4H_2O\}_n$ [23] for instance shows *N*-(4-carboxyphenyl)iminodiacetic acid molecules (H3cpida) alternating with Cu^{II} units. (Figure A-14)

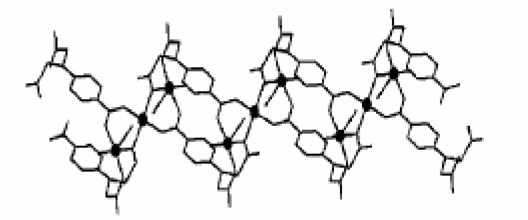

Figure A-14: One-dimensional motif of $Cu_3(cpida)_2(H_2O)_4]\cdot 4H_2O\}_n$ (Copper atoms are represented with black circles)

Although the one-dimensional chain organisation seems to be simple, there are many possible permutations in the packing taking into account the interactions during the crystal formation. Janiak *et al*. have reported two one-dimensional chains based on terephthalate dianions: $\{[M(\mu\text{-}C_{12}H_{30}N_6O_2)(NH_3)_2]\}_n$ (M=Cu^{II}, Cd^{II}) obtained by slow evaporation. [24] While the two systems seem to be similar, they differ from the coordination sphere of the cations. In the copper compound, Cu^{II} (Figure A-15a/b) is square-planar coordinated by two ammin and two ligand molecules in a monodentate way, leading to a *trans*-arrangement of the ligand molecules and linear chains, whereas in the second compound the ligand acts as a bidentate pincer. (Figure A-15c/d) The Cd^{II} ion is thus coordinated with six atoms in a trigonal-prismatic way; the ligand molecules are in *cis*-position on one side of the cadmium ion, and the ammin molecules on the other. Some **zig-zag chains** are thus formed in this second case due to the difference in the coordination orientations of the two metal ions.

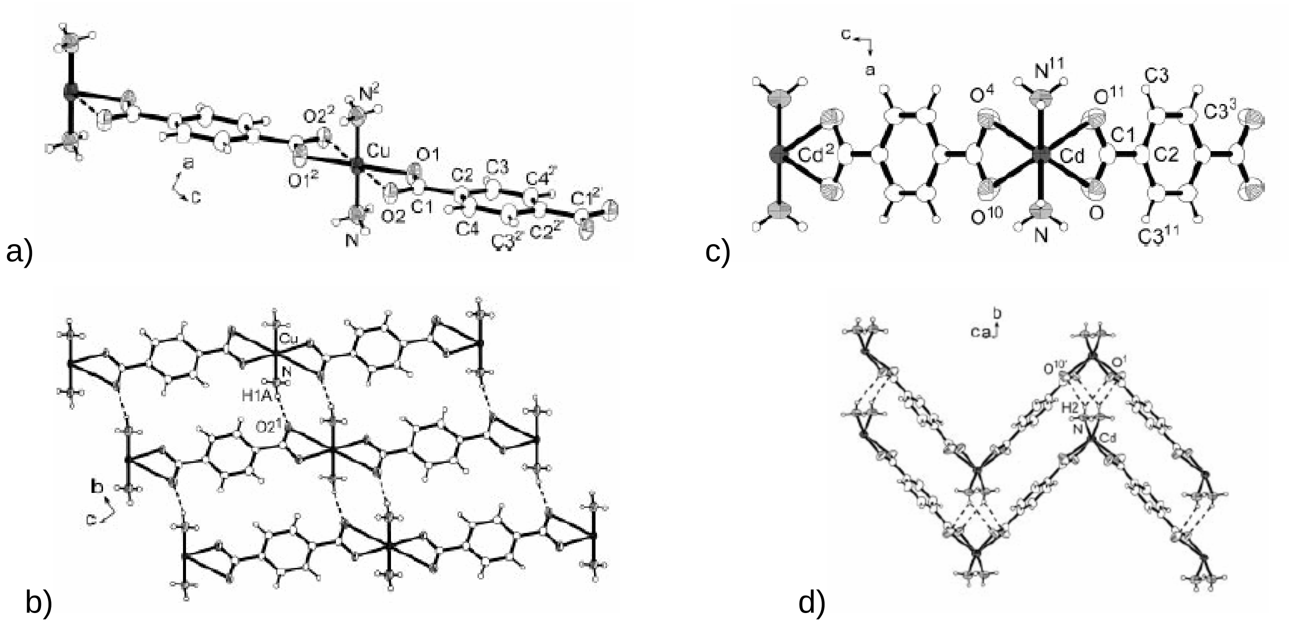

Figure A-15: a) and b) {[Cu(μ-$C_{12}H_{30}N_6O_2$)($(NH_3)_2$)]}$_n$; c) and d) {[Cd(μ-$C_{12}H_{30}N_6O_2$)($(NH_3)_2$)]}$_n$

A similar arrangement of cadmium cations with terephthalate dianions as connecting ligands is reported by Qiu [25] with phenantroline molecules instead of ammin ones.

The formation of zig-zag chains can be explained by the shape of the ligand molecules. A first simple example will rationalize this fact: in comparison of the coordination polymers obtained from $Cu(HCO_2)_2 \cdot yH_2O$ and pyrazine (pyz) or pyrimidine (pym) [26]. The difference of these two ligands is the relative position of the two N-donor atoms on the ring. As shown on Figure A-16 pyrazine ligand molecules lead to linear chains whereas zig-zag chains occur by use of pyrimidine ligand molecules.

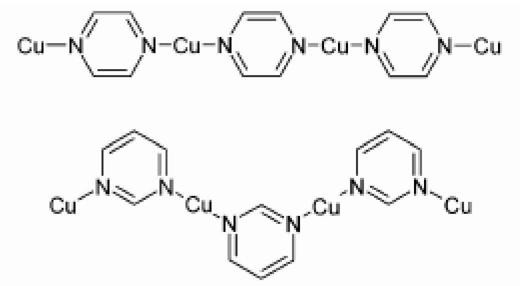

Figure A-16: Schematic representation of the skeleton of one dimensional coordination polymers {[Cu(L)($(HCO_2)_2$)]}$_n$ (L=pyz, pym)

This second example shows the similar influence of the position of the two N-donor atoms on the ring. Under similar experimental conditions acetylene-bridged *N,N'*-bidentate ligands with different positions of the nitrogen atoms on the rings (*N,N'*-dpa) coordinate with cobalt ions. The coordination polymer containing 3,3'-dpa shows a zig-zag chain motif (Figure A-17a) whereas the compound with 4,4'-dpa shows a one-dimensional ladder-like organisation (Figure A-17b). [27, 28]

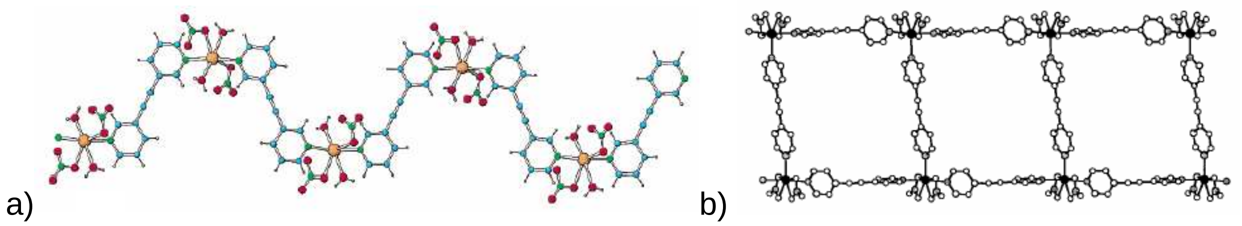
a) b)

Figure A-17:a) {[Cd(3,3'-dpa)$(NO_3)_2(H_2O)_2$]}$_n$; b) {[Cd$(NO_3)_2$(4,4'-dpa)$_{1.5}$]}$_n$

Comparable zig-zag chains can be also obtained with longer bent ligand molecules or with flexible ligand molecules. The coordination polymer {[Cu(dtmp)(dmf)Cl_2]dmf}$_n$ (dtmp = 1,6-di(triazole-1-yl-methyl)-4-methylphenol) self-assembles in the reaction mixture and shows a zig-zag chain motif. (Figure A-18) [29] The flexibility of the ligand allows its *cis* conformation. Cu^{II} ions are five coordinated with two nitrogen atoms of two different ligand molecules, two terminal chloride anions and one oxygen atom of the coordinated dmf molecules.

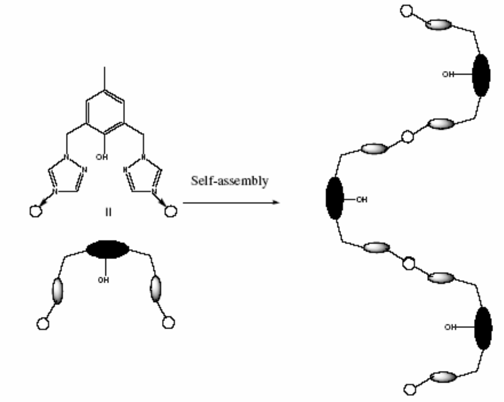

Figure A-18: zig-zag coordination polymers {[Cu(dtmp)(dmf)Cl_2]dmf}$_n$

A solution of 2,2'-bis(4-pyridylmethyleneoxy)-1,1'-biphenylene (4,4'-bpp) in methanol diffuses into an aqueous solution of $ZnCl_2$ or $ZnBr_2$ in order to lead to crystals showing zig-zag chains: the Zn atoms are tetra-coordinated with two different bend ligand molecules and with two terminal halide atoms as shown on Figure A-19 [30].

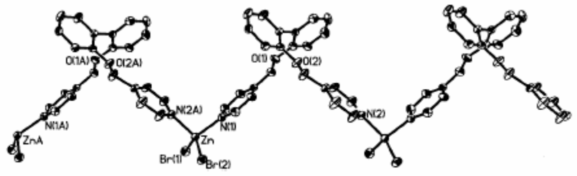

Figure A-19: one-dimensional polymeric chain of {[Zn(4,4'-bpp)Br_2]}$_n$

From a high-dilution synthesis, crystals [Cu(2,3-pydcH)$_2$] are obtained. [31] The ligand 2,3-pyridine dicarboxylic acid (2,3-pydcH_2) is a bidentate asymmetric molecule. The repeating units of this coordination polymer are metallacycles: two ligand molecules bridge two closest copper atoms in the chain. (Figure A-20) Each Cu^{II} atom has a distorted octahedral coordination sphere; the apical positions are occupied by the oxygen atoms of the non-deprotonated 3-carboxyl groups; the equatorial ones with two nitrogen atoms and two oxygen atoms of the deprotonated 2-carboxyl groups. This motif is called a **double chain** motif.

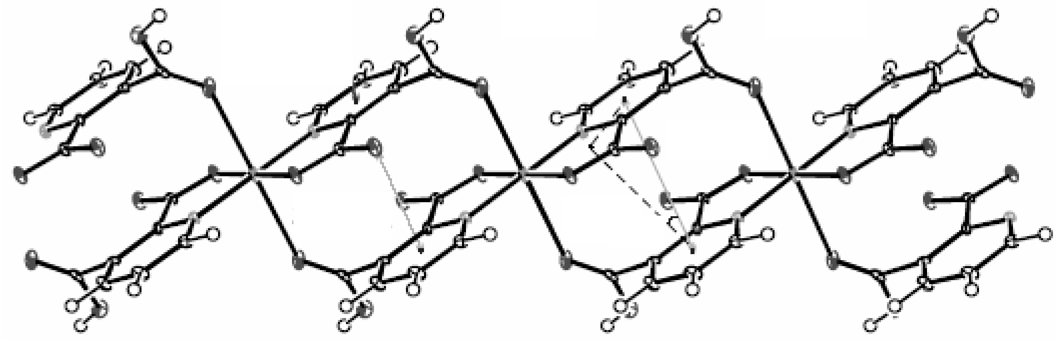

Figure A-20: double chain motifs in [Cu(2,3-pydcH)$_2$]

Recrystallization of Zn^{II} salts and 4,4'-dipyridyl disulfide (4pds) coordination polymers in different solvents leads to double chain structural motifs [32]. Zn^{II} is hexa-coordinated and the equatorial positions are occupied with four nitrogen atoms of four different ligand molecules and the apical ones with counter anions or solvent molecules. The repeating unit is a Zn$_2$L$_2$ ring. Figure A-21 shows for instance the compound {[Zn(SCN)$_2$(4pds)$_2$](dmf)$_2$}$_n$. The torsion angle C-S-S-C is of ca. 90°, thus the bend shape of the ligand molecules explains the rhombohedral chains. In this series of Zn^{II} coordination polymers derived from 4dps ligands, an important additional feature appears, as the ligand can adopt two forms of enantiomers. The double chains can be achiral or chiral.

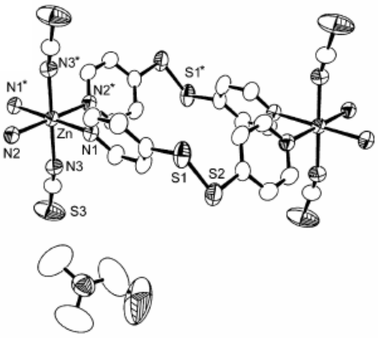

Figure A-21: The loop Zn$_2$L$_2$ in {[Zn(SCN)$_2$(4pds)$_2$](dmf)$_2$}$_n$

Double chain motif can also be found in compounds based on polydentate ligand molecules. 1,2,7,8-benzenetetracarboxylic acid molecules (H$_4$bta) self-assemble with Mn^{II} ions in presence of 4,4'-bipyridine (bpy) in a basic solution affording crystals with a double chain structural motif. (Figure A-22) The Hbta molecules act as tridentate ligand molecules on an octahedral Mn^{II} ion, the coordination sphere of Mn^{II} ion being completed with two water molecules and one Hbyp molecule [33]. Double chain motifs can also appear with flexible or well-shaped ligand molecules in association with a large variety of metal centers.

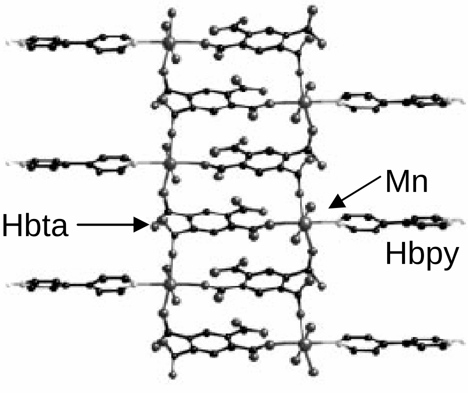

Figure A-22: double chain motif in {[Mn(Hbta)(Hbyp)(H_2O)$_2$]}$_n$

Ladder-like one-dimensional motifs can also be formed. A great example is shown on Figure A-17b. The hepta-coordinated cadmium ions are coordinated with three different ligand molecules leading to a “T-shape” organisation of the ligand molecules around the metal center; the other sites of the coordination sphere are blocked with the counter anions avoiding the extension of the structure in further direction. Another ladder-like organisation is found in the compound {[Cu(2,3-dimethylpyrazine)Br_2]}$_n$ [34]. This compound co-crystallises as main product of the slow diffusion between methanolic solutions of the ligand and $CuBr_2$. In this case two “rails” formed by bridging 2,3-dimethylpyrazine between the Cu^{II} ions are linked together by bridging bromide ions. (Figure A-23) The additional bromide anions are terminal ones.

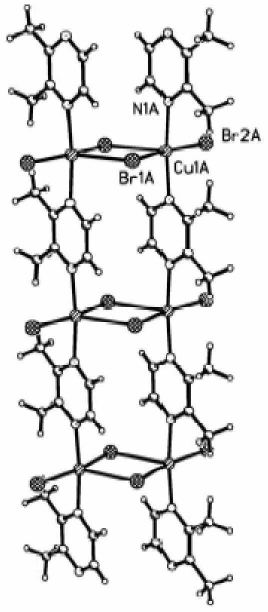

Figure A-23: ladder-like arrangement in the compound {[Cu(2,3-dimethylpyrazine)Br_2]}$_n$

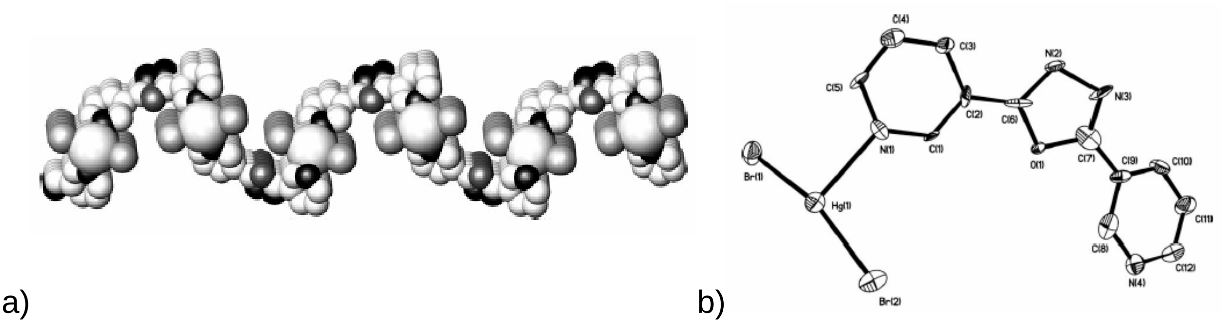

Figure A-24: {[HgBr$_2$(2,5-bis(3-pyridyl)-1,3,4-oxadiazole)]}$_n$ a) helical chain; b) coordination of Hg^{II} and shape of the ligand

The least common one-dimensional motif is the **helical chain**. {[HgBr$_2$(2,5-bis(3-pyridyl)-1,3,4-oxadiazole)]}$_n$ crystals appear after the slow diffusion of the ligand solution in methanol into an aqueous solution of HgBr$_2$. [35] The Hg^{II} has a distorted tetrahedral environment consisting of two nitrogen atoms of two ligand molecules and of two terminal bromide atoms. The HgBr$_2$ and the ligand units alternate in order to form a one-dimensional chain. The bent shape of the ligand molecules and its coordination at the Hg^{II} centers give a helical twist to the chain. (Figure A-24) In comparison, the coordination polymer obtained with HgI$_2$ and the similar 2,5-bis(4-pyridyl)-1,3,4-oxadiazole ligand (except for the position of the nitrogen atoms on the ring) shows a one-dimensional zig-zag motif, as the ligand coordination orientation is different. Some other examples of helical chains can be found [36], for instance the anion bis[3-(2-pyridyl)pyrazol-1-yl)]phosphinate crystallizes with Ag^I or Tl^I in order to form helical strands (Figure A-25) [37]; the complex {[Ag(*N*,*N*'-di(2-pyridyl)oxamide)]NO$_3$}$_n$ crystallizes also in single-twist helices. [38]

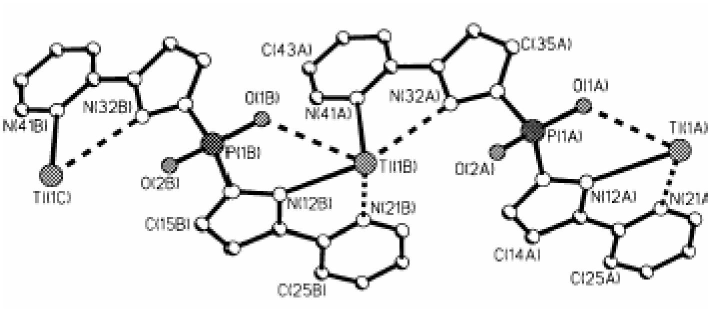

Figure A-25: Crystal structure of the one-dimensional helical chain of {[Tl(bis[3-(2-pyridyl)pyrazol-1-yl)]phosphinate)]·MeOH}$_n$

Some few double helical motifs are related, especially if there are several kinds of donor groups in the ligand molecule or with flexible ligands. For instance, the ligand 1,3-bis(4-pyridyl)propane (bpp) reacts with AgCF$_3$SO$_3$ by diffusion technique. [39] The structure of the resulting product show double helical chains, as one-dimensional chains are intertwined. The contacts between the two chains are Ag-Ag interactions and π-stacking as shown on Figure A-26.

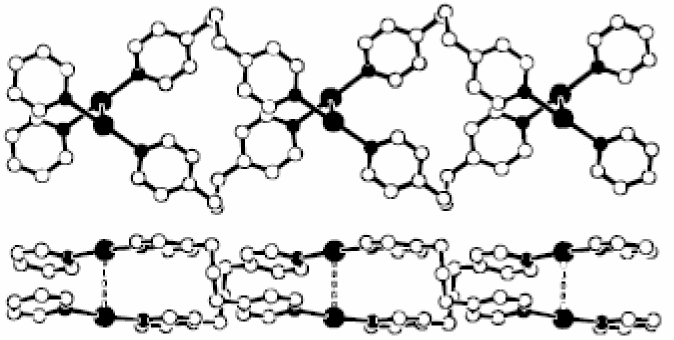

Figure A-26: double helical motif in the compound {[Ag(bpp)](CF_3SO_3)}$_n$

In the one-dimensional chain motif, ligand and node centers alternate in one direction so that the repeating unit is form with one node and one ligand and the proportion metal to ligand is 1:1 (except for the double chain motifs).

II.4 - Two-dimensional motifs

Square grid networks are the simplest example of the two-dimensional motifs. In these coordination polymers the proportion metal to ligand usually is 1:2. The metal centers are coordinated with four different ligand molecules and the repetition of this unit allows the propagation of the structure in two dimensions.

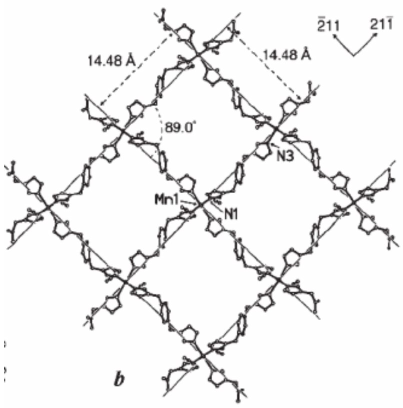

Figure A-27: square grid network in {[Mn(N_3)$_2$(bix)$_2$]}$_n$

The ligand 1,4-bis(imidazol-1-ylmethyl)benzene (bix) molecules react with Mn^{II} ions in order to form single crystals in which the motifs are perfect square grid layers. (Figure A-27) [40] The metal ions have an octahedral environment: the equatorial positions are occupied by the nitrogen atoms of four ligand molecules and the apical ones by the counter anions (azide or dicyanamide anions). A similar example affords a square grid motif [41]: the metal node is an Uranyl^{VI} ion and the bridging ligand is 1-oxo-4-

pyridylcarboxylate (opyca). Single crystals appear during the hydrolysis reaction of $UO_2(NO_3)_2$ with the 1-oxo-4-cyanopyridine under hydrothermal conditions. (Figure A-28)

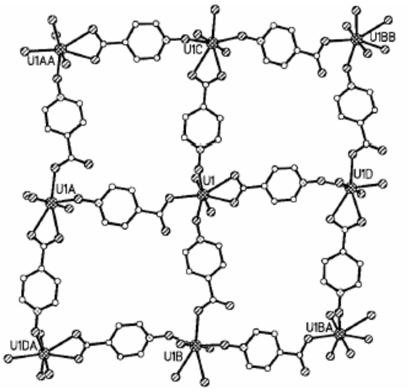

Figure A-28: 2D square grid motif in $\{[UO_2(opca)_2]\}_n$

A lot of two-dimensional networks based on square grid motifs can be found in the literature, but also a lot of derived motifs such as **rhombic** or **rectangular grids**. [41-44] In these cases, the metal centers are also linked with four ligand molecules.

In the other hand, if the metal ions are only coordinated with three ligand molecules giving a “T-shape” around the node, layers are formed and the motifs are called **honeycomb grid**, **brick wall**, **herringbone** motifs or other **parquet floor** architectures. Some of these motifs are shown by Necas *et al*. [45] with coordination polymers containing lanthanides centers and the ligand $Ph_2P(O)$-CH_2CH_2-$P(O)Ph_2$ ($dppeO_2$). (Figure A-29) In these cases the proportion metal:ligand is 1:1,5. To generate “T-shaped” connectors, some coordination sites of the metal center have to be blocked by highly coordinating counter anions such as halide anions or sometimes nitrate anions or by additional terminal ligand molecules.

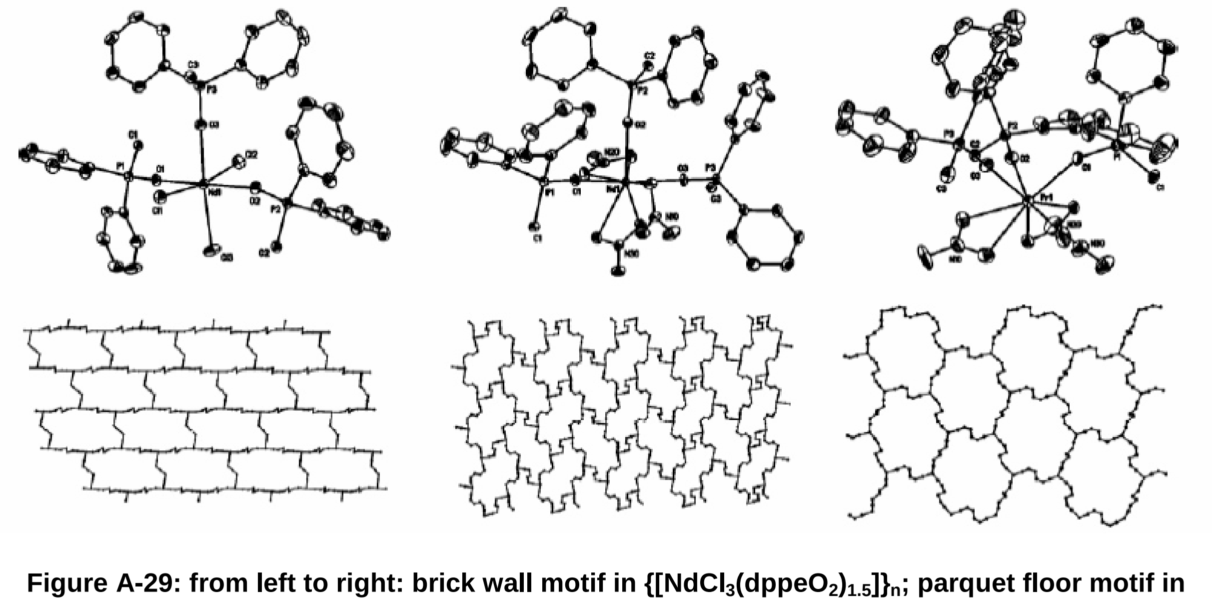

Figure A-29: from left to right: brick wall motif in $\{[NdCl_3(dppeO_2)_{1.5}]\}_n$; parquet floor motif in $\{[Nd(NO_3)_3(dppeO_2)_{1.5}]\}_n$; pseudo-honeycomb motif in $\{[Pr(NO_3)_3(dppeO_2)_{1.5}]\}_n$

Another motif containing “T-shaped” metal centers is the **bilayer** one. $\{[Cu(bipy)_{2.5}(H_2O)](ClO_4)_2\cdot(H_2O)\cdot(CH_3OH)_{1.5}\}_n$ presents this structural motif. [46] Each Cu^{II} center has a distorted square planar geometry surrounded by four nitrogen atoms in the equatorial positions: three of the bidentate bridging bipyridine molecules and one of the monodentate terminal ligand connector, the apical coordination sites being occupied with weakly coordinated water molecules. (Figure A-30) The proportion metal:ligand is now 1:2,5.

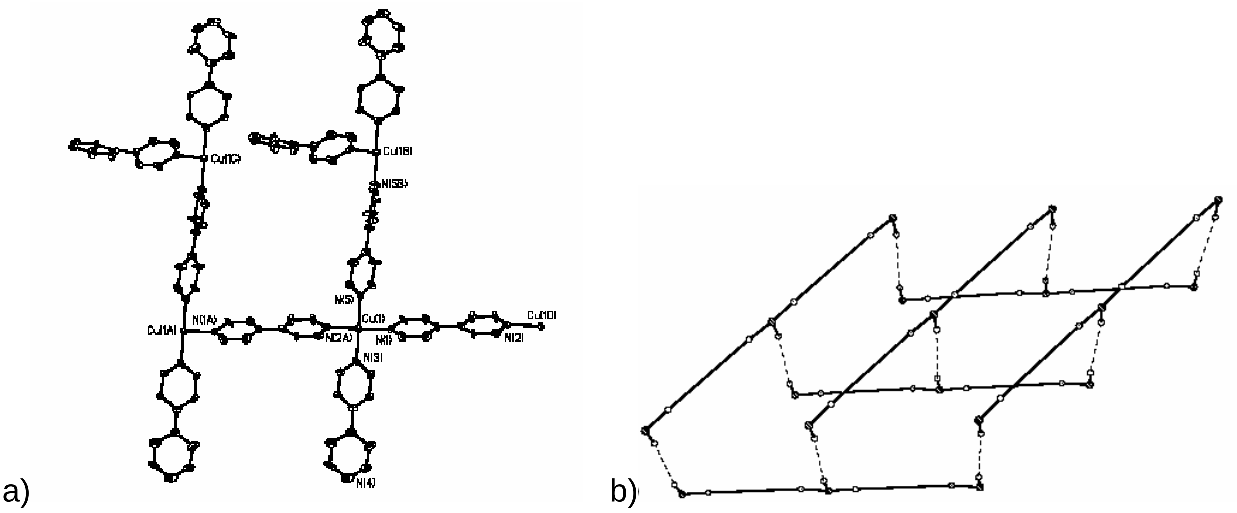

Figure A-30: bilayer structural motif in $\{[Cu(bipy)_{2.5}(H_2O)](ClO_4)_2\cdot(H_2O)\cdot(CH_3OH)_{1.5}\}_n$ (water, perchlorate and methanol molecules are omitted for clarity): a)coordination mode of the Cu^{II} ion; b)bilayer architecture (terminal ligands are omitted, solid lines-“chain makers”-, dashed lines-“linker between the chains”- symbolized the bridging ligands and black circles the Cu^{II} centers)

Thus, the two-dimensional structures are reached when three or four ligand molecules act as connectors between the node centers. The potential remaining coordination sites of the centers are occupied with other building blocks (counter-ions, solvent molecules or additional organic molecules). The proportions metal to ligand are no more 1:1 as in the one-dimensional networks (except for double chain motifs), but $ML_{1,5}$, ML_2 or $ML_{2,5}$. A large variety of nodes can be found in such complexes. These kinds of constructions show cavities; the remaining space is filled with guest molecules (counter ions or solvent molecules), by adequate stacking of the sheets or thanks to interpenetration.

II.5 - Three-dimensional motifs

Now, this is quite easy to imagine the requirements to build three-dimensional complexes. The extension has to occur in the tree dimensions from the nodes and thanks to the ligand connectors. The geometry of such compounds is more complex.

One of the well-known and frequently found three-dimensional motifs is the **diamondoid** network. Each node is connected to four bridging ligands in a tetrahedral way, leading to a three-dimensional diamond-like network. This motif can be found in the structure obtained from Cd^{II} centers as node and the dicarboxylate 3,3'-azodibenzoate (3,3'-azdb) as connector. [47] The cadmium ions are eight-coordinate but they act as four-connecting nodes, as the carboxylate groups are bidentate. On Figure A-31, it can be noted that this arrangement creates large cavities (in this case, the average distances between the cadmium atoms are 15 Å inside a cavity). When the intraframework voids are relatively large, interpenetration of a network by other independent networks is a common phenomenon. The degree of interpenetration depends on the length of the cavity's edge *i.e.* of the ligand molecule. In this structure, six independent interwoven diamondoid networks coexist.

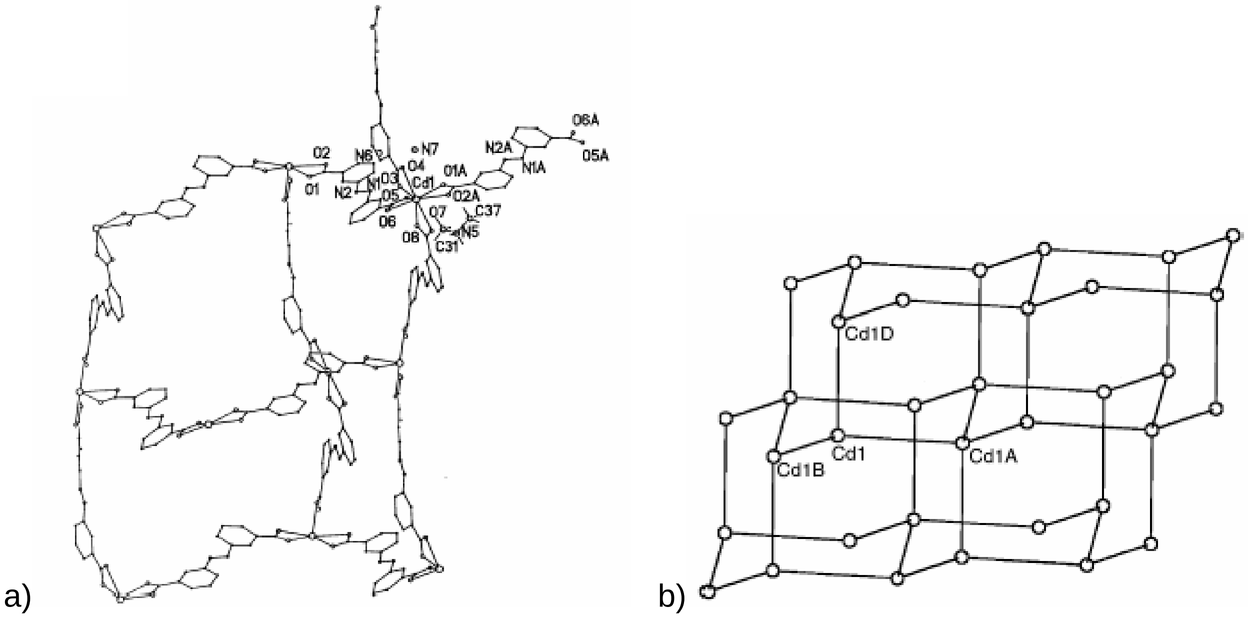

Figure A-31: a) adamantine unit in {[Cd(3,3'-azdb)$_2$](H$_2$NMe$_2$)(NH$_4$)}$_n$; b) schematic representation of the diamondoid network in {[Cd(3,3'-azdb)$_2$](H$_2$NMe$_2$)(NH$_4$)}$_n$.

Examples affording this motif are numerous. Lin's group relates two examples of diamondoid structures formed of Zn^{II} or Cd^{II} ions linked by the asymmetric ligand (4-[2-(4-pyridyl)ethenyl]benzoate = L). [48] The metal ions have a distorted octahedral or tetrahedral environment so that the diamondoid structure can appear. In this case, the number of interpenetration is eight. (Figure A-32)

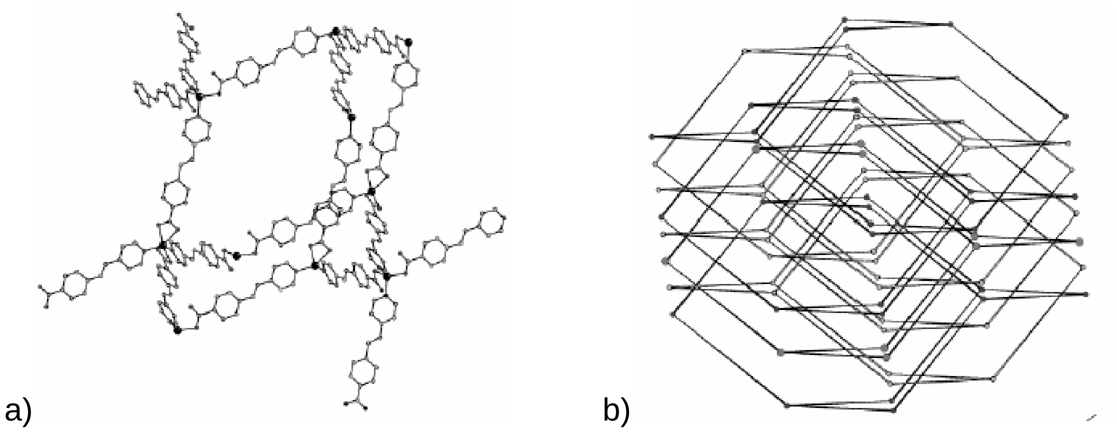

Figure A-32: $\{[Zn(L)_2]\}_n$ a) the diamondoid structure; b) schematic 8-fold interpenetration

This motif is sometimes distorted in correlation with the coordination way of the nodes centers. For instance the crystal structure obtained from the octahedral Cu^{II} associated with the ligand 2,5-bis(4-pyridyl)-1,3,4-oxadiazole (L) presents a distorted diamondoid motif. [49] The adamantane cages are elongated in one direction as shown on Figure A-33, as the four molecules coordinate the copper center in the equatorial positions.

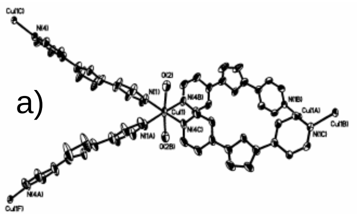

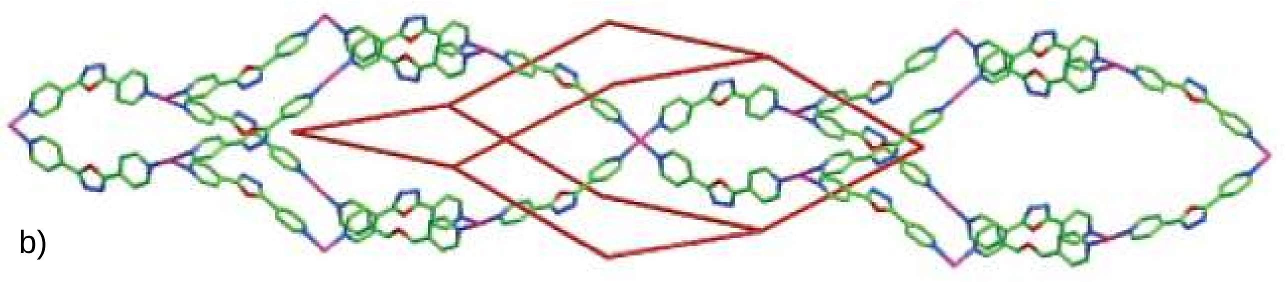

Figure A-33: a) coordination geometry around the Cu^{II} center and b) the distorted adamantine cages in $\{[Cu(L)_2(H_2O)_2](ClO_4)(OH)(H_2O)_{2,5}]\}_n$

Some other diamondoid metal-organic frameworks based on Ag^I as well as interpenetration structures are presented by Ciani *et al*. [50].

Octahedral motifs are based on the extension of the framework in the three directions from the octahedral nodes. It is very difficult to coordinate six ligand molecules around one metal center and generally the apical positions of the octahedral metal centers are occupied by water molecules, other solvent molecules or counter ions, and the resulting network is of lowest dimensionality. Indeed the apical positions are less often coordinated bond sites (Jahn-Teller distortion).

One of the strategies is to use two different molecules in order to build the edge of the cubical unit. SiF_6^{2-} anions for instance can link the metal atoms more easily than water molecules. These anions act thus as linkers between square-grid layers made with the metal ions and the ligand molecules as seen in the former chapter. Moreover the resulting three-dimensional framework is more robust as there is no uncoordinated counter anion in the structure.

The compound $\{[Cu(SiF_6)(4,4'\text{-bpy})_2]\cdot 8H_2O\}_n$ shows this organisation. [51] This compound was obtained thanks to slow diffusion of the ligand solution (in ethylene glycol) into an aqueous ethylene glycol solution containing a mixture of $Cu(BF_4)_2\cdot 6H_2O$ and $(NH_4)_2SiF_6$. The Cu^{II} center is coordinated to four ligand molecules in the equatorial positions leading to a square-grid layer. The layers are stacked together thanks to the bridging bidentate SiF_6^{2-} anions, F atoms occupying the apical sites of the Cu^{II} ions. (Figure A-34-a) There is no possible interpenetration in this case; channels are formed and filled with uncoordinated water molecules. (Figure A-34-b) This framework is very robust and remains organised even after removal of the water molecules under strong conditions (373K, reduced pressure).

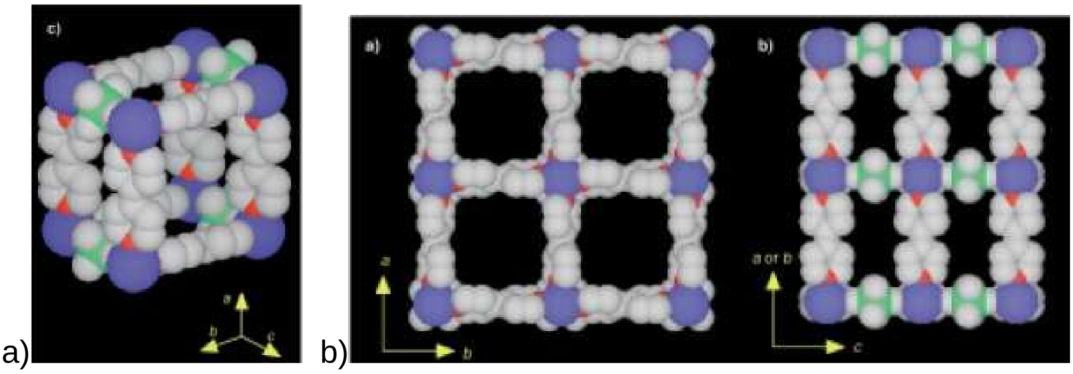

a) b)

Figure A-34: a) cubical unit in $\{[Cu(SiF_6)(4,4'\text{-bpy})_2]\cdot 8H_2O\}_n$; b) view of the cavities in $\{[Cu(SiF_6)(4,4'\text{-bpy})_2]\cdot 8H_2O\}_n$ (water molecules omitted for clarity) (Cu ions in blue, Si atom in green and nitrogen atoms in red)

The construction of octahedral motifs is also possible if the nodes are made with binuclear subunits. For example in the compound $\{[Co(\text{terephthalate})(4,4'\text{-bipy})]\}_n$ [52] one layer is formed with terephthalate dianions capping the cobalt binuclear unit as shown on Figure A-35-a/b (the carboxylate groups are coordinated to the cobalt ions in the equatorial sites). The bipyridine molecules are linked to the cobalt anions through the apical positions for the expansion of the structure in the third direction (Figure A-35-c). This system is twofold interpenetrated.

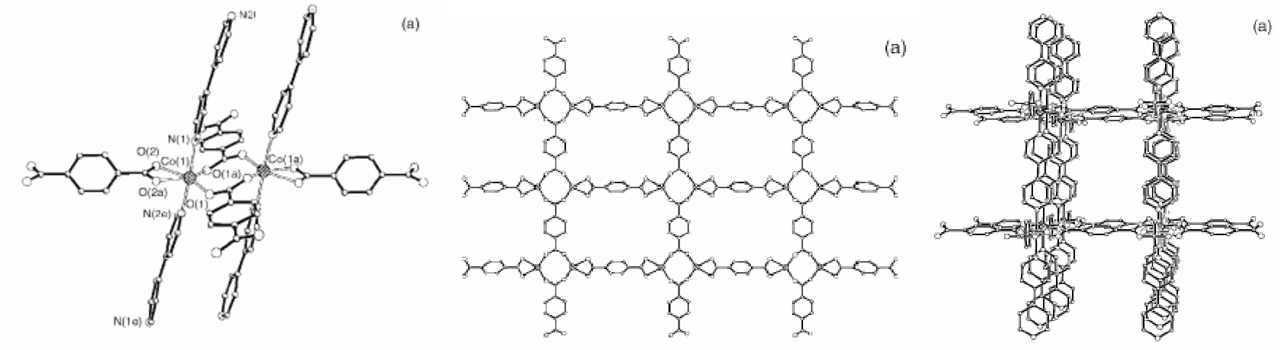

Figure A-35: Coordination polymers {[Co(terephthalate)(4,4'-bipy)]}$_n$: a) coordination environment of the cobalt binuclear unit; b) Co(terephthalate) sheet; c) perceptive view of the three dimensional motif.

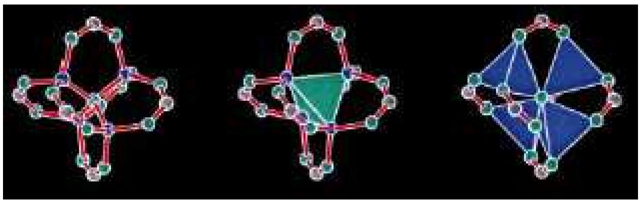

Another approach to build such three dimensional octahedral coordination polymers is to introduce metal clusters as connecting nodes. For instance Yaghi *et al*. present of lot of cuboidal frameworks {[$Zn_4O(L)_3$]}$_n$ in which the ligand molecules are dicarboxylate anions. [53, 54] The nodes are tetranuclear supertetrahedral cluster motifs Zn_4O, these oxide centred clusters appear by combination of metal cations with carboxylic acids in appropriate conditions. This synthetic path was successfully extended to dicarboxylic acids. In the compound {[$Zn_4O(bdc)_3$](dmf)$_8$(C_6H_5Cl)}$_n$ the core of the cluster consists of one oxygen atom bonded to four Zn atoms. Each edge of the Zn_4O tetrahedron is then capped by –CO_2 groups of a bridging ligand molecule (1,4-benzenedicarboxylate: bdc) (Figure A-36). This core represents a secondary building block unit (SBU) interconnected thanks to the ligands leading to the octahedral three-dimensional network. Here as well, the framework maintains its morphology and crystallinity after heating to 300°C for one day and thus desolvatation of the crystal.

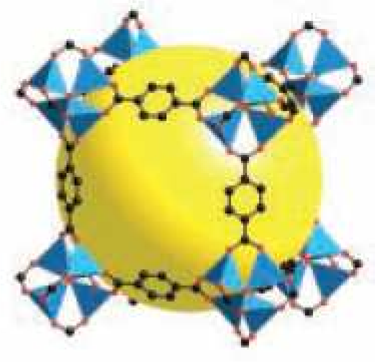

Figure A-36: cubical unit in {[$Zn_4O(bdc)_3$](dmf)$_8$(C_6H_5Cl)}$_n$ the corners are the Zn_4O clusters and the edges the ligand molecules. The yellow sphere represents the internal volume; the available space in the crystal is 80% of the crystal volume.

An important number of other three dimensional motifs have been observed: NbO-, $ThSi_2$-, PtS-, $SrSi_2$-, $CdSO_4$-like motifs or some intriguing and unique architectures with amazing names like ribbon-candy-like, chicken-wire-like, wave-like, accordion-like cages or other pipe-like architectures. All of these coordination polymers show a high stability; they present more or less large cavities filled with non coordinating solvent molecules and/or with other similar networks by interpenetration.

III - Polymorphism and other isomerism

Crystallization and crystallization product studies have allowed the description of various solid-state forms achieved from the same and/or different building blocks. The solids can be classified towards their composition and structure: they are defined by the repeating molecular patterns and the long-range order. This is true for the supramolecular chemistry field from pharmaceutical solids to coordination polymers ones. Some definitions for polymorphism and supramolecular isomerism were proposed in the literature for assemblies governed by molecular recognition [6, 13, 55-57]. The classification is not always well-defined and the following definition will be used in this thesis.

If the composition of several supramolecular networks is the same, the different structures are supramolecular isomers (by comparison to molecular isomerism). Different subsets of supramolecular isomerism can be found. In the other hand, if differences in the nature and stoechiometry of included molecules in the networks (obtained from the same ligand, metal ion and counter anion) contribute to the formation of several metal-organic frameworks, the term pseudo-polymorphism is used.

Supramolecular isomerism is the ability of a substance to exist in more than one type of network superstructure for the same molecular building blocks. Networks are generated by different supramolecular synthons or molecular assemblies. The metal moiety and the exofunctional organic ligands remain the same but combine to give a different superstructure. There is a lot of subsets to supramolecular isomerism.

Conformational supramolecular isomerism occurs when flexible molecular components are used. The change of ligand conformation can lead to similar motifs in which the conformation of the ligand is different from one structure to the other. For instance, Hanton and co-workers report two $[Cd(L)(NO_3)_2]$ (L = 1,4-bis(2-pyridylmethylsulfanylmethyl)benzene) compounds showing one-dimensional chain motifs [58]. They differ in the conformation of the ligand (Figure A-37), the inclusion solvent molecules not being the same in both cases. The coordination sphere of the metal ion remains the same in the two networks.

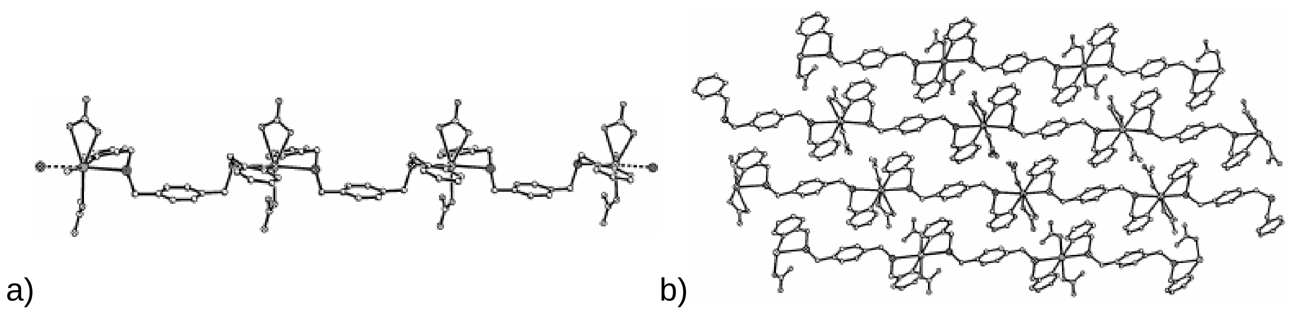

Figure A-37: one-dimensional motif in a) $\{[Cd(L)(NO_3)_2]\cdot CH_2Cl_2\}_n$ and b) $\{[Cd(L)(NO_3)_2]\cdot 4/3CH_3CN\}_n$ (L = 1,4-bis(2-pyridylmethylsulfanylmethyl)benzene)

Structural supramolecular isomers are different long-ranged organisations of the same synthons. For instance, $\{[Cu_2(\mu_2\text{-}(p\text{-benzoquinone}))(\mu_2\text{-Oac})_2]\}_n$ can be found under three different phases [59], the coordination of the ligands around Cu^{II} remaining the same but these synthons interacting differently (Figure A-38).

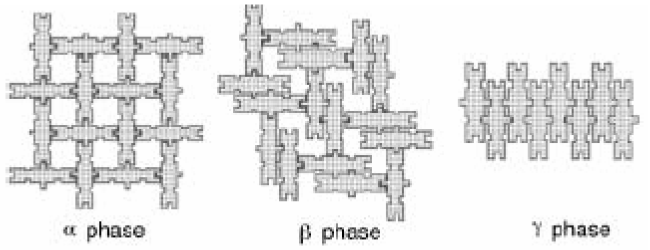

Figure A-38: the schematic representation of the three structural supramolecular isomers of $\{[Cu_2(\mu_2\text{-}(p\text{-benzoquinone}))(\mu_2\text{-Oac})_2]\}_n$ (each synthon is represented by the “rectangular” form)

Structural isomerism is the most widely found isomerism in which the coordination sphere of the metal cation differs between the two isomers [60-64] The two compounds $\{[Co(1\text{-methyl-}1'\text{-}(3\text{-pyridyl})\text{-}2\text{-}(4\text{-pyridyl})\text{ethene})_2(NCS)_2]\}_n$ can grow concomitantly or not during the slow diffusion of two solutions of each reagent, depending on the used solvents [64]. The motif of both coordination polymers is different: one-dimensional double chain in one case and two-dimensional sheet in the other (Figure A-39).

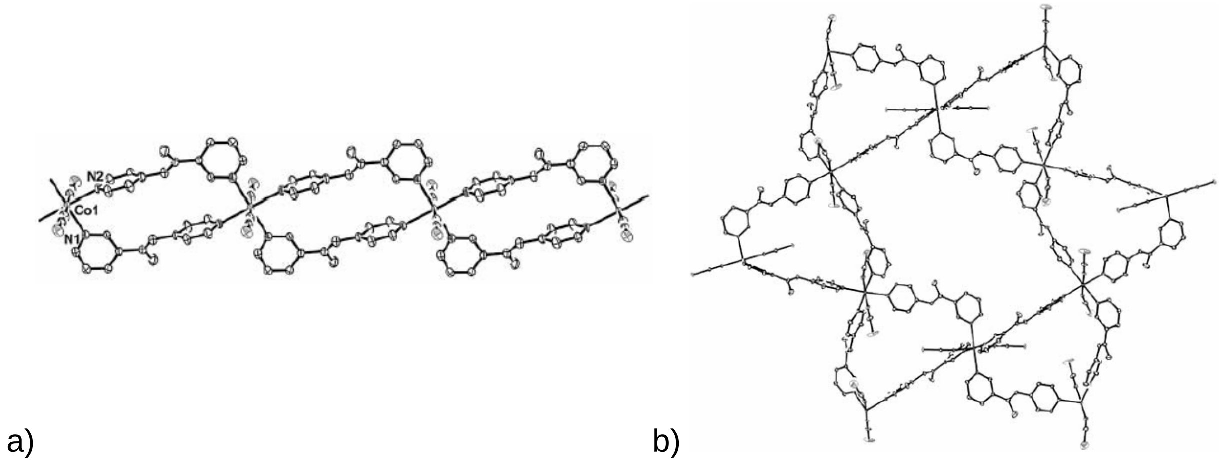

Figure A-39: the two structural supramolecular isomers of $\{[Co(1\text{-methyl-}1'\text{-}(3\text{-pyridyl})\text{-}2\text{-}(4\text{-pyridyl})\text{ethene})_2(NCS)_2]\}_n$: a) double chain and b) sheet

Polymorphism is the existence of the same chemical substance in more than one crystalline modification for molecular crystals. Polymorphism is scarce in coordination chemistry field [65] and is regarded as a subset of supramolecular isomerism: the same molecular components generate different supramolecular synthons, in other words, materials with the same chemical composition differ in the lattice structures and/or molecular conformation.

Pseudo-polymorphism is a term that refers to crystalline forms with solvent molecules as an integral part of the structure (isolated lattice sites, lattice channels or metal-ion coordinated solvates) [66-70]. The pseudo-polymorphs are obtained in crystalline forms that differ in nature or stoechiometry of included solvent molecules. Unlike polymorphs, pseudo-polymorphs are distinct chemical and structural entities. Zaworotko *et al.* present pseudo-polymorphs of $[Zn(nicotinate)_2]$ obtained under different conditions (solvent and crystallization techniques) [71]. They differ in the included solvent molecules: methanol/water or naphthalene or nitrobenzene. The motifs and dimensionalities of these compounds are very different and influenced by the reaction conditions.

During crystallization the traditional thermodynamic vs. kinetic game plays an important role. The different solid-state forms can appear under different conditions [60, 62, 64, 66-68, 71, 72] or as a mixture in the same batch [61, 64, 70, 73]. In some examples, isomers are found in the same crystal with two concomitant motifs [74].

Such phenomena could be regarded as drawback and one more difficulty in the prediction of molecular recognition, but they should be seen as a better understanding of the building blocks, the self-assembly process. They allow us to know the finite number of possible structures. These phenomena appear also quite frequently with more flexible systems and more functionalized groups.

IV - Possible Applications

One of the interests in building coordination polymers is the creation of new tuneable functional materials. In this part, we will see how metal-organic frameworks are promising as materials for applications in gas storage, anion exchange (due to the porosity and zeolitic-like behaviour), catalysis, conductivity, luminescence, chirality, magnetism, spin transition behaviour, NLO or deposition of thin films.

IV.1 - Porous materials

Controlled porosity in materials is a widely studied topic in chemistry, as open frameworks with micro-, or nanometre-sized spaces can be used in gas and liquid separation, gas storage, sensors, molecular recognition, anions/cations exchange, heterogeneous catalysis... [75] Indeed porous materials allow the reversible passage of host molecules through the guest materials *via* the surface holes. Some inorganic materials are commonly used such as zeolites and activated carbons. Zeolites are microporous crystalline solids containing generally silicon and aluminium oxides. They are extensively used in a lot of industrial processes. Activated carbons are twisted networks of defective hexagonal carbon layers, cross linked by aliphatic bridging groups showing a high open porosity and a high specific surface area. The advantage of introducing organic molecules in such frameworks is the control of the material design: architecture choice, functionality of the pores, increasing selectivity.

The coordination polymers have to be highly crystalline and porous, but it is well known that free space is against nature in crystals. When cavities appear in these frameworks, they are filled with counter anions, solvents molecules or additional co-crystallized organic molecules (or interpenetration). These molecules can be regarded as template molecules determining the pore shapes and sizes. As the metal-organic frameworks bonds are non-covalent bonds, the removal of the template molecules can lead to structure collapsing. That’s why scientist research metal-organic frameworks with permanent crystalline structures even after the removal or exchange of the guest molecules.

Porous coordination materials can be divided in three categories:

- the **first generation** porous materials contain cavities, and/or channels but these structures lose their crystallinity after removal of the guest molecules (collapsing) and are not useful for the following applications. (see further)
- the **second generation** metal-organic frameworks remain crystalline and stable as they are totally desolvated and they have a zeolitic behaviour.
- the **third generation** frameworks are dynamic and flexible ones which respond to external stimuli (like light, electric field, magnetic field, guest molecules) in changing their structures.

The transformation during the removal of the guest molecules is regarded as a “crystal-to-amorphous transformation” in the first generation metal-organic frameworks, whereas the transformations in the two other cases are named “crystal-to-crystal” ones. [76]

Gas storage is one of the applications for these materials. As seen previously the compound $\{[Zn_4O(dcx)_3]\}_n$ (dcx=dicarboxylate) [53] shows large channels. The channel sizes can be choosen by the use of convenient ligand molecules. In the compound $\{[Zn_4O(bdc)_3](dmf)_8(C_6H_5Cl)\}_n$ obtained with 1,4-benzenedicarboxylate (bdc) molecules as ligands, the dmf and chlorobenzene molecules can be removed. The total crystal desolvation and desolvated crystal stability was proven; the sorption behaviour was studied with nitrogen, argon and organic vapours of molecules such as CH_2Cl_2, $CHCl_3$, CCl_4, C_6H_6 and C_6H_{12}. Yaghi *et al.* report also other coordination polymers based on bis-, and tris-bidentate carboxylate linkers copolymerized with Zn^{II}. In these compounds the nodes are rigid metal carboxylate clusters, which allow the stability of the porous materials. The sorption processes are well studied affording efficient and robust materials for gas storage or liquid separation. [54, 77-79]

The compound $\{[Cu(SiF_6)(4,4'\text{-bpy})_2]\cdot 8H_2O\}_n$ described below (Figure A-34) presents similarly a robust three-dimensional network. The methane absorption experiments show high adsorption ability and good morphology/crystallinity retention [51].

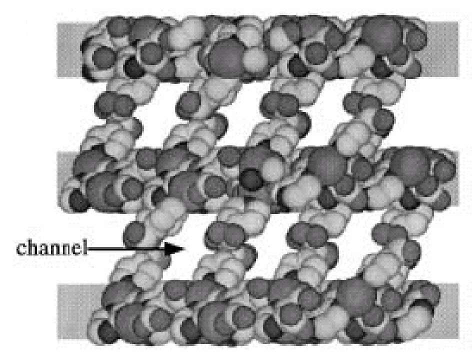

Figure A-40: 3D view of the layers, pillars and channels in $\{[Cu_2(pzdc)_2(dpyg)]8H_2O\}_n$ (water molecules omitted for clarity)

Kitagawa *et al.* report a third generation pillared-layer coordination polymer able of solvent removal and specific guest molecule re-inclusion. [80] The structure of this compound is made by two-dimensional layers $Cu_2(pzdc)_2$ (pzdc = pyrazine-2,3-dicarboxylate) connected with additional dpyg molecules (dpyg = 1,2-dipyridylglycol) in order to build a porous three-dimensional coordination polymer, the free space being initially filled with water molecules. (Figure A-40) The material is able to loose the co-crystallized water molecules (at 60°C) and a X-Ray Powder Diffraction (XRPD) study shows two guest-free phases: the anhydrous one I (same structure without the water molecules) and the apohost II (in which the inter-layer distances are smaller). Adsorption isotherm measurements prove that phase II can selectively adsorb CH_3OH and H_2O but not CCl_4, and that the final product (including the guest molecules) has the initial structure. In the absence of guest molecules, the layers get also closer to each other, the material adjusting to avoid the free space.

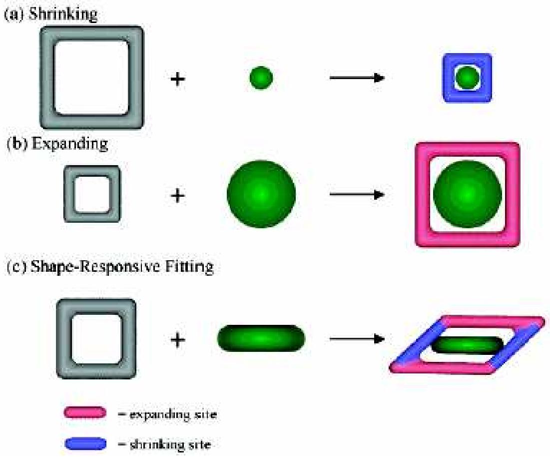

Figure A-41: schematic representation of the responsible coordination polymer networks

The Kitagawa group works on materials capable of structural changes in response to the guest-molecules: the cavities or channels adapt their shapes in order to fit around the guest-molecules. [81, 82] A schematic representation is shown on Figure A-41. These materials do not lose their robustness and are potential candidates for target molecule recognition or separation.

Another type of third generation metal-organic framework is presented by Wright *et al.* with compounds made from zinc^{II} benzene-dicarboxylates. [83] A series of [Zn(bdc)] coordination polymers is reported with solid-state transformations by removal or replacement of strongly hydrogen-bonded molecules: DMF, methanol, ethanol or water as resumed on the Figure A-42. All of these compounds have characteristic structures implying a lot of structural changes during the transformations.

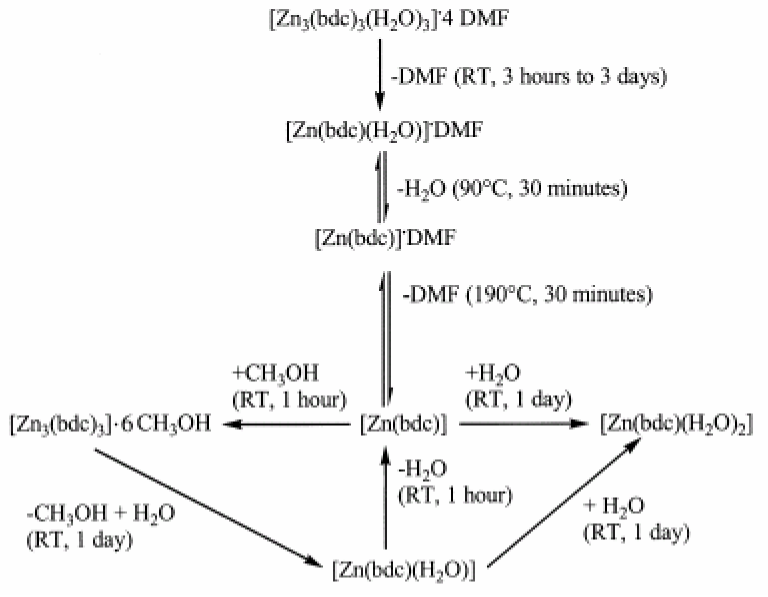

Figure A-42: desolvation and re-solvation reaction summary for the zinc^{II} benzenedicarboxylates

Soldatov and Ripmeester report species able of gas inclusion. [84, 85] The $\{[Cu(L)_2]\}_n$ (L = $CF_3COCHCOC(OMe)Me_2$) complex exists in two forms: the α-form containing no pores in the structure and the β-one having channels of about 6 Å in diameter. (Figure A-43)

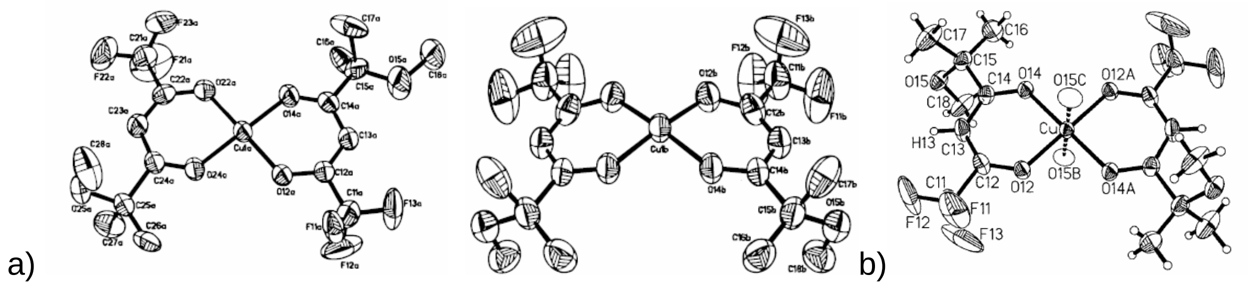

Figure A-43: a) α-form (there is two crystallographically independent complex units) and b) β-form of $\{[Cu(CF_3COCHCOC(OMe)Me_2)_2]\}_n$

Exposed to alcohol vapors, the α-form can transform itself simultaneously with the inclusion of the alcoholic guest molecules, although this form does not have any pores. Two phenomena are observed: in the case of methanol and ethanol exposures, new compounds appear in which the guest molecules coordinate the unsaturated copper atoms leading respectively to the compounds $[Cu(L)_2(MeOH)_2]$ and $\{[Cu(L)_2(MeOH)]_2[Cu(L)_2]\}_n$. (Figure A-44) There are no free voids in these structures.

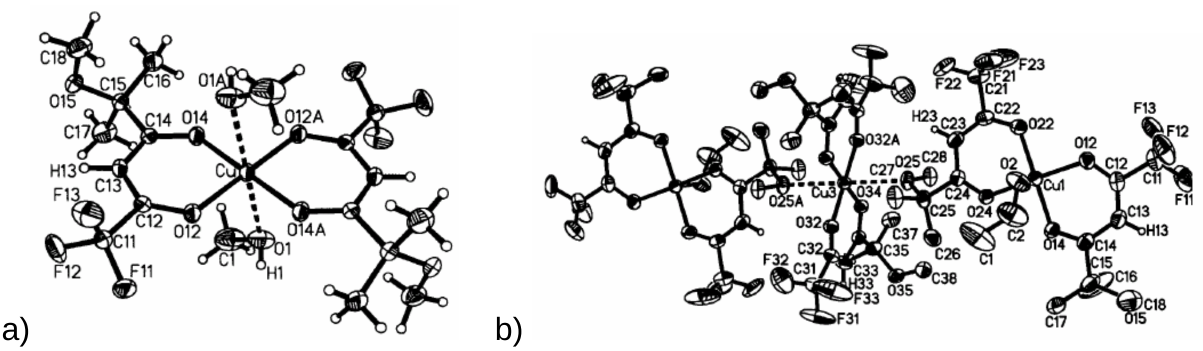

Figure A-44: a) the molecule $[Cu(L)_2(MeOH)_2]$, the overall structure is a two-dimensional structure achieved trough hydrogen bonds; b) the trinuclear unit of one-dimensional coordination polymer $\{[Cu(L)_2(MeOH)]_2[Cu(L)_2]\}_n$

Under longer alcohol gas exposure, the α-form transforms into the cavities containing β-form with inclusion of the alcohol molecules in the free spaces. The two phenomena are described as chemical or physical inclusions depending on the role of the hydrophobic part in the alcohol molecules able of more or less strong Van der Waals interactions with the wall cavities. The material can catalytically switch between dense or open forms. The same observation is made in wetting the α-form in different saturated solutions of guest molecules. Depending on the guest molecules the α-to-β transformations is observed, or new $[CuL_2Guest_2]$ compounds appear.

Upon the few examples of dynamic systems the following example is interesting. Ciani *et al.* synthesize a three-dimensional coordination polymer thanks to the self-assembly of Cu^{II} sulphate salt and 1,3-bis(4-pyridyl)propane (bpp) ligand molecules: $\{[Cu_5(bpp)_8(SO_4)_4(EtOH)(H_2O)_5](SO_4)\cdot EtOH\cdot 25{,}5H_2O\}_n$. [86] The three-dimensional structure is achieved with the entanglement of a one-dimensional motif within a two-dimensional one. (Figure A-45a)

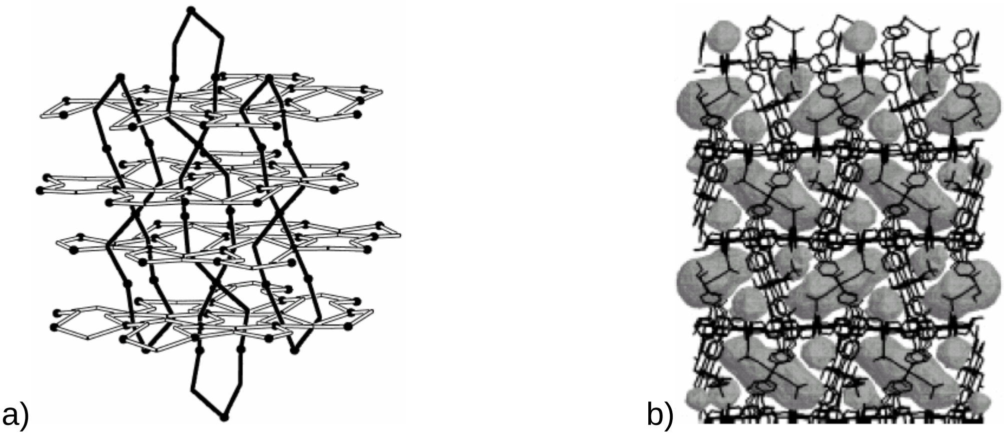

Figure A-45: $\{[Cu_5(bpp)_8(SO_4)_4(EtOH)(H_2O)_5](SO_4)\cdot EtOH\cdot 25{,}5H_2O\}_n$: a) schematic view of the entanglement of the 1D motif (in black) and the 2D motif (in white); b) distribution of the empty cavities (their limiting surface are show in grey)

About ¼ of the cell volume is constituted of large voids containing the solvated molecules of ethanol and water. (Figure A-45b) The loss of these solvent molecules was followed by thermogravimetric analysis (TGA). The desolvation is accompanied with a loss of order, but in presence of water vapors the crystallinity reappears. The process is also reversible. The re-hydration was followed by observation of the crystal surfaces (atomic force microscopy-AFM).

Another type of exchange is related by Navarro *et al*. [87]. The compound $\{[Cu(pymo\text{-}N1,N3)_2]\cdot NH_4ClO_4$ = **1**$\cdot NH_4ClO_4$ (Hpymo = 2-hydroxypyrimidine) shows an open framework. The free voids are organized in order to form a diamondoid network containing water, ammoniac and perchlorate molecules. (Figure A-46)

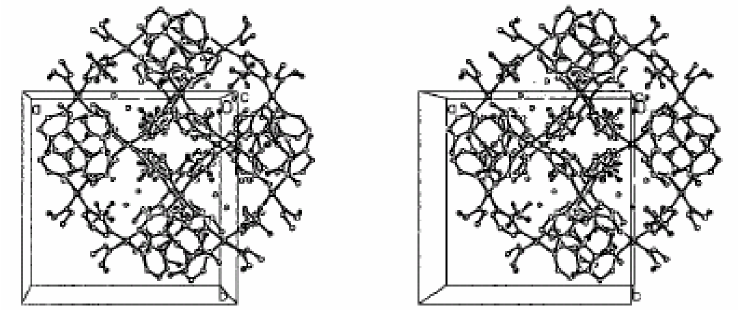

Figure A-46: View of the three-dimensional void network in $\{[Cu(pymo\text{-}N1,N3)_2]\cdot NH_4ClO_4$

By heating, the crystals can lose NH_3 molecules leading to the crystalline **1**·$HClO_4$ and are recovered by exposure to gaseous NH_3. A salt inclusion is possible too. Indeed, if the isolated compound **1** is exposed to $AClO_4$ aqueous solutions (A = NH_4^+, Li^+, Na^+, K^+ and Rb^+), **1**·$AClO_4$ is formed undergoing phase changes. This compound belongs to the third generation open metal-organic frameworks and is a rare example of **salt sorption**.

Finally **exchange of anions** can be performed as well using these open metal-organic frameworks. Zeolites are anionic frameworks and can only be used as cations exchangers. By using cationic ions and neutral ligand molecules, it is however possible to get cationic networks and to create anionic exchangers.

The process of anion exchange takes place at a solid-liquid interface and is a solid-state transformation. In this context, Min and Shu report coordination polymers based on ethylenediaminetetrapropionitrile ligand molecules (EDTPN) and silver salts (nitrate, perchlorate and triflate). [88] Some anion exchanges happen during the immersion of the crystals in appropriate aqueous solutions of $NaNO_3$, $NaClO_4$ or $LiCF_3SO_3$. As shown on the Figure A-47, the triflate anions can be quantitatively and reversibly exchanged with the nitrate anions. The triflate anions can also be exchanged with the perchlorate anions, and the nitrate compound can change its structure in including perchlorate anions. It is worth noting that these exchanges and structural transformations occur in the solid state. They were followed by XRPD and IR measurements.

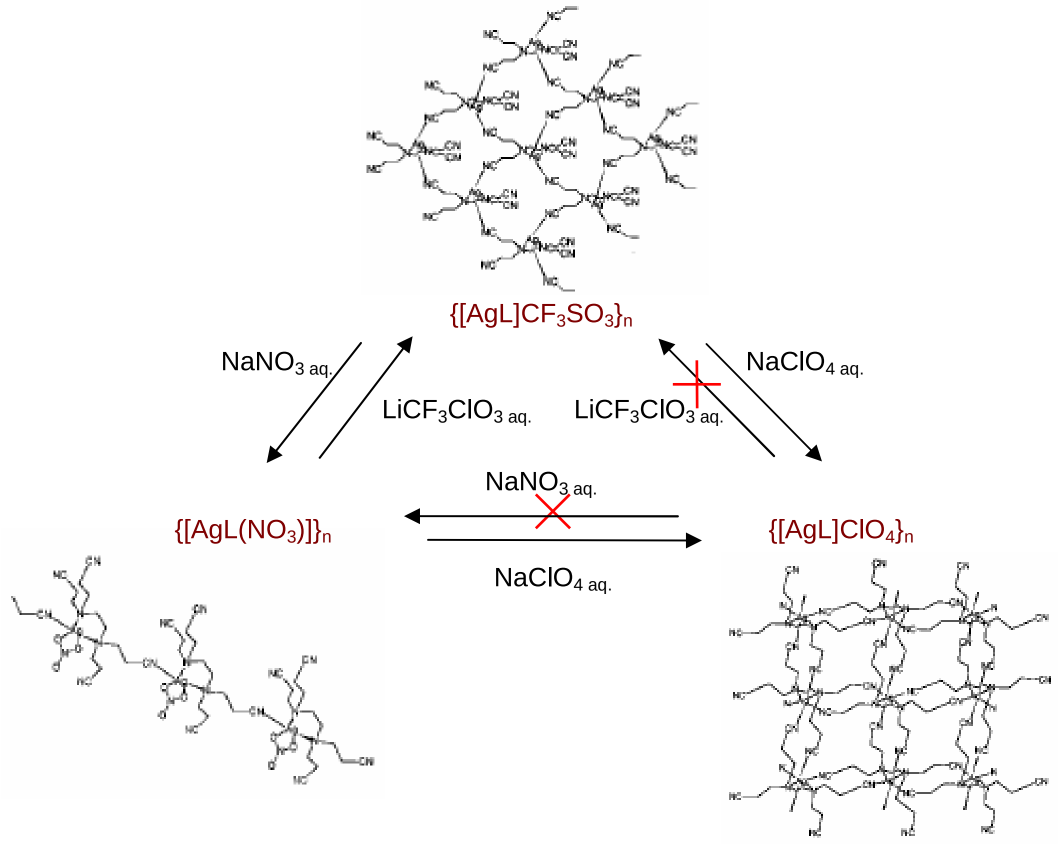

Figure A-47

An important application of the metal-organic frameworks is the **catalysis**. The coordination polymers may be helpful as 1) they can be porous; 2) they can contain catalytically active transition metal centers; 3) they can be designed in order to offer metal centers and specific organic groups to the reagents. Some non-porous coordination polymers are nevertheless also known for their catalytical properties. Heterogeneous catalysis is obviously considered with the use of the coordination polymer in crystalline form. A notable drawback in the use of these compounds for heterogeneous catalysis is their stability in the liquid phase: they should not dissolve or degrade at all during the catalytic cycle; otherwise ligand molecules and metal centers would react or interact.

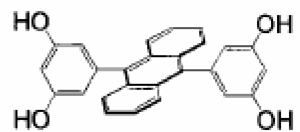

1

Only few examples of such materials with an efficient catalytic activity can be found in the literature. Coordination polymers based on anthracenebisresorcinol (H_4L) treated with $Al(CH_3)_3$, $Ti(O^iPr)_2Cl_2$, $Zr(O^tBu)_4$ or $La(O^iPr)_3$ are studied by Aoyama *et al*. and show catalytic activies. [89-92] For instance the Zr host compound $\{[Zr_2(L)(O^tBu)_2]\}_n$, whose structure is unknown (as it is insoluble in all common organic solvents), is described as a microporous framework. It can act as a reversible guest molecule acceptor (ethylacetate, benzene, hexane...) and as catalyst for Diels-Alder reactions (Equation A-1) with a good selectivity (endo:exo = 95:5), and there is no contamination of the catalytic solution.

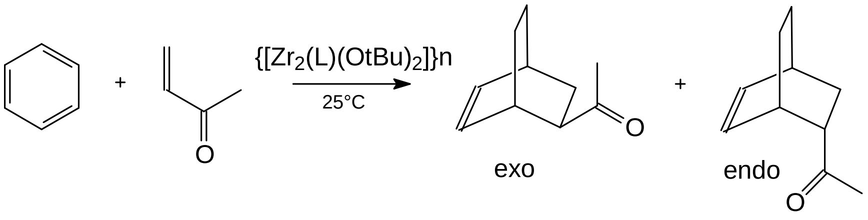

Equation A-1

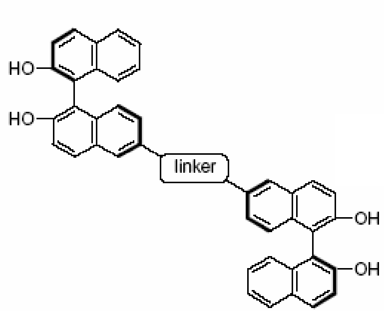

Recently several groups discovered metal-organic frameworks suitable for heterogeneous asymmetric catalysis. [93] The aim of these materials is to provide cavities walled with chiral environments for enantioselective control and with available metal ions as catalytic active centers. The groups of Sasai and Ding [94, 95] generate chiral metal-organic coordination polymers thanks to the self-assembly of a chiral ligand containing two 1,1'-2,2'-binaphtol units and Al^{3+}, Ti^{2+} ions. These compounds are highly insoluble in common organic solvents. The compound $\{[Ti_2(\mu\text{-}O)_2(binol)]\}_n$ (Figure A-48) is employed as catalyst in the asymmetric carbonyl-ene reaction shown on Equation A-2. The product was obtained with results comparable to those reached with the classical homogeneous catalyst.

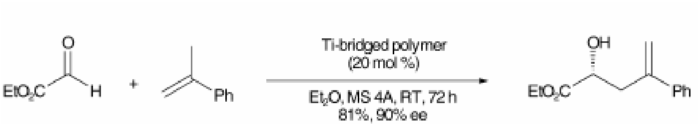

Equation A-2

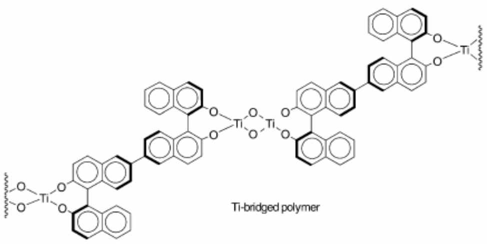

Figure A-48: coordination mode of {[Ti_2(μ-O)$_2$(binol)]}$_n$ obtained with the reaction of the ligand in which the linker is a single bond with Ti(O^{i}Pr)$_4$.

The non-porous coordination polymer {[$In_2(OH)_3(bdc)_{1,5}$]}$_n$ (Figure A-49) shows a catalytic activity for the hydrogenation of nitroaromatics (Equation A-3a) and oxidation of sulfide reactions (Equation A-3b). Although the catalytic mechanism is not totally understood, it must take place at the surface and involves coordinative unsaturations either with ligand dissociation or with increase in the coordination number of indium. [96]

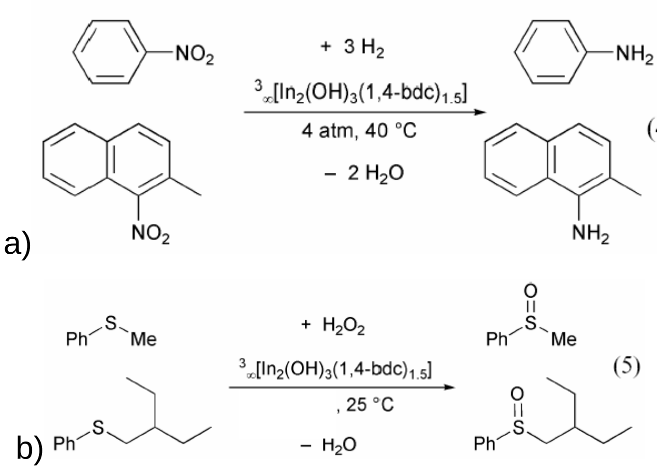

Equation A-3

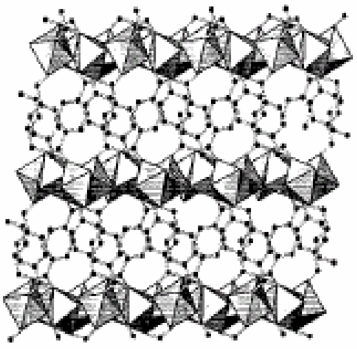

Figure A-49: The three-dimensional network of {[$In_2(OH)_3(bdc)_{1,5}$]}$_n$ is made of two-dimensional {[$In_2(OH)_3$]$^{2+}$}$_n$ sheets pillared with the bdc ligand molecules.

IV.2 - Conductivity

Conductivity may be an interesting research topic providing that short inorganic or conjugated organic bridges exist in the metal-organic framework.

Some one-dimensional coordination polymers $\{[ML(\mu\text{-}L')]\}_n$ built as shown on Figure A-50 with or without doping with iodine exhibit conductivity in a range of 1.10^{-6} S.cm^{-1} to 2.10^{-1} S.cm^{-1} [97]. (Conductivity of metals is 10^4-10^5 S.cm^{-1} and increases with decreasing temperature.) The conductivity is due to the interaction between the metal d-orbital and the π* level of the bridging ligand L'.

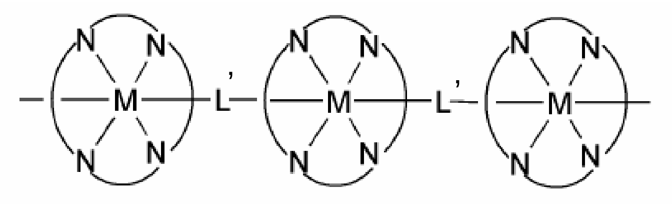

Figure A-50: $\{[ML(\mu\text{-}L')]\}_n$ coordination polymers with M = Fe, Ru, Os; L = octaethylporphyrinato (oep), phthalocyaninato (pc); L' = pyrazine (pyz), 4,4'-bipyridine, dabco.

In some cases coordination polymers can have semi-conductor behaviour. The three-dimensional polymer $\{[Ag(H_2btc)_2][Ag_2(Hbtc)]\}_n$ (H_3btc = benzene-1,3,5-tricarboxylate) [98] presents weak semi-conductivity (conductivity of $1,06.10^{-6}$ S.cm^{-1} and increase of conductivity with temperature) due to the presence short Ag-Ag contacts as the whole structure can be regarded as parallel Ag chains connected by the H_2btc^- and $Hbtc^{2-}$ molecules. (Figure A-51) The Ag-Ag contacts, ranging from 2.9626 to 3.2782 Å, are known for giving semi-conductivity properties to the materials.

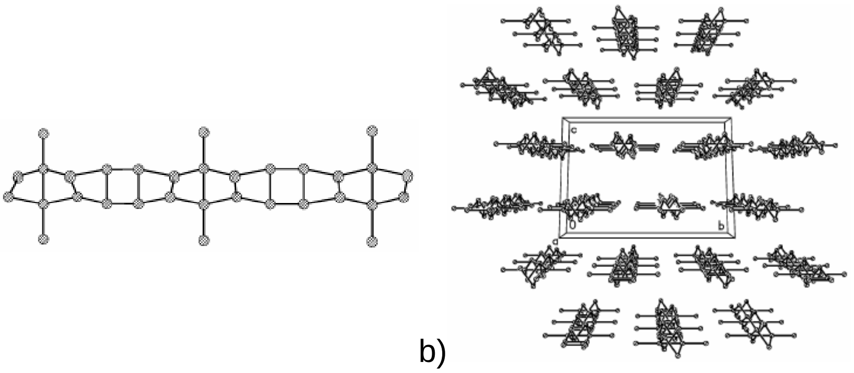

a) b)

Figure A-51: the Ag chains in $\{[Ag(H_2btc)_2][Ag_2(Hbtc)]\}_n$ (organic spacers omitted for clarity)

The semi-conductivity is better for the compound Ag_2.CA (CA = cyanuric acid, $C_3H_3N_3O_3$) being an organic-inorganic hybrid. It is composed of Ag sheets with the cyanuric acid as linkers between the sheets. The conductivity is furthermore anisotropic in this case: 5.10^{-3} parallel to the sheets; 2.10^{-5} S.cm^{-1} perpendicular to the sheets. [99]

Semi-conductivity was also found in the compound $\{[Ni_2(\text{pyrimidine-2-thiolate})]\}_n$ which exhibits two-dimensional motifs based on Ni_2S_2 units spaced out by the ligand molecules

[100]. (Figure A-52) There are therefore short distances between the metal centers of 3.774 Å. Its conductivity is of 5.10^{-3} $S.cm^{-1}$ at 28°C and increases with temperature. The semi-conductivity provides evidence for nickel and pyridine ring interactions.

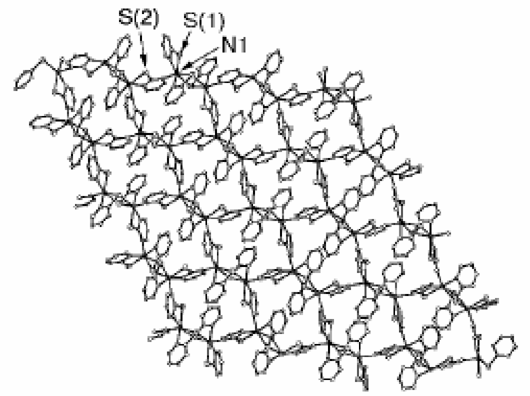

Figure A-52: View of the lamellar structure of {[Ni_2(pyrimidine-2-thiolate)]}$_n$

IV.3 - Luminescence

Luminescent supramolecular architectures have recently attracted much interest because of their potential applications in optoelectronic devices or as fluorescent sensors and probes. Indeed inorganic-organic coordination polymers afford more stability (thermal-, solvent-resistant) than the pure organic ligands and may affect the emission wavelength of these organic molecules.

Determination of the fluorescence is made in the solid state and mostly at room temperature. In some cases fluorescence measurements are also made in solution in order to prove the existence of oligomeric fragments. [101, 102] Different phenomena can explain the luminescence observed in related luminescent coordination polymers, they will be discussed in the following chapter.

Emissions may be assigned in a significant number of examples to ligand-to-metal charge transfer (LMCT), if the luminescence is due to the metal-ligand complex formation. [98, 103-109] The intense photoluminescence emission of these materials can be used in order to design potential candidates for emitting diode devices. The two compounds $\{[Tb(O_2CPh)_3(CH_3OH)_2(H_2O)]\}_n$ and $\{[Tb_2(O_2CPh)_6(4,4'\text{-bipyridine})]\}_n$ (Figure A-53a/b) present strong bright green emission and their emission spectra are almost identical. (Figure A-53c/d) The emission is due to LMCT processes. [108] Indeed the emission bands of the ligand molecules don't appear in the spectra. Thus, the ligand transfers the excitation energy efficiently to the Tb^{III} ions, the four bands corresponding respectively (from left to right) to the transitions $^5D_4 \rightarrow {}^7F_6$, $^5D_4 \rightarrow {}^7F_5$, $^5D_4 \rightarrow {}^7F_4$ and $^5D_4 \rightarrow {}^7F_3$.

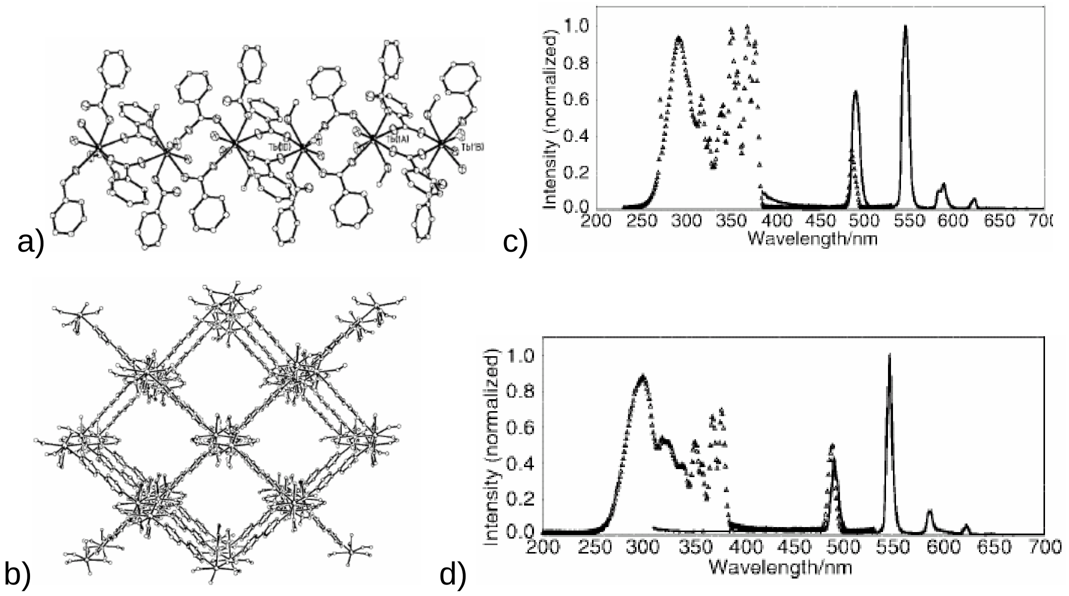

Figure A-53: a) 1D chain in $\{[Tb(O_2CPh)_3(CH_3OH)_2(H_2O)]\}_n$: the Tb ions are octa-coordinated by the benzoates, the methanol and the water molecules. b) 3D grid architecture in $\{[Tb_2(O_2CPh)_6(4,4'\text{-bipyridine})]\}_n$: Tb ions and benzoates molecules form 1D chains linked through the bipyridine molecules. c) excitation (triangles) and emission (solid line) of $\{[Tb(O_2CPh)_3(CH_3OH)_2(H_2O)]\}_n$; excitation at 300 or 368 nm. d) excitation (triangles) and emission (solid line) of $\{[Tb_2(O_2CPh)_6(4,4'\text{-bipyridine})]\}_n$; excitation at 300 nm.

In some other cases the fluorescence intensity can be significantly enhanced in the polymeric compound in comparison to the one of the pure organic molecules without change in the emission wavelength [110-114]. It is only due to contribution of the organic part, the enhancement coming from the increase in the rigidity of the ligand molecules in the complexes and/or the decrease of the symmetry within the ligand molecules. Sometimes red-, or blue-shift is observed due to particular interactions (π-π stacking) or to (de)protonation of the ligand. The emission of the compound $\{[Cd(\text{terephthalato})(\text{pyridine})]\}_n$ occurs at 464 nm while the terephthalato acid emits at 466 nm. But the intensity of the complex emission is 100 times larger than that of the free ligand. The emission is due to intraligand π-π* transitions [110]. The same observation is made with the compound $[Cu(PPh_3)(N,N\text{-}(2\text{-pyridyl})(4\text{-pyridylmethyl})\text{amine})_{1,5}]$-$\cdot 0,5CHCl_3\cdot ClO_4\}_n$: the free ligand emits at 460 nm whereas the complex emits at 490 nm with an intensity 10 times larger. The weak bathochromic shift is probably due to the increase of aromatic π-π stacking in the crystalline metal-organic frameworks [113].

Silver coordination polymers displays scarcely intense luminescence at room temperature [115]. They are known to be greater emitting materials at low temperature [116], with an enhancement of the emitting intensity towards the ligand [72] and/or a shift of the emission wavelength [116]. In the particular case of coordination polymers containing silver-silver contacts, the luminescence properties may be assigned to the short metal-metal contacts.

[117-119] In the series of polymers based on AgX (X = PF_6^-, ClO_4^-, OTs^-, NO_3^-, BF_4^-) and 4,4'-dipyridylsulfide (4-PDS), only the compound $\{[Ag(4\text{-}PDS)]OTs\}_n$ has Ag-Ag interactions. No fluorescence is observed for the coordination polymers except for $\{[Ag(4\text{-}PDS)]OTs\}_n$. The band at 600 nm is attributed to the Ag-Ag contact [117].

IV.4 - Nonlinear Optical properties

For the construction of nonlinear optical (NLO) materials, a noncentrosymmetric arrangement in the solid-state is required and this consists in an interesting challenge. These materials should also contain organic ligands with large molecular first hyperpolarizabilities, β, ideally chromophores with a good electron donor and a good electron acceptor connected through a conjugated bridge. Metal-organic framework building is used to order asymmetric chromophores which are highly dipolar and thus difficult to align in a noncentrosymmetric way. (dipole-dipole repulsions) Some examples of metal-organic frameworks showing frequency conversion (intensity modulation of light: second harmonic generation (SHG) processes) can be found in the literature [120-126]. The SHG is studied by the use of the 1064 nm fundamental wavelength of a Nd:YAG laser using the Kurtz-Perry powder method.

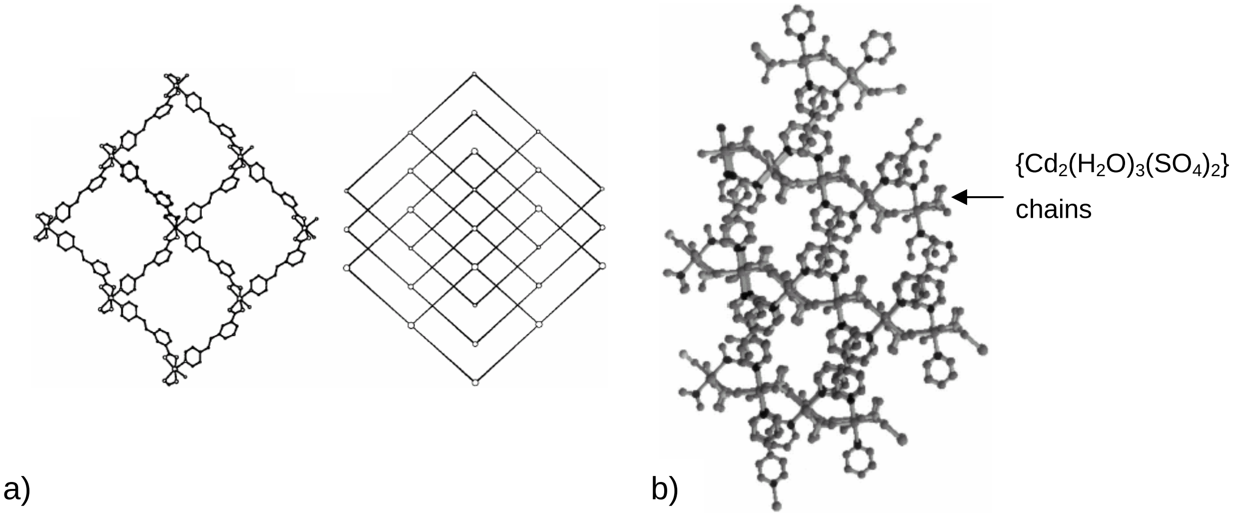

Figure A-54: a) A example of 2D NLO network: $\{[Cd(3\text{-}(2\text{-}(4\text{-pyridyl})ethenyl)benzoate)_2]\}_n$ with the interweaving of three independent rhombohedral grids; b) $\{[Cd_2(4,4'\text{-bipy})_2(H_2O)_3(SO_4)_2]\cdot 3H_2O\}_n$: the three-dimensional interwoven network

Lin *et al*. have outlined strategies to build noncentrosymmetric metal-organic frameworks [125]. They use *p*- or *m*-pyridinecarboxylate linear, rigid and nonsymmetric organic ligands as linkers between d^{10} metal centers (Zn^{2+}, Cd^{2+}: tetrahedral or pseudo-tetrahedral) in hydro(solvo)thermal conditions. The building blocks lead to the construction of three-dimensional diamondoid networks or two-dimensional frameworks (Figure A-54a). Even with weak electron donor/acceptor combinations, it is possible to obtain efficiently NLO properties, as the well chosen complexation can allow a good alignment and cooperation between the molecules. The powder SHG intensity of some compounds is comparable or higher than that of technologically important $LiNbO_3$. Furthermore they get a relatively good thermal resistance and are optically transparent. Huang and co-workers synthesize a noncentrosymmetric coordination polymer including the symmetric 4,4'-bipyridine ligand. The compound $\{[Cd_2(4,4'\text{-bipy})_2(H_2O)_3(SO_4)_2]\cdot 3H_2O\}_n$ crystallizes in the noncentrosymmetric space group *C*2. It consists of one-dimensional chains containing two types of Cd centers coordinated by μ_2- and μ_3-SO_4^{2-} anions and water molecules in the equatorial coordination sites. The chains are connected together with the bipyridine ligands coordinated in the apical sites of the Cd centers. (Figure A-54b) This compound shows powder SHG intensity.

A remaining problem in the use of such compounds is their poor stability in the laser light.

IV.5 - Magnetism

Coordination polymers strategy is furthermore employed for the design of molecular-based magnets. Indeed antiferromagnetism, ferrimagnetism and ferromagnetism are cooperative phenomena of the magnetic spins within a solid. They require an interaction or coupling between the spins of the paramagnetic centres. And the building of metal-organic frameworks allows the choice of the coupling parameters.

The magnetic coordination polymer has to own a residual permanent magnetization at zero-field for an as high as possible T_c (critical temperature). Its structure should allow parallel coupling of the spins (↑↑↑↑, ferromagnetism) or an anti-parallel coupling of inequal spins (↑↓↑↓, ferrimagnetism) of neighbouring paramagnetic spin carriers, so that a non-zero spin of the bulk material results. Some antiparallel couplings of spins (↑↓↑↓, antiferromagnetism) are found in numerous examples as the state of low-spin multiplicity is often more stable than the state of high-spin multiplicity.

An efficient coupling in magnetic materials occurs through open shell organic ligands. Materials with oxo, cyano or azido bridges show a strong coupling between the metal centres and these unpaired electrons. As example, the review of Batten and Murray focuses on the correlation between structures and magnetic properties of coordination polymers containing dicyanamide and tricyanomethanide [127].

Magnetic behaviour is found for coordination polymers built up with carboxylate group containing ligand [128-130]. Mixed metal (Cu^{II}, Mn^{II} or Fe^{II}) two-dimensional coordination polymers exhibit ferromagnetism due to the one-dimensional repeating motif (-M-O-C-O-

Cu-O-C-O-M-) [128] (Figure A-55). With the use of such ligands, metal-carboxylate subunits are often formed reinforcing the framework stability and the coupling [131-134]. Zaworotko and co-workers present a scarce example of ferromagnetic coordination polymer ($\{[Cu_2(pyridine)_2(bdc)_2)_3]\}_n$) even at room temperature [134].

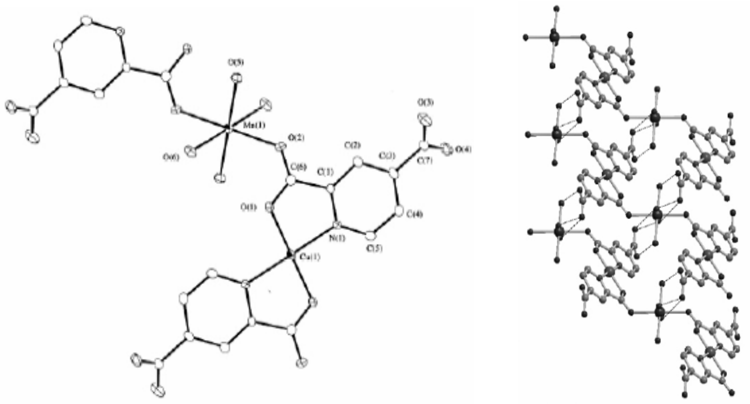

Figure A-55: $\{[Mn([Cu(pyridine\text{-}2,4\text{-}dicarboxylate)])_4(H_2O)_4]\}_n$

The examples of magnetic coordination polymers with polytopic nitrogen-based ligands exist but are much scarcer. For instance, the complex $\{[Fe_2($*trans*-4,4'-azopyridine$)_4(NCS)_4]\cdot EtOH\}_n$ presents a temperature dependant magnetic moment due to spin-crossover behaviour [135]. The long ligands avoid or lower the coupling between the metal centres. The complexes $\{[Cu(L)(H_2O)(SO_4)]\cdot 2H_2O\}_n$ and $\{[Co(L)_2(NCS)_2]\cdot 2{,}5H_2O\}_n$ (L = 2,5-bis(4-pyridyl)-1,3,4-thiadiazole) show very weak antiferromagnetic coupling [136].

Co-ligands (*N,N*-donors and carboxylic) are also used [26]. The carboxylic ligands are used as pillars between metal-*N-N'*-donors ligands motifs, allowing the required coupling. The $\{[M(oxalate)(4,4'\text{-}bipyridine)]\}_n$ (M = Fe^{II}, Co^{II} or Ni^{II}) (Figure A-56) revealed spontaneous antiferromagnetic ordering, attributed to the strong exchange interactions between the one-dimensional bridged metal ions through oxalate organic ligands and weaker interchain magnetic interactions [137].

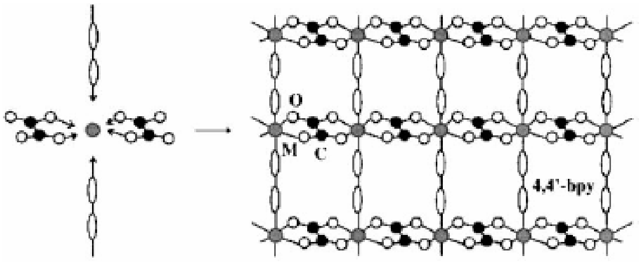

Figure A-56: $\{[M(oxalate)(4,4'\text{-}bipyridine)]\}_n$

Another example of mixed ligands coordination polymer can well illustrate the magnetic behaviour of metal-organic frameworks [138]. The complex $\{[Cu(N_3)_2((1\text{-}R)\text{-}6,6\text{-}dimethyl\text{-}5,7\text{-}methano\text{-}2\text{-}(2\text{-}pyridinyl)\text{-}4,5,6,7\text{-}tetrahydroquinoline)]\}_n$ presents weak antiferromagnetic interactions between the Cu^{II} ions through the azide bridge.

V - Choice of the working conditions

As previously seen, a large amount of coordination polymers involves bipyridyl (*N*-donors) ligands. They include pyrazine [20, 139, 140] and derivates [26, 34, 87, 141], 4,4'-bipyridine [46, 51, 120, 121, 142-145] and longer bridged bipyridyl ligands [28-30, 32, 39, 44, 49, 73, 102, 117, 146-154] as linkers with a large diversity of the metal centers as nodes.

V.1 - Bidentate bipyridyl ligands

The most important factors during the construction of coordination polymers are the coordination preferences of the metal center and the ligand functionality.

The studies of bipyridine based coordination polymers started with the complexation of 4,4'-bipyridine ligands with a large variety of metal centres changing also the experimental conditions. This ligand was widely and is still extensively studied, giving a lot of new materials (more than 300 articles relate coordination polymers built up with 4,4'-bipyridine among other building blocks). The 4,4'-bipyridine ligand can bridge a lot of metal centres in a numerous number of structural motifs: linear or zig-zag chains [9, 11, 155-159], ladder-like chains [160], bilayers [46], square grid layers [161], hexagonal sheets [143], diamondoid [143, 162], other three-dimensional motifs [51, 120, 121, 142, 144]. The characteristic of this organic ligand is its rigidity, it bridges the metal ions spacing them out to *ca.* 10 Å. The main interactions in such coordination polymers are obviously the coordination bonding, as well as π-stacking (ring···ring, ring···M or C-H···ring). Depending on the experimental conditions (solvent, stoechiometry, counter anions...), some other hydrogen bonding can occur [145, 160].

The first derivative of 4,4'-bipyridine is bipyridine molecules in which the position of the nitrogen atoms in the rings differs. For instance, the use of 2,4'-bipyridine instead of 4,4'-bipyridine with $AgNO_3$ favours the formation of helical chains rather than linear ones [142, 144, 150].

Research on bridging bidentate bipyridyl based complexes is also of interest. Indeed the introduction of linkers between the two N-donors groups allows a larger diversity, *i.e.* a larger potentiality in the resulting coordination polymer topologies. The bridging part of the ligands confers to the ligand some specificity: linearity, determined shape, rigidity/flexibility, specific functionality, increasing the ligand adaptability and the number of possible interactions. Due to the

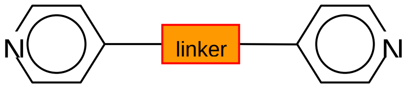

attraction towards these systems, bipyridine based coordination polymers are widely reviewed [9-11, 145, 163, 164].

Firstly some ligands with alkyl chains as linkers were used, introducing flexibility and particularly the fact that the ligand may assume different conformations in the crystal packing [39, 165, 166]. New structural motifs appeared, for instance, the double helix in the $\{[Ag(1,3\text{-bis(4-pyridyl)propane})](CF_3SO_3)\}_n$ (Figure A-26). The use of -CH=CH- or -C≡C- as linkers allows to conserve the rigidity of the ligand and at the same time to increase the distances between the nodes [152, 167]. This strategy combined with tetrahedral or octahedral metal centres is used in the elaboration of interpenetrated frameworks [168].

The next step in the studies of bipyridyl derivatives coordination polymers was the introduction of heteroatoms (N, S or O) in the bridging part.

Functions like -CR=N-R'-N=CR- (R and R' being other groups, for instance, -H, $-CH_3$, $-(CH_2)_n$-...) [102, 146, 169-173] confer to the ligands more N-donors sites as well as new hydrogen bond acceptors. The consequence on the final coordination polymers is the simultaneous coordination of the ligand to several metal ions, allowing the construction of less known supramolecular architectures with stabilization of the system. Bonding of organic guest molecules within framework cavities is also favoured, the imine functions offering sites for interactions with guest molecules. Reaction between *N,N'*-bis(4-acetylpyridine)idene 1,3-diaminopropane (L) and $AgClO_4$ in methanol gives crystals of the composition $\{[Ag_3(L)_2](ClO_4)_3\}_n$ [173] (Figure A-57). The high flexibility of the central propyl residue allows this ligand to bend and to optimize the metal coordination. There are two silver coordination environments: *i)* one Ag^I is coordinated by two outer nitrogen atoms (pyridyl ones) in a linear way; *ii)* the other Ag^I is coordinated by three nitrogen atoms (one outer nitrogen atom and two inner nitrogen atoms from the di-imino site in the bridge) in a nearly trigonal symmetry. In $\{[Co(1,4\text{-bis(3-pyridyl)-2,3-diaza-1,3-butadiene})(NCS)_2](CH_2Cl_2)_2\}_n$, weak hydrogen bonds between dichloromethane and inner N atoms stabilize the overall structure [171].

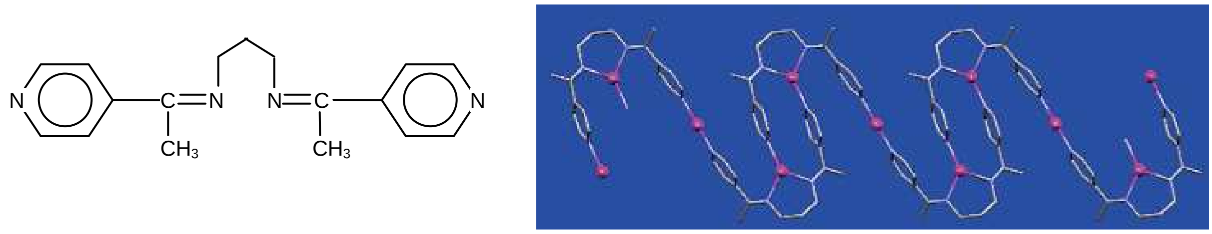

Figure A-57: ligand and one-dimensional polymer with two coordination modes of Ag^I in $\{[Ag_3($*N,N'*-bis(4-acetylpyridine)idene 1,3-diaminopropane$)_2](ClO_4)_3\}_n$ (silver in rose and ligand in gray)

Some other kind of ligands are chosen to self-assemble coordination polymers with specific networks, among them bipyridyl ligands containing five-membered heterocyclic rings [174, 175] or S-donors groups [36, 176-178].

More recently, the design of coordination polymers with bridged bipyridyl ligands containing carbonyl [179], and amide [38, 153, 180, 181] groups have also started to be studied. Few examples of ligands with ester functions in the bridge have been employed [179, 182, 183].

V.2 - Influence of the conditions on coordination polymers

Solvent All building blocks included in one coordination polymer have particular interactions with the solvents, according to their polarity, hydrophilic/hydrophobic groups.... The solvent can have a role as coordinating molecules [184] or template molecules [178]. Compounds $\{[Ag_2(L)_3(ClO_4)_2]\}_n$ and $\{[Ag_2(L)_3(ClO_4)_2 \cdot MeOH]\}_n$ (L = 1,4-bis(phenylthio)butane) are able to crystallize by diffusion of a mixture of L and $AgClO_4$ in acetone/chloroform into ether or methanol [184]. In the second compound, a methanol molecule coordinates the silver ions instead of a perchlorate anion as in the first one. $\{[Ag_2(L)_2](ClO_4)_2(CHCl_3)\}_n$ and $\{[Ag(L)](ClO_4)(C_3H_6O)\}_n$ (L = 1,4-bis(2-pyridylthio)butane) complexes crystallize under the same conditions (diffusion of a solution of silver salt into a solution of ligand in chloroform) except that MeOH was used to obtain the first compound and acetone for the second [178]. All used solvents are not coordinating. The authors assume that the differences in size and shape affect the self-assembly and result in different two-dimensional frameworks.

Counter-anions One example among numerous shows the influence of the counter ions on the final structure [38], *via* the achievement of four different coordination polymers by reaction between the ligand *N,N'*-di(2-pyridyl)oxamide with AgX (X = NO_3^-, ClO_4^-, PF_6^- and BF_4^-) under the same conditions (CH_3CN solution of the products layered with diethyl ether). The coordination force of the counter anions avoids or allows Ag-N bond formation with the ligands or the solvent molecules (CH_3CN).

Stoechiometry In some examples, the reaction of same compounds (ligand and metal salts) in the same conditions by changing the reaction stoechiometry leads to compounds of different dimensionalities: a stoechiometry M:L 1:1 leading to one-dimensional motifs, a stoechiometry M:L 1:2 giving two-dimensional motifs [185].

V.3 - Ethanediyl bis(isonicotinate)

The work on coordination polymers in our group follows the synthesis of homo- and mixed compounds of group 1 and 2 metals with the aim to synthesise new precursors for CVD and sol-gel techniques used for oxide materials. [186-195] In order to obtain better performing and single source precursors, mixed metal compounds containing transition metal, as well as group 1 and 2 metal ions began to be investigated. The formation of coordination polymers is thus an efficient way to get a good distribution of the metals within the materials.

With regard to the field of coordination polymers, the ligand ethanediyl bis(isonicotinate) (Figure A-58) was therefore chosen because it *i)* is flexible (structurally adaptative), *ii)* contains different functional groups allowing coordination of two different metal ions, and *iii)* can be prepared easily, which makes potential applications possible.

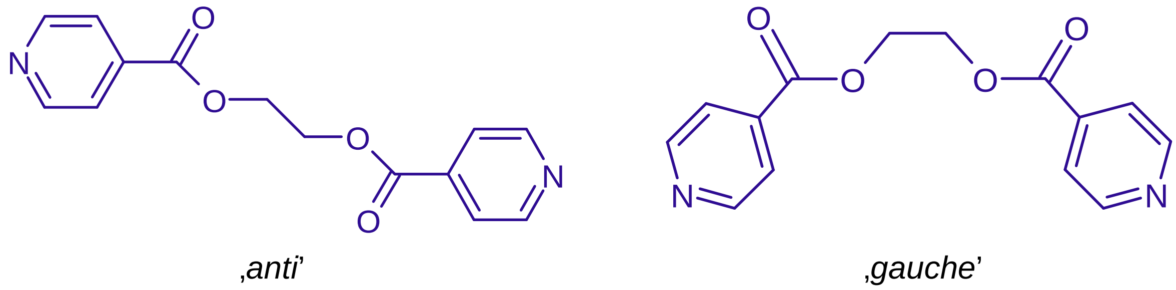

Figure A-58: ethanediyl bis(isonicotinate) and its two conformations

The ethanediyl bis(isonicotinate) can adopt two main conformations, *gauche* or *anti*, due to the free rotation around the ethlyl group C-C bond (Figure A-58). Obviously, different conformations of the ligand in the coordination polymers can drastically change the resulting framework architecture. Several ligands with the same flexibility have already been used [166, 170, 196]. In most cases, only one conformation per framework is observed.

It is worthwhile to note that only one coordination polymer with a similar ligand to ethanediyl bis(isonicotinate) was related at the beginning of this work [183]. Since, Song *et al*. presented coordination polymers built up with ethanediyl bis(isonicotinate) and Cu^{I} or Co^{II} [147, 197], while the Stang and Hosseini groups report the self-assembly of metallacycles with ethanediyl bis(isonicotinate) and respectively Pd^{II}, Pt^{II} [182] or Zn^{II}, Hg^{II}, Co^{II} [198]. The metallacycles are formed by two ligand molecules and two metal ions (two ligands coordinate each metal center through their nitrogen atoms). As the metal ions have a tetrahedral coordination geometry, the coordination sites not involved in M-N coordination bonds are occupied by additional ligand molecules (phosphine) [182] or coordinating anions (Cl) [198].

V.4 - Cu^I

The d^{10} metals (Ag^I, Cu^I, Zn^{II}...) are generally used in the coordination polymer engineering as their coordination spheres are flexible, with less constraints around the metal centers. Ag^I, Cu^I based networks are attractive, as they readily coordinate to unsaturated, bidentate nitrogen ligands (soft-soft bonding preference). The combination of conjugated ligands, electron-rich metal centers and the high degree of covalency inherent in soft-soft bonding can produce low-energy electronic interactions between metal centers and ligands (with possible optical or electronic properties).

A lot of coordination structures are obtained with CuX (X = Cl, Br, I) [139, 141, 143, 146-148, 199-208]. This strategy allows mainly the formation of neutral networks, as halile counter anions are generally strongly coordinated to the Cu^I. These networks are quite stable, as there are no counter anions between the coordination polymer skeleton. Furthermore, combinations of Cu halide with bidentate bridging ligands result in one-dimensional or two-dimensional networks, usually through the linking of Cu_2X_2 rings or $(CuX)_n$ chains by the ligand [204, 206].

V.5 - Ag^I

The coordination polymers derived from Ag^I with N-donor ligands are well-known for making simple one-dimensional motifs when the two-coordinate metal ion reacts with a bipyridine-type ligand [9, 11]. Ag^I has a preference for linear geometry in these cases. Nevertheless, as the coordination sphere of Ag^I is very flexible, it can adopt coordination number between two and six, the geometry changing from linear to octahedral. The coordination geometries of Ag^I are often distorted owing to the inherent lack of ligand field stabilization effects (Soft Lewis Acid).

The reaction of silver salt with the linear 4,4’-bipyridine ligand affords either linear geometry [152, 209, 210] or tetrahedral geometry [162], depending upon the ratio of 4,4’-bipyridine to silver, 1:1 or 2:1 respectively. The same compounds can also lead to other architecture with a “T-shaped” moiety by changing the reaction conditions. [142, 144] The number of N atoms coordinating the silver ions is a major factor for the motif construction.

With other bridged bipyridine ligands, Ag^I has also demonstrated its ability to adopt several coordination modes: linear geometry [9, 11] (Figure A-59a), trigonal planar [36] (Figure A-59b), tetrahedral [146, 166, 168, 169, 174] (Figure A-59c) which can be highly distorted. The coordination of silver centers with N-donors ligands seems to avoid the high coordination number for Ag^I, unlike O-donors ligands [211] (Figure A-60).

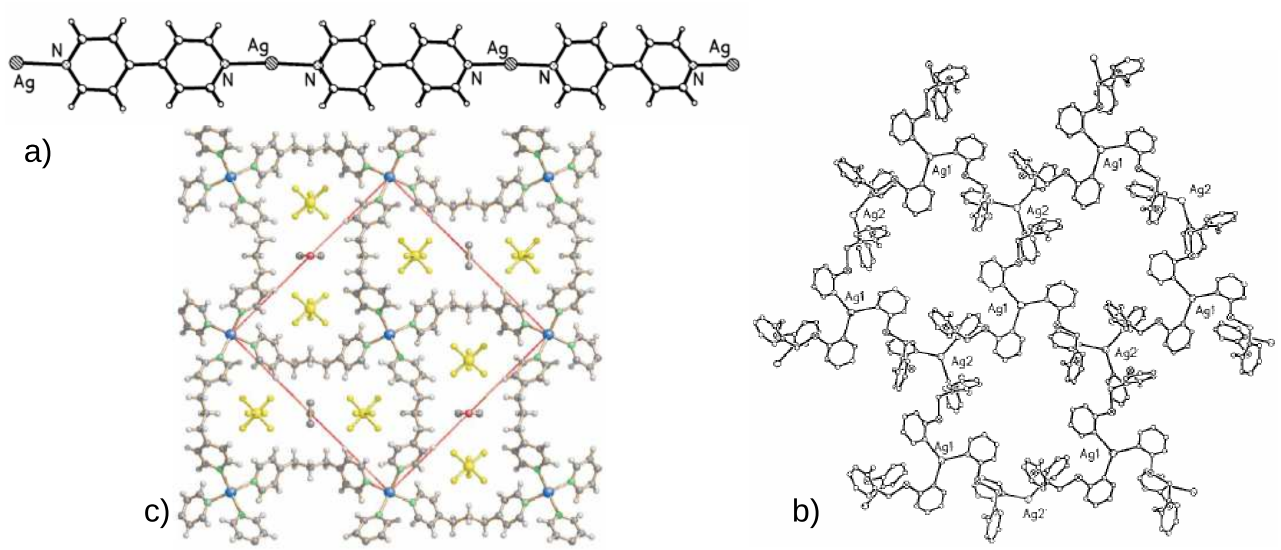

Figure A-59: the three main coordination of N-donors ligands around Ag^I : a) $\{[Ag(4,4'\text{-bipyridine})]BF_4\}_n$ [9]; b) $\{[Ag_2(1,2\text{-bis}((2\text{-pyrimidinyl})\text{sulfanylmethyl})\text{-benzene}))_3](ClO_4)_2\}_n$ [36]; c) $\{[Ag(1,3\text{-bis}(4\text{-pyridyl})\text{propane})_2]SbF_6\}_n$ [166]

This flexibility of the Ag^I ion is used to investigate the role played by the weak interactions (described in I.2 -) during the crystal formation. The lability of the silver-donor atom bonds allow furthermore to build totally reversible complexes, so that the process of coordination polymer formation is totally reversible.

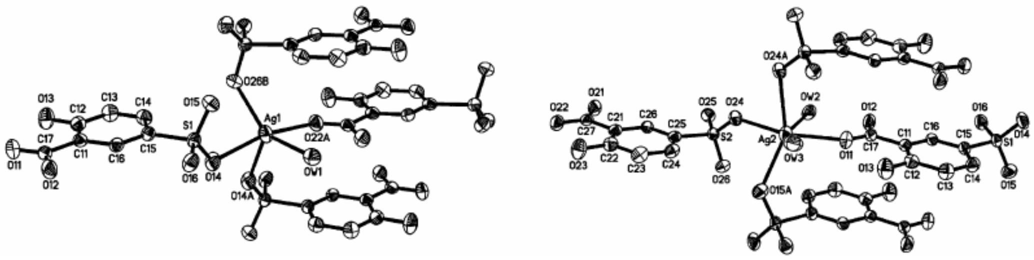

Figure A-60: five- and six-coordinated Ag in $\{[Ag_2(HL)_2(H_2O)_3]\cdot H_2O\}_n$ (H_2L = 5-sulfosalicylic acid)

V.6 - Cu^{II}

The Cu^{II} ion has a more rigid coordination sphere: octahedral [49, 212-215] (Figure A-61a), square pyramidal [27, 213, 216] (Figure A-61b), square planar [217], tetrahedral [218] (Figure A-61c), trigonal bipyramidal [164, 219] (Figure A-61d) or a mixed geometry in the same compound [86] can be found in the Cu^{II} coordination polymers.

In these examples, the coordination sphere of Cu^{II} is usually occupied with two to four N-donors groups, the other position being occupied with counter anions, water molecules or other organic molecules. More ligands around the copper ion are found in the cases of bifunctional ligands (for instance pyridine/carboxylate groups), the copper cations being coordinated with both ligand functions [216].

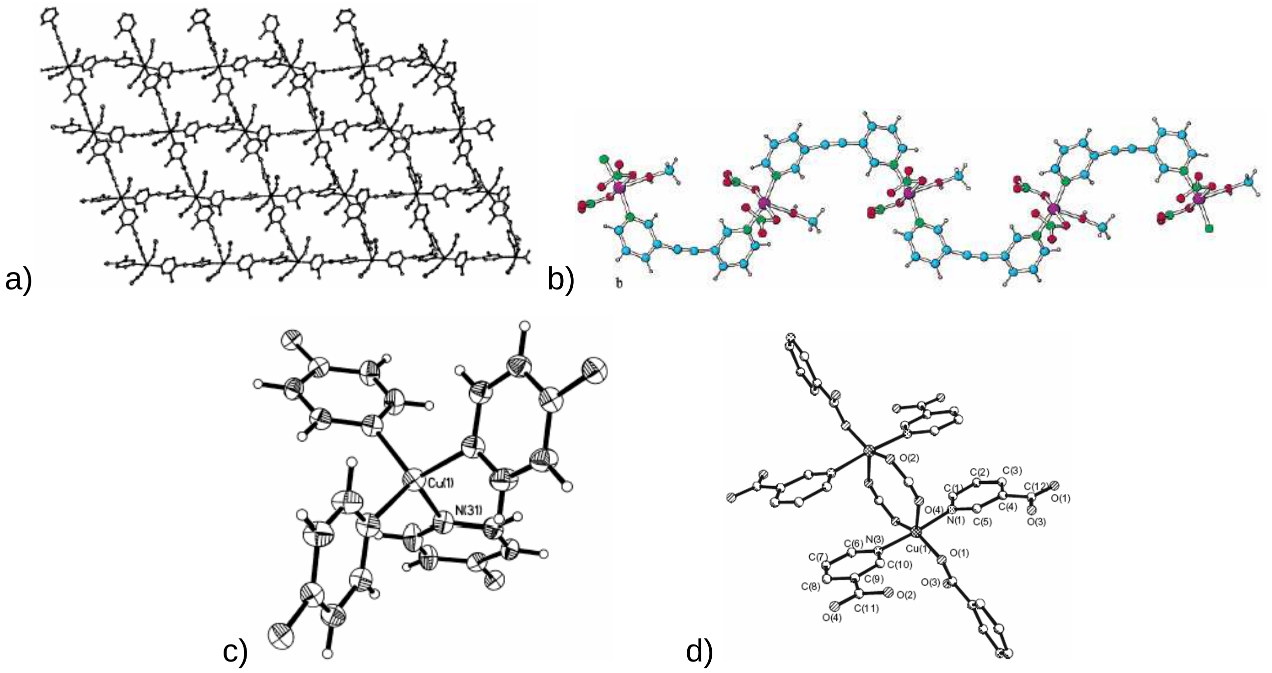

Figure A-61: several motif built up with a) octahedral [214] b) (pseudo-) square pyramidal [27] c) tetrahedral [218] or d) trigonal [164] Cu^{II} centres

Polymeric complexes featuring paramagnetic transition metal ions such as Cu^{II} are of great importance for the development of magnetic materials such as molecule-based magnets [67] (see also the chapter about magnetism).

V.7 - Aim of the thesis

The aim of this thesis is first to optimize the synthesis of the ligand in order to improve its availability, and, secondly to use it for the synthesis of coordination polymers with Cu^{I}, Ag^{I} and Cu^{II}. The strategies are the use of d^{10} metals to investigate the driving interactions during the coordination polymer building (The higher the flexibility of the building blocks, the more subtle the role of weak interactions, inclusion molecules-templating effects-.), the possibility of constructing mixed metal compounds and the use of Cu^{II} to study the behavior of **L** toward a less flexible cation and to make the construction of magnetic materials possible. The influence of the experimental conditions such as solvents, temperature and counter ions as well as the ligand conformation in the formed polymeric structures will be studied in the contest of crystal engineering.

B - Results and discussion

I - Ligand

I.1 - Two synthetic pathways

Synthetic pathways for **L** were described in the literature before [220-222], but did not give satisfactory yields. We therefore optimized the synthesis using either of the following reactions:

- *Reaction 1* (Equation B-1) Thionylchloride is carefully added to a stirred mixture of isonicotinic acid and DMF. After gas evolution (exothermic reaction with temperature increase from room temperature to 40°C), the solution is stirred for about 12 hours. Excess thionylchloride is then removed *in vacuo*. Dried ethylene glycol in stoechiometric ratio (1:2) is added to the isonicotinic acid chloride. The reaction is exothermic; after gas evolution, the mixture is heated to 150°C for a few hours to yield a white solid. The latter is then dissolved in a large amount of water, then NH_4OH is added. The white precipitate is filtered off and recrystallized from ethyl acetate.

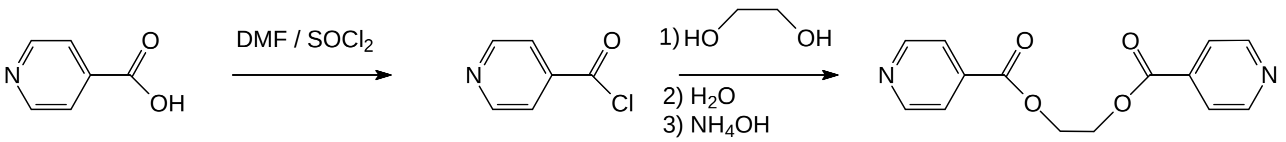

Equation B-1

- *Reaction 2* (Equation B-2) Ethylene glycol is added to isonicotinic acid in dichloromethane in stoechiometric ratio (1:2). A solution of 1,3-Dimethyl-2-chloroimidazolium chloride (DMC) in dichloromethane is added dropwise to the mixture. After a few minutes of stirring, pyridine as solvent is added in order to dissolve the crude solid white product. The reaction is refluxed for 2 hours and turns from yellow to dark yellow with the precipitation of a dark solid. The product remains in the liquid phase and is evaporated. It is then dissolved in dichloromethane and purified on a chromatography column with hexane:ethyl acetate (4:1) and ethyl acetate as eluents.

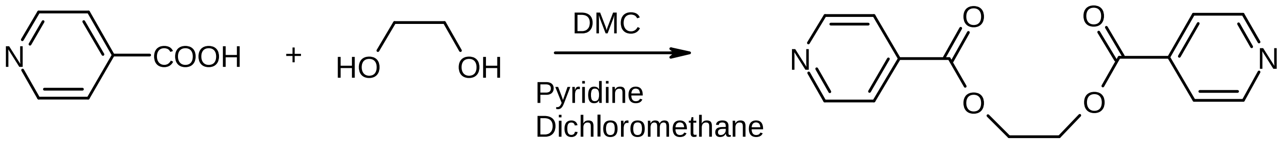

Equation B-2

I.2 - Crystallographic structure

Recrystallizing the crude product from ethyl acetate yields single crystals of **L**. **L** crystallizes in the monoclinic space group *P*2_1/*c* (no.14) with two molecules (four asymmetric units) per unit cell. The asymmetric unit consists of half a molecule as an inversion center is found in the geometrical middle of **L**; that is between C7 and C7$^{\#1}$. (Figure B-1) The most important distances and angles are given in Table B-1.

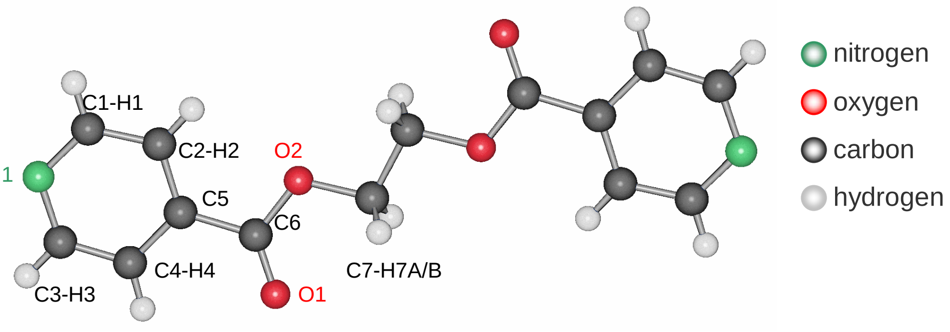

Figure B-1: Molecular structure of the ligand L (Color codes given for all following figures.)

Within a molecule the two pyridine rings lie therefore in parallel planes that are at a distance of *ca*. 0.01 Å to each other. The carbonyl groups of a ligand molecule are in *anti*-arrangement to each other, and the ethyl group is in a staggered conformation, featuring a dihedral angle of ca. 60°. The mean plane of the pyridine ring forms an angle of 4.56(3)° to the plane through C6, O1 and O2 of the neighbouring ester function.

In the crystal the molecules lie parallel to each other with a distance of 3.468(4) Å, allowing thus a π-stacking contribution between the pyridine ring of one ligand and the ester group of the adjacent ligand. (Figure B-2)

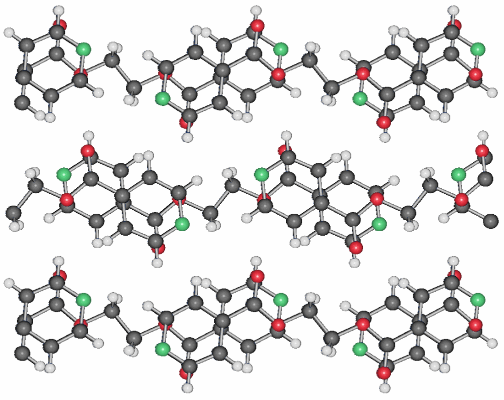

Figure B-2: packing in L and arrangement of the ligand molecules in chains and layers

In addition, several different hydrogen bonding motifs can be found in the structure. The corresponding bond lengths are given in Table B-2. Inter-molecularly the nitrogen atoms of the pyridine ring and the protons H3 of the pyridine ring of two ligand molecules lying in the same plane form a six-membered H-bonded ring involving C3, H3 and N1 and leading to chains of ligands. Complementary to the π-stacking, inter-chain hydrogen bonding occurs between O1 and H4 or H7B and between N1 and H7A of two parallel chains leading to sheets (Figure B-3a). H-bonding is also observed between the sheets involving O1 and the hydrogen atoms of C7[#1] of the ethyl group as well as H4 of a pyridine ring. (Figure B-3b) The chains are thus interconnected to each other, perpendicular to the chain propagation. Similar hydrogen bonds (C-H···N) have been used throughout the literature in order to engineer organic assemblies between structurally compatible H-bond donors and acceptors, leading to very stable supramolecular constructions. [223-225]

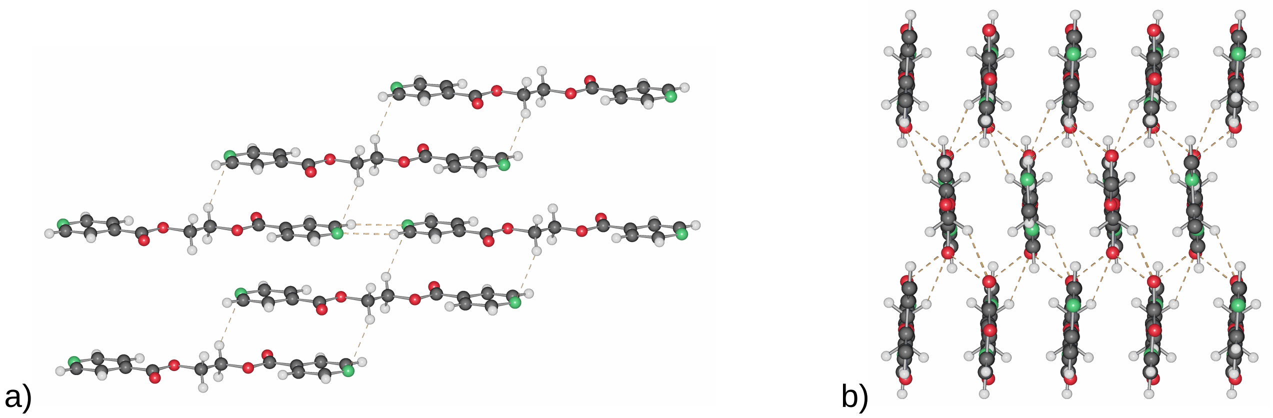

Figure B-3: H-bonds in L a) inter-layers; b) between the sheets

Table B-1: Most important bond lengths (Å) and angles (°) in L

C-N	1.343(2), 1.332(2)	C-N-C	116.8(1)

Table B-2: Hydrogen bond data for L [lengths (Å) and angles (°)]

D-H···A	*d*(D-H)	*d*(H···A)	*d*(D···A)	Angle D-H···A
C3-H3···N1[#1]	0.93	2.76	3.598(2)	151.2
C7-H7A···N1[#2]	0.97	2.85	3.571(2)	132.3
C4-H4···O1[#3]	0.93	2.72	3.252(2)	117.3
C7-H7B···O1[#4]	0.97	2.90	3.686(2)	139.2

Symmetry transformations used to generate equivalent atoms: #1 -X+1, -Y+2, -Z+1; #2 -X, -Y+2, -Z; #3 X, -Y+3/2, Z+1/2; #4 X, -Y+3/2, Z-1/2.

II - Cu^I coordination polymers

Our first attempts to make coordination polymers with the ligand ethanediyl bis(isonicotinate) was by using Cu^I metal compounds, *i.e.* CuCl.

II.1 - Preparation

CuCl was directly reacted with **L** in different solvents and proportions, leading to mostly orange insoluble powders of variable composition. (Table B-3) It was only possible with elemental analysis to find hints as to the composition of the precipitates, showing large excess of CuCl in some cases. The large amount of CuCl may be explained by the presence of mixtures of several compounds and/or compounds containing Cu_xCl_x clusters and polymers. Single crystals were obtained only in one case, for the reaction with the proportion metal to **L** 1:2 in acetonitrile, where yellow-orange crystals {[CuCl(**L**)]}$_n$, **1**, were obtained in very low yield.

Table B-3: Resume of the reaction L/CuCl with the reaction stoechiometry, the experimental conditions, the products and their apparition speeds

M: L	solvent		Experiment	Time	Product
	L	CuCl			
1:2	Dry THF	Dry ether	Direct reaction	Inst.	Orange precipitate: {Cu_4Cl_4(**L**)}
4:1	Dry THF	Dry ether	Direct reaction	Inst.	Orange precipitate: {Cu_8Cl_8(**L**)}
1:2	Dry THF	Dry THF	Direct reaction	Inst.	Orange precipitate: {$Cu_{23}Cl_{23}$(**L**)(THF)}
1:2	Dry CH_3CN	Dry CH_3CN	Direct reaction	3 months	Yellow-orange crystals: {CuCl(**L**)}
1:2	Dry THF	Dry CH_3CN	"U-shaped" tube	Few days	Red crystals: {CuCl(**L**)$(THF)_{0.5}$}
1:1	Dry THF	Dry CH_3CN	Direct reaction	2 H	Red crystals: {CuCl(**L**)$(THF)_{0.5}$}

At the same time, we started to use another strategy to get single crystals in a "U-shaped" tube (Figure B-4): a solution of CuCl in dry acetonitrile was introduced in one arm of the tube and a solution of **L** in dry THF in the other (proportion M:L = 1:2). The solutions were thus allowed to slowly diffuse into each other through a fritt. The same experiment was made, but this time with frozen THF as separator between the two solutions. After warming, the two solutions diffuse through the THF. In both cases, red crystals of {[CuCl(**L**)]·0.5THF}$_n$ **2** appear after a couple of days. The red crystals were suitable for single crystal X-rays diffraction.

Taking account of these two results (proportions metal to ligand of 1:1 in the final compound and incorporation of THF molecules into one of the structures), direct self-assembly of the **L** and CuCl was tested. We found that a mixture of **L** in dry THF and CuCl in dry acetonitrile in the proportion 1:1 and with the adequate concentration of 7.10^{-3}

mol.L^{-1} allows us to obtain the red crystals **2** within two hours. An important observation was finally made: if these red crystals of **2** stay for several weeks in the mother liquor, they transform into the yellow-orange ones of **1**. When isolated from the mother liquor, **2** is stable staying in air, although it contains unstable Cu^{I}.

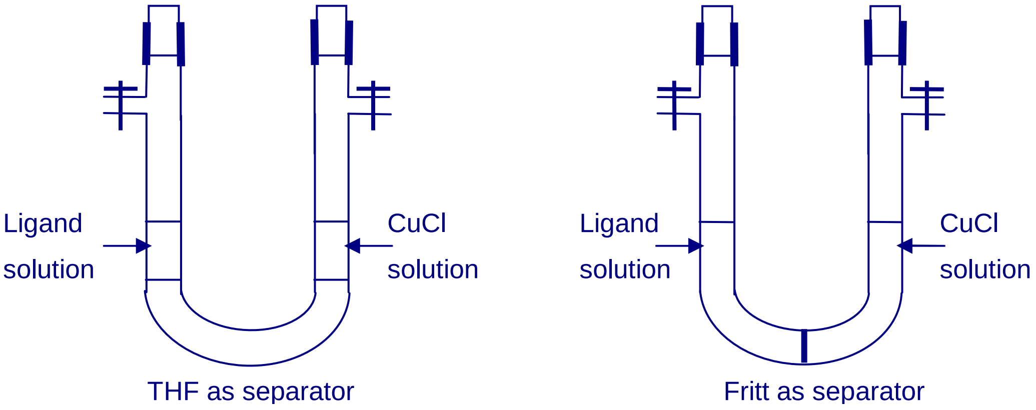

Figure B-4: "U-tube"

Both compounds were characterized in the solid-state (single crystal X-rays diffraction). Further characterization in the solid-state (elementary analysis, IR) was only possible for **2**, because of the low yield of **1** and its poor stability in air. Electrospray-ionization mass spectroscopy was also performed with a solution of **2** in dichloromethane, and the oligomeric fragments $[\mathrm{Cu}\mathbf{L}]^+$; $[\mathrm{Cu}\mathbf{L}_2]^+$; $[\mathrm{CuCl}\mathbf{L}\mathrm{H}]^+$; $[\mathrm{Cu_3Cl_2}\mathbf{L}]^+$ and $[\mathrm{Cu_4Cl_4}\mathbf{L}\mathrm{H}]^+$ were found. The absorption wavelengths for **2** are 211 and 274 nm. Emission (solid state) is only observed when **2** is excited at 240 nm (see experimental part). The emission spectra of **2** features almost unshifted bands compared to **L** but enhancement of bands. Mechanisms of absorption and emission are similar in both compounds and characteristic for the ligand.

II.2 - Structure description

II.2.a - {[CuCl(L)]}$_n$ 1

{[CuCl(**L**)]}$_n$ **1** crystallizes in the monoclinic space group *C*2/*c* (no.15). The asymmetric unit consists of one half of a ligand molecule, one copper cation (50% occupation) and one chloride anion (50% occupation). (Figure B-5) There are four asymmetric units and thus two [CuCl(**L**)] moieties per unit cell. The most important distances and angles for **1** are reported in Table B-4. (The complete list can be found in the crystallographic data part.)

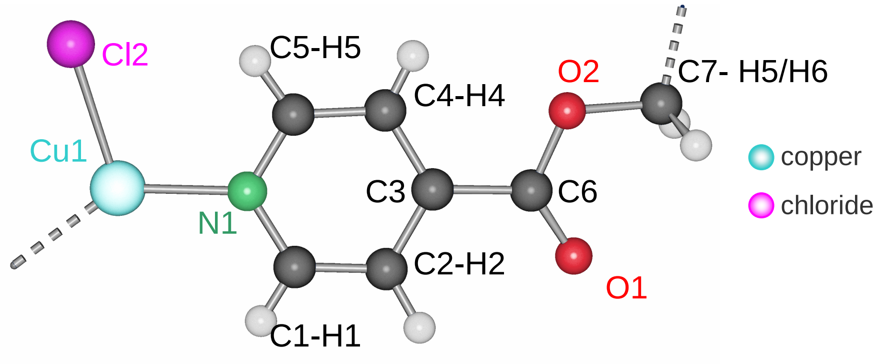

Figure B-5: asymmetric unit in 1 (Colors codes given for all following figures)

Compound **1** forms one-dimensional chains of copper atoms linked *via* the ligand, the latter coordinating through the nitrogen donor atoms. (Figure B-6) The distance between to copper atoms within one chain is 17.2(1) Å. The copper ion, having a trigonal planar arrangement of ligands (angle sum = 360°), is coordinated by two nitrogen atoms of two different ligands and a chloride. The Cu-N bonds are identical due to symmetry and are 1.955(3) Å long. The anion is bonded to the metal cation with a distance of 2.309(1) Å. This leads to an overall neutral one-dimensional coordination polymer. The copper atom as well as the chloride ion of a repeating unit are found on a crystallographic two fold axis (0, *y*, ¼ (e)). Additionally, an inversion center can be found in the geometrical middle of the C7-C7$^{\#1}$ bond of **L**. Each pyridine ring of one ligand molecule is therefore parallel to its symmetrical equivalent, in planes that are 0.30(1) Å apart.

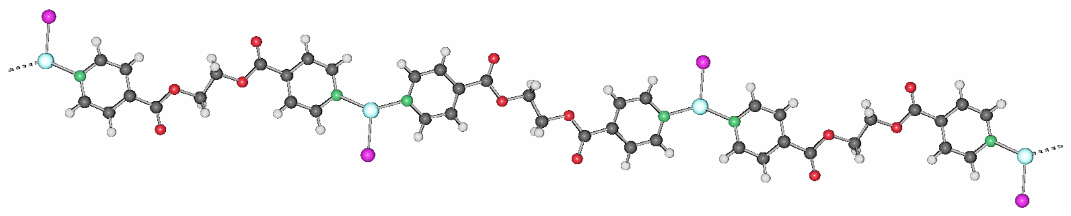

Figure B-6: One-dimensional chain in 1

The pyridine units are in *anti* position of the ethyl linking units that are staggered with a torsion angle of ~60°, with the two carbonyl groups pointing alternatingly up and down. The conformation of the ligand in this compound is thus the same as in the crystalline free ligand **L**. Compared to **L**, the N-C bonds are slightly elongated by 0.01-0.02 Å, the other distances and angles in the pyridine ring are similar on average.

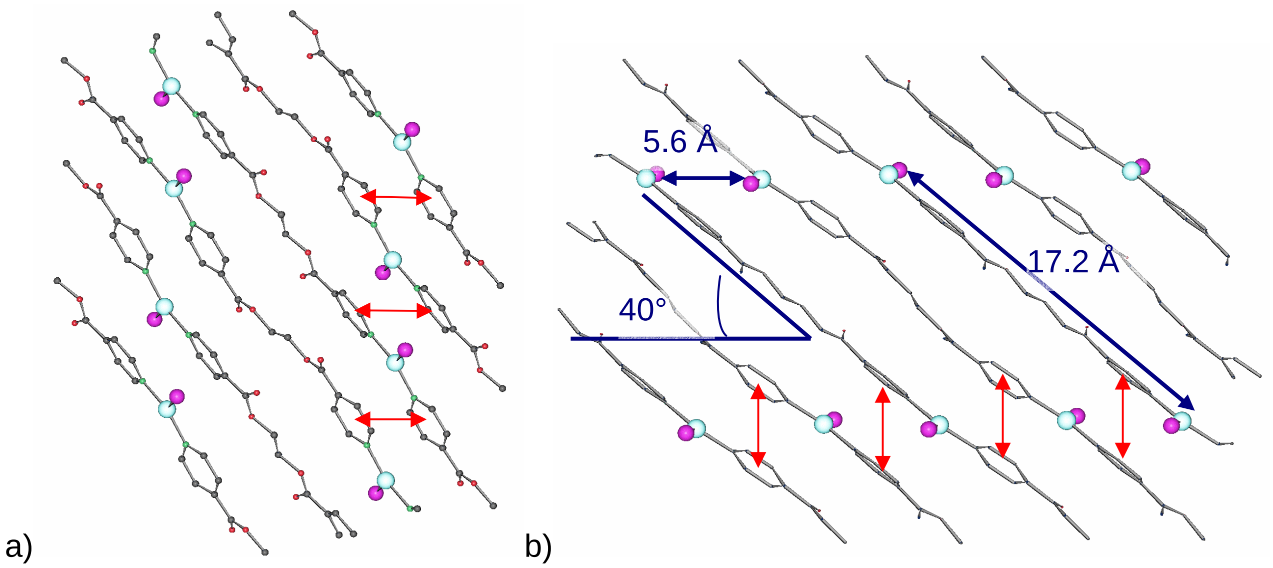

Figure B-7: a) view of the inter-chains π-stacking leading to the twist between the pyridine plans on each part of one copper atom in 1; b) View of the chains-sheet in 1 (Hydrogen atoms omitted for clarity)

Whereas the two pyridine rings within one ligand are parallel, they are tilted by 12.4(1)° to each other from one ligand to the next within a chain. This is due to the π-stacking influence in the packing, where one pyridine unit of the ligand stacks with the ring of another chain on one side, whereas the second pyridine unit is packed parallel to the ring of a chain on the opposite side. (Figure B-7) The π-stacked rings are not fully superposed, the nitrogen atom of one being over the middle of the neighbour ring (offset of 2.168 Å), but the shortest distance between the mean planes of the two pyridine ring is 3.247 Å (Table B-6). These π-π interactions lead to the formation of sheets constituted of the stacked chains.

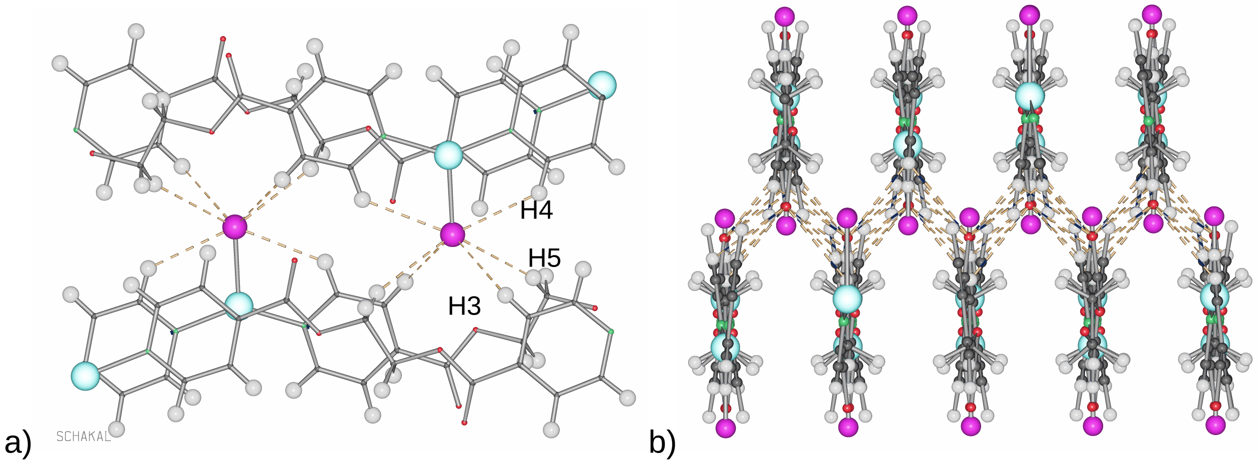

Figure B-8: View of the inter-sheet H-bonds between a) the chloride atom and protons of ligand molecules and b) between the ligand molecules in 1

Another influence on the overall arrangement is the formation of six weak H-bonds between the chloride atom and protons of **L** surrounding the anion. These interactions are part of the linking forces between the sheets. Four contacts are found between the H3 of a pyridine unit and H5 of the ethyl group and their symmetry equivalents of the two closest neighbour chains, with distances of 2.81(5) (H5) and 2.88(6) (H3). The shortest contact Cl-H is the one with H4 (2.80(5) Å) and its symmetrical equivalent, which belongs to pyridine units bonded to the same copper atom than the anion. (Figure B-8a) The chloride ion has thus a trigonal prismatic hydrogen coordination environment. Even though the contacts are rather long [226], the electrostatic attractive forces might still play a role in the formation of a structure, since it is usually the sum of all weak forces that contribute to a supramolecular array.

Furthermore O1 has contacts with four pyridine H-atoms, H3, H4, as well as H1 of two different ligand molecules (2.76(5), 2.95(4), 2.65(5) and 2.85(5) Å respectively). This inter-chain hydrogen-bonding strengthens the interconnection between the layers of chains. (Figure B-8b)

The structure can also be described as layers of copper atoms that are linked diagonally via ligands at approximately 40° as shown on Figure B-7b. The distances between the copper atoms within these layers are 5.6 Å and the ones between two adjacent layers are *ca*. 17.2 Å.

Table B-4: Most important bond lengths (Å) and angles (°) in 1

Cu-Cl	2.309(1)		
Cu-N	1.955(3)	N-Cu-N	141.6(2)
C-N	1.350(4), 1.352(4)	C-N-C	116.9(3)

Table B-5: Hydrogen bond data for 1 [lengths (Å) and angles (°)]

D-H···A	*d*(D-H)	*d*(H···A)	*d*(D···A)	Angle D-H···A
CH···O Hydrogen interactions				
C4-H3···O1[#1]	0.92(6)	2.76(5)	3.248(4)	114(4)
C5-H4···O1[#1]	1.00(4)	2.95(4)	3.353(4)	105(3)
C1-H1···O1[#2]	0.96(5)	2.85(5)	3.506(4)	126(3)
C1-H1···O1[#3]	0.96(5)	2.65(5)	3.533(4)	152(4)
CH···Cl Hydrogen interactions				
C5-H4···Cl2	1.00(4)	2.80(5)	3.533(4)	131(3)
C7-H5···Cl2[#4]	1.06(4)	2.81(5)	3.716(4)	143(3)
C4-H4···Cl2[#5]	0.92(6)	2.88(6)	3.670(4)	145(4)

Symmetry transformations used to generate equivalent atoms: #1 -X-1/2, Y+1/2, -Z+1/2; #2 -X-1/2, -Y-1/2, -Z; #3 X+1/2, -Y-1/2, -Z+1/2; #4 X-1/2, Y-1/2, Z-1; #5 X-1/2, -Y+1/2, -Z.

Table B-6: π-π interactions lengths (Å) and angles (°) in 1 (definition of parameters given in A -I.2 -)

π-π interactions	d_{R-R}	pd_{R-R}	β	α
Ring (N1, C1, C2, C3, C4, C5)··· Ring (N1, C1, C2, C3, C4, C5)#1	3.90	3.247	33.7	0
Symmetry transformations used to generate equivalent atoms: #1 -X, -Y, -Z.				

No analogous structure is known from literature with Cu^I having a trigonal planar environment and Cl anions being terminal. Similar supramolecular compounds with trigonal arrangement around the copper atoms are also scarce. [199] **1** may best be compared to $\{[Cu(4,7\text{-phenanthroline})(MeCN)]BF_4\}_n$, where the chloride has formally been replaced by MeCN and the ligand **L** by 4,7-phenanthroline [227]. The literature compound has all MeCN groups oriented to one side only of the chain, whereas in **1** the anions are arranged alternatingly up and down along the chain. In addition, the literature compound is charged, the anions not being bonded to the metal ion, while compound **1** is neutral. The distances Cu-N are however in the same order of magnitude in the two compounds. It is interesting to compare the angles at the copper ion. In **1**, the N-Cu-N angles are rather large with 141.6(2)° compared to 107° in the literature compound. The N-Cu-Cl angles in **1** are 109.2° and smaller than the corresponding ones in the literature compound (131 and 122°). This can be explained by the different ligands used in the two compounds. A second example of coordination polymer with trigonal Cu^I is presented by Xiong and *al*. [200]: the chain is also charged with *N*,*N*-(2-pyridyl)(4-pyridylmethyl)amine as bridging ligand and triphenylphosphine as terminal ligand, the counter anions being perchlorate.

II.2.b - $\{[CuCl(L)]\cdot 0.5THF\}_n$ 2

$\{[CuCl(\mathbf{L})]\cdot 0.5THF\}_n$ **2** crystallizes in the triclinic space group *P*-1 (no.2). Apart from the solvent molecule in the chemical formula, it seems in principle to be the same compound as **1**. However, not only colour, but also the structure of **2** differs dramatically from **1**. The most important distances and angles for **2** are listed in Table B-7.

The asymmetric unit consists of one ligand molecule, one copper atom, one chloride atom and one half of a THF molecule. A one-dimensional compound is now obtained by repeating units of copper atoms that are, two by two, alternatingly bridged by two chloride anions and two ligands, respectively. (Figure B-9) Each copper cation is therefore tetrahedrally coordinated by two N-atoms of two different ligand molecules and two chloride ions. The Cu-N distances are with 1.998(2) and 2.033(3) Å slightly longer than in **1**. This is due to the higher coordination number of the copper atoms with four in **2** than in **1** where it is three, which is also reflected in shorter N-C bonds in the pyridine ring in **2** than in **1**. The N-C bonds in **2** are thus in the same range than the ones in **L**, with a difference of less than 0.01 Å. The Cu-Cl bonds are very asymmetric with 2.3255(9) and 2.546(1) Å. The shorter Cu-Cl bond is only by 0.025 Å longer than the terminal Cu-Cl in **1**, indicating that the Cu(μ-Cl)$_2$Cu unit might be interpreted as a dimer of two Cu-Cl fragments. The plane through the copper atom and the two anions forms an angle of 89.53(6)° with the plane formed by the copper atom and the two bonded nitrogen atoms. The N-Cu-N angle is 122.9(1)° wide, the Cl-Cu-Cl angle amounts to 109.74(3)°, whereas N-Cu-Cl angles are 119.10(8) and 104.50(8)° wide, resulting in a distorted tetrahedral environment for the cation.

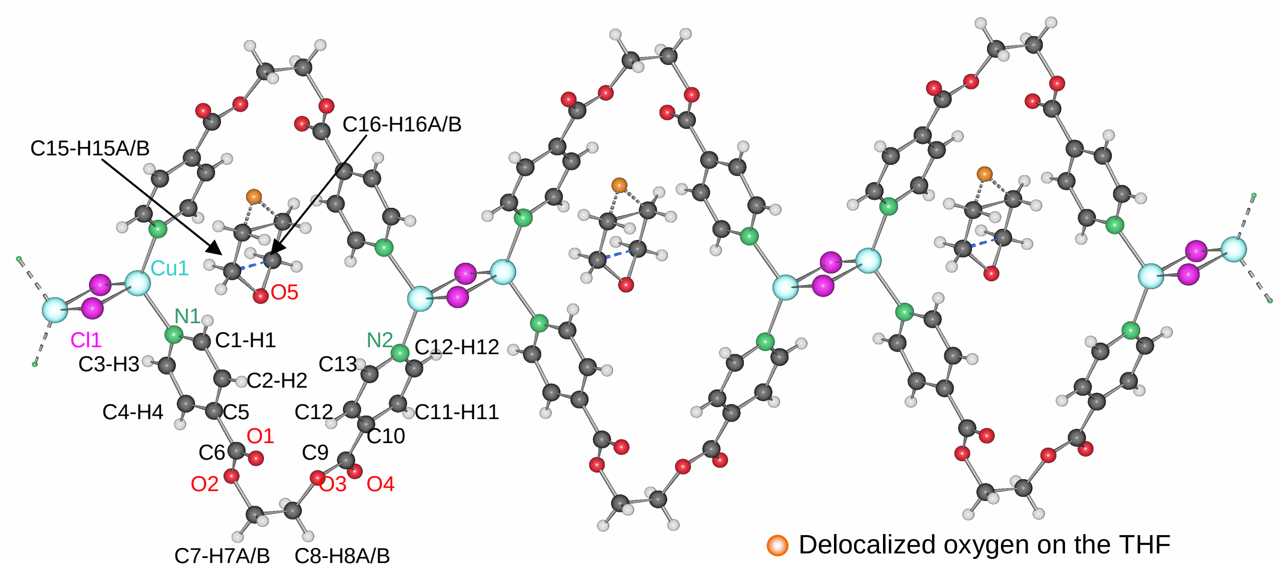

Figure B-9: View of the one-dimensional double chain in 2 showing the disorder of the THF molecule

An inversion centre is situated in the geometrical middle of the Cu(μ-Cl)$_2$Cu ring as well as in the centre of the Cu(μ-**L**)$_2$Cu unit. The Cu–Cu distance between the two chloride-bridged metal ions is with 2.809(1) Å rather short compared to what is known from literature [201] and is similar to the sum of the Cu^{I} Van der Waals radii (2.8 Å).

The emission spectrum of **2** shows more intense emission bands than **L**, with a blue-shift of the band at 409 nm (**L**) to 385 nm (**2**). The existence of Cu^{I}-Cu^{I} interactions in Cu$_2$X$_2$ cores is controversly discussed [228-230]: a two-dimensional coordination polymer sheet based on Cu$_2$I$_2$ cores linked with 4,4'-bipyridylsulfide has an enhanced emission intensity towards the ligand in addition to a red-shift of the emission maximum (both ligand and complex are excited at the same wavelengths) [72]. This phenomenon is attributed to cluster centred, a mixture of halide to copper charge transfer and metal centred d to s excited states. The Cu-Cu distances (2.647(1) Å) also support the cluster centred emission. In such complexes, low energy LMCT and MLCT transitions exist which can also mix with intraligand transitions, which adds more complexicity to the assignment. In **2**, where the Cu-Cu distance is longer (of about 0.15 Å), we observe the same differences between the emission spectra of **L** and **2** (see experimental part).

The Cu(μ-**L**)$_2$Cu ring forms a cavity with a diameter of approximately 5 Å, the corresponding copper atoms being separated by 9.167(7) Å. This much shorter Cu–Cu distance than in **1** is due to the ligand conformation. The ligand has no longer a linear form with the isonicotinic groups in an *anti* conformation, but adopts a U-shape. The ethyl unit is still staggered, but the ester groups are now arranged *syn* to each other. The pyridine rings within a ligand molecule form an angle of 40.5° to each other. The planes of the ester groups are tilted by 7.4(2) and 11.1(4)°, respectively, to the plane of the neighbour pyridine ring.

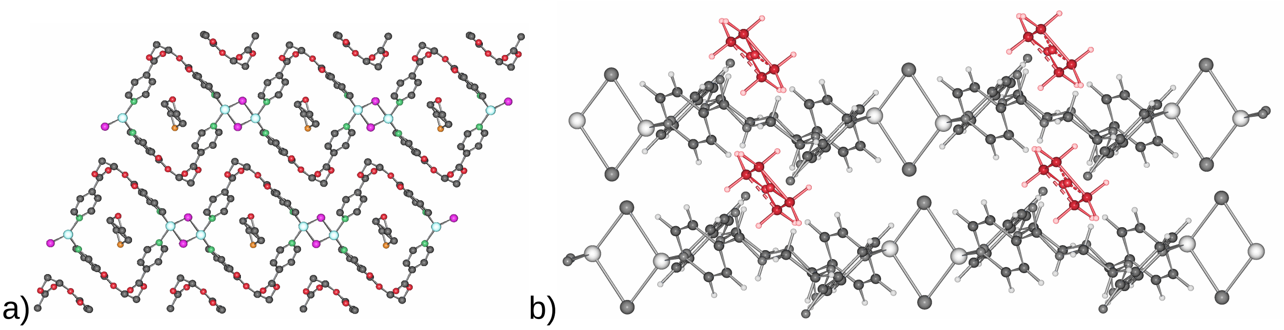

Figure B-10: View of the alignment of the chains in 2: b) View along the cavities containing the THF molecules; a) View of the stacking of the chains with the THF molecules in between the chains

The so-formed chains are stacked on top of each other so that the cavities in the centre of the Cu(μ-**L**)$_2$Cu rings form channels in which the disordered solvent molecules (THF) are located. (Figure B-10a) The THF molecules are however not exactly in the middle of the Cu(μ-**L**)$_2$Cu unit, or, otherwise described, in the same plane as the copper atoms and the two ligand molecules, but are placed in between the chains. (Figure B-10b) Due to the presence of an inversion centre, the oxygen atom of the THF molecule is placed on two positions. So apparently, the presence of the THF molecules *i)* keeps the chains apart from each other, and *ii)* therefore, no π-stacking is observed in **2**.

However, hydrogen bonding can be observed between C–H and oxygen atoms of the ligand or solvent molecules. The H-bonding is shown on Figure B-11a, the bond lengths being cited in Table B-8. In addition to this type of H-bonding, close contacts are also found between H-atoms and chloride ions. This H-bonding motif in **2** is based on the chloride atom and H-atoms vicinal to the nitrogen atom of the pyridine rings, so no ethyl-groups are involved as in compound **1** (Figure B-11b).

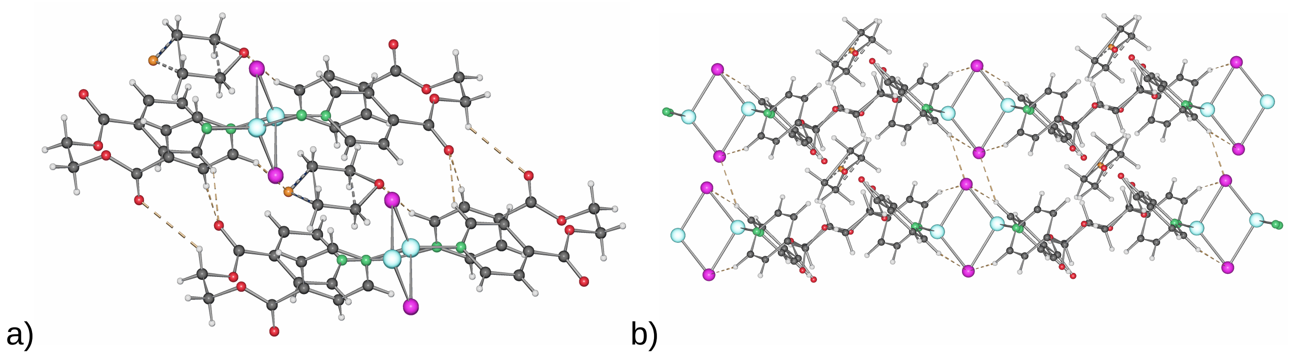

Figure B-11: H-bonding network in 2: a) C-H···O between two chains (view parallel to the chains); b) C-H···Cl between the chains (view of perpendicular the channels)

Apparently, the presence of solvent in the structure also influences the conformation of the ligand. **2** slowly transforms into **1** when the crystals remain in the mother liquor, giving rise to the assumption that **1** is the thermodynamically more stable product obtained by diffusion of THF out of the structure and following reorganisation. Indeed, during the transformation, ‘‘zwitter’’ crystals are observed that possess a red core (**2**) surrounded by bushes of yellow crystals (**1**). Unfortunately, we could not take pictures of this process as the crystals were difficult to focus on in the mother solution, and crystals deteriorate after a while when taken out of solution and exposed to air. The poor stability of this compound can perhaps be due to the coordination number of Cu^{I} in **1**.

Table B-7: Most important bond lengths (Å) and angles (°) in 2

Cu-Cu	2.809(1)		
Cu-Cl	2.3251(9)	Cu-Cl-Cu	70.25(3)
	2.547(1)	Cl-Cu-Cl	109.75(3)
Cu-N	1.998(2), 2.033(3)	N-Cu-N	122.9(1)
C-N	1.342(4), 1.348(4)	C-N-C	117.0(2)
	1.343(3), 1.347(4)		116.6(3)

Table B-8: Hydrogen bond data for 2 [lengths (Å) and angles(°)]

D-H···A	*d*(D-H)	*d*(H···A)	*d*(D···A)	Angle D-H···A
C-H···O Hydrogen interactions				
C8-H8A···O4	0.97	2.31	2.708(4)	103.4
C4-H4···O4	0.93	2.75	3.648(4)	162.2
C14-H14···O5	0.93	2.45	3.239(6)	142.1
C3-H3···O1$^{\#1}$	0.93	2.49	3.272(4)	141.8
C13-H13···O1$^{\#2}$	0.93	2.82	3.737(5)	167.4
C7-H7A···O4$^{\#3}$	0.97	2.87	3.579(4)	130.7
C-H···Cl Hydrogen interactions				
C1-H1···Cl2	0.93	2.82	3.487(3)	129.4
C12-H12···Cl2$^{\#1}$	0.93	2.94	3.653(3)	134.3
C12-H12···Cl2$^{\#5}$	0.93	2.93	3.540(3)	124.3

Symmetry transformations used to generate equivalent atoms: #1 X+1, Y, Z; #2 –X, -Y+1, -Z+1; #3 X-1, Y, Z; #4 X-1, Y-1, Z-1; #5 –X+1, -Y+1, -Z+2.

Some examples of coordination polymers involving Cu^{I} cations with a tetrahedral environment, pyridine or similar nitrogen donor ligands [146, 231] and halide counter-anions can be found in the literature. [143, 147, 202, 203] In the latter three compounds, $Cu_2(\mu\text{-}Cl)_2$ cores in double chains or molecules are present. The distances Cu-N usually range from 1.90 to 2.10 Å. The distances in **2** are consistent with the literature data.

Batten and co-workers report on $\{[Cu(4,4'\text{-bipyridine})X]\}_n$ (X = Cl, Br, I) coordination polymers, one of them showing a similar $Cu_2(\mu\text{-}Cl)_2$ core. Each $Cu_2(\mu\text{-}Cl)_2$ core also coordinates four bipyridine ligands, and acts as a trigonal node of a two-dimensional net. The motif is thus a two-dimensional hexagonal sheet with larger cavities than in compound **2**, allowing interpenetration instead of solvent inclusion: each hexagonal ring is penetrated by three separate sheets. [143]

After we determined the structure of **2**, Song *et al*. published two Cu^{I} coordination polymers with the same ligand **L** but with bromide as counter ion: $\{[Cu_2(\mu\text{-}Br)_2(\mathbf{L})_2]\cdot 2H_2O\}_n$ and $\{[Cu_2(\mu\text{-}Br)_2(\mathbf{L})_2]\cdot 0.5THF\cdot 0.5H_2O\}_n$ [147]. The structure of these compounds is similar with to that of **2**, *i.e.* possesses a double chain motif. The distances Cu-Br and Cu-Cu are on average longer that in **2**, as expected for the larger bromine anions. These two compounds grew from acetone/DMSO or THF/DMSO systems, the solvents being used without further distillation. It is the reason why THF molecules but also water molecules are included in the structures by Song. The synthesis of **2** was therefore attempted using non dried solvents, but after only a few minutes, the oxidation of the mixture was observed, the solution turning green.

The same double chain motif as in **2** is found in the compound {[Cu(1,3-benzotriazolyl)propane)Cl]}$_n$ with two bridging chloride alternating with two bridging ligand molecules between the copper atoms along the chain [203]. The distances Cu-Cl are more symmetric than in **2** with 2.372(1) and 2.429(1) Å whereas the Cu-Cu distances in both compounds are similar. In this compound there are no cavities and thus no inclusion solvent molecules due to the shape of the ligand molecules. There is furthermore π-stacking between the chains, whereas the THF molecules avoid π-stacking in **2**.

II.3 - Ring opening process

Copper halides are known to form {Cu_xX_y}$_n$ polymeric and cluster structures [139, 141, 148, 204-208, 232]. Associated to organic ligands, these {Cu_xX_y}$_n$ polymers or part of them retain their structure and the ligands act as linkers between the {Cu_xX_y}$_n$ motifs, ranging from mononuclear species through dinuclear and tetranuclear discrete molecular moieties to polymeric structures (chains, ladder-like motifs... (Figure B-12) [139, 141, 148, 204-206, 232] or chains of clusters [207, 208]). The less sterically demanding the ligand is, the greater the complexity of the Cu^I halide architectures. In our crystalline compounds **1** and **2** on the other hand, such behaviour is not observed. This is apparently due to the sterically more important and more flexible ligand **L** compared for instance to the simply functionalised pyridine ligands described by Aakeröy *et al*. [205], or the dipyridyl cations used by Place *et al*. [208]. Another reason for the absence of {Cu_xX_y}$_n$ polymers is probably also the implication of the chloride ions in H-bonding as it occurs on our both compounds **1** and **2**. However the existence of such species containing {Cu_xX_y}$_n$ motifs in the orange powders obtained from the direct reaction of **L** and CuCl couldn't be proven. The presence of clusters could explain the high proportion of CuCl in the precipitates.

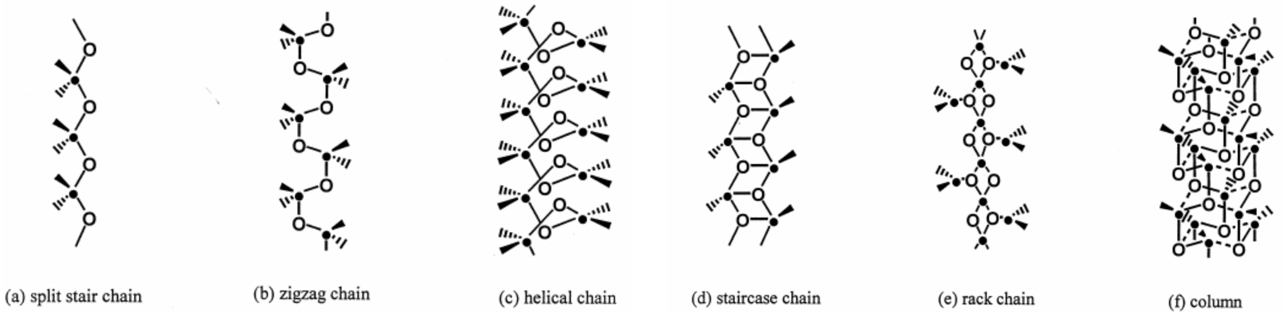

Figure B-12: Structural motifs observed for Cu^I halides based coordination polymers (filled circles = Cu; empty circles = Cl)

We are thus in presence of two pseudo-polymorphs built up from Cu^I cations, chloride counter-ions and **L** and eventually THF inclusion molecules as building blocks. As described above, it seems that compound **1** is formed out of compound **2** after several days in the mother liquor. How can this transformation be accounted for? Even though the transformation relies on severe rearrangements taking place in solution, one can propose at least a structural relationship. Structurally speaking, one has to formally cut one Cu-**L** bond (Figure B-13). The ligand would then bend over to the other side in order to adopt a stretched out *anti*-conformation and displace a chloride at the next copper atom. One Cu-Cl bond at each copper atom is thus formally cut as well, and the structure of **2** can thus be transformed into compound **1**. It is clear, that very probably the longer Cu-Cl contact of the two will be broken, considering that we have a dimerisation point in the Cu(μ-Cl)$_2$Cu ring and that the shorter Cu-Cl bond is similar to the one in **1**. Since the process takes place in solution and stops when the crystals are taken out of the mother liquor, the mechanism seems to be a solvent assisted one, as has been proposed for anion exchange in silver coordination compounds. [233]

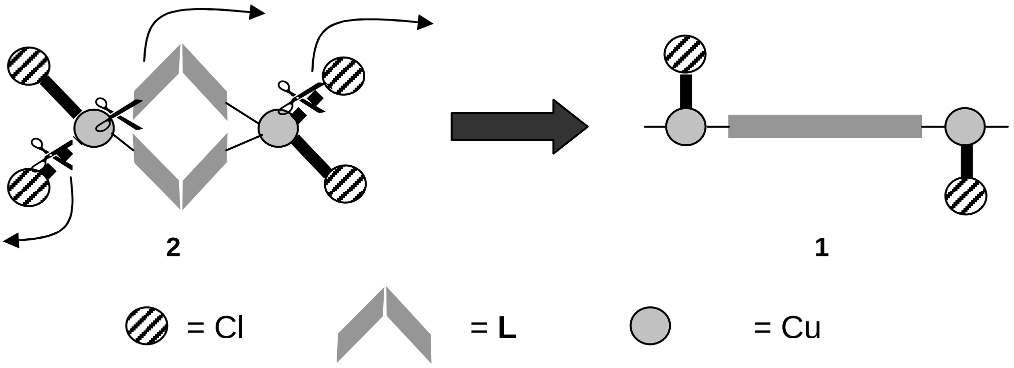

Figure B-13: Possible structural relationship between 2 and 1

James *et al.* reports ring-opening polymerisation, mostly transformations in solution: ligands and metal ions form rings or cages in solution, and coordination polymers crystallize from these solutions thanks to ring or cage opening. [234]

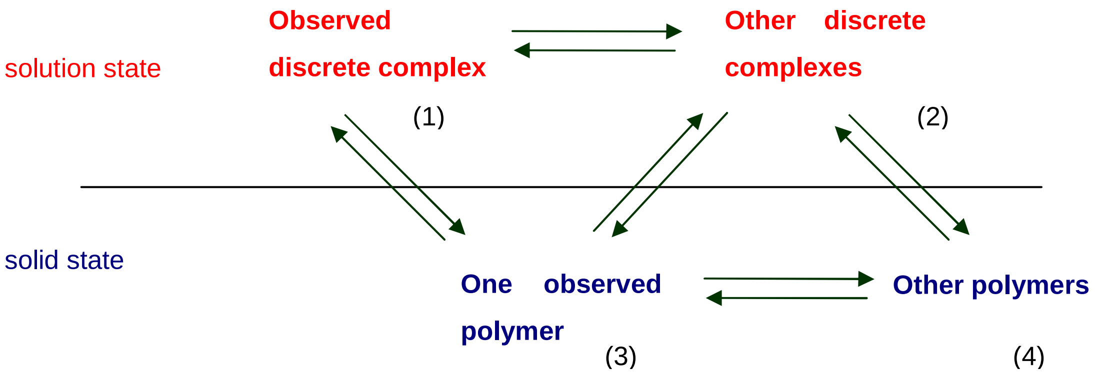

Figure B-14: potential equilibria involved in the formation of a coordination polymer

Ring opening polymerisations lead usually to kinetically stabilised compounds. In the case of coordination polymers, one has to remember that the formation of M-L bonds is always more or less reversible. It’s necessary to consider that the direct conversion of observed solution-based species into observed polymers (1 → 3) (Figure B-14) isn’t the unique pathway; indirect conversions can take place particularly between non-observed intermediates. [234, 235] In the case of the characterization of **1** and **2**, only discrete species such as $[\text{Cu}\mathbf{L}]^+$; $[\text{Cu}\mathbf{L}_2]^+$; $[\text{CuCl}\mathbf{L}\text{H}]^+$; $[\text{Cu}_3\text{Cl}_2\mathbf{L}]^+$ and $[\text{Cu}_4\text{Cl}_4\mathbf{L}\text{H}]^+$ species and two coordination polymers were observed as well as the solvent mediated reaction 3 → 4.

III - Ag^I coordination polymers

Ag^I was the second metal ion used to build coordination polymers and to study the influence on the architecture of crystallization conditions (solvent influence, counter anions influence, temperature, crystallization techniques). Darkness is required for the silver compounds because silver is light sensitive.

III.1 - Pseudo-polymorphism

Coordination polymer synthesis and crystallization based on **L** and $AgNO_3$ was first attempted in THF/water, using the "H-shaped" tube technique (Figure B-15). This method is convenient for making single crystals avoiding precipitation of insoluble powders: a solution of **L** in THF is introduced in one side of the tube, a solution of $AgNO_3$ in water being introduced on the other side. Both solutions are frozen and the diffusion solvent THF is added to connect both. The tube stays then at room temperature in darkness and diffusion can occur. Under these conditions, crystals of **{**[Ag(**L**)](NO_3)}$_n$ **3**, **{**[Ag(**L**)]$(NO_3)(H_2O)$}$_n$ **4** and **{**[Ag(**L**)]$(NO_3)(H_2O)_2$}$_n$ **5** are obtained in different sample, as well as a mixture of these compounds. The compounds **3**, **4** and **5** apparently only differ by the number of inclusion water molecules. Nevertheless their crystallographic structures are different (cf. the crystal descriptions below).

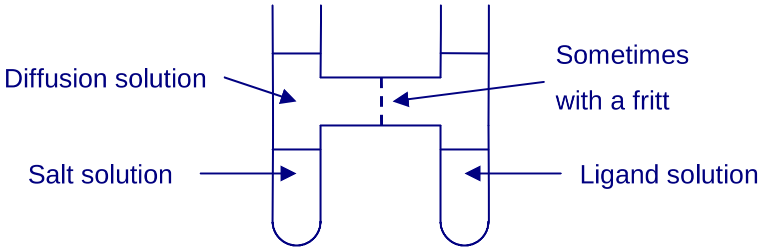

Figure B-15: "H-shaped" tube

Compound **3** is obtained purely by crystallisation from an **L**/$AgNO_3$ mixture in THF/water after slow evaporation of the solution. Elementary analysis for **3** shows a composition: Ag:NO_3:**L** of 1:1:1. TGA/SDTA (Thermo-Gravimetric Analysis/ Scanning Differential Thermal Analysis) measurements were performed on a sample of **3**. No loss/gain of weight and no phase transition before the decomposition of the product at 260°C are observed. The absorption bands of **3** in solution are found at 212 and 273 nm, the absorption spectrum is similar to the absorption spectrum of **L**. The luminescence spectrum is the same than the one for the ligand. The strongest emission occurs at 406 nm (409 nm for the ligand) when the sample is excited at 232 nm (234 nm for **L**), the measurement being done at 77K. The intensity in both spectra is similar.

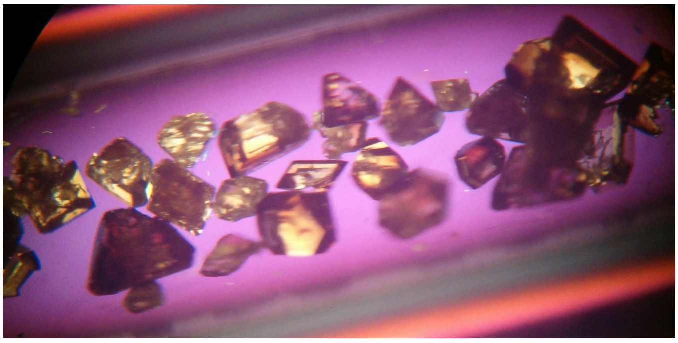

Picture B-1: crystals of 4

Compound **4** appears as major product in one batch (“H-shaped” tube). The characteristic crystal shape of **4** (Picture B-1) allows sorting them out under microscope light. The TGA/SDTA curve shows an exothermal loss of one water molecule at 117°C (loss of weight: 3.2%; calculated: 3.9%). Between the starting temperature and the water loss temperature, weight loss (3%) is also observed corresponding to adsorbed solvent as crystals are not fully dried before the measurement for maintaining the structure and the inclusion molecules. (Graph B-1) The loss of weight was calculated taking into account the sample weight after desadsorption of the solvent molecules. An error on the measure was estimated for the weight loss: 0.08(2) mg.

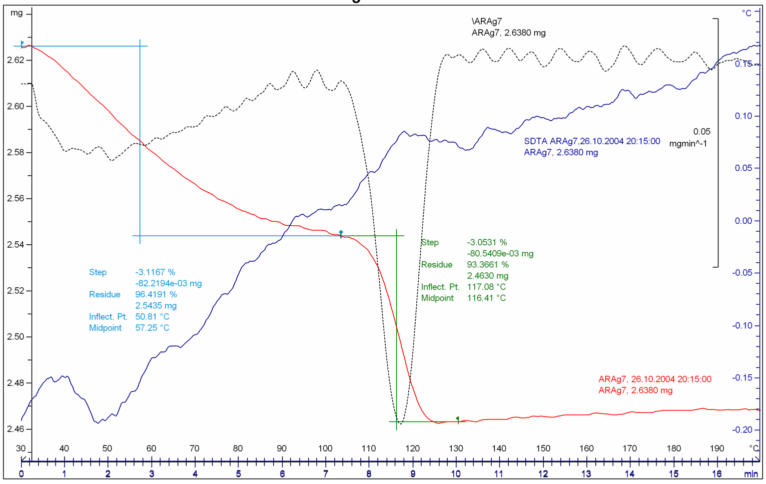

Graph B-1: DTA/SDTA analysis of 4: temperature ranged from 25 to 200°C.

Compound **4** shows no particular emission. Its emission spectrum (excitation at 230nm) looks like the one of **L** at 77K. The signal intensity is enhanced in the silver compound and particularly in the region of 350 nm. (Graph B-2) The luminescence may be assigned to intra-ligand transitions, as the excitation wavelengths are unchanged between **L** and **4** [24, 236]. The existence of the shoulder at 348 nm can be due to the stronger π-stacking in **4** than in **L** allowing charge delocalisation.

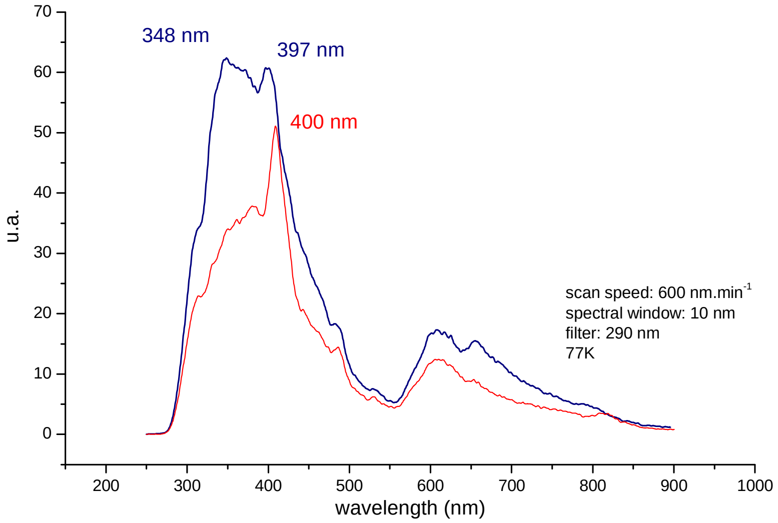

Graph B-2: luminescence spectra of L (red) and 4 (blue) collected a 77K

5 crystallizes in an "H-shaped" tube, but unfortunately it was not possible to isolate it in large amounts. Elementary analysis, IR measurement, TGA/SDTA analyses and luminescence measurement were performed in addition to single crystal X-rays diffraction. The luminescence signal of **5** is highly enhanced compared to **L** with similar excitation wavelengths. According to the TGA/SDTA measurement, an endothermal loss of two water molecules between 25 and 70°C (loss of weight: 7.44%; calculated: 7.52%) occurs. The compound decomposes at 220°C.

Further tests were made to get the pure compounds **3**, **4** and **5**. A mixture of **L** and $AgNO_3$ in THF/water was heated and the cooling time was modified by putting the solution directly into the refrigerator for a fast cooling or by leaving the solution in the heating bath for a slow cooling. During the fast cooling, the highly polycrystalline compound was suitable for powder X-ray diffraction: the powder X-ray spectrum shows that it is pure compound **3**.

The solid-state reaction was also investigated by grinding solid ligand with solid $AgNO_3$ in powder, but the powder X-rays diffraction shows only a mixture of the ligand and $AgNO_3$ structures.

The crystal structure of each compound, **3**, **4** and **5,** are now described to show their differences, and to understand the different driving forces leading to one or another structure.

III.1.a - $\{[Ag(L)](NO_3)\}_n$ 3

The crystal shapes of **3** are thin plates or trapezoidal prisms. **3** crystallizes in the monoclinic space group $P2_1/n$ (no.14). There are four asymmetric units per unit cell, made of one ligand molecule, one silver atom and one nitrate anion. (Figure B-16) The pyridine rings coordinate to the silver ions creating a one-dimensional motif: a chain with alternating silver ions and ligand molecules -Ag-L-Ag-L, the silver atoms being coordinated by two nitrogen atoms of two different ligand molecules. (Figure B-17)

The important distances of the structure are reported in Table B-9. The distances C-N within the ligand are on average 1.339 Å and the angle C-N-C is 117.7(2)°. These distances are similar to the ones in **L** (1.337 Å). This difference can not be seen in the IR-spectrum, where the band shift of the ν(ArC-C, C=N) are found at 1412 cm^{-1} for both **L** and **3**.

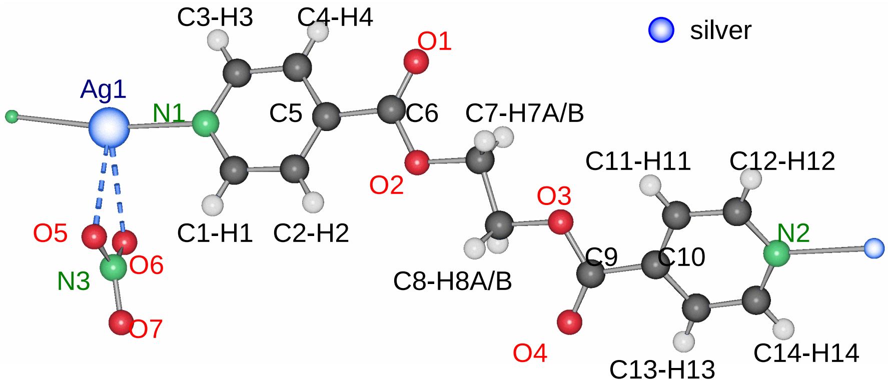

Figure B-16: asymmetric unit in 3 (Color codes given for all following figures)

The conformation of the ligand within the coordination polymer of **3** is the *anti* one, the same as in the crystalline ligand alone and as in compound **1**. The chain has an undulating form because the direction of the ligand molecules changes after each silver cation, going "up-to-down" and then "down-to-up" (Figure B-17). The distance between two silver ions within the chain is 17.74(3) Å which is in accordance with the *anti*-conformation of the ligand and usual distances and angles within one ligand molecule.

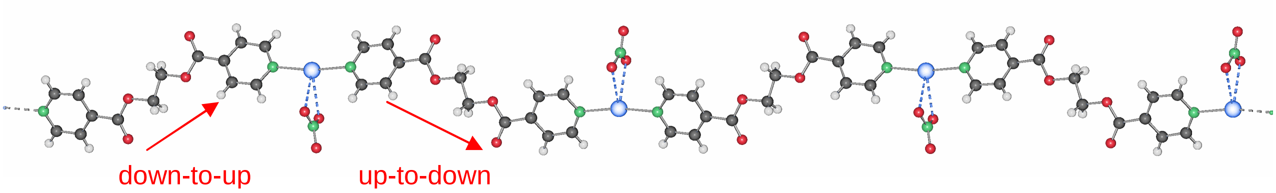

Figure B-17: chain motif in 3

The silver-nitrogen distances are 2.232(2) and 2.239(2) Å long and the angle N-Ag-N is 170.25(9)°. This non-180° angle at the silver cation is due to the asymmetric coordination of the nitrate counter anion. Each nitrate anion is connected with two silver atoms and each silver atom with two nitrate anions: the nitrate anions act as linkers between the silvers atoms, perpendicular to the chain propagation direction ····Ag-L-Ag-L···· (Figure B-18a). Each silver ion reaches thus a coordination number of five: the two nitrogen atoms occupy the axial positions of the distorted trigonal bipyramid, whereas three nitrate oxygen atoms occupy the equatorial ones. (Figure B-18b) One of the nitrate anions is coordinated to the silver in an anisobidentate way with silver-oxygen distances of 2.669(2) and 2.724(2) Å and the other nitrate anion is coordinated to the same silver atom in a monodentate way with silver-oxygen distances of 2.800(3) Å. The “silver-nitrate” distances are usually found from 2.3 to 2.6 Å, as the nitrate anion is a moderate good coordinating counter anion [9, 11]. The longer distances in **3** indicate a weaker coordinating effect. The delocalized charge allows generally a bridging or chelating action of the nitrate anion. The interaction nitrate-silver in **3** is however strong enough to deform the N-Ag-N angle (170.2°) to the side of the bidentate coordination.

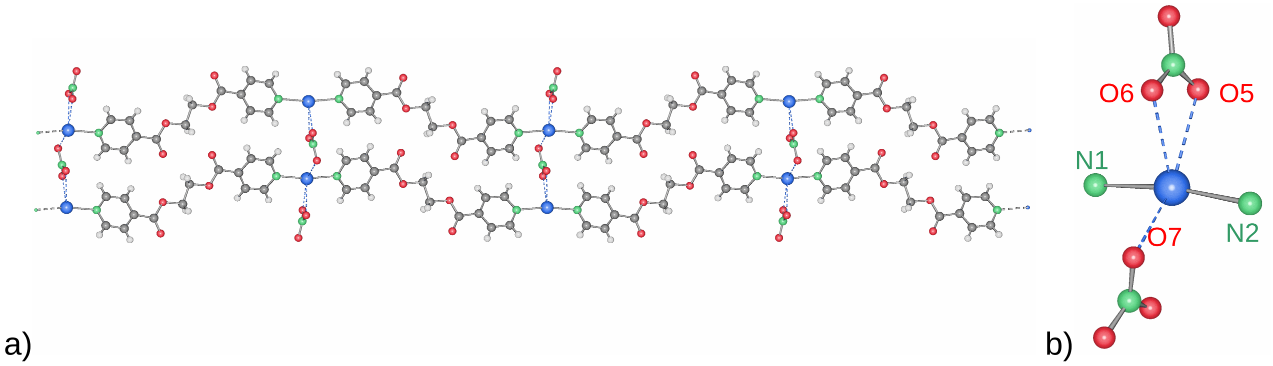

Figure B-18: a) the nitrate anions acts as linkers between the chains in 3; b) coordination sphere of the silver atom in 3

Another coordination polymer based on silver nitrate and the rigid ligand 1,2-bis(4-pyridyl)ethane (bpe) affords a similar sheet with bridging nitrate between the linear chains. However the coordination geometry of the Ag^I nodes is slightly different with a {AgN_2O_2} unit instead of a {AgN_2O_3} silver coordination sphere in **3** [149].

Between so close chains, some other interactions appear. (Figure B-19) i*)* Hydrogen bonding occurs between the C=O groups of one chain and the CH_2 moieties of the parallel ones with H···O contacts of 2.57 and 2.75 Å. (Figure B-19) The hydrogen bonds are listed in Table B-10. *ii)* The two closest pyridine rings seem to be tilted in order to generate C-H···π interactions, also called "face-to-edge" interactions [16]. They occur between the tilted pyridine ring and the H1 atom of the next of pyridine group at 3.33 Å, offset by 0.47 Å. (Table B-11) This interaction explains the bending within the ligand molecules: the pyridine planes are tilted with an angle of 50.25(7)°, and the planes containing the pyridine group and those of the corresponding ester function form angles of 16.5(3) and 20.9(2)°. The chains have thus a "bow-shaped" form if regarded along the propagation direction (Figure B-20) and the so-made sheets are not linear but undulating.

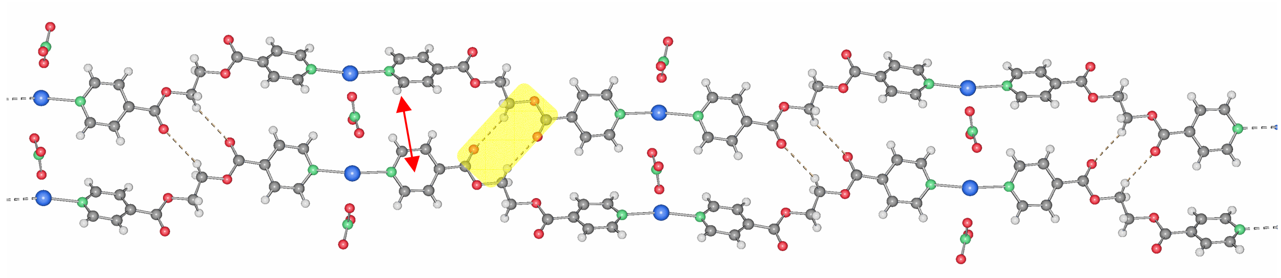

Figure B-19: other interactions between two chains in 3 (C-H···π: red arrow; H-bonds: yellow)

Additionally to the already described interactions between the chains, other interactions complete the overall structure. *i)* Hydrogen bonding occurs between close ligand molecules (C11-H1···O4 and C12-H12···O4) and between the nitrate anions and pyridine hydrogen atoms or ethyl hydrogen atoms. (Table B-10) (Figure B-20) *ii)* π-stacking of rings at a distance of 3.62 Å and offset by 1.61 Å is also observed. (Table B-11) The closest distances between to silver atoms are 8.02(3) Å, so that no silver-silver contacts can be discussed.

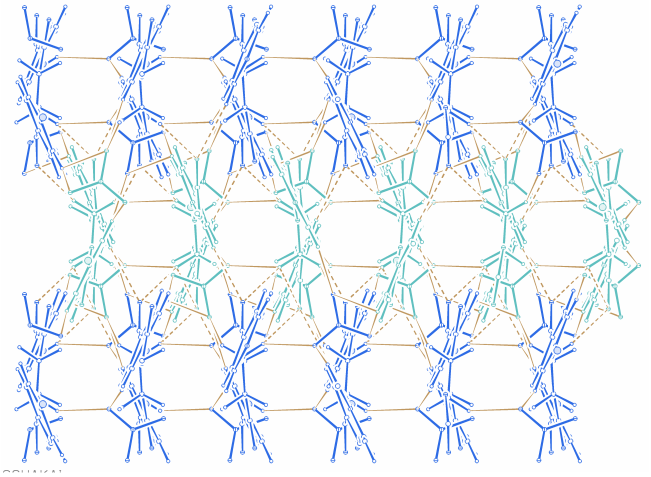

Figure B-20: View of the three-dimensional structure of 3 along the chain propagation (dashed lines: hydrogen bonds between the ligand molecules; full lines: hydrogen bonds involving nitrate anions)

Table B-9: Most important bond lengths (Å) and angles (°) in 3

Ag-N	2.232(2), 2.239(2)	N-Ag-N	170.25(9)
Ag-O(O_2N)	2.669(2), 2.724(2)	O-Ag-O	47.05(6)
	2.800 (3)		149.70(7), 103.32(6)
C-N	1.337(3), 1.343(4)	C-N-C	117.7(2)
	1.340(3), 1.335(4)		117.7(2)

Table B-10: Hydrogen bond data for 3 [lengths (Å) and angles (°)]

D-H···A	*d*(D-H)	*d*(H···A)	*d*(D···A)	Angle D-H···A
Inter-ligand hydrogen bonds				
C7-H7A···O1$^{\#1}$	0.97	2.75	3.543(4)	139.8
C8-H8A···O4$^{\#2}$	0.97	2.57	3.457(4)	152.9
C11-H11···O4$^{\#3}$	0.93	2.77	3.367(3)	122.8
C12-H12···O4$^{\#3}$	0.93	2.68	3.337(3)	128.0
hydrogen interactions between the nitrate anions and the ligand molecules				
C1-H1···O5	0.93	2.74	3.450(4)	133.9
C12-H12···O5$^{\#4}$	0.93	2.80	3.496(4)	132.6
C3-H3···O6$^{\#5}$	0.93	2.46	3.290(3)	148.4
C14-H14··O6$^{\#2}$	0.93	2.51	3.333(3)	148.2
C2-H2···O7$^{\#6}$	0.93	2.54	3.461(4)	172.5
C8-H8B···O7$^{\#6}$	0.97	2.61	3.346(4)	133.1
Symmetry transformations used to generate equivalent atoms: #1 -X+3, -Y, -Z+1; #2 -X+3, -Y+1, -Z+1; #3 -X+7/2, Y-1/2, -Z+3/2; #4 X+3/2, -Y+1/2, Z+1/2; #5 -X+3/2, Y-1/2, -Z+1/2; #6 -X+2, -Y+1, -Z+1.				

Table B-11: pyridine ring interactions lengths (Å) and angles (°) in 3 (definition of parameters given in A -I.2 -)

C-H···π interactions	d_{H-R}	pd_{H-R}	β	α
Ring (N2, C10, C11, C12, C14, C14)···H1$^{\#1}$	3.33	3.30	8.2	123.3
π-π interactions	d_{R-R}	pd_{R-R}	β	α
Ring (N1, C1, C2, C3, C4, C5)··· Ring (N1, C1, C2, C3, C4, C5)$^{\#2}$	3.62	3.24	26.5	0.02
Symmetry transformations used to generate equivalent atoms: #1 X+1/2, -Y+1/2, Z+1/2; #2 -X, -Y, -Z+1.				

III.1.b - $\{[Ag(L)](NO_3)(H_2O)\}_n$ 4

Compound **4** crystallizes in the orthorhombic space group *Ccca* (no.68). The asymmetric unit is formed of one silver atom, one ligand molecule, one nitrate counter anion and one water molecule, and all atoms are found on general positions. (Figure B-21) The most important geometrical data are listed in Table B-12.

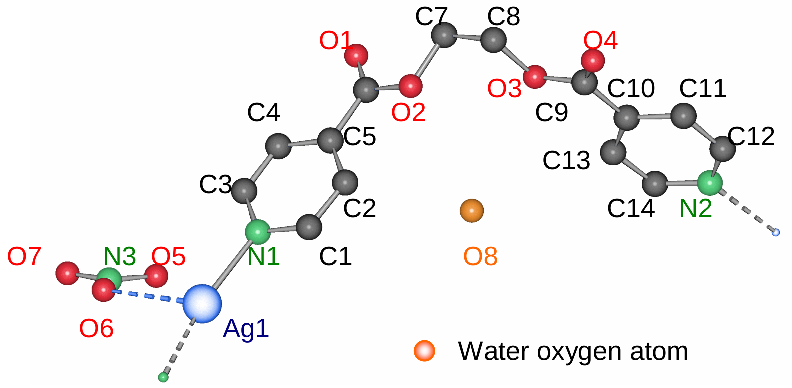

Figure B-21: asymmetric unit in 4 (hydrogen atoms omitted for clarity)

The silver cation is coordinated by two different ligands through their nitrogen atoms leading to a one-dimensional chain. (Figure B-22) The ligand adopts the *gauche*-conformation with a torsion angle between its two pyridine planes of 81.8(1)° giving to the strand an undulating zig-zag structure; the ester containing planes form angles of 8.1(6) and 14.7(8)° with the corresponding plane of the adjacent pyridine group. The distance between two silver atoms in a chain is 13.974(4) Å long in accordance with the strong bending of the ligand molecules and compared to the stretched out ligand with *ca.* 17.5 Å. The metal-metal distance is however longer than in **2** (9.167(7) Å), which presents the same ligand conformation but with a more important bending of **L**. The distances C-N in the pyridine ring are longer than in **L** and **3** (*ca.* 0.02 Å) which is reflected in the IR-spectrum with a band shift at 1419 cm^{-1} in **4** compared to 1412 cm^{-1} in **L**.

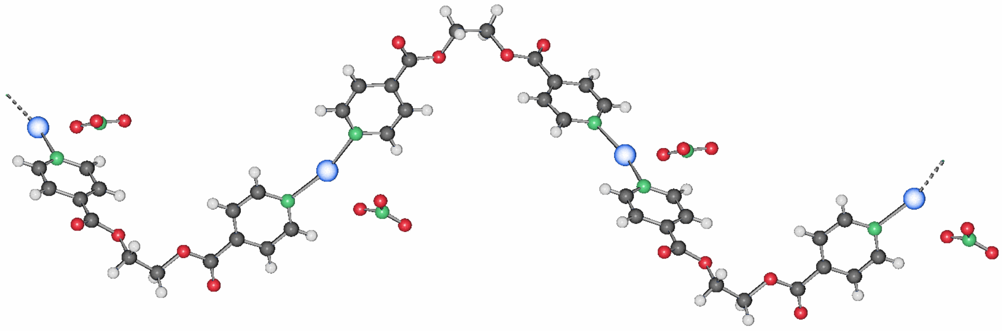

Figure B-22: chain motif in 4

The distances silver-nitrate in **4** are 2.171(4) and 2.189(4) Å long, which is shorter than in the chains of **3**. The N-Ag-N angle is with 161.1(2)° smaller than in **3**. These differences are due to the different environment around the silver ions in the two structures. Indeed the coordination number of the silver cation in **4** is four with two nitrogen atoms and two oxygen atoms of the nitrate counter anions (silver oxygen distances: 2.671(8) and 2.874(5) Å). Furthermore silver-silver interactions are observed at a distance of 3.136(1) Å. (Figure B-23a) These contacts are the shortest distances between two chains which stack almost perfectly parallel giving pairs of chains (Figure B-23b). A crystallographic inversion center is found in the middle of the Ag-Ag contact.

The arrangement in pairs is possible because the nitrate anions act as bridging linkers between the chains capping the silver-silver contacts. The distances silver-oxygen are longer than in **3** (by 0.04 Å) indicating a weaker coordination to the metal ions.

Another difference with **3** is that the third oxygen atom O7 of the nitrate anion is not involved in coordination bonding to another silver atom. In **3**, the negative charge of the anions is distributed over the three oxygen atoms. However in **4**, the negative charge is only distributed over two oxygen atoms, which partially compensate for the positive charge on each silver ion. The silver cations are thus allowed to approach each other more closely. This arrangement is finally reinforced by π-π interactions between the head-to-head ligands on each side of the silver pair system, the centroid-centroid distances being 3.79 Å and the offset 1.92 Å (Table B-14).

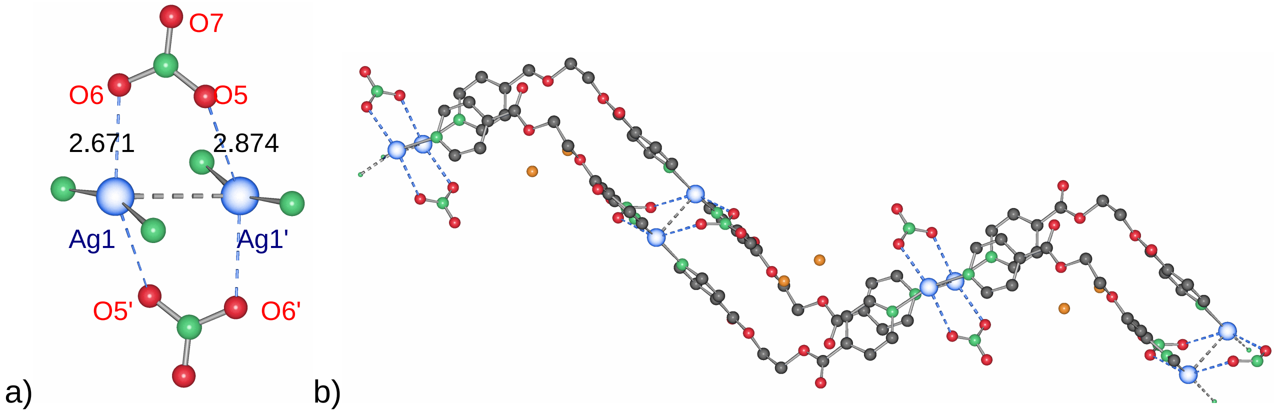

Figure B-23: a) The silver environment in 4 b) leading to the formation of pair of chains (hydrogen atoms omitted for clarity

The pairs of chains cross each other once in the solid-state structure of **4** at an angle of about 80° (Figure B-24a), one running in the (203)-direction, the other in the (-203)-direction leading to an open three-dimensional framework (Figure B-24b). There are some π-stacking interactions (Table B-14) between the pairs as well as hydrogen bonds (Table B-13).

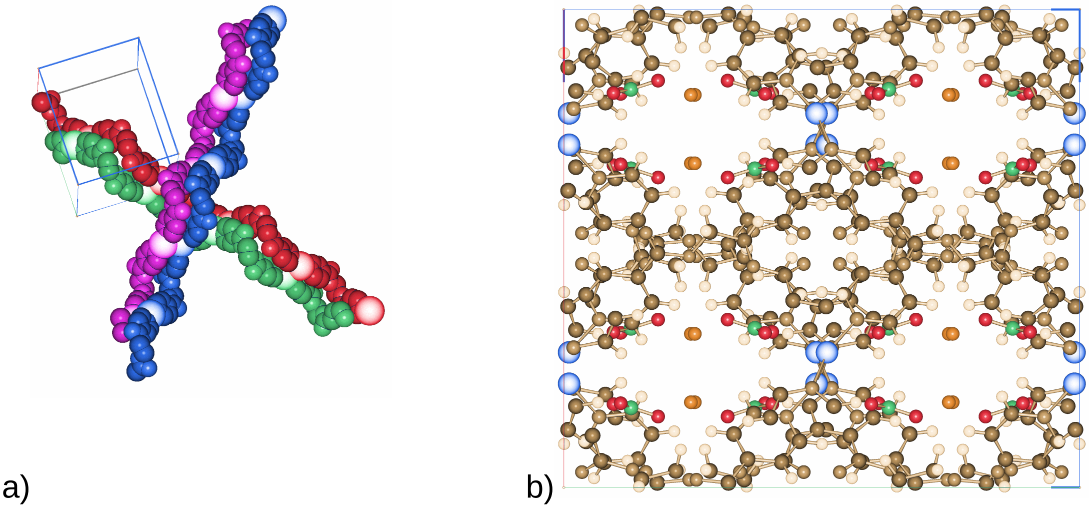

Figure B-24: View a) of the two propagation directions in 4 and b) of the open three dimensional framework along the *a*-axis

Local cavities are thus obtained along the direction of the *a*-axis in which four water molecules, *i.e.* O8, O9 and their symmetry equivalents, form discrete hydrogen-bonded clusters with O-O distances of 2.77(1) and 2.81(1) Å (Figure B-25). Unfortunately the positions of the water hydrogen atoms could not be located on the Fourier map. The square of water molecules is parallel to the *bc*-plane, and these water clusters are isolated except for some interactions with O6 and O7 of the nitrate anion (3.329(9) and 3.243(9) Å), as well as weak interactions with O3 and O2 of the ester functions in the ligand (3.662(7) and 3.401(7) Å). Closest contacts of O8 to hydrogen atoms of the ligand are also observed: 2.79 and 2.63 Å to H11 and 2.92 Å to H4 of three pyridine groups.

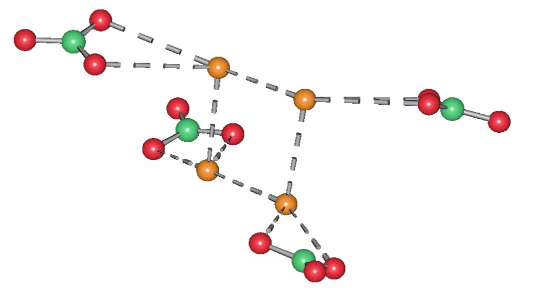

Figure B-25: View of the isolated water cluster in 4 with the nitrate anions

Table B-12: Most important bond lengths (Å) and angles (°) in 4

Ag-Ag	3.136(1)		
Ag-N	2.171(4), 2.189(4)	N-Ag-N	161.1(2)
Ag-O(O_2N)	2.671(8), 2.874(5)		
C-N	1.357(6), 1.359(6)	C-N-C	117.1(4)
	1.350(6), 1.332(7)		117.2(4)
O(H_2)-O(H_2)	2.77(1), 2.81(1)		
O(H_2)-O(O_2N)	3.329(9), 3.243(9)		

Table B-13: Hydrogen bond data for 4 [lengths (Å) and angles (°)]

D-H···A	*d*(D-H)	*d*(H···A)	*d*(D···A)	Angle D-H···A
Inter-ligand hydrogen bonds				
C2-H2···O4$^{\#1}$	0.93	2.27	3.075(6)	144.2
C7-H7A···O1$^{\#2}$	0.97	2.96	3.781(6)	142.7
Hydrogen bonding between water molecules and ligand molecules				
C11-H11···O8$^{\#3}$	0.93	2.79	3.587(7)	144.5
C11-H11···O8	0.93	2.63	3.348(7)	134.1
C4-H4···O8	0.93	2.92	3.334(6)	108.3
hydrogen interactions between the nitrate anions and the ligand molecules				
C12-H12···O6	0.93	2.46	3.185(7)	134.8
C7-H7B···O7$^{\#4}$	0.97	2.68	3.421(9)	133.5
C4-H4···O7$^{\#5}$	0.93	2.31	3.224(6)	168.8
C8-H8A··O5$^{\#6}$	0.97	2.82	3.563(7)	134.2
C1-H1···O5	0.93	2.62	3.335(7)	134.2

Symmetry transformations used to generate equivalent atoms: #1 X-1/2, Y-1/2, Z; #2 -X, Y, -Z+1/2; #3 X+1/2, -Y+1/2, Z+1/2; #4 X, -Y, Z-1/2; #5 -X+1/2, Y, Z-1/2; #6 X+1/2, Y+1/2, Z.

Table B-14: pyridine ring interactions lengths (Å) and angles (°) in 4

π-π interactions	d_{R-R}	pd_{R-R}	β	α
intra-pairs				
Ring (N1, C1, C2, C3, C4, C5)···Ring (N2, C10, C11, C12, C13, C14)$^{\#1}$	3.79	3.26	30.4	6.25
inter-pairs				
Ring (N1, C1, C2, C3, C4, C5)···Ring (N1, C1, C2, C3, C4, C5)$^{\#2}$	4.19	3.28	38.5	7.6
Ring (N2, C10, C11, C12, C13, C14)···Ring (N2, C10, C11, C12, C13, C14)$^{\#3}$	3.62	3.24	26.5	0.02
Symmetry transformations used to generate equivalent atoms: #1 -X, Y+1/2, -Z+1/2; #2 -X+1/2, -Y, Z; #3 -X, -Y+1/2, Z.				

III.1.c - $\{[Ag(L)](NO_3)(H_2O)_2\}_n$ 5

The single crystals of **5** are plates or twinned plates. On Picture B-2, one can see a crystal of **5** as well as a damaged one: the crystal has lost its inclusion water molecules and only the sheets are retained.

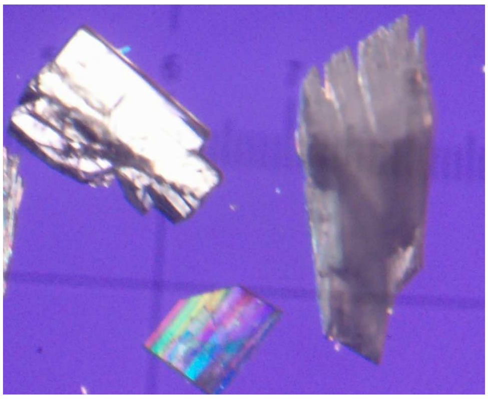

Picture B-2: View of one 5 crystal (left) and of one damaged crystal of 5 (right)

Compound **5** crystallizes in the triclinic space group P-1 (no.2) The asymmetric unit (one ligand molecule, one silver ion, one nitrate counter anion and two water molecules for which the hydrogen atom positions could not be determined) is shown on the Figure B-26.

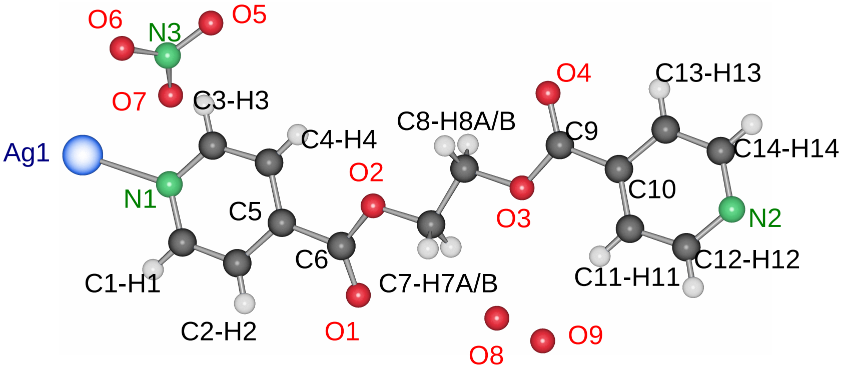

Figure B-26: asymmetric unit in 5

The motif of **5** is a one-dimensional chain in which silver atoms and ligand molecules alternate, the silver ion being coordinated with two nitrogen atoms of two different ligand molecules. (Figure B-27) The characteristic distances and angles are listed in Table B-15.

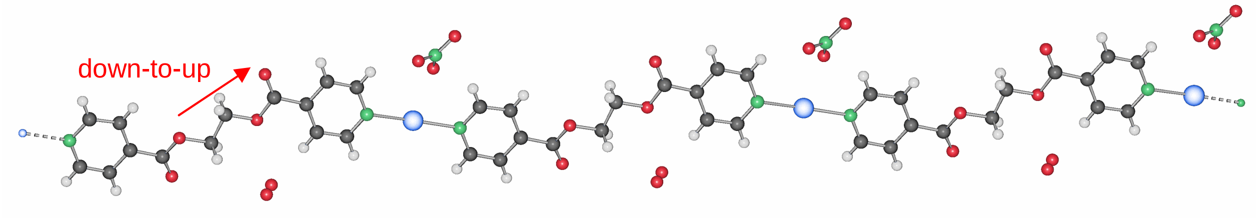

Figure B-27: the chain motif in 5

The ligand molecules are in the *anti*-conformation as in **3**, with the pyridine planes within a ligand lying in almost parallel planes (6.4(1)°). These two planes are shifted by 1.26(1) Å. The two angles between the plane containing the carbonyl group of the isonicotinic units and the plane of the corresponding mean pyridine ring are relatively different, 19.2(3)° and 8.4(4)°. The distance from one silver atom to the next within one chain is determined by the ligand in the *anti*-conformation, and is, with 17.604(8) Å, compatible with the other one-dimensional compounds with silver and copper (**3** and **1**). Contrary to **1** and **3**, the direction of the ligand is always the same along the chain: “down-to-up” (Figure B-27).

The coordination environment of silver in **5** is similar to the one in **4**. However the angle N-Ag-N is with 173.20(8)° larger, the distances Ag-N (2.150(2) and 2.154(2) Å) shorter and the silver-silver distance longer with 3.4079(6) Å than in **4**. This is due to a decrease of coordination by the nitrate anions towards the cations. Indeed, the silver-oxygen distances are with 2.704(2) and 2.892(2) rather longer on average in **5** than in **4**. The chains are also organised in pairs of chains with the nitrate anions acting as pincers between the chains. (Figure B-28) An inversion center is found in the middle of the silver-silver contact. This arrangement induces "head-to-head" π-π stacking with a spacing of 3.70 Å between two adjacent rings, taking into account the distances between the ring centers. The aromatic rings are not perfectly superposed, but offset by 1.42 Å to each other, allowing an energetically more efficient stacking (Table B-17) [16].

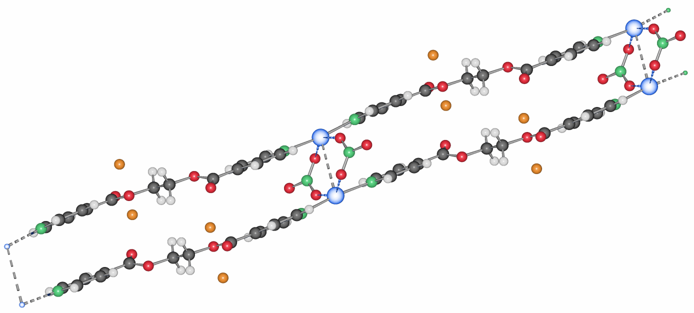

Figure B-28: organisation of the chains in 5 with the fourth-coordinated silver atoms and the nitrate bridging anions

As in **4** the shortest distance between the two chains is the silver-silver contact, it is however longer in **5** with 3.4079(6) Å than in **4**. The O5 oxygen atom of the nitrate counter-anions is not involved in coordination bonds to silver, but in a hydrogen bonding network with the water molecules (Figure B-29), the distances between O5 and O8, O9 are respectively 2.827(3) and 3.196(3) Å. From these interactions results a nitrate-water network. The O5 atom also forms hydrogen bonds with H3 and H4 of neighbour pyridine rings and H7B of a close ethyl group. (Table B-16) The nitrate oxygen atoms O6 and O7 are moreover involved in hydrogen bonding to O9 and O8 with distances of 2.974(3) and 3.503(3) Å respectively. The presence of crystalline water molecules is confirmed by the IR-spectrum, with a broad band between 3540 and 3300 cm^{-1}.

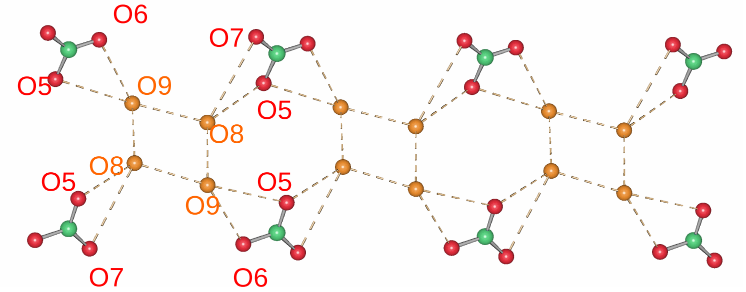

Figure B-29: nitrate-water network in 5

These nitrate-water ribbon-like networks are placed between the pairs of chains, which are stacked in a parallel fashion in the crystal lattice (Figure B-30) with the previously described interactions and additional hydrogen bonds between the ligand hydrogen atoms and the O6 and O7 nitrate oxygen atoms (Table B-16). The loss of the water molecules occurs between 25 and 70°C, whereas it happens at 117°C in **4**. Indeed, the water molecules in **5** are localized in channels and can be more easily removed than in **4**, in which they are located in local cavities.

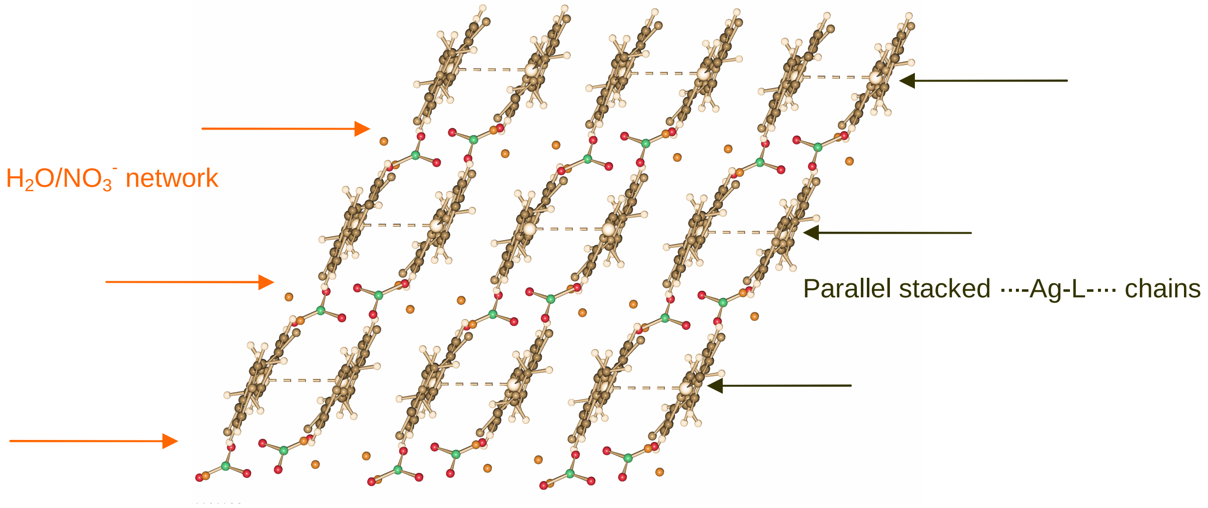

Figure B-30: three-dimensional arrangement in 5: the pairs are stacked parallel in the (-10 20 24)-direction

Further interactions are observed between the pairs of chains in **5**. *i)* Silver-aromatic ring interactions take place between the silver atom and the (N2, C10…C14) ring of the next pair of chains with a distance of 3.48 Å between silver atom and ring center (offset of 0.5 Å). (Table B-17) This kind of interaction is found in other silver coordination polymers with a range of silver-centroid distances of 2.89-3.37 Å. In **5**, the silver-ring interaction is thus weaker [11]. *ii)* The layers are also maintained by π-π interactions between two adjacent pairs (Table B-17). *iii)* Finally hydrogen interactions complete the weak interaction system between the pairs (Table B-16). The two interactions C13-H13···O1 and C2-H2···O4 take place where the ligand molecules are closer, separating the channels in **5** along the (17 1 1)-direction (Figure B-31).

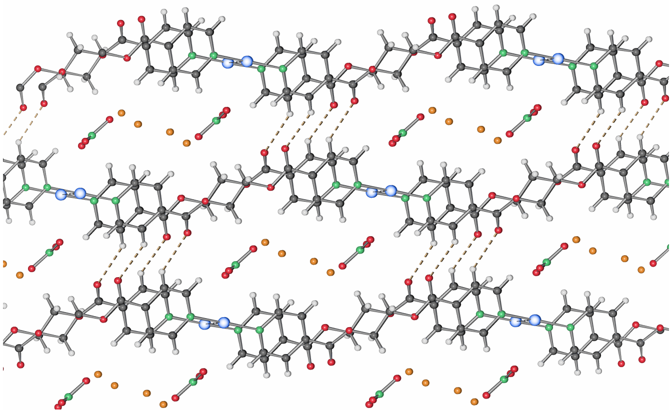

Figure B-31: View of the channels along the (17 1 1)-direction in 5

Table B-15: Most important bond lengths (Å) and angles (°) in 5

Ag-Ag	3.4079(6)		
Ag-N	2.150(2), 2.154(2)	N-Ag-N	173.2(8)
Ag-O(O_2N)	2.704(2), 2.892(2)		
C-N	1.343(3), 1.347(3)	C-N-C	117.7(2)
	1.345(3), 1.350(3)		118.1(2)
O(H_2)-O(H_2)	2.761(3), 2.779(4)		
O(H_2)-O(O_2N)	2.827(3), 3.196(3)		
	2.974(3), 3.503(3)		

Table B-16: Hydrogen bond data for 5 [lengths (Å) and angles (°)]

D-H···A	*d*(D-H)	*d*(H···A)	*d*(D···A)	Angle D-H···A
Inter-pairs hydrogen bonds				
C13-H13···O1$^{\#1}$	0.93	2.49	3.257(3)	140.4
C8-H8B···O2$^{\#2}$	0.97	2.70	3.632(3)	162.5
C2-H2···O4$^{\#3}$	0.93	2.42	3.184(3)	139.6
hydrogen interactions between the nitrate anions (O6, O7) and the ligand molecules				
C1-H1···O7$^{\#4}$	0.93	2.57	3.346(3)	141.7
C12-H12···O7$^{\#5}$	0.93	2.67	3.410(3)	137.0
C8-H8A···O6$^{\#6}$	0.97	2.95	3.712(3)	136.7
C3-H3···O6	0.93	2.83	3.470(3)	127.3
C14-H14···O6$^{\#7}$	0.93	2.50	3.192(3)	131.1
hydrogen interactions between the nitrate anions (O5) and the ligand molecules				
C4-H4··O5$^{\#6}$	0.93	2.44	3.349(3)	167.1
C3-H3··O5	0.93	2.88	3.555(3)	130.6
C7-H7B··O5$^{\#8}$	0.97	2.60	3.486(4)	151.3

Symmetry transformations used to generate equivalent atoms: #1 X, Y, Z+1; #2 -X+1, -Y+2, -Z+2; #3 X, Y, Z-1; #4 -X+1, -Y+1, -Z+1; #5 -X, -Y+2, -Z+2; #6 -X+1, -Y+1, -Z+2; #7 X-1, Y+1, Z+1; #8 X, Y+1, Z.

Table B-17: pyridine ring interactions lengths (Å) and angles (°) in 5

π-π interactions	d_{R-R}	pd_{R-R}	β	α
intra-pairs				
Ring (N1, C1, C2, C3, C4, C5)···Ring (N2, C10, C11, C12, C13, C14)$^{\#1}$	3.70	3.40	22.5	6.4
inter-pairs				
Ring (N1, C1, C2, C3, C4, C5)···Ring (N2, C10, C11, C12, C13, C14)$^{\#2}$	4.73	3.33	45.3	6.4
Ag-π interactions	d_{M-R}	pd_{M-R}	β	
Ring (N2, C10, C11, C12, C13, C14)···Ag1$^{\#3}$	3.48	3.44	8.4	

Symmetry transformations used to generate equivalent atoms: #1 -X, -Y, -Z; #2 –X+1, -Y, -Z; #3 -X+1, -Y, -Z.

III.1.d - Conclusion on compounds 3, 4 and 5

The three compounds **3**, **4** and **5**, which can grow from the same batch, have different structures and the three compounds do not contain the same number of co-crystallized solvent molecules. They are pseudo-polymorphs. What are the main similarities and differences between them?

Motif

The three compounds have in principal one general structural feature in common: the presence of one-dimensional coordination polymer chains made of Ag and **L**. The silver-nitrogen distances evolve from the longer average values of 2.23(2) Å (in **3**) to the shortest distance of 2.15(2) Å (in **5**). This is in the range of the silver-nitrogen distances in other comparable compounds with similar coordination sphere for the silver cations. For instance, in $\{[Ag(pyrazine)]NO_3\}_n$ the average silver-nitrogen distance is 2.21(1) Å [140], in $\{[Ag(2,4'\text{-bipyridine})]NO_3\}_n$ it is 2.19 Å long [150]. The smallest N-Ag-N angle is found in **4** with 161.1(1)°, which is to our knowledge the second smallest angle for this type of coordination, only the one in $\{[Ag(pyrazine)]NO_3\}_n$ is smaller by 2° [140].

Anion bonds

Whereas in **3**, all of the nitrate oxygen atoms are involved in coordination bonds, in **4** and **5**, each nitrate anion forms H-bonds towards water molecules: one of the nitrate oxygen atoms is completely involved in the hydrogen bonding system. From the examples stated in the literature, nitrate counter anions are generally rather strong coordinating anions towards the silver cation, with silver-oxygen distances in the range from 2.3 to 2.6 Å [237, 238]. They can act as monodentate anions for one silver cation [151, 152, 180] or as bridging aniso- or iso-bidentate anion for two metal ions [142, 151]. In some cases, the nitrate anions are not coordinated to the silver atom and have apparently a template effect on the conformation of the silver polymer in comparison to the same polymer formed for instance with triflate anions. [73]

Ag-Ag contact and nitrate anions as bidentate pincers

It has also been stated that the nitrate anion is unable to delocalize the positive charges of two silver ions in an Ag-Ag pair in order to allow metal-metal interactions and thus closer contacts between the metal atoms. [152]

In our compounds, the nitrate anion acts as tridentate ligand towards two silver atoms in **3**, whereas it plays the role of bidentate ligand bridging two silver cations in **4** and **5**. The latter coordination leads to a better delocalisation of the positive charge on silver and allows two metal ions to approach and form pairs of chains in **4** and **5**. The two compounds are quite similar as far as the pincer role of the anions is concerned. The H-bonding system in which the nitrate anions are involved leads to distortion of the nitrate anions in **5**, weakening the bridging effect over the two silver cations. Thus the positive charge on the metal ions in **5** is probably less well compensated by the anions than in the case of **4**, and the resulting Ag-Ag contact is therefore longer by 0.27 Å than that in **4**.

Although controversially debated, Ag-Ag contacts can be of considerable influence in the structure formation. Their energy has been roughly estimated to 5-12 $kJ.mol^{-1}$ [11], sometimes more energetic than Ag···ring interactions. Compared to Ag-Ag distances known from literature (Table B-18), the one in **4** is among the shorter or medium strong interactions, whereas the metal-metal contact in **5** is rather weak. Both are, however, shorter than the Van der Waals diameter for silver (3.44 Å). [239, 240]

Table B-18: Ag-Ag contacts in silver coordination polymers with the Ag-Ag distances, the nature of the Ag-Ag contact, the motif built up with the Ag-Ag interaction and if known, the characterization of the Ag-Ag interaction thanks to luminescence (— if the luminescence spectrometry was not performed)

Compound	Ag···Ag (Å)	Counter-anion supported?	Motiv	Lumin.?	Ref.
{[Ag$_2$(4,5-diazospirobifluorene)$_2$(ClO$_4$)$_2$](CH$_3$CN)}$_n$	2.776(1)	non-bridging ClO$_4$	chain	no	[241]
{[Ag$_2$(2,2'-bipyrazine)(NO$_3$)$_2$]}$_n$	2.8754(7)	ligand supported	Layers	yes	[115]
{[Ag(4,4'-bipyridine)]NO$_3$}$_n$	2.977(1)	non-bridging NO$_3$	3-D T-shaped MOF	—	[142]
{[Ag(4-4'-dipyridyldisulfide)](p-toluenesulfonate)}$_n$	3.044(2)	bridging OTs	2-D sheet	yes	[117]
{[Ag(OAc)(4-2,5-bis(4-pyridyl)pyrazine]}$_n$	3.077(3)	bridging acetate	Double chain	—	[242]
{[Ag(1,3-bis(4-pyridyl)propane)]PF$_6$}$_n$	3.0852(9)	bridging PF$_6$	Double chain	—	[165]
{[Ag(1,3-bis(4-pyridyl)propane](CF$_3$SO$_3$)}$_n$	3.089(1)	non-bridging CF$_3$SO$_3$	Double helicate	—	[39]
{[Ag$_4$(3-cyanopyridine)$_8$(SiF$_6$)$_2$(H$_2$O)$_2$}$_n$	3.3072(5), 3.0242(6)	bridging SiF$_6$	Tetranuclear cluster	—	[243]
4	3.136(1)	bridging NO$_3$	Double chain	no	
{[Ag(1,4-bis(4-pyridyl)butadiyne)MeCO$_2$·2.5H$_2$O}$_n$	3.1371(5)	bridging MeCO$_2$	Double chain	—	[152]
{[Ag(2,4'-bipyridine)]ClO$_4$}$_n$	3.1526(6)	non-bridging ClO$_4$	2-D sheet	—	[150]
{[Ag(1,4-bis(4-pyridyl)butadiyne)PO$_2$F$_2$·MeCN}$_n$	3.193(1)	bridging PO$_2$F$_2$	Double chain	—	[152]
{[Ag$_2$(N-(4-pyridinylmethyl)-4-pyridinecarboxamide)$_2$(ox)](H$_2$O)$_9$}$_n$	3.202(1)	bridging oxalate	Double chain	—	[153]
{[Ag(μ-3,6-bis(pyridin-3-yl)-1,2,4,5-tetrazine)]CF$_3$SO$_3$}$_n$	3.220(1)	bridging triflate	Double chain	—	[244]
{[Ag(1,3-bis(4-pyridyl)propane)]ClO$_4$}$_n$	3.221(1)	bridging ClO$_4$	Double chain	—	[165]
{[Ag$_2$(4,4'-dipyridylsulfide)$_2$](ClO$_4$)$_2$(MeCN)}$_n$	3.240(1)	bridging ClO$_4$	Double chain	no	[72]
{[Ag(1,1'-(4-dipyridinethio)ferrocene)]PF$_6$}$_n$	3.2670(8)	non-bridging PF$_6$	Double chain	no	[245]
{[Ag(*trans*-4,4'-azopyridine)]NO$_3$·MeOH·H$_2$O}$_n$	3.295	bridging NO$_3$	Double chain	—	[246]
5	3.4079(6)	bridging NO$_3$	Double chain	no	
{[Ag(2,4'-bipyridine)]NO$_3$}$_n$	3.987	bridging NO$_3$	Double helicate	—	[150]

Concerning nitrate as bridging ligand for pairs of silver atoms, there are to our knowledge only three other examples: in the first one, metal-oxygen distances are asymmetric with 2.66(0)-2.903(3) Å, bridging a relatively long Ag-Ag contact of 3.987 Å [150], all of the nitrate oxygen atoms being involved in silver-interactions. In the second, metal oxygen distances are similar to the ones in our compounds (2.878(3) and 2.966(3) Å) but the metal-metal distance (5.287 Å) is too long for attractive interactions. [143] The third example exhibits pairs of chains formed with silver cations and 4,4'-azopyridine. Metal-oxygen distances are 2.923 Å and 2.797 Å allowing pair wise silver-silver interactions at a distance of 3.295 Å. [246] Some examples show Ag-Ag contacts with other bridging anions, such as triflate [244] (Ag-O: 2.740(4) and 2.839(4), Ag-Ag: 3.220(1) Å) or acetate [242] (Ag-O: 2.636(3) and 2.621 Å for a Ag-Ag separation of 3.077(3) Å). Some Ag-Ag contacts are known to be supported by strong coordinating anions such as MeCO$_2^-$ or

$PF_2CO_2^-$ [11, 152]. In **4** and **5**, the negative charge distribution on the nitrate anions can be compared to the one on the $MeCO_2^-$ or $PF_2CO_2^-$ anions. This is due to the involvement of the nitrate anions in hydrogen bonding.

The existence of attractive interactions is not unanimously recognized, since a Van der Waals radius of 1.33 Å for Ag^+ is also stated, avoiding Ag-Ag interactions. [247, 248]

It is extremely difficult to find an experimental evidence for Ag-Ag contacts in coordination polymers. The existence of metal-metal bonded excited state for d^{10} metals was proven by luminescence. The emission properties of $M(d^{10})$-$M(d^{10})$ containing complexes are consistent with the presence of the ndσ*→(n+1)pσ transitions. [249-252] Luminescence properties of coordination polymers showing Ag-Ag contacts are sometimes explained by the short contacts [115, 117-119], while other so-called argentophilic interactions can not be proven by luminescence measurements [72, 241, 245, 253]. The typical emission wavelengths for Ag-Ag interactions occurs usually around 600 nm [115, 117]. Additionally, the overall supramolecular interactions can influence and increase the emission intensity of the intraligand transitions [72]. Increase of the intensity is relevant for all coordination polymers [116, 236]. The emission spectroscopy of **3**, **4** and **5** shows no new emission band or new excitation wavelength. In the case of **4**, the emission spectrum is similar to the one of **L**, with only a shoulder at 348 nm (larger than in **L**) The same **L**-Ag compound emission differences is reported by Wang *et al.* [241] and the shoulder is attributed to a π-stacking effect. In **5**, the enhancement of the emission intensity compared to **L** is more important than in **3** and **4**.

Che *et al*. afford the first spectroscopic verification of the existence of Ag-Ag attractive interactions in coordination compounds, with identification of a silver-silver bonded excited state, using Raman and luminescence measurements. [249]

Water clusters

The presence and the number of water molecules in **4** and **5** lead to severe changes in the arrangement of the chains with respect to each other compared to **3**, as well as in the ligand conformation as far as **4** is concerned. Thus, compounds **4** and **5** both feature short metal–metal distances, leading to pairs of chains. Weak interactions are, in their sum, responsible for their formation. Aromatic π-π-stacking is observed in all three compounds.

However, two major facts can be found which are responsible for the formation of different solid state structures. One is evidenced in the ligand conformation. In **5**, it adopts an *anti*-conformation, whereas in **4**, a *gauche*-arrangement is observed. The second point is the presence of different amounts of water molecules per asymmetric unit. Thus, the factor influencing the overall arrangement of the double-chains to each other in the crystal seems to be the number of water molecules and the resulting number of possible hydrogen bonds. The H-bonds also influence the fact that the chains run parallel in **5**, or cross each other in **4**, and that the ligand adopts two different conformations in **4** and **5**. However, the latter influence can be discussed in several ways, and it cannot be said if the ligand in **4** adopts *gauche*-conformation because of the H-bonds or if the H-bonds result out of the ligand conformation.

Some coordination polymers including non-coordinated water molecules can be found in the literature. The inclusion water molecules form mostly so-called water clusters with at least six water molecules. The water clusters can be regarded as “glue” which allows the assembly of low-dimensional motifs to a three-dimensional packing. [254-256] “Glue” means that the water molecules can adapt their structures and interactions in order to fit and optimize the attractive forces in the framework, the rigidity of the overall structure being enhanced. [257] This role is also found for water molecules permitting the agglomeration of motifs showing both hydrophobic and hydrophilic faces [37]. Liu *et al*. consider however that the water clusters not only fill the voids but also contribute to the total lattice energy. [112] Nonetheless, when the water molecules are evacuated from the structure [254-256], the overall arrangement is breaking down, showing the importance of water clusters in the packing. The water loss usually occurs between 60°C and 150°C, and at 117°C for **4**. A similar nitrate-water-methanol network is found in {[Ag(*trans*-4,4’-azopyridine)]$NO_3 \cdot MeOH \cdot H_2O\}_n$ between the double chains organized in layers as in **5**. But no strong network forces are outlined. [246]

Very probably, the Ag-π contacts in **5** are also responsible for inducing the parallel packing of the chains in this structure. Energies of such stacking interactions may be comparable to coordinate bond energies for some heavy metals such as Tl, Ag and Pb, and have roughly been estimated to up to 40 kJ.mol^{-1}. [73, 258, 259] From the Cu^{I} coordination compounds **1** and **2** and from the Ag^{I} compounds **4**, it can be concluded that the H-bonds toward solvent molecules such as THF or H_2O may induce deformation of the ligand **L**, whereas in absence of solvent molecules, the ligand has so far always adopted the *anti*-conformation as in the free ligand.

Calculation

To corroborate the findings, additional electronic structure calculations were carried out in collaboration with the group of Prof. Markus Meuwly, using the GAUSSIAN03 suite of programs [260]. The silver atoms were treated with a LANL2DZ effective core potential [261] while for all other atoms the basis set was 6-31G(d,p). Correlation was described with the B3LYP density functional. The total wave function was converged to better than

10^{-7} and structural optimizations used the default values for convergence. The numerical integration of the functional was carried out with the grid = ultrafine option.

For the ligand a *gauche*- and an *anti*-conformation are relevant. First, the structures of the two ligand conformations were optimized. Their energies differ weakly by 0.8 kcal mol^{-1}. Consequently, the size of the model including the silver atoms and the counter ion could be reduced and only the part of the ligand directly ligated to the Ag atoms was retained. The reduced system is shown in Figure B-32. In the calculations for **4** and **5**, the Ag–Ag and Ag–N bond lengths and the relevant angles were optimized. The positions of the NO_3^- ions were kept fixed, as found in the single crystal structure. Structural optimizations establish that the Ag–Ag distance for fragment **5** is longer by 0.15 Å than for **4**, in quite a good agreement with experiment (0.27 Å). However, the distances do not compare quantitatively; they are 3.34 Å for **4** and 3.49 Å for **5** compared with 3.136 and 3.408 Å from experiment, respectively. Most likely, correlation effects beyond the density functional theory would have to be included to better describe the interaction between the pyridine rings. The validity of B3LYP/LANL2DZ for the present approach was tested for isolated $(Ag)_2$ and $(Ag)_2^+$: the optimized bond lengths are 2.62 Å and 2.82 Å which compares with 2.69 Å and 2.84 Å from recent CCSD(T) calculations. [262]

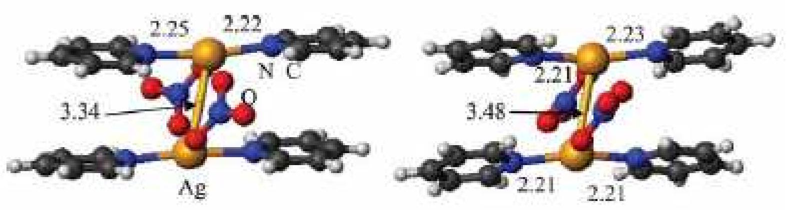

Compound **4** Compound **5**

Figure B-32: Models used for calculations with relevant calculated bond lengths Å

To further understand the difference in the total energy of **4** and **5**, the potential energy was calculated while scanning the Ag-Ag distance. Figure B-33 shows the behaviour of the total energy as a function of the Ag-Ag separation. The equilibrium of each curve was shifted to 0 to allow more direct comparison of the curves. The repulsive wall for compound **5** is steeper, which indicates, together with the longer Ag-Ag interaction, that the repulsion between the π-stacked pyridine rings is likely to make the major contribution to the elongated Ag-Ag contact. Superimposed in Figure B-33 are the potential energy curves for $(Ag)_2$ and $(Ag)_2^+$. It is interesting to note that the $(Ag)_2$ potential has a considerably larger curvature around the minimum than the one for $(Ag)_2^+$ which, in turn, is rather similar to the curves for **4** and **5**. This suggests that the Ag atoms should behave like $(Ag)_2^+$ rather than $(Ag)_2$. Indeed, calculating nuclear charges for the minimized structures of **4** and **5** using the natural bond orbital (NBO) method reveals that the Ag atoms carry 0.73*e* of nuclear charge. This rationalizes the even flatter potential energy curves for **4** and **5**, compared to $(Ag)_2^+$ in Figure B-33.

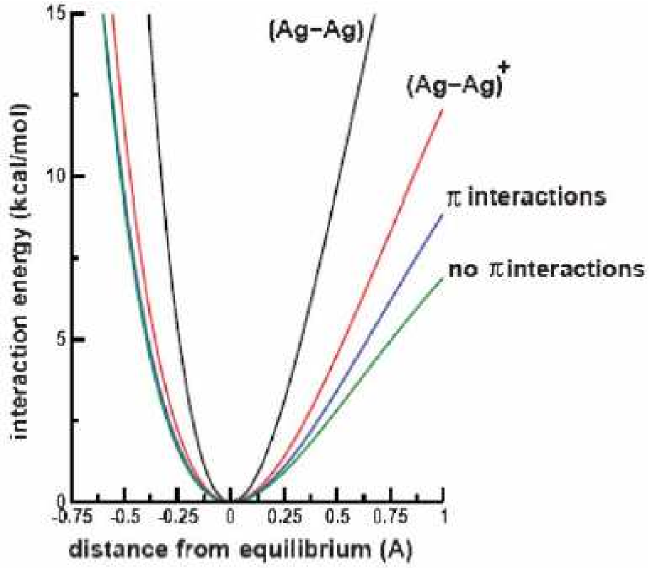

Figure B-33: Behaviour of the total energy as a function of the Ag-Ag separation

Computational calculations allow thus confirmation of structures **4** and **5**, and explain qualitatively the impact of metal-metal and π-interactions.

Pseudo-polymorphism

The three coordination polymers **3**, **4** and **5** with the same {Ag(**L**)(NO_3)} components, but with different amounts of co-crystallizing water molecules ({[Ag(**L**)(NO_3)]·xH_2O}$_n$, x = 0, 1, 2) are pseudo-polymorphs. Without water in the crystal structure, simple 1-D chains are obtained in which the nitrate anions bridge the silver cations using all three oxygen atoms. As soon as water co-crystallizes, the good solvating capacity of water towards the nitrate anions is revealed by hydrogen-bonding interactions to at least one oxygen atom of the anion. Thus, the anion acts as bidentate pincer, bridging two metal ions and allowing the generation of pairs of chains. Metal-metal contacts and π-interactions play also a role in the construction of the structures and the arrangement of the pairs of chains with respect to each other.

The three compounds can appear concomitantly, as often observed [72, 73, 166]. The flexibility of the building blocks can explain the presence of different compounds [73]. Indeed the resulting compounds have close potential energy (as seen in the calculations on **4** and **5**) avoiding the formation of pure phases [56]. It is worthy to note that the compounds without inclusion water molecules (**3**) can be obtained purely. It must be the thermodynamically more stable compound.

III.2 - Solvent influence

The coordination of **L** to $AgNO_3$ was also studied for building other Ag^I coordination polymers under other conditions, particularly the change of the solvents.

III.2.a - $\{[Ag_2(NO_3)_2(L)]\}_n$ 6

$\{[Ag_2(NO_3)_2(\mathbf{L})]\}_n$ **6** grow in a “H-shaped” tube. (Figure B-15) With the proportion **L**:Ag = 1:1, **L** in THF and silver nitrate in ethanol instead of water are put each in one arm of the tube, the solutions are frozen by immersion of the tube in liquid nitrogen and finally the diffusion solvent (THF) is added. The slow diffusion can take place in order to yield high quality crystals of **6** at the interface EtOH/THF after several months**.** Unfortunately the yield was not high enough to perform more characterizations than the crystallographic one. Only few crystals grow in each batch. The results of performed reactions in order to get **6** in higher quantity are resumed in Table B-19.

Table B-19: experiments and products of reaction L + $AgNO_3$ (1:1) with ethanol

ligand	$AgNO_3$	Experiment	Diffusion solvent	Product	Concentration ($mol.L^{-1}$)
THF	EtOH	“H-shaped” tube	THF	**6**	3.10^{-3}
THF	EtOH	“H-shaped” tube	THF	**6**	$1,5.10^{-3}$
THF	EtOH	“H-shaped” tube	THF	cotton-like precipitate: $\{Ag\mathbf{L}NO_3\}$	6.10^{-3}
EtOH	EtOH	“H-shaped” tube	EtOH	**3**	3.10^{-3}
EtOH	H_2O	“H-shaped” tube	EtOH	**5**	3.10^{-3}
EtOH	EtOH	direct		White precipitate: $\{Ag\mathbf{L}NO_3\}$	

Compound **6** crystallizes in the monoclinic space group *C2/c* (no.15). There are eight asymmetric units (one silver atom, one nitrate molecule and one half ligand) in each unit cell. (Figure B-34) There are thus two silver atoms for one ligand molecule.

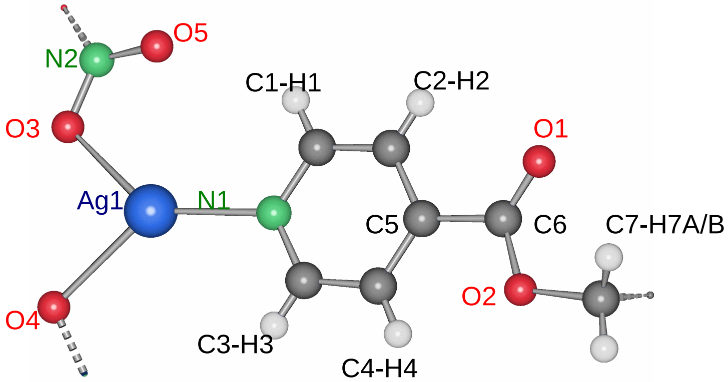

Figure B-34: asymmetric unit in 6

Ligand molecules, silver atoms and nitrate counter anions are organized so that a neutral two-dimensional motif appears. This motif is called "fishbone"-like layer. (Figure B-35a)

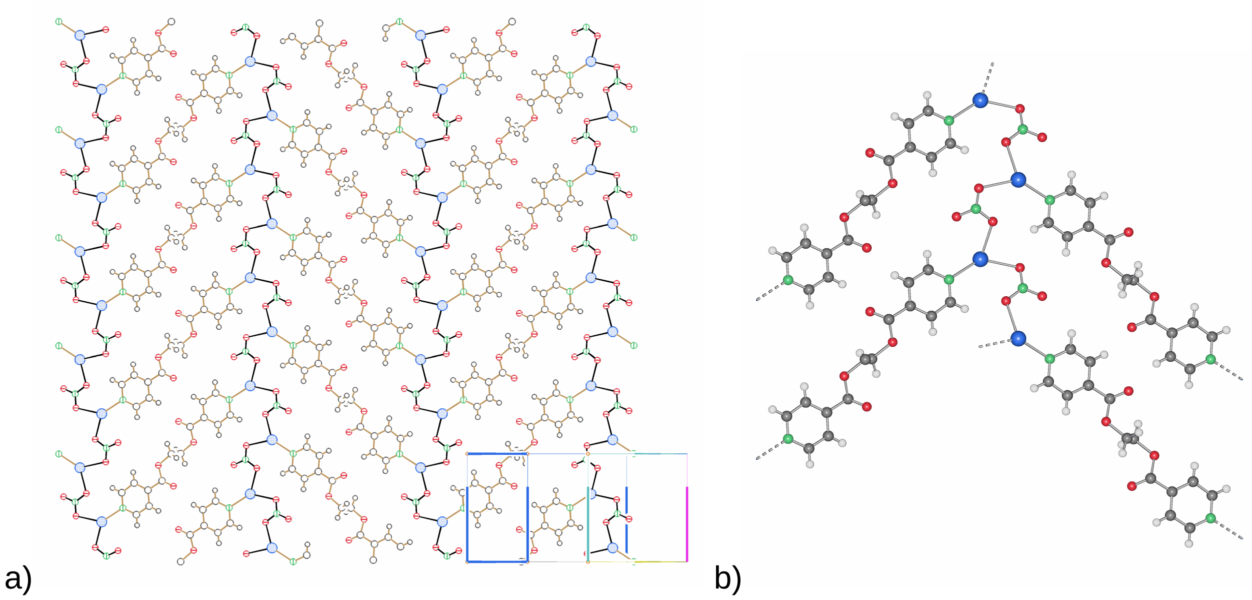

Figure B-35: a) the two-dimensional "fishbone" motif in 6; b) detail around the silver atoms

It is evident that the motif is constituted by silver-nitrate chains (in the *c* direction), which are linked through the ligand molecules. Each silver atom is coordinated with one ligand molecule (the distance Ag-N is with 2.226(7) Å in the same range than in **3**, **4** or **5**) and with two nitrate counter anions (the distances Ag-O are 2.354(5) and 2.390(7) Å long) This corresponds to short silver nitrate distances showing a strong coordination bond (Figure B-35b). The silver-oxygen distances belong to the shortest ones known from the literature [184, 263, 264]. The ligand molecules are running in symmetric directions on both sides of the silver-nitrate chain, explaining the "fishbone" name. The main structure is made of -Ag-NO_3-Ag-NO_3- chains, arrangement probably due to the poor solubility of $AgNO_3$ in ethanol unable to completely dissolve the silver nitrate contacts.

The conformation of the ligand is *anti* as in the free ligand. The pyridine planes within a ligand molecule are parallel as there is an inversion center in the middle of the C7-C7$^{\#1}$ bond, the two planes being separated by 0.46(5) Å. The plane containing the pyridine ring and the plane containing the adjacent ester group form an angle of 10.1(8)°. There is one hydrogen bond between the oxygen atom O1 and the hydrogen atom H7B within a ligand molecule. (Table B-20) This intra-ligand hydrogen bond can appear as the ligand is highly distorted with a O2-C7-C7$^{\#1}$ angle of 77(3)°. (Figure B-36) The position of O2 is distorted: this atom position was spilt into two positions with 50% occupancy (O2A and O2B in the crystallographic data). In spite of this distortion, the distance silver-silver is 17.76 Å long, corresponding to the same silver-silver distance observed in the coordination polymers with the *anti*-conformation of **L**, **3** and **5**. The distortion is compensated by longer bonds oxygen-carbon of *ca.* 0.04 Å compared to **3** and **5**.

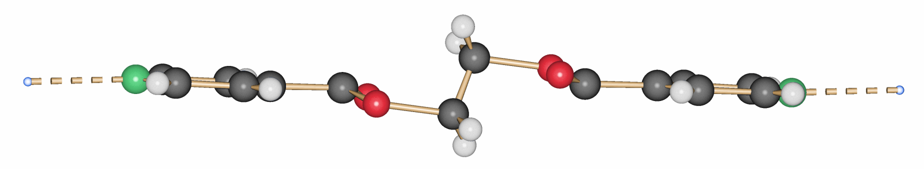

Figure B-36: top view of the ligand in 6 with the distortion

Some other weak interactions can be observed within the layer (Figure B-37, Table B-21): *i)* There are hydrogen bonds between two parallel ligand molecules (2.38 Å). *ii)* Furthermore the nitrate anions are involved in hydrogen bonding to the surrounding pyridyl hydrogen atoms, ranging from 2.46 to 2.89 Å.

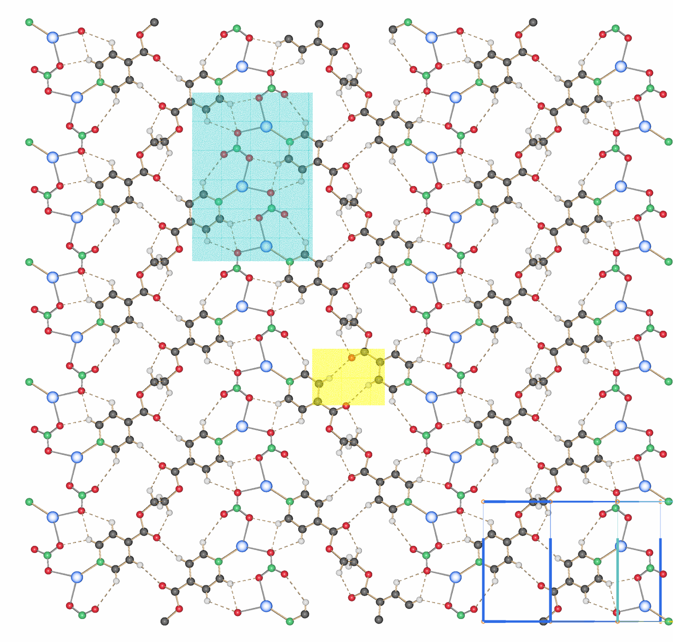

Figure B-37: intra-sheets interactions in 6: hydrogen bonds between ligand molecules in yellow and hydrogen bonds involving the nitrate counter anions in blue

The layers are stacked parallel to each other to form the overall three-dimensional structure. (Figure B-38a) The layers are flat; however the silver atoms don't exactly lie in the mean plane of the layers. If one considers the three atoms around one silver atom (N1, O3 and O4), the sum of the three angles (O3-Ag-N1, N1-Ag-O4, O4-Ag-O3) is smaller that 360° (358°) indicating a weak deformation of the trigonal planar coordination sphere of the silver atom. Indeed the silver atoms coordinate perpendicularly to the layer plane with nitrate O5 atoms at a distance of 2.72(1) Å. This distance Ag-O is longer than the ones with O3 and O4 but is in the range of those of weak coordinating nitrate anions.

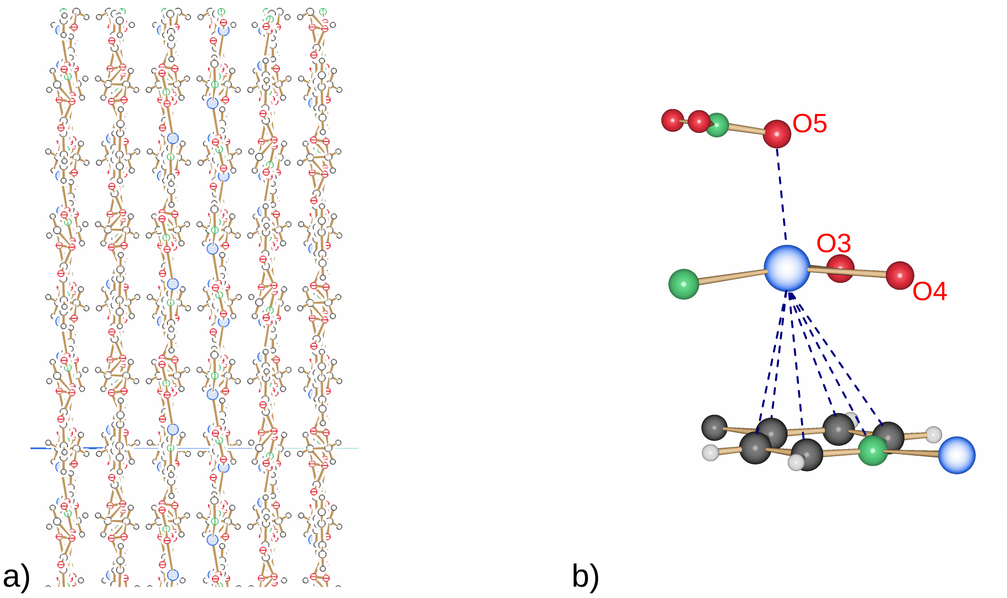

a) b)

Figure B-38: a) three-dimensional structure of 3 in the direction (11 0 10); b) coordination environment around silver atoms in 6

Furthermore there is a metal-ring interaction on the other side of the silver atom. (Figure B-38b, Table B-22) No other interactions were found between two layers except these interactions involving silver atoms.

Table B-20: Most important bond lengths (Å) and angles (°) in 6

Ag-N	2.226(7)	O-Ag-N	138.2(3), 135.3(2)
		O-Ag-O	84.6(2)
Ag-O(O_2N)	2.354(5), 2.390(7)		
	2.72(1)		
C-N	1.334(8), 1.35(1)	C-N-C	118.6(6)

Table B-21: Hydrogen bond data for 6 [lengths (Å) and angles (°)]

D-H···A	*d*(D-H)	*d*(H···A)	*d*(D···A)	Angle D-H···A
Intra-ligand				
C7-H7B···O1$^{\#1}$	0.97	2.37	2.98(3)	120.6
Intra-sheets hydrogen interactions				
C2-H2···O1$^{\#2}$	0.93	2.38	3.27(1)	161.2
C3-H3···O3$^{\#3}$	0.93	2.49	3.29(1)	143.7
C3-H3···O4$^{\#3}$	0.93	2.46	3.167(9)	132.9
C4-H4···O4$^{\#3}$	0.93	2.89	3.37(1)	113.0
C1-H1···O5	0.93	2.80	3.55(1)	137.8

Symmetry transformations used to generate equivalent atoms: #1 -X, -Y-1, -Z; #2 -X, -Y, -Z; #3 -X+1/2, Y-1/2, -Z+3/2.

Table B-22: Ag···pyridine ring interactions lengths (Å) and angles (°) in 6

	$d_{M\text{-}R}$	$pd_{M\text{-}R}$	β
Ring (N1, C1, C2, C3, C4, C5)···Ag1[#1]	3.472	3.357	14.77
Symmetry transformations used to generate equivalent atoms: #1 X, -Y, Z+1/2			

To our knowledge, this is the first example of two-dimensional neutral silver coordination polymer, with a trigonal planar coordination of silver $\{AgO_2N\}$ and this motif. Some $[\text{-Ag-}(NO_3)\text{-}]_n$ are found in the compound $\{[Ag(1,4\text{-bis(phenylthio)butane})(NO_3)]\}_n$ [184], in which the Ag^I center is tetrahedrally coordinated to two S atoms from the ligand and two O atoms from nitrate anions. The structure may be described as $[\text{-Ag-}(NO_3)\text{-}]_n$ linked *via* the ligands as in **6**, but with a different coordination environment for the silver ion and longer silver-nitrate distances (2.452(6) and 2.557(6) Å).

III.2.b - $\{[Ag(L)](NO_3)\}_n$ 7

The crystallization of silver polymers using silver nitrate was also performed in acetonitrile. Both solutions of **L** and silver nitrate in acetonitrile are mixed, stirred and then left at room temperature (C = 5.10^{-3} mol.L^{-1}). Self-assembly between silver and **L** occurs in the darkness giving colorless single crystals of $\{[Ag(L)]NO_3\}_n$ **7** suitable for X-ray diffraction. The quantity of crystals was not sufficient to perform other analyses on this sample. However the reaction of **L** and $AgNO_3$ in dichloromethane gives a white polycrystalline precipitate. Its powder X-ray spectrum was compared to the calculated one (from single crystal data) showing that the precipitate is isostructural to **7**. This precipitate was thus used for the further characterizations.

In order to get information on the existence of coordination polymers or oligomers in solution, electrospray-ionization mass spectroscopy was performed. With a solution of compound Ag(**L**)NO_3 in CH_3CN, no species were detected, except $[Ag(CH_3CN)]^+$ and $[Ag(CH_3CN)_2]^+$ (149 and 190 m/z respectively). Acetonitrile can easily coordinate the silver ions and the main species in solution are silver-acetonitrile complexes. Nevertheless, if we use a solvent mixture CH_3CN/CH_2Cl_2 (10/1) peaks are found at well identifiable m/z with a good isotopic resolution: 273.2, [**L**H]$^+$; 379.1, [**L**Ag]$^+$; 549.9 [**L**$Ag_2(NO_3)$]$^+$; 650.9 [$\mathbf{L}_2$Ag]$^+$; 718.6 [**L**$Ag_3(NO_3)_2$]$^+$; 821.7 [$\mathbf{L}_2Ag_2(NO_3)$]$^+$; 990 [$\mathbf{L}_2Ag_3(NO_3)_2$]$^+$; 1161.3 [$\mathbf{L}_2Ag_4(NO_3)_3$]$^+$; 1262.2 [$\mathbf{L}_3Ag_3(NO_3)_2$]$^+$; 1432.6 [$\mathbf{L}_3Ag_4(NO_3)_3$]$^+$ m/z.

Other electrospray ionization mass spectroscopy studies were performed in order to follow the evolution of the distribution of the above species in solution as a function of time and ligand to metal proportion. Solutions with $M_2\mathbf{L}$, $M\mathbf{L}$, $M\mathbf{L}_2$ proportions were prepared and measured just after mixing **L** and $AgNO_3$ and after 24 hours. The results are shown in Table B-23.

Table B-23: Resume of the detected peaks (the main peaks are presented with the relative abundance ratio (%)) for the three tested solutions at 0 and 24H.

	M_2L		ML		ML_2	
	0	24 H	0	24 H	0	24 H
$[LH]^+$	ø	ø	√(2%)	ø	√(6%)	√(11%)
$[LAg]^+$	√(11%)	√(7%)	√(3%)	ø	√(1%)	√(4%)
$[LAg_2(NO_3)]^+$	**√(100%)**	**√(100%)**	**√(34%)**	**√(37%)**	√(18%)	√(26%)
$[L_2Ag]^+$	ø	ø	√(9%)	√(19%)	√(18%)	**√(69%)**
$[LAg_3(NO_3)_2]^+$	**√(52%)**	**√(69%)**	√(14%)	**√(37%)**	√(2%)	√(5%)
$[L_2Ag_2(NO_3)]^+$	**√(80%)**	**√(31%)**	**√(100%)**	**√(100%)**	**√(100%)**	**√(100%)**
$[L_2Ag_3(NO_3)_2]^+$	**√(45%)**	√(24%)	**√(30%)**	**√(60%)**	√(12%)	√(19%)
$[L_2Ag_4(NO_3)_3]^+$	**√(62%)**	**√(36%)**	√(18%)	**√(60%)**	√(5%)	√(7%)
$[L_3Ag_3(NO_3)_2]^+$	ø	ø	√(2%)	√(10%)	√(3%)	√(3%)
$[L_3Ag_4(NO_3)_3]^+$	√(18%)	√(8%)	√(7%)	**√(30%)**	√(3%)	√(4%)

Almost all species were found in each solution and a all times. For each solution, the main species are found whatever the reaction time: the distribution of the compounds in the solution is similar at t = 0 and t=24 H. In the solution $M_2\mathbf{L}$, the main species is $[\mathbf{L}Ag_2(NO_3)]^+$ and species containing more Ag than **L** are favoured; in the solution $M\mathbf{L}$, a more important variety of species is observed; in the solution $M\mathbf{L}_2$, only compounds $[\mathbf{L}_2Ag]^+$ and $[\mathbf{L}_2Ag_2(NO_3)]^+$ are mainly found.

These results indicate that in all cases oligomeric fragments of coordination polymers are formed. This is in agreement with the fact that only the compound $\{[Ag(\mathbf{L})]NO_3\}_n$ is obtained by changing the metal to ligand stoechiometry for the reaction. Indeed the fact that many species are present indicates a fast complexation exchange. The acetonitrile is in concurrence with the pyridine groups of the ligand for the complexation of silver. The peaks corresponding to $[Ag(CH_3CN)]^+$ and $[Ag(CH_3CN)_2]^+$ (149 and 190 m/z respectively) are in fact found in the mass spectra.

Compound **7** crystallizes in the triclinic space group *P*-1 (no.2). The asymmetric unit is composed of one ligand molecule, one silver atom and one nitrate anion (Figure B-39) and there are two of such moieties in the unit cell. The most important bond lengths and angles are listed in Table B-24.

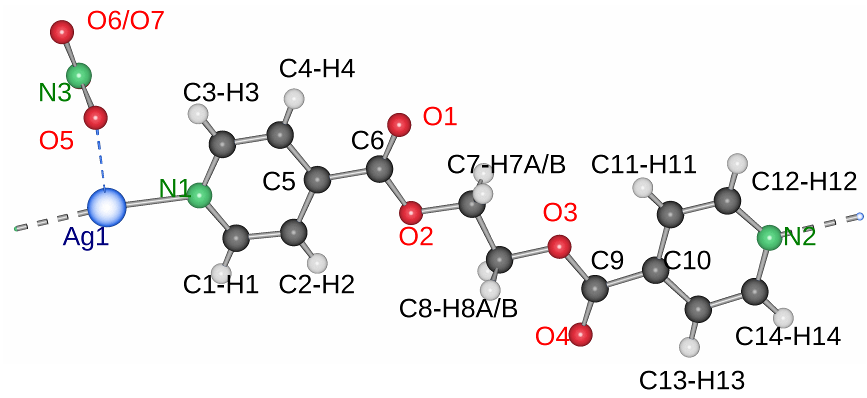

Figure B-39: asymmetric unit in 7

In this case the silver atoms are coordinated by two different ligands through their nitrogen atoms. The ligand molecules act thus as connectors between the silver atoms, the final motif being a charged one-dimensional chain. (Figure B-40) The distances silver-nitrogen are 2.183(4) and 2.189(4) Å long and the N-Ag-N angle is 169.8(2)°.

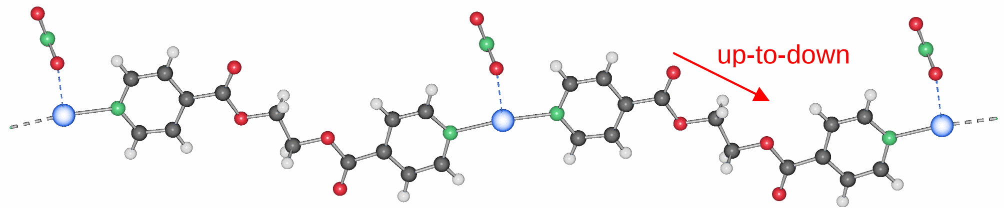

Figure B-40: The linear motif in 7

The linearity in the chain is due to the *anti*-conformation adopted by the ligand molecules. The ligand molecules alternating with the silver atoms have all the same direction: “up-to-down”. The distance silver-silver within the chain is thus 17.66 Å long as in **1**, **3**, **5** and **6** where the ligand is in *anti* conformation. The coordination sphere of the silver atoms is completed thanks to interactions with the nitrate counter-anions. All three nitrate oxygen atoms are linked to silver atoms, that means that the nitrate anions stay as linkers in between the chains (Figure B-41). The silver-oxygen distances range from 2.599(5) to 3.122(4) Å. These distances in **7** are by 0.25 Å longer on average than in **6** and smaller than in **3**, **4** and **5**. The N-Ag-N deformation from 180° is due to the stronger Ag1-O5 interactions (2.599(5) Å). Some hydrogen bonds (C8-H8B···O1) allow the alignment of the chains and thus the formation of the neutral layer. The shortest distance between the silver atoms in the layer is 6.159(1) Å.

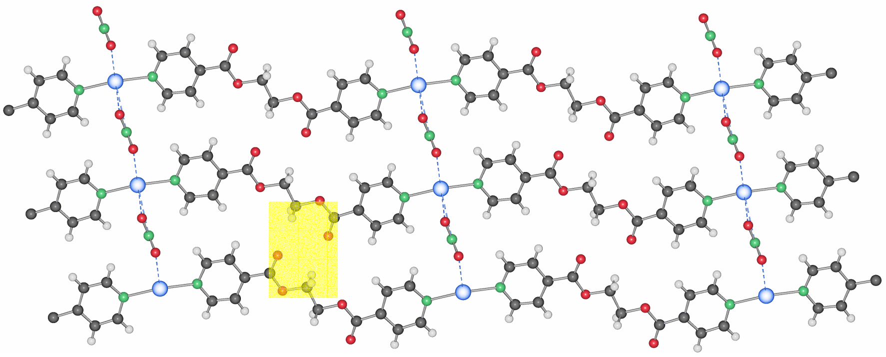

Figure B-41: alignment of the chains in 7 with the nitrate as linkers and the hydrogen bond region in yellow

As shown on Figure B-42a, the chains are ordered in the direction (-12 10 22) with a slight inclination of the molecular mean plane compared to this direction, the counter anions lying only on one side of the chains. Indeed the coordination of the nitrate molecules is not distributed all around the silver atoms but they are found only on one side. (Figure B-42b) In the three-dimensional structure of **7**, the layers stack parallel together in alternating their orientations: the nitrate anions are pointing in one direction and in the next layer they are pointing in the opposite one. (Figure B-42c)

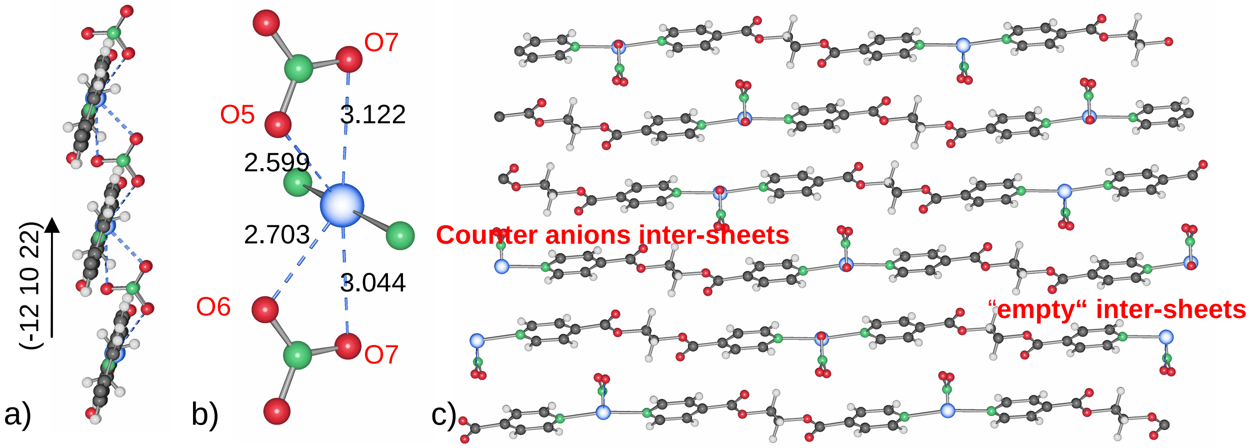

Figure B-42: a) organisation of the chains and the nitrate anions within a layer; b) coordination of silver; c) stacking of the layers in the structure of 4

Two types of inter-sheet areas are thus created: in the first one the anions are found, and in the next one the chains are simply parallel to each other, as described in the Figure B-43b.

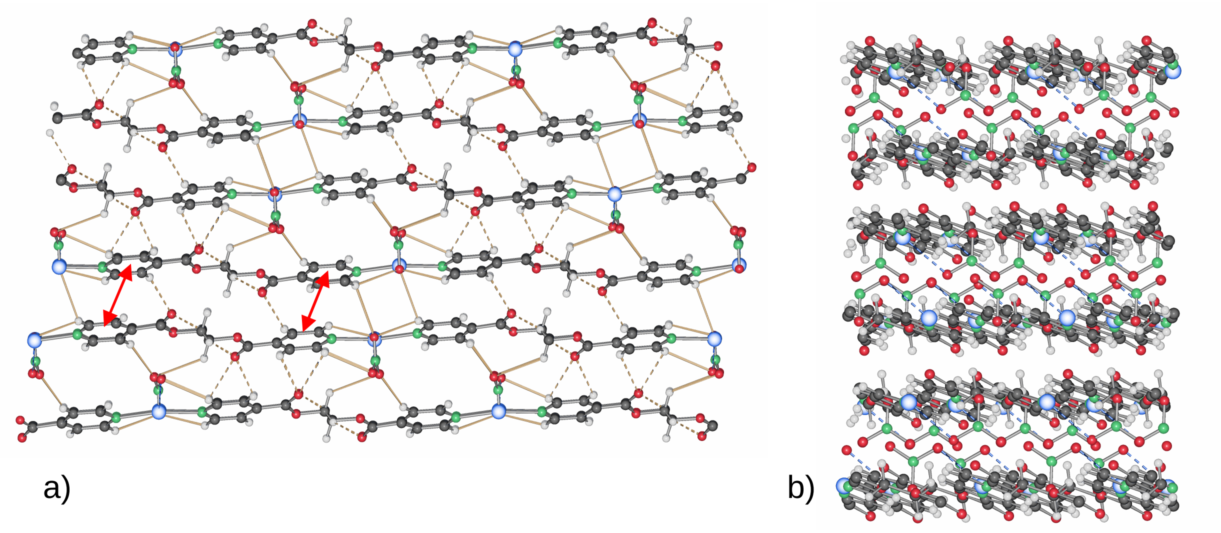

Figure B-43: a) three-dimensional structure of 7 with the inter-sheets interactions (red arrows: π-stacking in the empty inter-sheets; dashed lines: hydrogen bonds between ligands; full lines: hydrogen bonding involving the nitrate anions) b) View of the stacked layers in 7

As there are two types of inter-sheets, there are various complementary interactions between the layers. (Figure B-43a) In the “empty” inter-sheets, the layers interact thanks to π-stacking (Table B-26) between the rings N1, C1…C5 and N2, C10…C14 with a center-center distance of 3.82 Å and an offset of 1.5 Å. The silver-silver distances are 4.017(2) Å long and are not the shortest contact between two chains as in **4** and **5**. The same pairs of chains than in **4** and **5** appear but as the counter ion role is different, only the π-stacking remains. The much shorter Ag-Ag distances of **4** and **5** need thus to be supported by the nitrate anions.

The overall arrangement is strengthened with hydrogen bonds between the ligand molecules of two close layers and also between the nitrate anions and neighbouring ligand molecules (Figure B-43a). These interactions take place in the two kinds of inter-sheet layers (Table B-25).

Table B-24: Most important bond lengths (Å) and angles (°) in 7

Ag-Ag	4.017(2)		
Ag-N	2.183(4), 2.189(4)	N-Ag-N	169.8(2)
Ag-O(O_2N)	2.599(5), 2.703(7)		
	3.044(4), 3.122(4)		
C-N	1.342(5), 1.343(7)	C-N-C	117.5(4)
	1.352(6), 1.347(5)		116.6(4)

Table B-25: Hydrogen bond data for 7 [lengths (Å) and angles (°)]

D-H···A	*d*(D-H)	*d*(H···A)	*d*(D···A)	Angle D-H···A
Inter-chains interactions				
C8-H8B···O1[#1]	0.97	2.64	3.580(7)	163.4
intra-sheets hydrogen interactions				
C11-H11···O1[#2]	0.93	2.79	3.648(7)	153.2
C13-H13···O3[#3]	0.93	2.63	3.195(7)	119.3
C14-H14···O4[#3]	0.93	2.85	3.316(6)	112.3
C7-H7A···O4[#4]	0.97	2.50	3.436(7)	161.9
Hydrogen bonds involving nitrate anions				
C1-H1···O7[#4]	0.93	2.65	3.403(7)	138.9
C12-H12···O7[#4]	0.93	2.58	3.309(8)	135.3
C1-H1···O7[#5]	0.93	2.80	3.38(1)	121.3
C4-H4···O6[#3]	0.93	2.53	3.390(8)	154.7
C8-H8A···O6[#3]	0.97	2.83	3.494(7)	126.5
C14-H14···O5	0.93	2.65	3.308(9)	128.3

Symmetry transformations used to generate equivalent atoms: #1 X+1, Y, Z; #2 -X, -Y+2, -Z+2; #3 -X+2, -Y+1, Z+1; #4 X-1, Y, Z; #5 -X+1, -Y+2, -Z+2.

Table B-26: ring interactions lengths (Å) and angles (°) in 7

π-π interactions	d_{R-R}	pd_{R-R}	β	α
Ring (N1, C1, C2, C3, C4, C5)···Ring (N2, C10, C11, C12, C13, C14)[#1]	3.82	3.49	24.0	2.1

Symmetry transformations used to generate equivalent atoms: #1 -X+2, -Y+1, -Z+1.

Compound **7** is a structural supramolecular isomer of **3** (same Ag-ligand-nitrate system), showing apparently the same arrangement: one-dimensional chain, nitrate anions in between the chains. But paradoxically, the structure of **7** is closer to the structure of **5**. Both one-dimensional motifs are similar, the apparition of pairs of chains with π-stacking within the pairs, the parallel stacking of the pairs of chains with other π-stacking and the overall parallel stacking in order to build the three-dimensional network are also very similar. (Figure B-44) It seems that the presence of water molecules in **5** has just increased the separation between the layers, the structural changes in **5** and **7** may be compared to the swelling of clays in case of water infiltration.

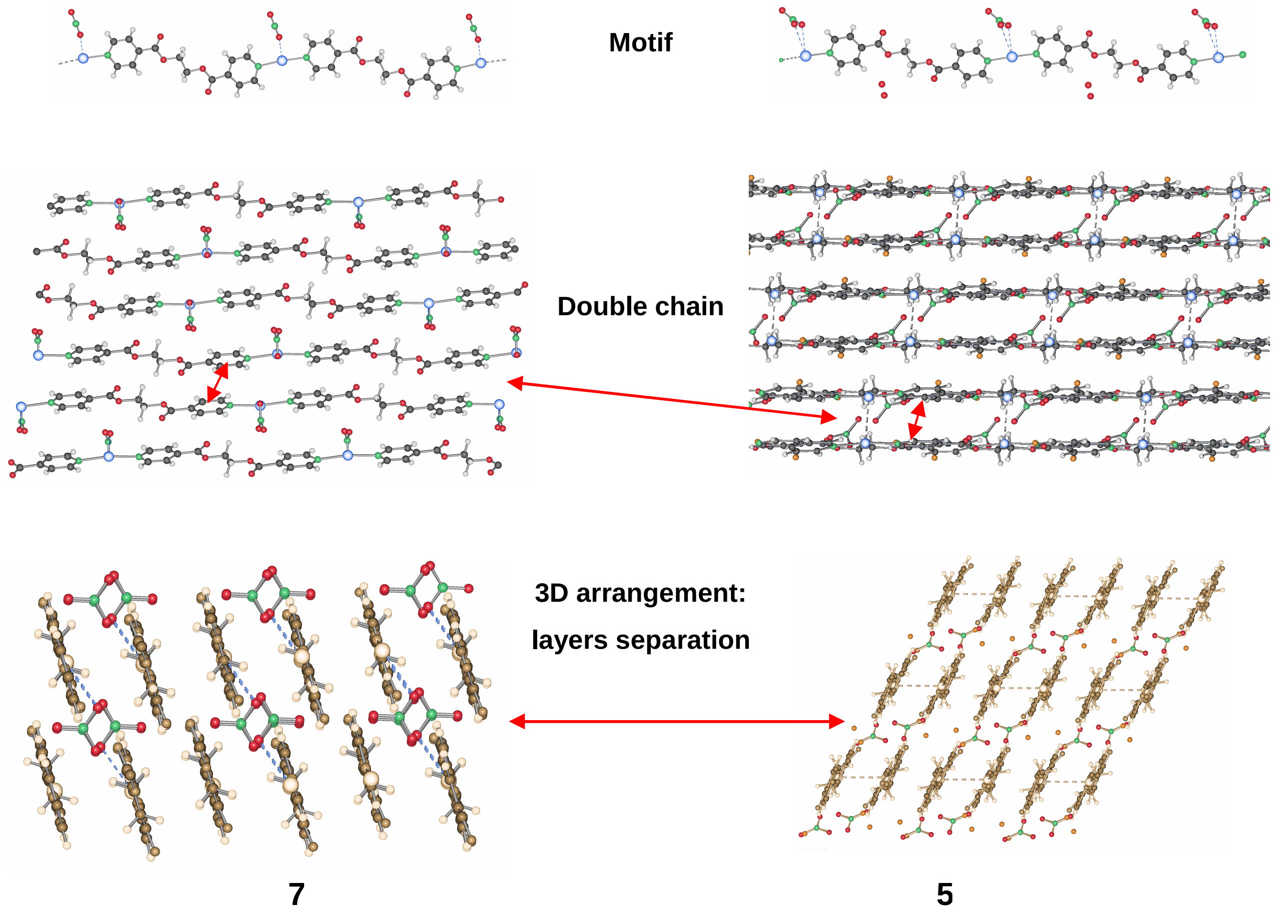

Figure B-44: structural comparisons between 7 and 5

It can be thus assumed that the interactions nitrate-water molecules are the only ones responsible for the structural differences in **7** and **5**. However, the cell parameters for **5** and **7** do not show any correlation which means that more than simple water elimination is necessary to explain the transformation of one to another.

III.2.c - Solvent influence

It has been stated that the silver coordination polymer one-dimensional motifs including linear ligands with a poor delocalized π-system and moderately coordinating counter anions (such as nitrate) tend to arrange themselves parallel in the structure and that the coulombic repulsion between the Ag^I centers cannot be compensated by a strong face-to-face ligand stacking or by the coordination of the counter-anions to silver. [11] So, which is the behaviour of **L** in the $AgNO_3$ coordination polymers when diverse solvent conditions are applied?

It is worthy noting that silver nitrate has different solubilities in the used crystallization solvents, allowing more or less good solvatation of the ions. The comparison of the average silver-nitrate distances in the solid and the solubility of the silver salt in the different solvents is shown on Graph B-3.

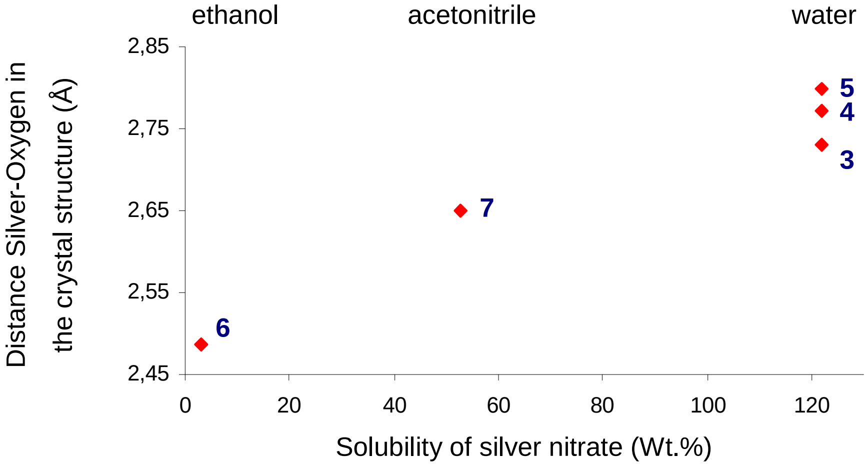

Graph B-3: average distances Ag-O(NO_2) in compounds 3 to 7 in function of $AgNO_3$ solubility

There is thus a link between these silver-nitrate distances and the solubility of silver nitrate in mother liquor. The worst solvent for silver nitrate is ethanol and the best is water. This bad solubility of $AgNO_3$ in ethanol can explain the short distances Ag-nitrate in the solid state in **6** and also the existence of the silver nitrate chains. On the other hand, the good solubility of $AgNO_3$ in water prevents Ag and nitrate to be so close. According to these results, it can be said that the solubility seems to be a major parameter for the crystallization. As far as we know this dependence has never been outlined in the literature.

However the importance of the solvent choice is known, without being clearly studied. The solvents are usually classified in two categories: the coordinating and the non coordinating ones. In compounds **4** or **5**, the solvent molecules co-crystallize without being cation coordinating solvents. Weak solvation of the anions by the solvent remains.

In the literature, numerous examples of silver coordination polymers with solvent molecules in the first coordination sphere can be found. The coordinated solvent molecules are water [73, 151, 170, 265], acetonitrile [72, 154, 244, 266-270] or methanol [184]. Water molecules can be directly coordinated to silver ions even in the presence of nitrate as counter anion. In $\{[Ag(1,3\text{-bis(2-pyridylethynyl)-2-methyl-benzene})(NO_3)(H_2O)]\}_n$, there are two crystallographically and chemically different silver ions: both have a distorted tetrahedral coordination sphere containing two ligand nitrogen atoms in addition with either an anisobidentate nitrate anion or a monodentate nitrate anion and a water molecule. [151] This compound grows from mixture of a solution of ligand in acetone and a solution of silver nitrate in water, illustrating the possible competition in coordination between the water molecules and the nitrate anions.

Acetonitrile has a favourable affinity toward silver ions in the liquid phase, it is also more easily involved in the coordination sphere of silver in the resulting coordination polymer structure. Reger *et al.* state that if compounds are crystallized from the coordinating solvent acetonitrile, the anions have less effect on the structure. [268] For instance, the silver ion has a {AgN(pyridyl)$_2$N(acetonitrile)O(nitrate)$_2$} coordination sphere in the compound {[Ag(2,2',3"-tripyridylamine)(NO_3)(CH_3CN)]$_n$ [270]. When crystals grow from the mixture **L**/$AgNO_3$ in acetonitrile, we do not observe the formation of such compounds in the solid state. Crystals of **7** do not contain any acetonitrile molecule.

The used solvents are not the unique important factor but also the crystallization techniques have to be carefully regarded. The "H-shaped" tubes allow the slow diffusion of the reagents, and mostly the crystals are of better quality. The drawbacks of this technique are the weak concentration and the non-homogeneous conditions depending on the localization in the tube. Indeed the crystallization can occur in one or the other arm, on the fritt if present, at the solvent/air interface, in the curved part etc... where the concentration and the ratio metal to ligand can be locally different. However, we always get pure phases during the direct mixing: **3** crystallizes in a THF/water solution of L and $AgNO_3$; **7** is obtained in a solution of both reagents in acetonitrile. The comparison between the diffusion techniques and the direct self-assembly methods is made by Champness and Schröder [271]. Contrary to us, their recommended method is the diffusion technique. They obtained mixtures of products with direct methods.

Another solvent influence in the formation of coordination polymers based on flexible organic ligand is the correlation between the presence of inclusion solvent molecules in the structures and the conformation of the ligand. In **2** and **4**, the presence of respectively THF or water molecules coincide with the *gauche*-conformation. However in **5**, water molecules co-crystallize and the ligand has the *anti*-conformation. In all other products, the ligand adopts the *anti*-conformation as in free **L**. It can be concluded that the presence of co-crystallized solvent molecules (not coordinating) may induce the change of conformation of the ligands in the crystallographic structures from *anti* to *gauche*. This confirms previous findings [196].

III.3 - Counter ion influence

After this variety of **L** and $AgNO_3$ containing-coordination polymer structures, we also chose to vary the counter ions, using less coordinating ones than nitrate in order to investigate the differences and the similarities in the bond and interaction formation.

III.3.a - $\{[Ag(L)]CF_3SO_3\}_n$ 8

The coordination polymer based on silver triflate and **L** crystallizes in a “H-shaped” tube in the darkness at room temperature: a solution of **L** in THF diffuses into a solution of $AgCF_3SO_3$ in water through THF and a fritt. After one day, crystals of $\{[Ag(L)]CF_3SO_3\}_n$ **8** appear at the interface THF/water. They are suitable for single crystal X-ray diffraction, and they are obtained in a relative good yield.

8 are also obtained thanks to the direct reaction of **L** and $AgCF_3SO_3$ in dichloromethane. This mixture gives a white polycrystalline precipitate. Its powder X-ray spectrum and the theoretical spectrum for **8** (calculated from the single crystals X-ray data) show that the two compounds are isostructural (Figure B-45). The concordance between the two spectra is good, only a slight shift after 20° is observed.

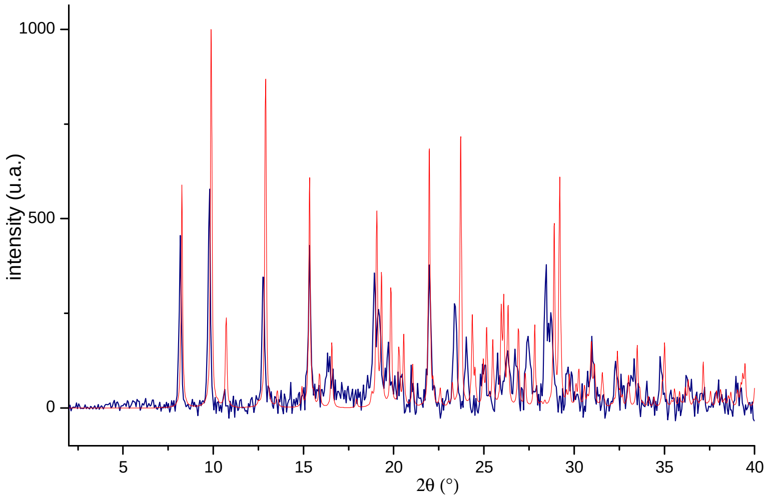

Figure B-45: comparison between the single crystal X-ray and the powder X-ray spectra of 8

8 crystallizes in a monoclinic space group $P2_1/c$ (no.14) as thin and colorless plates. The asymmetric unit is formed by one silver atom, one ligand molecule and one triflate molecule, the unit cell containing four asymmetric units. As shown on Figure B-46 there are two types of ligand molecules in the structure: *i)* the one numbered from N1 to $N1^{\#1}$ (symmetrical equivalent) called L1; *ii)* the second numbered from N1A to $N1A^{\#2}$ called L2. The important bond lengths and angles are listed in Table B-27.

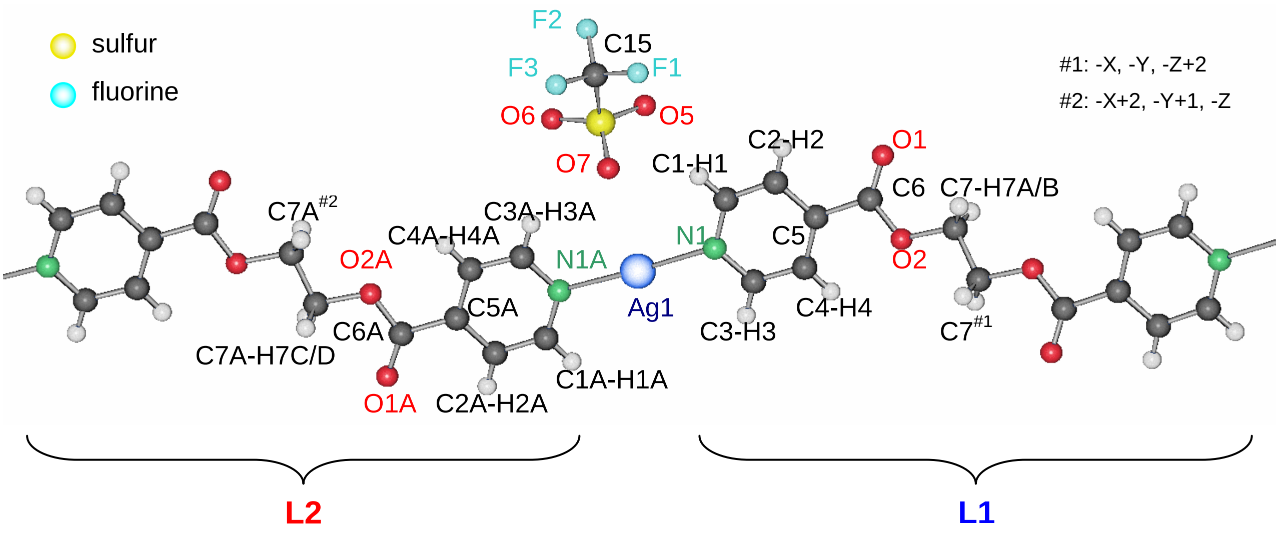

Figure B-46: unite asymmetric in 8 (S in yellow and F in blue)

The structural motif in **8** is a one-dimensional one: silver atoms and ligand molecules alternate in order to form a charged chain. (Figure B-47) The silver atoms are thus coordinated with two different ligand molecules. The angle N1-Ag1-N1A is 177.61(6) Å, and the distances Ag1-N1 and Ag1-N1A are similar with 2.159(2) Å. The counter anion triflate interacts only weakly with the silver atom *via* the O7 oxygen atom at a distance of 2.804(2) Å, the deformation of the angle N-Ag-N around Ag is not attributed to this interaction. In the literature, the distances silver-triflate are mainly ranged from 2.4 to 2.8 Å [167, 169, 178, 180, 270]. The silver-triflate interactions in **8** belong thus to the weakest ones. The distances silver-oxygen(counter ion) are in the same range than in **5**, in which the nitrate anions are the least coordinated of the $AgNO_3$ coordination polymers. The charge on silver has to be more compensated by the nitrogen donor ligand in the cases of poor coordinating anions, as it happens in **8** and **5**, in which the silver-nitrogen distances are the shortest.

Along the chain, the ligand molecule direction is always the same: “up-to-down”. The distance between two silver atoms in a chain is 17.46 Å, as the ligand is in the *anti*-conformation.

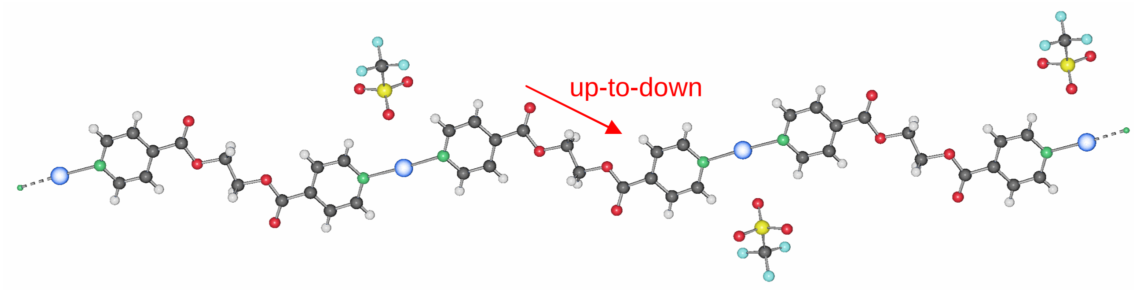

Figure B-47: chain motif in 8

The pyridine units are in *anti*-position of the ethyl linking units with the two carbonyl groups pointing alternatingly up and down. This conformation is similar to the conformation of the molecules in the structure of free **L**. The pyridyl groups within a ligand lie in parallel planes due to the inversion center in the geometrical middle of the C7-C7$^{\#1}$ (C7A-C7A$^{\#2}$) bonds. However it's worthy to note why two types of ligand are distinguished within the structure: in L1, the shift between the latter planes within a ligand is 0.299(8) Å, but in L2, it is 1.242(9) Å. (Figure B-48) The silver atoms are thus not perfectly aligned with a slight undulation of the chain due to the important difference in the angles between the plane containing the pyridine group and the adjacent plane containing the ester group (5.3(4)° in L1; 12.0(3)° in L2). The all-over chain motif is -Ag-L1-Ag-L2-Ag-L1-.

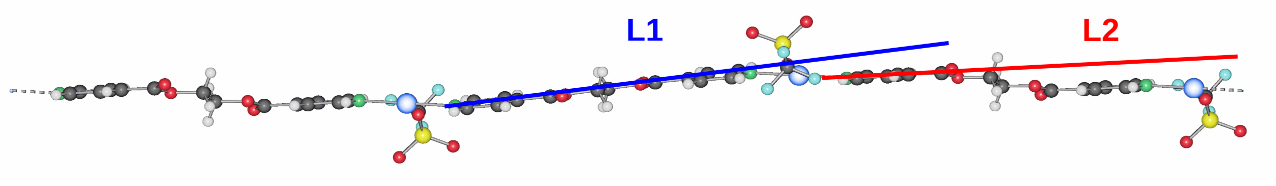

Figure B-48: chain motif in 8 with the deformation of L2 toward L1

The chains interact together to give firstly a two dimensional motif (Figure B-49a). In these layers, the chains remain parallel to each other and are connected thanks to two interaction types: *i)* Hydrogen bonding takes place between a ligand L1 and a ligand L2: C2A-H2A···O1 (2.81 Å) and C2-H2···O1A (2.68 Å) and form a 10-membered hydrogen bonding system. *ii)* The triflate anions act as linkers between the chains: a triflate anion is coordinated to a silver atom through an oxygen atom of the -SO_3 groups; this -SO_3 oxygen atom forms hydrogen bounds with the hydrogen atoms of the two pyridines coordinated to the same silver atom (C3-H3···O7 and C1A-H1A···O7 with 2.48 and 2.58 Å); the fluorine atoms of the considered triflate anion are furthermore involved in C-H···F bonds with the ethyl hydrogen atom (H7A) and pyridine hydrogen atom (H4) of the adjacent chain, with distances of 2.72, 2.81 and 2.82 Å. The interactions between the -CF_3 groups in the coordination polymers containing triflate ions are not well documented. In {[Ag(2,2',3''-tripyridylamine)(CF_3SO_3)]}$_n$, the triflate anions link two adjacent chains and the C(-H)···F distance is 3.60(2) Å long with an angle C-H···F of 136(1)° [270]. The H···F interaction parameters in **8** are in the same range (Table B-28). All hydrogen bond parameters are listed in the Table B-28. In the IR spectrum, the two ν(C-F) bands corresponding to the triflate molecule are shifted towards the bands in pure $AgCF_3SO_3$ salt (1249→1265 and 1176→1140 cm^{-1}), as well as the ν(S-O) band (1038→1026).

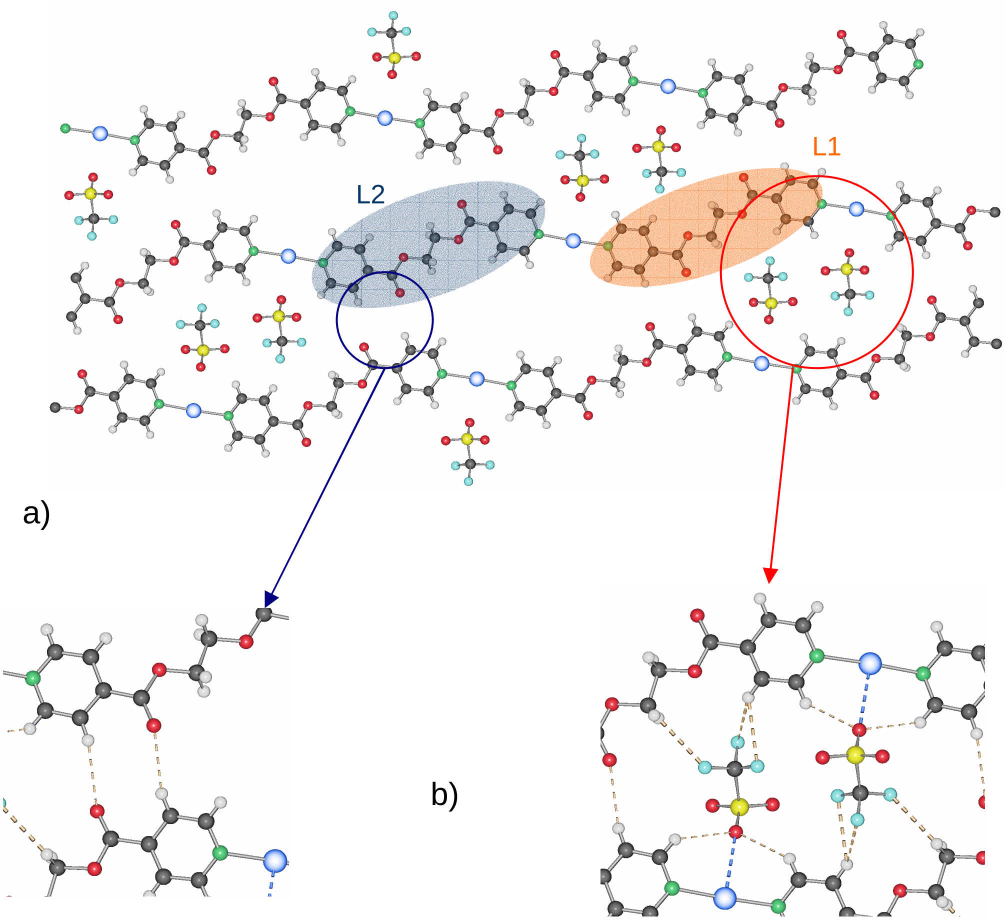

Figure B-49: a) arrangement of the chains in layers in 8: the ligands L1 are in front of the triflate molecules whereas the ligands L2 stay in front of the sheets cavities; b) details of the hydrogen networks

This weak interactions network creates some “cavities” in the layers whose size is *ca*. 6 Å × 15 Å. However this material is not porous, as the layers stack with triflate anions filling these cavities. Indeed, the layers stack parallel to each other and two adjacent layers are tilted by about 60°, the triflate anions of the first layer occupying the cavities of the next layer and so on. (Figure B-50a) The triflate anions do not lie in the plane of the sheets. (Figure B-51a) Each type of layers reappears after 4 superpositions. (Figure B-50b)

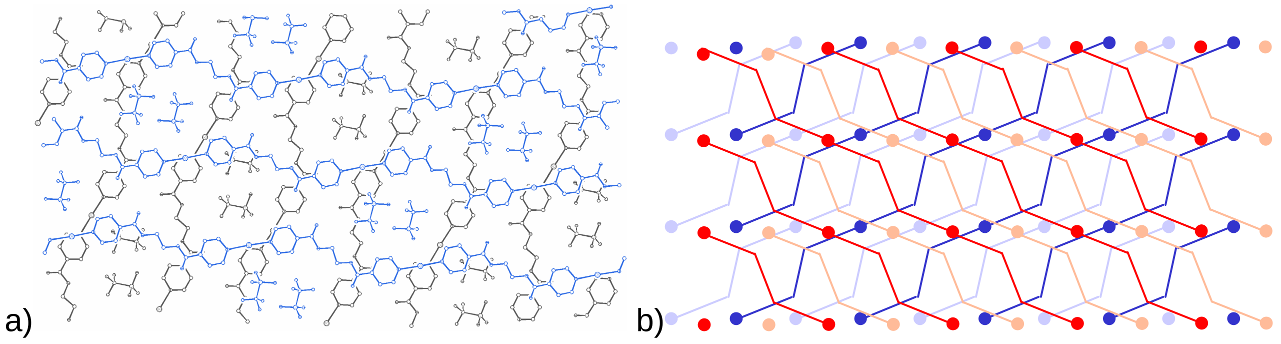

Figure B-50: a) two adjacent layers in 8, with the tilting angle and the position of the triflate anions in the cavities. b) Stacking of the layers in 8 (sheet S1 in red, sheets S2 in blue): S1A, S2B, S1C, S2D (A, B, C, D: stacking motifs of layers).

The average distance between two sheets is constant with 3.4 Å. There are several interactions between the layers: *i)* π-stacking takes place between a pyridine ring and a carbonyl group of the next layer (the average distance between the two groups is 3.5 Å). *ii)* Ag-pyridine ring interactions lead to the deformation of the N-Ag-N angle (Table B-29), the centroid-silver distances being *ca.* 3.5 Å long and the shift *ca.* 1.4 Å. *iii)* Weaker coordination bonds exist involving the O5 atom of a triflate anion (2.830(2) Å), the same triflate anion being already coordinated to a silver atom of another layer through its O7 atom. The triflate anion acts thus as bridge between two silver atoms, the distance silver-silver being however long (4.760(1) Å). The repulsion between the silver atoms avoids them to get closer to each other, as the triflate anion is not strongly coordinated to the silver ions as in the case of nitrate as counter anion in **4** and **5**. *iv)* Several hydrogen bonds are localized between the layers (Table B-28). The O5 atom coordinating the silver cations forms hydrogen bonds with the hydrogen atoms localized on the pyridine rings on each side of the involved silver. The triflate anions are also involved in hydrogen bonding through the O6 oxygen atom (which does not interact with Ag^{I} ions) with two ethyl hydrogen (H7B/D) and one pyridine hydrogen (H4A) of close ligands. The hydrogen bond network is completed with hydrogen bonds between ligand molecules of different layers (C1-H1···O1).

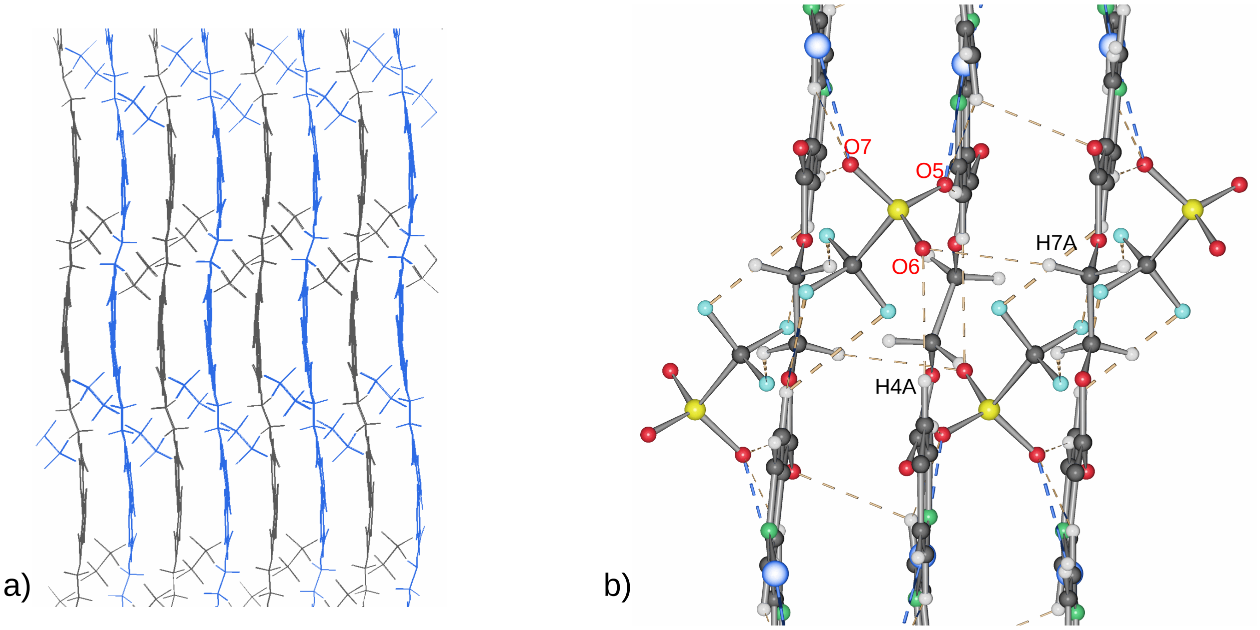

Figure B-51: a) View parallel to the layers in 8: the triflate anions stay in between the sheets; b) View of further interactions between the layers in 8

Table B-27: most important bond lengths (Å) and angles (°) in 8

Ag-N	2.159(2), 2.159(2)	N-Ag-N	177.61(6)
Ag-O(SO_2CF_3)	2.804(2), 2.830(2)		
C-N	1.343(3), 1.344(3)	C-N-C	118.2(2)
	1.343(2), 1.350(3)		118.4(2)

Table B-28: Hydrogen bond data for 8 [lengths (Å) and angles (°)]

D-H···A	*d*(D-H)	*d*(H···A)	*d*(D···A)	Angle D-H···A
intra-sheets hydrogen interactions				
C2-H2···O1A$^{\#1}$	0.93	2.68	3.579(3)	163.8
C2A-H2A···O1$^{\#2}$	0.93	2.81	3.708(3)	163.2
C7-H7A···F3$^{\#3}$	0.97	2.72	3.440(3)	131.2
C4-H4···F1	0.93	2.81	3.501(3)	131.9
C4-H4···F2	0.93	2.82	3.556(3)	136.9
C3-H3···O7$^{\#1}$	0.93	2.48	3.235(3)	138.0
C1A-H1A···O7$^{\#1}$	0.93	2.58	3.298(3)	134.7
C-H···O hydrogen interactions between the sheets				
C1-H1···O5$^{\#4}$	0.93	2.66	3.368(3)	133.8
C3A-H3A···O5$^{\#4}$	0.93	2.61	3.378(3)	140.4
C7A-H7D···O6$^{\#5}$	0.97	2.77	3.517(3)	134.4
C4A-H4A···O6$^{\#6}$	0.93	2.78	3.703(3)	173.6
C7-H7B···O6$^{\#7}$	0.97	2.74	3.554(4)	142.0
C1-H1···O1$^{\#8}$	0.93	2.70	3.239(3)	117.8

Symmetry transformations used to generate equivalent atoms: #1 X-1, Y, Z+1; #2 X+1, Y, Z-1; #3 -X, -Y, -Z+2; #4 –X+1, Y+1/2, -Z+3/2; #5 –X+2, Y+1/2, -Z+1/2; #6 X, -Y+1/2, Z-1/2 ; #7 -X+1, -Y, -Z+2 ; #8 X, -Y+1/2, Z-1/2.

Table B-29: Ag···pyridine rings interactions lengths (Å) and angles (°) in 8

	d_{M-R}	pd_{M-R}	β
Ring (N1, C1, C2, C3, C4, C5)···Ag1$^{\#1}$	3.317	3.159	17.55
Ring (N1A, C1A, C2A, C3A, C4A, C5A)···Ag1$^{\#2}$	3.606	3.098	30.78

Symmetry transformations used to generate equivalent atoms: #1 X, -Y+1/2, Z+1/2; #2 X, -Y+1/2, Z-1/2

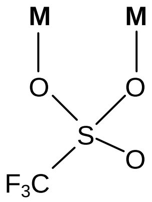

Triflate anions are regarded as “non-coordinating” anions, because the strong electron withdrawal of the -CF_3 moiety lowers the Lewis basicity of the -SO_3 group. Triflate anions can nonetheless weakly interact with Ag^I, due to its flexible coordination sphere [272]. The coordination mode for the sulfonate group in **8** was expected, as it is one of the known sulfonate coordination modes. The solid-state compound $[Ag(CF_3SO_3)(EtOH)_{0.5}]$ shows two-dimensional motifs, with two crystallographically different silver ions, respectively seven coordinate and nine-coordinate [273]. The triflate anions support silver-silver contacts of 3.327(2) and 3.060(1) Å, the silver-triflate distances ranging from 2.381(5) to 2.588(5) Å. A silver-silver contact supported by triflate anions remains in the structure of $\{[Ag(\mu$-3,6-bis(pyridin-3-yl)-1,2,4,5-tetrazine)]$(CF_3SO_3)\}_n$ [244], the silver-triflate distances being 2.740(4) and 2.839(4) Å. Triflate as bidentate ligand is also found in $\{[Ag($1,4-bis(2-pyridyl)butadiyne)$(CF_3SO_3)]\}_n$, with silver-triflate distances of 2.445(4) and 2.572(4) Å in order to build a two-dimensional motif [167] without silver-silver contacts.

According to the literature, the silver-triflate interactions occur with distances $Ag\cdots O(SO_2CF_3)$ ranging from 2.4 to 2.8 Å [167, 169, 178, 180, 270]. In these examples, triflate oxygen atoms are included in the coordination sphere of Ag^I, having a direct influence on the structural motif. Triflate anions have also an influence on the long range arrangement because of the $-CF_3$ moieties, which can lead to the formation of $F\cdots H-C$ interactions [270]. The triflate anions can thus act as pillars between the motifs. In **8** indeed, the triflate anions are linkers between the one-dimensional chains, even if the interactions with Ag^I is weak.

The motif in **8** is similar to the motif in **5** and **7**, but the long range organisation is rather different, due to the difference in size, shape and symmetry between nitrate and triflate. Yip and co-workers present two compounds {[Ag(*N,N*'-bis(3pyridinecarboxamide)-1,6-hexane)]$(NO_3)\}_n$ and {[Ag(*N,N*'-bis(3pyridinecarboxamide)-1,6-hexane)]$(CF_3SO_3)\}_n$ with similar zig-zag chains and similar packing in layers. The major difference between both coordination polymers is the inter-sheet distances, in correlation with the anion size.

Nevertheless, triflate counter anions are usually used to simply balance the charge in the lattice, the triflate anions acting as template [268, 270, 274]. Particularly, when the silver ion is coordinated by four ligand molecules, the triflate anion can not approach the silver ion due to steric inherence [275].

III.3.b - $\{[Ag(L)]ClO_4\}_n$ 9

The slow diffusion of a solution of **L** in THF into a solution of silver perchlorate in water leads to the formation of colorless and plate-like crystals of $\{[Ag(L)]ClO_4\}_n$, **9**. The crystals grow in the darkness after one day, they are suitable for single crystal X-ray diffraction.

Caution! Although no problem in handling perchlorate salts occurs, these should be treated with great caution, due to their potential explosive nature.

The space group of the crystals of **9** is monoclinic *I*2/*a* (no.15). The obtained crystals are constituted of two inseparable twins. The measurement was performed on a twinned crystal and the collected data were separated, according to their belonging to one or the other. The resolution was made on one part of the data collection.

The unit cell is constituted of four asymmetric units, consisting of one half silver atom, one half ligand molecule and one half of a perchlorate molecule. (Figure B-52) The silver atom is localized on an inversion center (0, ½, 0(b)) and the chlorine atoms on a two-fold axis (1/4, y, 0(e)). The most important bond lengths and angles are listed in Table B-30.

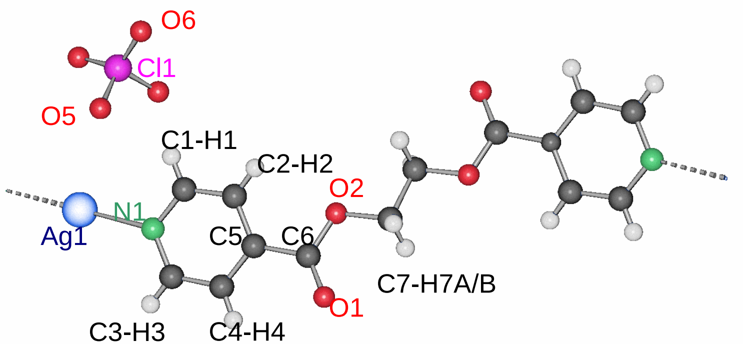

Figure B-52: asymmetric unit in 9

As an inversion center lies in the middle of the C7-C7$^{\#1}$, the pyridine rings within a ligand stay thus in parallel planes. They are separated by 1.49(3) Å as the ester groups are twisted towards the pyridine groups. The angle between the plane containing the pyridine and the one containing the ester groups is 16.0(8)°.

The general motif is the same as for compound **8** with formation of a chain, the *anti*-conformation of the ligand and the “up-to-down” direction of the ligand molecules along the chain (Figure B-53). The distances between two silver atoms in a chain is 17.47 Å. The distances Ag-N are 2.197(4) Å *i.e.* 0.04 Å longer than in **8**. The N-Ag-N angle is 180°, due to the symmetric influence of the coordinating perchlorate anions on this angle. The distance Ag-O(perchlorate) is 2.698(8) Å. This distance indicates a weak interaction between silver and perchlorate [178], the silver-perchlorate distances usually ranging from 2.50 to 2.80 Å.

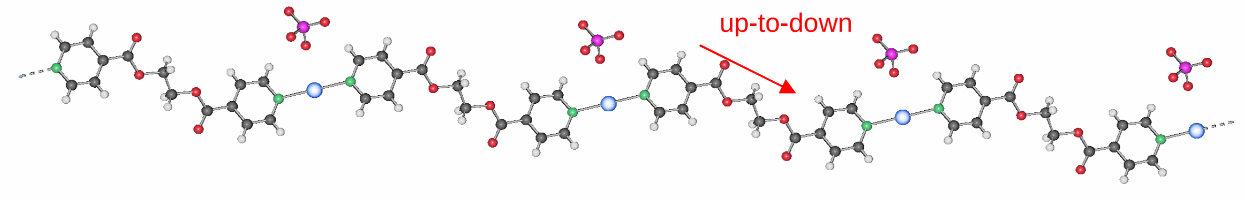

Figure B-53: one chain motif in 9

In **9**, the chains are parallel to each other with the counter anion between the chains. Two close chains are propagated in different directions tilted of about 30°. These two chains cross each other only once (Figure B-54). The overall arrangement is stabilized with the perchlorate counter anion. Indeed, the two oxygen atoms O5 of one perchlorate interact both with one silver atom of each chain. The distance silver-silver is 4.5410(6) Å long, the counter-anion does not support silver-silver contacts, the silver-perchlorate interaction being too weak. There is a weak Ag···ring interaction between one silver atom and a pyridine ring of the second chain, the silver-centroid distance being 3.511 Å with an offset of *ca.* 2 Å. (Table B-32)

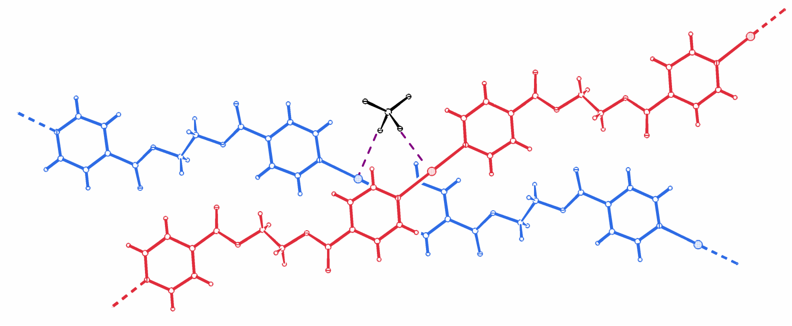

Figure B-54: chains crossing in 9 (the two different chain directions are shown in blue and in red, perchlorate atoms in black)

The three-dimensional structure can be understood as the stacking of these two kinds of chains (Figure B-55a). The undulation of the chains is due to the presence of the perchlorate counter anions.

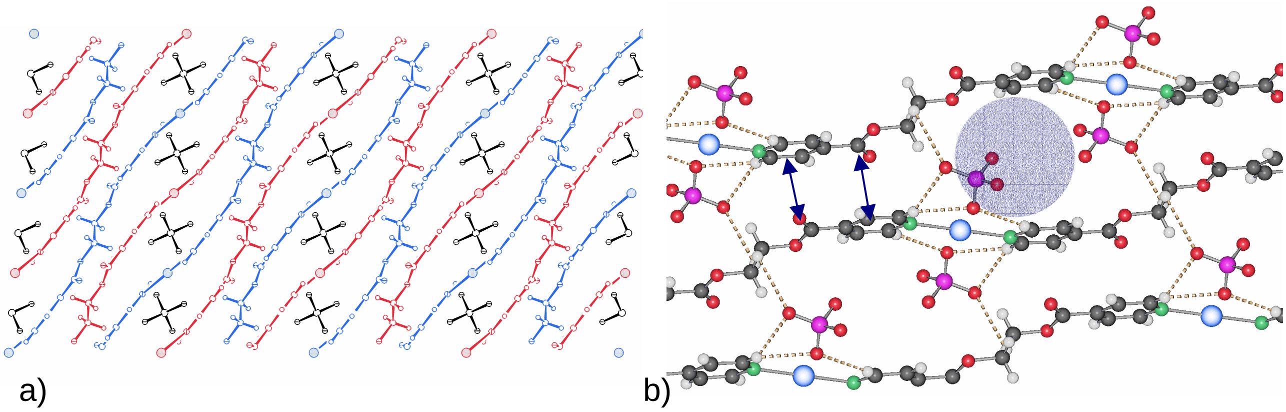

Figure B-55: a) top view of the overall structure (the colour has the same meaning as on previous figure) along the b-axis; b) detail of the interactions within a layer in 9: π-stacking (arrows) and hydrogen bonds (dashed lines)

Two adjacent chains running in the same direction are close enough to interact and to form layers. There are weak interactions within these layers and also between the layers.

Firstly, the interactions within a layer will be detailed (Figure B-55b): *i)* The perchlorate counter anions bridge two chains, being involved in coordination bonds (O5-Ag1) and hydrogen bonding (with the H1 and H3 hydrogen atoms of the pyridine rings coordinated to the Ag1 silver atom and with the H7B ethyl hydrogen atom of the adjacent chain) (Table

B-31.); *ii)* there is also π-stacking between the pyridine rings and the ester groups in the area where the chains are the closest (the shortest distance is 3.3 Å). On Figure B-55b, cavities (9.5 × 10 Å) between the perchlorate anions (region in blue) can be seen: the second kind of chains is going through these channels.

There are further interactions between the sheets: hydrogen bonds involving the O6 oxygen of the perchlorate anions and hydrogen bonds between the ligand molecules belonging to different layers (Table B-31). These hydrogen bonds are mostly involving the O1 oxygen atoms and pyridyl or ethyl hydrogen atoms of another layer.

Table B-30: most important bond lengths (Å) and angles (°) in 9

Ag-N	2.197(4)	N-Ag-N	180.000(1)
Ag-O(ClO_3)	2.698(8)		
C-N	1.346(7), 1.350(7)	C-N-C	117.5(5)

Table B-31: Hydrogen bond data for 9 [lengths (Å) and angles (°)]

D-H···A	*d*(D-H)	*d*(H···A)	*d*(D···A)	Angle D-H···A
intra-sheets hydrogen interactions				
C3-H3···O5	0.93	2.55	3.256(1)	133.6
C3-H3···O6	0.93	2.52	3.33(1)	145.1
C1-H1···O5$^{\#1}$	0.93	2.56	3.30(1)	137.7
C7-H7B···O6$^{\#2}$	0.97	2.89	3.47(2)	119.6
C-H···O hydrogen interactions between the sheets				
C4-H4···O6$^{\#3}$	0.93	2.47	3.31(1)	150.7
C7-H7B···O1$^{\#3}$	0.97	2.82	3.649(7)	143.9
C2-H2···O1$^{\#4}$	0.93	2.66	3.565(7)	164.0
C1-H1···O2$^{\#5}$	0.93	2.89	3.609(7)	134.7

Symmetry transformations used to generate equivalent atoms: #1 -X, -Y+2, -Z+1; #2 X+1, Y, Z; #3 X+1/2, -Y+1, Z; #4 -X+1, Y+1/2, -Z+1/2; #5 X-1/2, -Y+2, Z.

Table B-32: Ag···pyridine rings interactions lengths (Å) and angles (°) in 9

	d_{M-R}	pd_{M-R}	β
Ring (N1, C1, C2, C3, C4, C5)···Ag1$^{\#1}$	3.511	2.911	33.99

Symmetry transformations used to generate equivalent atoms: #1 -X+3/2, Y, -Z.

Perchlorate anions can be coordinating moieties (with silver-oxygen distances of about 2.5 Å) [178], or engage in weak interactions with Ag^{I} (with silver-oxygen distances of about 2.7

Å) [36, 38, 165, 180] or be templates for the formation of networks (silver and perchlorate are spaced by *ca.* 2.9 Å) [167, 169, 172, 175, 270].

In **9**, the motif is again a one-dimensional chain $\{Ag(\mathbf{L})\}^{+}_{n}$, with which the perchlorate anions are moderately interacting. The role of perchlorate may be regarded as a template: the chains can not be linear and lie exactly parallel, because of the presence of the counter anions, giving an undulation to the chains. Contrary to **8**, the chains in **9** tend to stack parallel as in the case of coordination polymers obtained with **L** and $AgNO_3$ (**3**, **4**, **5** and **7**).

III.3.c - $\{[Ag(L)]PF_6\}_n$ 10

As in some cases, the use of hexafluorophosphate instead of perchlorate as counter anions induces no or few changes in the structure [169, 270], the $\{[Ag(\mathbf{L})]ClO_4\}_n$, **9**, and $\{[Ag(\mathbf{L})]PF_6\}_n$, **10**, will be compared. Indeed, both counter anions have a similar shape, size and non-polarity. **10** was synthetized by Jorge Sagué in the Fromm group and the synthesis and the crystallographic structure will be here only resumed for comparison.

Crystals of **10** are obtained by slow diffusion between a solution of **L** in THF and a solution of $AgPF_6$ in water in an “H-shaped” tube in low yield.

The direct reaction between **L** and $AgPF_6$ in dichloromethane gives a white precipitate with the composition **L**:$AgPF_6$ 1:1. The IR spectrum indicates the presence of PF_6 and **L**, as well as the coordination of the ligand (shift of the ν(C=C) band from 1597 to 1618 cm^{-1}). The batch precipitate was not crystalline enough to collect a good powder X-ray spectrum.

10 crystallizes in the monoclinic space group *I*2/*a* (no.15) as does **9**. The cell parameters are similar for *a* and *b*, but the *c* axis is twice as longer in **10** than in **9** (34.6 and 17.3 Å respectively). This difference is due to the fact that in **10**, the asymmetric unit is bigger with one silver atom, one PF_6^- counter ion and one ligand molecule. No atom is lying on particular crystallographic positions.

The motif is, as in **9**, a chain with alternating silver atoms and **L** molecules, but the directions of **L** on each side of one silver atom are different (Figure B-56). The ligand is going alternatingly “up-to-down” and “down-to-up” so that a zig-zag chain is formed.

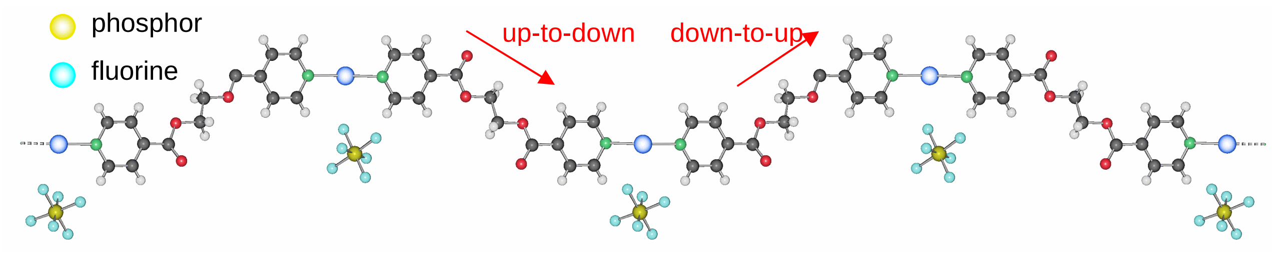

Figure B-56: chain motif in 10

The shape of the chain is the major difference between the structure of **9** and **10**. The overall arrangement of the chains is indeed the same in **9** and **10** (Figure B-57). The chains arrange parallel to each other, and there are two main directions for the chains in **10**, and the PF$_6^-$ counter anions have the same effect in the structure: they are responsible of the undulation of the chains. The PF$_6^-$ anions interact weakly with silver ions in the same way than perchlorate in **9**, *i.e.* PF$_6^-$ is bidentate with silver-fluorine distances of 2.894 and 3.093 Å. Weak Ag-PF$_6^-$ are usually found with silver-fluorine distances of *ca.* 3 Å [177], the shortest Ag-F(PF$_5$)$^-$ is found in {[Ag(1,3-bis(4-pyridyl)propane](PF$_6$)}$_n$ with 2.75 Å and the interaction is described as ionic [165].

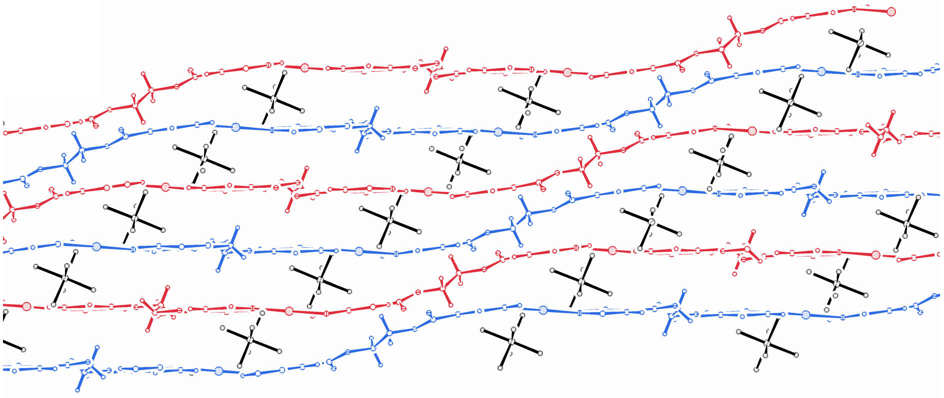

Figure B-57: parallel stacking of the chains in 10: the blue chains are going in one direction, the red ones in another and the hexafluorophosphate anions are drawn in black

The difference in the chain shape in **10** towards **9** induces another structural change: in **10**, the PF$_6^-$ anions are localized in channels, whereas **9** is not a porous material. Both three-dimensional structures of **10** and **9** are compared in Figure B-58.

The interactions within the packing are listed in Table B-33 The most important ones are the hydrogen bonds between the ligand molecules (The ester oxygen atoms form hydrogen bonds with pyridyl hydrogen atoms with distances of 2.52 and 2.58 Å.) and the more or less strong interactions between the PF$_6$ and the ligands (The fluorine hydrogen distances range from 2.49 to 2.86 Å.). For comparison, C-H···F interactions are found in {[Ag$_2$(*N,N'*-di(2-pyridyl)oxamide)$_3$(CH$_3$CN)$_2$](PF$_6$)$_2$}$_n$ between the fluorine atoms and pyridyl hydrogen atoms at 2.542 and 2.508 Å with angles of 143.4 and 152.7° respectively [38].

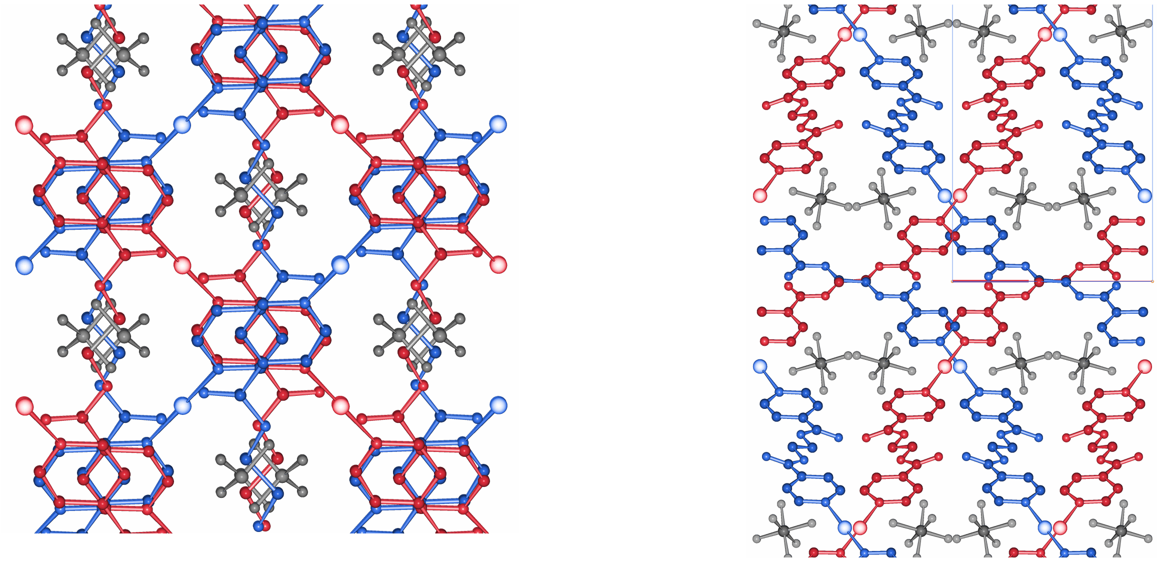

9 **10**

Figure B-58: Comparison of the 3D-dimensional structures of 9 and 10, the chains in different directions are shown in red and blue, anions in black

Table B-33: most important bond lengths (Å) and angles (°) in 10

Ag-N	2.138(5), 2.148(5)	N-Ag-N	178.9(3)
Ag-F(PF_5)	2.896(8), 3.096(8)		
C-N	1.39, 1.39	C-N-C	120

Table B-34: Hydrogen bond data for 10 [lengths (Å) and angles (°)]

D-H···A	*d*(D-H)	*d*(H···A)	*d*(D···A)	Angle D-H···A
Ligand-ligand hydrogen interactions				
C8-H8···O1$^{\#1}$	0.93	2.52	3.42(1)	163.6
C3-H3···O3$^{\#2}$	0.93	2.58	3.49(1)	163.9
C-H···F hydrogen interactions				
C7-H7···F1$^{\#3}$	0.93	2.61	3.43(1)	147.8
C1-H1···F2$^{\#3}$	0.93	2.62	3.36(1)	137.1
C7-H7···F2$^{\#3}$	0.93	2.49	3.27(1)	141.3
C2-H2···F3$^{\#4}$	0.93	2.54	3.30(1)	134.0
C6-H6···F3$^{\#4}$	0.93	2.86	3.57(1)	134.0
C5-H5···F1	0.93	2.59	3.46(1)	156.8
C1-H1···F4$^{\#3}$	0.93	2.50	3.25-1)	137.5
C14-H14B···F4$^{\#5}$	0.97	2.66	3.20(2)	115.6
C14-H14A···F4$^{\#2}$	0.97	2.74	3.35(2)	121.7
C6-H6···F5	0.93	2.76	3.69(1)	173.4
C10-H10···F6$^{\#6}$	0.93	2.45	3.21(1)	139.1

Symmetry transformations used to generate equivalent atoms: #1 -X+1, -Y+2, -Z; #2 -X-1, Y+1/2, -Z+1/2; #3 X+1/2, -Y+1, Z; #4 X, Y+1, Z; #5 X-1/2, -Y+1, Z; #6 X+1/2, -Y+2, Z.

Table B-35: Ag···pyridine rings interactions lengths (Å) and angles (°) in 10

	d_{M-R}	pd_{M-R}	β
Ring (N1, C1, C2, C3, C4, C5)···Ag1[#1]	3.88	2.89	41.9
Ring (N2, C6, C7, C8, C9, C10)···Ag1[#2]	3.27	3.17	14.6

Symmetry transformations used to generate equivalent atoms: #1 X-1/2, -Y, Z; #2 X+1/2, -Y, Z.

As expected, there are similarities between the coordination polymer based on **L** and silver perchlorate or hexafluorophosphate, but both structures are not identical as in some other reported cases [169, 270].

Jung *et al.* show some coordination polymers built with 3,3'-thiobispyridine and different silver salts [177]. The compounds obtained with ClO_4^- and PF_6^- have similar motifs, *i.e.* helicoidal chains, but the helical pitches are different according to the anions, although both anions have a similar shape and size. They assume that the crystal packing may be a more important factor than the volume of the counter anions. The difference in the structural motif in **9** and **10** can thus be explained by the difference in the weak interactions between the counter anions and the surrounding ligand.

III.3.d - $Ag(BF_4)$ + L

In order to continue our study of the counter anion influence, the crystallization of **L** with $AgBF_4$ was attempted. Unfortunately, it was not possible to obtain crystals. The direct reaction of **L** and $AgBF_4$ in dichloromethane gives a white precipitate. Its composition Ag:**L**:BF_4 is 1:1:1. The IR spectrum indicates the presence of BF_4 and **L**, as well as the coordination of the ligand (shift of the ν(C=C) band from 1597 to 1612 cm^{-1}). The presence of oligomeric species in solution was proven with ESI/MS in CH_3CN/CH_2Cl_2 (presence of [**L**H]$^+$, [**L**Ag]$^+$, [**L**HAg(BF_4)]$^+$, [$\mathbf{L}_2$Ag]$^+$ and [$\mathbf{L}_2Ag_2(BF_4)$]$^+$ at respectively 273.1, 379.1, 467.2, 650.9 and 846.8 m/z).

III.3.e - Ag_2SO_4 + L

Some other Ag^I coordination polymers were attempted with other more coordinating anions such as sulfate.

The reaction between Ag_2SO_4 and **L** (molar ratio 1:1) in dichloromethane gives a white precipitate. The analyses show a composition Ag:SO_4:L 2:1:3 in addition to solvent molecules (either 0.5 CH_2Cl_2 or 2 H_2O). The IR spectrum indicates the presence of the ligand and sulfate anions, but the proof of the coordination is not evident.

The different used techniques for the (re-)crystallization of this compound were unsuccessful: different solvents, different reaction temperatures, “H-shaped tube”. Generally, only Ag_2SO_4 crystallizes.

III.3.f - Counter ion influence

Motifs

It is worthy to notice that the linear environment around silver is the preferential coordination modes of **L** with Ag^I (except for **6**), the counter anions being more or less close to the silver centres for completing the Ag^I coordination sphere. This is in agreement with the important class of Ag^I-bipyridyl ligands already reviewed [9, 11]. Three- or four-coordinated silver centers with **L** were never obtained.

Ligand functionalities

Both pyridine groups of **L** are coordinating silver atoms in the presented compounds, *i.e.* there are only bridging ligands, **L**, and no terminal ones in these structures. Another important aspect is the implication of the ester groups in the building of the coordination polymers. The oxygen atoms of the carbonyl functions are always involved in hydrogen bonding and not involved in any interactions with silver ions. This implies the formation of layers by stacking of parallel chains.

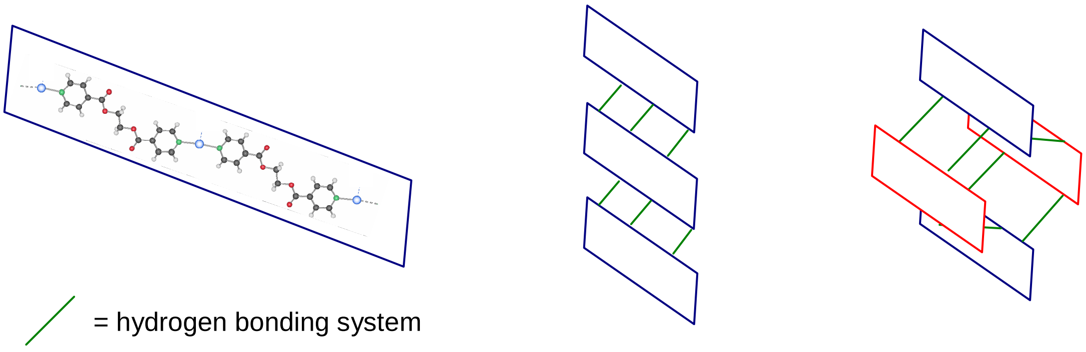

3, **5**, **7**, **8** **9**, **10**

Figure B-59: arrangement of the chains thanks to the hydrogen bonds involving C=O functions in 3, 5, 7, 8 (formation of layers) and in 9, 10 (interactions between layers)

In **3**, **5**, **7**, **8**, the ten-membered hydrogen bonding systems (···O=C-C-C-H···O=C-C-C-H) allow the “edge-to-edge” alignment of the chains (Figure B-59). These hydrogen bonds are moderate to weak [12] and involve either pyridyl hydrogen or ethyl hydrogen atoms. In **9** and **10**, C=O groups are also involved in hydrogen bonds, but as previously seen, these interactions are not the main factor of the sheet formation, layers in these structures being primarily formed by other interactions. In the two compounds **4** and **6**, such hydrogen bonds are also observed, even if the structures are strongly different. The ligand *N,N'*-di(2-

pyridyl)oxamide containing C=O bonds in the bridging part between the pyridine rings is also involved in hydrogen bonding in all the coordination polymers built with this ligand [38].

Anion bonding modes

The behaviour of the nitrate anions differs from the behaviour of the other counter ions, as its coordinating ability is flexible. In the compounds **3**, **4**, **5**, **6**, and **7**, the interactions between the silver cations and the nitrate anions vary from weak monodentate interaction to strong bidentate coordination. The nitrate anions always interact with two silver ions using two or three of their oxygen donor atoms. It is possible for nitrate to bridge metal-metal contacts (**4** and **5**).

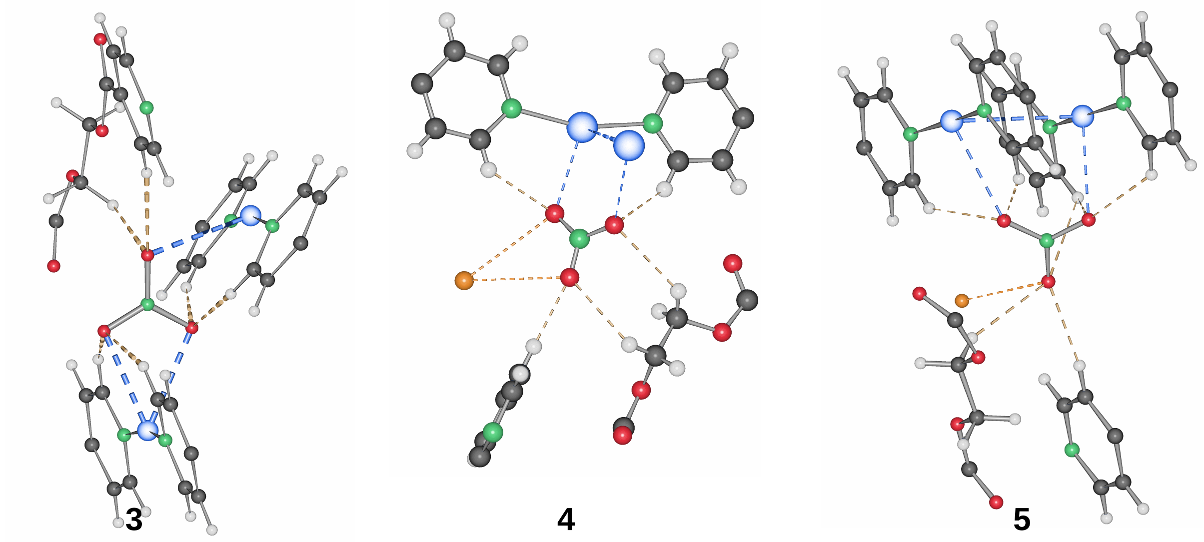

3 **4** **5**

Figure B-60: Nitrate interactions in 3, 4 and 5 (coordination bonds in blue, hydrogen bonds in brown, oxygen-oxygen contacts in orange)

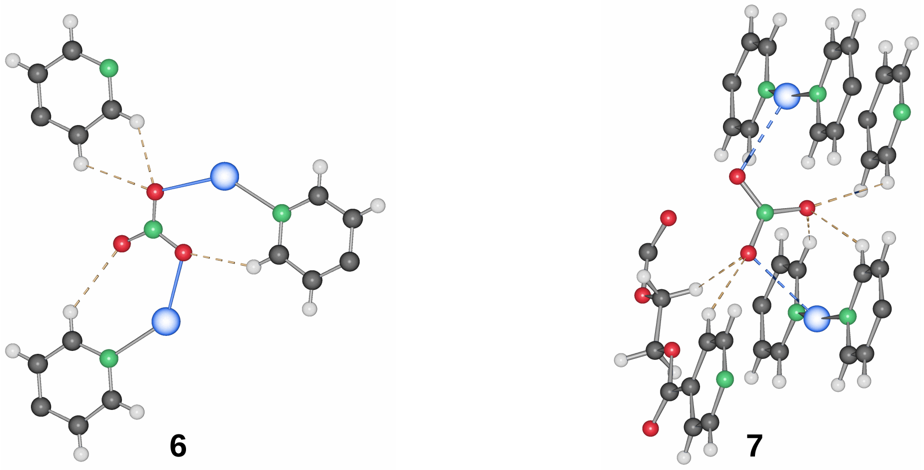

6 **7**

Figure B-61: Nitrate interactions in 6 and 7 (coordination bonds in blue, hydrogen bonds in brown)

The three other used counter anions are weakly coordinated to silver and act also as bidentate ligands between two chains.

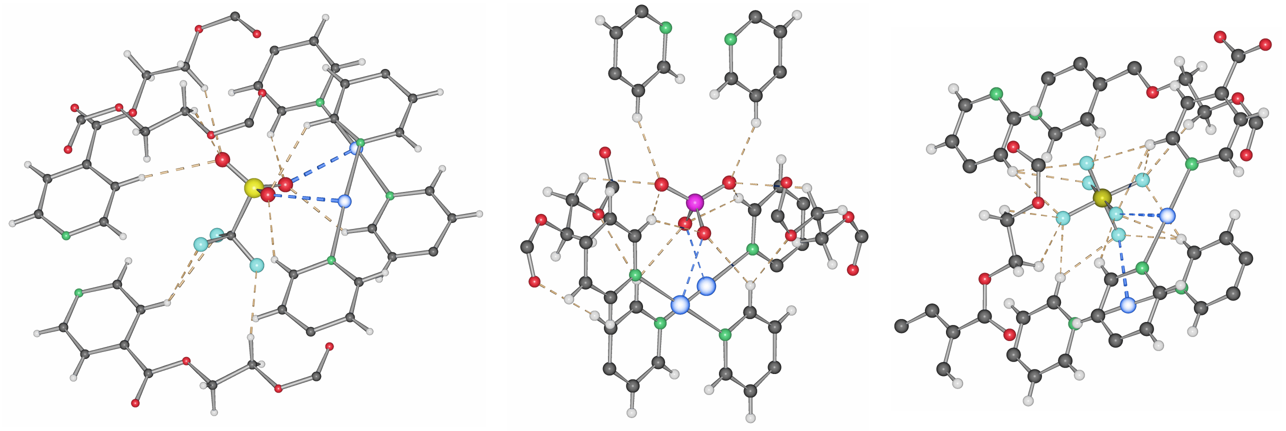

8 **9** **10**

Figure B-62: triflate, perchlorate and hexafluoroborate interactions in 8, 9 and 10 (coordination bonds in blue, hydrogen bonds in brown)

All donor atoms of the counter anions are furthermore involved in hydrogen bonding. Apart for **8** (triflate), the donor atoms of the counter anions are similar and the shapes of the counter anions are symmetric. The increasing number of the donor atoms in the counter anions increases the number of interactions with the environment. This difference can be directly seen as far as the compounds **9** and **10** are compared (Figure B-62). Both structures are equivalent except the direction of the ligand molecules within a chain. This can be attributed to the counter anion influence. Concerning the triflate counter anions, the main influence is the presence of two kinds of donor atoms, which allows the formation of either C-H···F or C-H···O interactions. The direct consequence is the apparition of two types of ligands within the chain motif: ligands without interactions with -CF_3 and ligand involved in hydrogen bonds with -CF_3.

Counter anion influence

The role of the counter anions seems to come in third place in these coordination polymer packing, after the coordination bonding (linear silver centres) and the ligand-ligand hydrogen bonding (except in **4** and **6**, in which the solvent influence is predominant).

The nitrate anions can bridge two silver atoms and generate pairs of chains. In the $AgNO_3$ compounds, the chains are parallel “face-to-face” in addition to the stacking described above (except for **6**, in which there is only parallel organisation within a pair of chains).

The use of less coordinating counter anions shows the tendency to a tilted organisation of the chains, perhaps for better adjusting the repulsive and attractive forces in the packing (Ag···Ag, ring···ring, C=O···C=O, C-H···O....). On the other hand, these counter anions bring obviously new interactions, particularly with the introduction of fluorine atoms in triflate.

IV - Cu^{II} coordination polymers

Coordination polymers based on ethanediyl bis(isonicotinate) are at last investigated by the use of Cu^{II} metal ions.

IV.1 - $\{[Cu(L)_2(NO_3)(H_2O)](THF)_2(NO_3)(H_2O)_x\}_n$ 11

The reaction between **L** and $Cu(NO_3)_2{\cdot}3H_2O$ in methanol gives a blue precipitate, of composition Cu:**L**:NO_3 1:1:2 whatever the reaction stoechiometry (M**L**, M**L**$_2$ or M_2**L**). The recrystallization of this powder in a mixture of solvents THF/water (50:50) yields few dark blue and poorly stable (when coming out from the mother liquor) single crystals suitable for single crystal X-ray diffraction : $\{[Cu(L)_2(NO_3)(H_2O)](THF)_2(NO_3)(H_2O)_x\}_n$, **11**. Some oligomeric fragments are present in solution: [**L**H]$^+$, [Cu**L**$(NO_3)_2(H_2O)_2(THF)_2]^{2+}$, [Cu**L**$(NO_3)]^+$, [$Cu_2$**L**$_2(NO_3)_2(H_2O)]^{2+}$, [Cu**L**$_2(NO_3)]^+$, [$Cu_2$**L**$_2(NO_3)_3]^+$.

The coordination polymer **11** crystallizes in the monoclinic space group *P*2/*c* (no.13). The asymmetric unit is composed of one copper atom (Cu1), two **L** molecules (labelling on Figure B-63), two nitrate counter anions (N5, O9, O10, O11 and disordered N6, O12, O13, O14 or N7, O15, O16), two THF molecules (O17-C29 to C32 and O18-C33 to C36), one coordinating water molecule (O40) and non coordinating water molecules (O19, O600, O700, O12). All atoms are found in general positions, except two atoms, which are localized on a two-fold axis (0, y, 1/4(e)): N7 and O15.

Figure B-63: labelling of the ligands in 11 (carbon atoms are going from C1 to C14 in L1, and from C15 to C28 in L2)

The Cu^{II} is hexa-coordinated by four nitrogen atoms of four different ligand molecules in equatorial positions and two oxygen atoms in apical positions: one from a water molecule (O40) and one from a nitrate anion (O9) (Figure B-64b). The repeating unit of a one-dimensional chain is a loop, in which the Cu^{II} atoms are pairwise bridged by two ligands and terminally bonded to one water and one anion (Figure B-64a).

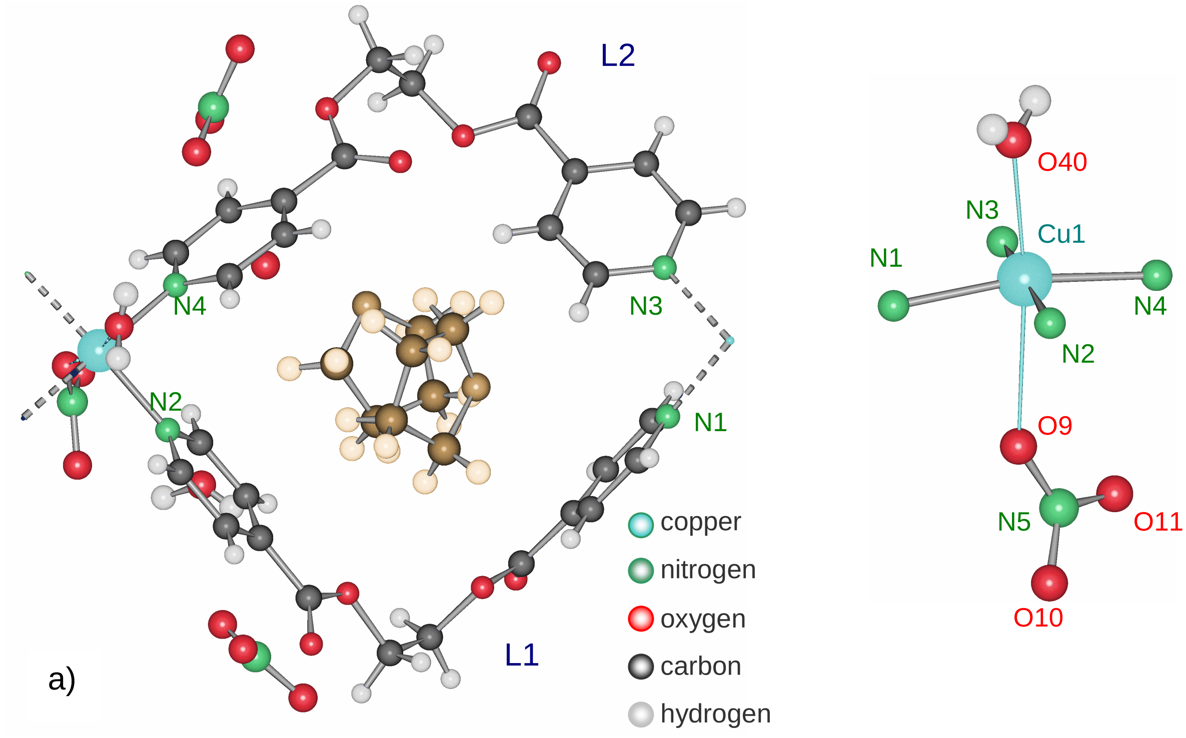

Figure B-64: a) repeating unit in 11 (color codes giving for all following figures, the THF molecules being shown in brown on this figure); b) coordinated atoms on Cu^{II}

In the $\{CuN_4O_2\}$ unit, the distances copper-nitrogen range from 2.026(2) to 2.051(2) Å (Table B-36). The sum of the N-Cu-N angles around a Cu^{II} centre is 359.46°; the four nitrogen atoms do not lie exactly in a plane and the Cu^{II} centre is found 0.116(1) Å above the mean plane through these four nitrogen atoms. There is thus a slight distortion of the equatorial positions, due to the relatively strong coordination of the water molecules on Cu^{II}. The distance Cu-water is 2.261(2) Å long, whereas the copper-nitrate distance is 2.673(2) Å long. The Cu-nitrogen distances are in an expected range (2.01-2.06 Å) for equivalent coordination of four nitrogen atoms on Cu^{II} in Cu^{II} coordination polymers [49, 276-278], so are the distances Cu-water (2.1-2.5 Å) [49, 277, 279, 280]. The nitrate anion is moderately coordinated to the Cu^{II} centre, like usually observed with nitrate monodentate ligands [161]. The Cu^{II} centre shows thus a Jahn-Teller distortion with the axial distances elongated in comparison to the equatorial distances. The distances C-N within the ligand are similar to the distances in the previous compound, whereas the C-C distances are *ca.* 0.01 Å smaller.

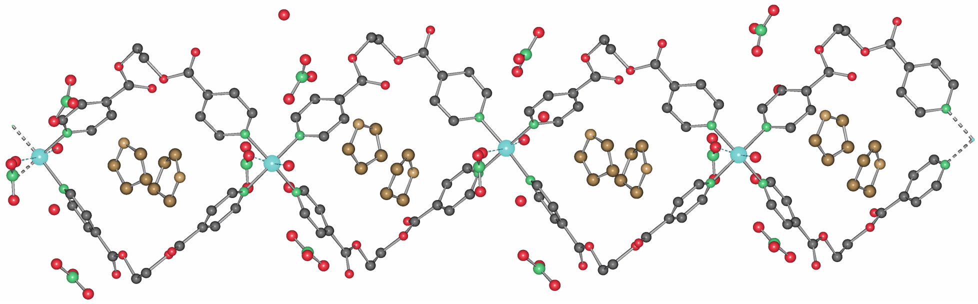

Figure B-65: one-dimensional motif in 11

The structural motif in **11** is a one dimensional double chain (Figure B-65), in which the ligand adopts the *gauche*-conformation. The planes containing the pyridine groups within a ligand form an angle of 83.35(7)° for L1 and 40.9(1)° for L2. This motif is similar to compound **2** with the formation of (Cu_2**L**$_2$)-loops. Unlike in **2**, there is no symmetry operation in the middle of the metallacycle and the two bridging ligands (L1 and L2) are not equivalent. The distance between two double-bridged Cu^{II} centres is 12.3611(7) Å, which is longer than in **2** by *ca.* 3 Å but smaller than in **4** by *ca.* 5 Å.

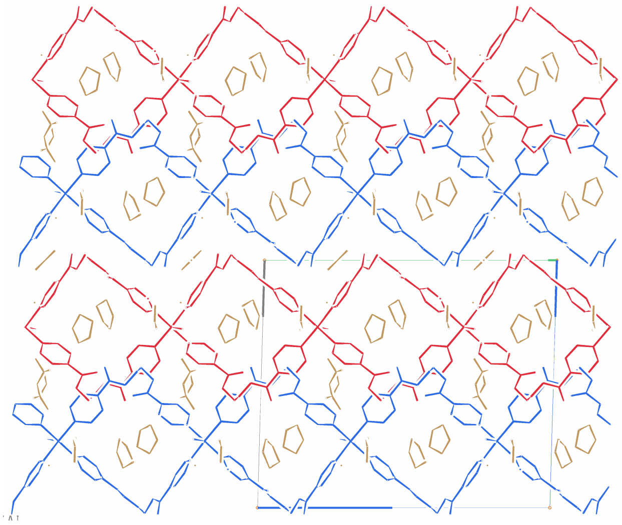

Figure B-66: the crystal packing along the *b*-axis (the two types of chains are shown in blue and red, the non-coordinating molecules in brown)

The cavities formed within the (Cu_2**L**$_2$)-loops have a size of about 7x8 Å. Along the *b*-axis, these cavities are stacked and the so-built channels contain the THF molecules (Figure B-66). The THF molecules are not found exactly between the ligand molecules, but below and above the chains as in **2** (Figure B-67). The THF molecules interact with the walls of the cavities through C-H···π interactions; the distance between THF hydrogen atoms and pyridine ring centres are 3.39 and 3.01 Å long, hydrogen atoms are not exactly vertical to the ring centres but offset of respectively 1.7 and 0.7 Å (Table B-37).

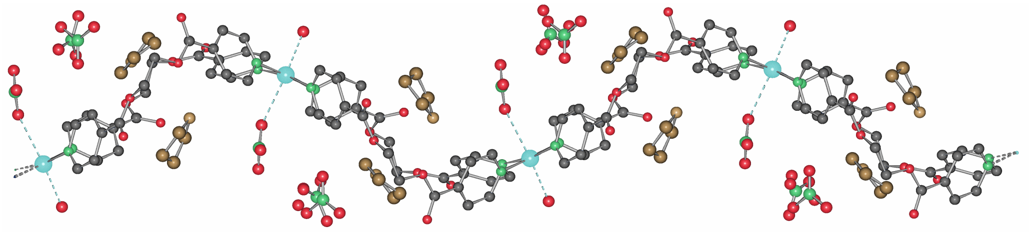

Figure B-67: the chains in 11 along the *a*-axis

The strong bending of the ligand molecules is also due to the fact that the chains in **11** are not linear but undulating if regarded along the *a*-axis (Figure B-67). This undulation is attributed to the presence of non-coordinating water molecules and nitrate anions. Indeed, these molecules are localized in a second kind of channels along the *a*-axis (Figure B-68).

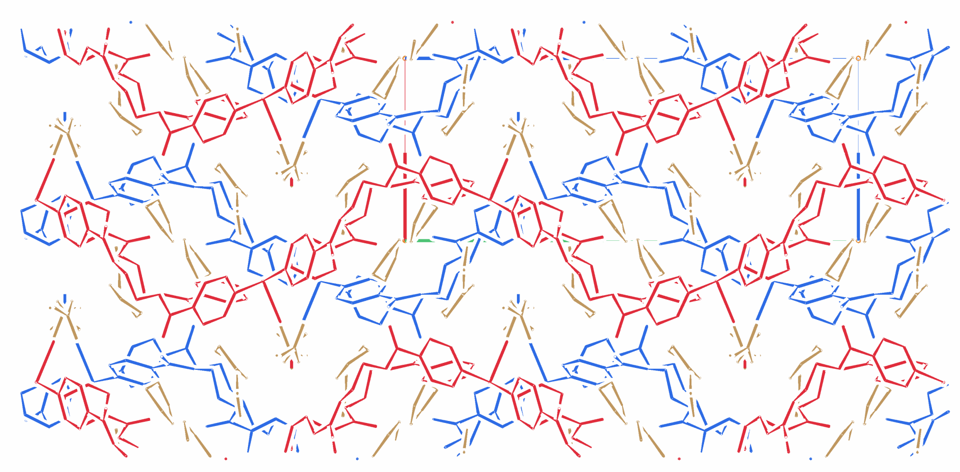

Figure B-68: Crystal packing along the *a*-axis (the two types of chains are shown in blue and red, the non-coordinating molecules in brown)

The two kinds of channels are supported by the skeleton of the structure: the double chains are arranged in a parallel way in the crystal packing. As shown on Figure B-66, the chains are assembled “two-by-two”.

Firstly they interact on the side of the L2 ligands: they are alternatingly stacked and some interactions occur between the chains. *i)* Hydrogen bonds are found between the ligands, oxygen and hydrogen being apart by 2.60 and 2.81 Å (Table B-38). *ii)* Other kinds of hydrogen bonds occur between THF molecules and ligand, the THF molecules acting thus as intermediates between the chains, the oxygen-hydrogen distances ranging from 2.76 to 2.89 Å (Table B-38). *iii)* The coordinating nitrate ions play the same role between the chains in this area with oxygen-hydrogen distances of 2.50 to 2.63 Å (Table B-38).

Secondly the ligands L1 are in front of each other in the second kind of stacking of the chains. There are few interactions between the chains in this part. The major interactions are *i)* hydrogen bonds between the coordinated nitrate ions and ligand molecules belonging to the adjacent chains group (2.50 Å) (Table B-38) and *ii)* interactions through the disordered nitrate/water molecules located between both groups of chains.

As previously described, the non-coordinating molecules (one water molecule (O19) and some disordered nitrate and water molecules) are localized in the channels along the *a*-axis, as well as the coordinating water molecules (O40). On the other hand, the THF molecules and the coordinating nitrates are embedded in the skeleton of the coordination polymer (Figure B-69a).

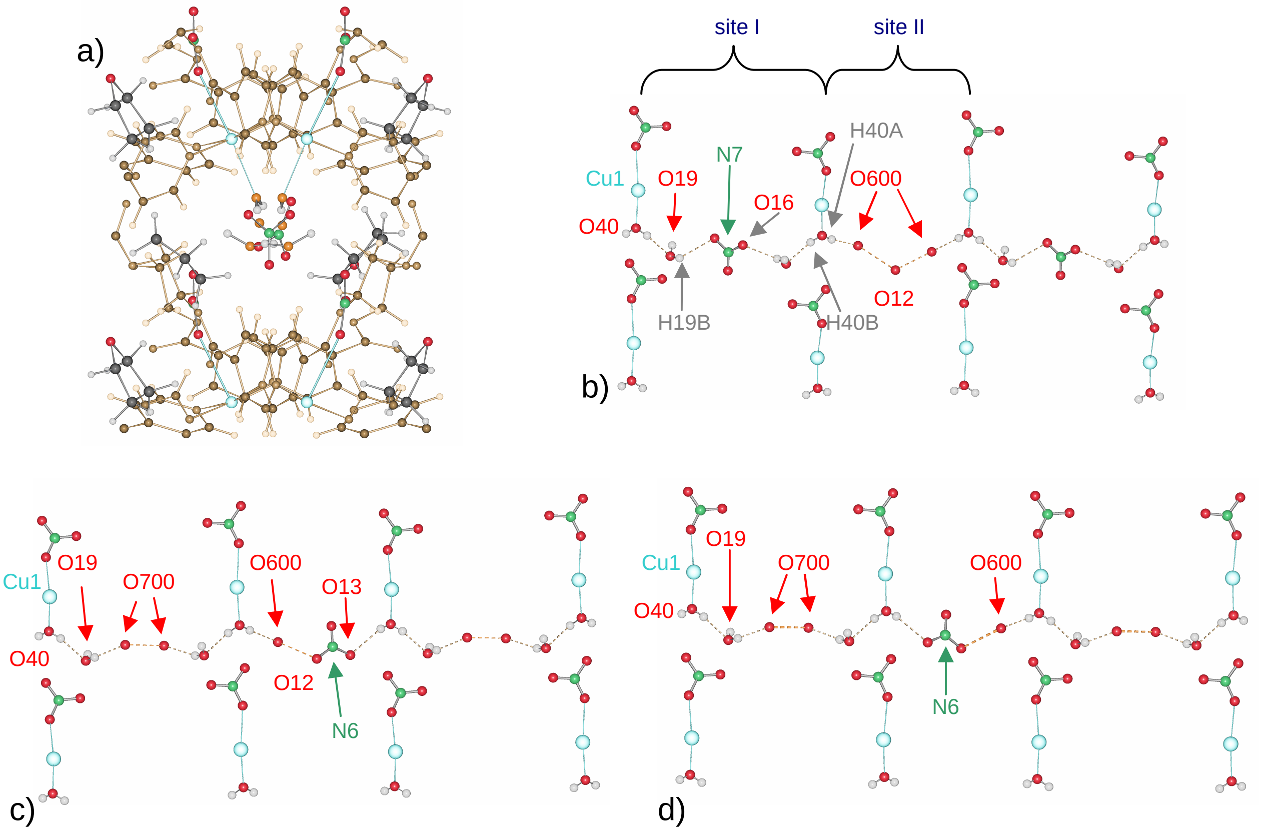

Figure B-69: a) detail of the channels along the *a*-axis in 11 (skeleton in brown, nitrogen of nitrate ions in green, oxygen of nitrate ions and THF in red, water oxygen atoms in orange, copper in blue); b,c,d) different nitrate and water positions in the channels

Two different crystallographic sites (sites I and II-Figure B-69b) were found to describe the disorder of the last nitrate anions. Both positions were refined at half site occupancy in order to establish the coherent charge balance. The Cu-Cu distances are different: 11.1 Å for site I, 9.4 Å for site II, implying different arrangement of the water and nitrate molecules in both sites.

Three cases can be distinguished. *i)* The nitrate (N7) is present in site I and forms hydrogen bonds with the water molecules (O19). The site II is therefore occupied by three water molecules linked *via* hydrogen bonds (distances oxygen-oxygen of 2.63(2) and 2.40(2) Å) (Figure B-69b, Table B-36, Table B-38). *ii)* Two water molecules (O700) are present in the site I, with hydrogen bonds between the several water molecules. In the site

II, the nitrate molecule (N6) and one water molecule (O600) are found with also strong hydrogen bonding (Figure B-69c). *iii)* The last situation is almost the same, but the positions of nitrate (N6) and O600 are exchanged, as there is a mirror in the middle of the site II (Figure B-69d, Table B-36, Table B-38). It is worthy to note that the channels are filled with hydrogen bonding chains (made up from the non coordinating nitrate molecules and water molecules) and that the coordinating nitrate anions and THF molecules do not participate to this network. There are also interactions between the considered network and the skeleton: hydrogen bonds between nitrate/water molecules and ligand (Table B-38). The total amount of water molecules per asymmetric unit is thus 1,5.

Table B-36: most important bond lengths (Å) and angles (°) in 11

Cu-N	2.026(2), 2.036(2)	N-Cu-N	90.24(8), 88.42(8)
	2.040(2), 2.051(2)		89.92(8), 90.88(8)
Cu-OH$_2$	2.261(2)	Cu-O(NO$_2$)	2.673(2)
C-N	1.336(3), 1.341(3)	C-N-C	118.8(2)
	1.333(3), 1.339(3)		118.0(2)
	1.340(3), 1.341(3)		118.0(2)
	1.337(3), 1.342(3)		118.3(2)
(H$_2$)O-O(H$_2$)	O700-0700	2.63(2)	
	O12-O600	2.41(2)	
	O12-O600	2.63(2)	

Table B-37: C-H···pyridine rings interactions lengths (Å) and angles (°) in 11

	d_{H-R}	pd_{H-R}	β	α
C31-H31B··· Ring(N1, C1, C2, C3, C4, C5)$^{\#1}$	3.39	2.94	29.8	145.4
C34-H34B··· Ring(N2, C10, C11, C12, C13, C14)$^{\#2}$	3.01	2.93	13.0	153.3
Symmetry transformations used to generate equivalent atoms: #1 X, Y, Z; #2 X, Y-1, Z.				

Table B-38: Hydrogen bond data for 11 [lengths (Å) and angles (°)]

D-H···A	*d*(D-H)	*d*(H···A)	*d*(D···A)	Angle D-H···A
inter-chains ligand-ligand hydrogen interactions				
C22-H22···O8$^{\#1}$	0.97	2.81	3.720(3)	157.5
C27-H27···O5$^{\#1}$	0.93	2.60	3.460(3)	153.0
C-H···O hydrogen interactions between ligand and THF				
C15-H15···O18$^{\#2}$	0.93	2.77	3.631(7)	153.9
C36-H36A···O8$^{\#2}$	0.97	2.84	3.676(8)	145.0
C34-H34B···O1$^{\#3}$	0.97	2.76	3.68(1)	158.8
C33-H33A···O3$^{\#2}$	0.97	2.89	3.832(9)	163.9
C-H···O hydrogen interactions between coordinated nitrate and ligand				
C1-H1···O10$^{\#4}$	0.93	2.63	3.462(4)	149.6
C22-H22B···O9$^{\#5}$	0.97	2.54	3.479(3)	164.2
C26-H26···O9$^{\#2}$	0.93	2.50	3.152(3)	127.5
C3-H3···O11$^{\#3}$	0.93	2.55	3.387(6)	149.4
C22-H22B···O11$^{\#5}$	0.97	2.51	3.352(6)	145.4
C8-H8A···O10$^{\#7}$	0.97	2.50	3.210(3)	129.8
C-H···O hydrogen interactions between channels and skeleton				
C17-H17···O14$^{\#8}$	0.93	2.33	3.208(9)	158.1
C25-H25···O12$^{\#9}$	0.93	2.79	3.67(1)	159.0
C7-H7B···O700$^{\#2}$	0.97	2.63	3.54(1)	155.8
C13-H13···O700$^{\#3}$	0.93	2.76	3.37(1)	123.6
hydrogen interactions between water				
O19-H19B···O16$^{\#3}$	0.83(5)	2.14(5)	2.831(6)	140(5)
O40-H40A···O13$^{\#8}$	0.66(3)	2.31(4)	2.940(6)	162(4)
O40-H40A···O600$^{\#8}$	0.66(3)	2.06(4)	2.69(1)	161(4)
O40-H40B···O19$^{\#6}$	0.87(4)	1.84(4)	2.696(3)	171(4)
O19-H19B···O700$^{\#8}$	0.83(5)	1.81(5)	2.632(8)	171(5)

Symmetry transformations used to generate equivalent atoms: #1 -X+1, -Y+2, -Z+2; #2 -X+1, Y, -Z+3/2; #3 -X+1, Y+1, -Z+3/2; #4 -X+1, -Y+2, -Z+1; #5 X, Y, Z+1; #6 -X+1, -Y+1, -Z+1; #7 X+1, Y, Z+1; #8 X, Y, Z; #9 -X+1, -Y+1, -Z+2; #10 X-1, Y-1, Z-1.

IV.2 - $\{[Cu(L)(NO_3)_2]\}_n$ 12

The slow diffusion between a solution of **L** in dichloromethane and a solution of $Cu(NO_3)_2 \cdot 3H_2O$ in methanol allows the formation of a blue polycrystalline compound, forming needles which grow as “urchins”. The polycrystalline powder is suitable for powder X-ray diffraction and the structure was solved from these data by Antonia Neels (Neuchâtel).

12 crystallizes in the triclinic space group *P*-1 (no.2). The asymmetric unit is composed of one copper atom (50% occupancy), two nitrate anions and one half of a ligand molecule (Figure B-70a). There are two asymmetric units per unit cell. The copper atom lies on an inversion center (0, 0, 1/2(*b*)).

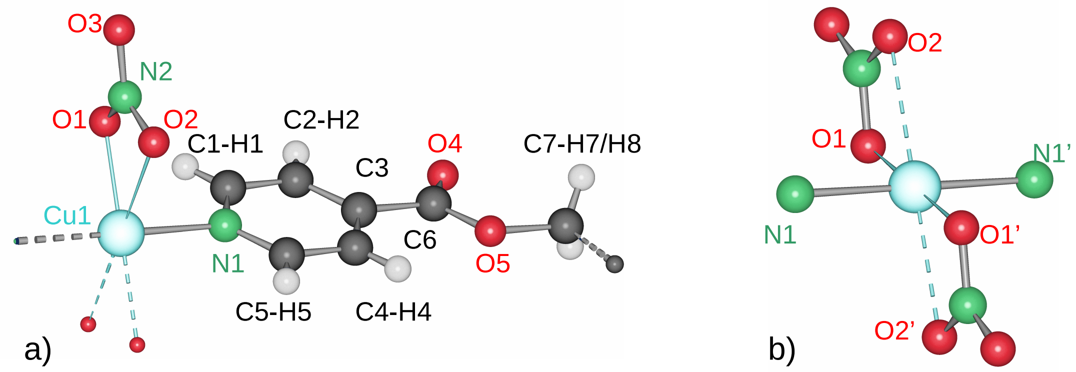

Figure B-70: a) asymmetric unit in 12: b) coordination around Cu^{II} centres

The Cu^{II} ion is coordinated by two nitrogen atoms of two different ligand molecules and two different nitrate anions in a pseudo-square planar coordination geometry, the distances copper-nitrogen being 2.002(5) Å long, the copper-oxygen 2.003(6) Å. The distortion of the coordination sphere is due to weak interactions of a second nitrate oxygen atom O2 to the copper centre (2.497(6) Å) (Figure B-70b). The nitrate anions act thus as anisobidentate ligands. Both copper-nitrogen and copper-oxygen bonds are smaller than in **11**. The strong bonding of nitrate on copper explains the shift of the nitrate stretching band on the IR-spectrum of **12**. Indeed this band is found between 1500 and 1450 cm^{-1}, whereas the “free” nitrate band usually appears at 1390 cm^{-1}. (In the silver-compounds in which the nitrate is moderately coordinating silver centers, the nitrate stretching bands also appear in the 1390 cm^{-1} region.) Such a shift has also been observed for similar copper compounds [281].

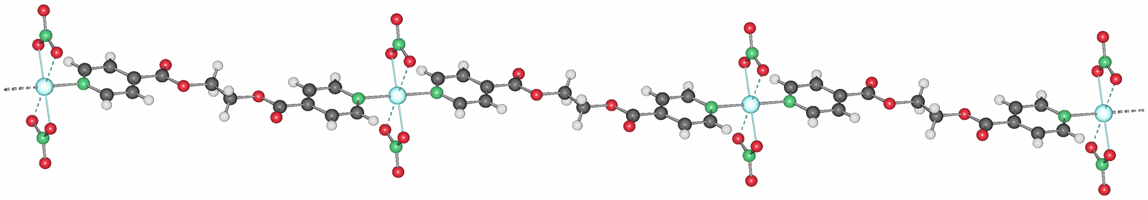

Figure B-71: chain motif in 12

The motif in **12** is a linear chain, in which the Cu^{II} ions are bridged by the ligand molecules in the *anti*-conformation (Figure B-71). The distances copper-copper within the chain are 17.20 Å, in agreement with the metal-metal distances in the other compounds with *anti*-conformation of the ligand, namely **1**, **3**, **5**, **7**, **8**, **9** and **10**.

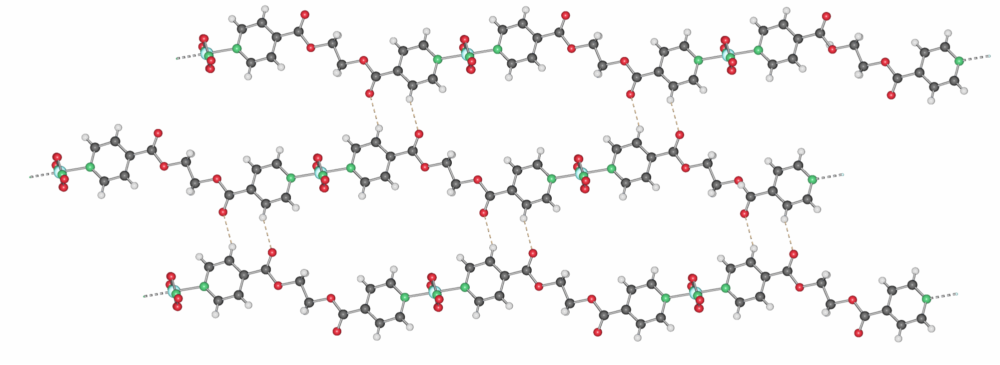

Figure B-72: layers in 12 supported by hydrogen bonds between the chains

The chains arrange parallel to each other supported by hydrogen bonds in order to build a layer. The hydrogen bond motif is a ten-membered ring including two hydrogen bonds: C2-H2···O4 with a hydrogen-oxygen distance of 2.41(1) Å. In the layers, cavities of 5x14 Å are formed, which are filled by the nitrate molecules of the adjacent layers, one of the above layer, the other from below. The layers are stacked parallel in the crystal packing (Figure B-73).

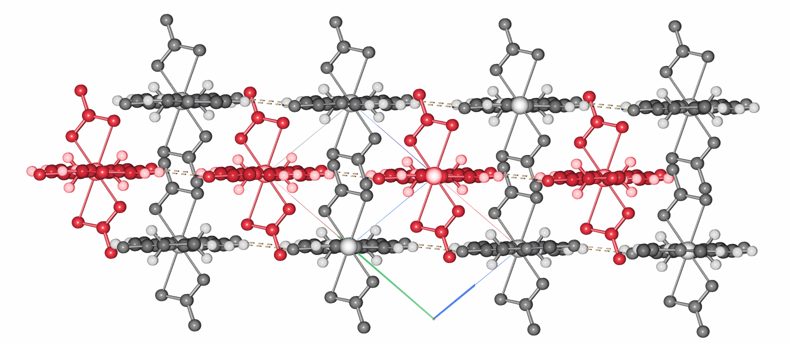

Figure B-73: the stacking of the layers in 12 (one layer in red, its adjacent ones in grey)

Only few interactions occur between the layers: hydrogen bond involving nitrate anions and ligand molecules (2.62 Å) (Table B-40). The smaller distance between to copper atoms in **12** is 5.193 Å.

Table B-39: most important bond lengths (Å) and angles (°) in 12

Cu-N	2.002(5)	N-Cu-N	180
Cu-O(NO_2)	2.003(6)		
	2.497(6)		
C-N	1.335(3), 1.330(4)	C-N-C	120.9(4)

Table B-40: Hydrogen bond data for 12 [lengths (Å) and angles (°)]

D-H···A	*d*(D-H)	*d*(H···A)	*d*(D···A)	Angle D-H···A
inter-chains ligand-ligand hydrogen interactions				
C2-H2···O4$^{\#1}$	0.928(9)	2.41(1)	3.256(8)	152(1)
C1-H1···O2$^{\#2}$	0.93	2.620		145.44
Symmetry transformations used to generate equivalent atoms: #1 -X-1, -Y+1, -Z; #2 -X-1, -Y, -Z+1.				

The two compounds based on **L** and $Cu(NO_3)_2$ strongly differ, underlining the influence of the crystallization method and solvent.

Cu^{II} coordination sphere

The main difference between the two compounds **11** and **12** is the coordination sphere of the Cu^{II} centers. The distorted octahedral Cu^{II} center (Jahn-Teller distortion) in **11** is coordinated by four ligand molecules (equatorial positions), one water molecule and one nitrate molecule (apical positions). In the other hand, the Cu^{II} center, in **12**, lies in a pseudo square planar coordination geometry formed by two ligand molecules and two nitrate counter anions. The distance copper-nitrogen are thus shorter in **12** than in **11** by *ca*. 0.04 Å. The nitrates are furthermore stronger coordinated in **12** than in **11**, with copper-nitrate distances smaller of more than 0.6 Å. They are monodentate ligands in **11** and anisobidentate ones in **12**. In these compounds, nitrate anions do not bridge two copper atoms, involving the three nitrate oxygen atoms in coordination bonds, as in some examples in the literature [10] or as in the silver compounds **3** and **7**.

As emphasized in the silver coordination polymers, the nitrate anions have flexible coordinating ability [10]. The use of this counter anion with a metal center like Cu^{II} (relatively rigid) and *N-N'*-donor bridging ligands can lead to bis-pyridyl metal coordination environment with *trans* monodentate nitrate anions and one-dimensional motifs [281, 282]. Other so-built frameworks can have tris-pyridyl metal environment with "T-shaped" connecting units, nitrate anions as *syn* terminal bidentate ligand and one- to -three dimensional networks [10]. The last possible configuration is the tetrakis-pyridyl metal environment with ligands in equatorial positions and nitrate anions in apical ones, giving two- or three-dimensional motifs [161, 217].

Compound **11** has a tetrakis-pyridyl metal environment, but with one water molecule and one nitrate anion in the apical positions. This situation is scarce in the literature [279, 283]. A similar motif is one of the motifs present in the compound $\{[Cu(L)_3(NO_3)_2]\cdot[Cu(L_2)(H_2O)(NO_3)](NO_3)\}_n$ (L = 1,6-bis(4-pyridyl)hexane) [283]. The motif is a double chain motif with $\{Cu_2L_2\}$ loops, with analogous coordination environment for

Cu^{II} than in **11**. On the other hand, second one-dimensional chains interlock the first kind of chains, passing through two loops: interpenetration occurs.

Compound **12** has a bis-pyridyl metal environment and some analogue compounds were already described [281, 282], for instance, with bipyridine as bridging ligand [282].

Long range order

The co-crystallisation of solvent molecules induces the *gauche*-conformation of the ligand molecules in **11**, whereas in **12**, the ligands adopt the *anti*-conformation as in the crystalline form of the ligand alone. Like in the silver coordination polymers based on **L**, the *gauche*-conformation is found in the compound containing solvent molecules. This is in correlation with the following statement: the co-crystallization of solvent molecules may induce the change in the ligand conformation, in order to create cavities or channels and to fit with the increasing number of possible interactions in the crystal packing. The reversible statement is not available.

The solvent crystallization plays also an important role, as the aqueous solution seems to favour the formation of tetrakis-metal environment, according to similar structures in the literature [161, 279]. Crystals formed in alcoholic solution mostly show the one-dimensional structural motif [281]. In $\{[Cu(1,2\text{-bis(3-pyridyl)ethyne})(NO_3)_2(MeOH)]\}_n$, the methanol molecule also coordinates to the copper ion, the copper ion having a pseudo-square pyramidal coordination environment, instead of the pseudo-square one [27].

IV.3 - $\{[Cu(L)_2(ClO_4)(H_2O)]_2(THF)_4(ClO_4)_2(H_2O)\}_n$ 13

Caution! Although no problem in handling perchlorate salts occurs, these should be treated with great caution, due to their potential explosive nature.

The reaction between **L** and $Cu(ClO_4)_2{\cdot}6H_2O$ in methanol gives a blue precipitate of composition Cu:**L**:ClO_4 1:2:2. This compound is insoluble in organic solvents, but soluble when organic solvents in addition with water are used. The recrystallization of the blue precipitate in a solvent mixture THF/water (50/50) yields to dark blue crystals (block-shape). The crystals are suitable for single crystal X-ray diffraction.

The determination of the total amount of water molecules in **13** was made thanks to the structure refinement in addition with TGA/SDTA measurement. For the latter, crystals were taken out of the mother liquor, slightly dried on a filter paper and quickly used for TGA/SDTA measurement. The loss of weight occurs instantaneously between the weighing of the sample and the beginning of the measurement (Figure B-74). The first exothermal loss of weight occurs between 25°C and 117°C (4.62%) corresponding to the loss of one THF molecule and one water molecule. This first step is followed by three other ones corresponding to the loss of three THF molecules between 117°C and 155°C (3.64%), 155°C and 173°C (3.82%) and 172 and 195°C (3.44%). (The calculated THF weight represents 3.68% of the total mass, water representing 0.92%.) The measurement should be stopped at 220°C before the decomposition of the organic part, in order to avoid explosion of the sample. Between 195°C and 220°C, the loss of one coordinating water molecule occurs (0.86%). Elementary analysis performed before and after the heating of the sample are in agreement with these results.

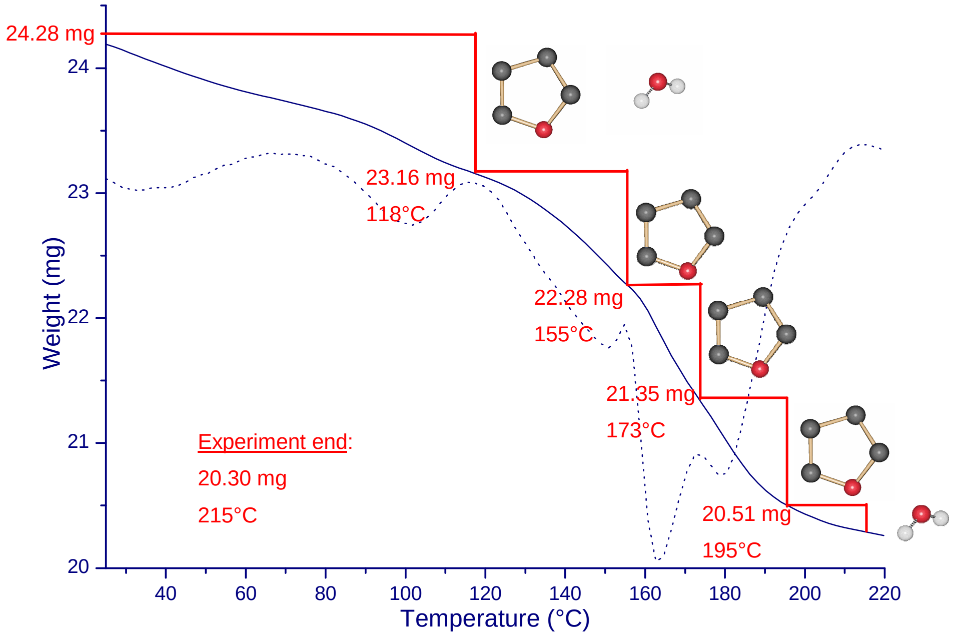

Figure B-74: TGA curve for 13 (and its derivative in dashed line)

The compound **13** crystallizes in the monoclinic space group $P2_1/c$ (no.14). The cell parameters of **13** are the same than the ones for **11**, except the *b*-axis parameter which is twice as long. Both compounds seem to be isomorphs, *i.e.* they have the same structural motifs. The only difference is in the number of included non-coordinating water molecules per $\{Cu(L)_2(X)(H_2O)\}$ unit: 1.5 for **11** and 0.5 for **13**.

The asymmetric unit in **13** is thus constituted of two copper ions (Cu1 and Cu2), four ligand molecules (labelled in the Figure B-75), four perchlorate counter anions (Cl1, O19, O20, O21, O22; Cl2, O23, O24, O25, O26; Cl3, O27, O28, O29, O30 and Cl4, O31, O32, O33, O34), three water molecules (O1, O2, O39/O40) and four THF molecules (O35, C350, C351, C352, C353; O36, C360, C361, C362, C363; O37, C370, C371, C372, C373 and O38, C380, C381, C382, C383). There are four asymmetric units per unit cell.

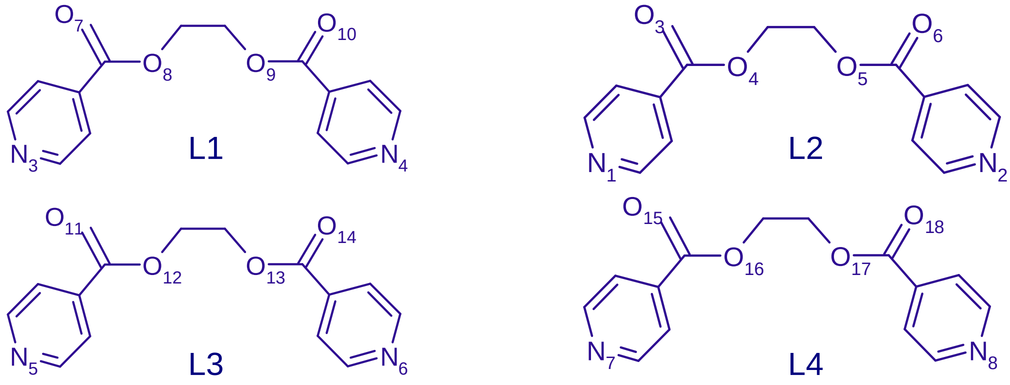

Figure B-75: Label of the ligand molecules in 13

The Cu1 copper ion is coordinated by four ligand molecules (L1 and L2) through the nitrogen atoms in equatorial positions, one water molecule (O1) and one perchlorate anion (Cl1) in apical positions of an octahedral coordination environment, in order to form double chain motifs similar to **11** (Figure B-76). Similar chains involve the Cu2 copper ions coordinated by the ligands L3 and L4, one water molecule (O2) and one perchlorate anion (Cl2). The coordination sphere of both copper ions is distorted with copper-nitrogen distances (2.02 to 2.05 Å) shorter than copper-oxygen distances (2.28 to 2.85 Å) (Table B-41). The Cu1 atom lies by 0.114(2) Å out of the plane formed by the nitrogen atoms, whereas the Cu2 atom is by 0.514(3) Å out of its corresponding plane. This is due to a stronger coordination of the water molecule on Cu2 (2.278(5) Å) than on Cu1 (2.311(4) Å).

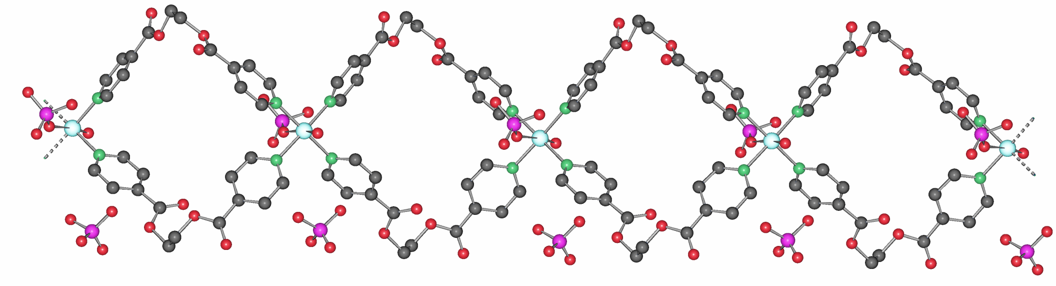

Figure B-76: double chain motif in 13 (uncoordinated water and THF molecules omitted for clarity)

Like in **11**, the chains organize themselves parallel in “groups” of chains, creating THF containing-channels along the *b*-axis (Figure B-77a). The chains are not fully stacked, but slightly offset, offset attributed to the presence of two kinds of chains. The same interactions (hydrogen bonds) between the chains are observed as in **11** (Table B-42). Only the C-H···π interactions between pyridyl rings and THF hydrogen atoms disappear, as some THF molecules are involved in other interactions in the channels.

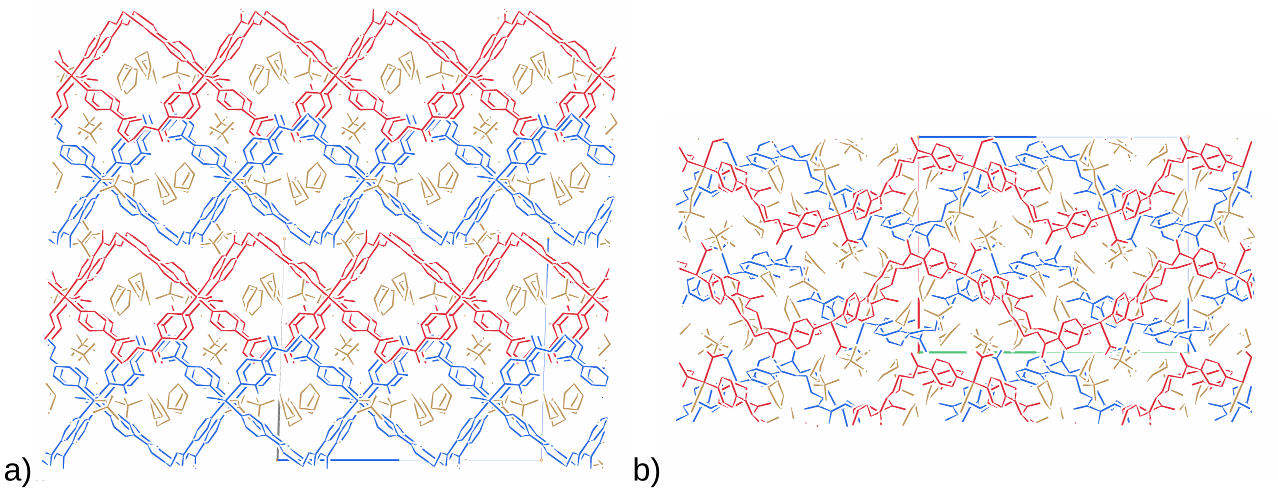

Figure B-77: Crystal packing in 13: a) along the *b*-axis and b) along the *a*-axis (stacked chains in red and blue; co-crystallized molecules in brown)

Along the *a*-axis, the stacking of the chains leads to the second kind of channels in which the non coordinating molecules (water, perchlorate) are localized, as well as the coordinating water molecules (Figure B-77b). Both compounds, **11** and **13**, differ in the organisation of the molecules in these channels. Whereas in **11**, the molecules form a hydrogen bonded network along the channels directions, a similar network is not present in **13**. Firstly, the coordinating perchlorate anions, as well as two of the THF molecules are involved in the channels interactions.

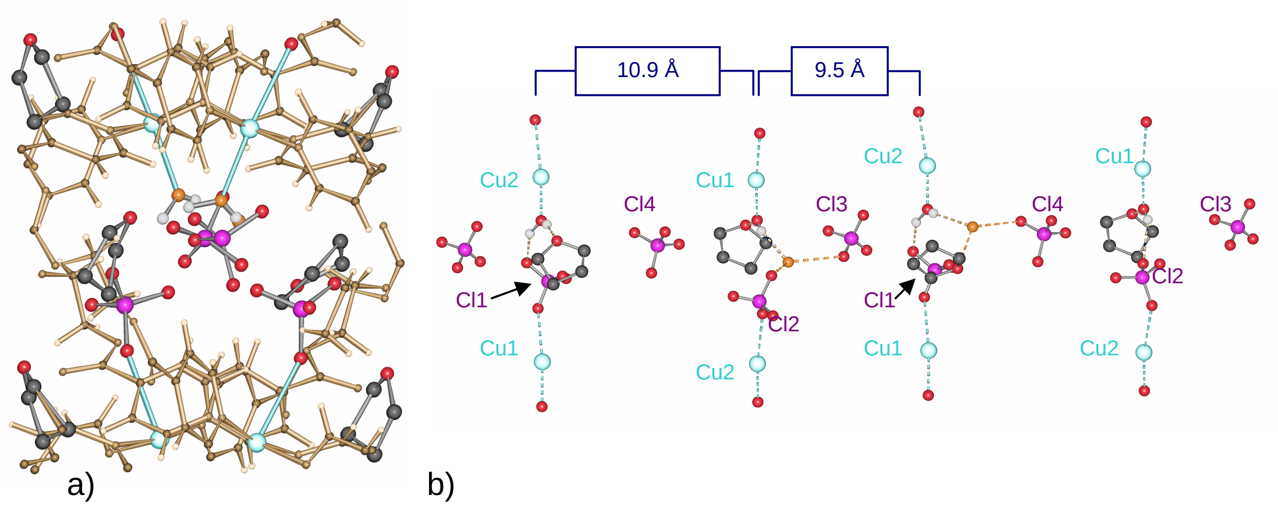

Figure B-78: a) detail of the molecules localized in the channels (skeleton in brown); b) organisation of the molecules in the channels in 13

The molecules located in the channels are the coordinating water molecules (O1, O2), the non-coordinating water molecules (O39/O40) and the non-coordinating perchlorate anions (Cl3 and Cl4). The other involved molecules (perchlorate-Cl1 and Cl2- and THF molecules-O35 and O36-) are also embedded in the organic skeleton (Figure B-78a). As shown on Figure B-78b, the molecules do not interact along the channel axis but are organized around the copper ions. Due to the disorder of some molecules and the non-coordinating water molecule, O39/O40, (both positions were refined at half site occupancy), different cases have to be distinguished.

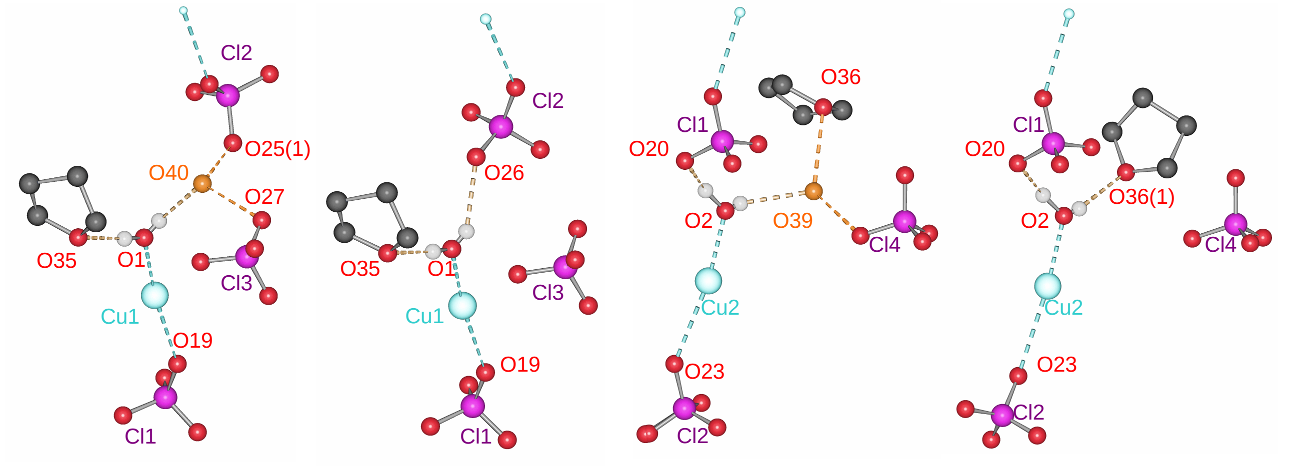

a) environment around O1-water molecules b) environment around O2-water molecules

Figure B-79: the different interactions in the channels in 13

- *environment around O1 water molecules* (Figure B-79a): The O1 water molecule forms one hydrogen bond with one THF molecule (O35) through its H1A atom. The other hydrogen atom (H1) is involved in one or the other of the following interactions: *i)* If the water molecule O40 is present, it is involved in hydrogen bonds with O25 (perchlorate coordinated to Cu2), O27 (non-coordinating perchlorate) and O1. *ii)* In the other case, the non-coordinating water molecule is not present, and there is a hydrogen bond between the water molecule and the Cl2 perchlorate anions. It is worthy to note that this perchlorate has two different positions in correlation with the presence or the absence of the non-coordinating water molecule.

- *environment around O2 water molecules* (Figure B-79b): The O2 water molecule always forms hydrogen bonds with the Cl1 perchlorate anion (coordinating Cu1) and with one non-coordinating water molecule or with one THF molecule according the cases: *i)* The presence of the non-coordinating water molecule (O39) leads to the formation of hydrogen bonds from this molecule to the coordinating water molecule, the THF molecule (O36) and the non-coordinating perchlorate anion (O39). *ii)* On the other hand, if the O39 water molecule is not present, there is a hydrogen bond between O2 and the THF molecule (O36). This molecule of THF is disordered, so that there are two possible positions in correlation with the presence of the O39 water molecule.

The distances corresponding to these interactions are listed in Table B-41 and Table B-42.

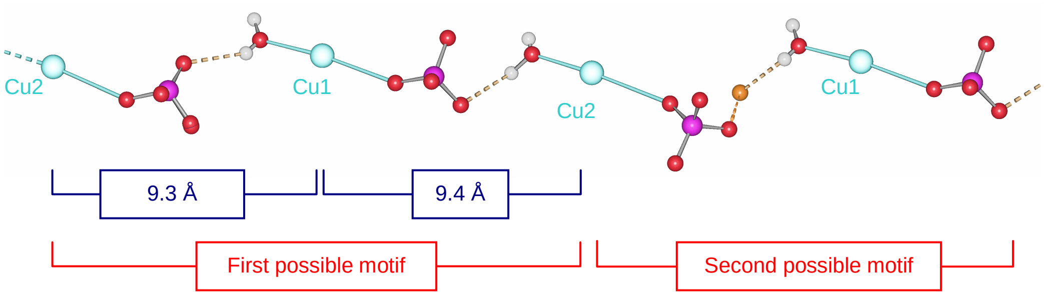

Figure B-80: perchlorate-water-copper networks in 13 along the *b*-axis

These interactions contribute to the bridging of the copper ions either through one water molecule and one perchlorate anion or through two water molecules and one perchlorate anion. The so-built interactions lead to the formation of perchlorate-water-copper networks running along the *b*-axis (Figure B-80).

Table B-41: most important bond lengths (Å) and angles (°) in 13

	Cu1		Cu2			Cu1	Cu2
Cu-N	2.025(4)		2.022(4)		N-Cu-N	90.3(2)	90.6(2)
	2.029(4)		2.035(4)			89.4(2)	88.9(2)
	2.041(4)		2.044(4)			88.4(2)	88.7(2)
	2.052(4)		2.055(4)			91.1(2)	91.0(2)
Cu-OH$_2$	2.311(4)		2.278(5)		Cu-O(ClO$_3$)	2.799(4)	2.85(2)
C-N	1.345(6)	to	1.346(6)	to	C-N-C	118.3(4)	118.9(4)
	1.366(6)		1.374(7)			118.1(4)	119.0(4)
						118.9(4)	118.3(4)
						119.3(4)	117.5(3)
(H$_2$)O-O(ClO$_3$)	O40-025(1)		2.78(2)		(H$_2$)O-O(THF)	O39-O36	2.79(1)
	O40-O27		2.89(1)				
	O39-O33		2.962(9)				

Table B-42: Hydrogen bond data for 13 [lengths (Å) and angles (°)]

D-H···A	*d*(D-H)	*d*(H···A)	*d*(D···A)	Angle D-H···A
inter-chains ligand-ligand hydrogen interactions				
C41-H41···O3$^{\#1}$	0.93	2.75	3.566(7)	147.2
C36-H36···O11$^{\#1}$	0.97	2.82	3.698(7)	150.5
C13-H13···O11$^{\#1}$	0.93	2.60	3.462(6)	153.5
C30-H30···O14	0.93	2.87	3.611(6)	137.2
C8-H8B···O14$^{\#1}$	0.97	2.80	3.715(7)	158.1
C15-H15···O18$^{\#2}$	0.93	2.44	3.026(6)	121.1
C-H···O hydrogen interactions between ligand and THF				
C14-H14···O35$^{\#1}$	0.93	2.41	3.308(7)	162.5
C42-H42···O361$^{\#1}$	0.93	2.43	3.33(1)	161.2
C-H···O hydrogen interactions between perchlorate and ligand				
C4-H4···O28$^{\#3}$	0.93	2.44	3.191(6)	137.8
C8-H8A···O23$^{\#1}$	0.97	2.56	3.50(2)	162.8
C8-H8A···O25$^{\#1}$	0.97	2.48	3.27(2)	138.4
C8-H8A···O251$^{\#3}$	0.97	2.53	3.34(2)	140.5
C11-H11···O27$^{\#4}$	0.93	2.54	3.457(7)	166.8
C17-H17··O25$^{\#5}$	0.93	2.55	3.28(2)	135.5
C17-H17···O251$^{\#5}$	0.93	2.53	3.25(2)	135.1
C22-H22B···O24$^{\#2}$	0.97	2.36	3.07(2)	130.1
C26-H26···O32$^{\#1}$	0.93	2.50	3.220(6)	134.3
C28-H28···O22$^{\#6}$	0.93	2.47	3.167(7)	131.7
C29-H29···O261$^{\#3}$	0.93	2.57	3.30(1)	135.8
C31-H31···O28$^{\#7}$	0.93	2.46	3.354(7)	160.6
C36-H36A···O20$^{\#1}$	0.97	2.59	3.367(6)	137.2
C43-H43···O20$^{\#3}$	0.93	2.48	3.373(7)	162.2
C54-H54···O26$^{\#8}$	0.93	2.40	3.26(1)	154.4
hydrogen interactions between water				
O1-H1···O40$^{\#5}$	0.68(7)	2.08(7)	2.66(1)	145(7)
O2-H2···O39$^{\#3}$	0.56(6)	2.32(7)	2.81(1)	150(9)
hydrogen interactions between water and perchlorate				
O1-H1···O26$^{\#5}$	0.68(7)	2.29(7)	2.88(1)	147(7)
O2-H2A···O20$^{\#3}$	0.99(9)	2.21(9)	3.085(6)	146(7)
hydrogen interactions between water and THF				
O2-H2···O361$^{\#7}$	0.56(6)	2.14(6)	2.76(1)	164(9)
O1-H1A···O35$^{\#9}$	0.97(8)	1.80(9)	2.752(6)	167(7)

Symmetry transformations used to generate equivalent atoms: #1 -X+1, -Y, -Z+1; #2 -X+2, -Y, -Z+1; #3 X, Y, Z; #4 -X+1, -Y+1, -Z+1; #5 X, Y+1, Z; #6 X, -Y+1/2, Z+1/2; #7 -X+1, Y-1/2, -Z+1/2; #8 X, -Y-1/2, Z+1/2; #9 -X+1, Y+1/2, -Z+1/2.

Copper perchlorate coordination polymers with bipyridine bridging ligands

The influence of the counter anions on Cu^{II} coordination polymers is less studied than in the case of Ag^{I}. The related compounds with perchlorate anions present a tetrakis-pyridyl metal environment, the coordination sphere being completed by water molecules, the counter anions being not coordinating [49, 276, 277, 280]. These structures show two-dimensional or three dimensional (diamondoid) motifs. For instance, the reaction between $Cu(ClO_4)_2{\cdot}6H_2O$ and bipyridine leads to the formation of a two-dimensional square grid framework [277] with the uncoordinated perchlorate anions and solvent molecules between the layers. This compound is obtained from an acetonitrile/water mixture of solvents.

To our knowledge, only one Cu^{II} coordination polymer exhibits a coordinating perchlorate anion [278]. This compound grows from a mixture methanol/dichloromethane, no water molecules are coordinating the copper centres. The structural motif is thus a one-dimensional double chain motif with an $\{CuN_4O\}$ square pyramidal coordination environment for the copper ions. The distance copper-oxygen is shorter than in **13**, due to the absence of other interactions in the crystal packing.

Comparison of 11 and 13

Both compounds **11** and **13** are very similar, if the motif, the chain packing is considered. But some differences have to be noticed. The distances in the one-dimensional chains are in the same range, particularly the copper-nitrogen distances. On the other hand, the distances copper-oxygen are longer in **13** than in **11**. This may be a consequence of the difference in the involvement of the coordinating water molecules and counter anions in the channels. Indeed, the coordinating nitrate anions do not participate to the hydrogen bonding network in **11**, allowing the nitrate anion to form a stronger coordination bond with Cu^{II} ions. The other main difference between both compounds is the organisation of the non-coordinating molecules in the channels: in **11**, a hydrogen bonding network allows the formation of a copper-water-nitrate system along the channel axis, whereas in **13**, a system copper-water-perchlorate appears perpendicularly to the channel direction. In the first case, the copper atoms are of 11.1 and 9.4 Å apart, in the second case, they are separated by distances of 9.3 and 9.4 Å.

C - Conclusion

This thesis reports the synthesis of the ligand ethanediyl bis(isonicotinate), **L**, as well as the building of coordination polymers based on **L** and Cu^I, Ag^I and Cu^{II} salts. The Figure C-1 resumes the obtained compounds.

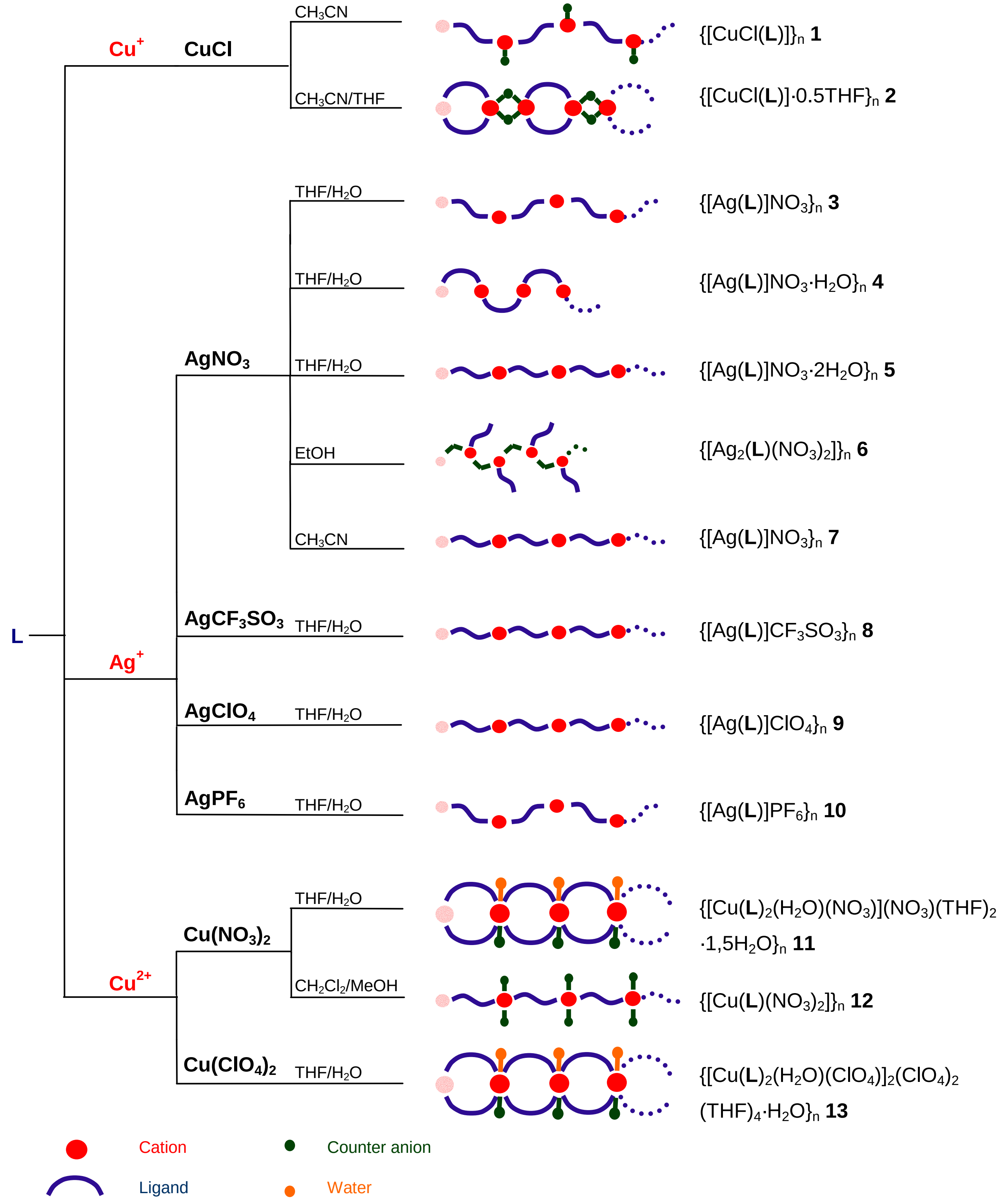

Figure C-1: summary scheme of the obtained coordination polymers with L and Cu^I, Ag^I and Cu^{II} ions

One-dimensional motifs

Construction of coordination polymers with ethanediyl bis(isonicotinate) and copper or silver shows a preference for one-dimensional structural motifs. Indeed, all obtained compounds (except **6**) present one-dimensional chains independently of the cation used: various linear chains or double chains with the ligand either in *anti-* or *gauche-*conformation. Such motifs were expected for the Ag^{I} complexes, as they are the most frequently found ones in coordination polymers with 4,4'-bipyridine-derived ligands [9, 11]. On the other hand, Cu^{II} metal cations allow the construction of coordination polymers of higher dimensionality. Such networks are in principle possible, but have never been observed along this thesis work.

Ligand functionalities

The role of the ligand in the coordination polymer construction may be described as follows: The ligand molecules always coordinate the metal ions through their two nitrogen atoms. The construction of the motifs is afterwards driven by the interactions involving the ligands, the counter anions and the solvents. The predominant interactions featured by the ligand involve the carbonyl groups (hydrogen bonding acceptors) and the isonicotinic groups (π-stacking, Ag···π interactions) (Figure C-2). During the crystal formation, there is competition between all possible interactions. The presence of some or the other interactions determines the conformation of the ligand and the long-range organisation.

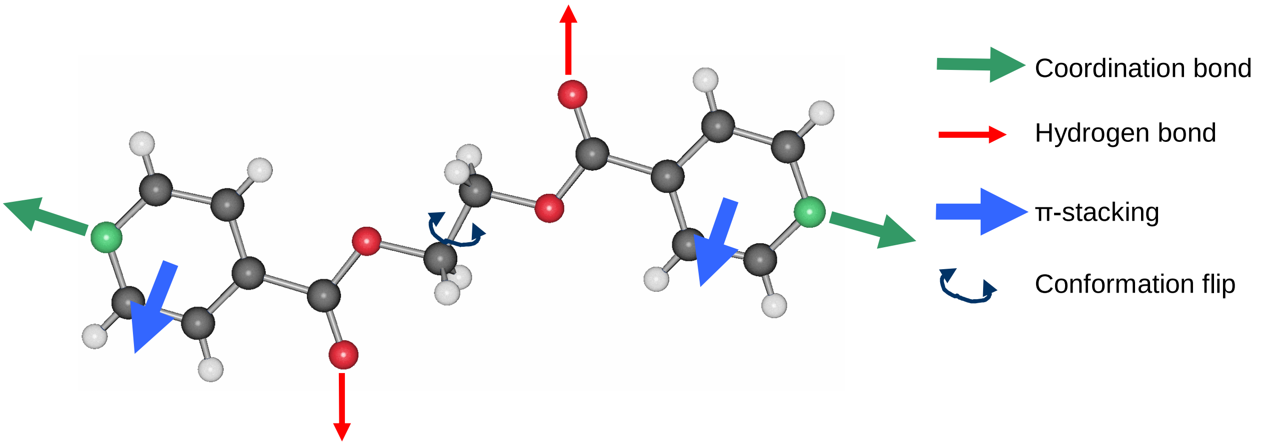

Figure C-2: predominant interactions with the ligand ethanediyl bis(isonicotinate)

For instance, the π-stacking between pyridyl rings of different ligands leads to the parallel organisation of the molecules in **5** and **7**. The interactions between ligand molecules thanks to hydrogen bonding contribute to the parallel stacking of the molecules for example in **3**, **7**, **8** and **12**. The inclusion of solvent molecules in the structures may furthermore induce the *gauche*-conformation of the ligand, like in **2**, **4**, **11** and **13**. The ability of the bridging part of the ligand to form hydrogen bonds and to rotate seems thus to favour the apparition of one-dimensional motifs.

Role of the counter anions

Another important parameter of the building of coordination polymers is the behavior of the counter anions. The coordination ability of the different counter anions was studied in the Ag^I coordination polymers. The nitrate anion is very flexible in its bridging mode and strength. It is therefore able to act as bridging ligand between two silver atoms as in **3** or **7** in which it links several chains together. It also shows its ability to support a metal-metal contact in **4** and **5**. Its coordination strength can be tuned by the number of hydrogen bonds it can be involved in with for instance water molecules. Thus, the silver-oxygen(nitrate) distances increase with the number of co-crystallizing solvent. Solvation of $AgNO_3$ also plays a role in Ag-NO_3 distances in the crystal structure (Graph C-1). In our Cu^{II} coordination polymers, the nitrate anion however only acts as a monodentate or anisobidentate ligand.

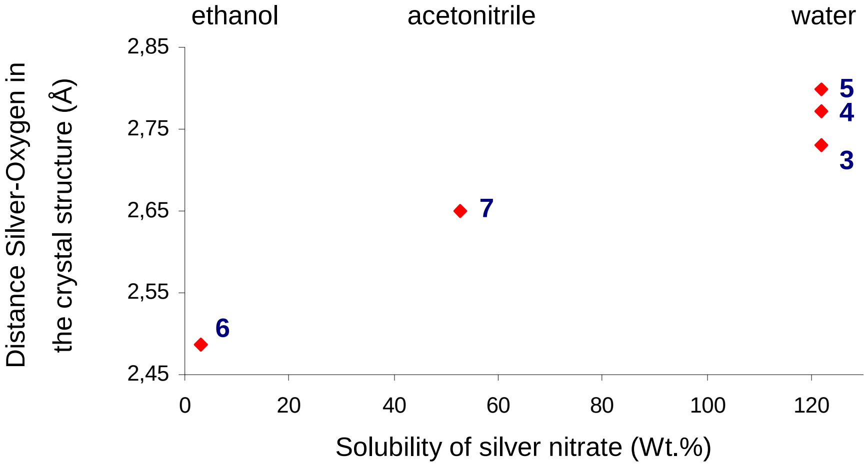

Graph C-1: dependence of distance silver-oxygen in the crystal structure for compounds 3 to 7 towards the silver nitrate salt solubility in the used crystallization solvent

Less coordinating counter anions change the nature and the number of interactions in the final packing. The counter anions are thus influencing the coordination sphere of the metal ions, as well as the long-range order.

The role of the counter anion in the Cu^{II} coordination polymers seems to be less important than the role of the crystallization conditions, as two almost isostructural complexes are obtained with either nitrate or perchlorate anions. However, no final conclusion can be derived from this as other non-coordinating anions have not been investigated.

Influence of the crystallization conditions

The influence of the solvent has been outlined with different compounds. Two solvent contributions can here be distinguished: the coordination ability of solvent molecules as in **11** and **13** and the different solvation of the reagents by the solvent in the crystallization process. In some cases, the interactions between solvent molecules and reagents remain in the solid state, and solvent molecules co-crystallize, as in **2**, **4**, **5**, **11** and **12**.

General conclusions

On a more general view, the synthezised compounds revealed to us the manifold structural modifications possible for Ag and Cu coordination polymer networks with our ligand ethanediyl bis(isonicotinate). By isolating several influences, we were able to gain a little insight in the type and mechanisms of interactions that lead to a certain structure.

Outlooks

After this study of the behavior of the ligand ethanediyl bis(isonicotinate) with copper and silver ions during coordination polymer construction, further investigations can be carried out.

Cu^{II} coordination polymers could be improved to get efficient coupling between the Cu^{II}, long-range magnetic ordering in low-dimensional metal complexes representing one of the most challenging research areas in chemistry and materials science.

Another research interest with the presented systems is to favour certain structures using the O-donors atoms, to coordinate NH_4^+ by hydrogen bonding or other metals ions. This approach should lead to crossing of chains for instance with the use of tetrahedral centres and the so-formed mixed metal compounds could be used as mixed metal precursors for oxide materials.

The coordination polymers allow the distribution of the metal centres at determined distances from each other (for example 17 Å between the silver ions in our one-dimensional Ag^I coordination polymers). If these species can be deposited on surfaces, local silver clusters could be formed by reduction or the biological activity of silver (sterilization of surfaces) could be investigated.

In a more fundamental way, the presented compounds may help in the understanding of polymorphism, and contribute on a long term to the control of the formation of such compounds. This may then be an important contribution to the highly interesting problem of structure prediction and crystal engineering.

D - Experimental

I - Reagents and solvents

The reagents were purchased and directly used without further purification, if described otherwise. CuCl was synthesized according to the literature description [284]. For the syntheses of **L** and Cu^{I} compounds, dried and distilled solvents were used under N_2 atmosphere: ethylene glycol (sodium), THF (sodium, benzophenone) and acetonitrile (CaH_2).

II - Equipments

Elementary analyses were performed by Dr. H. Eder, from the Laboratoire de Microchimie, University of Geneva, for **L**, **2**, **8** and **9** and by W. Kirsch, from the Mikrolabor, University of Basle for **L**, **3**, **4**, **5**, **7**, **10**, **11**, **12** and **13**.

IR-spectra were collected on a Perkin Elmer, Spectrum One FT-IR-spectrometer using KBr or CsBr plates, from 4000 to 250 cm^{-1}, at the University of Geneva for **L**, **2**, **8** and **9** and on a Shimazu FTIR-8400S equipped with Golden Gate ATR (attenuated total reflection) system at the University of Basle for **L**, **3**, **4**, **5**, **7**, **10**, **11**, **12** and **13**. Frequencies are given in cm^{-1}. Abbreviations used are: s, strong; m, medium and w, weak.

Luminescence curves were measured on a Perkin Elmer LS 50B at the University of Geneva for **L** and **2**, and on a Perkin Elmer LS 50B at the University of Basle for the other compounds. Measurements were collected on solid state samples in a capillary.

^{1}H-NMR analyses were performed on a Varian Gemini 300 spectrometer, at 298 K. The chemical shifts are given in ppm relative to tetramethylsilane (TMS) as an internal standard. Abbreviations used are: s, singulet and m, multiplet.

UV-Vis properties were analysed with a Varian Cary 1E at the University of Geneva.

Powder X-ray diffraction data for **7** and **8** was registered on a D 5000 Kristalloflex Siemens diffractometer (Bragg-Brentans geometry; CuK$_{\alpha}$ radiation) in the Mineralogie Fakultät, University of Basle.

TGA/SDTA measurements were performed on a Mettler Toledo TGA/SDTA851e Modul under N_2 (10cm^{3}/min) in aluminium crucibles.

ESI-MS spectra were recorded with a Finnigan-4000 and VG-7000E by the laboratoire de Spectrométrie de Masse, University of Geneva for **2** and **7** and on a Finnigan MAT LCQ at the University of Basle for **7**, **8**, **9**, **10**, **11** and **12**.

Fast Atom Bombardment Mass Spectroscopy of **7** was obtained on a Finnigan MAT 312, by Dr. H. Nadig, Massen-Spektroskopie Labor, University of Basle.

III - Synthetic part

III.1 - Ligand L

Synthesis I Isonicotinic acid (15 g, 0.122 mol) is strirred in $SOCl_2$ (40 mL) in the presence of DMF (0.6 mL) at 60°C for 12h. Excess thionyl chloride is removed *in vacuo*. Dried ethylene glycol (3.4 mL, 0.061 mol) is added. After the evolution of hydrogen chloride ends, the mixture is heated at 150°C for a few hours. The mixture is dissolved in water, and NH_4OH is added. After filtration, recrystallization in ethyl acetate gives white crystals of **L**. Yield 6 g (39%).

Analysis calculated for $C_{14}H_{12}N_2O_4$: C 61.76, H 4.44, N 10.29; found: C 61.12, H 4.52, N 10.11%.

^1H NMR (300MHz, THF, 293 K): δ(ppm) 8.73 (4 H, m, H-pyr), 7.82 (4H, m, H-pyr), 4.69 (4H, s, H-ethyl).

IR (KBr, cm^{-1}): ν(C=O) 1732s, ν(C=C) 1597 m, ν(ArC-C, C=N) 1412 s, ν(C-O) 1276 s, δ(ArC-H) 984 m. IR (CsBr, cm^{-1}): ν(ArC-H) 818 w, γ(ArC-H) 348 m.

UV-Vis (acetonitrile): 210, 271 nm.

Luminescence (77K): 409 nm (excitation at 234 nm)

Synthesis II Ethylene glycol (0.26 mL, 4 mmol) is added to isonicotinic acid (1 g, 8 mmol) in dichloromethane (10 mL) in stoechiometric ratio (1:2). A solution of 1,3-Dimethyl-2-chloroimidazolium chloride (DMC) (1.66 g, 8 mmol) in dichloromethane (5 mL) is added dropwise to the mixture. After a few minutes of stirring, pyridine as solvent (5 mL) is added in order to dissolve the crude white solid product. The reaction is refluxed for 2 hours and turns from yellow to dark yellow with the precipitation of a dark solid. The product remains in the liquid phase. After filtration, the solution is evaporated *in vacuo.* The product is dissolved in dichloromethane and purified on a chromatography column. The solvent mixture hexane/ethyl acetate (4:1) allows the elimination of the impurities, and ethyl acetate allows the elution of the pure product. The white product is obtained by *vacuo* elimination of solvent of the corresponding fractions. Yield 1.213 g (95%).

Analysis calculated for $C_{14}H_{12}N_2O_4$: C 61.76, H 4.44, N 10.29; found: C 61.58, H 4.72, N 9.76%.

^1H NMR (300MHz, THF, 293 K): δ(ppm) 8.77 (4 H, m, H-pyr), 7.83 (4H, m, H-pyr), 4.71 (4H, s, H-ethyl).

IR (GB, cm^{-1}): ν(C=O) 1720s, ν(C=C) 1597 m, ν(ArC-C, C=N) 1412 s, ν(C-O) 1257 s, δ(ArC-H) 980 m, ν(ArC-H) 848 w (Graph D-1).

UV-Vis (acetonitrile): 210, 271 nm.

Luminescence (77K): 409 nm (excitation at 234 nm)

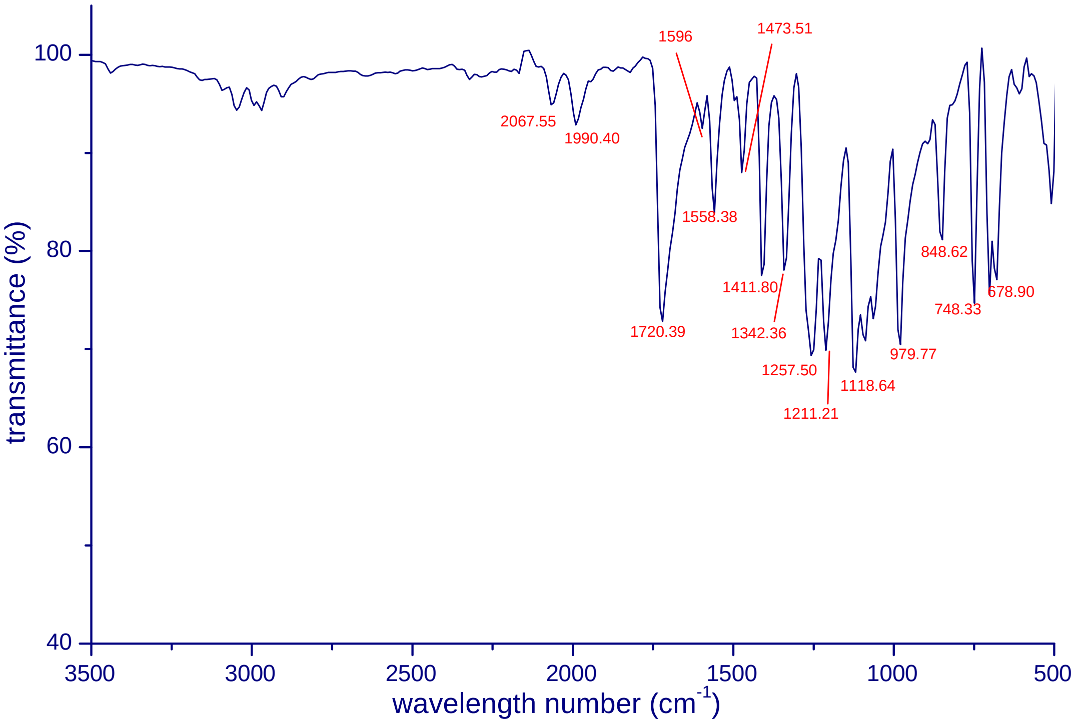

Graph D-1: IR spectrum of L

III.2 - {[CuCl(L)]}$_n$ 1

Reaction A: A solution of L (50,4 mg, 0,18 mmol) in dry acetonitrile (30 mL) is added to a solution of CuCl (9,1 mg, 0,09 mmol) in dry acetonitrile (10 mL). (molar ratio 2 : 1) giving a yellow solution. After concentration, the solution is left at room temperature for three months, then yellow-orange crystals **1** suitable for single crystal X-ray analysis appear in a low yield.

Reaction B: The mother liquor containing the crystals of **2** stays at room temperature for several weeks and transformation of **2** into the crystals **1** is observed.

Unfortunately the poor yield of these reactions and the poor stability of the crystals in air don't allow complementary characterization analyses.

III.3 - $\{[CuCl(L)]\cdot 0.5THF\}_n$ 2

Reaction A: The principle of the synthesis is the slow diffusion of the two solutions into each other. One arm of the tube is filled with a solution of CuCl (9.1 mg, 0,09 mmol) in dry acetonitrile (10 mL), and the other with a solution of **L** (50,4 mg, 0,18 mmol) in dry THF (10 mL). (molar ratio) In one case the two solutions are separated with a physical barrier (fritt). In the second case the separation is made with solvent (THF): THF is introduce in the "U-shaped" tube and frozen by immerging the tube into liquid nitrogen; then the two solutions are introduced carefully on the THF under nitrogen stream and after warming up of THF, the two solutions can diffuse. The crystals appear at the interface CH_3CN/THF as CuCl is not soluble in THF.

Reaction B: A solution of CuCl (7,8 mg, 0,08 mmol) in dry acetonitrile (5 mL) is added to a solution of **L** (21,6 mg, 0.08 mmol) in dry THF (6 mL). (molar ratio 1:1) The solutions is stirred for few minutes and red crystals of **2** appear after few hours. Yield: 8 mg (24%) The red crystals are stable in air after removal from mother liquor.

Analysis calculated for [CuCl(**L**)]·0,5(C_4H_8O): C 47.18, H 3.96, N 6.88; found: C 47.29 , H 3.97, N 6.81%.

IR (KBr, cm^{-1}): ν(C=O) 1731s, ν(C=C) 1603 w, ν(ArC-C, C=N) 1411 s, ν(C-O) 1269 s, δ(ArC-H) 1025 w. IR (CsBr, cm^{-1}): ν(ArC-H) 808 w, γ(ArC-H) 350 m, ν(Cu-N) 196 s.

Luminescence (solid state): emission at 385 nm for an excitation at 240 nm. (Graph D-2)

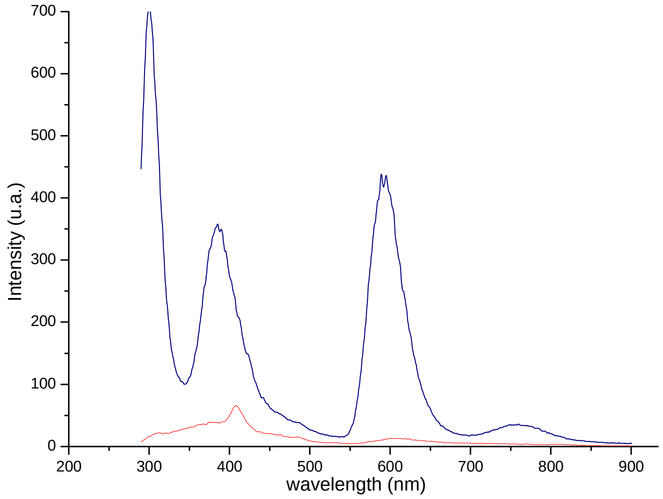

Graph D-2: emission spectrum of 2 (blue) compared to the emission spectrum of L (red)

ESI-MS (acetonitrile, m/z): 335.1, $[Cu\mathbf{L}]^+$; 435.0, $[Cu\mathbf{L}_2]^+$; 533.0, $[CuCl\mathbf{L}H]^+$; 607.2, $[Cu_3Cl_2\mathbf{L}]^+$; 666.7, $[Cu_4Cl_4\mathbf{L}H]^+$ (Graph D-3).

UV-Vis (acetonitrile): 211 and 274 nm.

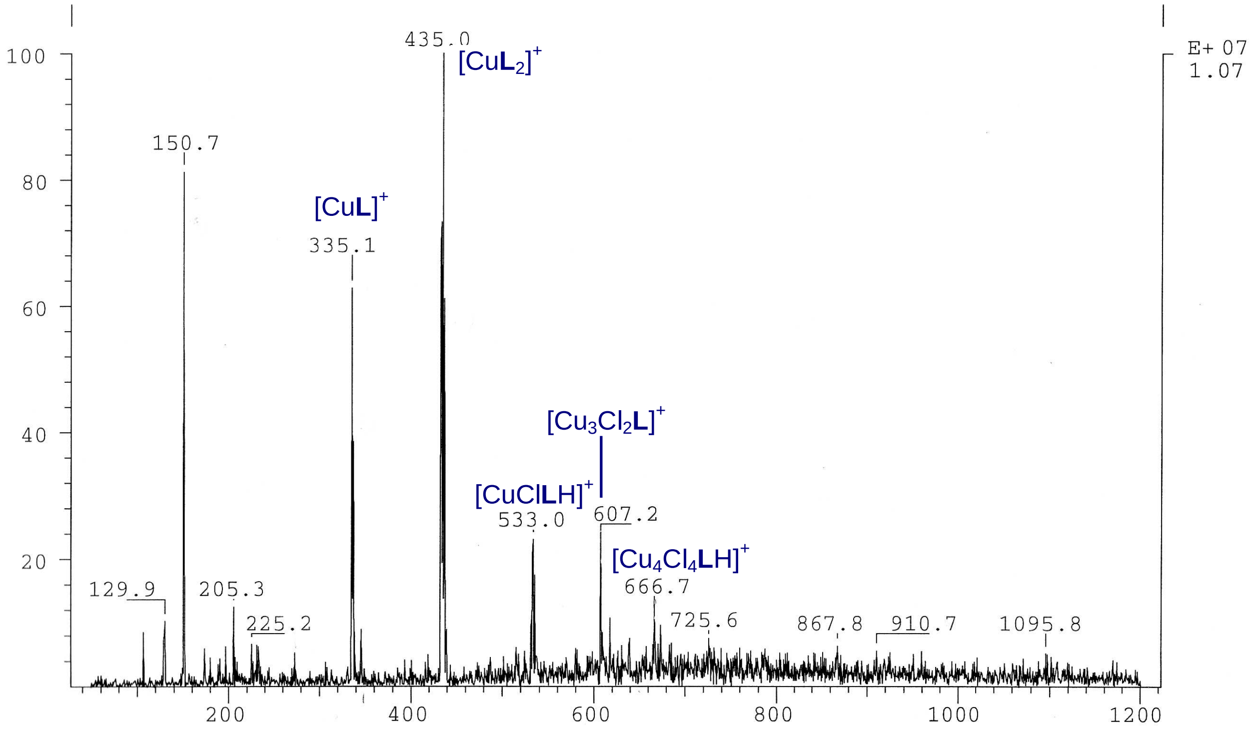

Graph D-3: ESI-MS (acetonitrile) of 2

III.4 - $\{[Ag(L)](NO_3)\}_n$ 3

Reaction A: Colorless crystals of **3** grew from a mixture of the solution of **L** (20mg, 0.04 mmol) in THF (5 mL) and a solution of $AgNO_3$ (12 mg, 0.07 mmol) in water (5mL) in darkness and at room temperature. Yield after drying: 23 mg (72 %).

Reaction B: Crystals of **3** are also obtained from a solution of **L** (50 mg, 0.18 mmol) and $AgNO_3$ (31 mg, 0.18 mmol) in THF (10 mL), heating to about 70°C, followed by fast cooling by putting it in the refrigerator at about 4°C just after the heating. Yield: 50 mg (62%).

Analysis calculated for $[Ag(\mathbf{L})]NO_3$: C 38.03, H 2.74, N 9.50; found: C 37.98, H 2.60, N 9.39%.

IR (GB, cm^{-1}): ν(C=O) 1720 s, ν(C=C) 1612 m, ν(ArC–C, C=N) 1412 s, ν(NO_3) 1365–1319 i, ν(C–O) 1265 s, δ(ArC–H) 980 m, ν(ArC–H) 856 w (Graph D-4).

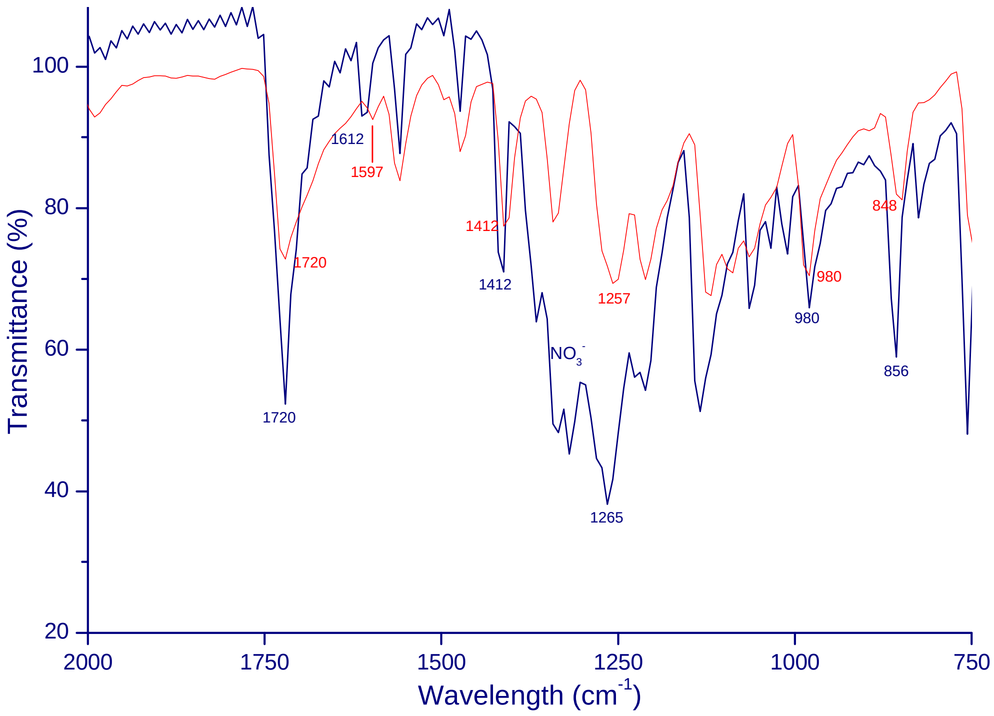

Graph D-4: Comparison between the IR-spectra of L (red) and 3 (blue)

TGA/SDTA: no loss/gain of weight and no phase transition before the decomposition of the product at 260°C.

UV-Vis (CH_3CN): absorption at 212 and 273 nm.

Luminescence (solid state): 406 nm (excitation at 232 nm) at 77K. (Graph D-5)

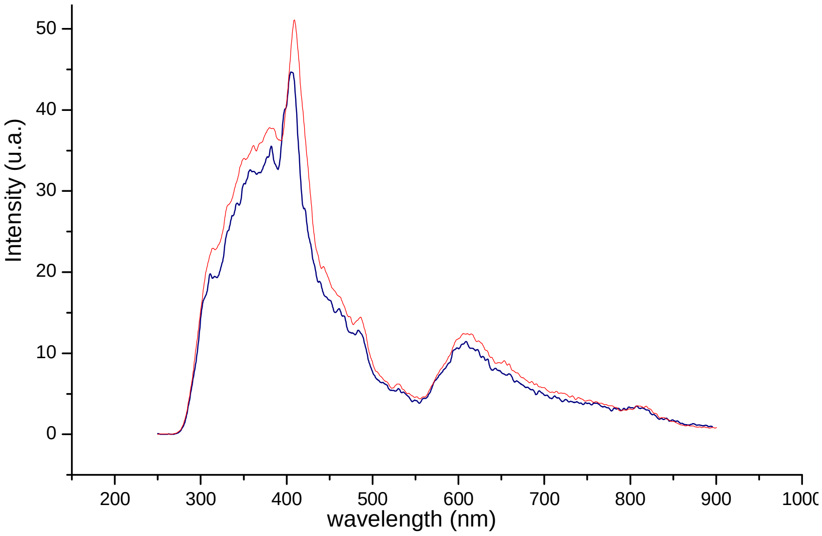

Graph D-5: emission spectrum of 3 (blue) compared to the emission spectrum of L (red)

III.5 - $\{[Ag(L)]NO_3(H_2O)\}_n$ 4

Crystals of **4** are obtained in an “H-shaped” tube. A solution of **L** (40 mg, 0.15 mmol) in THF (5 mL) is introduced in one tube arm, a solution of $AgNO_3$ (25 mg, 0.15 mmol) in water (5 mL) being introduced in the other arm. Both solutions are frozen and the diffusion solvent THF (~15 mL) is layered on top. The tube stays in the dark, and crystals appear after a couple of days. Crystals appear simultaneously with other crystals of **3** and **5** and polycrystalline powder. Yield after sorting: 12 mg (15%).

Analysis calculated for [Ag(**L**)]$NO_3(H_2O)$: C 36.54, H 3.07, N 9.13; found: C 36.47, H 2.98, N 9.07%.

IR (GB, cm^{-1}): ν(C=O) 1720 s, ν(C=C) 1612 m, ν(ArC–C, C=N) 1419 s, ν(NO_3) 1380–1330 i, ν(C–O) 1265 s, δ(ArC–H) 972 m.

TGA/SDTA: an exothermal loss of one water molecule at 117°C (loss of weight: 3.1%; calculated: 3.9%). (Between the starting temperature and the water loss temperature, weight loss (3%) is also observed but it corresponds to adsorbed solvent as we not fully dried the crystals before the measurement for maintaining its structure and the inclusion molecules.)

UV-Vis (CH_3CN): absorption at 212 and 273 nm.

Luminescence (solid state): 397 nm (excitation at 230 nm).

III.6 - $\{[Ag(L)]NO_3(H_2O)_2\}_n$ 5

Crystals of **5** appear during the slow diffusion using an “H-shaped” tube. A solution of **L** (40 mg, 0.15 mmol) in THF (5 mL) is introduced in one tube arm, a solution of $AgNO_3$ (25 mg, 0.15 mmol) in water (5 mL) being introduced in the other arm. Both solutions are frozen and the diffusion solvent THF (~15 mL) is layered onto the solutions. The tube stays at room temperature in darkness and crystals appear after a couple of weeks. Crystals appear simultaneously with other crystals of **3** and **4**, polycrystalline powder. Yield after sorting out: 9 mg (13%).

Analysis calculated for [Ag(**L**)]$NO_3(H_2O)_2$: C 35.17, H 3.37, N 8.79; found: C 35.34, H 3.36, N 8.61%.

IR (KBr, cm^{-1}): ν(water) 3540-3300 m, ν(C=O) 1728 s, ν(water) 1635 w ν(C=C) 1612 m, ν(ArC–C, C=N) 1420 s, ν(NO_3) 1380–1330 s, ν(C–O) 1265 s, δ(ArC–H) 980 m, ν(ArC–H) 864 w (Graph D-6).

TGA/SDTA: an endothermal loss of two water molecule between 25 and 70°C (loss of weight: 7.44%; calculated: 7.52%). The compound decomposes at 220°C.

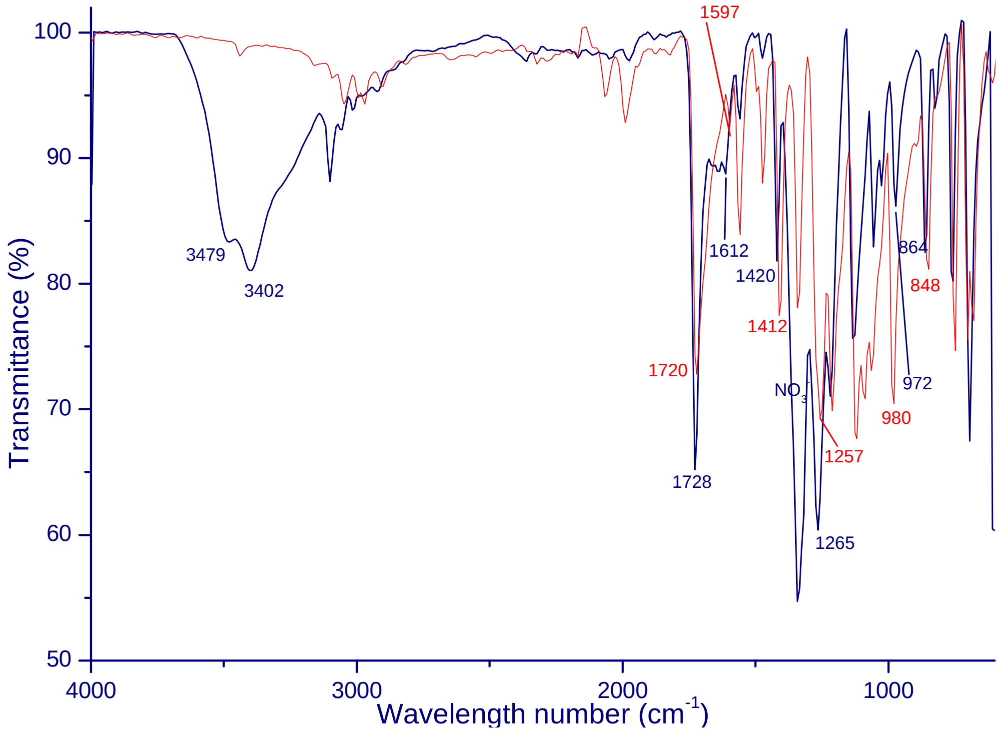

Graph D-6: Comparison between the IR-spectra of L (red) and 5 (blue)

Luminescence (solid state): 388 nm (excitation at 238 nm). (Graph D-7)

UV-Vis (CH_3CN): absorption at 212 and 273 nm.

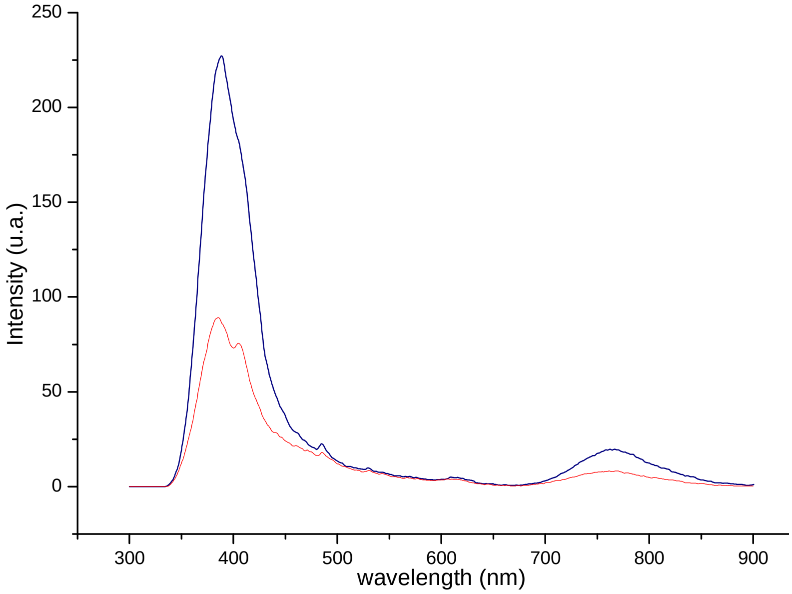

Graph D-7: emission spectrum of 5 (blue) compared to the emission spectrum of L (red)

III.7 - $\{[Ag_2(NO_3)_2(L)]\}_n$ 6

A solution of **L** (20 mg, 0.07 mmol) in THF (5 mL) is introduced in one arm of an “H-shaped” tube, a solution of $AgNO_3$ (12 mg, 0.07 mmol) in ethanol (5 mL) in the other one.

(molar ratio 1:1) The solutions are frozen in liquid nitrogen and THF is then layered into the tube in order to bridge the two reagent solutions. There is a fritt in the linking part of the tube. The slow diffusion occurs through the THF layer and the fritt. Crystals of **6** appear after several months at the interface EtOH/THF. After using some single crystals for X-ray diffraction, the product is collected. Yield: 4mg (11%). This quantity was not sufficient to perform a good elementary analysis.

III.8 - $\{(Ag(L)](NO_3)\}_n$ 7

Reaction A: Crystals of **7** are obtained at room temperature from a solution of **L** (13.6 mg, 0.05 mmol) and silver nitrate (8.5 mg, 0.05 mmol) in acetonitrile (10 mL). (Molar ratio 1:1) The crystals grow on the glass walls of the beaker at the solution surface after slow evaporation of the solution. The colorless crystals are suitable for single crystal X-rays diffraction and allow the resolution of the crystallographic structure. Not enough crystals were collected in order to make further investigations on this sample.

Reaction B: A polycrystalline white powder is obtained from a mixture of **L** (60 mg, 0.22 mmol) and $AgNO_3$ (37.5 mg, 0.22 mmol) in CH_2Cl_2 (a large volume as $AgNO_3$ is less well soluble in CH_2Cl_2). (Molar ratio 1:1) The powder X-ray spectrum of the compound shows that this polycrystalline precipitate has the same structure than **7**. The comparison of the experimental spectrum with the theoretical spectrum for **7** (calculated from the single crystals crystallographic data) in shown on Graph D-8. It's worth noting that if the molar ratio is changed, the same product is obtained. Yield: 79 mg (81 %)

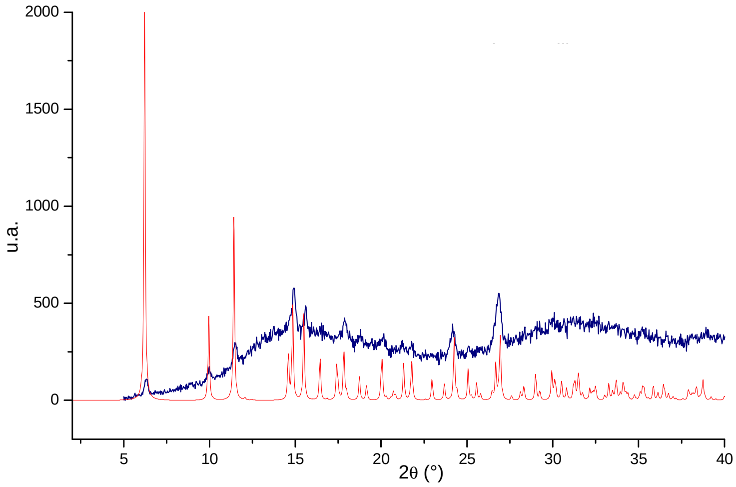

Graph D-8 : comparison of the spectrum of the polycrystalline precipitate (blue) obtained in dichloromethane and the theoretical spectrum for 7 (red)

Analysis calculated for [Ag(**L**)NO_3]: C 38.03, H 2.74, N 9.50; found C 37.26, H 2.64, N 9.4%. A certain amount of dichloromethane is adsorbed on the sample.

IR (GB, cm^{-1}): ν(C=O) 1726 s, ν(C=C) 1612 w, ν(ArC-C, C=N) 1412 w, ν(NO_3) 1380-1330 s, ν(C-O) 1272 s, δ(ArC-H) 985, 992 (split) m, ν(ArC-H) 825 m.

UV-Vis (CH_3CN): absorption at 212 and 273 nm.

Luminescence (solid state): 407 nm (excitation at 234 nm). (Graph D-9)

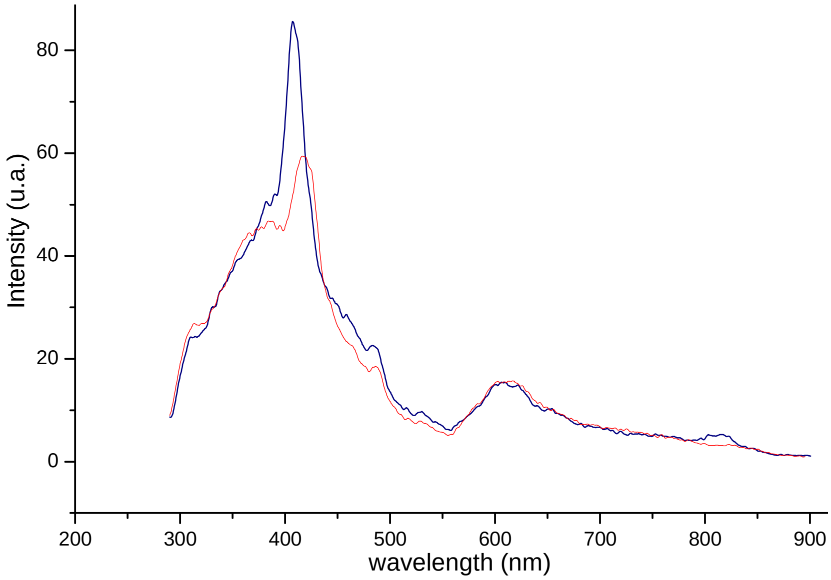

Graph D-9: emission spectrum of 7 (blue) compared to the emission spectrum of L (red)

ESI/MS (CH_3CN/CH_2Cl_2 10/1, m/z): 273.2, [**L**H]$^+$; 379.1, [**L**Ag]$^+$; 549.9, [**L**$Ag_2(NO_3)$]$^+$; 650.9, [**L**$_2$Ag]$^+$; 718.6, [**L**$Ag_3(NO_3)_2$]$^+$; 821.7, [**L**$_2Ag_2(NO_3)$]$^+$; 990, [**L**$_2Ag_3(NO_3)_2$]$^+$; 1161.3, [**L**$_2Ag_4(NO_3)_3$]$^+$; 1262.2, [**L**$_3Ag_3(NO_3)_2$]$^+$; 1432.6, [**L**$_3Ag_4(NO_3)_3$]$^+$ (Graph D-10).

FAB (Fast Atom Bombardment) Mass Spectroscopy (m/z): [**L**H]$^+$, [**L**Ag]$^+$, [**L**Ag_2NO_3]$^+$ and [**L**$_2$Ag]$^+$ at respectively 273, 379, 550 and 651.

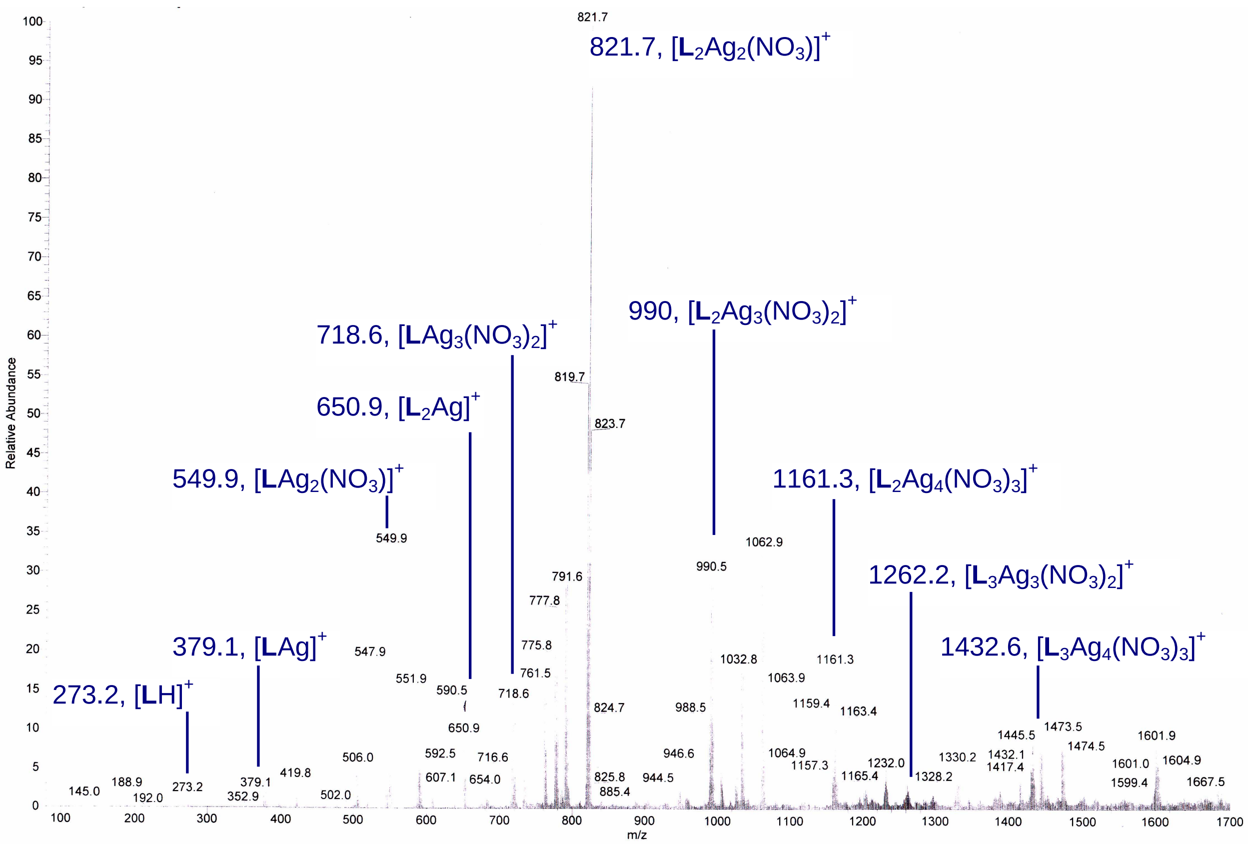

Graph D-10: ESI/MS (CH_3CN/CH_2Cl_2 10/1) for 7

III.9 - {(Ag(L)](CF$_3$SO$_3$)}$_n$ 8

Reaction A: A solution of **L** (40 mg, 0.15 mmol) in THF (5 mL) is introduced in one arm of an “H-shaped” tube, a solution of $AgCF_3SO_3$ (38 mg, 0.15 mmol) in water (4 mL) in the other one. (molar ratio 1:1) The solutions are frozen in liquid nitrogen and THF is then layered on top in order to bridge the two reagent solutions. There is a fritt in the linking part of the tube. The slow diffusion occurs through the THF layer and the fritt. Crystals of **8** appear after one day at the interface THF/water. After taking away some single crystals for the X-ray diffraction, the product is collected. Yield: 32mg (35%).

Analysis calculated for [Ag(**L**)CF_3SO_3]: C 34.04, H 2.28, N 5.29; found C 33.94, H 2.55, N 5.32%.

IR (KBr, cm^{-1}): ν(C=O) 1736s, ν(C=C) 1613 m, ν(ArC-C, C=N) 1425 s, ν(CF_3SO_3) 1300-1220 s, ν(CF_3SO_3) 1150-1140 s, δ(ArC-H) 983 m, ν(ArC-H) 804 w, γ(ArC-H) 366 m.

Reaction B: A polycrystalline white powder is obtained from a mixture of **L** (30 mg, 0.11 mmol) and $AgCF_3SO_3$ (28 mg, 0.11 mmol) in CH_2Cl_2. (Molar ratio 1:1) The powder X-ray spectrum of the compound shows that this polycrystalline precipitate has the same structure than **8**. Yield: 47 mg (81 %)

Analysis calculated for [Ag(**L**)CF_3SO_3]: C 34.04, H 2.28, N 5.29; found C 34.06, H 2.44, N 5.23%.

IR (GB, cm^{-1}): ν(C=O) 1732s, ν(C=C) 1614 m, ν(ArC-C, C=N) 1425 s, ν(CF_3SO_3) 1290-1210 s, ν(CF_3SO_3) 1160-1120 s, δ(ArC-H) 984 m, ν(ArC-H) 862 m.

ESI/MS (CH_3CN/CH_2Cl_2 10/1): 273.2 (14%) [**L**H]$^+$, 379.1 (2%) [**L**Ag]$^+$, 636.9 (31%) [**L**$Ag_2(CF_3SO_3)$]$^+$, 650.9 (20%) [**L**$_2$Ag]$^+$, 908.7 (100%) [**L**$_2Ag_2(CF_3SO_3)$]$^+$, 1164.4 (22%) [**L**$_2Ag_3(CF_3SO_3)_2$]$^+$.

III.10 - {(Ag(L)](ClO$_4$)}$_n$ 9

Crystals of **9** grow in an “H-shaped” tube, in which a solution of **L** (37 mg, 0.13 mmol) in THF (5 mL) can slowly diffuse into a solution of $AgClO_4$ (33 mg, 0.13 mmol) in water (4 mL) through THF (~15 mL). (molar ratio 1:1) Crystals suitable for single crystal X-ray diffraction appear after one day at the interface THF/water. Yield after drying: 24.6 mg (38%).

Analysis calculated for [Ag(**L**)ClO_4]: C 35.06, H 2.52, N 5.84; found C 35.36, H 2.79, N 5.71%.

IR (KBr, cm^{-1}): ν(C=O) 1733s, ν(C=C) 1613 m, ν(ArC-C, C=N) 1424 s, ν(C-O) 1268 s, ν(ClO_4) 1223 m, ν(ClO_4) 1130-1020 s, δ(ArC-H) 983 m, ν(ArC-H) 831 w, ν(ClO_4) 621 m, γ(ArC-H) 369 m.

Luminescence: emission at 409 nm for an excitation at 233 nm. (Graph D-11) (During this measure the ligand emits at 418 nm under an excitation at 233 nm.)

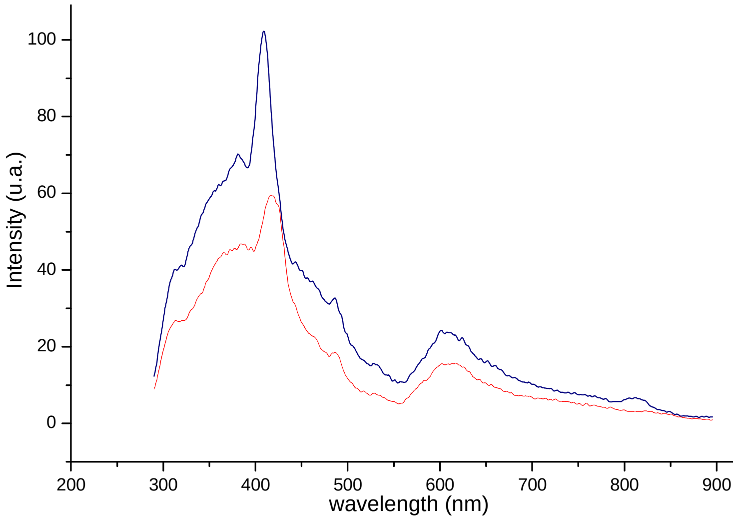

Graph D-11: emission spectrum of 9 (blue) compared to the emission spectrum of L (red)

ESI/MS (CH_3CN/CH_2Cl_2 10/1): 273.2 (18%) [**L**H]$^+$, 379.1 (6%) [**L**Ag]$^+$, 586.9 (100%) [**L**$Ag_2(ClO_4)$]$^+$, 858.9 (52%) [**L**$_2Ag_2(ClO_4)$]$^+$, 1066.6 (59%) [**L**$_2Ag_3(ClO_4)_2$]$^+$.

III.11 - $\{(Ag(L)](PF_6)\}_n$ 10

Reaction A: Single crystals of **10** are obtained by slow diffusion of a solution of **L** (20 mg, 0.07 mmol) in THF (5 mL) into a solution of $Ag(PF_6)$ (17.7 mg, 0.07 mmol) in water (5 mL) through THF (~15 mL). The reaction yields only small amount of crystals, which is not sufficient for further analyses.

Reaction B: The direct reaction of **L** (31.5 mg, 0.11 mmol) and $AgPF_6$ (28.7 mg, 0.11 mmol) in dichloromethane gives a white precipitate. (molar ratio 1:1) Yield: 36.7 mg (61%).

Analysis calculated for [Ag(**L**)PF_6]: C 32.02, H 2.30, N 5.34; found C 32.31, H 2.29, N 5.36%.

IR (GB, cm^{-1}): ν(C=O) 1727s, ν(C=C) 1618 m, ν(ArC-C, C=N) 1426 s, ν(C-O) 1280 s, δ(ArC-H) 977 m, ν(PF_6) 860-830 m.

ESI/MS (CH_3CN/CH_2Cl_2 10/1): 273.1 (30%) [**L**H]$^+$, 650.9 (14%) [$\mathbf{L}_2$Ag]$^+$, 904.8 (100%) [$\mathbf{L}_2Ag_2(PF_6)$]$^+$.

III.12 - $\{[Cu(L)_2(NO_3)(H_2O)](THF)_2(NO_3)(H_2O)_x\}_n$ 11

The reaction of **L** (60 mg, 0.22 mmol) and $Cu(NO_3)_2{\cdot}3H_2O$ (53.2 mg, 0.22 mmol) in methanol gives a blue precipitate (molar ratio 1:1). The same product is obtained with a molar ratio of 2:1 or 1:2. Yield: 80 mg (79%).

Analysis calculated for [Cu(**L**)$(NO_3)_2$]: C 36.57, H 2.63, N 12.18; found C 36.81, H 2.68, N 11.94%.

IR (GB, cm^{-1}): ν(C=O) 1727s, ν(C=C) 1622 w, ν(NO_3) 1500-1460 ν(ArC-C, C=N) 1427 m, ν(C-O) 1261 s, δ(ArC-H) 989 w, ν(ArC-H) 866 m.

ESI/MS (THF/H_2O 50/50): 273.2 (100%) [**L**H]$^+$, 352.7 (22%) [Cu**L**$(NO_3)_2(H_2O)_2(THF)_2$]$^{2+}$, 397.8 (12%) [Cu**L**(NO_3)]$^+$, 407.0 (23%) [$Cu_2\mathbf{L}_2(NO_3)_2(H_2O)$]$^{2+}$, 668.8 (14%) [Cu$\mathbf{L}_2(NO_3)$]$^+$, 859.8 (10%) [$Cu_2\mathbf{L}_2(NO_3)_3$]$^+$.

The blue precipitate is dissolved in a mixture of solvents THF/water (50/50) (minimum of solvents). And after some days, dark blue crystals suitable for single crystals X-ray diffraction grow. The yield of single crystals is very low. Furthermore, **L** and copper nitrate co-crystallize.

III.13 - $\{[Cu(L)(NO_3)_2]\}_n$ 12

The polycrystalline compound **12** grows by slow diffusion (“H-shaped” tube) of a solution of **L** (20 mg, 0.07 mmol) in dichloromethane (5mL) into a solution of $Cu(NO_3)_2{\cdot}3H_2O$ (17.7

mg, 0.07 mmol) in methanol (5mL) through dichloromethane (~15 mL) (molar ratio 1:1). Yield: 19 mg (56%). The polycrystalline powder is suitable of powder X-ray diffraction.

Analysis calculated for [Cu(**L**)$(NO_3)_2$]: C 36.57, H 2.63, N 12.18; found C 36.02, H 2.66, N 12.82%.

IR (GB, cm^{-1}): ν(C=O) 1728 m, ν(C=C) 1620 m, ν(NO_3) 1500-1450 m, ν(ArC-C, C=N) 1427 m, ν(C-O) 1257 s, δ(ArC-H) 1010 m, ν(ArC-H) 864 w (Graph D-12).

TGA/SDTA: an exothermal loss from 200°C corresponds to the loss of the organic material.

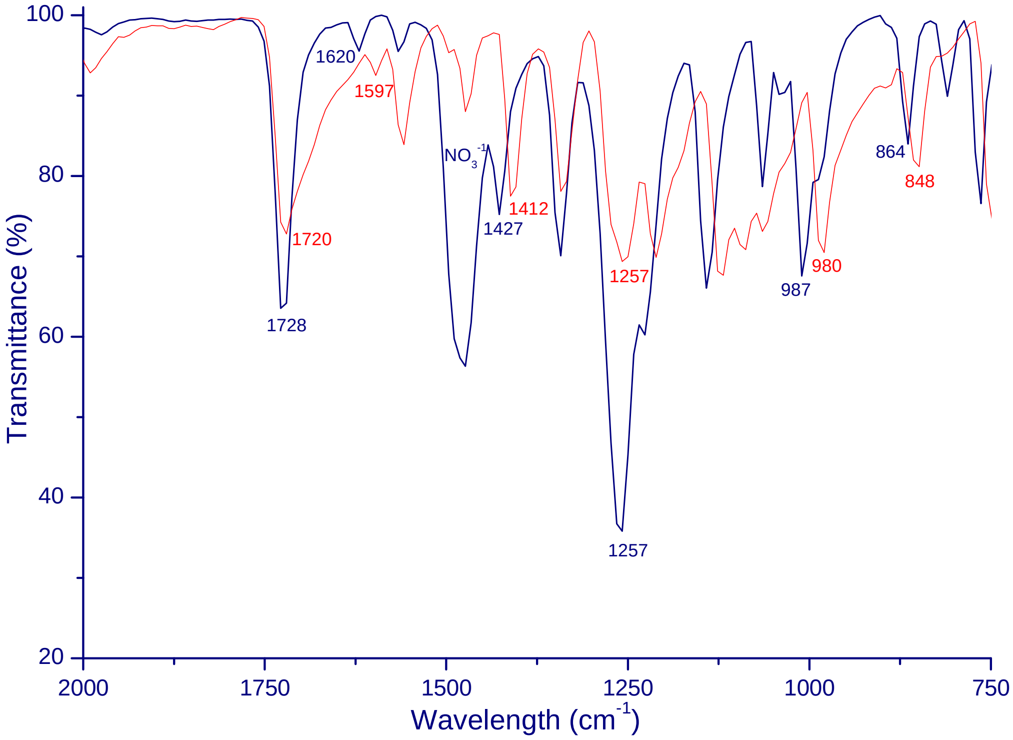

Graph D-12: Comparison between the IR-spectra of L (red) and 12 (blue)

III.14 - $\{[Cu(L)_2(ClO_4)(H_2O)]_2(THF)_4(ClO_4)_2(H_2O)\}_n$ 13

Caution! Although no problem in handling perchlorate salts occurs, these should be treated with great caution, owing their potential explosive nature.

The direct reaction of **L** (62.3 mg, 0.23 mmol) and $Cu(ClO_4)_2 \cdot 6H_2O$ (84.8 mg, 0.23 mmol) in methanol leads to a blue precipitate (molar ratio 1:1). Yield: 85.5 mg (43%).

Analysis calculated for [Cu(**L**)$_2(ClO_4)_2(H_2O)_3$]: C 39.06, H 3.51, N 6.51; found C 38.79, H 3.39, N 6.22%.

IR (GB, cm^{-1}): ν(C=O) 1728 s, ν(C=C) 1622 m, ν(ArC-C, C=N) 1423 s, ν(C-O) 1273 s, ν(ClO_4) 1230 w, ν(ClO_4) 1140-1000 s, ν(ArC-H) 860 m, ν(ClO_4) 621 s.

The recrystallization of the precipitate in the minimum of the solvent mixture THF/water (50/50) allows the formation of dark blue crystals, suitable for single crystal X-ray diffraction.

Analysis calculated for $[(Cu(\mathbf{L})_2(ClO_4)_2(H_2O))_2(H_2O)(C_4H_8O)_4]$: C 44.20, H 4.43, N 5.73; found C 43.98, H 4.30, N 5.87%.

IR (GB, cm^{-1}): v(C=O) 1728s, v(C=C) 1620 w, v(ArC-C, C=N) 1420 s, v(C-O) 1273 s, v(ClO_4) 1227 w, v(ClO_4) 1100-1000 s, v(ArC-H) 856 w, v(ClO_4) 617 m.

TGA/SDTA: exothermal loss between 25 and 118°C of one THF molecule and one water molecule, exothermal loss of three THF molecules respectively between 118°C and 155°C, 155°C and 172°C, 172°C and 195°C, exothermal loss of one water molecule between 172°C and 215°C. The measurement is stopped at 220°C to avoid the explosion of perchlorate.

E - Crystallographic Data

I - Single crystal X-ray diffraction

I.1 - Equipments

Crystals of **L**, **5**, **8** and **9** were measured at the University of Geneva by Gérald Bernardinelli, crystals of **1**, **2** and **4** at the University of Karlsruhe by Helmut Goesmann and crystals of **3**, **6**, **7, 10**, **11**, **11** and **13** on single crystals by myself at the University of Basle.

All diffractometers are STOE IPDS-II diffractometers with monochromated graphite Mo Kα radiation, λ = 0.71073 Å, equipped with an Oxford Cryosystems open flow cryostat [285], with an absorption correction by analytical integration [286]. The structures (except **12**) were solved with direct methods and refined by full-matrix least-square on F^2 with the SHELX-99 package [287]. Almost all heavy atoms could be refined anisotropically. Disorder was observed for the THF molecules included in the crystal structure of **2**, **11** and **13**, as well as for the water and counter anions in **11** and **13**. Crystallographic data for the structures **L**, **1**, **2**, **3**, **4** and **5** have been deposited with the Cambridge Crystallographic Data Center with the CCDC reference numbers 206524, 206525, 206593, 238163, 217748 and 217749 respectively. See http://www.rsc.org/suppdata/ce/b4/b413232g/ for crystallographic data in CIF or other format. Copies of the data can be obtained free of charge on application to CCDC, 12 Union Road, Cambridge CB21EZ, UK (fax: (+44)1223-336-033; e-mail: deposit@ccdc.cam.ac.uk).

The different representations of the compounds were drawn with the Schakal program.

Definitions of the factors R_{int}, R_1 and R_2:

$R_{int} = \Sigma \mid F_o^2 - F_o^2(\text{mean}) \mid / \Sigma [F_o^2]$

$R_1 = \Sigma \mid \mid F_o \mid - \mid F_c \mid \mid / \Sigma \mid F_o \mid$

$wR_2 = \{ \Sigma [w(F_o^2 - F_c^2)^2] / \Sigma [w(F_o^2)^2] \}^{1/2}$

I.2 - Crystal data and structure refinement for single crystal X-ray diffraction

I.2.a - Crystal data and structure refinement for L.

Empirical formula	C14 H12 N2 O4	
Formula weight	272.26	
Temperature	293(2) K	
Wavelength	0.71073 Å	
Crystal system	Monoclinic	
Space group	P2(1)/c	
Unit cell dimensions	a = 6.9688(11) Å	α = 90°.
	b = 10.6469(14) Å	β = 109.047(18)°.
	c = 8.8115(14) Å	γ = 90°.
Volume	617.99(16) Å^3	
Z	2	
Density (calculated)	1.463 Mg/m^3	
Absorption coefficient	0.109 mm^{-1}	
F(000)	284	
Crystal size	? x ? x ? mm^3	
Theta range for data collection	3.09 to 28.08°.	
Index ranges	-9<=h<=9, -14<=k<=14, -11<=l<=11	
Reflections collected	6383	
Independent reflections	1393 [R(int) = 0.0425]	
Completeness to theta = 28.08°	92.6 %	
Refinement method	Full-matrix least-squares on F^2	
Data / restraints / parameters	1393 / 0 / 91	
Goodness-of-fit on F^2	0.884	
Final R indices [I>2sigma(I)]	R1 = 0.0371, wR2 = 0.0926	
R indices (all data)	R1 = 0.0589, wR2 = 0.0983	
Largest diff. peak and hole	0.180 and -0.277 e.Å^{-3}	

Atomic coordinates (x 10^4) and equivalent isotropic displacement parameters (Å^{2}x 10^3) for **L**.U(eq) is defined as one third of the trace of the orthogonalized U^{ij} tensor.

	x	y	z	U(eq)
O(2)	1157(2)	10013(1)	-2857(1)	31(1)
O(1)	1635(2)	8073(1)	-1792(1)	41(1)
C(2)	2435(2)	11147(1)	109(1)	29(1)
C(1)	3133(2)	11667(1)	1641(2)	34(1)
C(3)	3863(2)	9742(1)	2816(2)	34(1)
C(4)	3204(2)	9131(1)	1344(2)	30(1)
C(5)	2479(2)	9855(1)	-40(1)	23(1)
C(6)	1732(2)	9194(1)	-1628(2)	26(1)
C(7)	337(2)	9454(1)	-4437(1)	33(1)
N(1)	3844(2)	10984(1)	2991(1)	35(1)

Bond lengths [Å] and angles [°] for **L**.

O(2)-C(6)	1.3450(16)	C(6)-O(2)-C(7)	115.35(10)
O(2)-C(7)	1.4492(15)	C(5)-C(2)-C(1)	118.43(11)
O(1)-C(6)	1.2015(16)	C(5)-C(2)-H(2)	120.8
C(2)-C(5)	1.3832(17)	C(1)-C(2)-H(2)	120.8
C(2)-C(1)	1.3919(17)	N(1)-C(1)-C(2)	123.66(13)
C(2)-H(2)	0.9300	N(1)-C(1)-H(1)	118.2
C(1)-N(1)	1.3435(18)	C(2)-C(1)-H(1)	118.2
C(1)-H(1)	0.9300	N(1)-C(3)-C(4)	124.04(12)
C(3)-N(1)	1.3320(18)	N(1)-C(3)-H(3)	118.0
C(3)-C(4)	1.3883(18)	C(4)-C(3)-H(3)	118.0
C(3)-H(3)	0.9300	C(3)-C(4)-C(5)	118.36(12)
C(4)-C(5)	1.3904(17)	C(3)-C(4)-H(4)	120.8
C(4)-H(4)	0.9300	C(5)-C(4)-H(4)	120.8
C(5)-C(6)	1.4995(16)	C(2)-C(5)-C(4)	118.75(11)
C(7)-C(7)#1	1.501(3)	C(2)-C(5)-C(6)	122.89(10)
C(7)-H(7A)	0.9700	C(4)-C(5)-C(6)	118.34(11)
C(7)-H(7B)	0.9700	O(1)-C(6)-O(2)	123.80(12)
		O(1)-C(6)-C(5)	124.54(12)
		O(2)-C(6)-C(5)	111.66(11)
		O(2)-C(7)-C(7)#1	104.89(13)
		O(2)-C(7)-H(7A)	110.8
		C(7)#1-C(7)-H(7A)	110.8
		O(2)-C(7)-H(7B)	110.8
		C(7)#1-C(7)-H(7B)	110.8
		H(7A)-C(7)-H(7B)	108.8
		C(3)-N(1)-C(1)	116.77(12)

Symmetry transformations used to generate equivalent atoms: #1 -x,-y+2,-z-1

Anisotropic displacement parameters (Å^{2}x 10^3) for **L**. The anisotropic displacement factor exponent takes the form: $-2\pi^2$[$h^2a^{*2}U^{11}$ + ... + 2 h k a* b* U^{12}]

	U^{11}	U^{22}	U^{33}	U^{23}	U^{13}	U^{12}
O(2)	45(1)	27(1)	15(1)	-1(1)	3(1)	-1(1)
O(1)	66(1)	26(1)	26(1)	-2(1)	9(1)	3(1)
C(2)	35(1)	30(1)	19(1)	2(1)	6(1)	0(1)
C(1)	44(1)	29(1)	26(1)	-2(1)	7(1)	-2(1)
C(3)	39(1)	39(1)	20(1)	4(1)	5(1)	1(1)
C(4)	34(1)	28(1)	24(1)	2(1)	7(1)	0(1)
C(5)	22(1)	30(1)	19(1)	-1(1)	7(1)	-1(1)
C(6)	29(1)	28(1)	20(1)	1(1)	8(1)	2(1)
C(7)	49(1)	29(1)	16(1)	-3(1)	5(1)	-1(1)
N(1)	41(1)	39(1)	22(1)	-3(1)	5(1)	-1(1)

Hydrogen coordinates (x 10^4) and isotropic displacement parameters (Å^{2}x 10^3) for **L**.

	x	y	z	U(eq)
H(2)	1950	11656	-794	34
H(1)	3105	12536	1735	41
H(3)	4347	9253	3738	40
H(4)	3247	8260	1285	35
H(7A)	-801	8909	-4494	39
H(7B)	1366	8967	-4695	39

Torsion angles [°] for **L**.

C(5)-C(2)-C(1)-N(1)	-0.2(2)
N(1)-C(3)-C(4)-C(5)	0.0(2)
C(1)-C(2)-C(5)-C(4)	0.4(2)
C(1)-C(2)-C(5)-C(6)	178.90(13)
C(3)-C(4)-C(5)-C(2)	-0.3(2)
C(3)-C(4)-C(5)-C(6)	-178.87(14)
C(7)-O(2)-C(6)-O(1)	1.7(2)
C(7)-O(2)-C(6)-C(5)	-177.67(12)
C(2)-C(5)-C(6)-O(1)	-175.28(14)
C(4)-C(5)-C(6)-O(1)	3.2(2)
C(2)-C(5)-C(6)-O(2)	4.04(19)
C(4)-C(5)-C(6)-O(2)	-177.47(13)
C(6)-O(2)-C(7)-C(7)#1	175.49(15)
C(4)-C(3)-N(1)-C(1)	0.2(2)
C(2)-C(1)-N(1)-C(3)	0.0(2)

Symmetry transformations used to generate equivalent atoms: #1 -x,-y+2,-z-1

Hydrogen bonds for **L** [Å and °].

D-H...A	d(D-H)	d(H...A)	d(D...A)	<(DHA)
C(3)-H(3)...N(1)#2	0.93	2.76	3.5981(18)	151.2
C(7)-H(7A)...N(1)#3	0.97	2.85	3.571(2)	132.3
C(4)-H(4)...O(1)#4	0.93	2.72	3.2519(17)	117.3
C(7)-H(7B)...O(1)#5	0.97	2.90	3.6859(17)	139.2

Symmetry transformations used to generate equivalent atoms: #1 -x,-y+2,-z-1 #2 -x+1,-y+2,-z+1 #3 -x,-y+2,-z #4 x,-y+3/2,z+1/2 #5 x,-y+3/2,z-1/2

I.2.b - Crystal data and structure refinement for 1.

Empirical formula	C28 H24 Cl2 Cu2 N4 O8	
Formula weight	371.26	
Temperature	293(2) K	
Wavelength	0.71073 Å	
Crystal system	Monoclinic	
Space group	C2/c	
Unit cell dimensions	a = 11.4740(11) Å	α = 90°.
	b = 11.5821(14) Å	β = 106.670(18)°.

	c = 10.9650(14) Å	γ = 90°.
Volume	1395.9(3) Å^3	
Z	2	
Density (calculated)	1.766 Mg/m^3	
Absorption coefficient	1.775 mm^{-1}	
F(000)	752	
Crystal size	? x ? x ? mm^3	
Theta range for data collection	2.55 to 28.26°.	
Index ranges	-15<=h<=15, -15<=k<=15, -14<=l<=14	
Reflections collected	5896	
Independent reflections	1655 [R(int) = 0.0596]	
Completeness to theta = 28.26°	95.6 %	
Refinement method	Full-matrix least-squares on F^2	
Data / restraints / parameters	1655 / 0 / 126	
Goodness-of-fit on F^2	0.990	
Final R indices [I>2sigma(I)]	R1 = 0.0467, wR2 = 0.1147	
R indices (all data)	R1 = 0.0617, wR2 = 0.1221	
Extinction coefficient	0.0063(11)	
Largest diff. peak and hole	0.642 and -0.808 e.Å^{-3}	

Atomic coordinates (x 10^4) and equivalent isotropic displacement parameters (Å^{2}x 10^3) for **1**. U(eq) is defined as one third of the trace of the orthogonalized U^{ij} tensor.

	x	y	z	U(eq)
Cu(1)	0	597(1)	2500	32(1)
Cl(2)	0	2591(1)	2500	35(1)
N(1)	-1001(2)	42(2)	847(3)	31(1)
C(1)	-1079(3)	-1080(3)	501(3)	32(1)
C(2)	-1802(3)	-1473(3)	-660(3)	32(1)
C(3)	-2486(3)	-679(3)	-1525(3)	31(1)
C(4)	-2395(3)	488(3)	-1203(4)	33(1)
C(5)	-1648(3)	805(3)	-18(3)	32(1)
C(6)	-3350(3)	-1102(3)	-2737(3)	33(1)
C(7)	-4775(3)	-562(3)	-4670(3)	34(1)
O(1)	-3619(2)	-2111(2)	-2956(3)	41(1)
O(2)	-3823(2)	-244(2)	-3539(2)	35(1)

Bond lengths [Å] and angles [°] for **1**.

Cu(1)-N(1)	1.955(3)	N(1)-Cu(1)-N(1)#1	141.63(17)
Cu(1)-N(1)#1	1.955(3)	N(1)-Cu(1)-Cl(2)	109.19(8)
Cu(1)-Cl(2)	2.3094(13)	N(1)#1-Cu(1)-Cl(2)	109.19(8)
N(1)-C(1)	1.350(4)	C(1)-N(1)-C(5)	116.9(3)
N(1)-C(5)	1.352(4)	C(1)-N(1)-Cu(1)	123.5(2)
C(1)-C(2)	1.382(5)	C(5)-N(1)-Cu(1)	119.6(2)

C(1)-H(1)	0.96(5)	N(1)-C(1)-C(2)	123.4(3)
C(2)-C(3)	1.390(5)	N(1)-C(1)-H(1)	116(3)
C(2)-H(2)	1.02(4)	C(2)-C(1)-H(1)	121(3)
C(3)-C(4)	1.394(5)	C(1)-C(2)-C(3)	118.9(3)
C(3)-C(6)	1.495(5)	C(1)-C(2)-H(2)	121(2)
C(4)-C(5)	1.385(5)	C(3)-C(2)-H(2)	120(2)
C(4)-H(3)	0.92(6)	C(2)-C(3)-C(4)	118.8(3)
C(5)-H(4)	1.00(4)	C(2)-C(3)-C(6)	119.4(3)
C(6)-O(1)	1.215(5)	C(4)-C(3)-C(6)	121.7(3)
C(6)-O(2)	1.335(4)	C(5)-C(4)-C(3)	118.4(3)
C(7)-O(2)	1.446(4)	C(5)-C(4)-H(3)	120(3)
C(7)-C(7)#2	1.507(7)	C(3)-C(4)-H(3)	122(3)
C(7)-H(5)	1.06(4)	N(1)-C(5)-C(4)	123.6(3)
		N(1)-C(5)-H(4)	113(3)
		C(4)-C(5)-H(4)	123(3)
		O(1)-C(6)-O(2)	123.6(3)
		O(1)-C(6)-C(3)	123.8(3)
		O(2)-C(6)-C(3)	112.5(3)
		O(2)-C(7)-C(7)#2	105.2(3)
		O(2)-C(7)-H(5)	109(2)
		C(7)#2-C(7)-H(5)	114(3)
		C(6)-O(2)-C(7)	116.1(3)

Symmetry transformations used to generate equivalent atoms: #1 -x,y,-z+1/2 #2 -x-1,-y,-z-1

Anisotropic displacement parameters (Å^{2}x 10^3) for **1**. The anisotropic displacement factor exponent takes the form: $-2\pi^2[h^2a^{*2}U^{11} + ... + 2 h k a^* b^* U^{12}]$

	U^{11}	U^{22}	U^{33}	U^{23}	U^{13}	U^{12}
Cu(1)	31(1)	36(1)	26(1)	0	3(1)	0
Cl(2)	38(1)	33(1)	32(1)	0	6(1)	0
N(1)	30(1)	34(2)	27(2)	-1(1)	6(1)	0(1)
C(1)	31(2)	35(2)	28(2)	2(1)	4(1)	0(1)
C(2)	31(2)	34(2)	29(2)	-1(1)	5(1)	-1(1)
C(3)	29(1)	37(2)	25(2)	0(1)	5(1)	0(1)
C(4)	31(2)	36(2)	30(2)	3(1)	6(1)	2(1)
C(5)	31(1)	32(2)	32(2)	0(1)	5(1)	0(1)
C(6)	27(1)	41(2)	29(2)	0(1)	6(1)	1(1)
C(7)	30(2)	42(2)	25(2)	-2(1)	-1(1)	-2(1)
O(1)	45(1)	34(1)	37(2)	-1(1)	0(1)	-5(1)
O(2)	35(1)	37(1)	25(1)	-3(1)	-2(1)	-1(1)

Hydrogen coordinates (x 10^4) and isotropic displacement parameters (Å^{2}x 10^3) for **1**.

	x	y	z	U(eq)
H(1)	-590(40)	-1610(40)	1120(50)	48(13)
H(2)	-1810(30)	-2320(30)	-900(40)	27(9)
H(3)	-2810(50)	1050(50)	-1760(50)	56(13)
H(4)	-1500(40)	1630(30)	260(40)	34(10)
H(5)	-4410(40)	-1130(40)	-5220(40)	42(11)
H(6)	-4540(30)	960(30)	-5570(40)	22(8)

Torsion angles [°] for **1**.

N(1)#1-Cu(1)-N(1)-C(1)	-7.2(2)
Cl(2)-Cu(1)-N(1)-C(1)	172.8(2)
N(1)#1-Cu(1)-N(1)-C(5)	173.5(3)
Cl(2)-Cu(1)-N(1)-C(5)	-6.5(3)
C(5)-N(1)-C(1)-C(2)	-1.8(5)
Cu(1)-N(1)-C(1)-C(2)	179.0(2)

N(1)-C(1)-C(2)-C(3)	0.2(5)
C(1)-C(2)-C(3)-C(4)	1.6(5)
C(1)-C(2)-C(3)-C(6)	-174.9(3)
C(2)-C(3)-C(4)-C(5)	-1.6(5)
C(6)-C(3)-C(4)-C(5)	174.7(3)
C(1)-N(1)-C(5)-C(4)	1.7(5)
Cu(1)-N(1)-C(5)-C(4)	-179.0(3)
C(3)-C(4)-C(5)-N(1)	0.0(5)
C(2)-C(3)-C(6)-O(1)	9.9(5)
C(4)-C(3)-C(6)-O(1)	-166.4(3)
C(2)-C(3)-C(6)-O(2)	-171.9(3)
C(4)-C(3)-C(6)-O(2)	11.7(4)
O(1)-C(6)-O(2)-C(7)	5.2(5)
C(3)-C(6)-O(2)-C(7)	-173.0(3)
C(7)#2-C(7)-O(2)-C(6)	174.6(3)

Symmetry transformations used to generate equivalent atoms: #1 -x,y,-z+1/2 #2 -x-1,-y,-z-1

Hydrogen bonds for **1** [Å and °].

D-H...A	d(D-H)	d(H...A)	d(D...A)	<(DHA)
C(4)-H(3)...O(1)#3	0.92(6)	2.76(5)	3.248(4)	114(4)
C(5)-H(4)...O(1)#3	1.00(4)	2.95(4)	3.353(4)	105(3)
C(1)-H(1)...O(1)#4	0.96(5)	2.85(5)	3.506(4)	126(3)
C(1)-H(1)...O(1)#5	0.96(5)	2.65(5)	3.533(4)	152(4)
C(5)-H(4)...Cl(2)	1.00(4)	2.80(5)	3.533(4)	131(3)
C(7)-H(5)...Cl(2)	1.06(4)	2.81(5)	3.716(4)	143(3)
C(4)-H(3)...Cl(2)#6	0.92(6)	2.88(6)	3.670(4)	145(4)

Symmetry transformations used to generate equivalent atoms: #1 -x,y,-z+1/2 #2 -x-1,-y,-z-1 #3 -x-1/2,y+1/2,-z-1/2 #4 -x-1/2,-y-1/2,-z #5 x+1/2,-y-1/2,z+1/2 #6 -x-1/2,-y+1/2,-z

I.2.c - Crystal data and structure refinement for 2.

Empirical formula	Cu2 Cl2 C32 H32 N4 O9	
Formula weight	814.60	
Temperature	293(2) K	
Wavelength	0.71073 Å	
Crystal system	Triclinic	
Space group	P-1	
Unit cell dimensions	a = 6.9874(10) Å	α = 112.339(17)°.
	b = 11.7096(19) Å	β = 96.728(17)°.
	c = 11.8247(17) Å	γ = 102.930(18)°.
Volume	850.0(2) Å^3	
Z	1	
Density (calculated)	1.591 Mg/m^3	
Absorption coefficient	1.468 mm^{-1}	
F(000)	416	

Crystal size	0.49 x 0.11 x 0.07 mm^3
Theta range for data collection	3.07 to 26.07°.
Index ranges	-8<=h<=8, -14<=k<=14, -14<=l<=14
Reflections collected	7365
Independent reflections	3106 [R(int) = 0.0387]
Completeness to theta = 26.07°	92.3 %
Refinement method	Full-matrix least-squares on F^2
Data / restraints / parameters	3106 / 0 / 226
Goodness-of-fit on F^2	0.785
Final R indices [I>2sigma(I)]	R1 = 0.0328, wR2 = 0.0800
R indices (all data)	R1 = 0.0525, wR2 = 0.0879
Largest diff. peak and hole	0.339 and -0.388 e.Å^{-3}

Atomic coordinates (x 10^4) and equivalent isotropic displacement parameters (Å^{2}x 10^3) for **2**. U(eq) is defined as one third of the trace of the orthogonalized U^{ij} tensor.

	x	y	z	U(eq)
Cu(1)	4684(1)	4626(1)	8699(1)	42(1)
Cl(2)	3186(1)	6127(1)	10287(1)	36(1)
N(1)	2223(3)	3366(2)	7413(2)	35(1)
C(1)	367(4)	3408(3)	7597(3)	37(1)
C(2)	-1358(4)	2647(3)	6681(3)	40(1)
C(3)	2334(4)	2516(3)	6295(3)	39(1)
C(4)	677(4)	1720(3)	5338(3)	36(1)
C(5)	-1223(4)	1802(3)	5528(3)	33(1)
C(6)	-3090(4)	1055(3)	4498(3)	39(1)
O(1)	-4722(3)	1196(3)	4592(2)	74(1)
O(2)	-2703(3)	241(2)	3480(2)	41(1)
C(7)	-4318(4)	-455(3)	2363(3)	42(1)
C(8)	-3367(4)	-918(3)	1277(3)	42(1)
O(3)	-2062(3)	190(2)	1183(2)	42(1)
C(9)	-85(4)	482(3)	1655(3)	38(1)
O(4)	695(3)	-133(2)	2067(2)	49(1)
C(10)	8931(4)	8304(3)	8398(3)	35(1)
C(11)	9732(4)	7690(3)	9048(3)	37(1)
C(12)	8514(4)	6578(3)	9040(3)	35(1)
C(13)	6924(4)	7743(3)	7738(3)	44(1)
C(14)	5826(4)	6645(3)	7784(3)	47(1)
N(2)	6570(3)	6049(2)	8429(2)	37(1)
O(5)	2143(9)	6223(7)	5590(6)	77(2)
C(15)	362(8)	5834(6)	6024(5)	94(2)
C(16)	1609(11)	4986(6)	4777(7)	135(3)

Bond lengths [Å] and angles [°] for **2**.

Cu(1)-N(1)	1.998(2)	C(5)-C(6)	1.503(4)
Cu(1)-N(2)	2.033(3)	C(6)-O(1)	1.200(4)
Cu(1)-Cl(2)#1	2.3251(9)	C(6)-O(2)	1.323(4)
Cu(1)-Cl(2)#1	2.3251(9)	O(2)-C(7)	1.450(3)
Cu(1)-Cl(2)	2.5472(10)	C(9)-C(10)#2	1.497(4)
Cu(1)-Cu(1)#1	2.8092(10)	C(10)-C(11)	1.385(4)

Cl(2)-Cu(1)#1	2.3251(9)
N(1)-C(3)	1.342(4)
N(1)-C(1)	1.348(4)
C(1)-C(2)	1.379(4)
C(1)-H(1)	0.9300
C(2)-C(5)	1.376(4)
C(2)-H(2)	0.9300
C(3)-C(4)	1.378(4)
C(3)-H(3)	0.9300
C(4)-C(5)	1.390(4)
C(4)-H(4)	0.9300
C(7)-C(8)	1.489(5)
C(7)-H(7A)	0.9700
C(7)-H(7B)	0.9700
C(8)-O(3)	1.460(3)
C(8)-H(8A)	0.9700
C(8)-H(8B)	0.9700
O(3)-C(9)	1.341(3)
C(9)-O(4)	1.198(4)
C(10)-C(13)	1.396(4)
C(10)-C(9)#2	1.497(4)
C(11)-C(12)	1.383(4)
C(11)-H(11)	0.9300
C(12)-N(2)	1.343(3)
C(12)-H(12)	0.9300
C(13)-C(14)	1.366(5)
C(13)-H(13)	0.9300
C(14)-N(2)	1.347(4)
C(14)-H(14)	0.9300
O(5)-C(16)	1.332(8)
O(5)-C(15)	1.447(8)
C(15)-C(16)#3	1.458(8)
C(15)-C(16)	1.869(10)
C(15)-H(15A)	0.9700
C(15)-H(15B)	0.9700
C(16)-C(15)#3	1.458(8)
C(16)-H(16A)	0.9700
C(16)-H(16B)	0.9700

N(1)-Cu(1)-N(2)	122.93(10)
N(1)-Cu(1)-Cl(2)#1	119.12(7)
N(2)-Cu(1)-Cl(2)#1	104.46(7)
N(1)-Cu(1)-Cl(2)#1	119.12(7)
N(2)-Cu(1)-Cl(2)#1	104.46(7)
Cl(2)#1-Cu(1)-Cl(2)#1	0.00(3)
N(1)-Cu(1)-Cl(2)	101.99(7)
N(2)-Cu(1)-Cl(2)	95.36(8)
Cl(2)#1-Cu(1)-Cl(2)	109.75(3)
Cl(2)#1-Cu(1)-Cl(2)	109.75(3)
N(1)-Cu(1)-Cu(1)#1	126.24(8)
N(2)-Cu(1)-Cu(1)#1	106.94(8)
Cl(2)#1-Cu(1)-Cu(1)#1	58.58(3)
Cl(2)#1-Cu(1)-Cu(1)#1	58.58(3)
Cl(2)-Cu(1)-Cu(1)#1	51.17(2)
Cu(1)#1-Cl(2)-Cu(1)	70.25(3)
C(3)-N(1)-C(1)	117.0(2)
C(3)-N(1)-Cu(1)	121.93(18)
C(1)-N(1)-Cu(1)	120.8(2)
N(1)-C(1)-C(2)	122.5(3)
N(1)-C(1)-H(1)	118.8
C(2)-C(1)-H(1)	118.8
C(5)-C(2)-C(1)	119.9(3)
C(5)-C(2)-H(2)	120.0
C(1)-C(2)-H(2)	120.0
N(1)-C(3)-C(4)	123.7(3)
N(1)-C(3)-H(3)	118.1
C(4)-C(3)-H(3)	118.1
C(3)-C(4)-C(5)	118.5(3)
C(3)-C(4)-H(4)	120.7
C(5)-C(4)-H(4)	120.7
C(2)-C(5)-C(4)	118.2(2)
C(2)-C(5)-C(6)	119.8(3)
C(4)-C(5)-C(6)	122.0(3)
O(1)-C(6)-O(2)	124.6(3)
O(1)-C(6)-C(5)	123.7(3)
O(2)-C(6)-C(5)	111.7(2)
C(6)-O(2)-C(7)	118.0(2)
O(2)-C(7)-C(8)	107.1(2)
O(2)-C(7)-H(7A)	110.3
C(8)-C(7)-H(7A)	110.3
O(2)-C(7)-H(7B)	110.3
C(8)-C(7)-H(7B)	110.3
H(7A)-C(7)-H(7B)	108.5
O(3)-C(8)-H(8B)	109.8
C(7)-C(8)-H(8B)	109.8
H(8A)-C(8)-H(8B)	108.3
C(9)-O(3)-C(8)	116.3(2)
O(4)-C(9)-O(3)	125.6(3)
O(4)-C(9)-C(10)#2	123.2(3)
O(3)-C(9)-C(10)#2	111.3(3)
C(11)-C(10)-C(13)	117.7(3)
C(11)-C(10)-C(9)#2	124.3(2)
C(13)-C(10)-C(9)#2	118.0(3)
C(12)-C(11)-C(10)	119.2(3)
C(12)-C(11)-H(11)	120.4
C(10)-C(11)-H(11)	120.4
N(2)-C(12)-C(11)	123.4(3)
N(2)-C(12)-H(12)	118.3
C(11)-C(12)-H(12)	118.3
C(14)-C(13)-C(10)	119.3(3)
C(14)-C(13)-H(13)	120.3
C(10)-C(13)-H(13)	120.3
N(2)-C(14)-C(13)	123.8(3)
N(2)-C(14)-H(14)	118.1
C(13)-C(14)-H(14)	118.1
C(12)-N(2)-C(14)	116.6(3)
C(12)-N(2)-Cu(1)	122.3(2)
C(14)-N(2)-Cu(1)	120.14(19)
C(16)-O(5)-C(15)	84.4(6)
O(5)-C(15)-C(16)#3	125.5(6)
O(5)-C(15)-C(16)	45.2(4)
C(16)#3-C(15)-C(16)	90.1(5)
O(5)-C(15)-H(15A)	105.9
C(16)#3-C(15)-H(15A)	105.9
C(16)-C(15)-H(15A)	149.7
O(5)-C(15)-H(15B)	105.9
C(16)#3-C(15)-H(15B)	105.9
C(16)-C(15)-H(15B)	93.3
H(15A)-C(15)-H(15B)	106.3
O(5)-C(16)-C(15)#3	128.9(6)
O(5)-C(16)-C(15)	50.4(4)
C(15)#3-C(16)-C(15)	89.9(5)
O(5)-C(16)-H(16A)	105.1
C(15)#3-C(16)-H(16A)	105.1
C(15)-C(16)-H(16A)	89.4
O(5)-C(16)-H(16B)	105.1
C(15)#3-C(16)-H(16B)	105.1

O(3)-C(8)-C(7)	109.3(2)	C(15)-C(16)-H(16B)	154.5
O(3)-C(8)-H(8A)	109.8	H(16A)-C(16)-H(16B)	105.9
C(7)-C(8)-H(8A)	109.8		

Symmetry transformations used to generate equivalent atoms: #1 -x+1,-y+1,-z+2 #2 -x+1,-y+1,-z+1 #3 -x,-y+1,-z+1

Anisotropic displacement parameters ($Å^2$x 10^3) for **2**. The anisotropic displacement factor exponent takes the form: $-2\pi^2[h^2a^{*2}U^{11} + ... + 2 h k a^* b^* U^{12}]$

	U^{11}	U^{22}	U^{33}	U^{23}	U^{13}	U^{12}
Cu(1)	27(1)	44(1)	43(1)	13(1)	3(1)	0(1)
Cl(2)	27(1)	32(1)	41(1)	9(1)	6(1)	6(1)
N(1)	29(1)	36(1)	37(2)	14(1)	7(1)	6(1)
C(1)	29(1)	44(2)	29(2)	8(1)	7(1)	6(1)
C(2)	26(1)	45(2)	38(2)	11(1)	8(1)	6(1)
C(3)	28(1)	44(2)	39(2)	12(1)	9(1)	11(1)
C(4)	29(1)	36(2)	35(2)	7(1)	7(1)	10(1)
C(5)	28(1)	36(2)	30(2)	9(1)	7(1)	7(1)
C(6)	28(1)	39(2)	37(2)	7(1)	4(1)	5(1)
O(1)	29(1)	104(2)	48(2)	-11(1)	1(1)	22(1)
O(2)	30(1)	41(1)	35(1)	1(1)	3(1)	6(1)
C(7)	33(1)	38(2)	37(2)	4(1)	-1(1)	-1(1)
C(8)	42(2)	31(2)	40(2)	9(1)	8(1)	-2(1)
O(3)	36(1)	38(1)	43(1)	15(1)	3(1)	-1(1)
C(9)	40(2)	34(2)	33(2)	9(1)	8(1)	8(1)
O(4)	50(1)	42(1)	59(2)	24(1)	10(1)	14(1)
C(10)	32(1)	35(2)	33(2)	11(1)	7(1)	6(1)
C(11)	27(1)	41(2)	34(2)	12(1)	3(1)	2(1)
C(12)	29(1)	37(2)	35(2)	14(1)	7(1)	7(1)
C(13)	35(2)	46(2)	50(2)	21(2)	2(1)	10(1)
C(14)	32(2)	51(2)	51(2)	21(2)	1(1)	6(1)
N(2)	26(1)	42(1)	36(1)	13(1)	5(1)	6(1)
O(5)	75(4)	98(5)	62(4)	35(3)	8(3)	36(3)
C(15)	103(4)	132(5)	65(3)	41(3)	30(3)	62(3)
C(16)	139(6)	109(5)	136(6)	34(4)	-28(5)	60(4)

Hydrogen coordinates (x 10^4) and isotropic displacement parameters ($Å^2$x 10^3) for **2**.

	x	y	z	U(eq)
H(1)	247	3972	8372	44
H(2)	-2613	2705	6843	47
H(3)	3601	2461	6160	47
H(4)	826	1140	4581	43
H(7A)	-5087	109	2263	51
H(7B)	-5221	-1180	2423	51
H(8A)	-2583	-1469	1391	50
H(8B)	-4402	-1419	511	50
H(11)	11072	8021	9483	44
H(12)	9070	6175	9480	42
H(13)	6341	8113	7272	53
H(14)	4488	6289	7345	57
H(15A)	144	6627	6581	113
H(15B)	732	5414	6547	113
H(16A)	1991	4534	5263	162
H(16B)	2514	4944	4210	162

Torsion angles [°] for **2**.

N(1)-Cu(1)-Cl(2)-Cu(1)#1	127.22(8)	C(6)-O(2)-C(7)-C(8)	160.5(3)
N(2)-Cu(1)-Cl(2)-Cu(1)#1	-107.46(7)	O(2)-C(7)-C(8)-O(3)	-61.6(3)
Cl(2)#1-Cu(1)-Cl(2)-Cu(1)#1	0.0	C(7)-C(8)-O(3)-C(9)	99.7(3)
Cl(2)#1-Cu(1)-Cl(2)-Cu(1)#1	0.0	C(8)-O(3)-C(9)-O(4)	5.1(5)
N(2)-Cu(1)-N(1)-C(3)	64.5(3)	C(8)-O(3)-C(9)-C(10)#2	-175.2(2)
Cl(2)#1-Cu(1)-N(1)-C(3)	-70.0(2)	C(13)-C(10)-C(11)-C(12)	-1.5(5)
Cl(2)#1-Cu(1)-N(1)-C(3)	-70.0(2)	C(9)#2-C(10)-C(11)-C(12)	179.4(3)
Cl(2)-Cu(1)-N(1)-C(3)	169.1(2)	C(10)-C(11)-C(12)-N(2)	0.1(5)
Cu(1)#1-Cu(1)-N(1)-C(3)	-140.7(2)	C(11)-C(10)-C(13)-C(14)	1.7(5)
N(2)-Cu(1)-N(1)-C(1)	-110.1(2)	C(9)#2-C(10)-C(13)-C(14)	-179.1(3)
Cl(2)#1-Cu(1)-N(1)-C(1)	115.4(2)	C(10)-C(13)-C(14)-N(2)	-0.6(6)
Cl(2)#1-Cu(1)-N(1)-C(1)	115.4(2)	C(11)-C(12)-N(2)-C(14)	1.1(5)
Cl(2)-Cu(1)-N(1)-C(1)	-5.6(2)	C(11)-C(12)-N(2)-Cu(1)	-168.1(2)
Cu(1)#1-Cu(1)-N(1)-C(1)	44.7(3)	C(13)-C(14)-N(2)-C(12)	-0.8(5)
C(3)-N(1)-C(1)-C(2)	-1.8(5)	C(13)-C(14)-N(2)-Cu(1)	168.6(3)
Cu(1)-N(1)-C(1)-C(2)	173.1(2)	N(1)-Cu(1)-N(2)-C(12)	-155.4(2)
N(1)-C(1)-C(2)-C(5)	0.2(5)	Cl(2)#1-Cu(1)-N(2)-C(12)	-15.4(2)
C(1)-N(1)-C(3)-C(4)	1.5(5)	Cl(2)#1-Cu(1)-N(2)-C(12)	-15.4(2)
Cu(1)-N(1)-C(3)-C(4)	-173.4(2)	Cl(2)-Cu(1)-N(2)-C(12)	96.6(2)
N(1)-C(3)-C(4)-C(5)	0.5(5)	Cu(1)#1-Cu(1)-N(2)-C(12)	45.6(2)
C(1)-C(2)-C(5)-C(4)	1.8(5)	N(1)-Cu(1)-N(2)-C(14)	35.8(3)
C(1)-C(2)-C(5)-C(6)	-175.0(3)	Cl(2)#1-Cu(1)-N(2)-C(14)	175.8(2)
C(3)-C(4)-C(5)-C(2)	-2.1(5)	Cl(2)#1-Cu(1)-N(2)-C(14)	175.8(2)
C(3)-C(4)-C(5)-C(6)	174.6(3)	Cl(2)-Cu(1)-N(2)-C(14)	-72.2(2)
C(2)-C(5)-C(6)-O(1)	4.1(5)	Cu(1)#1-Cu(1)-N(2)-C(14)	-123.2(2)
C(4)-C(5)-C(6)-O(1)	-172.5(3)	C(16)-O(5)-C(15)-C(16)#3	-45.2(8)
C(2)-C(5)-C(6)-O(2)	-176.6(3)	C(15)-O(5)-C(16)-C(15)#3	47.9(10)
C(4)-C(5)-C(6)-O(2)	6.7(4)	C(16)#3-C(15)-C(16)-O(5)	144.7(7)
O(1)-C(6)-O(2)-C(7)	5.3(5)	O(5)-C(15)-C(16)-C(15)#3	-144.7(7)
C(5)-C(6)-O(2)-C(7)	-173.9(3)	C(16)#3-C(15)-C(16)-C(15)#3	0.0

Symmetry transformations used to generate equivalent atoms: #1 -x+1,-y+1,-z+2 #2 -x+1,-y+1,-z+1 #3 -x,-y+1,-z+1

Hydrogen bonds for **2** [Å and °].

D-H...A	d(D-H)	d(H...A)	d(D...A)	<(DHA)
C(4)-H(4)...O(4)	0.93	2.75	3.648(4)	162.2
C(8)-H(8A)...O(4)	0.97	2.31	2.708(4)	103.4
C(14)-H(14)...O(5)	0.93	2.45	3.239(6)	142.1
C(3)-H(3)...O(1)#4	0.93	2.49	3.272(4)	141.8
C(13)-H(13)...O(1)#3	0.93	2.82	3.737(5)	167.4
C(7)-H(7A)...O(4)#5	0.97	2.87	3.579(4)	130.7
C(1)-H(1)...Cl(2)	0.93	2.82	3.487(3)	129.4
C(12)-H(12)...Cl(2)#4	0.93	2.94	3.653(3)	134.3
C(12)-H(12)...Cl(2)#1	0.93	2.93	3.540(3)	124.3

Symmetry transformations used to generate equivalent atoms: #1 -x+1,-y+1,-z+2 #2 -x+1,-y+1,-z+1 #3 -x,-y+1,-z+1 #4 x+1,y,z #5 x-1,y,z #6 x-1,y-1,z-1

I.2.d - Crystal data and structure refinement for 3.

Empirical formula	C14 H12 Ag N3 O7	
Formula weight	442.14	
Temperature	240(2) K	
Wavelength	0.71073 Å	
Crystal system	Monoclinic	
Space group	P2(1)/n	
Unit cell dimensions	a = 11.6742(8) Å	α = 90°.
	b = 11.0728(6) Å	β = 99.019(6)°.
	c = 12.1813(9) Å	γ = 90°.
Volume	1555.16(18) $Å^3$	
Z	4	
Density (calculated)	1.888 Mg/m^3	
Absorption coefficient	1.341 mm^{-1}	
F(000)	880	
Crystal size	0.3 x 0.24 x 0.17 mm^3	
Theta range for data collection	2.50 to 27.05°.	
Index ranges	-14<=h<=14, -14<=k<=13, -15<=l<=15	
Reflections collected	13875	
Independent reflections	3246 [R(int) = 0.0672]	
Completeness to theta = 27.05°	95.3 %	
Absorption correction	Numerical	
Max. and min. transmission	0.8999 and 0.5860	
Refinement method	Full-matrix least-squares on F^2	
Data / restraints / parameters	3246 / 0 / 226	
Goodness-of-fit on F^2	1.180	
Final R indices [I>2sigma(I)]	R1 = 0.0345, wR2 = 0.0948	
R indices (all data)	R1 = 0.0363, wR2 = 0.0960	
Largest diff. peak and hole	0.442 and -0.528 e.$Å^{-3}$	

Atomic coordinates (x 10^4) and equivalent isotropic displacement parameters ($Å^2$x 10^3) for **3**. U(eq) is defined as one third of the trace of the orthogonalized U^{ij} tensor.

	x	y	z	U(eq)
Ag(1)	7264(1)	1566(1)	3155(1)	40(1)
N(1)	9156(2)	1401(2)	3823(2)	34(1)
C(1)	9749(2)	2266(2)	4443(2)	36(1)
C(2)	10929(2)	2195(2)	4824(2)	35(1)
C(3)	9742(2)	424(2)	3583(2)	33(1)
C(4)	10917(2)	272(2)	3940(2)	33(1)
C(5)	11521(2)	1180(2)	4567(2)	30(1)
C(6)	12789(2)	994(2)	4952(2)	35(1)
O(1)	13260(2)	34(2)	4953(3)	59(1)
O(2)	13310(2)	2023(2)	5291(2)	39(1)
C(7)	14540(2)	1920(3)	5702(3)	45(1)
C(8)	14933(2)	3212(3)	5910(3)	37(1)
O(3)	16139(2)	3091(2)	6400(2)	34(1)
C(9)	16729(2)	4122(2)	6515(2)	29(1)
O(4)	16315(2)	5113(2)	6361(2)	39(1)
C(10)	17993(2)	3901(2)	6888(2)	28(1)
C(11)	18423(2)	2841(2)	7404(2)	32(1)
C(12)	19606(2)	2730(2)	7736(2)	33(1)
C(13)	18767(2)	4798(2)	6720(3)	37(1)
C(14)	19935(2)	4606(2)	7062(3)	39(1)
N(2)	20360(2)	3598(2)	7571(2)	34(1)
N(3)	7385(2)	4322(2)	3607(2)	33(1)
O(5)	7059(3)	3605(2)	4277(2)	56(1)
O(6)	7536(2)	3940(2)	2667(2)	46(1)
O(7)	7556(2)	5393(2)	3848(2)	57(1)

Bond lengths [Å] and angles [°] for **3**.

Ag(1)-N(2)#1	2.232(2)	C(7)-H(7B)	0.9700
Ag(1)-N(1)	2.239(2)	C(8)-O(3)	1.446(3)
Ag(1)-O(5)	2.669(2)	C(8)-H(8A)	0.9700
Ag(1)-O(6)	2.724(2)	C(8)-H(8B)	0.9700
Ag(1)-O(7)#2	2.800(3)	O(3)-C(9)	1.329(3)
N(1)-C(3)	1.337(3)	C(9)-O(4)	1.202(3)
N(1)-C(1)	1.343(4)	C(9)-C(10)	1.494(3)
C(1)-C(2)	1.385(4)	C(10)-C(13)	1.380(4)
C(1)-H(1)	0.9300	C(10)-C(11)	1.388(4)
C(2)-C(5)	1.380(4)	C(11)-C(12)	1.383(3)
C(2)-H(2)	0.9300	C(11)-H(11)	0.9300
C(3)-C(4)	1.382(4)	C(12)-N(2)	1.340(3)
C(3)-H(3)	0.9300	C(12)-H(12)	0.9300
C(4)-C(5)	1.387(4)	C(13)-C(14)	1.378(4)
C(4)-H(4)	0.9300	C(13)-H(13)	0.9300
C(5)-C(6)	1.495(3)	C(14)-N(2)	1.335(4)
C(6)-O(1)	1.198(4)	C(14)-H(14)	0.9300
C(6)-O(2)	1.326(3)	N(2)-Ag(1)#3	2.232(2)
O(2)-C(7)	1.449(3)	N(3)-O(7)	1.231(3)
C(7)-C(8)	1.511(4)	N(3)-O(5)	1.240(3)
C(7)-H(7A)	0.9700	N(3)-O(6)	1.259(3)
N(2)#1-Ag(1)-N(1)	170.25(9)	C(8)-C(7)-H(7B)	111.0
N(2)#1-Ag(1)-O(5)	93.84(9)	H(7A)-C(7)-H(7B)	109.0
N(1)-Ag(1)-O(5)	92.60(9)	O(3)-C(8)-C(7)	103.4(2)
N(2)#1-Ag(1)-O(6)	98.83(7)	O(3)-C(8)-H(8A)	111.1
N(1)-Ag(1)-O(6)	90.91(7)	C(7)-C(8)-H(8A)	111.1
O(5)-Ag(1)-O(6)	47.05(6)	O(3)-C(8)-H(8B)	111.1
N(2)#1-Ag(1)-O(7)#2	83.79(8)	C(7)-C(8)-H(8B)	111.1
N(1)-Ag(1)-O(7)#2	94.29(8)	H(8A)-C(8)-H(8B)	109.0

O(5)-Ag(1)-O(7)#2	149.70(7)
O(6)-Ag(1)-O(7)#2	103.32(6)
C(3)-N(1)-C(1)	117.7(2)
C(3)-N(1)-Ag(1)	119.74(18)
C(1)-N(1)-Ag(1)	122.58(18)
N(1)-C(1)-C(2)	123.1(2)
N(1)-C(1)-H(1)	118.5
C(2)-C(1)-H(1)	118.5
C(5)-C(2)-C(1)	118.5(2)
C(5)-C(2)-H(2)	120.7
C(1)-C(2)-H(2)	120.7
N(1)-C(3)-C(4)	123.1(2)
N(1)-C(3)-H(3)	118.5
C(4)-C(3)-H(3)	118.5
C(3)-C(4)-C(5)	118.6(2)
C(3)-C(4)-H(4)	120.7
C(5)-C(4)-H(4)	120.7
C(2)-C(5)-C(4)	119.0(2)
C(2)-C(5)-C(6)	123.2(2)
C(4)-C(5)-C(6)	117.8(2)
O(1)-C(6)-O(2)	125.0(3)
O(1)-C(6)-C(5)	123.7(3)
O(2)-C(6)-C(5)	111.2(2)
C(6)-O(2)-C(7)	114.9(2)
O(2)-C(7)-C(8)	104.0(2)
O(2)-C(7)-H(7A)	111.0
C(8)-C(7)-H(7A)	111.0
O(2)-C(7)-H(7B)	111.0
C(9)-O(3)-C(8)	114.8(2)
O(4)-C(9)-O(3)	125.3(2)
O(4)-C(9)-C(10)	123.4(2)
O(3)-C(9)-C(10)	111.3(2)
C(13)-C(10)-C(11)	118.5(2)
C(13)-C(10)-C(9)	118.4(2)
C(11)-C(10)-C(9)	123.1(2)
C(12)-C(11)-C(10)	118.7(2)
C(12)-C(11)-H(11)	120.6
C(10)-C(11)-H(11)	120.6
N(2)-C(12)-C(11)	122.9(2)
N(2)-C(12)-H(12)	118.6
C(11)-C(12)-H(12)	118.6
C(14)-C(13)-C(10)	119.0(2)
C(14)-C(13)-H(13)	120.5
C(10)-C(13)-H(13)	120.5
N(2)-C(14)-C(13)	123.2(2)
N(2)-C(14)-H(14)	118.4
C(13)-C(14)-H(14)	118.4
C(14)-N(2)-C(12)	117.7(2)
C(14)-N(2)-Ag(1)#3	119.69(18)
C(12)-N(2)-Ag(1)#3	122.61(18)
O(7)-N(3)-O(5)	121.0(3)
O(7)-N(3)-O(6)	120.0(2)
O(5)-N(3)-O(6)	119.0(2)
N(3)-O(5)-Ag(1)	98.22(16)
N(3)-O(6)-Ag(1)	95.06(16)

Symmetry transformations used to generate equivalent atoms: #1 x-3/2,-y+1/2,z-1/2 #2 -x+3/2,y-1/2,-z+1/2 #3 x+3/2,-y+1/2,z+1/2

Anisotropic displacement parameters ($Å^2$x 10^3) for **3**. The anisotropic displacement factor exponent takes the form: $-2\pi^2[h^2a^{*2}U^{11} + ... + 2 h k a^* b^* U^{12}]$

	U^{11}	U^{22}	U^{33}	U^{23}	U^{13}	U^{12}
Ag(1)	22(1)	40(1)	54(1)	-1(1)	-6(1)	-1(1)
N(1)	23(1)	38(1)	39(1)	1(1)	-3(1)	-4(1)
C(1)	27(1)	32(1)	48(2)	-3(1)	-2(1)	0(1)
C(2)	27(1)	32(1)	43(1)	-3(1)	-3(1)	-3(1)
C(3)	28(1)	37(1)	32(1)	-3(1)	-1(1)	-4(1)
C(4)	30(1)	34(1)	35(1)	-2(1)	5(1)	0(1)
C(5)	23(1)	33(1)	32(1)	4(1)	2(1)	-4(1)
C(6)	25(1)	36(1)	42(1)	4(1)	0(1)	-1(1)
O(1)	33(1)	39(1)	101(2)	-4(1)	-3(1)	5(1)
O(2)	21(1)	38(1)	55(1)	2(1)	-5(1)	-2(1)
C(7)	21(1)	45(2)	64(2)	9(1)	-9(1)	-3(1)
C(8)	18(1)	41(1)	47(2)	-6(1)	-4(1)	3(1)
O(3)	19(1)	38(1)	42(1)	2(1)	-4(1)	-1(1)
C(9)	24(1)	34(1)	30(1)	-2(1)	3(1)	1(1)
O(4)	31(1)	35(1)	49(1)	-3(1)	2(1)	8(1)
C(10)	22(1)	31(1)	28(1)	-2(1)	0(1)	-1(1)
C(11)	24(1)	32(1)	40(1)	3(1)	1(1)	-3(1)
C(12)	26(1)	32(1)	40(1)	4(1)	-1(1)	1(1)
C(13)	29(1)	30(1)	51(2)	7(1)	2(1)	1(1)
C(14)	26(1)	33(1)	57(2)	5(1)	3(1)	-4(1)
N(2)	22(1)	34(1)	43(1)	0(1)	-2(1)	0(1)
N(3)	23(1)	34(1)	42(1)	0(1)	1(1)	3(1)
O(5)	77(2)	46(1)	48(1)	3(1)	24(1)	-9(1)
O(6)	52(1)	48(1)	39(1)	-1(1)	9(1)	-1(1)
O(7)	63(2)	36(1)	74(2)	-10(1)	19(1)	-7(1)

Hydrogen coordinates (x 10^4) and isotropic displacement parameters ($Å^2$x 10^3) for **3**.

	x	y	z	U(eq)
H(1)	9349	2945	4624	44
H(2)	11313	2817	5243	42
H(3)	9340	-183	3156	39
H(4)	11294	-425	3764	39
H(7A)	14943	1541	5154	54
H(7B)	14676	1452	6383	54
H(8A)	14854	3665	5221	44
H(8B)	14492	3610	6416	44
H(11)	17924	2216	7525	39
H(12)	19891	2022	8089	40
H(13)	18506	5521	6381	44
H(14)	20452	5209	6931	47

Torsion angles [°] for **3**.

N(2)#1-Ag(1)-N(1)-C(3)	43.7(6)	C(8)-O(3)-C(9)-C(10)	-172.7(2)
O(5)-Ag(1)-N(1)-C(3)	175.0(2)	O(4)-C(9)-C(10)-C(13)	-21.0(4)
O(6)-Ag(1)-N(1)-C(3)	-137.9(2)	O(3)-C(9)-C(10)-C(13)	160.1(2)
O(7)#2-Ag(1)-N(1)-C(3)	-34.5(2)	O(4)-C(9)-C(10)-C(11)	158.4(3)
N(2)#1-Ag(1)-N(1)-C(1)	-138.0(5)	O(3)-C(9)-C(10)-C(11)	-20.5(3)
O(5)-Ag(1)-N(1)-C(1)	-6.7(2)	C(13)-C(10)-C(11)-C(12)	0.5(4)
O(6)-Ag(1)-N(1)-C(1)	40.4(2)	C(9)-C(10)-C(11)-C(12)	-178.9(2)
O(7)#2-Ag(1)-N(1)-C(1)	143.8(2)	C(10)-C(11)-C(12)-N(2)	-0.7(4)
C(3)-N(1)-C(1)-C(2)	0.9(4)	C(11)-C(10)-C(13)-C(14)	0.5(4)
Ag(1)-N(1)-C(1)-C(2)	-177.4(2)	C(9)-C(10)-C(13)-C(14)	179.9(2)
N(1)-C(1)-C(2)-C(5)	-0.9(4)	C(10)-C(13)-C(14)-N(2)	-1.3(5)
C(1)-N(1)-C(3)-C(4)	-0.1(4)	C(13)-C(14)-N(2)-C(12)	1.2(4)
Ag(1)-N(1)-C(3)-C(4)	178.2(2)	C(13)-C(14)-N(2)-Ag(1)#3	-177.2(2)
N(1)-C(3)-C(4)-C(5)	-0.7(4)	C(11)-C(12)-N(2)-C(14)	-0.1(4)
C(1)-C(2)-C(5)-C(4)	0.0(4)	C(11)-C(12)-N(2)-Ag(1)#3	178.1(2)
C(1)-C(2)-C(5)-C(6)	-178.8(2)	O(7)-N(3)-O(5)-Ag(1)	-171.6(2)
C(3)-C(4)-C(5)-C(2)	0.8(4)	O(6)-N(3)-O(5)-Ag(1)	8.6(3)
C(3)-C(4)-C(5)-C(6)	179.6(2)	N(2)#1-Ag(1)-O(5)-N(3)	-103.2(2)
C(2)-C(5)-C(6)-O(1)	162.9(3)	N(1)-Ag(1)-O(5)-N(3)	84.1(2)
C(4)-C(5)-C(6)-O(1)	-15.8(4)	O(6)-Ag(1)-O(5)-N(3)	-4.74(16)
C(2)-C(5)-C(6)-O(2)	-16.9(4)	O(7)#2-Ag(1)-O(5)-N(3)	-19.0(3)
C(4)-C(5)-C(6)-O(2)	164.4(2)	O(7)-N(3)-O(6)-Ag(1)	171.9(2)
O(1)-C(6)-O(2)-C(7)	-1.0(4)	O(5)-N(3)-O(6)-Ag(1)	-8.4(3)
C(5)-C(6)-O(2)-C(7)	178.8(2)	N(2)#1-Ag(1)-O(6)-N(3)	91.67(16)
C(6)-O(2)-C(7)-C(8)	174.1(3)	N(1)-Ag(1)-O(6)-N(3)	-88.05(16)
O(2)-C(7)-C(8)-O(3)	175.7(2)	O(5)-Ag(1)-O(6)-N(3)	4.64(15)
C(7)-C(8)-O(3)-C(9)	170.8(2)	O(7)#2-Ag(1)-O(6)-N(3)	177.32(15)
C(8)-O(3)-C(9)-O(4)	8.4(4)		

Symmetry transformations used to generate equivalent atoms: #1 x-3/2,-y+1/2,z-1/2 #2 -x+3/2,y-1/2,-z+1/2 #3 x+3/2,-y+1/2,z+1/2

Hydrogen bonds for **3** [Å and °].

D-H...A	d(D-H)	d(H...A)	d(D...A)	<(DHA)
C(7)-H(7A)...O(1)#4	0.97	2.75	3.543(4)	139.8
C(8)-H(8A)...O(4)#5	0.97	2.57	3.457(4)	152.9
C(11)-H(11)...O(4)#6	0.93	2.77	3.367(3)	122.8
C(12)-H(12)...O(4)#6	0.93	2.68	3.337(3)	128.0
C(1)-H(1)...O(5)	0.93	2.74	3.450(4)	133.9
C(12)-H(12)...O(5)#3	0.93	2.80	3.496(4)	132.6
C(2)-H(2)...O(7)#8	0.93	2.54	3.461(4)	172.5

C(8)-H(8B)...O(7)#8	0.97	2.61	3.346(4)	133.1
C(3)-H(3)...O(6)#2	0.93	2.46	3.290(3)	148.4
C(14)-H(14)...O(6)#5	0.93	2.51	3.333(3)	148.2

Symmetry transformations used to generate equivalent atoms: #1 x-3/2,-y+1/2,z-1/2 #2 -x+3/2,y-1/2,-z+1/2 #3 x+3/2,-y+1/2,z+1/2 #4 -x+3,-y,-z+1 #5 -x+3,-y+1,-z+1 #6 -x+7/2,y-1/2,-z+3/2 #7 x+1,y,z #8 -x+2,-y+1,-z+1

I.2.e - Crystal data and structure refinement for 4.

Empirical formula	C14 H14 Ag N3 O8	
Formula weight	462.16	
Temperature	293(2) K	
Wavelength	0.71073 Å	
Crystal system	Orthorhombic	
Space group	Ccca	
Unit cell dimensions	a = 17.463(4) Å	α = 90°.
	b = 19.599(4) Å	β = 90°.
	c = 21.204(4) Å	γ = 90°.
Volume	7257(3) Å^3	
Z	16	
Density (calculated)	1.677 Mg/m^3	
Absorption coefficient	1.157 mm^{-1}	
F(000)	3648	
Crystal size	0.4 x 0.2 x 0.15 mm^3	
Theta range for data collection	1.83 to 27.01°.	
Index ranges	0<=h<=22, 0<=k<=25, 0<=l<=27	
Reflections collected	3972	
Independent reflections	3972 [R(int) = ?]	
Completeness to theta = 27.01°	99.9 %	
Absorption correction	Spherical	
Refinement method	Full-matrix least-squares on F^2	
Data / restraints / parameters	3972 / 0 / 236	
Goodness-of-fit on F^2	1.045	
Final R indices [I>2sigma(I)]	R1 = 0.0674, wR2 = 0.2181	
R indices (all data)	R1 = 0.0760, wR2 = 0.2388	
Extinction coefficient	0.00048(13)	

Largest diff. peak and hole	1.720 and -0.932 e.Å^{-3}

Atomic coordinates (x 10^4) and equivalent isotropic displacement parameters (Å^{2}x 10^3) for **4**. U(eq) is defined as one third of the trace of the orthogonalized U^{ij} tensor.

	x	y	z	U(eq)
Ag(1)	3310(1)	2172(1)	4899(1)	75(1)
N(1)	2649(2)	1478(2)	4316(2)	58(1)
C(1)	2222(3)	967(2)	4569(2)	58(1)
C(2)	1792(2)	531(2)	4220(2)	53(1)
C(3)	1792(2)	595(2)	3562(2)	47(1)
C(4)	2227(2)	1120(2)	3297(2)	52(1)
C(5)	2633(3)	1548(3)	3680(2)	58(1)
C(6)	1338(2)	97(2)	3191(2)	51(1)
O(1)	917(2)	-326(2)	3412(2)	71(1)
O(2)	1470(2)	162(2)	2570(1)	55(1)
C(7)	1129(3)	-348(2)	2170(2)	61(1)
C(8)	6284(3)	5169(2)	6504(2)	58(1)
O(3)	5768(2)	4626(2)	6329(1)	52(1)
C(9)	5799(3)	4439(2)	5718(2)	56(1)
O(4)	6248(3)	4677(2)	5351(2)	89(1)
C(10)	5225(2)	3911(2)	5555(2)	52(1)
C(11)	4828(2)	3536(2)	5998(2)	50(1)
C(12)	4308(2)	3055(2)	5804(2)	52(1)
C(13)	5073(3)	3789(3)	4917(2)	60(1)
C(14)	4542(3)	3298(3)	4766(2)	65(1)
N(2)	4163(2)	2927(2)	5190(2)	58(1)
O(8)	791(3)	1784(4)	2463(3)	131(2)
N(3)	2621(2)	1669(2)	6300(2)	58(1)
O(5)	2061(3)	1744(2)	5961(3)	100(2)
O(6)	3263(3)	1763(3)	6100(4)	115(2)
O(7)	2554(5)	1486(5)	6825(2)	173(4)

Bond lengths [Å] and angles [°] for **4**.

Ag(1)-N(1)	2.171(4)	C(8)-H(8A)	0.9700
Ag(1)-N(2)	2.189(4)	C(8)-H(8B)	0.9700
Ag(1)-O(6)	2.671(8)	O(3)-C(9)	1.347(5)
Ag(1)-Ag(1)#1	3.1356(10)	C(9)-O(4)	1.199(6)
Ag(1)-O(5)	3.246(6)	C(9)-C(10)	1.482(6)
N(1)-C(5)	1.357(6)	C(10)-C(11)	1.379(6)
N(1)-C(1)	1.359(6)	C(10)-C(13)	1.400(6)
C(1)-C(2)	1.356(7)	C(11)-C(12)	1.372(6)
C(1)-H(1)	0.9300	C(11)-H(11)	0.9300
C(2)-C(3)	1.402(6)	C(12)-N(2)	1.350(6)
C(2)-H(2)	0.9300	C(12)-H(12)	0.9300
C(3)-C(4)	1.397(6)	C(13)-C(14)	1.374(8)
C(3)-C(6)	1.485(6)	C(13)-H(13)	0.9300
C(4)-C(5)	1.366(6)	C(14)-N(2)	1.332(7)
C(4)-H(4)	0.9300	C(14)-H(14)	0.9300
C(5)-H(5)	0.9300	O(8)-O(8)#4	2.766(11)
C(6)-O(1)	1.203(5)	O(8)-O(8)#5	2.812(15)
C(6)-O(2)	1.341(5)	O(8)-O(3)#2	3.662(7)
O(2)-C(7)	1.439(5)	N(3)-O(7)	1.175(6)
O(2)-O(8)	3.401(7)	N(3)-O(6)	1.213(6)
C(7)-C(8)#2	1.482(7)	N(3)-O(5)	1.223(5)
C(7)-H(7A)	0.9700	O(5)-Ag(1)#1	2.874(5)
C(7)-H(7B)	0.9700	O(6)-O(8)#6	3.329(9)
C(8)-O(3)	1.442(5)	O(6)-Ag(1)#1	4.048(7)
C(8)-C(7)#3	1.482(7)	O(7)-O(8)#6	3.243(9)

N(1)-Ag(1)-N(2)	161.13(16)
N(1)-Ag(1)-O(6)	109.76(17)
N(2)-Ag(1)-O(6)	87.45(17)
N(1)-Ag(1)-Ag(1)#1	81.66(10)
N(2)-Ag(1)-Ag(1)#1	107.40(11)
O(6)-Ag(1)-Ag(1)#1	88.02(11)
N(1)-Ag(1)-O(5)	82.87(13)
N(2)-Ag(1)-O(5)	115.91(15)
O(6)-Ag(1)-O(5)	40.55(13)
Ag(1)#1-Ag(1)-O(5)	53.49(8)
C(5)-N(1)-C(1)	117.1(4)
C(5)-N(1)-Ag(1)	120.9(3)
C(1)-N(1)-Ag(1)	122.0(3)
C(2)-C(1)-N(1)	123.6(4)
C(2)-C(1)-H(1)	118.2
N(1)-C(1)-H(1)	118.2
C(1)-C(2)-C(3)	119.1(4)
C(1)-C(2)-H(2)	120.5
C(3)-C(2)-H(2)	120.5
C(4)-C(3)-C(2)	117.9(4)
C(4)-C(3)-C(6)	124.2(4)
C(2)-C(3)-C(6)	118.0(4)
C(5)-C(4)-C(3)	119.7(4)
C(5)-C(4)-H(4)	120.2
C(3)-C(4)-H(4)	120.2
N(1)-C(5)-C(4)	122.7(4)
N(1)-C(5)-H(5)	118.7
C(4)-C(5)-H(5)	118.7
O(1)-C(6)-O(2)	123.6(4)
O(1)-C(6)-C(3)	124.9(4)
O(2)-C(6)-C(3)	111.5(3)
C(6)-O(2)-C(7)	116.1(4)
C(6)-O(2)-O(8)	95.4(3)
C(7)-O(2)-O(8)	117.8(3)
O(2)-C(7)-C(8)#2	108.7(4)
O(2)-C(7)-H(7A)	109.9
C(8)#2-C(7)-H(7A)	109.9
O(2)-C(7)-H(7B)	109.9
C(8)#2-C(7)-H(7B)	109.9
H(7A)-C(7)-H(7B)	108.3
O(3)-C(8)-C(7)#3	107.8(4)
O(3)-C(8)-H(8A)	110.1
C(7)#3-C(8)-H(8A)	110.1
O(3)-C(8)-H(8B)	110.1
C(7)#3-C(8)-H(8B)	110.1
C(12)-C(11)-H(11)	120.2
C(10)-C(11)-H(11)	120.2
H(8A)-C(8)-H(8B)	108.5
C(9)-O(3)-C(8)	115.0(3)
O(4)-C(9)-O(3)	123.0(4)
O(4)-C(9)-C(10)	124.2(4)
O(3)-C(9)-C(10)	112.8(3)
C(11)-C(10)-C(13)	118.1(4)
C(11)-C(10)-C(9)	123.6(4)
C(13)-C(10)-C(9)	118.3(4)
C(12)-C(11)-C(10)	119.7(4)
N(2)-C(12)-C(11)	122.7(4)
N(2)-C(12)-H(12)	118.6
C(11)-C(12)-H(12)	118.6
C(14)-C(13)-C(10)	118.2(4)
C(14)-C(13)-H(13)	120.9
C(10)-C(13)-H(13)	120.9
N(2)-C(14)-C(13)	124.1(4)
N(2)-C(14)-H(14)	118.0
C(13)-C(14)-H(14)	118.0
C(14)-N(2)-C(12)	117.2(4)
C(14)-N(2)-Ag(1)	121.1(3)
C(12)-N(2)-Ag(1)	121.7(4)
O(8)#4-O(8)-O(8)#5	89.82(3)
O(8)#4-O(8)-O(2)	110.14(12)
O(8)#5-O(8)-O(2)	158.37(15)
O(8)#4-O(8)-O(3)#2	91.52(18)
O(8)#5-O(8)-O(3)#2	142.2(3)
O(2)-O(8)-O(3)#2	48.89(11)
O(7)-N(3)-O(6)	118.0(6)
O(7)-N(3)-O(5)	121.0(6)
O(6)-N(3)-O(5)	121.0(6)
N(3)-O(5)-Ag(1)#1	129.9(4)
N(3)-O(5)-Ag(1)	84.3(3)
Ag(1)#1-O(5)-Ag(1)	61.29(11)
N(3)-O(6)-Ag(1)	114.1(5)
N(3)-O(6)-O(8)#6	99.0(5)
Ag(1)-O(6)-O(8)#6	143.93(19)
N(3)-O(6)-Ag(1)#1	68.5(4)
Ag(1)-O(6)-Ag(1)#1	50.73(12)
O(8)#6-O(6)-Ag(1)#1	141.7(2)
N(3)-O(7)-O(8)#6	104.6(5)

Symmetry transformations used to generate equivalent atoms: #1 -x+1/2,-y+1/2,-z+1 #2 x-1/2,-y+1/2,z-1/2 #3 x+1/2,-y+1/2,z+1/2 #4 -x,y,-z+1/2 #5 x+0,-y+1/2,-z+1/2 #6 -x+1/2,y,z+1/2

Anisotropic displacement parameters ($Å^2 x 10^3$) for **4**. The anisotropic displacement factor exponent takes the form: $-2\pi^2[h^2 a^{*2} U^{11} + ... + 2 h k a^* b^* U^{12}]$

	U^{11}	U^{22}	U^{33}	U^{23}	U^{13}	U^{12}
Ag(1)	59(1)	86(1)	79(1)	-25(1)	-19(1)	5(1)
N(1)	55(2)	69(2)	50(2)	-9(2)	-6(2)	7(2)
C(1)	65(2)	71(3)	39(2)	2(2)	-6(2)	11(2)
C(2)	57(2)	57(2)	44(2)	6(2)	2(2)	6(2)
C(3)	47(2)	53(2)	41(2)	2(2)	1(1)	10(2)
C(4)	51(2)	67(2)	39(2)	4(2)	3(2)	3(2)
C(5)	53(2)	69(3)	53(2)	0(2)	3(2)	-1(2)
C(6)	49(2)	56(2)	46(2)	4(2)	0(2)	4(2)
O(1)	74(2)	76(2)	63(2)	4(2)	2(2)	-11(2)

O(2)	60(2)	60(2)	44(1)	-2(1)	-3(1)	-4(1)
C(7)	64(3)	58(2)	60(2)	-7(2)	-10(2)	-3(2)
C(8)	56(2)	66(2)	53(2)	10(2)	-5(2)	-12(2)
O(3)	50(2)	63(2)	44(1)	5(1)	2(1)	-6(1)
C(9)	59(2)	70(3)	40(2)	11(2)	0(2)	4(2)
O(4)	101(3)	113(3)	52(2)	13(2)	12(2)	-38(2)
C(10)	50(2)	65(2)	40(2)	5(2)	-2(2)	6(2)
C(11)	48(2)	61(2)	41(2)	1(2)	-5(2)	5(2)
C(12)	43(2)	65(2)	48(2)	-2(2)	-5(2)	5(2)
C(13)	67(3)	71(3)	41(2)	6(2)	-5(2)	7(2)
C(14)	63(3)	83(3)	48(2)	-3(2)	-12(2)	7(2)
N(2)	48(2)	69(2)	55(2)	-5(2)	-13(2)	8(2)
O(8)	109(4)	215(7)	70(3)	-4(4)	0(3)	71(4)
N(3)	59(2)	67(2)	48(2)	9(2)	-7(2)	-4(2)
O(5)	101(3)	100(3)	100(3)	0(3)	-52(3)	6(3)
O(6)	75(3)	117(4)	153(6)	-18(4)	34(3)	-13(2)
O(7)	198(7)	258(9)	64(3)	66(4)	-28(4)	-81(7)

Hydrogen coordinates (x 10^4) and isotropic displacement parameters ($Å^2$x 10^3) for **4**.

	x	y	z	U(eq)
H(1)	2226	912	5004	70
H(2)	1500	195	4416	63
H(4)	2241	1177	2861	63
H(5)	2909	1902	3497	70
H(7A)	581	-368	2243	73
H(7B)	1345	-793	2266	73
H(8A)	6203	5562	6235	70
H(8B)	6811	5020	6456	70
H(11)	4913	3609	6426	60
H(12)	4045	2807	6109	63
H(13)	5325	4033	4603	72
H(14)	4440	3220	4342	78

Torsion angles [°] for **4**.

N(2)-Ag(1)-N(1)-C(5)	-20.2(7)	N(1)-Ag(1)-N(2)-C(14)	15.2(7)
O(6)-Ag(1)-N(1)-C(5)	-175.0(3)	O(6)-Ag(1)-N(2)-C(14)	171.5(4)
Ag(1)#1-Ag(1)-N(1)-C(5)	100.2(3)	Ag(1)#1-Ag(1)-N(2)-C(14)	-101.4(4)
O(5)-Ag(1)-N(1)-C(5)	154.2(4)	O(5)-Ag(1)-N(2)-C(14)	-158.6(4)
N(2)-Ag(1)-N(1)-C(1)	161.3(4)	N(1)-Ag(1)-N(2)-C(12)	-167.4(4)
O(6)-Ag(1)-N(1)-C(1)	6.5(4)	O(6)-Ag(1)-N(2)-C(12)	-11.0(4)
Ag(1)#1-Ag(1)-N(1)-C(1)	-78.4(3)	Ag(1)#1-Ag(1)-N(2)-C(12)	76.1(4)
O(5)-Ag(1)-N(1)-C(1)	-24.4(3)	O(5)-Ag(1)-N(2)-C(12)	18.8(4)
C(5)-N(1)-C(1)-C(2)	0.2(7)	C(6)-O(2)-O(8)-O(8)#4	-73.8(4)
Ag(1)-N(1)-C(1)-C(2)	178.7(3)	C(7)-O(2)-O(8)-O(8)#4	49.5(4)
N(1)-C(1)-C(2)-C(3)	1.4(7)	C(6)-O(2)-O(8)-O(8)#5	82.4(8)
C(1)-C(2)-C(3)-C(4)	-1.4(6)	C(7)-O(2)-O(8)-O(8)#5	-154.2(8)
C(1)-C(2)-C(3)-C(6)	177.8(4)	C(6)-O(2)-O(8)-O(3)#2	-147.4(3)
C(2)-C(3)-C(4)-C(5)	-0.1(6)	C(7)-O(2)-O(8)-O(3)#2	-24.1(3)
C(6)-C(3)-C(4)-C(5)	-179.2(4)	O(7)-N(3)-O(5)-Ag(1)#1	136.2(7)
C(1)-N(1)-C(5)-C(4)	-1.7(7)	O(6)-N(3)-O(5)-Ag(1)#1	-46.0(8)
Ag(1)-N(1)-C(5)-C(4)	179.7(3)	O(7)-N(3)-O(5)-Ag(1)	-179.2(7)
C(3)-C(4)-C(5)-N(1)	1.7(7)	O(6)-N(3)-O(5)-Ag(1)	-1.4(5)
C(4)-C(3)-C(6)-O(1)	-174.3(4)	N(1)-Ag(1)-O(5)-N(3)	133.0(3)
C(2)-C(3)-C(6)-O(1)	6.5(6)	N(2)-Ag(1)-O(5)-N(3)	-49.1(3)
C(4)-C(3)-C(6)-O(2)	7.3(6)	O(6)-Ag(1)-O(5)-N(3)	0.9(3)
C(2)-C(3)-C(6)-O(2)	-171.8(4)	Ag(1)#1-Ag(1)-O(5)-N(3)	-142.2(3)
O(1)-C(6)-O(2)-C(7)	-5.4(6)	N(1)-Ag(1)-O(5)-Ag(1)#1	-84.88(12)
C(3)-C(6)-O(2)-C(7)	173.0(3)	N(2)-Ag(1)-O(5)-Ag(1)#1	93.10(13)

O(1)-C(6)-O(2)-O(8)	119.2(4)	O(6)-Ag(1)-O(5)-Ag(1)#1	143.0(3)
C(3)-C(6)-O(2)-O(8)	-62.5(3)	O(7)-N(3)-O(6)-Ag(1)	179.8(6)
C(6)-O(2)-C(7)-C(8)#2	175.8(4)	O(5)-N(3)-O(6)-Ag(1)	1.9(7)
O(8)-O(2)-C(7)-C(8)#2	63.6(4)	O(7)-N(3)-O(6)-O(8)#6	-15.0(8)
C(7)#3-C(8)-O(3)-C(9)	175.2(4)	O(5)-N(3)-O(6)-O(8)#6	167.2(4)
C(8)-O(3)-C(9)-O(4)	3.8(7)	O(7)-N(3)-O(6)-Ag(1)#1	-157.3(7)
C(8)-O(3)-C(9)-C(10)	-176.5(4)	O(5)-N(3)-O(6)-Ag(1)#1	24.9(4)
O(4)-C(9)-C(10)-C(11)	165.3(5)	N(1)-Ag(1)-O(6)-N(3)	-52.4(5)
O(3)-C(9)-C(10)-C(11)	-14.4(6)	N(2)-Ag(1)-O(6)-N(3)	135.5(5)
O(4)-C(9)-C(10)-C(13)	-15.1(7)	Ag(1)#1-Ag(1)-O(6)-N(3)	28.0(4)
O(3)-C(9)-C(10)-C(13)	165.3(4)	O(5)-Ag(1)-O(6)-N(3)	-1.0(3)
C(13)-C(10)-C(11)-C(12)	0.6(6)	N(1)-Ag(1)-O(6)-O(8)#6	152.8(4)
C(9)-C(10)-C(11)-C(12)	-179.8(4)	N(2)-Ag(1)-O(6)-O(8)#6	-19.3(4)
C(10)-C(11)-C(12)-N(2)	0.1(6)	Ag(1)#1-Ag(1)-O(6)-O(8)#6	-126.8(4)
C(11)-C(10)-C(13)-C(14)	-0.5(6)	O(5)-Ag(1)-O(6)-O(8)#6	-155.7(6)
C(9)-C(10)-C(13)-C(14)	179.9(4)	N(1)-Ag(1)-O(6)-Ag(1)#1	-80.41(11)
C(10)-C(13)-C(14)-N(2)	-0.4(8)	N(2)-Ag(1)-O(6)-Ag(1)#1	107.52(11)
C(13)-C(14)-N(2)-C(12)	1.1(7)	O(5)-Ag(1)-O(6)-Ag(1)#1	-28.9(2)
C(13)-C(14)-N(2)-Ag(1)	178.7(4)	O(6)-N(3)-O(7)-O(8)#6	15.7(8)
C(11)-C(12)-N(2)-C(14)	-1.0(7)	O(5)-N(3)-O(7)-O(8)#6	-166.5(4)
C(11)-C(12)-N(2)-Ag(1)	-178.5(3)		

Symmetry transformations used to generate equivalent atoms: #1 -x+1/2,-y+1/2,-z+1 #2 x-1/2,-y+1/2,z-1/2 #3 x+1/2,-y+1/2,z+1/2 #4 -x,y,-z+1/2 #5 x+0,-y+1/2,-z+1/2 #6 -x+1/2,y,z+1/2

Hydrogen bonds for **4** [Å and °].

D-H...A	d(D-H)	d(H...A)	d(D...A)	<(DHA)
C(11)-H(11)...O(8)#3	0.93	2.79	3.587(7)	144.5
C(11)-H(11)...O(8)	0.93	2.63	3.348(7)	134.1
C(4)-H(4)...O(8)	0.93	2.92	3.334(6)	108.3
C(2)-H(2)...O(4)#7	0.93	2.27	3.075(6)	144.2
C(7)-H(7A)...O(1)#4	0.97	2.96	3.781(6)	142.7
C(12)-H(12)...O(6)	0.93	2.46	3.185(7)	134.8
C(7)-H(7B)...O(7)#9	0.97	2.68	3.421(9)	133.5
C(4)-H(4)...O(7)#10	0.93	2.31	3.224(6)	168.8
C(8)-H(8A)...O(5)#11	0.97	2.82	3.563(7)	134.2
C(1)-H(1)...O(5)	0.93	2.62	3.335(7)	134.2

Symmetry transformations used to generate equivalent atoms: #1 -x+1/2,-y+1/2,-z+1 #2 x-1/2,-y+1/2,z-1/2 #3 x+1/2,-y+1/2,z+1/2 #4 -x,y,-z+1/2 #5 x+0,-y+1/2,-z+1/2 #6 -x+1/2,y,z+1/2 #7 x-1/2,y-1/2,z #8 -x+1,-y+1/2,z #9 x,-y,z-1/2 #10 -x+1/2,y,z-1/2 #11 x+1/2,y+1/2,z

I.2.f - Crystal data and structure refinement for 5.

Empirical formula	C14 H16 Ag1 N3 O9	
Formula weight	478.16	
Temperature	240(2) K	
Wavelength	0.71073 Å	
Crystal system	Triclinic	
Space group	P-1	
Unit cell dimensions	a = 8.1061(9) Å	α = 80.155(13)°.
	b = 9.9873(11) Å	β = 87.947(13)°.

	c = 11.0040(12) Å	γ = 87.234(13)°.
Volume	876.38(17) Å^3	
Z	2	
Density (calculated)	1.812 Mg/m^3	
Absorption coefficient	1.205 mm^{-1}	
F(000)	480	
Crystal size	0.30 x 0.17 x 0.09 mm^3	
Theta range for data collection	2.52 to 28.08°.	
Index ranges	-10<=h<=10, -12<=k<=13, 0<=l<=14	
Reflections collected	3917	
Independent reflections	3917 [R(int) = ?]	
Completeness to theta = 28.08°	91.5 %	
Absorption correction	Spherical	
Refinement method	Full-matrix least-squares on F^2	
Data / restraints / parameters	3917 / 0 / 244	
Goodness-of-fit on F^2	0.805	
Final R indices [I>2sigma(I)]	R1 = 0.0244, wR2 = 0.0514	
R indices (all data)	R1 = 0.0372, wR2 = 0.0531	
Largest diff. peak and hole	0.476 and -0.277 e.Å^{-3}	

Atomic coordinates (x 10^4) and equivalent isotropic displacement parameters (Å^{2}x 10^3) for **5**. U(eq) is defined as one third of the trace of the orthogonalized U^{ij} tensor.

	x	y	z	U(eq)
Ag(1)	6976(1)	5288(1)	5333(1)	30(1)
N(1)	5558(3)	6747(2)	6213(2)	23(1)
C(1)	4731(3)	7798(2)	5540(2)	24(1)
C(2)	3789(3)	8749(2)	6062(2)	23(1)
C(3)	5459(3)	6638(2)	7451(2)	24(1)
C(4)	4547(3)	7546(2)	8053(2)	23(1)
C(5)	3696(3)	8632(2)	7342(2)	20(1)
C(6)	2673(3)	9673(2)	7896(2)	22(1)
O(1)	1613(3)	10402(2)	7355(2)	37(1)
O(2)	3079(2)	9687(2)	9055(1)	26(1)
C(7)	2185(3)	10686(2)	9672(2)	28(1)
C(8)	2445(3)	10224(2)	11021(2)	26(1)
O(3)	1557(2)	11235(2)	11621(1)	25(1)
C(9)	1613(3)	11030(2)	12847(2)	22(1)
O(4)	2381(2)	10110(2)	13454(2)	31(1)
C(10)	600(3)	12093(2)	13392(2)	20(1)
C(11)	-127(3)	13232(2)	12680(2)	27(1)
C(12)	-1080(3)	14141(2)	13254(2)	27(1)
C(13)	354(3)	11916(2)	14668(2)	25(1)
C(14)	-623(3)	12856(2)	15176(2)	27(1)
N(2)	-1351(3)	13957(2)	14483(2)	25(1)

N(3)	5327(3)	3279(2)	7752(2)	33(1)
O(5)	5066(3)	3193(2)	8882(2)	52(1)
O(6)	6777(3)	3304(2)	7333(2)	53(1)
O(7)	4142(3)	3372(2)	7054(2)	61(1)
O(8)	1998(3)	14312(2)	9619(2)	54(1)
O(9)	-1125(3)	13321(3)	9493(3)	76(1)

Bond lengths [Å] and angles [°] for **5**.

Ag(1)-N(1)	2.150(2)	C(8)-H(8B)	0.9700
Ag(1)-N(2)#1	2.154(2)	O(3)-C(9)	1.332(3)
Ag(1)-O(6)	2.704(2)	C(9)-O(4)	1.202(3)
Ag(1)-O(7)#2	2.892(2)	C(9)-C(10)	1.502(3)
Ag(1)-Ag(1)#2	3.4079(6)	C(10)-C(11)	1.385(3)
N(1)-C(1)	1.343(3)	C(10)-C(13)	1.394(3)
N(1)-C(3)	1.347(3)	C(11)-C(12)	1.383(3)
C(1)-C(2)	1.378(3)	C(11)-H(11)	0.9300
C(1)-H(1)	0.9300	C(12)-N(2)	1.345(3)
C(2)-C(5)	1.393(3)	C(12)-H(12)	0.9300
C(2)-H(2)	0.9300	C(13)-C(14)	1.377(3)
C(3)-C(4)	1.384(3)	C(13)-H(13)	0.9300
C(3)-H(3)	0.9300	C(14)-N(2)	1.350(3)
C(4)-C(5)	1.393(3)	C(14)-H(14)	0.9300
C(4)-H(4)	0.9300	N(2)-Ag(1)#3	2.154(2)
C(5)-C(6)	1.496(3)	N(3)-O(7)	1.242(3)
C(6)-O(1)	1.205(3)	N(3)-O(5)	1.243(3)
C(6)-O(2)	1.331(3)	N(3)-O(6)	1.247(3)
O(2)-C(7)	1.451(3)	O(5)-O(8)#4	2.827(3)
C(7)-C(8)	1.496(3)	O(5)-O(9)#5	3.196(3)
C(7)-H(7A)	0.9700	O(6)-O(9)#5	2.974(3)
C(7)-H(7B)	0.9700	O(7)-O(8)#4	3.503(3)
C(8)-O(3)	1.448(3)	O(8)-O(9)#6	2.761(3)
C(8)-H(8A)	0.9700	O(8)-O(9)#7	2.779(4)
N(1)-Ag(1)-N(2)#1	173.20(8)	O(3)-C(8)-H(8A)	110.7
N(1)-Ag(1)-O(6)	93.43(7)	C(7)-C(8)-H(8A)	110.7
N(2)#1-Ag(1)-O(6)	88.36(7)	O(3)-C(8)-H(8B)	110.7
N(1)-Ag(1)-O(7)#2	90.43(7)	C(7)-C(8)-H(8B)	110.7
N(2)#1-Ag(1)-O(7)#2	91.11(7)	H(8A)-C(8)-H(8B)	108.8
O(6)-Ag(1)-O(7)#2	151.55(8)	C(9)-O(3)-C(8)	115.75(17)
N(1)-Ag(1)-Ag(1)#2	77.55(6)	O(4)-C(9)-O(3)	124.4(2)
N(2)#1-Ag(1)-Ag(1)#2	109.06(6)	O(4)-C(9)-C(10)	123.6(2)
O(6)-Ag(1)-Ag(1)#2	89.16(6)	O(3)-C(9)-C(10)	112.0(2)
O(7)#2-Ag(1)-Ag(1)#2	64.20(6)	C(11)-C(10)-C(13)	118.4(2)
C(1)-N(1)-C(3)	117.7(2)	C(11)-C(10)-C(9)	122.9(2)
C(1)-N(1)-Ag(1)	120.71(15)	C(13)-C(10)-C(9)	118.7(2)
C(3)-N(1)-Ag(1)	121.55(16)	C(12)-C(11)-C(10)	119.2(2)
N(1)-C(1)-C(2)	122.8(2)	C(12)-C(11)-H(11)	120.4
N(1)-C(1)-H(1)	118.6	C(10)-C(11)-H(11)	120.4
C(2)-C(1)-H(1)	118.6	N(2)-C(12)-C(11)	122.6(2)
C(1)-C(2)-C(5)	119.1(2)	N(2)-C(12)-H(12)	118.7
C(1)-C(2)-H(2)	120.4	C(11)-C(12)-H(12)	118.7
C(5)-C(2)-H(2)	120.4	C(14)-C(13)-C(10)	119.3(2)
N(1)-C(3)-C(4)	123.3(2)	C(14)-C(13)-H(13)	120.4
N(1)-C(3)-H(3)	118.3	C(10)-C(13)-H(13)	120.4
C(4)-C(3)-H(3)	118.3	N(2)-C(14)-C(13)	122.5(2)
C(3)-C(4)-C(5)	118.2(2)	N(2)-C(14)-H(14)	118.8
C(3)-C(4)-H(4)	120.9	C(13)-C(14)-H(14)	118.8
C(5)-C(4)-H(4)	120.9	C(12)-N(2)-C(14)	118.1(2)
C(2)-C(5)-C(4)	118.7(2)	C(12)-N(2)-Ag(1)#3	121.69(16)
C(2)-C(5)-C(6)	118.5(2)	C(14)-N(2)-Ag(1)#3	120.12(16)
C(4)-C(5)-C(6)	122.7(2)	O(7)-N(3)-O(5)	119.6(3)
O(1)-C(6)-O(2)	124.6(2)	O(7)-N(3)-O(6)	120.9(2)

O(1)-C(6)-C(5)	123.8(2)	O(5)-N(3)-O(6)	119.4(2)
O(2)-C(6)-C(5)	111.6(2)	N(3)-O(5)-O(8)#4	116.14(18)
C(6)-O(2)-C(7)	116.14(18)	N(3)-O(5)-O(9)#5	94.42(18)
O(2)-C(7)-C(8)	105.71(18)	O(8)#4-O(5)-O(9)#5	137.52(10)
O(2)-C(7)-H(7A)	110.6	N(3)-O(6)-Ag(1)	109.13(15)
C(8)-C(7)-H(7A)	110.6	N(3)-O(6)-O(9)#5	105.44(16)
O(2)-C(7)-H(7B)	110.6	Ag(1)-O(6)-O(9)#5	120.50(10)
C(8)-C(7)-H(7B)	110.6	N(3)-O(7)-O(8)#4	82.20(16)
H(7A)-C(7)-H(7B)	108.7	O(9)#6-O(8)-O(9)#7	99.36(10)
O(3)-C(8)-C(7)	105.00(17)		

Symmetry transformations used to generate equivalent atoms: #1 x+1,y-1,z-1 #2 -x+1,-y+1,-z+1 #3 x-1,y+1,z+1 #4 x,y-1,z #5 x+1,y-1,z #6 -x,-y+3,-z+2 #7 x,y,z

Anisotropic displacement parameters (Å^{2}x 10^3) for **5**. The anisotropic displacement factor exponent takes the form: $-2\pi^2[h^2a^{*2}U^{11} + ... + 2 h k a^* b^* U^{12}]$

	U^{11}	U^{22}	U^{33}	U^{23}	U^{13}	U^{12}
Ag(1)	31(1)	30(1)	32(1)	-16(1)	6(1)	6(1)
N(1)	25(1)	25(1)	22(1)	-10(1)	2(1)	1(1)
C(1)	29(2)	28(1)	17(1)	-7(1)	2(1)	0(1)
C(2)	26(2)	24(1)	18(1)	-5(1)	-2(1)	3(1)
C(3)	29(2)	21(1)	22(1)	-5(1)	-2(1)	5(1)
C(4)	28(2)	26(1)	17(1)	-6(1)	-1(1)	1(1)
C(5)	20(1)	23(1)	19(1)	-9(1)	2(1)	-1(1)
C(6)	25(2)	22(1)	20(1)	-7(1)	1(1)	0(1)
O(1)	43(1)	42(1)	27(1)	-14(1)	-7(1)	21(1)
O(2)	29(1)	31(1)	20(1)	-13(1)	-1(1)	10(1)
C(7)	31(2)	28(1)	25(1)	-11(1)	5(1)	9(1)
C(8)	27(2)	29(1)	24(1)	-13(1)	0(1)	11(1)
O(3)	30(1)	29(1)	17(1)	-9(1)	2(1)	11(1)
C(9)	21(1)	26(1)	20(1)	-7(1)	1(1)	0(1)
O(4)	37(1)	33(1)	23(1)	-8(1)	-3(1)	14(1)
C(10)	19(1)	24(1)	20(1)	-8(1)	2(1)	0(1)
C(11)	32(2)	31(1)	16(1)	-5(1)	2(1)	5(1)
C(12)	32(2)	25(1)	24(1)	-4(1)	2(1)	6(1)
C(13)	26(2)	27(1)	19(1)	-3(1)	0(1)	6(1)
C(14)	30(2)	34(1)	18(1)	-8(1)	1(1)	4(1)
N(2)	25(1)	26(1)	27(1)	-11(1)	1(1)	3(1)
N(3)	44(2)	27(1)	25(1)	-5(1)	3(1)	6(1)
O(5)	40(1)	94(2)	20(1)	-6(1)	1(1)	-1(1)
O(6)	48(2)	55(1)	49(1)	2(1)	26(1)	16(1)
O(7)	71(2)	81(2)	35(1)	-22(1)	-22(1)	22(1)
O(8)	50(2)	53(1)	55(1)	-6(1)	8(1)	5(1)
O(9)	56(2)	67(2)	112(2)	-36(2)	-24(2)	8(1)

Hydrogen coordinates (x 10^4) and isotropic displacement parameters (Å^{2}x 10^3) for **5**.

	x	y	z	U(eq)
H(1)	4797	7890	4684	29
H(2)	3222	9458	5567	27
H(3)	6033	5915	7924	29
H(4)	4504	7435	8910	28
H(7A)	1019	10723	9495	33
H(7B)	2614	11582	9403	33
H(8A)	2008	9332	11293	32
H(8B)	3611	10183	11199	32
H(11)	23	13383	11826	32
H(12)	-1551	14910	12771	33
H(13)	844	11171	15172	29

H(14)	-787	12727	16028	32

Torsion angles [°] for **5**.

N(2)#1-Ag(1)-N(1)-C(1)	99.2(7)	O(4)-C(9)-C(10)-C(13)	-8.6(4)
O(6)-Ag(1)-N(1)-C(1)	-155.66(19)	O(3)-C(9)-C(10)-C(13)	171.4(2)
O(7)#2-Ag(1)-N(1)-C(1)	-3.86(19)	C(13)-C(10)-C(11)-C(12)	-0.6(4)
Ag(1)#2-Ag(1)-N(1)-C(1)	-67.28(18)	C(9)-C(10)-C(11)-C(12)	178.2(2)
N(2)#1-Ag(1)-N(1)-C(3)	-81.2(8)	C(10)-C(11)-C(12)-N(2)	-0.9(4)
O(6)-Ag(1)-N(1)-C(3)	24.0(2)	C(11)-C(10)-C(13)-C(14)	1.3(4)
O(7)#2-Ag(1)-N(1)-C(3)	175.8(2)	C(9)-C(10)-C(13)-C(14)	-177.6(2)
Ag(1)#2-Ag(1)-N(1)-C(3)	112.33(19)	C(10)-C(13)-C(14)-N(2)	-0.4(4)
C(3)-N(1)-C(1)-C(2)	-0.5(4)	C(11)-C(12)-N(2)-C(14)	1.8(4)
Ag(1)-N(1)-C(1)-C(2)	179.10(19)	C(11)-C(12)-N(2)-Ag(1)#3	-174.1(2)
N(1)-C(1)-C(2)-C(5)	0.7(4)	C(13)-C(14)-N(2)-C(12)	-1.1(4)
C(1)-N(1)-C(3)-C(4)	0.3(4)	C(13)-C(14)-N(2)-Ag(1)#3	174.8(2)
Ag(1)-N(1)-C(3)-C(4)	-179.29(19)	O(7)-N(3)-O(5)-O(8)#4	-25.2(3)
N(1)-C(3)-C(4)-C(5)	-0.3(4)	O(6)-N(3)-O(5)-O(8)#4	153.01(18)
C(1)-C(2)-C(5)-C(4)	-0.7(4)	O(7)-N(3)-O(5)-O(9)#5	-174.8(2)
C(1)-C(2)-C(5)-C(6)	179.8(2)	O(6)-N(3)-O(5)-O(9)#5	3.5(2)
C(3)-C(4)-C(5)-C(2)	0.5(4)	O(7)-N(3)-O(6)-Ag(1)	43.6(3)
C(3)-C(4)-C(5)-C(6)	180.0(2)	O(5)-N(3)-O(6)-Ag(1)	-134.6(2)
C(2)-C(5)-C(6)-O(1)	19.0(4)	O(7)-N(3)-O(6)-O(9)#5	174.4(2)
C(4)-C(5)-C(6)-O(1)	-160.5(3)	O(5)-N(3)-O(6)-O(9)#5	-3.9(3)
C(2)-C(5)-C(6)-O(2)	-161.1(2)	N(1)-Ag(1)-O(6)-N(3)	45.16(18)
C(4)-C(5)-C(6)-O(2)	19.4(3)	N(2)#1-Ag(1)-O(6)-N(3)	-141.41(18)
O(1)-C(6)-O(2)-C(7)	-1.6(4)	O(7)#2-Ag(1)-O(6)-N(3)	-52.1(2)
C(5)-C(6)-O(2)-C(7)	178.6(2)	Ag(1)#2-Ag(1)-O(6)-N(3)	-32.31(17)
C(6)-O(2)-C(7)-C(8)	162.4(2)	N(1)-Ag(1)-O(6)-O(9)#5	-76.93(11)
O(2)-C(7)-C(8)-O(3)	179.63(18)	N(2)#1-Ag(1)-O(6)-O(9)#5	96.50(11)
C(7)-C(8)-O(3)-C(9)	179.9(2)	O(7)#2-Ag(1)-O(6)-O(9)#5	-174.19(12)
C(8)-O(3)-C(9)-O(4)	2.6(4)	Ag(1)#2-Ag(1)-O(6)-O(9)#5	-154.40(10)
C(8)-O(3)-C(9)-C(10)	-177.5(2)	O(5)-N(3)-O(7)-O(8)#4	18.2(2)
O(4)-C(9)-C(10)-C(11)	172.5(3)	O(6)-N(3)-O(7)-O(8)#4	-160.1(2)
O(3)-C(9)-C(10)-C(11)	-7.4(3)		

Symmetry transformations used to generate equivalent atoms: #1 x+1,y-1,z-1 #2 -x+1,-y+1,-z+1
#3 x-1,y+1,z+1 #4 x,y-1,z #5 x+1,y-1,z #6 -x,-y+3,-z+2 #7 x,y,z

Hydrogen bonds for **5** [Å and °].

D-H...A	d(D-H)	d(H...A)	d(D...A)	<(DHA)
C(13)-H(13)...O(1)#8	0.93	2.49	3.257(3)	140.4
C(8)-H(8B)...O(2)#9	0.97	2.70	3.632(3)	162.5
C(2)-H(2)...O(4)#10	0.93	2.42	3.184(3)	139.6
C(1)-H(1)...O(7)#2	0.93	2.57	3.346(3)	141.7
C(12)-H(12)...O(7)#11	0.93	2.67	3.410(3)	137.0
C(8)-H(8A)...O(6)#12	0.97	2.95	3.712(3)	136.7
C(3)-H(3)...O(6)	0.93	2.83	3.470(3)	127.3
C(14)-H(14)...O(6)#3	0.93	2.50	3.192(3)	131.1
C(4)-H(4)...O(5)#12	0.93	2.44	3.349(3)	167.1
C(3)-H(3)...O(5)	0.93	2.88	3.555(3)	130.6
C(7)-H(7B)...O(5)#13	0.97	2.60	3.486(4)	151.3

Symmetry transformations used to generate equivalent atoms: #1 x+1,y-1,z-1 #2 -x+1,-y+1,-z+1
#3 x-1,y+1,z+1 #4 x,y-1,z #5 x+1,y-1,z #6 -x,-y+3,-z+2 #7 x,y,z #8 x,y,z+1 #9 -x+1,-y+2,-z+2
#10 x,y,z-1 #11 -x,-y+2,-z+2 #12 -x+1,-y+1,-z+2 #13 x,y+1,z

I.2.g - Crystal data and structure refinement for 6.

Empirical formula	C7 H6 Ag1 N2 O5	
Formula weight	306.01	
Temperature	293(2) K	
Wavelength	0.71073 Å	
Crystal system	Monoclinic	
Space group	C2/c	
Unit cell dimensions	a = 20.976(7) Å	α = 90°.
	b = 9.3460(17) Å	β = 106.98(2)°.
	c = 9.903(3) Å	γ = 90°.
Volume	1856.7(9) Å^3	
Z	8	
Density (calculated)	2.189 Mg/m^3	
Absorption coefficient	2.174 mm^{-1}	
F(000)	1192	
Crystal size	0.20 x 0.07 x 0.07 mm^3	
Theta range for data collection	2.40 to 31.94°.	
Index ranges	-26<=h<=3, -12<=k<=13, -6<=l<=14	
Reflections collected	1972	
Independent reflections	1452 [R(int) = 0.0777]	
Completeness to theta = 31.94°	45.2 %	
Absorption correction	Spherical	
Refinement method	Full-matrix least-squares on F^2	
Data / restraints / parameters	1452 / 0 / 147	
Goodness-of-fit on F^2	0.868	
Final R indices [I>2sigma(I)]	R1 = 0.0733, wR2 = 0.1742	
R indices (all data)	R1 = 0.0854, wR2 = 0.1885	
Largest diff. peak and hole	0.208 and -0.182 e.Å^{-3}	

Atomic coordinates (x 10^4) and equivalent isotropic displacement parameters (Å^{2}x 10^3) for **6**. U(eq) is defined as one third of the trace of the orthogonalized U^{ij} tensor.

	x	y	z	U(eq)
Ag(1)	2278(1)	1292(1)	6290(1)	62(1)
N(1)	1614(5)	14(6)	4541(8)	54(2)
C(1)	1215(6)	623(7)	3357(10)	62(3)

C(2)	834(6)	-167(8)	2249(10)	61(3)
C(3)	1652(5)	-1410(6)	4614(10)	56(3)
C(4)	1291(5)	-2287(7)	3521(9)	55(2)
C(5)	881(5)	-1649(7)	2321(9)	52(2)
C(6)	459(8)	-2493(9)	1113(12)	75(4)
O(1)	169(6)	-2006(8)	-24(10)	87(5)
O(2A)	641(11)	-3929(11)	1229(19)	61(4)
O(2B)	326(19)	-3818(16)	1530(20)	63(7)
C(7)	294(15)	-4980(20)	-30(30)	112(8)
O(3)	2365(5)	3663(5)	7124(8)	62(2)
N(2)	2023(5)	4465(6)	6179(8)	56(2)
O(4)	3033(5)	757(5)	8555(7)	65(3)
O(5)	1747(6)	3967(7)	4991(9)	74(3)

Bond lengths [Å] and angles [°] for **6**.

Ag(1)-N(1)	2.226(7)	C(5)-C(6)	1.489(12)
Ag(1)-O(3)	2.354(5)	C(6)-O(1)	1.201(12)
Ag(1)-O(4)	2.390(7)	C(6)-O(2B)	1.360(17)
Ag(1)-O(5)#1	2.716(13)	C(6)-O(2A)	1.391(15)
N(1)-C(3)	1.334(8)	O(2A)-C(7)	1.59(4)
N(1)-C(1)	1.351(11)	O(2B)-C(7)	1.87(4)
C(1)-C(2)	1.369(12)	C(7)-C(7)#2	1.25(6)
C(1)-H(1)	0.9300	C(7)-H(7A)	0.9700
C(2)-C(5)	1.389(10)	C(7)-H(7B)	0.9700
C(2)-H(2)	0.9300	O(3)-N(2)	1.249(10)
C(3)-C(4)	1.392(10)	N(2)-O(5)	1.240(10)
C(3)-H(3)	0.9300	N(2)-O(4)#3	1.249(8)
C(4)-C(5)	1.383(12)	O(4)-N(2)#4	1.249(8)
C(4)-H(4)	0.9300		

N(1)-Ag(1)-O(3)	138.2(3)	O(1)-C(6)-O(2B)	122.5(12)
N(1)-Ag(1)-O(4)	135.27(19)	O(1)-C(6)-O(2A)	119.7(11)
O(3)-Ag(1)-O(4)	84.6(2)	O(2B)-C(6)-O(2A)	34.1(13)
N(1)-Ag(1)-O(5)#1	88.5(3)	O(1)-C(6)-C(5)	124.8(8)
O(3)-Ag(1)-O(5)#1	104.8(3)	O(2B)-C(6)-C(5)	111.4(10)
O(4)-Ag(1)-O(5)#1	92.1(3)	O(2A)-C(6)-C(5)	111.1(10)
C(3)-N(1)-C(1)	118.6(6)	C(6)-O(2A)-C(7)	118.8(13)
C(3)-N(1)-Ag(1)	118.6(6)	C(6)-O(2B)-C(7)	103.9(18)
C(1)-N(1)-Ag(1)	122.5(4)	C(7)#2-C(7)-O(2A)	103(3)
N(1)-C(1)-C(2)	122.5(6)	C(7)#2-C(7)-O(2B)	77(3)
N(1)-C(1)-H(1)	118.8	O(2A)-C(7)-O(2B)	25.3(11)
C(2)-C(1)-H(1)	118.8	C(7)#2-C(7)-H(7A)	111.3
C(1)-C(2)-C(5)	118.7(8)	O(2A)-C(7)-H(7A)	111.3
C(1)-C(2)-H(2)	120.6	O(2B)-C(7)-H(7A)	123.3
C(5)-C(2)-H(2)	120.6	C(7)#2-C(7)-H(7B)	111.3
N(1)-C(3)-C(4)	122.4(7)	O(2A)-C(7)-H(7B)	111.2
N(1)-C(3)-H(3)	118.8	O(2B)-C(7)-H(7B)	119.4
C(4)-C(3)-H(3)	118.8	H(7A)-C(7)-H(7B)	109.2
C(5)-C(4)-C(3)	118.4(6)	N(2)-O(3)-Ag(1)	109.5(5)
C(5)-C(4)-H(4)	120.8	O(5)-N(2)-O(4)#3	121.1(7)
C(3)-C(4)-H(4)	120.8	O(5)-N(2)-O(3)	119.5(6)
C(4)-C(5)-C(2)	119.4(7)	O(4)#3-N(2)-O(3)	119.4(7)
C(4)-C(5)-C(6)	122.5(7)	N(2)#4-O(4)-Ag(1)	108.8(5)
C(2)-C(5)-C(6)	118.1(8)		

Symmetry transformations used to generate equivalent atoms: #1 -x+1/2,-y+1/2,-z+1 #2 -x,-y-1,-z
#3 -x+1/2,y+1/2,-z+3/2 #4 -x+1/2,y-1/2,-z+3/2

Anisotropic displacement parameters ($Å^2$x 10^3) for **6**. The anisotropic displacement factor exponent takes the form: $-2\pi^2$[$h^2a^{*2}U^{11}$ + ... + 2 h k a* b* U^{12}]

	U^{11}	U^{22}	U^{33}	U^{23}	U^{13}	U^{12}
Ag(1)	74(1)	50(1)	55(1)	-7(1)	6(1)	-4(1)
N(1)	61(6)	47(3)	50(3)	-4(2)	9(4)	-4(2)
C(1)	70(7)	47(3)	60(5)	-2(3)	6(5)	0(3)
C(2)	60(7)	60(4)	54(4)	1(3)	4(5)	8(3)
C(3)	57(6)	49(3)	51(4)	-3(2)	-2(5)	-3(2)
C(4)	59(6)	49(3)	52(4)	-1(2)	8(4)	-7(2)
C(5)	50(6)	57(3)	51(4)	-4(2)	17(4)	-7(3)
C(6)	86(10)	62(4)	61(6)	0(3)	-5(7)	-16(4)
O(1)	98(11)	79(4)	62(4)	0(3)	-12(7)	-5(4)
O(2A)	51(11)	65(7)	72(9)	-15(4)	25(9)	-10(5)
O(2B)	80(20)	51(7)	43(8)	-9(5)	4(12)	-23(8)
C(7)	80(20)	135(11)	162(17)	46(11)	89(15)	40(11)
O(3)	75(6)	49(3)	56(3)	4(2)	11(4)	1(2)
N(2)	62(6)	50(3)	49(3)	-3(2)	7(4)	-2(2)
O(4)	74(6)	47(3)	67(4)	-1(2)	9(4)	0(2)
O(5)	74(8)	76(4)	59(4)	-11(3)	-2(5)	-3(3)

Hydrogen coordinates (x 10^4) and isotropic displacement parameters ($Å^2$x 10^3) for **6**.

	x	y	z	U(eq)
H(1)	1199	1616	3291	74
H(2)	549	280	1464	73
H(3)	1928	-1832	5425	67
H(4)	1326	-3277	3596	66
H(7A)	318	-4614	-925	135
H(7B)	496	-5926	127	135

Torsion angles [°] for **6**.

O(3)-Ag(1)-N(1)-C(3)	-165.2(9)	C(4)-C(5)-C(6)-O(2A)	-13(2)
O(4)-Ag(1)-N(1)-C(3)	-7.5(12)	C(2)-C(5)-C(6)-O(2A)	170.0(17)
O(5)#1-Ag(1)-N(1)-C(3)	84.0(9)	O(1)-C(6)-O(2A)-C(7)	-17(3)
O(3)-Ag(1)-N(1)-C(1)	20.3(12)	O(2B)-C(6)-O(2A)-C(7)	88(3)
O(4)-Ag(1)-N(1)-C(1)	178.1(9)	C(5)-C(6)-O(2A)-C(7)	-174.6(19)
O(5)#1-Ag(1)-N(1)-C(1)	-90.4(10)	O(1)-C(6)-O(2B)-C(7)	46(3)
C(3)-N(1)-C(1)-C(2)	2(2)	O(2A)-C(6)-O(2B)-C(7)	-49.9(19)
Ag(1)-N(1)-C(1)-C(2)	176.4(10)	C(5)-C(6)-O(2B)-C(7)	-146.3(16)
N(1)-C(1)-C(2)-C(5)	-3(2)	C(6)-O(2A)-C(7)-C(7)#2	-67(3)
C(1)-N(1)-C(3)-C(4)	-0.5(19)	C(6)-O(2A)-C(7)-O(2B)	-72(2)
Ag(1)-N(1)-C(3)-C(4)	-175.2(9)	C(6)-O(2B)-C(7)-C(7)#2	-114(3)
N(1)-C(3)-C(4)-C(5)	-0.1(18)	C(6)-O(2B)-C(7)-O(2A)	62(2)
C(3)-C(4)-C(5)-C(2)	-0.8(18)	N(1)-Ag(1)-O(3)-N(2)	-17.0(11)
C(3)-C(4)-C(5)-C(6)	-178.0(12)	O(4)-Ag(1)-O(3)-N(2)	178.5(9)
C(1)-C(2)-C(5)-C(4)	2(2)	O(5)#1-Ag(1)-O(3)-N(2)	87.8(8)
C(1)-C(2)-C(5)-C(6)	179.5(13)	Ag(1)-O(3)-N(2)-O(5)	-5.0(15)
C(4)-C(5)-C(6)-O(1)	-168.9(16)	Ag(1)-O(3)-N(2)-O(4)#3	175.3(9)
C(2)-C(5)-C(6)-O(1)	14(3)	N(1)-Ag(1)-O(4)-N(2)#4	-7.9(11)
C(4)-C(5)-C(6)-O(2B)	24(3)	O(3)-Ag(1)-O(4)-N(2)#4	157.4(9)
C(2)-C(5)-C(6)-O(2B)	-153(2)	O(5)#1-Ag(1)-O(4)-N(2)#4	-97.9(8)

Symmetry transformations used to generate equivalent atoms: #1 -x+1/2,-y+1/2,-z+1 #2 -x,-y-1,-z
#3 -x+1/2,y+1/2,-z+3/2 #4 -x+1/2,y-1/2,-z+3/2

Hydrogen bonds for **6** [Å and °].

D-H...A	d(D-H)	d(H...A)	d(D...A)	<(DHA)
C(7)-H(7B)...O(1)#2	0.97	2.37	2.98(3)	120.6
C(2)-H(2)...O(1)#5	0.93	2.38	3.271(11)	161.2
C(3)-H(3)...O(3)#4	0.93	2.49	3.286(12)	143.7
C(3)-H(3)...O(4)#4	0.93	2.46	3.167(9)	132.9
C(4)-H(4)...O(4)#4	0.93	2.89	3.367(10)	113.0
C(1)-H(1)...O(5)	0.93	2.80	3.547(10)	137.8

Symmetry transformations used to generate equivalent atoms: #1 -x+1/2,-y+1/2,-z+1 #2 -x,-y-1,-z #3 -x+1/2,y+1/2,-z+3/2 #4 -x+1/2,y-1/2,-z+3/2 #5 -x,-y,-z

I.2.h - Crystal data and structure refinement for 7.

Empirical formula	C14 H12 Ag1 N3 O7	
Formula weight	442.14	
Temperature	293(2) K	
Wavelength	0.71073 Å	
Crystal system	Triclinic	
Space group	P-1	
Unit cell dimensions	a = 6.1591(13) Å	α = 93.15(2)°.
	b = 8.895(3) Å	β = 99.898(16)°.
	c = 14.439(3) Å	γ = 91.43(2)°.
Volume	777.6(4) Å^3	
Z	2	
Density (calculated)	1.888 Mg/m^3	
Absorption coefficient	1.341 mm^{-1}	
F(000)	440	
Crystal size	? x ? x ? mm^3	
Theta range for data collection	2.87 to 27.01°.	
Index ranges	-7<=h<=7, -8<=k<=1, -17<=l<=17	
Reflections collected	1565	
Independent reflections	1494 [R(int) = 0.0213]	
Completeness to theta = 27.01°	43.9 %	
Refinement method	Full-matrix least-squares on F^2	
Data / restraints / parameters	1494 / 0 / 226	
Goodness-of-fit on F^2	1.070	
Final R indices [I>2sigma(I)]	R1 = 0.0312, wR2 = 0.0686	

R indices (all data)	R1 = 0.0408, wR2 = 0.0732
Largest diff. peak and hole	0.189 and -0.216 e.Å^{-3}

Atomic coordinates (x 10^4) and equivalent isotropic displacement parameters (Å^{2}x 10^3) for **7**. U(eq) is defined as one third of the trace of the orthogonalized U^{ij} tensor.

	x	y	z	U(eq)
Ag(1)	3781(1)	8572(1)	8897(1)	49(1)
N(1)	4261(6)	7603(7)	10271(3)	43(2)
C(1)	2640(7)	7678(9)	10784(4)	44(2)
C(2)	2768(7)	6994(9)	11629(4)	44(2)
C(3)	6036(7)	6821(9)	10603(4)	47(2)
C(4)	6300(7)	6112(8)	11433(4)	39(2)
C(5)	4635(6)	6248(8)	11977(3)	35(2)
C(6)	4813(7)	5602(8)	12918(3)	34(2)
O(1)	3504(5)	5801(6)	13440(2)	48(2)
O(2)	6664(5)	4857(6)	13125(2)	39(1)
C(7)	6991(7)	4117(8)	13993(3)	37(2)
C(8)	9208(7)	3434(8)	14021(3)	39(2)
O(3)	9710(5)	2733(6)	14909(2)	39(1)
C(9)	11566(7)	1982(8)	15032(3)	35(2)
O(4)	12742(6)	1850(7)	14446(3)	55(2)
C(10)	2027(7)	11288(8)	5949(3)	32(2)
C(11)	568(7)	11285(8)	6592(3)	41(2)
C(12)	1128(7)	10589(9)	7408(4)	41(2)
C(13)	4018(7)	10595(8)	6197(3)	41(2)
C(14)	4455(7)	9904(8)	7031(3)	38(2)
N(2)	3037(6)	9872(7)	7644(3)	39(2)
N(3)	8575(6)	7523(8)	8492(3)	40(2)
O(5)	6661(6)	7028(8)	8165(3)	63(2)
O(6)	10157(6)	6753(10)	8340(4)	77(3)
O(7)	8869(6)	8723(10)	8943(3)	65(2)

Bond lengths [Å] and angles [°] for **7**.

Ag(1)-N(1)	2.183(4)
Ag(1)-N(2)	2.189(4)
Ag(1)-O(5)	2.599(5)
Ag(1)-O(6)#1	2.703(7)
Ag(1)-O(7)	3.122(4)
Ag(1)-Ag(1)#2	4.0170(17)
Ag(1)-Ag(1)#3	6.1591(13)
Ag(1)-Ag(1)#4	17.659(4)
N(1)-C(1)	1.342(5)
N(1)-C(3)	1.343(7)
C(1)-C(2)	1.384(7)
C(1)-H(1)	0.9300
C(2)-C(5)	1.375(6)
C(2)-H(2)	0.9300
C(3)-C(4)	1.372(7)
C(3)-H(3)	0.9300
C(4)-C(5)	1.398(5)
C(4)-H(4)	0.9300
C(5)-C(6)	1.493(6)
C(6)-O(1)	1.204(5)
C(6)-O(2)	1.331(5)
O(2)-C(7)	1.434(5)
C(7)-C(8)	1.503(6)
C(7)-H(7A)	0.9700
C(7)-H(7B)	0.9700
C(8)-O(3)	1.445(5)
C(8)-H(8A)	0.9700
C(8)-H(8B)	0.9700
O(3)-C(9)	1.329(6)
C(9)-O(4)	1.208(5)
C(9)-C(10)#5	1.479(7)
C(10)-C(13)	1.386(6)
C(10)-C(11)	1.398(5)
C(10)-C(9)#4	1.479(7)
C(11)-C(12)	1.358(7)
C(11)-H(11)	0.9300
C(12)-N(2)	1.352(6)
C(12)-H(12)	0.9300
C(13)-C(14)	1.370(7)
C(13)-H(13)	0.9300
C(14)-N(2)	1.347(5)
C(14)-H(14)	0.9300
N(3)-O(7)	1.213(10)
N(3)-O(6)	1.248(7)
N(3)-O(5)	1.251(7)
O(6)-Ag(1)#3	2.703(7)
O(7)-Ag(1)#3	3.044(4)

N(1)-Ag(1)-N(2)	169.8(2)	O(1)-C(6)-O(2)	124.7(4)
N(1)-Ag(1)-O(5)	98.02(18)	O(1)-C(6)-C(5)	124.1(4)
N(2)-Ag(1)-O(5)	91.59(17)	O(2)-C(6)-C(5)	111.1(3)
N(1)-Ag(1)-O(6)#1	89.6(2)	C(6)-O(2)-C(7)	116.9(3)
N(2)-Ag(1)-O(6)#1	92.1(2)	O(2)-C(7)-C(8)	103.4(3)
O(5)-Ag(1)-O(6)#1	99.91(17)	O(2)-C(7)-H(7A)	111.1
N(1)-Ag(1)-O(7)	90.63(15)	C(8)-C(7)-H(7A)	111.1
N(2)-Ag(1)-O(7)	94.21(15)	O(2)-C(7)-H(7B)	111.1
O(5)-Ag(1)-O(7)	42.67(19)	C(8)-C(7)-H(7B)	111.1
O(6)#1-Ag(1)-O(7)	142.13(17)	H(7A)-C(7)-H(7B)	109.0
N(1)-Ag(1)-Ag(1)#2	64.40(18)	O(3)-C(8)-C(7)	106.6(3)
N(2)-Ag(1)-Ag(1)#2	108.30(17)	O(3)-C(8)-H(8A)	110.4
O(5)-Ag(1)-Ag(1)#2	115.91(12)	C(7)-C(8)-H(8A)	110.4
O(6)#1-Ag(1)-Ag(1)#2	137.42(10)	O(3)-C(8)-H(8B)	110.4
O(7)-Ag(1)-Ag(1)#2	74.79(12)	C(7)-C(8)-H(8B)	110.4
N(1)-Ag(1)-Ag(1)#3	90.63(10)	H(8A)-C(8)-H(8B)	108.6
N(2)-Ag(1)-Ag(1)#3	94.62(9)	C(9)-O(3)-C(8)	115.0(3)
O(5)-Ag(1)-Ag(1)#3	40.04(13)	O(4)-C(9)-O(3)	123.5(5)
O(6)#1-Ag(1)-Ag(1)#3	139.45(12)	O(4)-C(9)-C(10)#5	123.1(4)
O(7)-Ag(1)-Ag(1)#3	2.68(14)	O(3)-C(9)-C(10)#5	113.4(3)
Ag(1)#2-Ag(1)-Ag(1)#3	77.19(2)	C(13)-C(10)-C(11)	117.3(4)
N(1)-Ag(1)-Ag(1)#4	164.53(11)	C(13)-C(10)-C(9)#4	118.8(3)
N(2)-Ag(1)-Ag(1)#4	8.19(9)	C(11)-C(10)-C(9)#4	123.9(4)
O(5)-Ag(1)-Ag(1)#4	97.24(12)	C(12)-C(11)-C(10)	119.3(4)
O(6)#1-Ag(1)-Ag(1)#4	85.29(14)	C(12)-C(11)-H(11)	120.3
O(7)-Ag(1)-Ag(1)#4	102.38(12)	C(10)-C(11)-H(11)	120.3
Ag(1)#2-Ag(1)-Ag(1)#4	110.67(3)	N(2)-C(12)-C(11)	123.7(3)
Ag(1)#3-Ag(1)-Ag(1)#4	102.755(17)	N(2)-C(12)-H(12)	118.1
C(1)-N(1)-C(3)	117.5(4)	C(11)-C(12)-H(12)	118.1
C(1)-N(1)-Ag(1)	119.1(3)	C(14)-C(13)-C(10)	119.8(3)
C(3)-N(1)-Ag(1)	123.1(3)	C(14)-C(13)-H(13)	120.1
N(1)-C(1)-C(2)	122.1(4)	C(10)-C(13)-H(13)	120.1
N(1)-C(1)-H(1)	118.9	N(2)-C(14)-C(13)	123.0(4)
C(2)-C(1)-H(1)	118.9	N(2)-C(14)-H(14)	118.5
C(5)-C(2)-C(1)	119.6(4)	C(13)-C(14)-H(14)	118.5
C(5)-C(2)-H(2)	120.2	C(14)-N(2)-C(12)	116.6(4)
C(1)-C(2)-H(2)	120.2	C(14)-N(2)-Ag(1)	119.9(3)
N(1)-C(3)-C(4)	124.1(3)	C(12)-N(2)-Ag(1)	123.3(3)
N(1)-C(3)-H(3)	117.9	O(7)-N(3)-O(6)	121.2(5)
C(4)-C(3)-H(3)	117.9	O(7)-N(3)-O(5)	120.4(5)
C(3)-C(4)-C(5)	117.7(4)	O(6)-N(3)-O(5)	118.4(7)
C(3)-C(4)-H(4)	121.2	N(3)-O(5)-Ag(1)	110.5(5)
C(5)-C(4)-H(4)	121.2	N(3)-O(6)-Ag(1)#3	105.3(5)
C(2)-C(5)-C(4)	118.8(4)	N(3)-O(7)-Ag(1)#3	89.3(3)
C(2)-C(5)-C(6)	119.0(3)	N(3)-O(7)-Ag(1)	85.3(3)
C(4)-C(5)-C(6)	122.2(4)	Ag(1)#3-O(7)-Ag(1)	174.6(3)

Symmetry transformations used to generate equivalent atoms: #1 x-1,y,z #2 -x+1,-y+2,-z+2
#3 x+1,y,z #4 x-1,y+1,z-1 #5 x+1,y-1,z+1

Anisotropic displacement parameters (Å^{2}x 10^3) for **7**. The anisotropic displacement factor exponent takes the form: $-2\pi^2[h^2a^{*2}U^{11} + ... + 2 h k a^* b^* U^{12}]$

	U^{11}	U^{22}	U^{33}	U^{23}	U^{13}	U^{12}
Ag(1)	52(1)	60(1)	37(1)	26(1)	6(1)	13(1)
N(1)	44(2)	56(7)	30(2)	20(2)	3(2)	11(2)
C(1)	42(2)	58(7)	35(3)	16(3)	6(2)	19(2)
C(2)	39(2)	59(7)	37(3)	15(3)	9(2)	17(2)
C(3)	41(2)	63(7)	42(3)	21(3)	15(2)	14(2)
C(4)	36(2)	43(7)	41(3)	17(3)	7(2)	9(2)
C(5)	32(2)	47(6)	27(2)	9(2)	3(2)	7(2)

C(6)	34(2)	37(6)	30(3)	12(2)	1(2)	5(2)
O(1)	51(2)	62(6)	36(2)	17(2)	15(2)	18(2)
O(2)	34(1)	53(5)	32(2)	21(2)	7(1)	11(2)
C(7)	38(2)	45(6)	29(3)	19(2)	2(2)	6(2)
C(8)	37(2)	54(7)	28(3)	20(2)	2(2)	7(2)
O(3)	40(2)	52(5)	29(2)	20(2)	6(1)	15(2)
C(9)	34(2)	39(6)	32(3)	12(2)	2(2)	7(2)
O(4)	53(2)	78(6)	44(2)	27(2)	23(2)	25(2)
C(10)	34(2)	32(6)	30(2)	9(2)	4(2)	4(2)
C(11)	32(2)	57(7)	36(3)	17(3)	8(2)	14(2)
C(12)	38(2)	51(6)	36(3)	16(3)	10(2)	12(2)
C(13)	34(2)	56(6)	36(3)	13(2)	10(2)	12(2)
C(14)	36(2)	41(7)	37(3)	15(2)	4(2)	12(2)
N(2)	39(2)	47(6)	32(2)	16(2)	4(2)	8(2)
N(3)	39(2)	44(6)	38(3)	12(3)	8(2)	5(2)
O(5)	41(2)	63(7)	82(3)	-4(3)	3(2)	4(2)
O(6)	47(2)	70(8)	112(4)	-11(4)	14(2)	21(3)
O(7)	59(2)	66(9)	67(3)	-6(3)	9(2)	1(3)

Hydrogen coordinates (x 10^4) and isotropic displacement parameters (Å^{2}x 10^3) for **7**.

	x	y	z	U(eq)
H(1)	1390	8207	10565	53
H(2)	1599	7038	11959	53
H(3)	7158	6755	10247	56
H(4)	7542	5560	11627	47
H(7A)	5849	3346	13993	44
H(7B)	7001	4832	14526	44
H(8A)	9164	2691	13500	47
H(8B)	10321	4206	13979	47
H(11)	-772	11756	6461	49
H(12)	142	10606	7830	49
H(13)	5054	10600	5799	49
H(14)	5793	9436	7181	45

Torsion angles [°] for **7**.

N(2)-Ag(1)-N(1)-C(1)	41.6(14)	C(11)-C(12)-N(2)-C(14)	1.8(11)
O(5)-Ag(1)-N(1)-C(1)	-157.7(6)	C(11)-C(12)-N(2)-Ag(1)	-174.0(6)
O(6)#1-Ag(1)-N(1)-C(1)	-57.8(6)	N(1)-Ag(1)-N(2)-C(14)	142.8(9)
O(7)-Ag(1)-N(1)-C(1)	160.1(6)	O(5)-Ag(1)-N(2)-C(14)	-18.0(6)
Ag(1)#2-Ag(1)-N(1)-C(1)	87.3(6)	O(6)#1-Ag(1)-N(2)-C(14)	-118.0(6)
Ag(1)#3-Ag(1)-N(1)-C(1)	162.8(6)	O(7)-Ag(1)-N(2)-C(14)	24.7(6)
Ag(1)#4-Ag(1)-N(1)-C(1)	12.6(11)	Ag(1)#2-Ag(1)-N(2)-C(14)	100.0(6)
N(2)-Ag(1)-N(1)-C(3)	-143.9(9)	Ag(1)#3-Ag(1)-N(2)-C(14)	22.0(6)
O(5)-Ag(1)-N(1)-C(3)	16.7(6)	Ag(1)#4-Ag(1)-N(2)-C(14)	-151.8(16)
O(6)#1-Ag(1)-N(1)-C(3)	116.6(6)	N(1)-Ag(1)-N(2)-C(12)	-41.5(13)
O(7)-Ag(1)-N(1)-C(3)	-25.5(6)	O(5)-Ag(1)-N(2)-C(12)	157.7(5)
Ag(1)#2-Ag(1)-N(1)-C(3)	-98.3(6)	O(6)#1-Ag(1)-N(2)-C(12)	57.7(5)
Ag(1)#3-Ag(1)-N(1)-C(3)	-22.8(6)	O(7)-Ag(1)-N(2)-C(12)	-159.7(5)
Ag(1)#4-Ag(1)-N(1)-C(3)	-173.0(5)	Ag(1)#2-Ag(1)-N(2)-C(12)	-84.3(5)
C(3)-N(1)-C(1)-C(2)	0.5(11)	Ag(1)#3-Ag(1)-N(2)-C(12)	-162.3(5)
Ag(1)-N(1)-C(1)-C(2)	175.3(6)	Ag(1)#4-Ag(1)-N(2)-C(12)	23.9(8)
N(1)-C(1)-C(2)-C(5)	2.1(12)	O(7)-N(3)-O(5)-Ag(1)	-12.4(8)
C(1)-N(1)-C(3)-C(4)	-0.7(11)	O(6)-N(3)-O(5)-Ag(1)	167.7(4)
Ag(1)-N(1)-C(3)-C(4)	-175.2(6)	N(1)-Ag(1)-O(5)-N(3)	-76.1(5)
N(1)-C(3)-C(4)-C(5)	-1.7(11)	N(2)-Ag(1)-O(5)-N(3)	100.6(4)
C(1)-C(2)-C(5)-C(4)	-4.4(11)	O(6)#1-Ag(1)-O(5)-N(3)	-167.0(4)
C(1)-C(2)-C(5)-C(6)	176.0(7)	O(7)-Ag(1)-O(5)-N(3)	6.1(4)
C(3)-C(4)-C(5)-C(2)	4.2(11)	Ag(1)#2-Ag(1)-O(5)-N(3)	-10.7(5)

C(3)-C(4)-C(5)-C(6)	-176.3(6)
C(2)-C(5)-C(6)-O(1)	-6.8(11)
C(4)-C(5)-C(6)-O(1)	173.6(7)
C(2)-C(5)-C(6)-O(2)	176.8(6)
C(4)-C(5)-C(6)-O(2)	-2.7(10)
O(1)-C(6)-O(2)-C(7)	6.5(10)
C(5)-C(6)-O(2)-C(7)	-177.1(6)
C(6)-O(2)-C(7)-C(8)	-178.6(5)
O(2)-C(7)-C(8)-O(3)	176.9(5)
C(7)-C(8)-O(3)-C(9)	175.9(5)
C(8)-O(3)-C(9)-O(4)	-1.8(9)
C(8)-O(3)-C(9)-C(10)#5	179.7(6)
C(13)-C(10)-C(11)-C(12)	-1.4(11)
C(9)#4-C(10)-C(11)-C(12)	178.6(7)
C(10)-C(11)-C(12)-N(2)	-0.5(11)
C(11)-C(10)-C(13)-C(14)	2.0(10)
C(9)#4-C(10)-C(13)-C(14)	-178.0(7)
C(10)-C(13)-C(14)-N(2)	-0.7(11)
C(13)-C(14)-N(2)-C(12)	-1.2(11)
C(13)-C(14)-N(2)-Ag(1)	174.8(5)
Ag(1)#3-Ag(1)-O(5)-N(3)	5.3(3)
Ag(1)#4-Ag(1)-O(5)-N(3)	106.5(4)
O(7)-N(3)-O(6)-Ag(1)#3	-10.6(7)
O(5)-N(3)-O(6)-Ag(1)#3	169.3(4)
O(6)-N(3)-O(7)-Ag(1)#3	9.0(6)
O(5)-N(3)-O(7)-Ag(1)#3	-170.8(5)
O(6)-N(3)-O(7)-Ag(1)	-170.5(5)
O(5)-N(3)-O(7)-Ag(1)	9.6(6)
N(1)-Ag(1)-O(7)-N(3)	95.3(4)
N(2)-Ag(1)-O(7)-N(3)	-93.7(5)
O(5)-Ag(1)-O(7)-N(3)	-5.9(4)
O(6)#1-Ag(1)-O(7)-N(3)	5.2(6)
Ag(1)#2-Ag(1)-O(7)-N(3)	158.5(4)
Ag(1)#3-Ag(1)-O(7)-N(3)	5(2)
Ag(1)#4-Ag(1)-O(7)-N(3)	-93.1(4)
N(1)-Ag(1)-O(7)-Ag(1)#3	90(2)
N(2)-Ag(1)-O(7)-Ag(1)#3	-99(2)
O(5)-Ag(1)-O(7)-Ag(1)#3	-11(2)
O(6)#1-Ag(1)-O(7)-Ag(1)#3	0(2)
Ag(1)#2-Ag(1)-O(7)-Ag(1)#3	153(2)
Ag(1)#4-Ag(1)-O(7)-Ag(1)#3	-98(2)

Symmetry transformations used to generate equivalent atoms: #1 x-1,y,z #2 -x+1,-y+2,-z+2
#3 x+1,y,z #4 x-1,y+1,z-1 #5 x+1,y-1,z+1

Hydrogen bonds for **7** [Å and °].

D-H...A	d(D-H)	d(H...A)	d(D...A)	<(DHA)
C(11)-H(11)...O(1)#6	0.93	2.79	3.648(7)	153.2
C(8)-H(8B)...O(1)#3	0.97	2.64	3.580(7)	163.4
C(13)-H(13)...O(4)#7	0.93	2.63	3.195(7)	119.3
C(14)-H(14)...O(4)#7	0.93	2.85	3.316(6)	112.3
C(7)-H(7A)...O(4)#1	0.97	2.50	3.436(7)	161.9
C(1)-H(1)...O(7)#1	0.93	2.65	3.403(7)	138.9
C(12)-H(12)...O(7)#1	0.93	2.58	3.309(8)	135.3
C(1)-H(1)...O(7)#2	0.93	2.80	3.377(11)	121.3
C(4)-H(4)...O(6)#7	0.93	2.53	3.390(8)	154.7
C(8)-H(8A)...O(6)#7	0.97	2.83	3.494(7)	126.5
C(14)-H(14)...O(5)	0.93	2.65	3.308(9)	128.3

Symmetry transformations used to generate equivalent atoms: #1 x-1,y,z #2 -x+1,-y+2,-z+2
#3 x+1,y,z #4 x-1,y+1,z-1 #5 x+1,y-1,z+1 #6 -x,-y+2,-z+2 #7 -x+2,-y+1,-z+2

I.2.i - Crystal data and structure refinement for 8.

Empirical formula	C15 H12 Ag1 F3 N2 O7 S	
Formula weight	529.20	
Temperature	293(2) K	
Wavelength	0.71073 Å	
Crystal system	monoclinic	
Space group	$P2_1/c$	
Unit cell dimensions	a = 8.9891(18) Å	α = 90°.
	b = 21.386(4) Å	β = 96.01(3)°.

	c = 9.4899(19) Å	γ = 90°.
Volume	1814.3(6) $Å^3$	
Z	4	
Density (calculated)	1.937 Mg/m^3	
Absorption coefficient	1.299 mm^{-1}	
F(000)	1048	
Crystal size	? x ? x ? mm^3	
Theta range for data collection	2.47 to 28.09°.	
Index ranges	-11<=h<=11, -28<=k<=28, -12<=l<=12	
Reflections collected	19223	
Independent reflections	4382 [R(int) = 0.0428]	
Completeness to theta = 28.09°	99.2 %	
Refinement method	Full-matrix least-squares on F^2	
Data / restraints / parameters	4382 / 0 / 262	
Goodness-of-fit on F^2	0.910	
Final R indices [I>2sigma(I)]	R1 = 0.0246, wR2 = 0.0591	
R indices (all data)	R1 = 0.0348, wR2 = 0.0611	
Largest diff. peak and hole	0.542 and -0.332 e.$Å^{-3}$	

Atomic coordinates (x 10^4) and equivalent isotropic displacement parameters ($Å^2$x 10^3) for **8**. U(eq) is defined as one third of the trace of the orthogonalized U^{ij} tensor.

	x	y	z	U(eq)
Ag(1)	4504(1)	2588(1)	4775(1)	34(1)
N(1)	2970(2)	2166(1)	6102(2)	26(1)
C(1)	2135(2)	2506(1)	6914(2)	26(1)
C(2)	1323(2)	2242(1)	7928(2)	25(1)
C(3)	3001(2)	1543(1)	6273(2)	28(1)
C(4)	2229(2)	1245(1)	7268(2)	27(1)
C(5)	1381(2)	1599(1)	8112(2)	24(1)
C(6)	521(2)	1302(1)	9211(2)	27(1)
O(1)	-165(2)	1587(1)	10021(2)	38(1)
O(2)	603(2)	681(1)	9132(2)	34(1)
C(7)	-138(3)	335(1)	10166(2)	37(1)
N(1A)	6067(2)	2970(1)	3425(2)	27(1)
C(1A)	6800(2)	2601(1)	2574(2)	28(1)
C(2A)	7660(2)	2838(1)	1573(2)	27(1)
C(3A)	6196(2)	3593(1)	3301(2)	28(1)
C(4A)	7040(2)	3868(1)	2324(2)	28(1)
C(5A)	7786(2)	3484(1)	1442(2)	24(1)
C(6A)	8747(2)	3745(1)	384(2)	26(1)
O(1A)	9260(2)	3446(1)	-520(2)	40(1)
O(2A)	8980(2)	4355(1)	616(2)	31(1)
C(7A)	9902(3)	4677(1)	-311(2)	30(1)
S(1)	5838(1)	-981(1)	7619(1)	34(1)
O(5)	5996(2)	-1225(1)	9047(2)	54(1)

O(6)	7041(2)	-600(1)	7256(3)	70(1)
O(7)	5284(3)	-1423(1)	6547(2)	61(1)
C(15)	4286(3)	-440(1)	7615(3)	48(1)
F(1)	4571(3)	16(1)	8539(2)	95(1)
F(2)	3960(3)	-174(1)	6364(2)	87(1)
F(3)	3073(2)	-726(1)	7953(3)	97(1)

Bond lengths [Å] and angles [°] for **8**.

Ag(1)-N(1A)	2.1590(17)	N(1A)-C(1A)	1.350(3)
Ag(1)-N(1)	2.1593(16)	C(1A)-C(2A)	1.382(3)
Ag(1)-O(7)#1	2.8041(17)	C(1A)-H(1A)	0.9300
Ag(1)-O(5)#2	2.8303(18)	C(2A)-C(5A)	1.394(3)
Ag(1)-Ag(1)#3	4.7598(10)	C(2A)-H(2A)	0.9300
N(1)-C(3)	1.343(3)	C(3A)-C(4A)	1.389(3)
N(1)-C(1)	1.344(3)	C(3A)-H(3A)	0.9300
C(1)-C(2)	1.387(3)	C(4A)-C(5A)	1.395(3)
C(1)-H(1)	0.9300	C(4A)-H(4A)	0.9300
C(2)-C(5)	1.388(3)	C(5A)-C(6A)	1.499(3)
C(2)-H(2)	0.9300	C(6A)-O(1A)	1.200(2)
C(3)-C(4)	1.384(3)	C(6A)-O(2A)	1.337(2)
C(3)-H(3)	0.9300	O(2A)-C(7A)	1.445(2)
C(4)-C(5)	1.387(3)	C(7A)-C(7A)#5	1.505(4)
C(4)-H(4)	0.9300	C(7A)-H(7C)	0.9700
C(5)-C(6)	1.502(3)	C(7A)-H(7D)	0.9700
C(6)-O(1)	1.200(3)	S(1)-O(6)	1.426(2)
C(6)-O(2)	1.334(2)	S(1)-O(7)	1.4387(19)
O(2)-C(7)	1.446(2)	S(1)-O(5)	1.4445(17)
C(7)-C(7)#4	1.492(4)	S(1)-C(15)	1.812(3)
C(7)-H(7A)	0.9700	C(15)-F(3)	1.318(4)
C(7)-H(7B)	0.9700	C(15)-F(1)	1.319(3)
N(1A)-C(3A)	1.343(2)	C(15)-F(2)	1.321(3)
N(1A)-Ag(1)-N(1)	177.61(6)	C(3A)-N(1A)-Ag(1)	119.69(14)
N(1A)-Ag(1)-O(7)#1	89.56(6)	C(1A)-N(1A)-Ag(1)	121.46(12)
N(1)-Ag(1)-O(7)#1	88.15(6)	N(1A)-C(1A)-C(2A)	122.73(17)
N(1A)-Ag(1)-O(5)#2	91.97(6)	N(1A)-C(1A)-H(1A)	118.6
N(1)-Ag(1)-O(5)#2	90.37(6)	C(2A)-C(1A)-H(1A)	118.6
O(7)#1-Ag(1)-O(5)#2	174.25(7)	C(1A)-C(2A)-C(5A)	118.72(18)
N(1A)-Ag(1)-Ag(1)#3	133.56(5)	C(1A)-C(2A)-H(2A)	120.6
N(1)-Ag(1)-Ag(1)#3	47.07(5)	C(5A)-C(2A)-H(2A)	120.6
O(7)#1-Ag(1)-Ag(1)#3	112.52(4)	N(1A)-C(3A)-C(4A)	122.49(18)
O(5)#2-Ag(1)-Ag(1)#3	70.14(4)	N(1A)-C(3A)-H(3A)	118.8
C(3)-N(1)-C(1)	118.23(16)	C(4A)-C(3A)-H(3A)	118.8
C(3)-N(1)-Ag(1)	118.58(14)	C(3A)-C(4A)-C(5A)	118.78(17)
C(1)-N(1)-Ag(1)	122.55(12)	C(3A)-C(4A)-H(4A)	120.6
N(1)-C(1)-C(2)	122.99(16)	C(5A)-C(4A)-H(4A)	120.6
N(1)-C(1)-H(1)	118.5	C(2A)-C(5A)-C(4A)	118.87(17)
C(2)-C(1)-H(1)	118.5	C(2A)-C(5A)-C(6A)	119.12(17)
C(1)-C(2)-C(5)	118.34(18)	C(4A)-C(5A)-C(6A)	122.00(16)
C(1)-C(2)-H(2)	120.8	O(1A)-C(6A)-O(2A)	124.91(18)
C(5)-C(2)-H(2)	120.8	O(1A)-C(6A)-C(5A)	124.91(17)
N(1)-C(3)-C(4)	122.26(18)	O(2A)-C(6A)-C(5A)	110.16(16)
N(1)-C(3)-H(3)	118.9	C(6A)-O(2A)-C(7A)	117.07(15)
C(4)-C(3)-H(3)	118.9	O(2A)-C(7A)-C(7A)#5	104.42(19)
C(3)-C(4)-C(5)	119.19(17)	O(2A)-C(7A)-H(7C)	110.9
C(3)-C(4)-H(4)	120.4	C(7A)#5-C(7A)-H(7C)	110.9
C(5)-C(4)-H(4)	120.4	O(2A)-C(7A)-H(7D)	110.9
C(4)-C(5)-C(2)	118.98(17)	C(7A)#5-C(7A)-H(7D)	110.9
C(4)-C(5)-C(6)	121.64(16)	H(7C)-C(7A)-H(7D)	108.9
C(2)-C(5)-C(6)	119.39(17)	O(6)-S(1)-O(7)	114.86(13)
O(1)-C(6)-O(2)	125.16(18)	O(6)-S(1)-O(5)	115.47(14)
O(1)-C(6)-C(5)	124.56(17)	O(7)-S(1)-O(5)	114.81(11)

O(2)-C(6)-C(5)	110.26(16)	O(6)-S(1)-C(15)	103.74(14)
C(6)-O(2)-C(7)	116.10(16)	O(7)-S(1)-C(15)	102.03(13)
O(2)-C(7)-C(7)#4	104.4(2)	O(5)-S(1)-C(15)	103.41(12)
O(2)-C(7)-H(7A)	110.9	F(3)-C(15)-F(1)	106.8(3)
C(7)#4-C(7)-H(7A)	110.9	F(3)-C(15)-F(2)	107.9(2)
O(2)-C(7)-H(7B)	110.9	F(1)-C(15)-F(2)	106.8(2)
C(7)#4-C(7)-H(7B)	110.9	F(3)-C(15)-S(1)	111.1(2)
H(7A)-C(7)-H(7B)	108.9	F(1)-C(15)-S(1)	112.0(2)
C(3A)-N(1A)-C(1A)	118.41(17)	F(2)-C(15)-S(1)	111.99(19)

Symmetry transformations used to generate equivalent atoms: #1 -x+1,-y,-z+1 #2 -x+1,y+1/2,-z+3/2
#3 x,-y+1/2,z+1/2 #4 -x,-y,-z+2 #5 -x+2,-y+1,-z

Anisotropic displacement parameters (Å^{2}x 10^3) for **8**. The anisotropic displacement factor exponent takes the form: $-2\pi^2[h^2a^{*2}U^{11} + ... + 2 h k a^* b^* U^{12}]$

	U^{11}	U^{22}	U^{33}	U^{23}	U^{13}	U^{12}
Ag(1)	33(1)	39(1)	31(1)	12(1)	11(1)	-11(1)
N(1)	27(1)	27(1)	25(1)	6(1)	5(1)	-8(1)
C(1)	29(1)	21(1)	29(1)	6(1)	2(1)	-5(1)
C(2)	26(1)	23(1)	26(1)	0(1)	5(1)	-3(1)
C(3)	30(1)	28(1)	27(1)	2(1)	10(1)	-2(1)
C(4)	30(1)	21(1)	32(1)	5(1)	9(1)	-3(1)
C(5)	23(1)	25(1)	23(1)	4(1)	5(1)	-6(1)
C(6)	30(1)	27(1)	25(1)	4(1)	7(1)	-7(1)
O(1)	45(1)	36(1)	36(1)	-1(1)	22(1)	-5(1)
O(2)	45(1)	26(1)	34(1)	8(1)	21(1)	-7(1)
C(7)	47(1)	33(1)	35(1)	11(1)	23(1)	-8(1)
N(1A)	27(1)	28(1)	26(1)	7(1)	6(1)	-7(1)
C(1A)	29(1)	23(1)	33(1)	5(1)	6(1)	-4(1)
C(2A)	26(1)	25(1)	31(1)	1(1)	6(1)	-3(1)
C(3A)	28(1)	29(1)	29(1)	2(1)	11(1)	-4(1)
C(4A)	28(1)	22(1)	34(1)	3(1)	10(1)	-4(1)
C(5A)	22(1)	26(1)	23(1)	4(1)	5(1)	-5(1)
C(6A)	26(1)	27(1)	27(1)	3(1)	8(1)	-4(1)
O(1A)	51(1)	34(1)	38(1)	-4(1)	24(1)	-8(1)
O(2A)	36(1)	26(1)	33(1)	4(1)	19(1)	-7(1)
C(7A)	33(1)	30(1)	31(1)	7(1)	16(1)	-7(1)
S(1)	39(1)	24(1)	41(1)	5(1)	20(1)	5(1)
O(5)	77(1)	44(1)	44(1)	13(1)	21(1)	24(1)
O(6)	43(1)	80(1)	88(2)	23(1)	19(1)	-14(1)
O(7)	102(2)	32(1)	56(1)	-14(1)	38(1)	-7(1)
C(15)	53(2)	48(1)	44(1)	-6(1)	3(1)	18(1)
F(1)	151(2)	51(1)	76(1)	-29(1)	-13(1)	49(1)
F(2)	107(2)	92(1)	59(1)	14(1)	-7(1)	51(1)
F(3)	41(1)	147(2)	107(2)	0(2)	31(1)	15(1)

Hydrogen coordinates (x 10^4) and isotropic displacement parameters (Å^{2}x 10^3) for **8**.

	x	y	z	U(eq)
H(1)	2100	2937	6790	32
H(2)	754	2491	8471	30
H(3)	3561	1303	5703	34
H(4)	2278	812	7369	33
H(7A)	-1201	425	10073	45
H(7B)	283	437	11121	45
H(1A)	6722	2170	2664	34
H(2A)	8146	2570	997	32
H(3A)	5701	3850	3891	34
H(4A)	7106	4301	2259	33

H(7C)	9411	4694	-1271	36
H(7D)	10861	4470	-323	36

Torsion angles [°] for **8**.

N(1A)-Ag(1)-N(1)-C(3)	4.8(15)	O(7)#1-Ag(1)-N(1A)-C(1A)	-8.36(15)
O(7)#1-Ag(1)-N(1)-C(3)	21.99(15)	O(5)#2-Ag(1)-N(1A)-C(1A)	177.18(15)
O(5)#2-Ag(1)-N(1)-C(3)	-163.57(15)	Ag(1)#3-Ag(1)-N(1A)-C(1A)	113.06(14)
Ag(1)#3-Ag(1)-N(1)-C(3)	-101.61(15)	C(3A)-N(1A)-C(1A)-C(2A)	-0.7(3)
N(1A)-Ag(1)-N(1)-C(1)	175.4(14)	Ag(1)-N(1A)-C(1A)-C(2A)	171.68(15)
O(7)#1-Ag(1)-N(1)-C(1)	-167.36(15)	N(1A)-C(1A)-C(2A)-C(5A)	0.4(3)
O(5)#2-Ag(1)-N(1)-C(1)	7.08(15)	C(1A)-N(1A)-C(3A)-C(4A)	0.6(3)
Ag(1)#3-Ag(1)-N(1)-C(1)	69.04(14)	Ag(1)-N(1A)-C(3A)-C(4A)	-171.93(16)
C(3)-N(1)-C(1)-C(2)	0.9(3)	N(1A)-C(3A)-C(4A)-C(5A)	-0.2(3)
Ag(1)-N(1)-C(1)-C(2)	-169.83(15)	C(1A)-C(2A)-C(5A)-C(4A)	0.0(3)
N(1)-C(1)-C(2)-C(5)	0.2(3)	C(1A)-C(2A)-C(5A)-C(6A)	178.50(18)
C(1)-N(1)-C(3)-C(4)	-1.2(3)	C(3A)-C(4A)-C(5A)-C(2A)	-0.1(3)
Ag(1)-N(1)-C(3)-C(4)	169.82(15)	C(3A)-C(4A)-C(5A)-C(6A)	-178.56(18)
N(1)-C(3)-C(4)-C(5)	0.6(3)	C(2A)-C(5A)-C(6A)-O(1A)	11.5(3)
C(3)-C(4)-C(5)-C(2)	0.4(3)	C(4A)-C(5A)-C(6A)-O(1A)	-170.1(2)
C(3)-C(4)-C(5)-C(6)	-179.91(18)	C(2A)-C(5A)-C(6A)-O(2A)	-167.04(17)
C(1)-C(2)-C(5)-C(4)	-0.8(3)	C(4A)-C(5A)-C(6A)-O(2A)	11.4(3)
C(1)-C(2)-C(5)-C(6)	179.55(17)	O(1A)-C(6A)-O(2A)-C(7A)	1.0(3)
C(4)-C(5)-C(6)-O(1)	175.8(2)	C(5A)-C(6A)-O(2A)-C(7A)	179.46(16)
C(2)-C(5)-C(6)-O(1)	-4.5(3)	C(6A)-O(2A)-C(7A)-C(7A)#5	-173.7(2)
C(4)-C(5)-C(6)-O(2)	-5.6(3)	O(6)-S(1)-C(15)-F(3)	-179.3(2)
C(2)-C(5)-C(6)-O(2)	174.06(17)	O(7)-S(1)-C(15)-F(3)	61.1(2)
O(1)-C(6)-O(2)-C(7)	-3.4(3)	O(5)-S(1)-C(15)-F(3)	-58.4(2)
C(5)-C(6)-O(2)-C(7)	177.99(18)	O(6)-S(1)-C(15)-F(1)	-59.9(2)
C(6)-O(2)-C(7)-C(7)#4	-179.8(2)	O(7)-S(1)-C(15)-F(1)	-179.5(2)
N(1)-Ag(1)-N(1A)-C(3A)	-179(39)	O(5)-S(1)-C(15)-F(1)	61.0(2)
O(7)#1-Ag(1)-N(1A)-C(3A)	163.92(15)	O(6)-S(1)-C(15)-F(2)	60.0(2)
O(5)#2-Ag(1)-N(1A)-C(3A)	-10.54(15)	O(7)-S(1)-C(15)-F(2)	-59.6(2)
Ag(1)#3-Ag(1)-N(1A)-C(3A)	-74.66(16)	O(5)-S(1)-C(15)-F(2)	-179.1(2)
N(1)-Ag(1)-N(1A)-C(1A)	8.8(15)		

Symmetry transformations used to generate equivalent atoms: #1 -x+1,-y,-z+1 #2 -x+1,y+1/2,-z+3/2
#3 x,-y+1/2,z+1/2 #4 -x,-y,-z+2 #5 -x+2,-y+1,-z

Hydrogen bonds for **8** [Å and °].

D-H...A	d(D-H)	d(H...A)	d(D...A)	<(DHA)
C(3)-H(3)...O(7)#1	0.93	2.48	3.235(3)	138.0
C(1A)-H(1A)...O(7)#1	0.93	2.58	3.298(3)	134.7
C(4)-H(4)...F(1)	0.93	2.81	3.501(3)	131.9
C(4)-H(4)...F(2)	0.93	2.82	3.556(3)	136.9
C(7)-H(7A)...F(3)#4	0.97	2.72	3.440(3)	131.2
C(2)-H(2)...O(1A)#6	0.93	2.68	3.579(3)	163.8
C(2A)-H(2A)...O(1)#7	0.93	2.81	3.708(3)	163.2
C(1)-H(1)...O(1)#8	0.93	2.70	3.239(3)	117.8
C(1)-H(1)...O(5)#2	0.93	2.66	3.368(3)	133.8
C(3A)-H(3A)...O(5)#2	0.93	2.61	3.378(3)	140.4
C(7A)-H(7D)...O(6)#9	0.97	2.77	3.517(3)	134.4
C(4A)-H(4A)...O(6)#8	0.93	2.78	3.703(3)	173.6
C(7)-H(7B)...O(6)#10	0.97	2.74	3.554(4)	142.0

Symmetry transformations used to generate equivalent atoms: #1 -x+1,-y,-z+1 #2 -x+1,y+1/2,-z+3/2
#3 x,-y+1/2,z+1/2 #4 -x,-y,-z+2 #5 -x+2,-y+1,-z #6 x-1,y,z+1 #7 x+1,y,z-1 #8 x,-y+1/2,z-1/2
#9 -x+2,y+1/2,-z+1/2 #10 -x+1,-y,-z+2

I.2.j - Crystal data and structure refinement for 9.

Empirical formula	C14 H12 Ag1 Cl1 N2 O8	
Formula weight	479.58	
Temperature	293(2) K	
Wavelength	0.71073 Å	
Crystal system	monoclinic	
Space group	I2/a	
Unit cell dimensions	a = 9.0820(12) Å	α = 90°.
	b = 10.1788(11) Å	β = 94.543(17)°.
	c = 17.343(3) Å	γ = 90°.
Volume	1598.2(4) Å^3	
Z	4	
Density (calculated)	1.993 Mg/m^3	
Absorption coefficient	1.478 mm^{-1}	
F(000)	952	
Crystal size	? x ? x ? mm^3	
Theta range for data collection	3.01 to 28.13°.	
Index ranges	-11<=h<=11, -13<=k<=13, -22<=l<=22	
Reflections collected	6160	
Independent reflections	1391 [R(int) = 0.0471]	
Completeness to theta = 28.13°	71.2 %	
Refinement method	Full-matrix least-squares on F^2	
Data / restraints / parameters	1391 / 0 / 120	
Goodness-of-fit on F^2	1.143	
Final R indices [I>2sigma(I)]	R1 = 0.0481, wR2 = 0.1395	
R indices (all data)	R1 = 0.0650, wR2 = 0.1497	
Largest diff. peak and hole	1.001 and -0.717 e.Å^{-3}	

Atomic coordinates (x 10^4) and equivalent isotropic displacement parameters (Å^{2}x 10^3) for **9**. U(eq) is defined as one third of the trace of the orthogonalized U^{ij} tensor.

	x	y	z	U(eq)
Ag(1)	0	10000	5000	34(1)
N(1)	1326(5)	8867(5)	4228(3)	25(1)
C(1)	2326(7)	9524(6)	3844(4)	27(1)
C(2)	3402(6)	8913(5)	3452(3)	24(1)
C(3)	1366(7)	7543(6)	4206(4)	29(1)

C(4)	2405(6)	6853(5)	3814(4)	27(1)
C(5)	3455(6)	7547(5)	3449(3)	20(1)
C(6)	4608(6)	6821(5)	3043(3)	22(1)
O(1)	4525(5)	5670(4)	2873(3)	37(1)
O(2)	5714(4)	7610(4)	2887(2)	25(1)
C(7)	6887(6)	6998(5)	2484(4)	28(1)
Cl(1)	-2500	6856(2)	5000	35(1)
O(5)	-1371(10)	7730(9)	5308(6)	107(3)
O(6)	-1935(10)	6210(12)	4382(9)	177(7)

Bond lengths [Å] and angles [°] for **9**.

Ag(1)-N(1)	2.197(4)	C(4)-H(4)	0.9300
Ag(1)-N(1)#1	2.197(4)	C(5)-C(6)	1.501(7)
Ag(1)-O(5)	2.698(8)	C(6)-O(1)	1.210(7)
Ag(1)-Ag(1)#2	4.5410(6)	C(6)-O(2)	1.331(6)
N(1)-C(1)	1.346(7)	O(2)-C(7)	1.459(6)
N(1)-C(3)	1.350(7)	C(7)-C(7)#3	1.510(11)
C(1)-C(2)	1.381(8)	C(7)-H(7A)	0.9700
C(1)-H(1)	0.9300	C(7)-H(7B)	0.9700
C(2)-C(5)	1.392(7)	Cl(1)-O(6)	1.390(9)
C(2)-H(2)	0.9300	Cl(1)-O(6)#4	1.390(9)
C(3)-C(4)	1.394(8)	Cl(1)-O(5)	1.429(8)
C(3)-H(3)	0.9300	Cl(1)-O(5)#4	1.429(8)
C(4)-C(5)	1.380(7)		
N(1)-Ag(1)-N(1)#1	180.000(1)	C(4)-C(5)-C(2)	118.9(5)
N(1)-Ag(1)-O(5)	87.4(2)	C(4)-C(5)-C(6)	119.8(5)
N(1)#1-Ag(1)-O(5)	92.6(2)	C(2)-C(5)-C(6)	121.3(5)
N(1)-Ag(1)-Ag(1)#2	53.40(13)	O(1)-C(6)-O(2)	124.6(5)
N(1)#1-Ag(1)-Ag(1)#2	126.60(13)	O(1)-C(6)-C(5)	124.0(5)
O(5)-Ag(1)-Ag(1)#2	118.5(2)	O(2)-C(6)-C(5)	111.4(4)
C(1)-N(1)-C(3)	117.5(5)	C(6)-O(2)-C(7)	115.6(4)
C(1)-N(1)-Ag(1)	117.7(4)	O(2)-C(7)-C(7)#3	104.9(5)
C(3)-N(1)-Ag(1)	124.0(4)	O(2)-C(7)-H(7A)	110.8
N(1)-C(1)-C(2)	123.4(5)	C(7)#3-C(7)-H(7A)	110.8
N(1)-C(1)-H(1)	118.3	O(2)-C(7)-H(7B)	110.8
C(2)-C(1)-H(1)	118.3	C(7)#3-C(7)-H(7B)	110.8
C(1)-C(2)-C(5)	118.6(5)	H(7A)-C(7)-H(7B)	108.8
C(1)-C(2)-H(2)	120.7	O(6)-Cl(1)-O(6)#4	123.5(13)
C(5)-C(2)-H(2)	120.7	O(6)-Cl(1)-O(5)	106.6(5)
N(1)-C(3)-C(4)	122.5(5)	O(6)#4-Cl(1)-O(5)	107.7(8)
N(1)-C(3)-H(3)	118.7	O(6)-Cl(1)-O(5)#4	107.7(8)
C(4)-C(3)-H(3)	118.7	O(6)#4-Cl(1)-O(5)#4	106.6(5)
C(5)-C(4)-C(3)	119.0(5)	O(5)-Cl(1)-O(5)#4	102.9(9)
C(5)-C(4)-H(4)	120.5	Cl(1)-O(5)-Ag(1)	142.0(7)
C(3)-C(4)-H(4)	120.5		

Symmetry transformations used to generate equivalent atoms: #1 -x,-y+2,-z+1 #2 -x+1/2,y,-z+1
#3 -x+3/2,-y+3/2,-z+1/2 #4 -x-1/2,y,-z+1

Anisotropic displacement parameters (Å^{2}x 10^3) for **9**. The anisotropic displacement factor exponent takes the form: $-2\pi^2[h^2a^{*2}U^{11} + ... + 2 h k a^* b^* U^{12}]$

	U^{11}	U^{22}	U^{33}	U^{23}	U^{13}	U^{12}
Ag(1)	29(1)	42(1)	32(1)	-2(1)	17(1)	11(1)
N(1)	18(2)	31(2)	27(2)	-4(2)	8(2)	7(2)
C(1)	24(3)	23(2)	35(3)	3(2)	13(3)	6(2)
C(2)	22(3)	24(3)	27(3)	1(2)	10(2)	0(2)
C(3)	20(3)	30(3)	38(3)	2(2)	13(3)	-2(2)
C(4)	24(3)	21(3)	37(3)	-2(2)	14(3)	0(2)

C(5)	16(3)	23(3)	22(3)	0(2)	7(2)	2(2)
C(6)	20(3)	20(2)	27(3)	0(2)	7(2)	2(2)
O(1)	32(3)	26(2)	56(3)	-14(2)	21(2)	-4(2)
O(2)	17(2)	22(2)	36(2)	-7(2)	16(2)	2(1)
C(7)	22(3)	26(3)	37(3)	-8(2)	18(3)	1(2)
Cl(1)	27(1)	32(1)	47(1)	0	15(1)	0
O(5)	117(7)	99(6)	112(7)	-43(5)	49(6)	-45(5)
O(6)	80(6)	186(11)	278(16)	-181(12)	91(8)	-46(6)

Hydrogen coordinates (x 10^4) and isotropic displacement parameters (Å^{2}x 10^3) for **9**.

	x	y	z	U(eq)
H(1)	2291	10437	3842	32
H(2)	4076	9405	3196	29
H(3)	675	7071	4462	34
H(4)	2390	5940	3799	33
H(7A)	6547	6800	1952	33
H(7B)	7219	6191	2739	33

Torsion angles [°] for **9**.

N(1)#1-Ag(1)-N(1)-C(1)	0(100)		
O(5)-Ag(1)-N(1)-C(1)	179.0(5)	C(1)-C(2)-C(5)-C(6)	-179.2(5)
Ag(1)#2-Ag(1)-N(1)-C(1)	-52.1(4)	C(4)-C(5)-C(6)-O(1)	15.6(9)
N(1)#1-Ag(1)-N(1)-C(3)	0(100)	C(2)-C(5)-C(6)-O(1)	-163.1(6)
O(5)-Ag(1)-N(1)-C(3)	-11.8(5)	C(4)-C(5)-C(6)-O(2)	-165.2(5)
Ag(1)#2-Ag(1)-N(1)-C(3)	117.1(5)	C(2)-C(5)-C(6)-O(2)	16.1(7)
C(3)-N(1)-C(1)-C(2)	-1.8(9)	O(1)-C(6)-O(2)-C(7)	-0.2(9)
Ag(1)-N(1)-C(1)-C(2)	168.1(5)	C(5)-C(6)-O(2)-C(7)	-179.3(5)
N(1)-C(1)-C(2)-C(5)	0.4(9)	C(6)-O(2)-C(7)-C(7)#3	-169.4(6)
C(1)-N(1)-C(3)-C(4)	0.9(9)	O(6)-Cl(1)-O(5)-Ag(1)	72.6(12)
Ag(1)-N(1)-C(3)-C(4)	-168.4(5)	O(6)#4-Cl(1)-O(5)-Ag(1)	-153.0(8)
N(1)-C(3)-C(4)-C(5)	1.5(10)	O(5)#4-Cl(1)-O(5)-Ag(1)	-40.6(6)
C(3)-C(4)-C(5)-C(2)	-3.0(9)	N(1)-Ag(1)-O(5)-Cl(1)	-79.9(8)
C(3)-C(4)-C(5)-C(6)	178.3(6)	N(1)#1-Ag(1)-O(5)-Cl(1)	100.1(8)
C(1)-C(2)-C(5)-C(4)	2.1(9)	Ag(1)#2-Ag(1)-O(5)-Cl(1)	-125.2(8)

Symmetry transformations used to generate equivalent atoms: #1 -x,-y+2,-z+1 #2 -x+1/2,y,-z+1
#3 -x+3/2,-y+3/2,-z+1/2 #4 -x-1/2,y,-z+1

Hydrogen bonds for **9** [Å and °].

D-H...A	d(D-H)	d(H...A)	d(D...A)	<(DHA)
C(3)-H(3)...O(5)	0.93	2.55	3.259(10)	133.6
C(3)-H(3)...O(6)	0.93	2.52	3.327(11)	145.1
C(1)-H(1)...O(5)#1	0.93	2.56	3.305(10)	137.7
C(7)-H(7B)...O(6)#5	0.97	2.89	3.474(18)	119.6
C(4)-H(4)...O(6)#6	0.93	2.47	3.310(11)	150.7
C(7)-H(7B)...O(1)#6	0.97	2.82	3.649(7)	143.9
C(1)-H(1)...O(2)#7	0.93	2.89	3.609(7)	134.7
C(2)-H(2)...O(1)#8	0.93	2.66	3.565(7)	164.0

Symmetry transformations used to generate equivalent atoms: #1 -x,-y+2,-z+1 #2 -x+1/2,y,-z+1
#3 -x+3/2,-y+3/2,-z+1/2 #4 -x-1/2,y,-z+1 #5 x+1,y,z #6 x+1/2,-y+1,z #7 x-1/2,-y+2,z
#8 -x+1,y+1/2,-z+1/2

I.2.k - Crystal data and structure refinement for 10.

Empirical formula	C14 H12 Ag1 F6 N2 O4 P1	
Formula weight	525.10	
Temperature	293(2) K	
Wavelength	0.71073 Å	
Crystal system	Monoclinic	
Space group	I2/a	
Unit cell dimensions	a = 9.3818(19) Å	α = 90°.
	b = 10.453(2) Å	β = 93.95(3)°.
	c = 34.673(7) Å	γ = 90°.
Volume	3392.4(12) $Å^3$	
Z	8	
Density (calculated)	2.056 Mg/m^3	
Absorption coefficient	1.372 mm^{-1}	
F(000)	2064	
Crystal size	? x ? x ? mm^3	
Theta range for data collection	2.92 to 24.96°.	
Index ranges	-10<=h<=10, -12<=k<=12, -40<=l<=39	
Reflections collected	3443	
Independent reflections	1214 [R(int) = 0.0949]	
Completeness to theta = 24.96°	40.8 %	
Refinement method	Full-matrix least-squares on F^2	
Data / restraints / parameters	1214 / 0 / 229	
Goodness-of-fit on F^2	1.043	
Final R indices [I>2sigma(I)]	R1 = 0.0476, wR2 = 0.0843	
R indices (all data)	R1 = 0.0908, wR2 = 0.0970	
Largest diff. peak and hole	0.301 and -0.290 e.$Å^{-3}$	

Atomic coordinates (x 10^4) and equivalent isotropic displacement parameters ($Å^2$x 10^3) for**10**. U(eq) is defined as one third of the trace of the orthogonalized U^{ij} tensor.

	x	y	z	U(eq)
Ag(1)	-34(1)	9619(1)	1287(1)	39(1)
P	-2443(4)	3428(3)	1236(1)	36(1)
F(1)	-1784(11)	3228(11)	832(3)	86(3)
F(2)	-3906(9)	2814(8)	1050(3)	55(2)
F(3)	-1911(10)	2034(8)	1354(3)	75(3)

F(4)	-3141(11)	3559(8)	1644(3)	67(3)
F(5)	-1022(10)	3981(9)	1429(3)	88(4)
F(6)	-2979(11)	4788(6)	1121(3)	79(3)
C(1)	-1447(7)	7328(6)	1687(2)	40(3)
N(1)	-1381(7)	8656(6)	1671(2)	32(2)
C(2)	-2382(8)	9390(5)	1849(2)	33(3)
C(3)	-3450(7)	8797(6)	2043(2)	21(2)
C(4)	-3516(7)	7469(6)	2058(2)	23(3)
C(5)	-2515(8)	6735(5)	1881(2)	30(3)
C(6)	1413(7)	11932(6)	911(2)	32(3)
N(2)	1278(7)	10608(6)	904(2)	29(2)
C(7)	2142(8)	9878(5)	680(2)	33(3)
C(8)	3142(7)	10472(6)	463(2)	29(3)
C(9)	3278(7)	11796(7)	470(2)	28(3)
C(10)	2414(8)	12526(5)	694(2)	35(3)
C(11)	4371(14)	12404(10)	233(4)	29(3)
O(1)	5265(11)	11806(7)	73(3)	40(3)
O(2)	4223(9)	13651(7)	226(3)	40(2)
C(12)	5255(16)	14334(12)	11(5)	58(5)
C(13)	-4671(13)	6787(12)	2243(4)	30(3)
O(3)	-4593(9)	5695(8)	2358(3)	44(2)
O(4)	-5762(10)	7575(7)	2311(3)	34(3)
C(14)	-6896(16)	7010(12)	2508(4)	31(3)

Bond lengths [Å] and angles [°] for **10**.

Ag(1)-N(2)	2.138(5)	C(6)-N(2)	1.3900
Ag(1)-N(1)	2.148(5)	C(6)-C(10)	1.3900
Ag(1)-F(2)#1	2.896(8)	C(6)-H(6)	0.9300
Ag(1)-F(3)#2	3.096(8)	N(2)-C(7)	1.3900
P-F(6)	1.552(8)	C(7)-C(8)	1.3900
P-F(5)	1.561(9)	C(7)-H(7)	0.9300
P-F(3)	1.585(8)	C(8)-C(9)	1.3900
P-F(1)	1.585(10)	C(8)-H(8)	0.9300
P-F(4)#3	1.604(9)	C(9)-C(10)	1.3900
P-F(4)	1.604(9)	C(9)-C(11)	1.498(12)
P-F(2)	1.610(9)	C(10)-H(10)	0.9300
F(4)-F(4)#3	0.00(3)	C(11)-O(1)	1.212(15)
C(1)-N(1)	1.3900	C(11)-O(2)	1.311(12)
C(1)-C(5)	1.3900	O(2)-C(12)	1.450(15)
C(1)-H(1)	0.9300	C(12)-C(12)#4	1.47(3)
N(1)-C(2)	1.3900	C(12)-H(12A)	0.9700
C(2)-C(3)	1.3900	C(12)-H(12B)	0.9700
C(2)-H(2)	0.9300	C(13)-O(3)	1.210(13)
C(3)-C(4)	1.3900	C(13)-O(4)	1.347(15)
C(3)-H(3)	0.9300	O(4)-C(14)	1.431(17)
C(4)-C(5)	1.3900	C(14)-C(14)#5	1.53(3)
C(4)-C(13)	1.478(13)	C(14)-H(14A)	0.9700
C(5)-H(5)	0.9300	C(14)-H(14B)	0.9700

N(2)-Ag(1)-N(1)	178.9(3)	N(1)-C(2)-C(3)	120.0
N(2)-Ag(1)-F(2)#1	90.6(3)	N(1)-C(2)-H(2)	120.0
N(1)-Ag(1)-F(2)#1	90.4(3)	C(3)-C(2)-H(2)	120.0
N(2)-Ag(1)-F(3)#2	90.4(3)	C(2)-C(3)-C(4)	120.0
N(1)-Ag(1)-F(3)#2	88.5(3)	C(2)-C(3)-H(3)	120.0
F(2)#1-Ag(1)-F(3)#2	163.4(2)	C(4)-C(3)-H(3)	120.0
F(6)-P-F(5)	91.3(6)	C(5)-C(4)-C(3)	120.0
F(6)-P-F(3)	179.5(6)	C(5)-C(4)-C(13)	117.6(7)
F(5)-P-F(3)	89.2(6)	C(3)-C(4)-C(13)	122.3(7)
F(6)-P-F(1)	91.8(6)	C(4)-C(5)-C(1)	120.0
F(5)-P-F(1)	93.0(6)	C(4)-C(5)-H(5)	120.0
F(3)-P-F(1)	88.4(6)	C(1)-C(5)-H(5)	120.0
F(6)-P-F(4)#3	90.3(5)	N(2)-C(6)-C(10)	120.0

F(5)-P-F(4)#3	88.9(6)
F(3)-P-F(4)#3	89.5(5)
F(1)-P-F(4)#3	177.2(6)
F(6)-P-F(4)	90.3(5)
F(5)-P-F(4)	88.9(6)
F(3)-P-F(4)	89.5(5)
F(1)-P-F(4)	177.2(6)
F(4)#3-P-F(4)	0.0(7)
F(6)-P-F(2)	90.5(5)
F(5)-P-F(2)	177.8(6)
F(3)-P-F(2)	89.0(5)
F(1)-P-F(2)	88.0(5)
F(4)#3-P-F(2)	90.0(5)
F(4)-P-F(2)	90.0(5)
F(4)#3-F(4)-P	0(10)
N(1)-C(1)-C(5)	120.0
N(1)-C(1)-H(1)	120.0
C(5)-C(1)-H(1)	120.0
C(2)-N(1)-C(1)	120.0
C(2)-N(1)-Ag(1)	117.4(4)
C(1)-N(1)-Ag(1)	121.5(3)
N(2)-C(6)-H(6)	120.0
C(10)-C(6)-H(6)	120.0
C(6)-N(2)-C(7)	120.0
C(6)-N(2)-Ag(1)	121.8(4)
C(7)-N(2)-Ag(1)	117.7(4)
C(8)-C(7)-N(2)	120.0
C(8)-C(7)-H(7)	120.0
N(2)-C(7)-H(7)	120.0
C(7)-C(8)-C(9)	120.0
C(7)-C(8)-H(8)	120.0
C(9)-C(8)-H(8)	120.0
C(10)-C(9)-C(8)	120.0
C(10)-C(9)-C(11)	121.4(6)
C(8)-C(9)-C(11)	118.6(6)
C(9)-C(10)-C(6)	120.0
C(9)-C(10)-H(10)	120.0
C(6)-C(10)-H(10)	120.0
O(1)-C(11)-O(2)	125.4(11)
O(1)-C(11)-C(9)	123.7(10)
O(2)-C(11)-C(9)	110.9(9)
C(11)-O(2)-C(12)	115.2(10)
O(2)-C(12)-C(12)#4	105.4(17)
O(2)-C(12)-H(12A)	110.7
C(12)#4-C(12)-H(12A)	110.7
O(2)-C(12)-H(12B)	110.7
C(12)#4-C(12)-H(12B)	110.7
H(12A)-C(12)-H(12B)	108.8
O(3)-C(13)-O(4)	123.3(12)
O(3)-C(13)-C(4)	124.6(11)
O(4)-C(13)-C(4)	111.7(10)
C(13)-O(4)-C(14)	115.5(9)
O(4)-C(14)-C(14)#5	106.3(12)
O(4)-C(14)-H(14A)	110.5
C(14)#5-C(14)-H(14A)	110.5
O(4)-C(14)-H(14B)	110.5
C(14)#5-C(14)-H(14B)	110.5
H(14A)-C(14)-H(14B)	108.7

Symmetry transformations used to generate equivalent atoms: #1 x+1/2,-y+1,z #2 x,y+1,z #3 x,y,z #4 -x+1,-y+3,-z #5 -x-3/2,-y+3/2,-z+1/2

Anisotropic displacement parameters (Å^{2}x 10^3) for **10**. The anisotropic displacement factor exponent takes the form: $-2\pi^2[h^2a^{*2}U^{11} + ... + 2 h k a^* b^* U^{12}]$

	U^{11}	U^{22}	U^{33}	U^{23}	U^{13}	U^{12}
Ag(1)	34(1)	44(1)	41(1)	6(1)	17(1)	-11(1)
P	39(2)	29(2)	42(2)	1(2)	14(2)	-1(2)
F(1)	66(7)	133(9)	65(8)	-10(6)	41(6)	-16(6)
F(2)	37(5)	62(5)	67(7)	-1(5)	4(5)	-8(4)
F(3)	89(8)	50(6)	85(8)	6(5)	1(6)	22(5)
F(4)	76(7)	79(7)	50(7)	-9(5)	21(5)	-4(5)
F(5)	50(6)	99(8)	115(11)	-36(7)	3(7)	-36(6)
F(6)	112(8)	27(5)	99(6)	10(4)	13(6)	16(5)
C(1)	45(8)	50(9)	27(8)	10(6)	14(7)	5(7)
N(1)	31(6)	29(6)	37(7)	-2(5)	10(5)	-13(5)
C(2)	37(7)	30(6)	32(7)	-6(5)	13(6)	4(6)
C(3)	26(6)	26(6)	14(6)	0(5)	14(5)	9(6)
C(4)	30(7)	15(6)	24(7)	5(5)	12(6)	-3(5)
C(5)	32(7)	13(5)	48(9)	2(6)	18(7)	-4(6)
C(6)	29(7)	32(7)	34(8)	-5(6)	0(6)	-2(6)
N(2)	29(5)	30(5)	29(5)	9(5)	6(5)	-4(5)
C(7)	38(6)	17(6)	45(7)	6(6)	6(5)	-8(6)
C(8)	32(6)	24(6)	32(7)	-7(6)	5(5)	-5(6)
C(9)	29(7)	29(6)	25(7)	8(6)	-2(6)	-5(6)
C(10)	36(7)	36(7)	36(8)	3(6)	17(6)	-11(6)
C(11)	31(7)	19(7)	38(7)	8(6)	7(6)	3(6)
O(1)	44(6)	30(4)	48(8)	1(4)	26(5)	9(5)
O(2)	40(5)	22(5)	62(7)	9(4)	28(5)	-5(4)
C(12)	66(14)	41(8)	72(9)	15(9)	43(9)	-23(8)
C(13)	22(7)	37(7)	30(8)	-7(6)	0(6)	-11(6)

O(3)	44(5)	23(5)	68(7)	15(4)	26(5)	2(4)
O(4)	18(5)	26(5)	60(8)	10(5)	14(5)	-1(4)
C(14)	33(8)	49(9)	12(8)	-3(6)	20(7)	1(6)

Hydrogen coordinates (x 10^4) and isotropic displacement parameters (Å^{2}x 10^3) for **10**.

	x	y	z	U(eq)
H(1)	-777	6837	1568	48
H(2)	-2338	10278	1838	39
H(3)	-4120	9288	2162	26
H(5)	-2559	5847	1891	36
H(6)	835	12420	1062	38
H(7)	2051	8992	675	40
H(8)	3720	9984	312	35
H(10)	2505	13412	699	42
H(12A)	5297	13976	-246	70
H(12B)	6199	14289	143	70
H(14A)	-6580	6820	2774	37
H(14B)	-7212	6222	2382	37

Torsion angles [°] for **10**.

F(6)-P-F(4)-F(4)#3	0.0(8)	N(1)-Ag(1)-N(2)-C(7)	-150(16)
F(5)-P-F(4)-F(4)#3	0.0(8)	F(2)#1-Ag(1)-N(2)-C(7)	1.2(4)
F(3)-P-F(4)-F(4)#3	0.0(8)	F(3)#2-Ag(1)-N(2)-C(7)	-162.3(4)
F(1)-P-F(4)-F(4)#3	0(6)	C(6)-N(2)-C(7)-C(8)	0.0
F(2)-P-F(4)-F(4)#3	0.0(8)	Ag(1)-N(2)-C(7)-C(8)	-172.0(5)
C(5)-C(1)-N(1)-C(2)	0.0	N(2)-C(7)-C(8)-C(9)	0.0
C(5)-C(1)-N(1)-Ag(1)	-167.8(5)	C(7)-C(8)-C(9)-C(10)	0.0
N(2)-Ag(1)-N(1)-C(2)	-21(16)	C(7)-C(8)-C(9)-C(11)	179.7(9)
F(2)#1-Ag(1)-N(1)-C(2)	-172.2(4)	C(8)-C(9)-C(10)-C(6)	0.0
F(3)#2-Ag(1)-N(1)-C(2)	-8.8(4)	C(11)-C(9)-C(10)-C(6)	-179.7(9)
N(2)-Ag(1)-N(1)-C(1)	147(16)	N(2)-C(6)-C(10)-C(9)	0.0
F(2)#1-Ag(1)-N(1)-C(1)	-4.1(4)	C(10)-C(9)-C(11)-O(1)	170.3(10)
F(3)#2-Ag(1)-N(1)-C(1)	159.3(4)	C(8)-C(9)-C(11)-O(1)	-9.4(16)
C(1)-N(1)-C(2)-C(3)	0.0	C(10)-C(9)-C(11)-O(2)	-9.5(12)
Ag(1)-N(1)-C(2)-C(3)	168.3(5)	C(8)-C(9)-C(11)-O(2)	170.7(7)
N(1)-C(2)-C(3)-C(4)	0.0	O(1)-C(11)-O(2)-C(12)	-1.1(19)
C(2)-C(3)-C(4)-C(5)	0.0	C(9)-C(11)-O(2)-C(12)	178.7(11)
C(2)-C(3)-C(4)-C(13)	-176.8(9)	C(11)-O(2)-C(12)-C(12)#4	171.0(15)
C(3)-C(4)-C(5)-C(1)	0.0	C(5)-C(4)-C(13)-O(3)	24.1(15)
C(13)-C(4)-C(5)-C(1)	176.9(9)	C(3)-C(4)-C(13)-O(3)	-159.0(10)
N(1)-C(1)-C(5)-C(4)	0.0	C(5)-C(4)-C(13)-O(4)	-163.4(8)
C(10)-C(6)-N(2)-C(7)	0.0	C(3)-C(4)-C(13)-O(4)	13.4(13)
C(10)-C(6)-N(2)-Ag(1)	171.7(5)	O(3)-C(13)-O(4)-C(14)	-4.3(18)
N(1)-Ag(1)-N(2)-C(6)	38(16)	C(4)-C(13)-O(4)-C(14)	-176.8(10)
F(2)#1-Ag(1)-N(2)-C(6)	-170.7(4)	C(13)-O(4)-C(14)-C(14)#5	-170.5(14)
F(3)#2-Ag(1)-N(2)-C(6)	25.9(4)		

Symmetry transformations used to generate equivalent atoms: #1 x+1/2,-y+1,z #2 x,y+1,z #3 x,y,z #4 -x+1,-y+3,-z #5 -x-3/2,-y+3/2,-z+1/2

Hydrogen bonds for **10** [Å and °].

D-H...A	d(D-H)	d(H...A)	d(D...A)	<(DHA)
C(8)-H(8)...O(1)#6	0.93	2.52	3.425(11)	163.6
C(3)-H(3)...O(3)#7	0.93	2.58	3.487(10)	163.9
C(7)-H(7)...F(1)#1	0.93	2.61	3.429(12)	147.8
C(1)-H(1)...F(2)#1	0.93	2.62	3.363(11)	137.1

C(7)-H(7)...F(2)#1	0.93	2.49	3.271(10)	141.3
C(2)-H(2)...F(3)#2	0.93	2.54	3.298(10)	139.3
C(6)-H(6)...F(3)#2	0.93	2.86	3.572(11)	134.0
C(5)-H(5)...F(4)#3	0.93	2.59	3.461(10)	156.8
C(1)-H(1)...F(4)#1	0.93	2.50	3.251(12)	137.5
C(14)-H(14B)...F(4)#8	0.97	2.66	3.196(17)	115.6
C(14)-H(14A)...F(4)#7	0.97	2.74	3.355(16)	121.7
C(6)-H(6)...F(5)#2	0.93	2.76	3.687(12)	173.4
C(10)-H(10)...F(6)#9	0.93	2.45	3.207(10)	139.1

Symmetry transformations used to generate equivalent atoms: #1 x+1/2,-y+1,z #2 x,y+1,z #3 x,y,z
#4 -x+1,-y+3,-z #5 -x-3/2,-y+3/2,-z+1/2 #6 -x+1,-y+2,-z #7 -x-1,y+1/2,-z+1/2 #8 x-1/2,-y+1,z
#9 x+1/2,-y+2,z

I.2.l - Crystal data and structure refinement for 11.

Empirical formula	C36 H46 Cu1 N6 O19	
Formula weight	930.33	
Temperature	293(2) K	
Wavelength	0.71073 Å	
Crystal system	Monoclinic	
Space group	P2/c	
Unit cell dimensions	a = 19.6344(11) Å	α = 90°.
	b = 9.3190(4) Å	β = 91.634(5)°.
	c = 23.2805(14) Å	γ = 90°.
Volume	4258.0(4) Å^3	
Z	4	
Density (calculated)	1.451 Mg/m^3	
Absorption coefficient	0.597 mm^{-1}	
F(000)	1940	
Crystal size	? x ? x ? mm^3	
Theta range for data collection	1.75 to 26.87°.	
Index ranges	-24<=h<=24, -11<=k<=11, -29<=l<=29	
Reflections collected	25028	
Independent reflections	8457 [R(int) = 0.0365]	
Completeness to theta = 26.87°	92.3 %	
Refinement method	Full-matrix least-squares on F^2	
Data / restraints / parameters	8457 / 0 / 625	
Goodness-of-fit on F^2	0.983	
Final R indices [I>2sigma(I)]	R1 = 0.0611, wR2 = 0.1676	

R indices (all data)	R1 = 0.0777, wR2 = 0.1824
Largest diff. peak and hole	0.504 and -0.450 e.Å^{-3}

Atomic coordinates (x 10^4) and equivalent isotropic displacement parameters (Å^{2}x 10^3) for **11**. U(eq) is defined as one third of the trace of the orthogonalized U^{ij} tensor.

	x	y	z	U(eq)
Cu(1)	7300(1)	7768(1)	8124(1)	35(1)
O(40)	7228(1)	5533(2)	7750(1)	52(1)
N(1)	7968(1)	7118(2)	8751(1)	35(1)
C(1)	8451(1)	8021(3)	8951(1)	41(1)
C(2)	8878(1)	7661(3)	9408(1)	43(1)
C(3)	7915(1)	5826(3)	8994(1)	40(1)
C(4)	8331(1)	5397(3)	9450(1)	42(1)
C(5)	8815(1)	6342(3)	9669(1)	37(1)
C(6)	9251(1)	5912(3)	10176(1)	41(1)
O(1)	9318(1)	4696(2)	10337(1)	59(1)
O(2)	9544(1)	7042(2)	10425(1)	48(1)
C(7)	9986(1)	6760(4)	10926(1)	54(1)
C(8)	10216(1)	8178(4)	11152(1)	54(1)
O(3)	9640(1)	8830(2)	11425(1)	48(1)
C(9)	9751(1)	10118(3)	11649(1)	47(1)
O(4)	10259(1)	10789(3)	11597(1)	78(1)
C(10)	9156(1)	10614(3)	11989(1)	40(1)
C(11)	8666(1)	9676(3)	12166(1)	44(1)
C(12)	8138(1)	10198(3)	12487(1)	42(1)
C(13)	9114(1)	12032(3)	12148(1)	49(1)
C(14)	8579(1)	12473(3)	12473(1)	45(1)
N(2)	8089(1)	11574(2)	12637(1)	37(1)
N(3)	6511(1)	7470(2)	8670(1)	36(1)
C(15)	6563(1)	7883(3)	9221(1)	40(1)
C(16)	6053(1)	7665(3)	9606(1)	41(1)
C(17)	5936(1)	6816(3)	8490(1)	40(1)
C(18)	5402(1)	6569(3)	8850(1)	41(1)
C(19)	5460(1)	6987(2)	9419(1)	36(1)
C(20)	4873(1)	6765(3)	9804(1)	40(1)
O(5)	4323(1)	6361(3)	9635(1)	65(1)
O(6)	5038(1)	7048(2)	10349(1)	45(1)
C(21)	4490(1)	7115(3)	10749(1)	51(1)
C(22)	4342(1)	8650(3)	10886(1)	49(1)
O(7)	4832(1)	9197(2)	11311(1)	49(1)
C(23)	5364(1)	9932(3)	11125(1)	41(1)
O(8)	5473(1)	10196(2)	10631(1)	53(1)
C(24)	5806(1)	10444(3)	11620(1)	37(1)
C(25)	5816(1)	9782(3)	12151(1)	42(1)
C(26)	6246(1)	10323(3)	12582(1)	41(1)
C(27)	6225(1)	11614(3)	11535(1)	46(1)
C(28)	6636(1)	12086(3)	11983(1)	45(1)
N(4)	6647(1)	11462(2)	12503(1)	37(1)
N(5)	2472(1)	8472(3)	1302(1)	54(1)
O(9)	2751(1)	9661(2)	1370(1)	52(1)
O(10)	1844(1)	8368(3)	1303(1)	79(1)
O(11A)	2834(2)	7378(5)	1294(3)	123(2)
O(11B)	2778(5)	7492(8)	1100(5)	76(3)
N(6)	5479(3)	4147(6)	7442(2)	56(1)
O(12A)	5014(4)	3299(10)	7641(5)	103(5)
O(12B)	4987(6)	3381(14)	7216(5)	115(4)
O(13)	6020(3)	3666(5)	7752(2)	81(2)
O(14A)	5694(11)	5212(17)	7256(6)	154(5)
O(14B)	5423(5)	5388(8)	7301(4)	116(3)

O(600)	6066(6)	4489(15)	7268(5)	360(6)
N(7)	10000	15789(6)	12500	103(2)
O(15)	10000	17045(8)	12500	164(3)
O(16)	10391(3)	15103(6)	12174(2)	77(2)
O(700)	617(4)	5588(10)	2735(4)	156(3)
O(17)	3345(3)	7037(8)	3738(3)	200(3)
C(29)	2742(3)	7542(9)	3496(3)	149(3)
C(30)	2189(4)	6766(11)	3750(4)	192(4)
C(31)	2447(5)	5994(12)	4158(5)	289(5)
C(32)	3140(5)	5840(8)	4080(4)	238(4)
O(18)	2261(3)	9936(8)	4870(3)	218(3)
C(33)	1618(4)	10694(13)	4618(4)	230(5)
C(34)	1884(5)	11846(10)	4275(4)	207(4)
C(35)	2495(4)	12228(8)	4534(5)	176(4)
C(36)	2771(4)	10962(11)	4784(3)	178(3)
O(19)	1715(1)	6310(3)	2178(1)	87(1)

Anisotropic displacement parameters (Å^{2}x 10^3) for **11**. The anisotropic displacement factor exponent takes the form: $-2\pi^2[h^2a^{*2}U^{11} + ... + 2hka^*b^*U^{12}]$

	U^{11}	U^{22}	U^{33}	U^{23}	U^{13}	U^{12}
Cu(1)	28(1)	42(1)	34(1)	6(1)	0(1)	3(1)
O(40)	46(1)	41(1)	69(1)	-7(1)	-13(1)	9(1)
N(1)	29(1)	37(1)	40(1)	7(1)	-1(1)	0(1)
C(1)	39(1)	39(1)	45(1)	11(1)	-4(1)	-6(1)
C(2)	36(1)	43(1)	51(1)	3(1)	-5(1)	-7(1)
C(3)	37(1)	39(1)	44(1)	4(1)	-5(1)	-1(1)
C(4)	46(1)	37(1)	45(1)	7(1)	-3(1)	1(1)
C(5)	33(1)	41(1)	38(1)	2(1)	0(1)	8(1)
C(6)	38(1)	45(1)	40(1)	2(1)	0(1)	11(1)
O(1)	65(1)	54(1)	57(1)	9(1)	-16(1)	7(1)
O(2)	51(1)	51(1)	42(1)	-6(1)	-13(1)	15(1)
C(7)	48(1)	70(2)	43(1)	-10(1)	-13(1)	27(1)
C(8)	30(1)	82(2)	50(1)	-19(1)	-3(1)	12(1)
O(3)	29(1)	61(1)	53(1)	-19(1)	4(1)	4(1)
C(9)	37(1)	60(2)	45(1)	-11(1)	6(1)	-4(1)
O(4)	48(1)	89(2)	99(2)	-35(1)	33(1)	-25(1)
C(10)	32(1)	52(1)	38(1)	-8(1)	5(1)	-5(1)
C(11)	44(1)	40(1)	47(1)	-7(1)	9(1)	-4(1)
C(12)	39(1)	39(1)	49(1)	-6(1)	13(1)	-8(1)
C(13)	39(1)	48(2)	59(1)	-10(1)	13(1)	-14(1)
C(14)	42(1)	40(1)	55(1)	-8(1)	11(1)	-11(1)
N(2)	33(1)	41(1)	37(1)	-8(1)	4(1)	-5(1)
N(3)	32(1)	37(1)	40(1)	2(1)	0(1)	1(1)
C(15)	33(1)	44(1)	43(1)	-5(1)	1(1)	-7(1)
C(16)	41(1)	42(1)	39(1)	-4(1)	1(1)	-3(1)
C(17)	35(1)	45(1)	41(1)	-3(1)	-2(1)	-2(1)
C(18)	35(1)	43(1)	45(1)	-1(1)	-3(1)	-4(1)
C(19)	35(1)	30(1)	44(1)	2(1)	4(1)	-2(1)
C(20)	43(1)	31(1)	44(1)	2(1)	3(1)	-5(1)
O(5)	47(1)	92(2)	55(1)	-4(1)	8(1)	-32(1)
O(6)	39(1)	49(1)	46(1)	-7(1)	9(1)	-4(1)
C(21)	48(1)	59(2)	49(1)	-9(1)	15(1)	-16(1)
C(22)	29(1)	64(2)	54(1)	-21(1)	1(1)	-4(1)
O(7)	35(1)	66(1)	45(1)	-16(1)	1(1)	-11(1)
C(23)	36(1)	40(1)	46(1)	-9(1)	-2(1)	-1(1)
O(8)	57(1)	63(1)	39(1)	-1(1)	-8(1)	-15(1)
C(24)	30(1)	42(1)	39(1)	-6(1)	-1(1)	-1(1)
C(25)	37(1)	44(1)	43(1)	0(1)	2(1)	-10(1)
C(26)	37(1)	47(1)	40(1)	3(1)	-2(1)	-11(1)
C(27)	51(1)	49(1)	37(1)	3(1)	-3(1)	-13(1)

C(28)	47(1)	48(1)	40(1)	3(1)	-4(1)	-16(1)
N(4)	31(1)	44(1)	36(1)	-4(1)	0(1)	-5(1)
N(5)	38(1)	51(1)	73(1)	13(1)	5(1)	-6(1)
O(9)	46(1)	50(1)	60(1)	-5(1)	6(1)	-8(1)
O(10)	32(1)	82(2)	122(2)	29(1)	-2(1)	-10(1)
O(11A)	60(2)	58(2)	254(6)	52(3)	27(3)	12(2)
O(11B)	63(5)	17(3)	150(8)	-27(4)	29(5)	-5(3)
N(6)	53(3)	55(3)	59(3)	-10(2)	-10(2)	-3(2)
O(12A)	59(4)	53(4)	190(14)	35(5)	-107(7)	-29(4)
O(12B)	85(6)	142(8)	117(6)	-53(6)	-9(6)	-1(6)
O(13)	112(4)	48(2)	84(3)	12(2)	-8(3)	-6(3)
O(14A)	318(14)	112(8)	27(6)	35(5)	-73(8)	-207(8)
O(14B)	177(7)	59(4)	109(6)	9(4)	-70(5)	45(5)
N(7)	57(2)	87(4)	167(5)	0	39(3)	0
O(15)	176(6)	123(5)	195(7)	0	33(5)	0
O(16)	67(3)	67(3)	96(3)	0(3)	17(2)	21(2)
O(700)	117(5)	147(7)	207(7)	65(5)	93(5)	35(5)
O(17)	117(3)	242(6)	238(6)	34(5)	-25(4)	24(4)
C(29)	106(4)	197(7)	143(5)	50(5)	0(4)	22(4)
C(30)	100(4)	267(9)	209(7)	106(7)	12(5)	18(5)
C(31)	219(9)	323(9)	328(9)	240(7)	58(8)	82(8)
C(32)	324(9)	106(5)	273(9)	10(5)	-162(7)	75(6)
O(18)	204(5)	255(6)	191(5)	70(5)	-46(4)	-70(5)
C(33)	108(4)	359(14)	221(9)	35(9)	-22(5)	-98(6)
C(34)	256(9)	141(6)	216(8)	-4(6)	-118(7)	-29(7)
C(35)	117(5)	122(5)	289(11)	-21(6)	29(6)	-20(4)
C(36)	135(5)	250(9)	150(5)	58(6)	2(4)	-63(6)
O(19)	62(1)	81(2)	120(2)	27(2)	18(1)	18(1)

Bond lengths [Å] and angles [°] for **11**.

Cu(1)-N(1)	2.0261(19)	C(20)-O(5)	1.200(3)
Cu(1)-N(4)#1	2.0356(19)	C(20)-O(6)	1.326(3)
Cu(1)-N(2)#1	2.0401(19)	O(6)-C(21)	1.444(3)
Cu(1)-N(3)	2.051(2)	C(21)-C(22)	1.496(4)
Cu(1)-O(40)	2.261(2)	C(21)-H(21A)	0.9700
Cu(1)-O(9)#2	2.673(2)	C(21)-H(21B)	0.9700
Cu(1)-Cu(1)#3	12.3611(7)	C(22)-O(7)	1.453(3)
O(40)-H(40A)	0.66(3)	C(22)-H(22A)	0.9700
O(40)-H(40B)	0.87(4)	C(22)-H(22B)	0.9700
N(1)-C(3)	1.336(3)	O(7)-C(23)	1.332(3)
N(1)-C(1)	1.341(3)	C(23)-O(8)	1.200(3)
C(1)-C(2)	1.377(3)	C(23)-C(24)	1.500(3)
C(1)-H(1)	0.9300	C(24)-C(27)	1.383(4)
C(2)-C(5)	1.379(4)	C(24)-C(25)	1.383(3)
C(2)-H(2)	0.9300	C(25)-C(26)	1.387(3)
C(3)-C(4)	1.382(3)	C(25)-H(25)	0.9300
C(3)-H(3)	0.9300	C(26)-N(4)	1.337(3)
C(4)-C(5)	1.382(4)	C(26)-H(26)	0.9300
C(4)-H(4)	0.9300	C(27)-C(28)	1.375(4)
C(5)-C(6)	1.494(3)	C(27)-H(27)	0.9300
C(6)-O(1)	1.199(3)	C(28)-N(4)	1.342(3)
C(6)-O(2)	1.326(3)	C(28)-H(28)	0.9300
O(2)-C(7)	1.456(3)	N(4)-Cu(1)#3	2.0356(19)
C(7)-C(8)	1.489(4)	N(5)-O(11B)	1.196(9)
C(7)-H(7A)	0.9700	N(5)-O(10)	1.237(3)
C(7)-H(7B)	0.9700	N(5)-O(11A)	1.242(5)
C(8)-O(3)	1.447(3)	N(5)-O(9)	1.245(3)
C(8)-H(8A)	0.9700	O(13)-O(600)	1.369(13)
C(8)-H(8B)	0.9700	O(14B)-O(14B)#4	0.000(19)
O(3)-C(9)	1.324(3)	O(14B)-O(600)#4	1.520(15)
C(9)-O(4)	1.186(3)	O(14B)-O(600)	1.520(15)
C(9)-C(10)	1.502(3)	O(600)-O(600)#4	0.00(4)

C(10)-C(11)	1.372(4)
C(10)-C(13)	1.375(4)
C(11)-C(12)	1.383(3)
C(11)-H(11)	0.9300
C(12)-N(2)	1.333(3)
C(12)-H(12)	0.9300
C(13)-C(14)	1.375(4)
C(13)-H(13)	0.9300
C(14)-N(2)	1.339(3)
C(14)-H(14)	0.9300
N(2)-Cu(1)#3	2.0401(19)
N(3)-C(17)	1.340(3)
N(3)-C(15)	1.341(3)
C(15)-C(16)	1.378(3)
C(15)-H(15)	0.9300
C(16)-C(19)	1.383(3)
C(16)-H(16)	0.9300
N(6)-O(14A)	1.166(15)
N(6)-O(14B)#4	1.206(9)
N(6)-O(14B)	1.206(9)
N(6)-O(12A)#5	1.261(10)
N(6)-O(600)#4	1.273(13)
N(6)-O(600)	1.273(13)
N(6)-O(12A)	1.303(11)
N(6)-O(12B)	1.300(13)
N(6)-O(13)#4	1.344(7)
N(6)-O(13)	1.344(7)
N(6)-O(12B)#5	1.424(12)
O(12A)-O(12A)#5	0.66(2)
O(12A)-N(6)#5	1.261(10)
O(12A)-O(600)#5	2.409(16)
O(12B)-O(12B)#5	1.32(2)
O(12B)-N(6)#5	1.424(12)
O(12B)-O(600)#5	2.634(17)
O(13)-O(13)#4	0.000(14)
O(13)-O(600)#4	1.369(13)
C(17)-C(18)	1.379(3)
C(17)-H(17)	0.9300
C(18)-C(19)	1.384(3)
C(18)-H(18)	0.9300
C(19)-C(20)	1.495(3)
O(600)-O(13)#4	1.369(13)
O(600)-O(14B)#4	1.520(15)
N(7)-O(15)	1.170(9)
N(7)-O(16)	1.269(6)
N(7)-O(16)#6	1.269(6)
N(7)-O(700)#7	1.329(9)
N(7)-O(700)#8	1.329(9)
O(16)-O(700)#7	1.440(11)
O(700)-O(700)#4	0.000(18)
O(700)-N(7)#9	1.329(9)
O(700)-O(16)#9	1.440(11)
O(700)-O(700)#10	2.631(17)
O(17)-C(29)	1.380(8)
O(17)-C(32)	1.435(11)
C(29)-C(30)	1.446(10)
C(29)-H(29A)	0.9700
C(29)-H(29B)	0.9700
C(30)-C(31)	1.284(11)
C(30)-H(30A)	0.9700
C(30)-H(30B)	0.9700
C(31)-C(32)	1.385(13)
C(31)-H(31A)	0.9700
C(31)-H(31B)	0.9700
C(32)-H(32A)	0.9700
C(32)-H(32B)	0.9700
O(18)-C(36)	1.404(10)
O(18)-C(33)	1.548(11)
C(33)-C(34)	1.444(13)
C(33)-H(33A)	0.9700
C(33)-H(33B)	0.9700
C(34)-C(35)	1.375(11)
C(34)-H(34A)	0.9700
C(34)-H(34B)	0.9700
C(35)-C(36)	1.416(11)
C(35)-H(35A)	0.9700
C(35)-H(35B)	0.9700
C(36)-H(36A)	0.9700
C(36)-H(36B)	0.9700
O(19)-H(19A)	0.93(3)
O(19)-H(19B)	0.83(5)

N(1)-Cu(1)-N(4)#1	176.76(9)
N(1)-Cu(1)-N(2)#1	90.24(8)
N(4)#1-Cu(1)-N(2)#1	88.42(8)
N(1)-Cu(1)-N(3)	89.92(8)
N(4)#1-Cu(1)-N(3)	90.88(8)
N(2)#1-Cu(1)-N(3)	169.86(8)
N(1)-Cu(1)-O(40)	91.96(8)
N(4)#1-Cu(1)-O(40)	91.11(8)
N(2)#1-Cu(1)-O(40)	95.91(8)
N(3)-Cu(1)-O(40)	94.21(8)
N(1)-Cu(1)-O(9)#2	89.00(7)
N(4)#1-Cu(1)-O(9)#2	88.07(7)
N(2)#1-Cu(1)-O(9)#2	90.86(7)
N(3)-Cu(1)-O(9)#2	79.01(7)
O(40)-Cu(1)-O(9)#2	173.15(7)
N(1)-Cu(1)-Cu(1)#3	55.95(6)
N(4)#1-Cu(1)-Cu(1)#3	122.22(6)
N(2)#1-Cu(1)-Cu(1)#3	116.29(6)
N(3)-Cu(1)-Cu(1)#3	56.08(6)
O(40)-Cu(1)-Cu(1)#3	132.16(5)
O(9)#2-Cu(1)-Cu(1)#3	44.13(4)
Cu(1)-O(40)-H(40A)	129(3)
O(14A)-N(6)-O(600)	47.9(13)
O(14B)#4-N(6)-O(600)	75.5(8)
O(14B)-N(6)-O(600)	75.5(8)
O(12A)#5-N(6)-O(600)	143.9(9)
O(600)#4-N(6)-O(600)	0.0(12)
O(14A)-N(6)-O(12A)	155.8(13)
O(14B)#4-N(6)-O(12A)	128.2(8)
O(14B)-N(6)-O(12A)	128.2(8)
O(12A)#5-N(6)-O(12A)	29.7(10)
O(600)#4-N(6)-O(12A)	156.3(9)
O(600)-N(6)-O(12A)	156.3(9)
O(14A)-N(6)-O(12B)	126.1(10)
O(14B)#4-N(6)-O(12B)	110.8(8)
O(14B)-N(6)-O(12B)	110.8(8)
O(12A)#5-N(6)-O(12B)	15.3(8)
O(600)#4-N(6)-O(12B)	132.7(9)
O(600)-N(6)-O(12B)	132.7(9)
O(12A)-N(6)-O(12B)	44.9(6)
O(14A)-N(6)-O(13)#4	101.3(10)
O(14B)#4-N(6)-O(13)#4	122.0(6)
O(14B)-N(6)-O(13)#4	122.0(6)
O(12A)#5-N(6)-O(13)#4	117.7(6)

Cu(1)-O(40)-H(40B)	124(3)
H(40A)-O(40)-H(40B)	105(4)
C(3)-N(1)-C(1)	118.8(2)
C(3)-N(1)-Cu(1)	121.18(16)
C(1)-N(1)-Cu(1)	119.93(16)
N(1)-C(1)-C(2)	121.6(2)
N(1)-C(1)-H(1)	119.2
C(2)-C(1)-H(1)	119.2
C(1)-C(2)-C(5)	119.8(2)
C(1)-C(2)-H(2)	120.1
C(5)-C(2)-H(2)	120.1
N(1)-C(3)-C(4)	122.3(2)
N(1)-C(3)-H(3)	118.8
C(4)-C(3)-H(3)	118.8
C(5)-C(4)-C(3)	119.0(2)
C(5)-C(4)-H(4)	120.5
C(3)-C(4)-H(4)	120.5
C(2)-C(5)-C(4)	118.4(2)
C(2)-C(5)-C(6)	122.2(2)
C(4)-C(5)-C(6)	119.5(2)
O(1)-C(6)-O(2)	124.8(2)
O(1)-C(6)-C(5)	123.8(2)
O(2)-C(6)-C(5)	111.4(2)
C(6)-O(2)-C(7)	116.6(2)
O(2)-C(7)-C(8)	106.9(2)
O(2)-C(7)-H(7A)	110.3
C(8)-C(7)-H(7A)	110.3
O(2)-C(7)-H(7B)	110.3
C(8)-C(7)-H(7B)	110.3
H(7A)-C(7)-H(7B)	108.6
O(3)-C(8)-C(7)	107.2(2)
O(3)-C(8)-H(8A)	110.3
C(7)-C(8)-H(8A)	110.3
O(3)-C(8)-H(8B)	110.3
C(7)-C(8)-H(8B)	110.3
H(8A)-C(8)-H(8B)	108.5
C(9)-O(3)-C(8)	115.6(2)
O(4)-C(9)-O(3)	124.5(3)
O(4)-C(9)-C(10)	124.1(3)
O(3)-C(9)-C(10)	111.4(2)
C(11)-C(10)-C(13)	118.9(2)
C(11)-C(10)-C(9)	121.6(2)
C(13)-C(10)-C(9)	119.4(2)
C(10)-C(11)-C(12)	118.7(2)
C(10)-C(11)-H(11)	120.6
C(12)-C(11)-H(11)	120.7
N(2)-C(12)-C(11)	122.8(2)
N(2)-C(12)-H(12)	118.6
C(11)-C(12)-H(12)	118.6
C(14)-C(13)-C(10)	119.2(2)
C(14)-C(13)-H(13)	120.4
C(10)-C(13)-H(13)	120.4
N(2)-C(14)-C(13)	122.4(2)
N(2)-C(14)-H(14)	118.8
C(13)-C(14)-H(14)	118.8
C(12)-N(2)-C(14)	118.0(2)
C(12)-N(2)-Cu(1)#3	119.77(16)
C(14)-N(2)-Cu(1)#3	122.19(17)
C(17)-N(3)-C(15)	118.0(2)
C(17)-N(3)-Cu(1)	120.89(16)
C(15)-N(3)-Cu(1)	121.04(16)
N(3)-C(15)-C(16)	122.9(2)
N(3)-C(15)-H(15)	118.6
C(16)-C(15)-H(15)	118.6
O(600)#4-N(6)-O(13)#4	63.0(7)
O(600)-N(6)-O(13)#4	63.0(7)
O(12A)-N(6)-O(13)#4	99.1(6)
O(12B)-N(6)-O(13)#4	127.0(7)
O(14A)-N(6)-O(13)	101.3(10)
O(14B)#4-N(6)-O(13)	122.0(6)
O(14B)-N(6)-O(13)	122.0(6)
O(12A)#5-N(6)-O(13)	117.7(6)
O(600)#4-N(6)-O(13)	63.0(7)
O(600)-N(6)-O(13)	63.0(7)
O(12A)-N(6)-O(13)	99.1(6)
O(12B)-N(6)-O(13)	127.0(7)
O(13)#4-N(6)-O(13)	0.0(5)
O(14A)-N(6)-O(12B)#5	151.5(12)
O(14B)#4-N(6)-O(12B)#5	125.2(8)
O(14B)-N(6)-O(12B)#5	125.2(8)
O(12A)#5-N(6)-O(12B)#5	42.9(7)
O(600)#4-N(6)-O(12B)#5	155.1(9)
O(600)-N(6)-O(12B)#5	155.1(9)
O(12A)-N(6)-O(12B)#5	13.5(8)
O(12B)-N(6)-O(12B)#5	57.9(9)
O(13)#4-N(6)-O(12B)#5	92.5(6)
O(13)-N(6)-O(12B)#5	92.5(6)
O(12A)#5-O(12A)-N(6)#5	78.7(10)
O(12A)#5-O(12A)-N(6)	71.6(13)
N(6)#5-O(12A)-N(6)	96.3(8)
O(12A)#5-O(12A)-O(600)#5	92.2(13)
N(6)#5-O(12A)-O(600)#5	18.2(5)
N(6)-O(12A)-O(600)#5	112.4(7)
N(6)-O(12B)-O(12B)#5	65.7(9)
N(6)-O(12B)-N(6)#5	88.9(8)
O(12B)#5-O(12B)-N(6)#5	56.3(7)
N(6)-O(12B)-O(600)#5	100.6(7)
O(12B)#5-O(12B)-O(600)#5	63.3(9)
N(6)#5-O(12B)-O(600)#5	11.8(4)
O(13)#4-O(13)-N(6)	0(10)
O(13)#4-O(13)-O(600)#4	0(10)
N(6)-O(13)-O(600)#4	56.0(6)
O(13)#4-O(13)-O(600)	0(10)
N(6)-O(13)-O(600)	56.0(6)
O(600)#4-O(13)-O(600)	0.0(6)
O(14B)#4-O(14B)-N(6)	0(10)
O(14B)#4-O(14B)-O(600)#4	0(10)
N(6)-O(14B)-O(600)#4	54.2(6)
O(14B)#4-O(14B)-O(600)	0(10)
N(6)-O(14B)-O(600)	54.2(6)
O(600)#4-O(14B)-O(600)	0.0(13)
O(600)#4-O(600)-N(6)	0(10)
O(600)#4-O(600)-O(13)	0(10)
N(6)-O(600)-O(13)	61.0(7)
O(600)#4-O(600)-O(13)#4	0(10)
N(6)-O(600)-O(13)#4	61.0(7)
O(13)-O(600)-O(13)#4	0.0(6)
O(600)#4-O(600)-O(14B)	0(10)
N(6)-O(600)-O(14B)	50.2(6)
O(13)-O(600)-O(14B)	101.1(9)
O(13)#4-O(600)-O(14B)	101.1(9)
O(600)#4-O(600)-O(14B)#4	0(10)
N(6)-O(600)-O(14B)#4	50.2(6)
O(13)-O(600)-O(14B)#4	101.1(9)
O(13)#4-O(600)-O(14B)#4	101.1(9)
O(14B)-O(600)-O(14B)#4	0.0(8)
O(15)-N(7)-O(16)	120.3(3)
O(15)-N(7)-O(16)#6	120.3(3)

C(15)-C(16)-C(19)	118.9(2)
C(15)-C(16)-H(16)	120.5
C(19)-C(16)-H(16)	120.5
N(3)-C(17)-C(18)	122.3(2)
N(3)-C(17)-H(17)	118.8
C(18)-C(17)-H(17)	118.8
C(17)-C(18)-C(19)	119.4(2)
C(17)-C(18)-H(18)	120.3
C(19)-C(18)-H(18)	120.3
C(18)-C(19)-C(16)	118.4(2)
C(18)-C(19)-C(20)	119.4(2)
C(16)-C(19)-C(20)	122.1(2)
O(5)-C(20)-O(6)	124.7(2)
O(5)-C(20)-C(19)	123.3(2)
O(6)-C(20)-C(19)	111.9(2)
C(20)-O(6)-C(21)	117.2(2)
O(6)-C(21)-C(22)	109.4(2)
O(6)-C(21)-H(21A)	109.8
C(22)-C(21)-H(21A)	109.8
O(6)-C(21)-H(21B)	109.8
C(22)-C(21)-H(21B)	109.8
H(21A)-C(21)-H(21B)	108.2
O(7)-C(22)-C(21)	110.6(2)
O(7)-C(22)-H(22A)	109.5
C(21)-C(22)-H(22A)	109.5
O(7)-C(22)-H(22B)	109.5
C(21)-C(22)-H(22B)	109.5
H(22A)-C(22)-H(22B)	108.1
C(23)-O(7)-C(22)	118.0(2)
O(8)-C(23)-O(7)	125.4(2)
O(8)-C(23)-C(24)	123.7(2)
O(7)-C(23)-C(24)	110.8(2)
C(27)-C(24)-C(25)	119.1(2)
C(27)-C(24)-C(23)	118.3(2)
C(25)-C(24)-C(23)	122.6(2)
C(24)-C(25)-C(26)	118.5(2)
C(24)-C(25)-H(25)	120.7
C(26)-C(25)-H(25)	120.7
N(4)-C(26)-C(25)	122.5(2)
N(4)-C(26)-H(26)	118.7
C(25)-C(26)-H(26)	118.7
C(28)-C(27)-C(24)	118.8(2)
C(28)-C(27)-H(27)	120.6
C(24)-C(27)-H(27)	120.6
N(4)-C(28)-C(27)	122.7(2)
N(4)-C(28)-H(28)	118.6
C(27)-C(28)-H(28)	118.6
C(26)-N(4)-C(28)	118.3(2)
C(26)-N(4)-Cu(1)#3	122.93(16)
C(28)-N(4)-Cu(1)#3	118.77(17)
O(11B)-N(5)-O(10)	116.9(5)
O(11B)-N(5)-O(11A)	22.3(7)
O(10)-N(5)-O(11A)	120.4(3)
O(11B)-N(5)-O(9)	120.3(5)
O(10)-N(5)-O(9)	120.3(3)
O(11A)-N(5)-O(9)	118.8(3)
O(14A)-N(6)-O(14B)#4	27.7(12)
O(14A)-N(6)-O(14B)	27.7(12)
O(14B)#4-N(6)-O(14B)	0.0(11)
O(14A)-N(6)-O(12A)#5	139.5(10)
O(14B)#4-N(6)-O(12A)#5	119.6(7)
O(14B)-N(6)-O(12A)#5	119.6(7)
O(14A)-N(6)-O(600)#4	47.9(13)
O(14B)#4-N(6)-O(600)#4	75.5(8)
O(16)-N(7)-O(16)#6	119.5(7)
O(15)-N(7)-O(700)#7	98.1(5)
O(16)-N(7)-O(700)#7	67.3(5)
O(16)#6-N(7)-O(700)#7	104.1(5)
O(15)-N(7)-O(700)#8	98.1(5)
O(16)-N(7)-O(700)#8	104.1(5)
O(16)#6-N(7)-O(700)#8	67.3(5)
O(700)#7-N(7)-O(700)#8	163.8(10)
N(7)-O(16)-O(700)#7	58.3(4)
O(700)#4-O(700)-N(7)#9	0(10)
O(700)#4-O(700)-O(16)#9	0(10)
N(7)#9-O(700)-O(16)#9	54.4(4)
O(700)#4-O(700)-O(700)#10	0(10)
N(7)#9-O(700)-O(700)#10	8.1(5)
O(16)#9-O(700)-O(700)#10	50.7(4)
C(29)-O(17)-C(32)	103.9(6)
O(17)-C(29)-C(30)	108.0(6)
O(17)-C(29)-H(29A)	110.1
C(30)-C(29)-H(29A)	110.1
O(17)-C(29)-H(29B)	110.1
C(30)-C(29)-H(29B)	110.1
H(29A)-C(29)-H(29B)	108.4
C(31)-C(30)-C(29)	107.3(7)
C(31)-C(30)-H(30A)	110.3
C(29)-C(30)-H(30A)	110.3
C(31)-C(30)-H(30B)	110.2
C(29)-C(30)-H(30B)	110.3
H(30A)-C(30)-H(30B)	108.5
C(30)-C(31)-C(32)	109.3(9)
C(30)-C(31)-H(31A)	109.9
C(32)-C(31)-H(31A)	109.9
C(30)-C(31)-H(31B)	109.8
C(32)-C(31)-H(31B)	109.8
H(31A)-C(31)-H(31B)	108.3
C(31)-C(32)-O(17)	106.5(6)
C(31)-C(32)-H(32A)	110.4
O(17)-C(32)-H(32A)	110.4
C(31)-C(32)-H(32B)	110.5
O(17)-C(32)-H(32B)	110.4
H(32A)-C(32)-H(32B)	108.6
C(36)-O(18)-C(33)	102.2(7)
C(34)-C(33)-O(18)	104.2(6)
C(34)-C(33)-H(33A)	110.9
O(18)-C(33)-H(33A)	110.9
C(34)-C(33)-H(33B)	110.9
O(18)-C(33)-H(33B)	110.9
H(33A)-C(33)-H(33B)	108.9
C(35)-C(34)-C(33)	105.9(8)
C(35)-C(34)-H(34A)	110.6
C(33)-C(34)-H(34A)	110.5
C(35)-C(34)-H(34B)	110.6
C(33)-C(34)-H(34B)	110.6
H(34A)-C(34)-H(34B)	108.7
C(34)-C(35)-C(36)	106.5(7)
C(34)-C(35)-H(35A)	110.4
C(36)-C(35)-H(35A)	110.4
C(34)-C(35)-H(35B)	110.4
C(36)-C(35)-H(35B)	110.4
H(35A)-C(35)-H(35B)	108.6
O(18)-C(36)-C(35)	111.1(7)
O(18)-C(36)-H(36A)	109.4
C(35)-C(36)-H(36A)	109.4
O(18)-C(36)-H(36B)	109.4
C(35)-C(36)-H(36B)	109.4

O(14B)-N(6)-O(600)#4	75.5(8)	H(36A)-C(36)-H(36B)	108.0
O(12A)#5-N(6)-O(600)#4	143.9(9)	H(19A)-O(19)-H(19B)	94(4)

Symmetry transformations used to generate equivalent atoms: #1 x,-y+2,z-1/2 #2 -x+1,-y+2,-z+1
#3 x,-y+2,z+1/2 #4 x,y,z #5 -x+1,y,-z+3/2 #6 -x+2,y,-z+5/2 #7 x+1,y+1,z+1 #8 -x+1,y+1,-z+3/2
#9 x-1,y-1,z-1 #10 -x,y,-z+1/2

Hydrogen coordinates (x 10^4) and isotropic displacement parameters (Å^{2}x 10^3) for **11**.

	x	y	z	U(eq)
H(40A)	6955(17)	5150(40)	7681(14)	63(10)
H(40B)	7567(19)	4940(40)	7733(15)	80(11)
H(1)	8499	8912	8776	49
H(2)	9208	8307	9540	52
H(3)	7586	5193	8851	48
H(4)	8287	4487	9608	51
H(7A)	10375	6186	10818	65
H(7B)	9739	6243	11215	65
H(8A)	10591	8056	11428	65
H(8B)	10368	8781	10841	65
H(11)	8688	8707	12071	52
H(12)	7804	9563	12603	50
H(13)	9443	12684	12037	58
H(14)	8557	13430	12584	55
H(15)	6961	8338	9349	48
H(16)	6106	7968	9985	49
H(17)	5895	6518	8109	48
H(18)	5006	6125	8711	49
H(21A)	4619	6603	11098	62
H(21B)	4086	6663	10581	62
H(22A)	4361	9221	10539	59
H(22B)	3886	8728	11033	59
H(25)	5540	8992	12219	50
H(26)	6257	9877	12939	50
H(27)	6228	12072	11180	55
H(28)	6918	12871	11925	54
H(29A)	2735	7392	3083	179
H(29B)	2697	8561	3569	179
H(30A)	1858	7432	3900	230
H(30B)	1961	6163	3465	230
H(31A)	2230	5059	4157	347
H(31B)	2370	6448	4525	347
H(32A)	3233	4945	3885	285
H(32B)	3385	5841	4448	285
H(33A)	1347	10039	4383	276
H(33B)	1340	11067	4922	276
H(34A)	1951	11526	3884	248
H(34B)	1572	12653	4266	248
H(35A)	2425	12949	4827	211
H(35B)	2800	12616	4253	211
H(36A)	3111	10567	4533	214
H(36B)	2995	11194	5149	214
H(19A)	1586(17)	5840(40)	1839(15)	58(10)
H(19B)	1350(30)	6150(60)	2340(20)	124(18)

Torsion angles [°] for **11**.

N(4)#1-Cu(1)-N(1)-C(3)	162.3(13)	O(14B)-N(6)-O(12B)-O(600)#5	-65.3(8)
N(2)#1-Cu(1)-N(1)-C(3)	-132.17(19)	O(12A)#5-N(6)-O(12B)-O(600)#5	63(3)
N(3)-Cu(1)-N(1)-C(3)	57.97(19)	O(600)#4-N(6)-O(12B)-O(600)#5	-154.5(11)
O(40)-Cu(1)-N(1)-C(3)	-36.24(19)	O(600)-N(6)-O(12B)-O(600)#5	-154.5(11)

O(9)#2-Cu(1)-N(1)-C(3)	136.98(19)	O(12A)-N(6)-O(12B)-O(600)#5	58.5(8)
Cu(1)#3-Cu(1)-N(1)-C(3)	105.71(19)	O(13)#4-N(6)-O(12B)-O(600)#5	120.0(7)
N(4)#1-Cu(1)-N(1)-C(1)	-13.9(15)	O(13)-N(6)-O(12B)-O(600)#5	120.0(7)
N(2)#1-Cu(1)-N(1)-C(1)	51.62(19)	O(12B)#5-N(6)-O(12B)-O(600)#5	54.1(8)
N(3)-Cu(1)-N(1)-C(1)	-118.24(19)	O(14A)-N(6)-O(13)-O(13)#4	0.0(8)
O(40)-Cu(1)-N(1)-C(1)	147.55(19)	O(14B)#4-N(6)-O(13)-O(13)#4	0.0(8)
O(9)#2-Cu(1)-N(1)-C(1)	-39.23(18)	O(14B)-N(6)-O(13)-O(13)#4	0.0(8)
Cu(1)#3-Cu(1)-N(1)-C(1)	-70.50(18)	O(12A)#5-N(6)-O(13)-O(13)#4	0.0(6)
C(3)-N(1)-C(1)-C(2)	-1.7(4)	O(600)#4-N(6)-O(13)-O(13)#4	0.0(6)
Cu(1)-N(1)-C(1)-C(2)	174.6(2)	O(600)-N(6)-O(13)-O(13)#4	0.0(6)
N(1)-C(1)-C(2)-C(5)	0.3(4)	O(12A)-N(6)-O(13)-O(13)#4	0.0(7)
C(1)-N(1)-C(3)-C(4)	1.2(4)	O(12B)-N(6)-O(13)-O(13)#4	0.0(6)
Cu(1)-N(1)-C(3)-C(4)	-175.07(19)	O(12B)#5-N(6)-O(13)-O(13)#4	0.0(7)
N(1)-C(3)-C(4)-C(5)	0.8(4)	O(14A)-N(6)-O(13)-O(600)#4	-29.7(11)
C(1)-C(2)-C(5)-C(4)	1.7(4)	O(14B)#4-N(6)-O(13)-O(600)#4	-49.5(10)
C(1)-C(2)-C(5)-C(6)	-178.2(2)	O(14B)-N(6)-O(13)-O(600)#4	-49.5(10)
C(3)-C(4)-C(5)-C(2)	-2.2(4)	O(12A)#5-N(6)-O(13)-O(600)#4	139.1(11)
C(3)-C(4)-C(5)-C(6)	177.7(2)	O(600)-N(6)-O(13)-O(600)#4	0.000(4)
C(2)-C(5)-C(6)-O(1)	-163.2(3)	O(12A)-N(6)-O(13)-O(600)#4	163.6(10)
C(4)-C(5)-C(6)-O(1)	16.9(4)	O(12B)-N(6)-O(13)-O(600)#4	124.7(11)
C(2)-C(5)-C(6)-O(2)	17.3(3)	O(13)#4-N(6)-O(13)-O(600)#4	0(100)
C(4)-C(5)-C(6)-O(2)	-162.6(2)	O(12B)#5-N(6)-O(13)-O(600)#4	175.4(10)
O(1)-C(6)-O(2)-C(7)	0.8(4)	O(14A)-N(6)-O(13)-O(600)	-29.7(11)
C(5)-C(6)-O(2)-C(7)	-179.8(2)	O(14B)#4-N(6)-O(13)-O(600)	-49.5(10)
C(6)-O(2)-C(7)-C(8)	-176.2(2)	O(14B)-N(6)-O(13)-O(600)	-49.5(10)
O(2)-C(7)-C(8)-O(3)	73.2(3)	O(12A)#5-N(6)-O(13)-O(600)	139.1(11)
C(7)-C(8)-O(3)-C(9)	-179.4(2)	O(600)#4-N(6)-O(13)-O(600)	0.000(4)
C(8)-O(3)-C(9)-O(4)	6.3(4)	O(12A)-N(6)-O(13)-O(600)	163.6(10)
C(8)-O(3)-C(9)-C(10)	-172.4(2)	O(12B)-N(6)-O(13)-O(600)	124.7(11)
O(4)-C(9)-C(10)-C(11)	-162.2(3)	O(13)#4-N(6)-O(13)-O(600)	0(100)
O(3)-C(9)-C(10)-C(11)	16.5(3)	O(12B)#5-N(6)-O(13)-O(600)	175.4(10)
O(4)-C(9)-C(10)-C(13)	15.2(4)	O(14A)-N(6)-O(14B)-O(14B)#4	0(5)
O(3)-C(9)-C(10)-C(13)	-166.1(2)	O(12A)#5-N(6)-O(14B)-O(14B)#4	0(5)
C(13)-C(10)-C(11)-C(12)	1.4(4)	O(600)#4-N(6)-O(14B)-O(14B)#4	0(5)
C(9)-C(10)-C(11)-C(12)	178.8(2)	O(600)-N(6)-O(14B)-O(14B)#4	0(5)
C(10)-C(11)-C(12)-N(2)	-0.7(4)	O(12A)-N(6)-O(14B)-O(14B)#4	0(5)
C(11)-C(10)-C(13)-C(14)	-0.7(4)	O(12B)-N(6)-O(14B)-O(14B)#4	0(5)
C(9)-C(10)-C(13)-C(14)	-178.2(2)	O(13)#4-N(6)-O(14B)-O(14B)#4	0(5)
C(10)-C(13)-C(14)-N(2)	-0.8(4)	O(13)-N(6)-O(14B)-O(14B)#4	0(5)
C(11)-C(12)-N(2)-C(14)	-0.9(4)	O(12B)#5-N(6)-O(14B)-O(14B)#4	0(5)
C(11)-C(12)-N(2)-Cu(1)#3	-178.85(19)	O(14A)-N(6)-O(14B)-O(600)#4	-1.4(18)
C(13)-C(14)-N(2)-C(12)	1.6(4)	O(14B)#4-N(6)-O(14B)-O(600)#4	0(100)
C(13)-C(14)-N(2)-Cu(1)#3	179.6(2)	O(12A)#5-N(6)-O(14B)-O(600)#4	-144.4(10)
N(1)-Cu(1)-N(3)-C(17)	-135.48(19)	O(600)-N(6)-O(14B)-O(600)#4	0.000(3)
N(4)#1-Cu(1)-N(3)-C(17)	47.7(2)	O(12A)-N(6)-O(14B)-O(600)#4	-178.8(11)
N(2)#1-Cu(1)-N(3)-C(17)	133.6(4)	O(12B)-N(6)-O(14B)-O(600)#4	-130.6(9)
O(40)-Cu(1)-N(3)-C(17)	-43.52(19)	O(13)#4-N(6)-O(14B)-O(600)#4	44.4(8)
O(9)#2-Cu(1)-N(3)-C(17)	135.5(2)	O(13)-N(6)-O(14B)-O(600)#4	44.4(8)
Cu(1)#3-Cu(1)-N(3)-C(17)	176.9(2)	O(12B)#5-N(6)-O(14B)-O(600)#4	164.7(10)
N(1)-Cu(1)-N(3)-C(15)	42.4(2)	O(14A)-N(6)-O(14B)-O(600)	-1.4(18)
N(4)#1-Cu(1)-N(3)-C(15)	-134.4(2)	O(14B)#4-N(6)-O(14B)-O(600)	0(100)
N(2)#1-Cu(1)-N(3)-C(15)	-48.5(5)	O(12A)#5-N(6)-O(14B)-O(600)	-144.4(10)
O(40)-Cu(1)-N(3)-C(15)	134.39(19)	O(600)#4-N(6)-O(14B)-O(600)	0.000(3)
O(9)#2-Cu(1)-N(3)-C(15)	-46.58(19)	O(12A)-N(6)-O(14B)-O(600)	-178.8(11)
Cu(1)#3-Cu(1)-N(3)-C(15)	-5.21(16)	O(12B)-N(6)-O(14B)-O(600)	-130.6(9)
C(17)-N(3)-C(15)-C(16)	-0.1(4)	O(13)#4-N(6)-O(14B)-O(600)	44.4(8)
Cu(1)-N(3)-C(15)-C(16)	-178.0(2)	O(13)-N(6)-O(14B)-O(600)	44.4(8)
N(3)-C(15)-C(16)-C(19)	0.1(4)	O(12B)#5-N(6)-O(14B)-O(600)	164.7(10)
C(15)-N(3)-C(17)-C(18)	0.5(4)	O(14A)-N(6)-O(600)-O(600)#4	0.0(14)
Cu(1)-N(3)-C(17)-C(18)	178.4(2)	O(14B)#4-N(6)-O(600)-O(600)#4	0.0(13)
N(3)-C(17)-C(18)-C(19)	-1.0(4)	O(14B)-N(6)-O(600)-O(600)#4	0.0(13)
C(17)-C(18)-C(19)-C(16)	1.0(4)	O(12A)#5-N(6)-O(600)-O(600)#4	0.0(7)
C(17)-C(18)-C(19)-C(20)	177.9(2)	O(12A)-N(6)-O(600)-O(600)#4	0.0(17)
C(15)-C(16)-C(19)-C(18)	-0.6(4)	O(12B)-N(6)-O(600)-O(600)#4	0.0(8)

C(15)-C(16)-C(19)-C(20)	-177.4(2)
C(18)-C(19)-C(20)-O(5)	-7.2(4)
C(16)-C(19)-C(20)-O(5)	169.6(3)
C(18)-C(19)-C(20)-O(6)	171.9(2)
C(16)-C(19)-C(20)-O(6)	-11.4(3)
O(5)-C(20)-O(6)-C(21)	-11.3(4)
C(19)-C(20)-O(6)-C(21)	169.6(2)
C(20)-O(6)-C(21)-C(22)	-103.6(3)
O(6)-C(21)-C(22)-O(7)	-79.9(3)
C(21)-C(22)-O(7)-C(23)	96.8(3)
C(22)-O(7)-C(23)-O(8)	0.6(4)
C(22)-O(7)-C(23)-C(24)	178.6(2)
O(8)-C(23)-C(24)-C(27)	20.9(4)
O(7)-C(23)-C(24)-C(27)	-157.1(2)
O(8)-C(23)-C(24)-C(25)	-158.3(3)
O(7)-C(23)-C(24)-C(25)	23.7(3)
C(27)-C(24)-C(25)-C(26)	0.2(4)
C(23)-C(24)-C(25)-C(26)	179.4(2)
C(24)-C(25)-C(26)-N(4)	0.5(4)
C(25)-C(24)-C(27)-C(28)	-0.3(4)
C(23)-C(24)-C(27)-C(28)	-179.5(2)
C(24)-C(27)-C(28)-N(4)	-0.2(4)
C(25)-C(26)-N(4)-C(28)	-1.0(4)
C(25)-C(26)-N(4)-Cu(1)#3	-178.20(19)
C(27)-C(28)-N(4)-C(26)	0.9(4)
C(27)-C(28)-N(4)-Cu(1)#3	178.2(2)
O(14A)-N(6)-O(12A)-O(12A)#5	81(2)
O(14B)#4-N(6)-O(12A)-O(12A)#5	83.7(12)
O(14B)-N(6)-O(12A)-O(12A)#5	83.7(12)
O(600)#4-N(6)-O(12A)-O(12A)#5	-93(2)
O(600)-N(6)-O(12A)-O(12A)#5	-93(2)
O(12B)-N(6)-O(12A)-O(12A)#5	2.4(12)
O(13)#4-N(6)-O(12A)-O(12A)#5	-132.3(9)
O(13)-N(6)-O(12A)-O(12A)#5	-132.3(9)
O(12B)#5-N(6)-O(12A)-O(12A)#5	166(3)
O(14A)-N(6)-O(12A)-N(6)#5	5(2)
O(14B)#4-N(6)-O(12A)-N(6)#5	7.9(11)
O(14B)-N(6)-O(12A)-N(6)#5	7.9(11)
O(12A)#5-N(6)-O(12A)-N(6)#5	-75.9(10)
O(600)#4-N(6)-O(12A)-N(6)#5	-169.3(19)
O(600)-N(6)-O(12A)-N(6)#5	-169.3(19)
O(12B)-N(6)-O(12A)-N(6)#5	-73.5(10)
O(13)#4-N(6)-O(12A)-N(6)#5	151.8(6)
O(13)-N(6)-O(12A)-N(6)#5	151.8(6)
O(12B)#5-N(6)-O(12A)-N(6)#5	90(3)
O(14A)-N(6)-O(12A)-O(600)#5	-4(2)
O(14B)#4-N(6)-O(12A)-O(600)#5	-0.9(12)
O(14B)-N(6)-O(12A)-O(600)#5	-0.9(12)
O(12A)#5-N(6)-O(12A)-O(600)#5	-84.6(10)
O(600)#4-N(6)-O(12A)-O(600)#5	-178.1(16)
O(600)-N(6)-O(12A)-O(600)#5	-178.1(16)
O(12B)-N(6)-O(12A)-O(600)#5	-82.2(10)
O(13)#4-N(6)-O(12A)-O(600)#5	143.1(6)
O(13)-N(6)-O(12A)-O(600)#5	143.1(6)
O(12B)#5-N(6)-O(12A)-O(600)#5	82(3)
O(14A)-N(6)-O(12B)-O(12B)#5	-145.8(15)
O(14B)#4-N(6)-O(12B)-O(12B)#5	-119.4(8)
O(14B)-N(6)-O(12B)-O(12B)#5	-119.4(8)
O(12A)#5-N(6)-O(12B)-O(12B)#5	9(3)
O(600)#4-N(6)-O(12B)-O(12B)#5	151.4(13)
O(600)-N(6)-O(12B)-O(12B)#5	151.4(13)
O(12A)-N(6)-O(12B)-O(12B)#5	4.4(10)
O(13)#4-N(6)-O(12B)-O(12B)#5	65.9(10)
O(13)-N(6)-O(12B)-O(12B)#5	65.9(10)
O(13)#4-N(6)-O(600)-O(600)#4	0.0(12)
O(13)-N(6)-O(600)-O(600)#4	0.0(12)
O(12B)#5-N(6)-O(600)-O(600)#4	0(2)
O(14A)-N(6)-O(600)-O(13)	139.1(12)
O(14B)#4-N(6)-O(600)-O(13)	138.3(7)
O(14B)-N(6)-O(600)-O(13)	138.3(7)
O(12A)#5-N(6)-O(600)-O(13)	-100.9(13)
O(600)#4-N(6)-O(600)-O(13)	0(100)
O(12A)-N(6)-O(600)-O(13)	-44(2)
O(12B)-N(6)-O(600)-O(13)	-116.7(11)
O(13)#4-N(6)-O(600)-O(13)	0.000(5)
O(12B)#5-N(6)-O(600)-O(13)	-11(2)
O(14A)-N(6)-O(600)-O(13)#4	139.1(12)
O(14B)#4-N(6)-O(600)-O(13)#4	138.3(7)
O(14B)-N(6)-O(600)-O(13)#4	138.3(7)
O(12A)#5-N(6)-O(600)-O(13)#4	-100.9(13)
O(600)#4-N(6)-O(600)-O(13)#4	0(100)
O(12A)-N(6)-O(600)-O(13)#4	-44(2)
O(12B)-N(6)-O(600)-O(13)#4	-116.7(11)
O(13)-N(6)-O(600)-O(13)#4	0.000(5)
O(12B)#5-N(6)-O(600)-O(13)#4	-11(2)
O(14A)-N(6)-O(600)-O(14B)	0.9(11)
O(14B)#4-N(6)-O(600)-O(14B)	0.000(4)
O(12A)#5-N(6)-O(600)-O(14B)	120.9(14)
O(600)#4-N(6)-O(600)-O(14B)	0(100)
O(12A)-N(6)-O(600)-O(14B)	178(2)
O(12B)-N(6)-O(600)-O(14B)	105.1(12)
O(13)#4-N(6)-O(600)-O(14B)	-138.3(7)
O(13)-N(6)-O(600)-O(14B)	-138.3(7)
O(12B)#5-N(6)-O(600)-O(14B)	-149(2)
O(14A)-N(6)-O(600)-O(14B)#4	0.9(11)
O(14B)-N(6)-O(600)-O(14B)#4	0.000(4)
O(12A)#5-N(6)-O(600)-O(14B)#4	120.9(14)
O(600)#4-N(6)-O(600)-O(14B)#4	0(100)
O(12A)-N(6)-O(600)-O(14B)#4	178(2)
O(12B)-N(6)-O(600)-O(14B)#4	105.1(12)
O(13)#4-N(6)-O(600)-O(14B)#4	-138.3(7)
O(13)-N(6)-O(600)-O(14B)#4	-138.3(7)
O(12B)#5-N(6)-O(600)-O(14B)#4	-149(2)
O(13)#4-O(13)-O(600)-O(600)#4	0.0
N(6)-O(13)-O(600)-O(600)#4	0(4)
O(13)#4-O(13)-O(600)-N(6)	0.0(13)
O(600)#4-O(13)-O(600)-N(6)	0(93)
N(6)-O(13)-O(600)-O(13)#4	0(100)
O(600)#4-O(13)-O(600)-O(13)#4	0(100)
O(13)#4-O(13)-O(600)-O(14B)	0.0(12)
N(6)-O(13)-O(600)-O(14B)	31.4(6)
O(600)#4-O(13)-O(600)-O(14B)	0(100)
O(13)#4-O(13)-O(600)-O(14B)#4	0.0(12)
N(6)-O(13)-O(600)-O(14B)#4	31.4(6)
O(600)#4-O(13)-O(600)-O(14B)#4	0(100)
O(14B)#4-O(14B)-O(600)-O(600)#4	0.0
N(6)-O(14B)-O(600)-O(600)#4	0.0(8)
O(14B)#4-O(14B)-O(600)-N(6)	0.0(6)
O(600)#4-O(14B)-O(600)-N(6)	0(100)
O(14B)#4-O(14B)-O(600)-O(13)	0.0(3)
N(6)-O(14B)-O(600)-O(13)	-36.4(7)
O(600)#4-O(14B)-O(600)-O(13)	0(100)
O(14B)#4-O(14B)-O(600)-O(13)#4	0.0(3)
N(6)-O(14B)-O(600)-O(13)#4	-36.4(7)
O(600)#4-O(14B)-O(600)-O(13)#4	0(100)
N(6)-O(14B)-O(600)-O(14B)#4	0(100)
O(600)#4-O(14B)-O(600)-O(14B)#4	0(100)
O(15)-N(7)-O(16)-O(700)#7	86.2(5)

O(14A)-N(6)-O(12B)-N(6)#5	-92.7(14)	O(16)#6-N(7)-O(16)-O(700)#7	-93.8(5)
O(14B)#4-N(6)-O(12B)-N(6)#5	-66.2(8)	O(700)#8-N(7)-O(16)-O(700)#7	-165.5(8)
O(14B)-N(6)-O(12B)-N(6)#5	-66.2(8)	C(32)-O(17)-C(29)-C(30)	7.1(9)
O(12A)#5-N(6)-O(12B)-N(6)#5	62(3)	O(17)-C(29)-C(30)-C(31)	7.0(12)
O(600)#4-N(6)-O(12B)-N(6)#5	-155.4(10)	C(29)-C(30)-C(31)-C(32)	-18.9(13)
O(600)-N(6)-O(12B)-N(6)#5	-155.4(10)	C(30)-C(31)-C(32)-O(17)	23.7(13)
O(12A)-N(6)-O(12B)-N(6)#5	57.6(8)	C(29)-O(17)-C(32)-C(31)	-18.0(10)
O(13)#4-N(6)-O(12B)-N(6)#5	119.1(8)	C(36)-O(18)-C(33)-C(34)	16.4(9)
O(13)-N(6)-O(12B)-N(6)#5	119.1(8)	O(18)-C(33)-C(34)-C(35)	-29.9(11)
O(12B)#5-N(6)-O(12B)-N(6)#5	53.2(8)	C(33)-C(34)-C(35)-C(36)	31.9(11)
O(14A)-N(6)-O(12B)-O(600)#5	-91.7(15)	C(33)-O(18)-C(36)-C(35)	2.3(10)
O(14B)#4-N(6)-O(12B)-O(600)#5	-65.3(8)	C(34)-C(35)-C(36)-O(18)	-21.4(11)

Symmetry transformations used to generate equivalent atoms: #1 x,-y+2,z-1/2 #2 -x+1,-y+2,-z+1
#3 x,-y+2,z+1/2 #4 x,y,z #5 -x+1,y,-z+3/2 #6 -x+2,y,-z+5/2 #7 x+1,y+1,z+1 #8 -x+1,y+1,-z+3/2
#9 x-1,y-1,z-1 #10 -x,y,-z+1/2

Hydrogen bonds for **11** [Å and °].

D-H...A	d(D-H)	d(H...A)	d(D...A)	<(DHA)
C(22)-H(22A)...O(8)#11	0.97	2.81	3.720(3)	157.5
C(27)-H(27)...O(5)#11	0.93	2.60	3.460(3)	153.0
C(15)-H(15)...O(18)#5	0.93	2.77	3.631(7)	153.7
C(36)-H(36A)...O(8)#5	0.97	2.84	3.676(8)	145.0
C(34)-H(34B)...O(1)#8	0.97	2.76	3.683(10)	158.8
C(33)-H(33A)...O(3)#5	0.97	2.89	3.832(9)	163.9
C(1)-H(1)...O(10)#2	0.93	2.63	3.462(4)	149.6
C(8)-H(8A)...O(10)#12	0.97	2.50	3.210(3)	129.8
C(22)-H(22B)...O(9)#13	0.97	2.54	3.479(3)	164.2
C(26)-H(26)...O(9)#5	0.93	2.50	3.152(3)	127.5
C(3)-H(3)...O(11A)#14	0.93	2.55	3.387(6)	149.4
C(22)-H(22B)...O(11A)#13	0.97	2.51	3.352(6)	145.4
C(17)-H(17)...O(14B)#4	0.93	2.33	3.208(9)	158.1
C(25)-H(25)...O(12B)#15	0.93	2.79	3.672(13)	159.0
C(7)-H(7B)...O(700)#5	0.97	2.63	3.541(10)	155.8
C(13)-H(13)...O(700)#8	0.93	2.76	3.366(10)	123.6
O(19)-H(19B)...O(16)#9	0.83(5)	2.14(5)	2.831(6)	140(5)
O(40)-H(40A)...O(13)#4	0.66(3)	2.31(4)	2.940(6)	162(4)
O(40)-H(40A)...O(600)#4	0.66(3)	2.06(4)	2.694(13)	161(4)
O(40)-H(40B)...O(19)#14	0.87(4)	1.84(4)	2.696(3)	171(4)
O(19)-H(19B)...O(700)#4	0.83(5)	1.81(5)	2.632(8)	171(5)

Symmetry transformations used to generate equivalent atoms: #1 x,-y+2,z-1/2 #2 -x+1,-y+2,-z+1
#3 x,-y+2,z+1/2 #4 x,y,z #5 -x+1,y,-z+3/2 #6 -x+2,y,-z+5/2 #7 x+1,y+1,z+1 #8 -x+1,y+1,-z+3/2
#9 x-1,y-1,z-1 #10 -x,y,-z+1/2 #11 -x+1,-y+2,-z+2 #12 x+1,y,z+1 #13 x,y,z+1 #14 -x+1,-y+1,-z+1
#15 -x+1,-y+1,-z+2

I.2.m - Crystal data and structure refinement for 13.

Empirical formula	C72 H86 Cl4 Cu2 N8 O39
Formula weight	1956.37
Temperature	293(2) K
Wavelength	0.71073 Å
Crystal system	Monoclinic
Space group	P21/c

Unit cell dimensions	a = 19.6910(11) Å	α = 90°.
	b = 18.6897(16) Å	β = 91.748(5)°.
	c = 23.5089(13) Å	γ = 90°.
Volume	8647.7(10) Å^{3}	
Z	4	
Density (calculated)	1.503 Mg/m^{3}	
Absorption coefficient	0.711 mm^{-1}	
F(000)	4048	
Crystal size	? x ? x ? mm^{3}	
Theta range for data collection	3.03 to 29.96°.	
Index ranges	-27<=h<=26, -11<=k<=25, -31<=l<=33	
Reflections collected	41387	
Independent reflections	21936 [R(int) = 0.0415]	
Completeness to theta = 29.96°	87.3 %	
Refinement method	Full-matrix least-squares on F^{2}	
Data / restraints / parameters	21936 / 0 / 1226	
Goodness-of-fit on F^{2}	1.073	
Final R indices [I>2sigma(I)]	R1 = 0.0882, wR2 = 0.2042	
R indices (all data)	R1 = 0.1305, wR2 = 0.2262	
Extinction coefficient	0.00132(12)	
Largest diff. peak and hole	1.629 and -0.952 e.Å^{-3}	

Atomic coordinates (x 10^{4}) and equivalent isotropic displacement parameters (Å^{2}x 10^{3}) for **13**. U(eq) is defined as one third of the trace of the orthogonalized U^{ij} tensor.

	x	y	z	U(eq)
Cu(1)	7315(1)	3611(1)	2967(1)	22(1)
O(1)	7230(2)	4778(2)	2648(2)	32(1)
Cu(2)	7378(1)	-1405(1)	3258(1)	23(1)
O(2)	7295(3)	-279(2)	2890(2)	38(1)
N(1)	6551(2)	3748(2)	3524(2)	23(1)
C(1)	6608(2)	3521(3)	4071(2)	24(1)
C(2)	6108(2)	3644(3)	4467(2)	25(1)
C(3)	5970(2)	4091(3)	3352(2)	24(1)
C(4)	5445(2)	4214(3)	3715(2)	25(1)
C(5)	5512(2)	3994(3)	4282(2)	23(1)
C(6)	4923(2)	4123(3)	4664(2)	24(1)
O(3)	4377(2)	4338(3)	4492(2)	46(1)
O(4)	5092(2)	3975(2)	5211(1)	29(1)
C(7)	4540(3)	3983(3)	5603(2)	30(1)
C(8)	4337(2)	3217(3)	5735(2)	30(1)
O(5)	4805(2)	2908(2)	6172(2)	29(1)
C(9)	5317(2)	2511(3)	5986(2)	24(1)
O(6)	5421(2)	2358(2)	5497(2)	31(1)

C(10)	5769(2)	2252(3)	6481(2)	23(1)
C(11)	5798(2)	2608(3)	7009(2)	26(1)
C(12)	6237(2)	2339(3)	7430(2)	25(1)
C(13)	6182(3)	1657(3)	6398(2)	29(1)
C(14)	6611(3)	1433(3)	6842(2)	29(1)
N(2)	6642(2)	1766(2)	7355(2)	24(1)
N(3)	7999(2)	3873(2)	3593(2)	24(1)
C(15)	8495(2)	3415(3)	3757(2)	27(1)
C(16)	8934(2)	3555(3)	4215(2)	26(1)
C(17)	7934(3)	4502(3)	3882(2)	28(1)
C(18)	8355(3)	4681(3)	4345(2)	29(1)
C(19)	8860(2)	4193(3)	4523(2)	25(1)
C(20)	9292(2)	4382(3)	5042(2)	24(1)
O(7)	9279(2)	4963(2)	5276(2)	33(1)
O(8)	9666(2)	3815(2)	5214(1)	29(1)
C(21)	10099(3)	3930(3)	5729(2)	32(1)
C(22)	10286(2)	3192(3)	5949(2)	33(1)
O(9)	9672(2)	2891(2)	6188(2)	27(1)
C(23)	9754(3)	2237(3)	6428(2)	31(1)
O(10)	10255(2)	1867(2)	6395(2)	47(1)
C(24)	9144(2)	2035(3)	6769(2)	25(1)
C(25)	9096(3)	1320(3)	6969(2)	28(1)
C(26)	8554(2)	1156(3)	7309(2)	25(1)
C(27)	8664(3)	2544(3)	6917(2)	30(1)
C(28)	8135(3)	2321(3)	7252(2)	27(1)
N(4)	8081(2)	1646(2)	7447(2)	24(1)
N(5)	6594(2)	-1252(2)	3796(2)	24(1)
C(29)	6633(2)	-1488(3)	4340(2)	23(1)
C(30)	6111(2)	-1378(3)	4716(2)	23(1)
C(31)	6024(3)	-903(3)	3610(2)	27(1)
C(32)	5487(2)	-773(3)	3963(2)	25(1)
C(33)	5524(2)	-1008(3)	4525(2)	23(1)
C(34)	4932(2)	-879(3)	4902(2)	23(1)
O(11)	4404(2)	-612(2)	4730(2)	28(1)
O(12)	5080(2)	-1087(2)	5440(1)	23(1)
C(35)	4521(3)	-1090(3)	5834(2)	30(1)
C(36)	4376(3)	-1859(3)	6010(2)	31(1)
O(13)	4875(2)	-2115(2)	6439(1)	29(1)
C(37)	5411(2)	-2487(3)	6261(2)	26(1)
O(14)	5519(2)	-2625(2)	5765(2)	34(1)
C(38)	5859(2)	-2735(3)	6751(2)	26(1)
C(39)	5851(3)	-2406(3)	7281(2)	28(1)
C(40)	6292(3)	-2665(3)	7713(2)	29(1)
C(41)	6302(3)	-3305(3)	6667(2)	29(1)
C(42)	6731(3)	-3531(3)	7116(2)	28(1)
N(6)	6719(2)	-3216(2)	7634(2)	25(1)
N(7)	8035(2)	-1096(2)	3896(2)	26(1)
C(43)	8037(3)	-396(3)	4077(2)	32(1)
C(44)	8455(3)	-168(3)	4529(2)	31(1)
C(45)	8451(3)	-1565(3)	4171(2)	29(1)
C(46)	8873(3)	-1369(3)	4632(2)	30(1)
C(47)	8877(2)	-659(3)	4808(2)	24(1)
C(48)	9313(2)	-396(3)	5306(2)	28(1)
O(15)	9386(2)	231(2)	5426(2)	35(1)
O(16)	9604(2)	-948(2)	5596(2)	32(1)
C(49)	10030(3)	-745(3)	6089(2)	34(1)
C(50)	10280(2)	-1426(3)	6366(2)	33(1)
O(17)	9705(2)	-1776(2)	6622(2)	38(1)
C(51)	9843(3)	-2402(3)	6886(2)	37(1)
O(18)	10389(2)	-2697(3)	6890(2)	48(1)
C(52)	9242(3)	-2684(3)	7194(2)	35(1)
C(53)	8716(3)	-2235(3)	7353(2)	34(1)
C(54)	8188(3)	-2531(3)	7651(2)	34(1)
C(55)	9217(3)	-3414(3)	7341(3)	41(2)

C(56)	8677(3)	-3658(3)	7648(2)	39(1)
N(8)	8159(2)	-3229(2)	7802(2)	30(1)
Cl(1)	7599(1)	1512(1)	3492(1)	28(1)
O(19)	7311(2)	2235(2)	3437(2)	32(1)
O(20)	7078(2)	1020(2)	3672(2)	38(1)
O(21)	8145(2)	1530(2)	3911(2)	48(1)
O(22)	7851(3)	1271(2)	2955(2)	62(2)
Cl(2)	7506(1)	-3563(1)	3738(1)	18(1)
O(23)	7267(9)	-2786(9)	3760(8)	25(4)
O(24)	8215(7)	-3590(9)	3833(10)	108(8)
O(25)	7135(7)	-3997(7)	4137(6)	37(5)
O(26)	7359(6)	-3824(7)	3162(5)	81(3)
Cl(21)	7529(2)	-3310(2)	4267(1)	46(1)
O(231)	7345(11)	-2875(11)	3769(10)	34(5)
O(241)	8189(6)	-3466(7)	4216(8)	75(5)
O(251)	7178(9)	-3982(9)	4114(8)	66(7)
O(261)	7296(6)	-3012(6)	4804(4)	69(3)
Cl(3)	4759(1)	5387(1)	2472(1)	32(1)
O(27)	5059(2)	5779(2)	2951(2)	43(1)
O(28)	4489(3)	4719(3)	2671(2)	61(2)
O(29)	4139(7)	5847(11)	2188(9)	32(3)
O(291)	4316(7)	5766(12)	2234(9)	38(3)
O(30)	5269(2)	5241(3)	2066(2)	59(1)
Cl(4)	184(1)	382(1)	2315(1)	39(1)
O(31)	-21(3)	1097(3)	2137(2)	54(1)
O(32)	810(2)	431(2)	2655(2)	41(1)
O(33)	-339(2)	82(3)	2666(2)	48(1)
O(34)	273(3)	-80(3)	1826(2)	64(1)
O(35)	2710(2)	126(3)	3486(2)	55(1)
C(350)	2102(4)	382(4)	3737(3)	59(2)
C(351)	2235(6)	1089(6)	4020(6)	112(4)
C(352)	2888(5)	1356(5)	3707(5)	91(3)
C(353)	3267(4)	658(7)	3646(4)	94(4)
O(36)	2270(5)	6060(5)	3673(3)	32(2)
C(360)	2919(9)	6331(11)	3487(8)	57(6)
C(361)	3445(7)	5862(10)	3849(6)	59(4)
C(362)	3030(6)	5324(8)	4186(6)	46(3)
C(363)	2344(7)	5677(7)	4222(5)	36(3)
O(361)	2530(5)	5077(5)	3198(4)	58(3)
C(364)	3081(8)	5507(10)	3455(7)	65(4)
C(365)	2744(14)	6154(10)	3718(10)	70(6)
C(366)	2046(10)	5793(10)	3921(9)	69(6)
C(367)	1860(7)	5337(8)	3354(7)	57(4)
O(37)	2532(4)	7385(3)	4865(3)	100(3)
C(370)	1862(5)	7647(5)	4707(4)	74(3)
C(371)	1981(4)	8377(4)	4413(3)	58(2)
C(372)	2601(3)	8678(4)	4758(3)	46(2)
C(373)	2974(4)	7989(4)	4978(3)	55(2)
O(38)	7778(6)	-2588(6)	5269(5)	71(3)
C(380)	7216(7)	-3063(8)	5348(6)	49(3)
C(381)	7563(7)	-3753(8)	5554(6)	51(3)
C(382)	8167(9)	-3539(11)	5865(7)	60(4)
C(383)	8460(9)	-2891(10)	5404(8)	71(5)
O(381)	9246(7)	-2864(8)	5915(6)	88(4)
C(384)	8575(10)	-2541(11)	5789(9)	82(5)
C(385)	8100(8)	-3114(10)	6084(7)	64(4)
C(386)	8413(10)	-3792(11)	5922(8)	71(5)
C(387)	9100(11)	-3553(12)	5784(9)	91(6)
O(39)	8292(4)	83(4)	2108(3)	34(2)
O(40)	6522(6)	-4131(7)	3059(5)	74(3)

Bond lengths [Å] and angles [°] for **13**.

Cu(1)-N(3)	2.025(4)	C(41)-C(42)	1.397(7)
Cu(1)-N(4)#1	2.029(4)	C(41)-H(41)	0.9300
Cu(1)-N(1)	2.041(4)	C(42)-N(6)	1.353(6)
Cu(1)-N(2)#1	2.052(4)	C(42)-H(42)	0.9300
Cu(1)-O(1)	2.311(4)	N(6)-Cu(2)#4	2.055(4)
Cu(1)-O(19)	2.799(4)	N(7)-C(45)	1.351(6)
Cu(1)-Cu(1)#2	12.4667(7)	N(7)-C(43)	1.374(7)
O(1)-H(1)	0.68(7)	C(43)-C(44)	1.391(7)
O(1)-H(1A)	0.97(8)	C(43)-H(43)	0.9300
Cu(2)-N(8)#3	2.022(4)	C(44)-C(47)	1.389(7)
Cu(2)-N(7)	2.035(4)	C(44)-H(44)	0.9300
Cu(2)-N(5)	2.044(4)	C(45)-C(46)	1.393(7)
Cu(2)-N(6)#3	2.055(4)	C(45)-H(45)	0.9300
Cu(2)-O(2)	2.278(5)	C(46)-C(47)	1.391(7)
Cu(2)-O(23)	2.850(17)	C(46)-H(46)	0.9300
Cu(2)-Cu(2)#4	12.4471(8)	C(47)-C(48)	1.513(7)
O(2)-H(2)	0.56(6)	C(48)-O(15)	1.213(7)
O(2)-H(2A)	0.99(9)	C(48)-O(16)	1.354(6)
N(1)-C(1)	1.355(6)	O(16)-C(49)	1.460(6)
N(1)-C(3)	1.362(6)	C(49)-C(50)	1.505(8)
C(1)-C(2)	1.395(7)	C(49)-H(49A)	0.9700
C(1)-H(1B)	0.9300	C(49)-H(49B)	0.9700
C(2)-C(5)	1.401(7)	C(50)-O(17)	1.454(6)
C(2)-H(2B)	0.9300	C(50)-H(50A)	0.9700
C(3)-C(4)	1.379(7)	C(50)-H(50B)	0.9700
C(3)-H(3)	0.9300	O(17)-C(51)	1.349(7)
C(4)-C(5)	1.398(7)	C(51)-O(18)	1.207(6)
C(4)-H(4)	0.9300	C(51)-C(52)	1.503(7)
C(5)-C(6)	1.507(7)	C(52)-C(53)	1.393(7)
C(6)-O(3)	1.205(6)	C(52)-C(55)	1.409(8)
C(6)-O(4)	1.347(6)	C(53)-C(54)	1.385(7)
O(4)-C(7)	1.447(6)	C(53)-H(53)	0.9300
C(7)-C(8)	1.521(8)	C(54)-N(8)	1.354(7)
C(7)-H(7A)	0.9700	C(54)-H(54)	0.9300
C(7)-H(7B)	0.9700	C(55)-C(56)	1.379(8)
C(8)-O(5)	1.476(6)	C(55)-H(55)	0.9300
C(8)-H(8A)	0.9700	C(56)-N(8)	1.356(7)
C(8)-H(8B)	0.9700	C(56)-H(56)	0.9300
O(5)-C(9)	1.335(6)	N(8)-Cu(2)#4	2.022(4)
C(9)-O(6)	1.209(6)	Cl(1)-O(21)	1.436(4)
C(9)-C(10)	1.522(6)	Cl(1)-O(22)	1.442(4)
C(10)-C(13)	1.395(7)	Cl(1)-O(20)#5	1.451(4)
C(10)-C(11)	1.407(7)	Cl(1)-O(20)	1.451(4)
C(11)-C(12)	1.389(7)	Cl(1)-O(19)	1.471(4)
C(11)-H(11)	0.9300	O(20)-O(20)#5	0.000(12)
C(12)-N(2)	1.352(6)	Cl(2)-O(24)	1.407(15)
C(12)-H(12)	0.9300	Cl(2)-O(25)	1.453(8)
C(13)-C(14)	1.389(7)	Cl(2)-O(26)	1.460(13)
C(13)-H(13)	0.9300	Cl(2)-O(23)	1.528(16)
C(14)-N(2)	1.355(6)	O(26)-O(40)	1.755(17)
C(14)-H(14)	0.9300	Cl(21)-O(241)	1.341(12)
N(2)-Cu(1)#2	2.052(4)	Cl(21)-O(231)	1.46(2)
N(3)-C(15)	1.345(6)	Cl(21)-O(261)#5	1.467(10)
N(3)-C(17)	1.366(6)	Cl(21)-O(261)	1.467(10)
C(15)-C(16)	1.386(7)	Cl(21)-O(251)	1.472(17)
C(15)-H(15)	0.9300	O(251)-O(40)	2.78(2)
C(16)-C(19)	1.404(7)	O(261)-O(261)#5	0.00(4)
C(16)-H(16)	0.9300	Cl(3)-O(291)	1.243(11)
C(17)-C(18)	1.388(7)	Cl(3)-O(30)	1.432(5)
C(17)-H(17)	0.9300	Cl(3)-O(28)#5	1.441(5)
C(18)-C(19)	1.404(7)	Cl(3)-O(28)	1.441(5)
C(18)-H(18)	0.9300	Cl(3)-O(27)	1.455(4)

C(19)-C(20)	1.508(7)
C(20)-O(7)	1.219(6)
C(20)-O(8)	1.347(6)
O(8)-C(21)	1.475(6)
C(21)-C(22)	1.515(8)
C(21)-H(21A)	0.9700
C(21)-H(21B)	0.9700
C(22)-O(9)	1.463(6)
C(22)-H(22A)	0.9700
C(22)-H(22B)	0.9700
O(9)-C(23)	1.354(6)
C(23)-O(10)	1.208(6)
C(23)-C(24)	1.511(7)
C(24)-C(27)	1.393(7)
C(24)-C(25)	1.420(7)
C(25)-C(26)	1.387(7)
C(25)-H(25)	0.9300
C(26)-N(4)	1.352(6)
C(26)-H(26)	0.9300
C(27)-C(28)	1.389(7)
C(27)-H(27)	0.9300
C(28)-N(4)	1.348(6)
C(28)-H(28)	0.9300
N(4)-Cu(1)#2	2.029(4)
N(5)-C(29)	1.354(6)
N(5)-C(31)	1.358(6)
C(29)-C(30)	1.391(6)
C(29)-H(29)	0.9300
C(30)-C(33)	1.407(6)
C(30)-H(30)	0.9300
C(31)-C(32)	1.386(7)
C(31)-H(31)	0.9300
C(32)-C(33)	1.392(7)
C(32)-H(32)	0.9300
C(33)-C(34)	1.506(7)
C(34)-O(11)	1.212(6)
C(34)-O(12)	1.347(6)
O(12)-C(35)	1.460(6)
C(35)-C(36)	1.525(8)
C(35)-H(35A)	0.9700
C(35)-H(35B)	0.9700
C(36)-O(13)	1.466(6)
C(36)-H(36A)	0.9700
C(36)-H(36B)	0.9700
O(13)-C(37)	1.341(6)
C(37)-O(14)	1.219(6)
C(37)-C(38)	1.505(7)
C(38)-C(39)	1.389(7)
C(38)-C(41)	1.395(7)
C(39)-C(40)	1.402(7)
C(39)-H(39)	0.9300
C(40)-N(6)	1.346(7)
C(40)-H(40)	0.9300
Cl(3)-O(29)	1.621(10)
O(28)-O(28)#5	0.000(13)
Cl(4)-O(33)	1.452(5)
Cl(4)-O(34)	1.452(5)
Cl(4)-O(32)	1.452(4)
Cl(4)-O(31)	1.454(5)
O(35)-C(350)	1.431(8)
O(35)-C(353)	1.519(11)
C(350)-C(351)	1.499(13)
C(351)-C(352)	1.581(13)
C(352)-C(353)	1.511(15)
O(36)-C(360)	1.454(17)
O(36)-C(363)	1.480(14)
C(360)-C(361)	1.59(2)
C(361)-C(362)	1.53(2)
C(362)-C(363)	1.508(17)
O(361)-C(367)	1.463(16)
O(361)-C(364)	1.47(2)
O(361)-O(39)#6	1.751(13)
C(364)-C(365)	1.52(3)
C(365)-C(366)	1.62(3)
C(366)-C(367)	1.61(3)
C(367)-O(39)#6	1.213(18)
O(37)-C(370)	1.445(11)
O(37)-C(373)	1.446(10)
C(370)-C(371)	1.551(11)
C(371)-C(372)	1.551(10)
C(372)-C(373)	1.563(10)
O(38)-C(380)	1.435(17)
O(38)-C(383)	1.48(2)
C(380)-C(381)	1.53(2)
C(381)-C(382)	1.43(2)
C(381)-C(386)	1.86(2)
C(381)-C(385)	2.00(2)
C(382)-C(386)	0.69(2)
C(382)-C(385)	0.96(2)
C(382)-C(383)	1.74(3)
C(382)-C(387)	1.85(3)
C(382)-C(384)	2.04(3)
C(383)-C(384)	1.14(2)
C(383)-C(385)	1.82(2)
C(383)-C(387)	1.96(3)
O(381)-C(387)	1.35(2)
O(381)-C(384)	1.47(2)
C(384)-C(385)	1.59(3)
C(385)-C(386)	1.46(3)
C(386)-C(387)	1.47(3)
O(39)-O(39)#5	0.00(2)
O(39)-C(367)#7	1.213(18)
O(39)-O(361)#7	1.751(13)
O(39)-O(36)#7	2.792(12)
O(39)-O(33)#8	2.962(9)
O(40)-O(27)#9	2.890(13)

N(3)-Cu(1)-N(4)#1	90.33(16)
N(3)-Cu(1)-N(1)	89.40(16)
N(4)#1-Cu(1)-N(1)	173.22(17)
N(3)-Cu(1)-N(2)#1	173.90(17)
N(4)#1-Cu(1)-N(2)#1	88.40(16)
N(1)-Cu(1)-N(2)#1	91.15(16)
N(3)-Cu(1)-O(1)	92.74(16)
N(4)#1-Cu(1)-O(1)	94.37(17)
N(1)-Cu(1)-O(1)	92.41(16)
N(2)#1-Cu(1)-O(1)	93.30(16)
C(40)-N(6)-C(42)	119.0(4)
C(40)-N(6)-Cu(2)#4	123.2(3)
C(42)-N(6)-Cu(2)#4	117.7(3)
C(45)-N(7)-C(43)	118.3(4)
C(45)-N(7)-Cu(2)	122.1(4)
C(43)-N(7)-Cu(2)	119.6(3)
N(7)-C(43)-C(44)	121.6(5)
N(7)-C(43)-H(43)	119.2
C(44)-C(43)-H(43)	119.2
C(47)-C(44)-C(43)	119.3(5)

N(3)-Cu(1)-O(19)	86.83(14)
N(4)#1-Cu(1)-O(19)	91.82(14)
N(1)-Cu(1)-O(19)	81.41(14)
N(2)#1-Cu(1)-O(19)	87.25(14)
O(1)-Cu(1)-O(19)	173.80(14)
N(3)-Cu(1)-Cu(1)#2	54.11(12)
N(4)#1-Cu(1)-Cu(1)#2	120.74(12)
N(1)-Cu(1)-Cu(1)#2	54.21(11)
N(2)#1-Cu(1)-Cu(1)#2	121.91(12)
O(1)-Cu(1)-Cu(1)#2	128.16(12)
O(19)-Cu(1)-Cu(1)#2	47.29(8)
Cu(1)-O(1)-H(1)	117(6)
Cu(1)-O(1)-H(1A)	123(5)
H(1)-O(1)-H(1A)	118(7)
N(8)#3-Cu(2)-N(7)	90.57(17)
N(8)#3-Cu(2)-N(5)	167.54(18)
N(7)-Cu(2)-N(5)	88.88(16)
N(8)#3-Cu(2)-N(6)#3	88.72(17)
N(7)-Cu(2)-N(6)#3	176.27(17)
N(5)-Cu(2)-N(6)#3	91.03(16)
N(8)#3-Cu(2)-O(2)	99.1(2)
N(7)-Cu(2)-O(2)	93.13(17)
N(5)-Cu(2)-O(2)	93.40(19)
N(6)#3-Cu(2)-O(2)	90.60(17)
N(8)#3-Cu(2)-O(23)	89.0(4)
N(7)-Cu(2)-O(23)	90.4(4)
N(5)-Cu(2)-O(23)	78.6(4)
N(6)#3-Cu(2)-O(23)	85.9(4)
O(2)-Cu(2)-O(23)	171.2(4)
N(8)#3-Cu(2)-Cu(2)#4	114.33(14)
N(7)-Cu(2)-Cu(2)#4	54.25(12)
N(5)-Cu(2)-Cu(2)#4	55.99(11)
N(6)#3-Cu(2)-Cu(2)#4	122.90(12)
O(2)-Cu(2)-Cu(2)#4	131.33(13)
O(23)-Cu(2)-Cu(2)#4	46.3(4)
Cu(2)-O(2)-H(2)	122(8)
Cu(2)-O(2)-H(2A)	122(5)
H(2)-O(2)-H(2A)	116(9)
C(1)-N(1)-C(3)	118.3(4)
C(1)-N(1)-Cu(1)	121.9(3)
C(3)-N(1)-Cu(1)	119.8(3)
N(1)-C(1)-C(2)	122.8(4)
N(1)-C(1)-H(1B)	118.6
C(2)-C(1)-H(1B)	118.6
C(1)-C(2)-C(5)	118.2(4)
C(1)-C(2)-H(2B)	120.9
C(5)-C(2)-H(2B)	120.9
N(1)-C(3)-C(4)	122.3(4)
N(1)-C(3)-H(3)	118.9
C(4)-C(3)-H(3)	118.9
C(3)-C(4)-C(5)	119.4(4)
C(3)-C(4)-H(4)	120.3
C(5)-C(4)-H(4)	120.3
C(4)-C(5)-C(2)	119.1(4)
C(4)-C(5)-C(6)	118.0(4)
C(2)-C(5)-C(6)	122.9(4)
O(3)-C(6)-O(4)	125.5(5)
O(3)-C(6)-C(5)	123.2(4)
O(4)-C(6)-C(5)	111.3(4)
C(6)-O(4)-C(7)	115.9(4)
O(4)-C(7)-C(8)	109.1(4)
O(4)-C(7)-H(7A)	109.9
C(8)-C(7)-H(7A)	109.9
O(4)-C(7)-H(7B)	109.9
C(47)-C(44)-H(44)	120.3
C(43)-C(44)-H(44)	120.3
N(7)-C(45)-C(46)	122.7(5)
N(7)-C(45)-H(45)	118.7
C(46)-C(45)-H(45)	118.7
C(47)-C(46)-C(45)	118.7(5)
C(47)-C(46)-H(46)	120.7
C(45)-C(46)-H(46)	120.7
C(44)-C(47)-C(46)	119.4(5)
C(44)-C(47)-C(48)	117.9(5)
C(46)-C(47)-C(48)	122.6(5)
O(15)-C(48)-O(16)	125.0(5)
O(15)-C(48)-C(47)	123.7(5)
O(16)-C(48)-C(47)	111.3(5)
C(48)-O(16)-C(49)	115.2(4)
O(16)-C(49)-C(50)	107.2(5)
O(16)-C(49)-H(49A)	110.3
C(50)-C(49)-H(49A)	110.3
O(16)-C(49)-H(49B)	110.3
C(50)-C(49)-H(49B)	110.3
H(49A)-C(49)-H(49B)	108.5
O(17)-C(50)-C(49)	108.1(4)
O(17)-C(50)-H(50A)	110.1
C(49)-C(50)-H(50A)	110.1
O(17)-C(50)-H(50B)	110.1
C(49)-C(50)-H(50B)	110.1
H(50A)-C(50)-H(50B)	108.4
C(51)-O(17)-C(50)	115.6(4)
O(18)-C(51)-O(17)	124.6(5)
O(18)-C(51)-C(52)	123.3(5)
O(17)-C(51)-C(52)	112.0(4)
C(53)-C(52)-C(55)	119.0(5)
C(53)-C(52)-C(51)	121.4(5)
C(55)-C(52)-C(51)	119.5(5)
C(54)-C(53)-C(52)	118.1(5)
C(54)-C(53)-H(53)	121.0
C(52)-C(53)-H(53)	121.0
N(8)-C(54)-C(53)	123.8(5)
N(8)-C(54)-H(54)	118.1
C(53)-C(54)-H(54)	118.1
C(56)-C(55)-C(52)	118.8(5)
C(56)-C(55)-H(55)	120.6
C(52)-C(55)-H(55)	120.6
N(8)-C(56)-C(55)	122.8(5)
N(8)-C(56)-H(56)	118.6
C(55)-C(56)-H(56)	118.6
C(54)-N(8)-C(56)	117.5(5)
C(54)-N(8)-Cu(2)#4	120.3(3)
C(56)-N(8)-Cu(2)#4	122.2(4)
O(21)-Cl(1)-O(22)	109.8(3)
O(21)-Cl(1)-O(20)#5	109.6(3)
O(22)-Cl(1)-O(20)#5	108.9(3)
O(21)-Cl(1)-O(20)	109.6(3)
O(22)-Cl(1)-O(20)	108.9(3)
O(20)#5-Cl(1)-O(20)	0.0(4)
O(21)-Cl(1)-O(19)	108.5(3)
O(22)-Cl(1)-O(19)	110.6(3)
O(20)#5-Cl(1)-O(19)	109.4(2)
O(20)-Cl(1)-O(19)	109.4(2)
Cl(1)-O(19)-Cu(1)	150.9(2)
O(20)#5-O(20)-Cl(1)	0(8)
O(24)-Cl(2)-O(25)	113.3(9)
O(24)-Cl(2)-O(26)	107.6(11)
O(25)-Cl(2)-O(26)	108.8(9)

C(8)-C(7)-H(7B)	109.9
H(7A)-C(7)-H(7B)	108.3
O(5)-C(8)-C(7)	110.4(4)
O(5)-C(8)-H(8A)	109.6
C(7)-C(8)-H(8A)	109.6
O(5)-C(8)-H(8B)	109.6
C(7)-C(8)-H(8B)	109.6
H(8A)-C(8)-H(8B)	108.1
C(9)-O(5)-C(8)	116.8(4)
O(6)-C(9)-O(5)	126.5(4)
O(6)-C(9)-C(10)	122.6(4)
O(5)-C(9)-C(10)	110.9(4)
C(13)-C(10)-C(11)	119.5(5)
C(13)-C(10)-C(9)	118.4(4)
C(11)-C(10)-C(9)	122.0(4)
C(12)-C(11)-C(10)	117.8(5)
C(12)-C(11)-H(11)	121.1
C(10)-C(11)-H(11)	121.1
N(2)-C(12)-C(11)	123.3(5)
N(2)-C(12)-H(12)	118.3
C(11)-C(12)-H(12)	118.3
C(14)-C(13)-C(10)	118.6(5)
C(14)-C(13)-H(13)	120.7
C(10)-C(13)-H(13)	120.7
N(2)-C(14)-C(13)	122.7(5)
N(2)-C(14)-H(14)	118.6
C(13)-C(14)-H(14)	118.6
C(12)-N(2)-C(14)	118.1(4)
C(12)-N(2)-Cu(1)#2	123.4(3)
C(14)-N(2)-Cu(1)#2	118.5(3)
C(15)-N(3)-C(17)	118.9(4)
C(15)-N(3)-Cu(1)	121.0(3)
C(17)-N(3)-Cu(1)	119.9(3)
N(3)-C(15)-C(16)	122.2(5)
N(3)-C(15)-H(15)	118.9
C(16)-C(15)-H(15)	118.9
C(15)-C(16)-C(19)	119.2(5)
C(15)-C(16)-H(16)	120.4
C(19)-C(16)-H(16)	120.4
N(3)-C(17)-C(18)	122.3(5)
N(3)-C(17)-H(17)	118.9
C(18)-C(17)-H(17)	118.9
C(17)-C(18)-C(19)	118.6(5)
C(17)-C(18)-H(18)	120.7
C(19)-C(18)-H(18)	120.7
C(18)-C(19)-C(16)	118.7(5)
C(18)-C(19)-C(20)	117.8(5)
C(16)-C(19)-C(20)	123.4(4)
O(7)-C(20)-O(8)	125.8(4)
O(7)-C(20)-C(19)	123.7(4)
O(8)-C(20)-C(19)	110.4(4)
C(20)-O(8)-C(21)	115.4(4)
O(8)-C(21)-C(22)	106.0(4)
O(8)-C(21)-H(21A)	110.5
C(22)-C(21)-H(21A)	110.5
O(8)-C(21)-H(21B)	110.5
C(22)-C(21)-H(21B)	110.5
H(21A)-C(21)-H(21B)	108.7
O(9)-C(22)-C(21)	106.6(4)
O(9)-C(22)-H(22A)	110.4
C(21)-C(22)-H(22A)	110.4
O(9)-C(22)-H(22B)	110.4
C(21)-C(22)-H(22B)	110.4
H(22A)-C(22)-H(22B)	108.6
O(24)-Cl(2)-O(23)	109.5(10)
O(25)-Cl(2)-O(23)	110.3(9)
O(26)-Cl(2)-O(23)	107.3(9)
Cl(2)-O(23)-Cu(2)	145.0(10)
Cl(2)-O(26)-O(40)	113.3(9)
O(241)-Cl(21)-O(231)	105.5(11)
O(241)-Cl(21)-O(261)#5	119.2(10)
O(231)-Cl(21)-O(261)#5	113.7(9)
O(241)-Cl(21)-O(261)	119.2(10)
O(231)-Cl(21)-O(261)	113.7(9)
O(261)#5-Cl(21)-O(261)	0.0(10)
O(241)-Cl(21)-O(251)	104.0(10)
O(231)-Cl(21)-O(251)	100.1(12)
O(261)#5-Cl(21)-O(251)	112.2(9)
O(261)-Cl(21)-O(251)	112.2(9)
Cl(21)-O(251)-O(40)	120.4(10)
O(261)#5-O(261)-Cl(21)	0(10)
O(291)-Cl(3)-O(30)	107.8(10)
O(291)-Cl(3)-O(28)#5	112.3(11)
O(30)-Cl(3)-O(28)#5	109.0(3)
O(291)-Cl(3)-O(28)	112.3(11)
O(30)-Cl(3)-O(28)	109.0(3)
O(28)#5-Cl(3)-O(28)	0.0(6)
O(291)-Cl(3)-O(27)	108.8(11)
O(30)-Cl(3)-O(27)	109.6(3)
O(28)#5-Cl(3)-O(27)	109.3(3)
O(28)-Cl(3)-O(27)	109.3(3)
O(291)-Cl(3)-O(29)	4.4(17)
O(30)-Cl(3)-O(29)	111.2(8)
O(28)#5-Cl(3)-O(29)	108.2(8)
O(28)-Cl(3)-O(29)	108.2(8)
O(27)-Cl(3)-O(29)	109.5(8)
O(28)#5-O(28)-Cl(3)	0(10)
O(33)-Cl(4)-O(34)	109.0(3)
O(33)-Cl(4)-O(32)	108.4(3)
O(34)-Cl(4)-O(32)	110.6(3)
O(33)-Cl(4)-O(31)	108.9(3)
O(34)-Cl(4)-O(31)	111.0(3)
O(32)-Cl(4)-O(31)	108.9(3)
C(350)-O(35)-C(353)	106.6(6)
O(35)-C(350)-C(351)	109.9(7)
C(350)-C(351)-C(352)	101.8(8)
C(353)-C(352)-C(351)	100.6(8)
C(352)-C(353)-O(35)	103.5(7)
C(360)-O(36)-C(363)	111.5(10)
O(36)-C(360)-C(361)	102.2(11)
C(362)-C(361)-C(360)	106.9(10)
C(363)-C(362)-C(361)	103.6(11)
O(36)-C(363)-C(362)	103.1(9)
C(367)-O(361)-C(364)	112.2(11)
C(367)-O(361)-O(39)#6	43.2(7)
C(364)-O(361)-O(39)#6	146.0(10)
O(361)-C(364)-C(365)	106.0(14)
C(364)-C(365)-C(366)	100.0(14)
C(367)-C(366)-C(365)	98.7(12)
O(39)#6-C(367)-O(361)	81.1(10)
O(39)#6-C(367)-C(366)	171.1(15)
O(361)-C(367)-C(366)	101.4(12)
C(370)-O(37)-C(373)	108.9(6)
O(37)-C(370)-C(371)	105.2(7)
C(372)-C(371)-C(370)	102.3(6)
C(371)-C(372)-C(373)	103.2(6)
O(37)-C(373)-C(372)	107.9(6)
C(380)-O(38)-C(383)	115.6(12)

C(23)-O(9)-C(22)	114.7(4)
O(10)-C(23)-O(9)	125.2(5)
O(10)-C(23)-C(24)	123.7(5)
O(9)-C(23)-C(24)	111.1(4)
C(27)-C(24)-C(25)	120.5(5)
C(27)-C(24)-C(23)	121.2(5)
C(25)-C(24)-C(23)	118.2(4)
C(26)-C(25)-C(24)	117.3(5)
C(26)-C(25)-H(25)	121.3
C(24)-C(25)-H(25)	121.3
N(4)-C(26)-C(25)	122.4(5)
N(4)-C(26)-H(26)	118.8
C(25)-C(26)-H(26)	118.8
C(28)-C(27)-C(24)	117.6(5)
C(28)-C(27)-H(27)	121.2
C(24)-C(27)-H(27)	121.2
N(4)-C(28)-C(27)	122.9(5)
N(4)-C(28)-H(28)	118.6
C(27)-C(28)-H(28)	118.6
C(28)-N(4)-C(26)	119.3(4)
C(28)-N(4)-Cu(1)#2	119.6(3)
C(26)-N(4)-Cu(1)#2	121.0(3)
C(29)-N(5)-C(31)	118.9(4)
C(29)-N(5)-Cu(2)	121.1(3)
C(31)-N(5)-Cu(2)	120.0(3)
N(5)-C(29)-C(30)	122.1(4)
N(5)-C(29)-H(29)	119.0
C(30)-C(29)-H(29)	119.0
C(29)-C(30)-C(33)	119.0(4)
C(29)-C(30)-H(30)	120.5
C(33)-C(30)-H(30)	120.5
N(5)-C(31)-C(32)	122.0(4)
N(5)-C(31)-H(31)	119.0
C(32)-C(31)-H(31)	119.0
C(31)-C(32)-C(33)	119.5(5)
C(31)-C(32)-H(32)	120.2
C(33)-C(32)-H(32)	120.2
C(32)-C(33)-C(30)	118.5(4)
C(32)-C(33)-C(34)	119.2(4)
C(30)-C(33)-C(34)	122.2(4)
O(11)-C(34)-O(12)	126.2(4)
O(11)-C(34)-C(33)	122.8(4)
O(12)-C(34)-C(33)	111.0(4)
C(34)-O(12)-C(35)	116.9(4)
O(12)-C(35)-C(36)	109.0(4)
O(12)-C(35)-H(35A)	109.9
C(36)-C(35)-H(35A)	109.9
O(12)-C(35)-H(35B)	109.9
C(36)-C(35)-H(35B)	109.9
H(35A)-C(35)-H(35B)	108.3
O(13)-C(36)-C(35)	111.5(4)
O(13)-C(36)-H(36A)	109.3
C(35)-C(36)-H(36A)	109.3
O(13)-C(36)-H(36B)	109.3
C(35)-C(36)-H(36B)	109.3
H(36A)-C(36)-H(36B)	108.0
C(37)-O(13)-C(36)	118.1(4)
O(14)-C(37)-O(13)	124.8(5)
O(14)-C(37)-C(38)	123.5(5)
O(13)-C(37)-C(38)	111.6(4)
C(39)-C(38)-C(41)	119.4(5)
C(39)-C(38)-C(37)	121.9(5)
C(41)-C(38)-C(37)	118.7(5)
C(38)-C(39)-C(40)	118.2(5)
O(38)-C(380)-C(381)	102.9(11)
C(382)-C(381)-C(380)	106.4(13)
C(382)-C(381)-C(386)	18.9(10)
C(380)-C(381)-C(386)	124.5(12)
C(382)-C(381)-C(385)	26.3(9)
C(380)-C(381)-C(385)	85.2(10)
C(386)-C(381)-C(385)	44.3(9)
C(386)-C(382)-C(385)	125(3)
C(386)-C(382)-C(381)	119(3)
C(385)-C(382)-C(381)	112(2)
C(386)-C(382)-C(383)	111(3)
C(385)-C(382)-C(383)	79.2(17)
C(381)-C(382)-C(383)	99.3(13)
C(386)-C(382)-C(387)	47(2)
C(385)-C(382)-C(387)	102.8(19)
C(381)-C(382)-C(387)	138.9(15)
C(383)-C(382)-C(387)	66.2(11)
C(386)-C(382)-C(384)	112(3)
C(385)-C(382)-C(384)	49.5(15)
C(381)-C(382)-C(384)	122.2(14)
C(383)-C(382)-C(384)	33.8(8)
C(387)-C(382)-C(384)	67.1(11)
C(384)-C(383)-O(38)	96.1(17)
C(384)-C(383)-C(382)	88.0(17)
O(38)-C(383)-C(382)	94.9(12)
C(384)-C(383)-C(385)	60.2(14)
O(38)-C(383)-C(385)	84.3(11)
C(382)-C(383)-C(385)	31.2(8)
C(384)-C(383)-C(387)	83.7(16)
O(38)-C(383)-C(387)	154.6(15)
C(382)-C(383)-C(387)	59.8(11)
C(385)-C(383)-C(387)	73.5(11)
C(387)-O(381)-C(384)	99.3(15)
C(383)-C(384)-O(381)	94.6(18)
C(383)-C(384)-C(385)	81.7(17)
O(381)-C(384)-C(385)	99.9(15)
C(383)-C(384)-C(382)	58.2(14)
O(381)-C(384)-C(382)	87.8(13)
C(385)-C(384)-C(382)	27.2(8)
C(382)-C(385)-C(386)	22.6(15)
C(382)-C(385)-C(384)	103.3(19)
C(386)-C(385)-C(384)	102.2(14)
C(382)-C(385)-C(383)	69.6(16)
C(386)-C(385)-C(383)	77.9(13)
C(384)-C(385)-C(383)	38.2(9)
C(382)-C(385)-C(381)	41.5(15)
C(386)-C(385)-C(381)	62.7(12)
C(384)-C(385)-C(381)	115.8(13)
C(383)-C(385)-C(381)	78.5(10)
C(382)-C(386)-C(385)	32(2)
C(382)-C(386)-C(387)	113(3)
C(385)-C(386)-C(387)	101.1(16)
C(382)-C(386)-C(381)	43(2)
C(385)-C(386)-C(381)	73.0(13)
C(387)-C(386)-C(381)	134.9(16)
O(381)-C(387)-C(386)	115.4(19)
O(381)-C(387)-C(382)	99.6(15)
C(386)-C(387)-C(382)	19.9(10)
O(381)-C(387)-C(383)	68.4(12)
C(386)-C(387)-C(383)	73.1(13)
C(382)-C(387)-C(383)	54.0(10)
O(39)#5-O(39)-C(367)#7	0(10)
O(39)#5-O(39)-O(361)#7	0(10)
C(367)#7-O(39)-O(361)#7	55.7(8)

C(38)-C(39)-H(39)	120.9	O(39)#5-O(39)-O(36)#7	0(10)
C(40)-C(39)-H(39)	120.9	C(367)#7-O(39)-O(36)#7	22.3(8)
N(6)-C(40)-C(39)	122.7(5)	O(361)#7-O(39)-O(36)#7	52.5(4)
N(6)-C(40)-H(40)	118.7	O(39)#5-O(39)-O(33)#8	0(10)
C(39)-C(40)-H(40)	118.7	C(367)#7-O(39)-O(33)#8	126.4(8)
C(38)-C(41)-C(42)	119.3(5)	O(361)#7-O(39)-O(33)#8	177.9(5)
C(38)-C(41)-H(41)	120.3	O(36)#7-O(39)-O(33)#8	129.0(3)
C(42)-C(41)-H(41)	120.3	O(26)-O(40)-O(251)	55.5(7)
N(6)-C(42)-C(41)	121.4(5)	O(26)-O(40)-O(27)#9	163.9(8)
N(6)-C(42)-H(42)	119.3	O(251)-O(40)-O(27)#9	121.3(6)
C(41)-C(42)-H(42)	119.3		

Symmetry transformations used to generate equivalent atoms: #1 x,-y+1/2,z-1/2 #2 x,-y+1/2,z+1/2 #3 x,-y-1/2,z-1/2 #4 x,-y-1/2,z+1/2 #5 x,y,z #6 -x+1,y+1/2,-z+1/2 #7 -x+1,y-1/2,-z+1/2 #8 x+1,y,z #9 x,y-1,z

Anisotropic displacement parameters ($Å^2$x 10^3) for **13**. The anisotropic displacement factor exponent takes the form: $-2\pi^2[h^2a^{*2}U^{11} + ... + 2 h k a^* b^* U^{12}]$

	U^{11}	U^{22}	U^{33}	U^{23}	U^{13}	U^{12}
Cu(1)	19(1)	25(1)	23(1)	-1(1)	0(1)	0(1)
O(1)	39(2)	26(2)	32(2)	1(2)	1(2)	0(2)
Cu(2)	23(1)	24(1)	23(1)	-2(1)	3(1)	0(1)
O(2)	63(3)	24(2)	26(2)	1(2)	-3(2)	-3(2)
N(1)	23(2)	22(2)	25(2)	1(2)	1(2)	0(2)
C(1)	25(2)	22(2)	26(2)	5(2)	0(2)	0(2)
C(2)	27(2)	22(2)	26(2)	2(2)	2(2)	-1(2)
C(3)	25(2)	27(3)	20(2)	4(2)	-2(2)	0(2)
C(4)	19(2)	31(3)	24(2)	0(2)	-3(2)	2(2)
C(5)	26(2)	19(2)	23(2)	1(2)	-2(2)	-3(2)
C(6)	28(2)	23(2)	22(2)	-2(2)	-3(2)	6(2)
O(3)	36(2)	68(3)	34(2)	6(2)	5(2)	26(2)
O(4)	29(2)	34(2)	25(2)	2(2)	2(1)	5(2)
C(7)	28(3)	39(3)	22(2)	3(2)	6(2)	8(2)
C(8)	17(2)	43(3)	31(3)	5(2)	1(2)	3(2)
O(5)	22(2)	37(2)	28(2)	5(2)	2(1)	7(2)
C(9)	21(2)	24(2)	26(2)	0(2)	-3(2)	-3(2)
O(6)	38(2)	33(2)	22(2)	-1(2)	-2(2)	7(2)
C(10)	21(2)	25(2)	24(2)	1(2)	2(2)	2(2)
C(11)	26(2)	24(3)	26(2)	-1(2)	1(2)	3(2)
C(12)	24(2)	27(3)	23(2)	-3(2)	3(2)	1(2)
C(13)	29(3)	32(3)	27(2)	-5(2)	4(2)	4(2)
C(14)	29(2)	31(3)	27(2)	-8(2)	4(2)	5(2)
N(2)	17(2)	29(2)	27(2)	2(2)	-1(2)	1(2)
N(3)	20(2)	22(2)	28(2)	-1(2)	0(2)	1(2)
C(15)	24(2)	29(3)	28(2)	-1(2)	4(2)	1(2)
C(16)	20(2)	26(3)	32(3)	3(2)	-1(2)	3(2)
C(17)	27(2)	24(3)	33(3)	1(2)	-5(2)	6(2)
C(18)	31(3)	21(3)	36(3)	1(2)	-1(2)	-1(2)
C(19)	20(2)	27(3)	28(2)	6(2)	1(2)	-4(2)
C(20)	19(2)	27(3)	25(2)	5(2)	1(2)	-1(2)
O(7)	32(2)	37(2)	30(2)	1(2)	-3(2)	1(2)
O(8)	33(2)	30(2)	24(2)	4(1)	-12(2)	-5(2)
C(21)	28(3)	40(3)	28(3)	10(2)	-10(2)	-7(2)
C(22)	20(2)	44(3)	37(3)	12(2)	-3(2)	-6(2)
O(9)	21(2)	27(2)	32(2)	8(2)	2(1)	-3(1)
C(23)	32(3)	29(3)	33(3)	8(2)	4(2)	1(2)
O(10)	36(2)	50(3)	57(3)	27(2)	19(2)	17(2)
C(24)	22(2)	27(3)	26(2)	2(2)	0(2)	0(2)
C(25)	28(2)	26(3)	29(2)	2(2)	3(2)	3(2)
C(26)	27(2)	20(2)	28(2)	2(2)	2(2)	2(2)
C(27)	32(3)	23(3)	33(3)	3(2)	4(2)	1(2)

C(28)	28(2)	23(3)	30(3)	2(2)	2(2)	4(2)
N(4)	24(2)	25(2)	24(2)	3(2)	0(2)	2(2)
N(5)	23(2)	25(2)	24(2)	0(2)	0(2)	1(2)
C(29)	22(2)	23(2)	25(2)	0(2)	-3(2)	1(2)
C(30)	25(2)	23(2)	20(2)	-1(2)	0(2)	1(2)
C(31)	30(2)	29(3)	22(2)	2(2)	2(2)	3(2)
C(32)	24(2)	22(2)	29(2)	5(2)	2(2)	1(2)
C(33)	22(2)	23(2)	25(2)	-3(2)	0(2)	0(2)
C(34)	27(2)	17(2)	25(2)	-1(2)	4(2)	-3(2)
O(11)	26(2)	31(2)	28(2)	-1(2)	3(1)	8(2)
O(12)	23(2)	25(2)	22(2)	2(1)	0(1)	2(1)
C(35)	30(3)	34(3)	26(2)	1(2)	5(2)	5(2)
C(36)	22(2)	37(3)	35(3)	5(2)	-1(2)	5(2)
O(13)	28(2)	33(2)	25(2)	4(2)	2(1)	4(2)
C(37)	24(2)	27(3)	28(2)	3(2)	1(2)	-7(2)
O(14)	35(2)	39(2)	26(2)	-1(2)	-3(2)	7(2)
C(38)	24(2)	23(2)	30(3)	7(2)	4(2)	-4(2)
C(39)	26(2)	28(3)	31(3)	1(2)	4(2)	1(2)
C(40)	33(3)	30(3)	22(2)	0(2)	-1(2)	0(2)
C(41)	34(3)	30(3)	23(2)	-2(2)	4(2)	3(2)
C(42)	32(3)	26(3)	26(2)	2(2)	3(2)	7(2)
N(6)	26(2)	23(2)	27(2)	0(2)	7(2)	-4(2)
N(7)	23(2)	25(2)	29(2)	-1(2)	6(2)	1(2)
C(43)	31(3)	24(3)	41(3)	3(2)	-4(2)	1(2)
C(44)	34(3)	25(3)	34(3)	0(2)	-1(2)	-1(2)
C(45)	29(3)	23(3)	35(3)	-1(2)	3(2)	5(2)
C(46)	28(2)	30(3)	33(3)	4(2)	0(2)	5(2)
C(47)	20(2)	27(3)	24(2)	5(2)	7(2)	-1(2)
C(48)	22(2)	37(3)	26(2)	5(2)	3(2)	-2(2)
O(15)	38(2)	30(2)	37(2)	0(2)	-8(2)	-1(2)
O(16)	32(2)	31(2)	34(2)	11(2)	1(2)	-3(2)
C(49)	28(3)	40(3)	33(3)	9(2)	-2(2)	-7(2)
C(50)	21(2)	51(4)	27(2)	8(2)	6(2)	-1(2)
O(17)	24(2)	48(2)	44(2)	22(2)	8(2)	8(2)
C(51)	32(3)	48(4)	32(3)	16(3)	11(2)	11(3)
O(18)	32(2)	60(3)	53(3)	28(2)	17(2)	19(2)
C(52)	27(3)	43(3)	36(3)	17(3)	8(2)	9(2)
C(53)	29(3)	29(3)	43(3)	15(2)	9(2)	10(2)
C(54)	25(2)	31(3)	46(3)	7(2)	9(2)	7(2)
C(55)	32(3)	45(4)	46(3)	20(3)	18(2)	20(3)
C(56)	38(3)	39(3)	41(3)	22(3)	13(2)	17(3)
N(8)	25(2)	30(2)	34(2)	10(2)	7(2)	6(2)
Cl(1)	29(1)	26(1)	29(1)	2(1)	3(1)	1(1)
O(19)	33(2)	24(2)	38(2)	0(2)	2(2)	3(2)
O(20)	28(2)	30(2)	54(2)	8(2)	4(2)	-4(2)
O(21)	28(2)	50(3)	65(3)	16(2)	-12(2)	0(2)
O(22)	114(4)	31(2)	43(3)	-2(2)	35(3)	4(3)
Cl(2)	17(1)	12(1)	23(1)	-2(1)	8(1)	-1(1)
O(23)	21(5)	12(5)	44(7)	9(4)	7(4)	12(4)
O(24)	34(6)	80(10)	220(20)	73(13)	74(11)	43(6)
O(25)	32(7)	27(8)	53(8)	31(6)	40(6)	-4(5)
Cl(21)	36(2)	46(2)	55(2)	-2(2)	-4(1)	3(1)
O(241)	26(5)	45(7)	157(15)	37(8)	53(8)	16(4)
O(251)	47(9)	50(11)	98(13)	-42(8)	-31(8)	26(7)
O(261)	107(9)	59(7)	42(5)	-16(5)	-6(6)	18(6)
Cl(3)	41(1)	31(1)	23(1)	0(1)	-4(1)	1(1)
O(27)	52(3)	39(2)	38(2)	-13(2)	-5(2)	3(2)
O(28)	90(4)	45(3)	47(3)	14(2)	-32(3)	-24(3)
O(29)	9(6)	51(7)	34(5)	20(4)	-18(5)	33(5)
O(291)	18(8)	59(7)	35(6)	13(5)	-18(6)	40(6)
O(30)	46(3)	87(4)	44(3)	-24(3)	4(2)	12(3)
Cl(4)	47(1)	34(1)	36(1)	10(1)	-8(1)	-4(1)
O(31)	67(3)	43(3)	51(3)	22(2)	-14(2)	7(2)
O(32)	36(2)	35(2)	53(3)	5(2)	-2(2)	1(2)

O(33)	43(2)	50(3)	51(3)	3(2)	-4(2)	-11(2)
O(34)	94(4)	56(3)	40(3)	-3(2)	-6(3)	3(3)
O(35)	57(3)	59(3)	47(3)	-21(2)	4(2)	3(2)
C(350)	47(4)	59(5)	72(5)	-18(4)	15(4)	5(3)
C(351)	111(9)	78(7)	150(11)	-31(7)	70(8)	-31(6)
C(352)	97(7)	65(6)	114(8)	-4(6)	54(6)	-20(5)
C(353)	37(4)	164(11)	83(6)	-40(7)	3(4)	-3(5)
O(36)	35(5)	36(5)	24(4)	-2(3)	-8(4)	-1(4)
C(360)	41(8)	77(13)	53(10)	35(9)	-5(7)	-24(8)
C(361)	30(6)	98(13)	50(8)	22(8)	7(6)	6(7)
C(362)	33(6)	58(8)	47(7)	11(6)	-6(5)	14(6)
C(363)	42(7)	34(7)	31(6)	3(5)	5(5)	4(5)
O(361)	65(6)	51(6)	57(6)	-2(5)	17(5)	4(5)
C(364)	65(10)	75(11)	55(9)	-24(8)	19(8)	7(8)
C(365)	93(19)	43(10)	73(15)	-24(10)	-39(13)	-6(10)
C(366)	87(14)	52(10)	71(12)	13(9)	52(12)	30(9)
C(367)	44(7)	55(9)	71(10)	7(8)	18(7)	16(7)
O(37)	147(6)	50(3)	97(5)	-17(3)	-78(5)	21(4)
C(370)	93(6)	57(5)	71(5)	19(4)	-36(5)	-18(5)
C(371)	67(5)	51(4)	55(4)	3(3)	-16(4)	6(4)
C(372)	49(4)	50(4)	40(3)	0(3)	5(3)	9(3)
C(373)	57(4)	60(5)	49(4)	13(3)	6(3)	13(4)

Hydrogen coordinates (x 10^4) and isotropic displacement parameters (Å^{2}x 10^3) for **13**.

	x	y	z	U(eq)
H(1)	7160(30)	5030(40)	2850(30)	30(20)
H(1A)	7180(40)	4910(40)	2250(40)	70(20)
H(2)	7390(30)	-210(40)	2680(30)	20(20)
H(2A)	7040(40)	110(50)	3080(40)	80(30)
H(1B)	6998	3273	4187	29
H(2B)	6169	3498	4843	30
H(3)	5925	4247	2977	29
H(4)	5051	4442	3584	30
H(7A)	4154	4239	5435	36
H(7B)	4682	4227	5951	36
H(8A)	3877	3209	5871	36
H(8B)	4348	2931	5391	36
H(11)	5532	3010	7073	31
H(12)	6252	2566	7783	30
H(13)	6170	1416	6051	35
H(14)	6888	1038	6786	35
H(15)	8544	2991	3556	32
H(16)	9274	3230	4318	31
H(17)	7596	4822	3764	34
H(18)	8303	5115	4532	35
H(21A)	9853	4194	6013	39
H(21B)	10504	4197	5638	39
H(22A)	10442	2894	5641	40
H(22B)	10646	3223	6239	40
H(25)	9415	976	6875	33
H(26)	8514	692	7447	30
H(27)	8696	3016	6796	36
H(28)	7804	2652	7346	33
H(29)	7020	-1731	4467	28
H(30)	6149	-1546	5088	28
H(31)	5994	-746	3235	32
H(32)	5103	-531	3825	30
H(35A)	4119	-882	5653	36
H(35B)	4642	-806	6168	36
H(36A)	3925	-1887	6163	37

H(36B)	4386	-2166	5678	37
H(39)	5560	-2025	7348	34
H(40)	6290	-2448	8068	34
H(41)	6312	-3532	6315	34
H(42)	7031	-3907	7058	34
H(43)	7752	-68	3893	38
H(44)	8452	308	4643	37
H(45)	8456	-2038	4048	35
H(46)	9147	-1707	4817	36
H(49A)	9769	-467	6355	40
H(49B)	10411	-458	5971	40
H(50A)	10476	-1737	6084	40
H(50B)	10627	-1319	6655	40
H(53)	8719	-1751	7262	40
H(54)	7834	-2233	7753	41
H(55)	9557	-3726	7233	49
H(56)	8669	-4137	7753	47

Torsion angles [°] for **13**.

N(3)-Cu(1)-N(1)-C(1)	-40.8(4)	O(261)#5-Cl(21)-O(251)-O(40)	125.8(9)
N(4)#1-Cu(1)-N(1)-C(1)	47.0(15)	O(261)-Cl(21)-O(251)-O(40)	125.8(9)
N(2)#1-Cu(1)-N(1)-C(1)	133.2(4)	O(241)-Cl(21)-O(261)-O(261)#5	0.0(6)
O(1)-Cu(1)-N(1)-C(1)	-133.5(4)	O(231)-Cl(21)-O(261)-O(261)#5	0.0(6)
O(19)-Cu(1)-N(1)-C(1)	46.1(4)	O(251)-Cl(21)-O(261)-O(261)#5	0.0(3)
Cu(1)#2-Cu(1)-N(1)-C(1)	3.6(3)	O(291)-Cl(3)-O(28)-O(28)#5	0.0(2)
N(3)-Cu(1)-N(1)-C(3)	137.7(4)	O(30)-Cl(3)-O(28)-O(28)#5	0.0(3)
N(4)#1-Cu(1)-N(1)-C(3)	-134.5(13)	O(27)-Cl(3)-O(28)-O(28)#5	0.0(3)
N(2)#1-Cu(1)-N(1)-C(3)	-48.4(4)	O(29)-Cl(3)-O(28)-O(28)#5	0.0(2)
O(1)-Cu(1)-N(1)-C(3)	45.0(4)	C(353)-O(35)-C(350)-C(351)	3.8(10)
O(19)-Cu(1)-N(1)-C(3)	-135.4(4)	O(35)-C(350)-C(351)-C(352)	21.4(12)
Cu(1)#2-Cu(1)-N(1)-C(3)	-178.0(4)	C(350)-C(351)-C(352)-C(353)	-37.8(11)
C(3)-N(1)-C(1)-C(2)	-2.1(7)	C(351)-C(352)-C(353)-O(35)	40.6(10)
Cu(1)-N(1)-C(1)-C(2)	176.4(4)	C(350)-O(35)-C(353)-C(352)	-28.9(9)
N(1)-C(1)-C(2)-C(5)	2.5(7)	C(363)-O(36)-C(360)-C(361)	19.1(17)
C(1)-N(1)-C(3)-C(4)	0.2(7)	O(36)-C(360)-C(361)-C(362)	3.6(18)
Cu(1)-N(1)-C(3)-C(4)	-178.3(4)	C(360)-C(361)-C(362)-C(363)	-23.7(17)
N(1)-C(3)-C(4)-C(5)	1.2(8)	C(360)-O(36)-C(363)-C(362)	-34.8(15)
C(3)-C(4)-C(5)-C(2)	-0.7(7)	C(361)-C(362)-C(363)-O(36)	34.3(13)
C(3)-C(4)-C(5)-C(6)	-178.7(5)	C(367)-O(361)-C(364)-C(365)	-9.1(19)
C(1)-C(2)-C(5)-C(4)	-1.0(7)	O(39)#6-O(361)-C(364)-C(365)	27(2)
C(1)-C(2)-C(5)-C(6)	176.9(5)	O(361)-C(364)-C(365)-C(366)	34.3(18)
C(4)-C(5)-C(6)-O(3)	7.8(8)	C(364)-C(365)-C(366)-C(367)	-44.8(16)
C(2)-C(5)-C(6)-O(3)	-170.1(5)	C(364)-O(361)-C(367)-O(39)#6	150.9(12)
C(4)-C(5)-C(6)-O(4)	-171.6(4)	C(364)-O(361)-C(367)-C(366)	-20.5(15)
C(2)-C(5)-C(6)-O(4)	10.5(7)	O(39)#6-O(361)-C(367)-C(366)	-171.4(16)
O(3)-C(6)-O(4)-C(7)	9.0(8)	C(365)-C(366)-C(367)-O(39)#6	-66(9)
C(5)-C(6)-O(4)-C(7)	-171.7(4)	C(365)-C(366)-C(367)-O(361)	39.6(15)
C(6)-O(4)-C(7)-C(8)	102.8(5)	C(373)-O(37)-C(370)-C(371)	30.3(9)
O(4)-C(7)-C(8)-O(5)	80.9(5)	O(37)-C(370)-C(371)-C(372)	-35.7(8)
C(7)-C(8)-O(5)-C(9)	-96.5(5)	C(370)-C(371)-C(372)-C(373)	27.3(7)
C(8)-O(5)-C(9)-O(6)	-2.8(7)	C(370)-O(37)-C(373)-C(372)	-12.2(9)
C(8)-O(5)-C(9)-C(10)	178.0(4)	C(371)-C(372)-C(373)-O(37)	-10.6(7)
O(6)-C(9)-C(10)-C(13)	-20.0(7)	C(383)-O(38)-C(380)-C(381)	-0.3(16)
O(5)-C(9)-C(10)-C(13)	159.2(4)	O(38)-C(380)-C(381)-C(382)	31.2(15)
O(6)-C(9)-C(10)-C(11)	157.8(5)	O(38)-C(380)-C(381)-C(386)	25.1(17)
O(5)-C(9)-C(10)-C(11)	-23.0(6)	O(38)-C(380)-C(381)-C(385)	47.0(11)
C(13)-C(10)-C(11)-C(12)	-1.0(7)	C(380)-C(381)-C(382)-C(386)	-164(3)
C(9)-C(10)-C(11)-C(12)	-178.7(4)	C(385)-C(381)-C(382)-C(386)	158(5)
C(10)-C(11)-C(12)-N(2)	1.3(7)	C(380)-C(381)-C(382)-C(385)	38(2)
C(11)-C(10)-C(13)-C(14)	0.2(7)	C(386)-C(381)-C(382)-C(385)	-158(5)
C(9)-C(10)-C(13)-C(14)	178.0(5)	C(380)-C(381)-C(382)-C(383)	-44.3(15)
C(10)-C(13)-C(14)-N(2)	0.4(8)	C(386)-C(381)-C(382)-C(383)	120(4)

C(11)-C(12)-N(2)-C(14)	-0.7(7)
C(11)-C(12)-N(2)-Cu(1)#2	177.7(4)
C(13)-C(14)-N(2)-C(12)	-0.1(8)
C(13)-C(14)-N(2)-Cu(1)#2	-178.7(4)
N(4)#1-Cu(1)-N(3)-C(15)	-52.0(4)
N(1)-Cu(1)-N(3)-C(15)	121.2(4)
N(2)#1-Cu(1)-N(3)-C(15)	26.0(17)
O(1)-Cu(1)-N(3)-C(15)	-146.4(4)
O(19)-Cu(1)-N(3)-C(15)	39.8(4)
Cu(1)#2-Cu(1)-N(3)-C(15)	76.8(4)
N(4)#1-Cu(1)-N(3)-C(17)	132.3(4)
N(1)-Cu(1)-N(3)-C(17)	-54.5(4)
N(2)#1-Cu(1)-N(3)-C(17)	-149.8(14)
O(1)-Cu(1)-N(3)-C(17)	37.9(4)
O(19)-Cu(1)-N(3)-C(17)	-135.9(4)
Cu(1)#2-Cu(1)-N(3)-C(17)	-98.9(4)
C(17)-N(3)-C(15)-C(16)	1.3(7)
Cu(1)-N(3)-C(15)-C(16)	-174.5(4)
N(3)-C(15)-C(16)-C(19)	0.4(7)
C(15)-N(3)-C(17)-C(18)	-1.2(7)
Cu(1)-N(3)-C(17)-C(18)	174.6(4)
N(3)-C(17)-C(18)-C(19)	-0.6(8)
C(17)-C(18)-C(19)-C(16)	2.2(7)
C(17)-C(18)-C(19)-C(20)	-177.5(5)
C(15)-C(16)-C(19)-C(18)	-2.1(7)
C(15)-C(16)-C(19)-C(20)	177.5(5)
C(18)-C(19)-C(20)-O(7)	-8.2(7)
C(16)-C(19)-C(20)-O(7)	172.2(5)
C(18)-C(19)-C(20)-O(8)	169.4(4)
C(16)-C(19)-C(20)-O(8)	-10.2(6)
O(7)-C(20)-O(8)-C(21)	-1.0(7)
C(19)-C(20)-O(8)-C(21)	-178.5(4)
C(20)-O(8)-C(21)-C(22)	162.3(4)
O(8)-C(21)-C(22)-O(9)	-72.1(5)
C(21)-C(22)-O(9)-C(23)	-177.3(4)
C(22)-O(9)-C(23)-O(10)	-9.5(8)
C(22)-O(9)-C(23)-C(24)	168.1(4)
O(10)-C(23)-C(24)-C(27)	163.0(6)
O(9)-C(23)-C(24)-C(27)	-14.6(7)
O(10)-C(23)-C(24)-C(25)	-12.9(8)
O(9)-C(23)-C(24)-C(25)	169.6(4)
C(27)-C(24)-C(25)-C(26)	0.5(7)
C(23)-C(24)-C(25)-C(26)	176.3(5)
C(24)-C(25)-C(26)-N(4)	0.5(7)
C(25)-C(24)-C(27)-C(28)	-1.5(8)
C(23)-C(24)-C(27)-C(28)	-177.2(5)
C(24)-C(27)-C(28)-N(4)	1.6(8)
C(27)-C(28)-N(4)-C(26)	-0.7(8)
C(27)-C(28)-N(4)-Cu(1)#2	176.8(4)
C(25)-C(26)-N(4)-C(28)	-0.4(7)
C(25)-C(26)-N(4)-Cu(1)#2	-177.9(4)
N(8)#3-Cu(2)-N(5)-C(29)	43.1(10)
N(7)-Cu(2)-N(5)-C(29)	-44.5(4)
N(6)#3-Cu(2)-N(5)-C(29)	131.8(4)
O(2)-Cu(2)-N(5)-C(29)	-137.6(4)
O(23)-Cu(2)-N(5)-C(29)	46.1(5)
Cu(2)#4-Cu(2)-N(5)-C(29)	1.7(3)
N(8)#3-Cu(2)-N(5)-C(31)	-137.5(7)
N(7)-Cu(2)-N(5)-C(31)	134.9(4)
N(6)#3-Cu(2)-N(5)-C(31)	-48.8(4)
O(2)-Cu(2)-N(5)-C(31)	41.8(4)
O(23)-Cu(2)-N(5)-C(31)	-134.5(6)
Cu(2)#4-Cu(2)-N(5)-C(31)	-178.9(4)
C(31)-N(5)-C(29)-C(30)	-0.6(7)
C(385)-C(381)-C(382)-C(383)	-82(2)
C(380)-C(381)-C(382)-C(387)	-109(2)
C(386)-C(381)-C(382)-C(387)	56(3)
C(385)-C(381)-C(382)-C(387)	-146(4)
C(380)-C(381)-C(382)-C(384)	-17.4(19)
C(386)-C(381)-C(382)-C(384)	147(4)
C(385)-C(381)-C(382)-C(384)	-55.2(19)
C(380)-O(38)-C(383)-C(384)	-112.4(17)
C(380)-O(38)-C(383)-C(382)	-23.9(16)
C(380)-O(38)-C(383)-C(385)	-53.3(14)
C(380)-O(38)-C(383)-C(387)	-24(4)
C(386)-C(382)-C(383)-C(384)	-98(3)
C(385)-C(382)-C(383)-C(384)	25(2)
C(381)-C(382)-C(383)-C(384)	136.5(18)
C(387)-C(382)-C(383)-C(384)	-83.9(16)
C(386)-C(382)-C(383)-O(38)	166(3)
C(385)-C(382)-C(383)-O(38)	-70.6(18)
C(381)-C(382)-C(383)-O(38)	40.5(15)
C(387)-C(382)-C(383)-O(38)	-179.8(14)
C(384)-C(382)-C(383)-O(38)	-96.0(18)
C(386)-C(382)-C(383)-C(385)	-123(4)
C(381)-C(382)-C(383)-C(385)	111(2)
C(387)-C(382)-C(383)-C(385)	-109.3(18)
C(384)-C(382)-C(383)-C(385)	-25(2)
C(386)-C(382)-C(383)-C(387)	-14(3)
C(385)-C(382)-C(383)-C(387)	109.3(18)
C(381)-C(382)-C(383)-C(387)	-139.7(16)
C(384)-C(382)-C(383)-C(387)	83.9(16)
O(38)-C(383)-C(384)-O(381)	179.2(13)
C(382)-C(383)-C(384)-O(381)	84.5(14)
C(385)-C(383)-C(384)-O(381)	99.4(14)
C(387)-C(383)-C(384)-O(381)	24.7(13)
O(38)-C(383)-C(384)-C(385)	79.9(13)
C(382)-C(383)-C(384)-C(385)	-14.8(12)
C(387)-C(383)-C(384)-C(385)	-74.6(11)
O(38)-C(383)-C(384)-C(382)	94.7(13)
C(385)-C(383)-C(384)-C(382)	14.8(12)
C(387)-C(383)-C(384)-C(382)	-59.8(10)
C(387)-O(381)-C(384)-C(383)	-38(2)
C(387)-O(381)-C(384)-C(385)	44.7(17)
C(387)-O(381)-C(384)-C(382)	20.2(15)
C(386)-C(382)-C(384)-C(383)	96(3)
C(385)-C(382)-C(384)-C(383)	-146(3)
C(381)-C(382)-C(384)-C(383)	-53(2)
C(387)-C(382)-C(384)-C(383)	81.1(17)
C(386)-C(382)-C(384)-O(381)	-1(3)
C(385)-C(382)-C(384)-O(381)	117(2)
C(381)-C(382)-C(384)-O(381)	-150.2(16)
C(383)-C(382)-C(384)-O(381)	-96.8(18)
C(387)-C(382)-C(384)-O(381)	-15.7(11)
C(386)-C(382)-C(384)-C(385)	-118(4)
C(381)-C(382)-C(384)-C(385)	93(2)
C(383)-C(382)-C(384)-C(385)	146(3)
C(387)-C(382)-C(384)-C(385)	-133(2)
C(381)-C(382)-C(385)-C(386)	156(5)
C(383)-C(382)-C(385)-C(386)	-108(4)
C(387)-C(382)-C(385)-C(386)	-46(3)
C(384)-C(382)-C(385)-C(386)	-90(4)
C(386)-C(382)-C(385)-C(384)	90(4)
C(381)-C(382)-C(385)-C(384)	-114.1(17)
C(383)-C(382)-C(385)-C(384)	-18.3(14)
C(387)-C(382)-C(385)-C(384)	44.0(19)
C(386)-C(382)-C(385)-C(383)	108(4)
C(381)-C(382)-C(385)-C(383)	-95.8(17)

Cu(2)-N(5)-C(29)-C(30)	178.8(4)
N(5)-C(29)-C(30)-C(33)	-0.1(7)
C(29)-N(5)-C(31)-C(32)	0.9(7)
Cu(2)-N(5)-C(31)-C(32)	-178.6(4)
N(5)-C(31)-C(32)-C(33)	-0.3(8)
C(31)-C(32)-C(33)-C(30)	-0.5(7)
C(31)-C(32)-C(33)-C(34)	-178.7(5)
C(29)-C(30)-C(33)-C(32)	0.7(7)
C(29)-C(30)-C(33)-C(34)	178.9(4)
C(32)-C(33)-C(34)-O(11)	4.1(7)
C(30)-C(33)-C(34)-O(11)	-174.0(5)
C(32)-C(33)-C(34)-O(12)	-174.8(4)
C(30)-C(33)-C(34)-O(12)	7.0(6)
O(11)-C(34)-O(12)-C(35)	9.6(7)
C(33)-C(34)-O(12)-C(35)	-171.4(4)
C(34)-O(12)-C(35)-C(36)	114.0(5)
O(12)-C(35)-C(36)-O(13)	78.0(5)
C(35)-C(36)-O(13)-C(37)	-95.2(5)
C(36)-O(13)-C(37)-O(14)	0.6(7)
C(36)-O(13)-C(37)-C(38)	-177.8(4)
O(14)-C(37)-C(38)-C(39)	160.2(5)
O(13)-C(37)-C(38)-C(39)	-21.3(7)
O(14)-C(37)-C(38)-C(41)	-18.8(7)
O(13)-C(37)-C(38)-C(41)	159.6(4)
C(41)-C(38)-C(39)-C(40)	-0.1(7)
C(37)-C(38)-C(39)-C(40)	-179.1(4)
C(38)-C(39)-C(40)-N(6)	-0.1(8)
C(39)-C(38)-C(41)-C(42)	-0.3(7)
C(37)-C(38)-C(41)-C(42)	178.8(5)
C(38)-C(41)-C(42)-N(6)	0.9(8)
C(39)-C(40)-N(6)-C(42)	0.7(7)
C(39)-C(40)-N(6)-Cu(2)#4	179.2(4)
C(41)-C(42)-N(6)-C(40)	-1.1(7)
C(41)-C(42)-N(6)-Cu(2)#4	-179.7(4)
N(8)#3-Cu(2)-N(7)-C(45)	-59.4(4)
N(5)-Cu(2)-N(7)-C(45)	108.1(4)
N(6)#3-Cu(2)-N(7)-C(45)	20(3)
O(2)-Cu(2)-N(7)-C(45)	-158.5(4)
O(23)-Cu(2)-N(7)-C(45)	29.6(5)
Cu(2)#4-Cu(2)-N(7)-C(45)	60.6(4)
N(8)#3-Cu(2)-N(7)-C(43)	124.0(4)
N(5)-Cu(2)-N(7)-C(43)	-68.4(4)
N(6)#3-Cu(2)-N(7)-C(43)	-157(2)
O(2)-Cu(2)-N(7)-C(43)	24.9(4)
O(23)-Cu(2)-N(7)-C(43)	-147.0(5)
Cu(2)#4-Cu(2)-N(7)-C(43)	-116.0(4)
C(45)-N(7)-C(43)-C(44)	0.3(8)
Cu(2)-N(7)-C(43)-C(44)	177.0(4)
N(7)-C(43)-C(44)-C(47)	-0.6(8)
C(43)-N(7)-C(45)-C(46)	0.7(7)
Cu(2)-N(7)-C(45)-C(46)	-175.9(4)
N(7)-C(45)-C(46)-C(47)	-1.4(8)
C(43)-C(44)-C(47)-C(46)	-0.1(8)
C(43)-C(44)-C(47)-C(48)	-178.7(5)
C(45)-C(46)-C(47)-C(44)	1.0(7)
C(45)-C(46)-C(47)-C(48)	179.5(4)
C(44)-C(47)-C(48)-O(15)	-10.5(7)
C(46)-C(47)-C(48)-O(15)	171.0(5)
C(44)-C(47)-C(48)-O(16)	169.2(4)
C(46)-C(47)-C(48)-O(16)	-9.3(6)
O(15)-C(48)-O(16)-C(49)	0.2(7)
C(47)-C(48)-O(16)-C(49)	-179.4(4)
C(48)-O(16)-C(49)-C(50)	177.7(4)
O(16)-C(49)-C(50)-O(17)	-69.6(5)
C(387)-C(382)-C(385)-C(383)	62.3(12)
C(384)-C(382)-C(385)-C(383)	18.3(14)
C(386)-C(382)-C(385)-C(381)	-156(5)
C(383)-C(382)-C(385)-C(381)	95.8(17)
C(387)-C(382)-C(385)-C(381)	158(2)
C(384)-C(382)-C(385)-C(381)	114.1(17)
C(383)-C(384)-C(385)-C(382)	28(2)
O(381)-C(384)-C(385)-C(382)	-65(2)
C(383)-C(384)-C(385)-C(386)	51.6(19)
O(381)-C(384)-C(385)-C(386)	-41.6(18)
C(382)-C(384)-C(385)-C(386)	23.2(15)
O(381)-C(384)-C(385)-C(383)	-93.2(18)
C(382)-C(384)-C(385)-C(383)	-28(2)
C(383)-C(384)-C(385)-C(381)	-13.8(19)
O(381)-C(384)-C(385)-C(381)	-107.0(14)
C(382)-C(384)-C(385)-C(381)	-42.2(16)
C(384)-C(383)-C(385)-C(382)	-150(2)
O(38)-C(383)-C(385)-C(382)	109.2(18)
C(387)-C(383)-C(385)-C(382)	-58.2(17)
C(384)-C(383)-C(385)-C(386)	-128.4(19)
O(38)-C(383)-C(385)-C(386)	131.2(14)
C(382)-C(383)-C(385)-C(386)	21.9(15)
C(387)-C(383)-C(385)-C(386)	-36.3(12)
O(38)-C(383)-C(385)-C(384)	-100.4(18)
C(382)-C(383)-C(385)-C(384)	150(2)
C(387)-C(383)-C(385)-C(384)	92.1(17)
C(384)-C(383)-C(385)-C(381)	167.4(17)
O(38)-C(383)-C(385)-C(381)	67.0(10)
C(382)-C(383)-C(385)-C(381)	-42.3(15)
C(387)-C(383)-C(385)-C(381)	-100.5(11)
C(380)-C(381)-C(385)-C(382)	-144(2)
C(386)-C(381)-C(385)-C(382)	10(2)
C(382)-C(381)-C(385)-C(386)	-10(2)
C(380)-C(381)-C(385)-C(386)	-153.9(13)
C(382)-C(381)-C(385)-C(384)	81(2)
C(380)-C(381)-C(385)-C(384)	-63.1(15)
C(386)-C(381)-C(385)-C(384)	90.8(16)
C(382)-C(381)-C(385)-C(383)	72(2)
C(380)-C(381)-C(385)-C(383)	-71.8(10)
C(386)-C(381)-C(385)-C(383)	82.2(12)
C(381)-C(382)-C(386)-C(385)	-155(5)
C(383)-C(382)-C(386)-C(385)	91(4)
C(387)-C(382)-C(386)-C(385)	73(4)
C(384)-C(382)-C(386)-C(385)	55(3)
C(385)-C(382)-C(386)-C(387)	-73(4)
C(381)-C(382)-C(386)-C(387)	132(2)
C(383)-C(382)-C(386)-C(387)	18(3)
C(384)-C(382)-C(386)-C(387)	-18(3)
C(385)-C(382)-C(386)-C(381)	155(5)
C(383)-C(382)-C(386)-C(381)	-114(3)
C(387)-C(382)-C(386)-C(381)	-132(2)
C(384)-C(382)-C(386)-C(381)	-150(4)
C(384)-C(385)-C(386)-C(382)	-95(4)
C(383)-C(385)-C(386)-C(382)	-66(4)
C(381)-C(385)-C(386)-C(382)	18(4)
C(382)-C(385)-C(386)-C(387)	116(4)
C(384)-C(385)-C(386)-C(387)	20.8(19)
C(383)-C(385)-C(386)-C(387)	50.5(15)
C(381)-C(385)-C(386)-C(387)	133.8(16)
C(382)-C(385)-C(386)-C(381)	-18(4)
C(384)-C(385)-C(386)-C(381)	-112.9(13)
C(383)-C(385)-C(386)-C(381)	-83.2(9)
C(380)-C(381)-C(386)-C(382)	18(4)
C(385)-C(381)-C(386)-C(382)	-14(3)

C(49)-C(50)-O(17)-C(51)	179.5(5)
C(50)-O(17)-C(51)-O(18)	-4.7(9)
C(50)-O(17)-C(51)-C(52)	173.5(5)
O(18)-C(51)-C(52)-C(53)	156.8(6)
O(17)-C(51)-C(52)-C(53)	-21.4(8)
O(18)-C(51)-C(52)-C(55)	-21.3(10)
O(17)-C(51)-C(52)-C(55)	160.5(6)
C(55)-C(52)-C(53)-C(54)	0.0(9)
C(51)-C(52)-C(53)-C(54)	-178.1(5)
C(52)-C(53)-C(54)-N(8)	0.8(9)
C(53)-C(52)-C(55)-C(56)	-1.2(9)
C(51)-C(52)-C(55)-C(56)	176.9(6)
C(52)-C(55)-C(56)-N(8)	1.8(10)
C(53)-C(54)-N(8)-C(56)	-0.3(9)
C(53)-C(54)-N(8)-Cu(2)#4	178.1(5)
C(55)-C(56)-N(8)-C(54)	-1.1(9)
C(55)-C(56)-N(8)-Cu(2)#4	-179.4(5)
O(21)-Cl(1)-O(19)-Cu(1)	85.1(5)
O(22)-Cl(1)-O(19)-Cu(1)	-35.4(6)
O(20)#5-Cl(1)-O(19)-Cu(1)	-155.3(4)
O(20)-Cl(1)-O(19)-Cu(1)	-155.3(4)
N(3)-Cu(1)-O(19)-Cl(1)	-85.2(5)
N(4)#1-Cu(1)-O(19)-Cl(1)	5.0(5)
N(1)-Cu(1)-O(19)-Cl(1)	-175.1(5)
N(2)#1-Cu(1)-O(19)-Cl(1)	93.3(5)
O(1)-Cu(1)-O(19)-Cl(1)	-171.4(11)
Cu(1)#2-Cu(1)-O(19)-Cl(1)	-126.8(5)
O(21)-Cl(1)-O(20)-O(20)#5	0.00(12)
O(22)-Cl(1)-O(20)-O(20)#5	0.00(4)
O(19)-Cl(1)-O(20)-O(20)#5	0.00(8)
O(24)-Cl(2)-O(23)-Cu(2)	61(2)
O(25)-Cl(2)-O(23)-Cu(2)	-174.0(17)
O(26)-Cl(2)-O(23)-Cu(2)	-56(2)
N(8)#3-Cu(2)-O(23)-Cl(2)	-9.4(19)
N(7)-Cu(2)-O(23)-Cl(2)	-100.0(19)
N(5)-Cu(2)-O(23)-Cl(2)	171.3(19)
N(6)#3-Cu(2)-O(23)-Cl(2)	79.4(19)
O(2)-Cu(2)-O(23)-Cl(2)	146.5(16)
Cu(2)#4-Cu(2)-O(23)-Cl(2)	-135(2)
O(24)-Cl(2)-O(26)-O(40)	158.3(10)
O(25)-Cl(2)-O(26)-O(40)	35.3(12)
O(23)-Cl(2)-O(26)-O(40)	-84.0(11)
O(241)-Cl(21)-O(251)-O(40)	-104.0(11)
O(231)-Cl(21)-O(251)-O(40)	4.9(13)
C(382)-C(381)-C(386)-C(385)	14(3)
C(380)-C(381)-C(386)-C(385)	32.1(16)
C(382)-C(381)-C(386)-C(387)	-75(4)
C(380)-C(381)-C(386)-C(387)	-57(3)
C(385)-C(381)-C(386)-C(387)	-89(2)
C(384)-O(381)-C(387)-C(386)	-36(2)
C(384)-O(381)-C(387)-C(382)	-22.7(16)
C(384)-O(381)-C(387)-C(383)	22.3(12)
C(382)-C(386)-C(387)-O(381)	40(4)
C(385)-C(386)-C(387)-O(381)	8(2)
C(381)-C(386)-C(387)-O(381)	85(3)
C(385)-C(386)-C(387)-C(382)	-32(3)
C(381)-C(386)-C(387)-C(382)	45(3)
C(382)-C(386)-C(387)-C(383)	-15(3)
C(385)-C(386)-C(387)-C(383)	-47.0(14)
C(381)-C(386)-C(387)-C(383)	30(2)
C(386)-C(382)-C(387)-O(381)	-144(4)
C(385)-C(382)-C(387)-O(381)	-18(2)
C(381)-C(382)-C(387)-O(381)	131(2)
C(383)-C(382)-C(387)-O(381)	54.3(14)
C(384)-C(382)-C(387)-O(381)	17.4(13)
C(385)-C(382)-C(387)-C(386)	126(4)
C(381)-C(382)-C(387)-C(386)	-85(4)
C(383)-C(382)-C(387)-C(386)	-162(4)
C(384)-C(382)-C(387)-C(386)	161(4)
C(386)-C(382)-C(387)-C(383)	162(4)
C(385)-C(382)-C(387)-C(383)	-71.9(19)
C(381)-C(382)-C(387)-C(383)	76(2)
C(384)-C(382)-C(387)-C(383)	-36.9(9)
C(384)-C(383)-C(387)-O(381)	-29.2(16)
O(38)-C(383)-C(387)-O(381)	-120(4)
C(382)-C(383)-C(387)-O(381)	-120.6(15)
C(385)-C(383)-C(387)-O(381)	-90.0(13)
C(384)-C(383)-C(387)-C(386)	97.7(18)
O(38)-C(383)-C(387)-C(386)	7(4)
C(382)-C(383)-C(387)-C(386)	6.4(13)
C(385)-C(383)-C(387)-C(386)	37.0(12)
C(384)-C(383)-C(387)-C(382)	91.3(17)
O(38)-C(383)-C(387)-C(382)	0(3)
C(385)-C(383)-C(387)-C(382)	30.6(9)
Cl(2)-O(26)-O(40)-O(251)	-19.9(7)
Cl(2)-O(26)-O(40)-O(27)#9	64(3)
Cl(21)-O(251)-O(40)-O(26)	50.0(11)
Cl(21)-O(251)-O(40)-O(27)#9	-111.2(11)

Symmetry transformations used to generate equivalent atoms: #1 x,-y+1/2,z-1/2 #2 x,-y+1/2,z+1/2 #3 x,-y-1/2,z-1/2 #4 x,-y-1/2,z+1/2 #5 x,y,z #6 -x+1,y+1/2,-z+1/2 #7 -x+1,y-1/2,-z+1/2 #8 x+1,y,z #9 x,y-1,z

Hydrogen bonds for **13** [Å and °].

D-H...A	d(D-H)	d(H...A)	d(D...A)	<(DHA)
C(41)-H(41)...O(3)#10	0.93	2.75	3.566(7)	147.2
C(36)-H(36B)...O(6)#10	0.97	2.82	3.698(7)	150.5
C(13)-H(13)...O(11)#10	0.93	2.60	3.462(6)	153.5
C(12)-H(12)...O(13)#11	0.93	2.98	3.639(6)	129.2
C(30)-H(30)...O(14)	0.93	2.87	3.611(6)	137.2
C(8)-H(8B)...O(14)#10	0.97	2.80	3.715(7)	158.1
C(15)-H(15)...O(18)#12	0.93	2.44	3.026(6)	121.1
C(14)-H(14)...O(35)#10	0.93	2.41	3.308(7)	162.5
C(42)-H(42)...O(361)#10	0.93	2.43	3.328(11)	161.2
C(4)-H(4)...O(28)#5	0.93	2.44	3.191(6)	137.8
C(8)-H(8A)...O(23)#10	0.97	2.56	3.501(19)	162.8

C(8)-H(8A)...O(25)#10	0.97	2.48	3.266(16)	138.4
C(8)-H(8A)...O(251)#10	0.97	2.53	3.337(18)	140.5
C(11)-H(11)...O(27)#13	0.93	2.54	3.457(7)	166.8
C(17)-H(17)...O(25)#14	0.93	2.55	3.281(16)	135.5
C(17)-H(17)...O(251)#14	0.93	2.53	3.254(18)	135.1
C(22)-H(22B)...O(24)#12	0.97	2.36	3.072(18)	130.1
C(22)-H(22B)...O(241)#12	0.97	2.60	3.081(13)	110.9
C(26)-H(26)...O(32)#10	0.93	2.50	3.220(6)	134.3
C(28)-H(28)...O(22)#2	0.93	2.47	3.167(7)	131.7
C(29)-H(29)...O(261)#5	0.93	2.57	3.304(12)	135.8
C(31)-H(31)...O(28)#7	0.93	2.46	3.354(7)	160.6
C(36)-H(36A)...O(20)#10	0.97	2.59	3.367(6)	137.2
C(43)-H(43)...O(20)#5	0.93	2.48	3.373(7)	162.2
C(54)-H(54)...O(26)#4	0.93	2.40	3.263(14)	154.4
C(56)-H(56)...O(39)#4	0.93	2.43	3.037(10)	122.8
O(1)-H(1)...O(26)#14	0.68(7)	2.29(7)	2.885(14)	147(7)
O(2)-H(2A)...O(20)#5	0.99(9)	2.21(9)	3.085(6)	146(7)
O(1)-H(1)...O(40)#14	0.68(7)	2.08(7)	2.666(13)	145(7)
O(2)-H(2)...O(39)#5	0.56(6)	2.32(7)	2.814(10)	150(9)
O(2)-H(2)...O(361)#7	0.56(6)	2.14(6)	2.676(11)	164(9)
O(1)-H(1A)...O(35)#6	0.97(8)	1.80(9)	2.752(6)	167(7)

Symmetry transformations used to generate equivalent atoms: #1 x,-y+1/2,z-1/2 #2 x,-y+1/2,z+1/2 #3 x,-y-1/2,z-1/2 #4 x,-y-1/2,z+1/2 #5 x,y,z #6 -x+1,y+1/2,-z+1/2 #7 -x+1,y-1/2,-z+1/2 #8 x+1,y,z #9 x,y-1,z #10 -x+1,-y,-z+1 #11 -x+1,y+1/2,-z+3/2 #12 -x+2,-y,-z+1 #13 -x+1,-y+1,-z+1 #14 x,y+1,z

II - Powder X-Ray diffraction

II.1 - Experiment

This experiment was carried out in collaboration with Dr. Antonia Neels from the University of Neuchâtel. The powder sample of **12** was inserted in a glass capillary of 0.5 mm diameter. The X-ray powder data (Graph E-1) were collected on a computer controlled STOE-STADIP focusing powder diffractometer [288] equipped with a curved Ge(111) monochromator, where the $CuK\alpha1$-line could be well separated (λ=1.5404 Å). A STOE linear position sensitive detector [289] was used. The compound was measured in the range of $6° \leq 2\theta \leq 80°$ using a step width of 0.01°. The indexing procedure was performed using TREOR [290] in the program EXPO2004 [291]. The structure solution was carried out using the program DASH introducing a structural model of the copper-ligand fragment ($Cu_{0.5}L_{0.5}$) and one nitrate anion. The obtained positions of the molecules in the given symmetry and unit cell was used for Rietveld refinement in GSAS/EXPGUI [292-294]. After the initial refinement of the scale, and unit cell constants, the atomic positions were refined using soft constraints defining the geometry of the molecule within some allowable errors [295]. Subsequent Rietveld refinement was carried out using gradually relaxing bond restraints. The copper atom position was refined anisotropically, while all remaining non-hydrogen atoms were refined isotropically applying an overall temperature factor for all carbon atoms and all nitrogen and oxygen atoms. The temperature factor of the H-atoms was fixed. In the final cycles of refinement, the shifts in all parameters were less than their estimated standard deviations. Neutral atom scattering factors were used for all atoms. No corrections were made for anomalous dispersion, absorption effects, or preferred orientation.

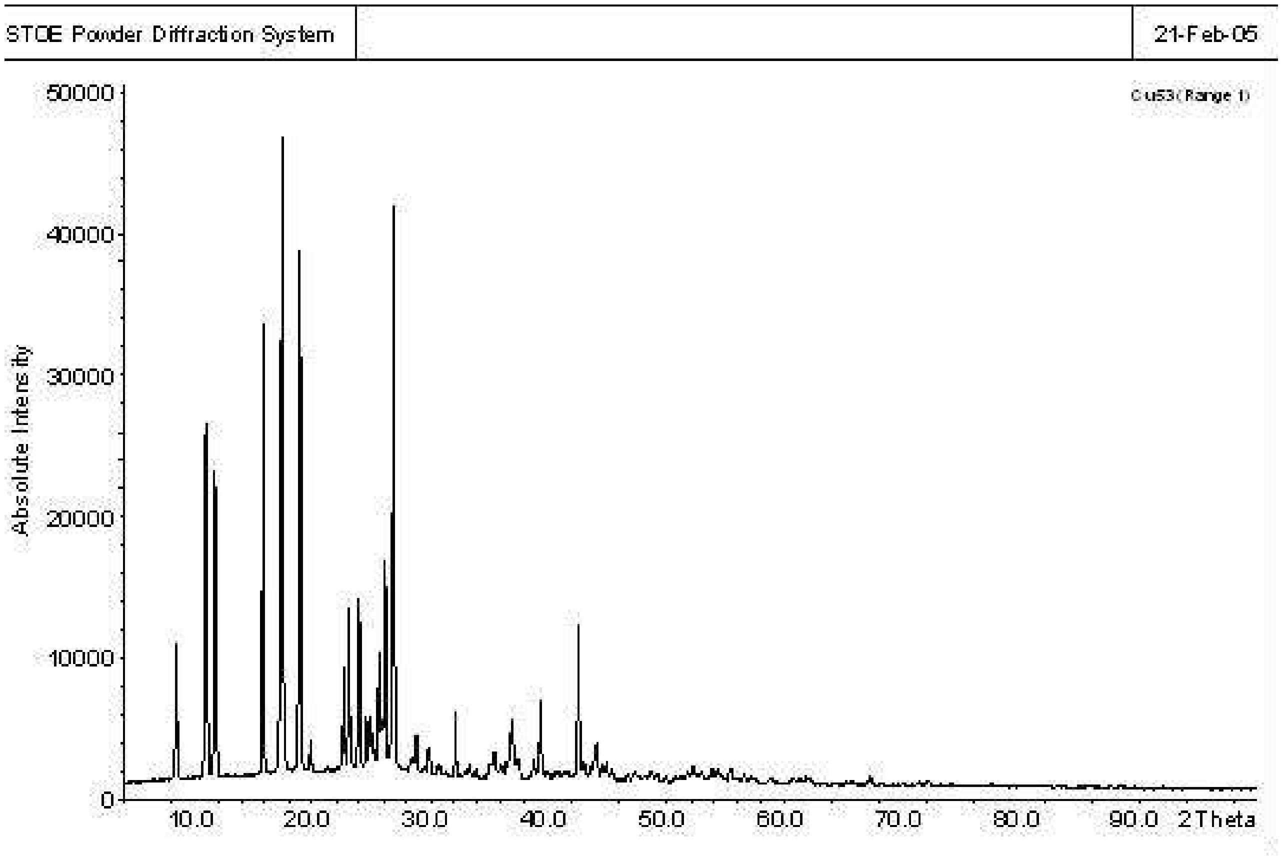

Graph E-1: Powder X-ray diffraction of 12

II.2 - Crystallographic data for 12

Empirical formula	$C_{14}H_{12}N_4O_{10}Cu_1$	
Formula weight	459.81	
Temperature	293 K	
Wavelength	1.5404 Å	
Crystal system	Triclinic	
Space group	P-1	
Unit cell dimensions	a = 5.19250(11) Å	α = 71.8835(16)°.
	b = 8.56689(19) Å	β = 83.5771(16)°.
	c = 10.8523(3) Å	γ = 77.9083(19)°.

Volume	448.07 (1)Å^{3}
Z	1
Density (calculated)	1.704 Mg/m^{3}
Absorption coefficient	2.336 mm^{-1}
Specimen form, colour	Cylinder (particle morphology: powder), green
Crystal size	0.5 × 5 × 0.5 mm^{3}
Diffractometer	Stoe STADIP
Data collection method	Specimen mounting: capillary; mode: transmission; scan method: step
Absorption correction	none
2θ (°)	$2\,\theta_{\mathrm{min}} = 6.0$, $2\,\theta_{\mathrm{max}} = 80.0$, increment = 0.01
Refinement on	I_{net}
R factors and goodness of fit	$R_p = 0.052$, $R_{\mathrm{wp}} = 0.068$, $R_{\mathrm{exp}} = 0.021$, $S = 3.36$
Profile function	pseudovoigt
No. of parameters	87
H-atom treatment	Constrained to parent site
$(\Delta/\sigma)_{\mathrm{max}}$	0.04

Computer programs: *WinXPow, Stoe & Cie* (1997); *EXPO04*; *GSAS*; *PLATON04*.

Atomic coordinates and displacement parameters for **12**

	x	y	z	U(iso or eq)	
Cu1	1.0	0.0	0.5	Uani	0.05911
C1	0.7957(14)	0.2408(7)	0.2735(5)	Uiso	0.0251(16)
C2	0.7364(11)	0.3905(8)	0.1758(4)	Uiso	0.0251(16)
C3	0.8528(12)	0.5197(6)	0.1737(4)	Uiso	0.0251(16)
C4	1.0214(11)	0.4998(7)	0.2677(5)	Uiso	0.0251(16)
C5	1.0742(11)	0.3489(8)	0.3644(4)	Uiso	0.0251(16)
C6	0.7989(11)	0.6844(6)	0.0713(4)	Uiso	0.0251(16)
C7	0.9062(11)	0.9555(6)	-0.0200(5)	Uiso	0.0251(16)
N2	0.6559(13)	0.1460(5)	0.6459(5)	Uiso	0.0491(13)
N1	0.9592(14)	0.2236(7)	0.3653(4)	Uiso	0.0491(13)
O1	0.8994(12)	0.1234(7)	0.6328(6)	Uiso	0.0491(13)
O2	0.5423(12)	0.0803(8)	0.5873(5)	Uiso	0.0491(13)
O3	0.5314(12)	0.2249(7)	0.7176(5)	Uiso	0.0491(13)
O4	0.6461(12)	0.7181(7)	-0.0112(5)	Uiso	0.0491(13)
O5	0.9472(12)	0.7912(6)	0.0789(4)	Uiso	0.0491(13)
H1	0.7134(22)	0.1538(10)	0.2728(8)	Uiso	0.05
H2	0.6210(13)	0.3993(14)	0.1135(6)	Uiso	0.05
H4	1.1022(19)	0.5867(11)	0.2683(8)	Uiso	0.05
H5	1.1904(14)	0.3405(14)	0.4270(6)	Uiso	0.05
H7	0.9319(34)	0.9540(13)	-0.1064(5)	Uiso	0.05
H8	0.7317(11)	1.0134(11)	-0.0272(16)	Uiso	0.05

Bond lengths [Å] and angles [°] for **12**.

Cu1	N1	2.002(5)	C7	O5	1.4710(35)
Cu1	N1	2.002(5)	C7	H7	0.9361(23)
Cu1	O1	2.003(6)	C7	H8	0.9362(23)
Cu1	O1	2.003(6)	N2	O1	1.237(4)
Cu1	O2	2.497(6)	N2	O2	1.230(4)
Cu1	O2	2.497(6)	N2	O3	1.230(4)
C1	C2	1.3879(34)	N1	CU1	2.002(5)
C1	N1	1.3349(35)	N1	C1	1.3349(35)
C1	H1	0.9359(22)	N1	C5	1.330(4)
C2	C1	1.3879(34)	O1	CU1	2.003(6)
C2	C3	1.3602(34)	O1	N2	1.237(4)
C2	H2	0.9286(22)	O2	CU1	2.497(6)
C3	C2	1.3602(34)	O2	N2	1.230(4)
C3	C4	1.3659(35)	O3	N2	1.230(4)
C3	C6	1.494(4)	O4	C6	1.190(4)
C4	C3	1.3659(35)	O5	C6	1.340(4)
C4	C5	1.3854(34)	O5	C7	1.4710(35)
C4	H4	0.9299(22)	H1	C1	0.9359(22)
C5	C4	1.3854(34)	H2	C2	0.9286(22)
C5	N1	1.330(4)	H4	C4	0.9299(22)
C5	H5	0.9347(22)	H5	C5	0.9347(22)
C6	C3	1.494(4)	H7	C7	0.9361(23)
C6	O4	1.190(4)	H7	H8	1.389(5)
C6	O5	1.340(4)	H8	C7	0.9362(23)
C7	C7	1.527(4)	H8	H7	1.389(5)

C2	C1	N1	121.12(34)	C7	C7	O5	101.9(4)
C2	C1	H1	117.0(5)	C7	C7	H7	114.3(5)
N1	C1	H1	121.8(5)	C7	C7	H8	114.2(5)
C1	C2	C3	118.61(32)	O5	C7	H7	115.8(5)
C1	C2	H1	24.70(17)	O5	C7	H8	115.7(5)
C1	C2	H2	119.3(5)	H7	C7	H8	95.8(5)
C3	C2	H1	143.31(31)	O1	N2	O2	116.9(5)
C3	C2	H2	122.0(5)	O1	N2	O3	122.2(6)
H1	C2	H2	94.7(5)	O2	N2	O3	120.8(6)
C2	C3	C4	119.60(33)	C1	N1	C5	120.9(4)
C2	C3	C6	121.6(5)	C1	N1	H1	23.50(18)
C4	C3	C6	118.8(5)	C1	N1	H5	144.0(4)
C3	C4	C5	120.22(32)	C5	N1	H1	144.3(4)
C3	C4	H4	120.9(5)	C5	N1	H5	23.13(19)
C3	C4	H5	144.73(31)	H1	N1	H5	167.48(34)
C5	C4	H4	118.9(5)	C6	O5	C7	115.8(4)
C5	C4	H5	24.51(17)	C1	H1	C2	38.29(31)
H4	C4	H5	94.4(5)	C1	H1	N1	34.66(32)
C4	C5	N1	119.59(34)	C2	H1	N1	72.94(21)
C4	C5	H5	117.5(5)	C4	H5	C5	37.95(31)
N1	C5	H5	122.9(5)	C4	H5	N1	71.94(21)
C3	C6	O4	124.5(5)	C5	H5	N1	34.00(32)
C3	C6	O5	112.9(4)	C7	H7	H8	42.11(25)
O4	C6	O5	122.6(5)	C7	H8	H7	42.10(25)

F - Bibliography

[1] A.Y. Robin, K.M. Fromm, H. Goesmann, G. Bernardinelli. *CrystEngComm*, **2003**, *5*, 405-410.

[2] A.Y. Robin, M. Meuwly, K.M. Fromm, H. Goesmann, G. Bernardinelli. *CrystEngComm*, **2004**, *6*, 336-343.

[3] K.M. Fromm, R. Bergougnant, W. Maudez, A.Y. Robin, J. Sagué. *Z. Anorg. Allg. Chem.*, **2005**, *631*, 1725-1740.

[4] J.C. Bailar, Jr. *Prep. Inorg. React.*, **1964**, *1*, 1-27.

[5] C. Janiak. *Dalton Trans.*, **2003**, (14), 2781-2804.

[6] B. Moulton, M.J. Zaworotko. *Chem. Rev.*, **2001**, *101*(6), 1629-1658.

[7] J.M. Lehn, *Supramolecular Chemistry: Concepts and Perspectives*. **1995**, VCH, Weinheim.

[8] S. Kitagawa, S. Noro. *Compreh. Coord. Chem.*, **2004**, *7*, 231-261.

[9] A.J. Blake, N.R. Champness, P. Hubberstey, W.-S. Li, M.A. Withersby, M. Schroder. *Coord. Chem. Rev.*, **1999**, *183*, 117-138.

[10] S.A. Barnett, N.R. Champness. *Coord. Chem. Rev.*, **2003**, *246*(1-2), 145-168.

[11] A.N. Khlobystov, A.J. Blake, N.R. Champness, D.A. Lemenovskii, A.G. Majouga, N.V. Zyk, M. Schroder. *Coord. Chem. Rev.*, **2001**, *222*, 155-192.

[12] T. Steiner. *Angew. Chem., Ed. Engl.*, **2002**, *41*(1), 48-76.

[13] A. Nangia. *CrystEngComm*, **2002**, *4*, 93-101.

[14] G. Aullon, D. Bellamy, A.G. Orpen, L. Brammer, E.A. Bruton. *Chem. Comm.*, **1998**, (6), 653-654.

[15] G.R. Desiraju. *Acc. Chem. Res*, **1996**, *29*(9), 441-449.

[16] C. Janiak. *Dalton Trans.*, **2000**, (21), 3885-3896.

[17] P. Pyykkö. *Chem. Rev.*, **1997**, *97*, 597-636.

[18] W. Clegg. *Compreh. Coord. Chem.*, **2004**, *1*, 579-583.

[19] L. Carlucci, G. Ciani, D.M. Proserpio. *Coord. Chem. Rev.*, **2003**, *246*(1-2), 247-289.

[20] K.T. Holman, H.H. Hammud, S. Isber, M. Tabbal. *Polyhedron*, **2005**, *24*(2), 221-228.

[21] H.J. Choi, M.P. Suh. *Inorg. Chem.*, **1999**, *38*(26), 6309-6312.

[22] G. De Munno, D. Armentano, T. Poerio, M. Julve, J.A. Real. *Dalton Trans.*, **1999**, (11), 1813-1818.

[23] G.-P. Yong, Z.-Y. Wang, Y. Cui. *Eur. J. Inorg. Chem.*, **2004**, (21), 4317-4323.

[24] B. Paul, B. Zimmermann, K.M. Fromm, C. Janiak. *Z. Anorg. Allg. Chem.*, **2004**, *630*(11), 1650-1654.

[25] X. Shi, G. Zhu, X. Wang, G. Li, Q. Fang, G. Wu, G. Tian, M. Xue, X. Zhao, R. Wang, S. Qiu. *Cryst. Grow. Des.*, **2005**, *5*(1), 207-213.

[26] J.L. Manson, T. Lancaster, L.C. Chapon, S.J. Blundell, J.A. Schlueter, M.L. Brooks, F.L. Pratt, C.L. Nygren, J.S. Qualls. *Inorg. Chem.*, **2005**, *44*(4), 989-995.

[27] M.B. Zaman, M.D. Smith, D.M. Ciurtin, H.-C. Zur Loye. *Inorg. Chem.*, **2002**, *41*(19), 4895-4903.

[28] Y.-B. Dong, R.C. Layland, M.D. Smith, N.G. Pschirer, U.H.F. Bunz, H.-C. Zur Loye. *Inorg. Chem.*, **1999**, *38*(13), 3056-3060.

[29] H. Zhu, C. Huang, W. Huang, S. Gou. *Inorg. Chem. Comm.*, **2004**, *7*(10), 1095-1099.

[30] R. Wang, L. Han, L. Xu, Y. Gong, Y. Zhou, M. Hong, A.S.C. Chan. *Eur. J. Inorg. Chem.*, **2004**, (18), 3751-3763.

[31] B.O. Patrick, C.L. Stevens, A. Storr, R.C. Thompson. *Polyhedron*, **2003**, *22*(22), 3025-3035.

[32] R. Horikoshi, M. Mikuriya. *Cryst. Grow. Des.*, **2005**, *5*(1), 223-230.

[33] C. Ruiz-Perez, P. Lorenzo-Luis, M. Hernandez-Molina, M.M. Laz, F.S. Delgado, P. Gili, M. Julve. *Eur. J. Inorg. Chem.*, **2004**, (19), 3873-3879.

[34] B.M. Wells, C.P. Landee, M.M. Turnbull, F.F. Awwadi, B. Twamley. *J. Mol. Catal. A*, **2005**, *228*(1-2), 117-123.

[35] J.-Y. Cheng, Y.-B. Dong, R.-Q. Huang, M.D. Smith. *Inorg. Chim. Acta*, **2005**, *358*(4), 891-902.

[36] M. Hong, W. Su, R. Cao, M. Fujita, J. Lu. *Chem. Eur. J.*, **2000**, *6*(3), 427-431.

[37] E. Psillakis, J.C. Jeffery, J.A. McCleverty, M.D. Ward. *Dalton Trans.*, **1997**, (9), 1645-1651.

[38] Y.-F. Hsu, J.-D. Chen. *Eur. J. Inorg. Chem.*, **2004**, (7), 1488-1493.

[39] L. Carlucci, G. Ciani, D.W. v. Gundenberg, D.M. Proserpio. *Inorg. Chem.*, **1997**, *36*(18), 3812-3813.

[40] E.-Q. Gao, Y.-X. Xu, C.-H. Yan. *CrystEngComm*, **2004**, *6*, 298-302.

[41] Y.-r. Xie, H. Zhao, X.-s. Wang, Z.-r. Qu, R.-g. Xiong, X. Xue, Z. Xue, X.-z. You. *Eur. J. Inorg. Chem.*, **2003**, (20), 3712-3715.

[42] K. Uemura, S. Kitagawa, K. Fukui, K. Saito. *J. Am. Chem. Soc.*, **2004**, *126*(12), 3817-3828.

[43] Z. Spichal, M. Necas, J. Pinkas, J. Novosad. *Inorg. Chem.*, **2004**, *43*(9), 2776-2778.

[44] X.-M. Ouyang, B.-L. Fei, T.-a. Okamura, H.-W. Bu, W.-Y. Sun, W.-X. Tang, N. Ueyama. *Eur. J. Inorg. Chem.*, **2003**, (4), 618-627.

[45] Z. Spichal, M. Necas, J. Pinkas. *Inorg. Chem.*, **2005**, *44*(6), 2074-2080.

[46] M. Du, X.-J. Zhao. *Inorg. Chem. Comm.*, **2004**, *7*(9), 1056-1060.

[47] Z.-F. Chen, R.-G. Xiong, B.F. Abrahams, X.-Z. You, C.-M. Che. *Dalton Trans.*, **2001**, (17), 2453-2455.

[48] W. Lin, L. Ma, O.R. Evans. *Chem. Comm.*, **2000**, (22), 2263-2264.

[49] M. Du, X.-H. Bu, Y.-M. Guo, H. Liu, S.R. Batten, J. Ribas, T.C.W. Mak. *Inorg. Chem.*, **2002**, *41*(19), 4904-4908.

[50] L. Carlucci, G. Ciani, D.M. Proserpio, S. Rizzato. *Chem. Eur. J.*, **2002**, *8*(7), 1519-1526.

[51] S. Noro, S. Kitagawa, M. Kondo, K. Seki. *Angew. Chem., Ed. Engl.*, **2000**, *39*(12), 2082-2084.

[52] J. Tao, M.-L. Tong, X.-M. Chen. *Dalton Trans.*, **2000**, (20), 3669-3674.

[53] H. Li, M. Eddaoudi, M. O'Keeffe, M. Yaghi. *Nature*, **1999**, *402*(6759), 276-279.

[54] M. Eddaoudi, J. Kim, N. Rosi, D. Vodak, J. Wachter, M. O'Keeffe, M. Yaghi Omar. *Science*, **2002**, *295*(5554), 469-472.

[55] C.V.K. Sharma. *Cryst. Grow. Des.*, **2002**, *2*(6), 465-474.

[56] J. Bernstein, R.J. Davey, J.-O. Henck. *Angew. Chem., Ed. Engl.*, **1999**, *38*(23), 3441-3461.

[57] B. Rodriguez-Spong, C.P. Price, A. Jayasankar, A.J. Matzger, N. Rodriguez-Hornedo. *Adv. Drug Deliv. Rev.*, **2004**, *56*(3), 241-274.

[58] D.B. Cordes, A.S. Bailey, P.L. Caradoc-Davies, D.H. Gregory, L.R. Hanton, K. Lee, M.D. Spicer. *Inorg. Chem.*, **2005**, *44*(7), 2544-2552.

[59] S. Masaoka, D. Tanaka, Y. Nakanishi, S. Kitagawa. *Angew. Chem., Ed. Engl.*, **2004**, *43*(19), 2530-2534.

[60] M.-L. Tong, S. Hu, J. Wang, S. Kitagawa, S.W. Ng. *Cryst. Grow. Des.*, **2005**, *5*(3), 837-839.

[61] P. Jensen, S.R. Batten, G.D. Fallon, D.C.R. Hockless, B. Moubaraki, K.S. Murray, R. Robson. *J. Solid State Chem.*, **1999**, *145*(2), 387-393.

[62] S.A. Barnett, A.J. Blake, N.R. Champness, J.E.B. Nicolson, C. Wilson. *Dalton Trans.*, **2001**, (5), 567-573.

[63] S.A. Barnett, A.J. Blake, N.R. Champness, C. Wilson. *Chem. Comm.*, **2002**, (15), 1640-1641.

[64] I.S. Lee, D.M. Shin, Y.K. Chung. *Chem. Eur. J.*, **2004**, *10*(13), 3158-3165.

[65] R.A. Heintz, H. Zhao, X. Ouyang, G. Grandinetti, J. Cowen, K.R. Dunbar. *Inorg. Chem.*, **1999**, *38*(1), 144-156.

[66] D.M. Shin, I.S. Lee, Y.K. Chung, M.S. Lah. *Chem. Comm.*, **2003**, (9), 1036-1037.

[67] A.V. Prokofiev, E. Dahlmann, F. Ritter, W. Assmus, G. Margraf, M. Wagner. *Crystal Research and Technology*, **2004**, *39*(11), 1014-1019.

[68] M.J. Hardie, C.L. Raston. *Cryst. Grow. Des.*, **2001**, *1*(1), 53-58.

[69] A. Deluzet, R. Rousseau, C. Guilbaud, I. Granger, K. Boubekeur, P. Batail, E. Canadell, P. Auban-Senzier, D. Jerome. *Chem. Eur. J.*, **2002**, *8*(17), 3884-3900.

[70] B.-Q. Ma, H.-L. Sun, S. Gao, G.-X. Xu. *Inorg. Chem.*, **2001**, *40*(24), 6247-6253.

[71] B. Rather, B. Moulton, R.D. Bailey Walsh, M.J. Zaworotko. *Chem. Comm.*, **2002**, (7), 694-695.

[72] S. Muthu, Z. Ni, J.J. Vittal. *Inorg. Chim. Acta*, **2005**, *358*(3), 595-605.

[73] S. Muthu, J.H.K. Yip, J.J. Vittal. *Dalton Trans.*, **2001**, (24), 3577-3584.

[74] L. Carlucci, G. Ciani, D.M. Proserpio, L. Spadacini. *CrystEngComm*, **2004**, *6*, 96-101.

[75] S. Kitagawa, R. Kitaura, S.-i. Noro. *Angew. Chem., Ed. Engl.*, **2004**, *43*(18), 2334-2375.

[76] S. Kitagawa, K. Uemura. *Chem. Soc. Rev.*, **2005**, *34*(2), 109-119.

[77] M. Eddaoudi, H. Li, O.M. Yaghi. *J. Am. Chem. Soc.*, **2000**, *122*(7), 1391-1397.

[78] N.L. Rosi, J. Kim, M. Eddaoudi, B. Chen, M. O'Keeffe, O.M. Yaghi. *J. Am. Chem. Soc.*, **2005**, *127*(5), 1504-1518.

[79] H.K. Chae, D.Y. Siberio-Perez, J. Kim, Y.B. Go, M. Eddaoudi, A.J. Matzger, M. O'Keeffe, O.M. Yaghi. *Nature*, **2004**, *427*(6974), 523-527.

[80] R. Kitaura, K. Fujimoto, S.-i. Noro, M. Kondo, S. Kitagawa. *Angew. Chem., Ed. Engl.*, **2002**, *41*(1), 133-135.

[81] R. Matsuda, R. Kitaura, S. Kitagawa, Y. Kubota, T.C. Kobayashi, S. Horike, M. Takata. *J. Am. Chem. Soc.*, **2004**, *126*(43), 14063-14070.

[82] Y. Kubota, M. Takata, R. Matsuda, R. Kitaura, S. Kitagawa, K. Kato, M. Sakata, T.C. Kobayashi*. Angew. Chem., Ed. Engl.*, **2005**, *44*(6), 920-923.

[83] M. Edgar, R. Mitchell, A.M.Z. Slawin, P. Lightfoot, P.A. Wright*. Chem. Eur. J.*, **2001**, *7*(23), 5168-5175.

[84] D.V. Soldatov, J.A. Ripmeester, S.I. Shergina, I.E. Sokolov, A.S. Zanina, S.A. Gromilov, Y.A. Dyadin*. J. Am. Chem. Soc.*, **1999**, *121*(17), 4179-4188.

[85] D.V. Soldatov, J.A. Ripmeester*. Chem. Mat.*, **2000**, *12*(7), 1827-1839.

[86] L. Carlucci, G. Ciani, M. Moret, D.M. Proserpio, S. Rizzato*. Angew. Chem., Ed. Engl.*, **2000**, *39*(8), 1506-1510.

[87] L.C. Tabares, J.A.R. Navarro, J.M. Salas*. J. Am. Chem. Soc.*, **2001**, *123*(3), 383-387.

[88] K.S. Min, M.P. Suh*. J. Am. Chem. Soc.*, **2000**, *122*(29), 6834-6840.

[89] T. Dewa, T. Saiki, Y. Aoyama*. J. Am. Chem. Soc.*, **2001**, *123*(3), 502-503.

[90] T. Dewa, Y. Aoyama*. J. Mol. Catal. A*, **2000**, *152*(1-2), 257-260.

[91] T. Sawaki, Y. Aoyama*. J. Am. Chem. Soc.*, **1999**, *121*(20), 4793-4798.

[92] T. Sawaki, T. Dewa, Y. Aoyama*. J. Am. Chem. Soc.*, **1998**, *120*(33), 8539-8540.

[93] L.-X. Dai*. Angew. Chem., Ed. Engl.*, **2004**, *43*(43), 5726-5729.

[94] S. Takizawa, H. Somei, D. Jayaprakash, H. Sasai*. Angew. Chem., Ed. Engl.*, **2003**, *42*(46), 5711-5714.

[95] H. Guo, X. Wang, K. Ding*. Tetrahedron Letters*, **2004**, *45*(9), 2009-2012.

[96] B. Gomez-Lor, E. Gutierrez-Puebla, M. Iglesias, M.A. Monge, C. Ruiz-Valero, N. Snejko*. Inorg. Chem.*, **2002**, *41*(9), 2429-2432.

[97] M. Hanack, S. Deger, A. Lange*. Coord. Chem. Rev.*, **1988**, *83*, 115-136.

[98] D. Sun, R. Cao, J. Weng, M. Hong, Y. Liang*. Dalton Trans.*, **2002**, (3), 291-292.

[99] C.N.R. Rao, A. Ranganathan, V.R. Pedireddi, A.R. Raju*. Chem. Comm.*, **2000**, (1), 39-40.

[100] Y. Zhao, M. Hong, Y. Liang, R. Cao, J. Weng, S. Lu, W. Li*. Chem. Comm.*, **2001**, (11), 1020-1021.

[101] M.-L. Tong, X.-M. Chen, B.-H. Ye, L.-N. Ji*. Angew. Chem., Ed. Engl.*, **1999**, *38*(15), 2237-2240.

[102] B.-L. Fei, W.-Y. Sun, T.-a. Okamura, W.-X. Tang, N. Ueyama*. NJC*, **2001**, *25*(2), 210-212.

[103] Z.-Y. Fu, X.-T. Wu, J.-C. Dai, S.-M. Hu, W.-X. Du, H.-H. Zhang, R.-Q. Sun*. Eur. J. Inorg. Chem.*, **2002**, (10), 2730-2735.

[104] Z.-Y. Fu, X.-T. Wu, J.-C. Dai, L.-M. Wu, C.-P. Cui, S.-M. Hu*. Chem. Comm.*, **2001**, (18), 1856-1857.

[105] J.-C. Dai, X.-T. Wu, Z.-Y. Fu, C.-P. Cui, S.-M. Hu, W.-X. Du, L.-M. Wu, H.-H. Zhang, R.-Q. Sun*. Inorg. Chem.*, **2002**, *41*(6), 1391-1396.

[106] S.Y. Yang, L.S. Long, R.B. Huang, L.S. Zheng*. Chem. Comm.*, **2002**, (5), 472-473.

[107] S.Y. Yang, L.S. Long, Y.B. Jiang, R.B. Huang, L.S. Zheng*. Chem. Mat.*, **2002**, *14*(8), 3229-3231.

[108] C. Seward, N.-X. Hu, S. Wang*. Dalton Trans.*, **2001**, (2), 134-137.

[109] G.-F. Liu, Z.-P. Qiao, H.-Z. Wang, X.-M. Chen, G. Yang*. NJC*, **2002**, *26*(6), 791-795.

[110] H.-K. Fun, S.S.S. Raj, R.-G. Xiong, J.-L. Zuo, Z. Yu, X.-Z. You*. Dalton Trans.*, **1999**, (12), 1915-1916.

[111] J. Zhang, W. Lin, Z.-F. Chen, R.-G. Xiong, B.F. Abrahams, H.-K. Fun*. Dalton Trans.*, **2001**, (12), 1806-1808.

[112] Q.-Y. Liu, L. Xu*. CrystEngComm*, **2005**, *7*, 87-89.

[113] Z.-F. Chen, R.-G. Xiong, J. Zhang, J.-L. Zuo, X.-Z. You, C.-M. Che, H.-K. Fun*. Dalton Trans.*, **2000**, (22), 4010-4012.

[114] Q. Ye, X.-B. Chen, Y.-M. Song, X.-S. Wang, J. Zhang, R.-G. Xiong, H.-K. Fun, X.-Z. You*. Inorg. Chim. Acta*, **2005**, *358*(4), 1258-1262.

[115] T.-T. Yeh, J.-Y. Wu, Y.-S. Wen, Y.-H. Liu, J. Twu, Y.-T. Tao, K.-L. Lu*. Dalton Trans.*, **2005**, (4), 656-658.

[116] Y.-B. Dong, Y. Geng, J.-P. Ma, R.-Q. Huang*. Inorg. Chem.*, **2005**, *44*(6), 1693-1703.

[117] R. Horikoshi, T. Mochida, N. Maki, S. Yamada, H. Moriyama*. Dalton Trans.*, **2002**, (1), 28-33.

[118] H. Zhang, J. Cai, X.-L. Feng, T. Li, X.-Y. Li, L.-N. Ji*. Inorg. Chem. Comm.*, **2002**, *5*(9), 637-641.

[119] H.-B. Zhou, W. Dong, M. Liang, D.-Z. Liao, Z.-H. Jiang, S.-P. Yan, P. Cheng*. Z. Anorg. Allg. Chem.*, **2004**, *630*(4), 498-500.

[120] S.D. Huang, R.-G. Xiong, J. Han, B.R. Weiner*. Inorg. Chim. Acta*, **1999**, *294*(1), 95-98.

[121] H. Hou, Y. Wei, Y. Fan, C. Du, Y. Zhu, Y. Song, Y. Niu, X. Xin*. Inorg. Chim. Acta*, **2001**, *319*(1,2), 212-218.

[122] H. Hou, X. Meng, Y. Song, Y. Fan, Y. Zhu, H. Lu, C. Du, W. Shao. *Inorg. Chem.*, **2002**, *41*(15), 4068-4075.

[123] H. Kishida, H. Matsuzaki, H. Okamoto, T. Manabe, M. Yamashita, Y. Taguchi, Y. Tokura. *Nature*, **2000**, *405*(6789), 929-932.

[124] E. Cariati, D. Roberto, R. Ugo, P.C. Ford, S. Galli, A. Sironi. *Chem. Mat.*, **2002**, *14*(12), 5116-5123.

[125] O.R. Evans, W. Lin. *Acc. Chem. Res*, **2002**, *35*(7), 511-522.

[126] K.M. Fromm. *Chem. Eur. J.*, **2001**, *7*(10), 2236-2244 *and unpublished results*.

[127] S.R. Batten, K.S. Murray. *Coord. Chem. Rev.*, **2003**, *246*(1-2), 103-130.

[128] S. Noro, H. Miyasaka, S. Kitagawa, T. Wada, T. Okubo, M. Yamashita, T. Mitani. *Inorg. Chem.*, **2005**, *44*(1), 133-146.

[129] H. Kumagai, C.J. Kepert, M. Kurmoo. *Inorg. Chem.*, **2002**, *41*(13), 3410-3422.

[130] H. Kumagai, M. Akita-Tanaka, K. Inoue, M. Kurmoo. *J. Mat. Chem.*, **2001**, *11*(9), 2146-2151.

[131] D. Maspoch, D. Ruiz-Molina, J. Veciana. *J. Mat. Chem.*, **2004**, *14*(18), 2713-2723.

[132] A. Grirrane, A. Pastor, E. Alvarez, C. Mealli, A. Ienco, P. Rosa, F. Montilla, A. Galindo. *Eur. J. Inorg. Chem.*, **2004**, *4*, 707-717.

[133] H. Srikanth, R. Hajndl, B. Moulton, M.J. Zaworotko. *J. App. Phys.*, **2003**, *93*(10), 7089-7091.

[134] B. Moulton, J. Lu, R. Hajndl, S. Hariharan, M.J. Zaworotko. *Angew. Chem., Ed. Engl.*, **2002**, *41*(15), 2821-2824.

[135] G.J. Halder, C.J. Kepert, B. Moubaraki, K.S. Murray, J.D. Cashion. *Science*, **2002**, *298*(5599), 1762-1765.

[136] Z. Huang, H.-B. Song, M. Du, S.-T. Chen, X.-H. Bu, J. Ribas. *Inorganic chemistry FIELD Publication Date:2004 Feb 9*, *43*(3), 931-944. FIELD Reference Number: FIELD Journal Code:0366543 FIELD Call Number:.

[137] T. Yuen, C.L. Lin, T.W. Mihalisin, M.A. Lawandy, J. Li. *J. App. Phys.*, **2000**, *87*(9, Pt. 3), 6001-6003.

[138] H.-R. Wen, J.-L. Zuo, W. Liu, Y. Song, X.-Z. You. *Inorg. Chim. Acta*, **2005**, *358*(8), 2565-2570.

[139] S. Kawata, S. Kitagawa, H. Kumagai, S. Iwabuchi, M. Katada. *Inorg. Chim. Acta*, **1998**, *267*(1), 143-145.

[140] R.G. Vranka, E.L. Amma. *Inorg. Chem.*, **1966**, *5*(6), 1020-1025.

[141] C. Naether, I. Jess. *Eur. J. Inorg. Chem.*, **2004**, (14), 2868-2876.

[142] O.M. Yaghi, H. Li. *J. Am. Chem. Soc.*, **1996**, *118*(1), 295-296.

[143] S.R. Batten, J.C. Jeffery, M.D. Ward. *Inorg. Chim. Acta*, **1999**, *292*(2), 231-237.

[144] F. Robinson, M.J. Zaworotko. *Chem. Comm.*, **1995**, (23), 2413-2414.

[145] H.W. Roesky, M. Andruh. *Coord. Chem. Rev.*, **2003**, *236*(1-2), 91-119.

[146] G.K. Patra, I. Goldberg. *Dalton Trans.*, **2002**, (6), 1051-1057.

[147] L.-C. Song, W.-X. Zhang, J.-Y. Wang, Q.-M. Hu. *Trans. Metal. Chem.*, **2002**, *27*(5), 526-531.

[148] A.J. Blake, N.R. Brooks, N.R. Champness, L.R. Hanton, P. Hubberstey, M. Schroder. *Pure Appl. Chem.*, **1998**, *70*(12), 2351-2357.

[149] R.L. LaDuca, Jr., R.S. Rarig, Jr., P.J. Zapf, J. Zubieta. *Sol. State Sci.*, **2000**, *2*(1), 39-45.

[150] M.-L. Tong, X.-M. Chen, B.-H. Ye, S.W. Ng. *Inorg. Chem.*, **1998**, *37*(20), 5278-5281.

[151] T. Kawano, C.-X. Du, T. Araki, I. Ueda. *Inorg. Chem. Comm.*, **2003**, *6*(2), 165-167.

[152] A.J. Blake, G. Baum, N.R. Champness, S.S.M. Chung, P.A. Cooke, D. Fenske, A.N. Khlobystov, D.A. Lemenovskii, W.-S. Li, M. Schroder. *Dalton Trans.*, **2000**, (23), 4285-4291.

[153] M.-L. Tong, Y.-M. Wu, J. Ru, X.-M. Chen, H.-C. Chang, S. Kitagawa. *Inorg. Chem.*, **2002**, *41*(19), 4846-4848.

[154] A.J. Blake, N.R. Champness, P.A. Cooke, J.E.B. Nicolson. *Chem. Comm.*, **2000**, (8), 665-666.

[155] L. Carlucci, G. Ciani, D.M. Proserpio, A. Sironi. *Dalton Trans.*, **1997**, (11), 1801-1803.

[156] M.-L. Tong, X.-M. Chen. *CrystEngComm*, **2000**, *2*, 1-5.

[157] M.A. Lawandy, X. Huang, R.-J. Wang, J. Li, J.Y. Lu, T. Yuen, C.L. Lin. *Inorg. Chem.*, **1999**, *38*(23), 5410-5414.

[158] M. Kondo, M. Shimamura, S.-I. Noro, T. Yoshitomi, S. Minakoshi, S. Kitagawa. *Chem. Lett.*, **1999**, (4), 285-286.

[159] J. Lu, C. Yu, T. Niu, T. Paliwala, G. Crisci, F. Somosa, A.J. Jacobson. *Inorg. Chem.*, **1998**, *37*(18), 4637-4640.

[160] B. Conerney, P. Jensen, P.E. Kruger, B. Moubaraki, K.S. Murray. *CrystEngComm*, **2003**, *5*, 454-458.

[161] M.L. Tong, S.L. Zheng, X.M. Chen. *Polyhedron*, **2000**, *19*(15), 1809-1814.

[162] L. Carlucci, G. Ciani, D.M. Proserpio, A. Sironi*. Chem. Comm.*, **1994**, (24), 2755-2756.
[163] J.-C. Dai, Z.-Y. Fu, X.-T. Wu*. Encyl. Nanosc. Nanotech.*, **2004**, *10*, 247-266.
[164] J.Y. Lu*. Coord. Chem. Rev.*, **2003**, *246*(1-2), 327-347.
[165] L. Pan, E.B. Woodlock, X. Wang, K.-C. Lam, A.L. Rheingold*. Chem. Comm.*, **2001**, (18), 1762-1763.
[166] L. Carlucci, G. Ciani, D.M. Proserpio, S. Rizzato*. CrystEngComm*, **2002**, *4*, 121-129.
[167] M. Maekawa, H. Konaka, Y. Suenaga, T. Kuroda-Sowa, M. Munakata*. Dalton Trans.*, **2000**, (22), 4160-4166.
[168] L. Carlucci, G. Ciani, D.M. Proserpio*. Chem. Comm.*, **1999**, (5), 449-450.
[169] Y.-B. Dong, X. Zhao, R.-Q. Huang, M.D. Smith, H.-C. Zur Loye*. Inorg. Chem.*, **2004**, *43*(18), 5603-5612.
[170] M. Sarkar, K. Biradha*. CrystEngComm*, **2004**, *6*, 310-314.
[171] Y.-B. Dong, M.D. Smith, H.-C. zur Loye*. J. Solid State Chem.*, **2000**, *155*(1), 143-153.
[172] H.-F. Zhu, L.-Y. Kong, T.-a. Okamura, J. Fan, W.-Y. Sun, N. Ueyama*. Eur. J. Inorg. Chem.*, **2004**, (7), 1465-1473.
[173] G.K. Patra, I. Goldberg*. Cryst. Grow. Des.*, **2003**, *3*(3), 321-329.
[174] Y.-B. Dong, H.-Y. Wang, J.-P. Ma, R.-Q. Huang, M.D. Smith*. Cryst. Grow. Des.*, **2005**, *5*(2), 789-800.
[175] Y.-B. Dong, J.-Y. Cheng, J.-P. Ma, R.-Q. Huang, M.D. Smith*. Cryst. Grow. Des.*, **2005**, *5*(2), 585-591.
[176] O.-S. Jung, S.H. Park, C.H. Park, J.K. Park*. Chem. Lett.*, **1999**, (9), 923-924.
[177] O.-S. Jung, Y.J. Kim, Y.-A. Lee, H.K. Chae, H.G. Jang, J. Hong*. Inorg. Chem.*, **2001**, *40*(9), 2105-2110.
[178] X.-H. Bu, Y.-B. Xie, J.-R. Li, R.-H. Zhang*. Inorg. Chem.*, **2003**, *42*(23), 7422-7430.
[179] S. Banfi, L. Carlucci, E. Caruso, G. Ciani, D.M. Proserpio*. Dalton Trans.*, **2002**, (13), 2714-2721.
[180] S. Muthu, J.H.K. Yip, J.J. Vittal*. Dalton Trans.*, **2002**, (24), 4561-4568.
[181] C. Jubert, A. Mohamadou, C. Gerard, S. Brandes, A. Tabard, J.-P. Barbier*. Dalton Trans.*, **2002**, (13), 2660-2669.
[182] B. Chatterjee, J.C. Noveron, M.J.E. Resendiz, J. Liu, T. Yamamoto, D. Parker, M. Cinke, C.V. Nguyen, A.M. Arif, P.J. Stang*. J. Am. Chem. Soc.*, **2004**, *126*(34), 10645-10656.
[183] B. Schmaltz, A. Jouaiti, M.W. Hosseini, A. De Cian*. Chem. Comm.*, **2001**, (14), 1242-1243.
[184] X.-H. Bu, W. Chen, W.-F. Hou, M. Du, R.-H. Zhang, F. Brisse*. Inorg. Chem.*, **2002**, *41*(13), 3477-3482.
[185] M. Oh, C.L. Stern, C.A. Mirkin*. Inorg. Chem.*, **2005**, *44*(8), 2647-2653.
[186] K.M. Fromm, E.D. Gueneau, G. Bernardinelli, H. Goesmann, J. Weber, M.J. Mayor-Lopez, P. Boulet, H. Chermette*. J. Am. Chem. Soc.*, **2003**, *125*(12), 3593-3604.
[187] K.M. Fromm*. CrystEngComm*, **2002**, *4*, 318-322.
[188] M. Mayor, M. Buschel, K.M. Fromm, J.-M. Lehn, J. Daub*. Chem. Eur. J.*, **2001**, *7*(6), 1266-1272.
[189] K.M. Fromm, E.D. Gueneau, H. Goesmann*. Chem. Comm.*, **2000**, (22), 2187-2188.
[190] K.M. Fromm, H. Goesmann*. Acta Cryst. C*, **2000**, *C56*(10), 1179-1180.
[191] K.M. Fromm, H. Goesmann, G. Bernardinelli*. Polyhedron*, **2000**, *19*(15), 1783-1789.
[192] K.M. Fromm, G. Bernardinelli, M.J. Mayor-Lopez, H. Goesmann*. Z. Anorg. Allg. Chem.*, **2000**, *626*(7), 1685-1691.
[193] K.M. Fromm*. Chem. Comm.*, **1999**, (17), 1659-1660.
[194] K.M. Fromm*. Angew. Chem., Ed. Engl.*, **1998**, *36*(24), 2799-2801.
[195] K. Fromm, G. Bernardinelli*. Z. Anorg. Allg. Chem.*, **2001**, *627*(7), 1626-1630.
[196] B. Li, X. Zhu, J. Zhou, Y. Peng, Y. Zhang*. Polyhedron*, **2004**, *23*(18), 3133-3141.
[197] L.-C. Song, W.-X. Zhang, Q.-M. Hu*. Chin. J. Chem.*, **2002**, *20*(11), 1421-1429.
[198] P. Grosshans, A. Jouaiti, V. Bulach, J.-M. Planeix, M.W. Hosseini, N. Kyritsakas*. Eur. J. Inorg. Chem.*, **2004**, (3), 453-458.
[199] E.D. Blue, T.B. Gunnoe, N.R. Brooks*. Angew. Chem., Ed. Engl.*, **2002**, *41*(14), 2571-2573.
[200] X.-F. Huang, Y.-H. Li, Q. Wu, Q. Ye, R.-G. Xiong*. Inorg. Chim. Acta*, **2005**, *358*(6), 2097-2100.
[201] G.A. Bowmaker, S.E. Boyd, J.V. Hanna, R.D. Hart, P.C. Healy, B.W. Skelton, A.H. White*. Dalton Trans.*, **2002**, (13), 2722-2730.
[202] E.W. Ainscough, A.M. Brodie, A.K. Burrell, G.H. Freeman, G.B. Jameson, G.A. Bowmaker, J.V. Hanna, P.C. Healy*. Dalton Trans.*, **2001**, (2), 144-151.

[203] P. Borsting, P.J. Steel. *Eur. J. Inorg. Chem.*, **2004**, (2), 376-380.

[204] P.M. Graham, R.D. Pike, M. Sabat, R.D. Bailey, W.T. Pennington. *Inorg. Chem.*, **2000**, *39*(22), 5121-5132.

[205] C.B. Aakeroy, A.M. Beatty, K.R. Lorimer. *Dalton Trans.*, **2000**, (21), 3869-3872.

[206] A.J. Blake, N.R. Brooks, N.R. Champness, P.A. Cooke, A.M. Deveson, D. Fenske, P. Hubberstey, W.-S. Li, M. Schroder. *Dalton Trans.*, **1999**, (13), 2103-2110.

[207] X. Xue, X.-S. Wang, R.-G. Xiong, X.-Z. You, B.F. Abrahams, C.-M. Che, H.-X. Ju. *Angew. Chem., Ed. Engl.*, **2002**, *41*(16), 2944-2946.

[208] H. Place, B. Scott, R.D. Willett. *Inorg. Chim. Acta*, **2001**, *319*(1,2), 43-48.

[209] W. Bi, D. Sun, R. Cao, M. Hong. *Acta Cryst. E*, **2002**, *E58*(7), m324-m325.

[210] J.H. Liao, P.L. Chen, C.C. Hsu. *J. Phys. Chem. Solids*, **2001**, *62*(9-10), 1629-1642.

[211] J.-F. Ma, J. Yang, S.-L. Li, S.-Y. Song, H.-J. Zhang, H.-S. Wang, K.-Y. Yang. *Cryst. Grow. Des.*, **2005**, *5*(2), 807-812.

[212] M.B. Zaman, K.A. Udachin, J.A. Ripmeester. *CrystEngComm*, **2002**, *4*(103), 613-617.

[213] L. Carlucci, G. Ciani, M. Moret, D.M. Proserpio, S. Rizzato. *Chem. Mat.*, **2002**, *14*(1), 12-16.

[214] X.-C. Su, S. Zhu, H.-K. Lin, X.-B. Leng, Y.-T. Chen. *Dalton Trans.*, **2001**, (21), 3163-3168.

[215] L. Carlucci, N. Cozzi, G. Ciani, M. Moret, D.M. Proserpio, S. Rizzato. *Chem. Comm.*, **2002**, (13), 1354-1355.

[216] J.Y. Lu, A.M. Babb. *Chem. Comm.*, **2002**, (13), 1340-1341.

[217] K.N. Power, T.L. Hennigar, M.J. Zaworotko. *Chem. Comm.*, **1998**, (5), 595-596.

[218] M.A. Withersby, A.J. Blake, N.R. Champness, P.A. Cooke, P. Hubberstey, A.L. Realf, S.J. Teat, M. Schroder. *Dalton Trans.*, **2000**, (19), 3261-3268.

[219] L.-G. Zhu, S. Kitagawa. *Inorg. Chem. Comm.*, **2002**, *5*(5), 358-360.

[220] L.R. Macgillivray, K.T. Holman, J.L. Atwood. *Cryst. Eng.*, **1998**, *1*(1), 87-96.

[221] C.O. Badgett, C.F. Woodward. *J. Am. Chem. Soc.*, **1947**, *69*, 2907.

[222] J.B. Christensen. *Molecules*, **2001**, *6*, 47-51.

[223] K.E. Schwiebert, D.N. Chin, J.C. MacDonald, G.M. Whitesides. *Journal of the American Chemical Society*, **1996**, *118*(17), 4018-4029.

[224] L.J. Prins, D.N. Reinhoudt, P. Timmerman. *Angewandte Chemie, International Edition*, **2001**, *40*(13), 2382-2426.

[225] S.F. Alshahateet, R. Bishop, D.C. Craig, M.L. Scudder. *Cryst. Grow. Des.*, **2004**, *4*(4), 837-844.

[226] T. Spaniel, H. Gorls, J. Scholz. *Angew. Chem., Ed. Engl.*, **1998**, *37*(13/14), 1862-1865.

[227] S. Lopez, S.W. Keller. *Inorg. Chem.*, **1999**, *38*(8), 1883-1888.

[228] S.W. Lee, W.C. Trogler. *Inorg. Chem.*, **1990**, *29*(9), 1659-1662.

[229] C. Koelmel, R. Ahlrichs. *J. Phys. Chem.*, **1990**, *94*(14), 5536-5542.

[230] M. Vitale, P.C. Ford. *Coord. Chem. Rev.*, **2001**, *219-221*, 3-16.

[231] S.P. Anthony, T.P. Radhakrishnan. *Cryst. Grow. Des.*, **2004**, *4*(6), 1223-1227.

[232] A.J. Blake, N.R. Brooks, N.R. Champness, P.A. Cooke, M. Crew, A.M. Deveson, L.R. Hanton, P. Hubberstey, D. Fenske, M. Schroder. *Cryst. Eng.*, **1999**, *2*(2/3), 181-195.

[233] A.N. Khlobystov, N.R. Champness, C.J. Roberts, S.J.B. Tendler, C. Thompson, M. Schroeder. *CrystEngComm*, **2002**, *4*, 426-431.

[234] S.L. James. *Macromol. Symp.*, **2004**, *209*, 119-131.

[235] P. Miller, M. Nieuwenhuyzen, J.P.H. Charmant, S.L. James. *CrystEngComm*, **2004**, *6*, 408-412.

[236] L. Han, R. Wang, D. Yuan, B. Wu, B. Lou, M. Hong. *J. Mol. Struc.*, **2005**, *737*(1), 55-59.

[237] F.H. Allen. *Chem. Des. Automat. News*, **1993**, *8*, 31.

[238] R.J. Lancashire. *Compreh. Coord. Chem.*, **1987**, *5*, 777.

[239] A. Bondi. *J. Phys. Chem.*, **1964**, *68*(3), 441-451.

[240] M. Jansen. *Angew. Chem.*, **1987**, *99*(11), 1136-1149.

[241] C.-C. Wang, C.-H. Yang, S.-M. Tseng, S.-Y. Lin, T.-Y. Wu, M.-R. Fuh, G.-H. Lee, K.-T. Wong, R.-T. Chen, Y.-M. Cheng, P.-T. Chou. *Inorg. Chem.*, **2004**, *43*(16), 4781-4783.

[242] O. Vallat, A. Neels, H. Stoeckli-Evans. *Journal of Chemical Crystallography*, **2003**, *33*(1), 39-50.

[243] P. Lin, R.A. Henderson, R.W. Harrington, W. Clegg, C.-D. Wu, X.-T. Wu. *Inorg. Chem.*, **2004**, *43*(1), 181-188.

[244] M.A. Withersby, A.J. Blake, N.R. Champness, P.A. Cooke, P. Hubberstey, W.-S. Li, M. Schroder. *Crystal Engineering*, **1999**, *2*(2/3), 123-136.

[245] R. Horikoshi, T. Mochida, H. Moriyama. *Inorg. Chem.*, **2002**, *41*(11), 3017-3024.

[246] C. He, B.-G. Zhang, C.-Y. Duan, J.-H. Li, Q.-J. Meng. *Eur. J. Inorg. Chem.*, **2000**, (12), 2549-2554.

[247] K. Singh, J.R. Long, P. Stavropoulos. *J. Am. Chem. Soc.*, **1997**, *119*(12), 2942-2943.

[248] A. Bayler, A. Schier, G.A. Bowmaker, H. Schmidbaur. *J. Am. Chem. Soc.*, **1996**, *118*(29), 7006-7007.

[249] C.-M. Che, M.-C. Tse, M.C.W. Chan, K.-K. Cheung, D.L. Phillips, K.-H. Leung. *J. Am. Chem. Soc.*, **2000**, *122*(11), 2464-2468.

[250] L.F. Veiros, M.J. Calhorda. *J. Organomet. Chem*, **1996**, *510*(1-2), 71-81.

[251] V.J. Catalano, H.M. Kar, B.L. Bennett. *Inorg. Chem.*, **2000**, *39*(1), 121-127.

[252] P.D. Harvey, H.B. Gray. *J. Am. Chem. Soc.*, **1988**, *110*(7), 2145-2147.

[253] R.-H. Uang, C.-K. Chan, S.-M. Peng, C.-M. Che. *Chem. Comm.*, **1994**, (22), 2561-2562.

[254] S.K. Ghosh, P.K. Bharadwaj. *Inorg. Chem.*, **2004**, *43*(22), 6887-6889.

[255] S.K. Ghosh, P.K. Bharadwaj. *Inorg. Chem.*, **2004**, *43*(17), 5180-5182.

[256] S. Neogi, G. Savitha, P.K. Bharadwaj. *Inorg. Chem.*, **2004**, *43*(13), 3771-3773.

[257] J.L. Atwood, L.J. Barbour, T.J. Ness, C.L. Raston, P.L. Raston. *J. Am. Chem. Soc.*, **2001**, *123*(29), 7192-7193.

[258] J.M. Harrowfield, B.J. Peachey, B.W. Skelton, A.H. White. *Aust. J. Chem.*, **1995**, *48*(7), 1349-1356.

[259] L. Troxler, J.M. Harrowfield, G. Wipff. *J. Phys. Chem. A*, **1998**, *102*(34), 6821-6830.

[260] M.J. Frisch, G.W. Trucks, H.B. Schlegel, G.E. Scuseria, M.A. Robb, J.R. Cheeseman, J. J. A. Montgomery, T. Vreven, K.N. Kudin, J.C. Burant, J.M. Millam, S.S. Iyengar, J. Tomasi, V. Barone, B. Mennucci, M. Cossi, G. Scalmani, N. Rega, G.A. Petersson, H. Nakatsuji, M. Hada, M. Ehara, K. Toyota, R. Fukuda, J. Hasegawa, M. Ishida, T. Nakajima, Y. Honda, O. Kitao, H. Nakai, M. Klene, X. Li, J.E. Knox, H.P. Hratchian, J.B. Cross, C. Adamo, J. Jaramillo, R. Gomperts, R.E. Stratmann, O. Yazyev, A.J. Austin, R. Cammi, C. Pomelli, J.W. Ochterski, P.Y. Ayala, K. Morokuma, G.A. Voth, P. Salvador, J.J. Dannenberg, V.G. Zakrzewski, S. Dapprich, A.D. Daniels, M.C. Strain, O. Farkas, D.K. Malick, A.D. Rabuck, K. Raghavachari, J.B. Foresman, J.V. Ortiz, Q. Cui, A.G. Baboul, S. Clifford, J. Cioslowski, B.B. Stefanov, G. Liu, A. Liashenko, P. Piskorz, I. Komaromi, R.L. Martin, D.J. Fox, T. Keith, M.A. Al-Laham, C.Y. Peng, A. Nanayakkara, M. Challacombe, P.M.W. Gill, B. Johnson, W. Chen, M.W. Wong, C. Gonzalez, J.A. Pople, Revision B.01.

[261] P.J. Hay, W.R. Wadt. *J. Chem. Phys.*, **1985**, *82*(1), 299-310.

[262] M.N. Huda, A.K. Ray. *Eur. Phys. J. D*, **2003**, *22*(2), 217-227.

[263] L. Yang, X. Shan, Q. Chen, Z. Wang, J.S. Ma. *Eur. J. Inorg. Chem.*, **2004**, (7), 1474-1477.

[264] G. Zhang, G. Yang, Q. Chen, J.S. Ma. *Cryst. Grow. Des.*, **2005**, *5*(2), 661-666.

[265] S.Q. Liu, T. Kuroda-Sowa, H. Konaka, Y. Suenaga, M. Maekawa, T. Mizutani, G.L. Ning, M. Munakata. *Inorg. Chem.*, **2005**, *44*(4), 1031-1036.

[266] N.S. Oxtoby, A.J. Blake, N.R. Champness, C. Wilson. *Proc. Natl. Acad. Sci. USA.*, **2002**, *99*(8), 4905-4910.

[267] J.J.M. Amoore, C.A. Black, L.R. Hanton, M.D. Spicer. *Cryst. Grow. Des.*, *5*(3), 1255-1261.

[268] D.L. Reger, R.F. Semeniuc, V. Rassolov, M.D. Smith. *Inorg. Chem.*, **2004**, *43*(2), 537-554.

[269] S.-L. Zheng, M.-L. Tong, S.-D. Tan, Y. Wang, J.-X. Shi, Y.-X. Tong, H.K. Lee, X.-M. Chen. *Organometallics*, **2001**, *20*(25), 5319-5325.

[270] C. Seward, J. Chan, D. Song, S. Wang. *Inorg. Chem.*, **2003**, *42*(4), 1112-1120.

[271] D.-L. Long, A.J. Blake, N.R. Champness, C. Wilson, M. Schroder. *Chem. Eur. J.*, **2002**, *8*(9), 2026-2033.

[272] A.P. Cote, G.K.H. Shimizu. *Coord. Chem. Rev.*, **2003**, *245*(1-2), 49-64.

[273] A.P. Cote, M.J. Ferguson, K.A. Khan, G.D. Enright, A.D. Kulynych, S.A. Dalrymple, G.K.H. Shimizu. *Inorg. Chem.*, **2002**, *41*(2), 287-292.

[274] L. Carlucci, G. Ciani, D.M. Proserpio, S. Rizzato. *CrystEngComm*, **2002**, *4*, 413-425.

[275] L. Mimassi, C. Guyard-Duhayon, L. Raehm, H. Amouri. *Eur. J. Inorg. Chem.*, **2002**, (9), 2453-2457.

[276] J.D. Woodward, R. Backov, K.A. Abboud, H. Ohnuki, M.W. Meisel, D.R. Talham. *Polyhedron*, **2003**, *22*(20), 2821-2830.

[277] M. Du, S.-T. Chen, X.-H. Bu, J. Ribas. *Inorg. Chem. Comm.*, **2002**, *5*(11), 1003-1006.

[278] Y.-B. Dong, J.-P. Ma, M.D. Smith, R.-Q. Huang, B. Tang, D.-S. Guo, J.-S. Wang, H.-C. zur Loye. *Sol. State Sci.*, **2003**, *5*(4), 601-610.

[279] L. Carlucci, G. Ciani, A. Gramaccioli, D.M. Prosperpio, S. Rizzato. *CrystEngComm*, **2000**, *29*, 154-163.

[280] M.-L. Tong, B.-H. Ye, J.-W. Cai, X.-M. Chen, S.W. Ng. *Inorg. Chem.*, **1998**, *37*(11), 2645-2650.

[281] T.X. Neenan, W.L. Driessen, J.G. Haasnoot, J. Reedijk. *Inorg. Chim. Acta*, **1996**, *247*(1), 43-49.

[282] J.Y. Lu, W.A. Fernandez, Z. Ge, K.A. Abboud. *NJC*, **2005**, *29*(3), 434-438.

[283] M.J. Plater, M.R.S.J. Foreman, T. Gelbrich, M.B. Hursthouse. *Cryst. Eng.*, **2001**, *4*(4), 319-328.

[284] R.N. Keller, H.D. Wycoff. *Inorg. Synth.*, **1946**, *2*, 1-4.

[285] J. Cosier, A.M. Glazer. *J. App. Cryst.*, **1986**, *19*(2), 105-107.

[286] E. Blanc, D. Schwarzenbach, H.D. Flack. *J. App. Cryst.*, **1991**, *24*(6), 1035-1041.

[287] G.M. Sheldrick. *SHELX-99, Program for Crystal Ctructure Refinement*, **1999**, University of Göttingen, Göttingen.

[288] E.R. Wolfel. *J. Appl. Crystallogr.*, **1981**, *14*, 291-296.

[289] E.R. Wolfel. *J. Appl. Crystallogr.*, **1983**, *16*, 341-348.

[290] P.E. Werner, L. Eriksson, M. Westdahl. *J. App. Cryst.*, **1985**, *18*(5), 367-370.

[291] A. Altomare, M. Camalli, R. Caliandro, C. Cuocci, C. Giacovazzo, A. Guagliardi, A.G.G. Moliterni, R. Rizzi, **2004,** EXPO2004. Program for Solving Crystal Structures from Powder Data by direct Methods.

[292] A.L. Spek. *J. App. Cryst.*, **2003**, *36*(1), 7-13.

[293] B.H. Toby. *J. App. Cryst.*, **2001**, *34*(2), 210-213.

[294] A. Larson, R. Von Dreele, **2000,** General Structure Analysis System (GSAS), Los Alamos National Laboratory Report LAUR.

[295] V.C. International Tables for X-ray Crystallography, Chap. 9, **1999,** Edt. Wilson, A. J. C.; Prince, E: Kluwer Academic Publishers, Dordrecht, The Netherlands.

G - Appendices

I - Abbreviations

DMC	1,3-dimethyl-2-chloroimidazolium chloride	**LMCT**	Ligand to Metal Charge Transfert
DMF	Dimethylformamide	**MeCN**	Acetonitrile
DMSO	Dimethylsulfoxide	**$MeCO_2^-$**	Acetate
EtOH	Ethanol	**MLCT**	Metal to Ligand Charge Transfert
ESI/MS	ElectroSpray Ionisation Mass Spectroscopy	**NMR**	Nuclear magnetic resonance
FT-IR spectro.	Fourier Transform InfraRed spectroscopy	**SDTA**	Scanning Differential Thermal Analysis
IR	InfraRed	**TGA**	Thermo-Gravimetric Analysis
L	Ethanediyl bis(isonicotinate)	**THF**	tetrahydrofurane

IR designations

ν	Stretching vibrations	**s**	strong
γ	Out of plane vibrations	**m**	medium
δ	In plane vibrations	**w**	weak

^{1}H-NMR desigantions

s	singulet
m	mutiplet

II - Summary

This thesis reports the synthesis of the ligand ethanediyl bis(isonicotinate), **L**, as well as the building of coordination polymers based on **L** and Cu^I, Ag^I and Cu^{II} salts.

Chapter A gives an overview on coordination polymers, their syntheses, structures, and applications. It describes the use of bidentate ligands with *N,N'*-donors with silver and copper cations for the building of such metal-organic frameworks.

Chapter B-I discusses the synthesis of the ligand ethanediyl bis(isonicotinate), **L**, and presents its characterizations and its crystallographic structure.

Chapter B-II describes coordination polymers obtained from **L** and CuCl. It is focused on the importance of the crystallization solvent, since two different compounds appear according to the chosen crystallization solvent.

Chapter B-III is devoted to the study of silver(I) coordination polymers based on **L** and silver salt. The numerous obtained silver coordination polymers allow finding some rules concerning the crystallization solvent influence or the counter ion influence.

Chapter B-IV presents some copper(II) coordination polymers build up with **L** and copper nitrate or perchlorate. With these compounds, the behaviour of the ligand **L** towards more “rigid” cations was studied.

Chapter C summarizes the related works, presents the outlooks to this project and especially the possible applications for the synthesized metal-organic frameworks.

H - Curriculum Vitae

PERSONNAL INFORMATIONS

Nationality	French
Date of birth	23rd August 1977 (Romilly/sur/Seine - France)
Gender	female

PROFESSIONAL

Studies towards PhD

2003-2005 University of Basle (Switzerland)
2001-2003 University of Geneva (Switzerland)
"Structural diversity of Cu(I), Ag(I) and Cu(II) coordination polymers with the ligand ethanediyl bis(isonicotinate)"
Assistant in Seminar and in Lab Classes
Group operator of single crystal X-ray diffractometer
Supervisor: Prof. Katharina M. FROMM

2001 **Preparation of a diploma in chemistry** (6 months)
GMI (Laboratory of inorganic chemistry) at IPCMS (Institute for Physic and Chemistry of Materials in Strasbourg)
"Cobalt-Ruthenium alloy nano-particles in an silicate ordered matrix"
Supervisor: Prof. J. L. Guille

2000-2001 **Micro-project**
Rohm&Haas (Alsace - France)
"Economic feasibility study in order to replace filters in an existing chemical process"

2000 **Training period** (4 months)
MTU (subsidiary company of Daimler-Chrysler; München - Germany)
"Powder X-ray diffraction study of a ceramic"

DIPLOMA

2005 **PhD awarded July 2005 (magna cum laude)**
University of Basle

2001 **Diplôme d'ingénieur (Master degree in Chemical Engineering)**
ECPM (European School of Chemistry, Polymers and Materials of Strasbourg)

2001 **DEA Chimie analytique et chimie des matériaux (French equivalent to the diploma in Chemistry of a master degree in Chemistry, specialized in materials)**
ECPM (European School of Chemistry, Polymers and Materials of Strasbourg)
GMI (Laboratory of inorganic chemistry) at IPCMS (Institute for Physic and Chemistry of Materials in Strasbourg)

PRESENTATIONS AT MEETINGS

- Posters at meetings of the Swiss Chemical Society in 2002, 2003 und 2004

- Poster at the International Conference on Coordination Chemistry Heidelberg (Germany) 2002

„*Toward low dimensional coordination polymers*“

- Poster and oral presentation at the Molecular Crystal Engineering Italy 2003 (Euresco Conferences)

„*Structural diversity of Ag(I) and Cu(I) coordination polymers with the ligand ethanediyl bis(isonicotinate)*“

- Oral presentation at the International Conference on Coordination Chemistry Merida (Mexico) 2004

„*Structural diversity of Ag(I) coordination polymers with the ligand ethanediyl bis(isonicotinate)“*

SCIENTIFIC PUBLICATIONS

- Structural relationship of two coordination polymers of Cu(I) with the ligand ethanediyl bis(isonicotinate), A. Y. Robin, K. M. Fromm, H. Goesmann, G. Bernardinelli, *CrystEngComm*, **2003**, *5*(71), 405–410.

- How many structures are there for {[AgL](NO_3)(H_2O)$_n$}? Water-content dependant variations in the structure of {[AgL](NO_3)(H_2O)$_n$}, n = 0, 1, 2; L = ethanediyl bis(isonicotinate), A. Y. Robin, M. Meuwly, K. M. Fromm, H. Goesmann, G. Bernardinelli, *CrystEngComm*, **2004**, *6*(60), 336-343.

- Recent advances in the chemistry of clusters and coordination polymers of alkali, alkaline earth metal and group11 compounds, K. M. Fromm, E. D. Gueneau, A. Y. Robin, W. Maudez, J. Sague, R. Bergougnant, *Z.Anorg.Allg.Chem*, **2005**, *671*, 1725-1740.

- Concomitant crystallization of two polymorphs-a ring and a helix: concentration effect on supramolecular isomerism, K.M. Fromm, J. L. Sagué Doimeadios, A. Y. Robin, *ChemComm*, **2005**, *36*, 4548-4550.

- „Hooked-on“ Calix[8]arenes: A (H_2O)$_{10}$ Cluster with an Unprecedented Structure, R.D. Bergougnant, A.Y. Robin, K.M. Fromm, **2005**, *5*(5), 1691-1694.

- Water trapped in dibenzo-18-crown-6: theoretical and spectroscopic (IR, Raman) studies, M. Dulak, R. Bergougnant, K. M. Fromm, H. R. Hagemann, A. Y. Robin, T. A. Wesolowski, *Spectrochimica Acta Part A: Molecular and Biomolecular Spectroscopy*, **2005**¸in press.

REFERENCES

Prof. Katharina M. FROMM	Prof. Edwin E. CONSTABLE
Department of Chemistry University of Basle Spitalstrasse 51 4056 Basel (CH) katharina.fromm@unibas.ch Phone: +41/(0)61 267 10 46	Department of Chemistry University of Basle Spitalstrasse 51 4056 Basel (CH) edwin.constable@unibas.ch Phone: +41/(0)61 267 10 01